THE FATE OF CANCER: FOCUSING ON PURE COMPOUNDS DERIVED FROM TRADITIONAL CHINESE MEDICINE

EDITED BY: Haiyang Yu, Lu Chen, Yuling Qiu and Shun-Fa Yang
PUBLISHED IN: Frontiers in Pharmacology and Frontiers in Oncology

frontiers Research Topics

frontiers

ISSN 1664-8714
ISBN 978-2-83250-109-2
DOI 10.3389/978-2-83250-109-2

About Frontiers

Frontiers is more than just an open-access publisher of scholarly articles: it is a pioneering approach to the world of academia, radically improving the way scholarly research is managed. The grand vision of Frontiers is a world where all people have an equal opportunity to seek, share and generate knowledge. Frontiers provides immediate and permanent online open access to all its publications, but this alone is not enough to realize our grand goals.

Frontiers Journal Series

The Frontiers Journal Series is a multi-tier and interdisciplinary set of open-access, online journals, promising a paradigm shift from the current review, selection and dissemination processes in academic publishing. All Frontiers journals are driven by researchers for researchers; therefore, they constitute a service to the scholarly community. At the same time, the Frontiers Journal Series operates on a revolutionary invention, the tiered publishing system, initially addressing specific communities of scholars, and gradually climbing up to broader public understanding, thus serving the interests of the lay society, too.

Dedication to Quality

Each Frontiers article is a landmark of the highest quality, thanks to genuinely collaborative interactions between authors and review editors, who include some of the world's best academicians. Research must be certified by peers before entering a stream of knowledge that may eventually reach the public - and shape society; therefore, Frontiers only applies the most rigorous and unbiased reviews.
Frontiers revolutionizes research publishing by freely delivering the most outstanding research, evaluated with no bias from both the academic and social point of view. By applying the most advanced information technologies, Frontiers is catapulting scholarly publishing into a new generation.

What are Frontiers Research Topics?

Frontiers Research Topics are very popular trademarks of the Frontiers Journals Series: they are collections of at least ten articles, all centered on a particular subject. With their unique mix of varied contributions from Original Research to Review Articles, Frontiers Research Topics unify the most influential researchers, the latest key findings and historical advances in a hot research area! Find out more on how to host your own Frontiers Research Topic or contribute to one as an author by contacting the Frontiers Editorial Office: frontiersin.org/about/contact

THE FATE OF CANCER: FOCUSING ON PURE COMPOUNDS DERIVED FROM TRADITIONAL CHINESE MEDICINE

Topic Editors:
Haiyang Yu, Tianjin University of Traditional Chinese Medicine, China
Lu Chen, Tianjin University of Traditional Chinese Medicine, China
Yuling Qiu, Tianjin Medical University, China
Shun-Fa Yang, Chung Shan Medical University, Taiwan

Citation: Yu, H., Chen, L., Qiu, Y., Yang, S.-F., eds. (2022). The Fate of Cancer: Focusing on Pure Compounds Derived From Traditional Chinese Medicine. Lausanne: Frontiers Media SA. doi: 10.3389/978-2-83250-109-2

Table of Contents

frontiers in Pharmacology

ORIGINAL RESEARCH
published: 29 April 2021
doi: 10.3389/fphar.2021.680589

Andrographolide Induces Noxa-Dependent Apoptosis by Transactivating ATF4 in Human Lung Adenocarcinoma Cells

*Junqian Zhang[1†], Chunjie Li[1†], Li Zhang[1†], Yongqing Heng[1], Tong Xu[1], Yunjing Zhang[1], Xihui Chen[1], Robert M Hoffman[2,3] and Lijun Jia[1]**

[1]Cancer Institute, Longhua Hospital, Shanghai University of Traditional Chinese Medicine, Shanghai, China, [2]Department of Surgery, University of California, San Diego, La Jolla, CA, United States, [3]Anticancer Inc., San Diego, CA, United States

Lung adenocarcinoma is the most common pathological type of lung cancer with poor patient outcomes; therefore, developing novel therapeutic agents is critically needed. Andrographolide (AD), a major active component derived from the traditional Chinese medicine (TCM) *Andrographis paniculate*, is a potential antitumor drug, but the role of AD in lung adenocarcinoma remains poorly understood. In the present study, we demonstrated that AD inhibited the proliferation of broad-spectrum lung cancer cell lines in a dose-dependent manner. Meanwhile, we found that a high dose of AD induced Noxa-dependent apoptosis in human lung adenocarcinoma cells (A549 and H1299). Further studies revealed that Noxa was transcriptionally activated by activating transcription factor 4 (ATF4) in AD-induced apoptosis. Knockdown of ATF4 by small interfering RNA (siRNA) significantly diminished the transactivation of Noxa as well as the apoptotic population induced by AD. These results of the present study indicated that AD induced apoptosis of human lung adenocarcinoma cells by activating the ATF4/Noxa axis and supporting the development of AD as a promising candidate for the new era of chemotherapy.

Keywords: TCM, andrographolide, lung adenocarcinoma, apoptosis, ATF4, noxa

OPEN ACCESS

Edited by:
Haiyang Yu,
Tianjin University of Traditional Chinese Medicine, China

Reviewed by:
Ping Chen,
Zhengzhou University, China
Zhen W Ang,
Chinese Academy of Medical Sciences, China

****Correspondence:***
Lijun Jia
ljjia@shutcm.edu.cn

[†]These authors have contributed equally to this work and share first authorship

Specialty section:
This article was submitted to Pharmacology of Anti-Cancer Drugs, a section of the journal Frontiers in Pharmacology

Received: *15 March 2021*
Accepted: *09 April 2021*
Published: *29 April 2021*

Citation:
Zhang J, Li C, Zhang L, Heng Y, Xu T, Zhang Y, Chen X, Hoffman RM and Jia L (2021) Andrographolide Induces Noxa-Dependent Apoptosis by Transactivating ATF4 in Human Lung Adenocarcinoma Cells. Front. Pharmacol. 12:680589. doi: 10.3389/fphar.2021.680589

INTRODUCTION

Lung adenocarcinoma is recalcitrant cancer with overall survival of less than 5 years (Denisenko et al., 2018). Intolerable side effects and multidrug resistance are still the main causes of the poor outcomes of patients with lung adenocarcinoma (Malhotra and Perry, 2003; Thomas et al., 2015; Jamal-Hanjani et al., 2017; Rotow and Bivona, 2017). Therefore, it is urgently needed to develop novel therapeutic agents with high efficiency and low toxicity to ameliorate patient outcomes.

Cell apoptosis is a process of programmed cell death, and inducing tumor cell apoptosis has become a strategy for cancer therapy (Gerl and Vaux, 2005; Hanahan and Weinberg, 2011). Among the apoptotic regulatory proteins, pro-apoptotic BH3-only (Bcl-2 homology domain 3) protein Noxa, a member of the Bcl-2 (B cell lymphoma-2) family proteins, has been defined as an antitumor drug target (Pérez-Galán et al., 2006; Albert et al., 2014; Guikema et al., 2017; Morsi et al., 2018). Inoue et al. reported that Noxa mediated HDAC (histone deacetylase) inhibitor-induced apoptosis and suggested that activated Noxa could be a potential clinical target for chronic lymphocytic leukemia and lymphoma therapy (Inoue et al., 2007). Shibue et al. reported that Noxa is necessary for irradiation-induced apoptosis and supported that upregulated Noxa may provide a new strategy for

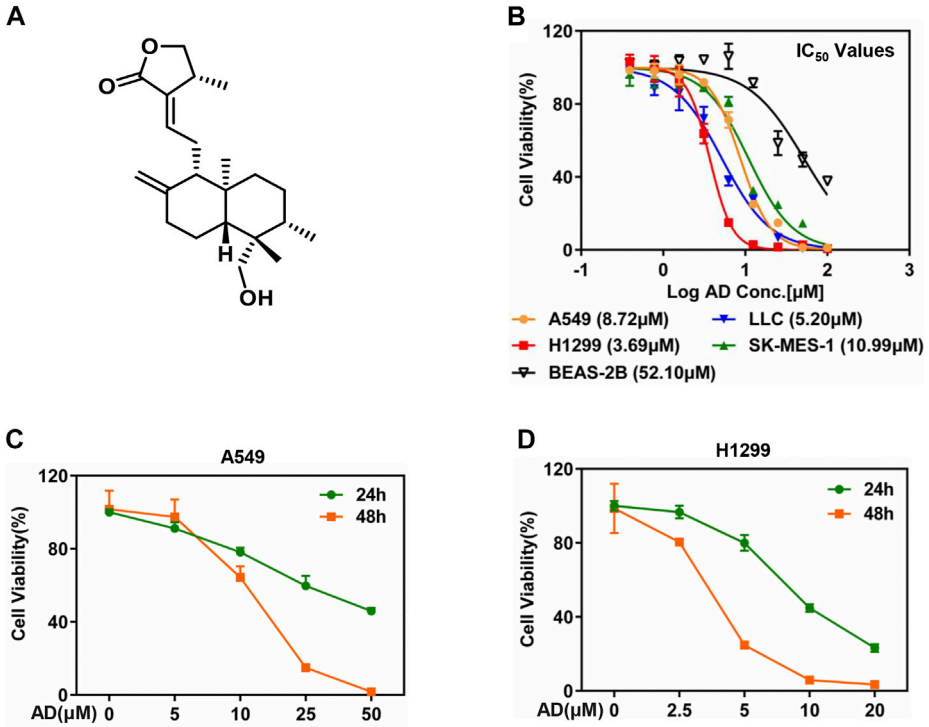

FIGURE 1 | Andrographolide inhibited the proliferation of lung cancer cells. **(A)** The chemical structure of AD. **(B)** Cells were seeded in ATPlite plates in triplicate, 2000 cells per well, cultured overnight, and treated with 1‰ DMSO or various concentrations of AD (100, 50, 25, 12.5, 6.25, 3.13, 1.56, and 0.78 μM) for 48 h. The ATPlite cell viability assay was used to determine the half-maximal inhibitory concentrations IC_{50} of A549, H1299, SK-MES-1, LLC, and BEAS-2B cells, respectively. **(C–D)** Cells were seeded in ATPlite plates in triplicate, 2000 cells per well, cultured overnight, and treated with 1‰ DMSO or indicated concentrations of AD for 24 h and 48 h, followed by the ATPlite cell viability assay.

cancer therapy (Shibue et al., 2003). Activating transcription factor 4 (ATF4) is a universal stress-responsive gene and could transcriptionally activate Noxa in response to chemotherapy. Armstrong et al. reported that apoptosis induced by fenretinide and bortezomib via upregulating Noxa was dependent on ATF4 (Armstrong et al., 2010). Chen et al. found the same mechanism in a small molecule compound MLN4924-treated human esophageal cancer cells (Chen et al., 2016). In conclusion, targeting ATF4/Noxa axis could be a promising strategy for cancer treatment (Zhu et al., 2012; Nunez-Vazquez et al., 2020).

There is currently a great interest in developing traditional Chinese medicine (TCM) into first-line therapy for cancer (Tang et al., 1999; Efferth et al., 2007; Lu et al., 2019). Andrographolide (AD) is one of the major active components of the TCM *Andrographis paniculate* (Zhao et al., 2002). Previous studies have reported that AD exhibits a broad-spectrum antitumor efficacy in various cancer cells (Banerjee et al., 2016; Kumar et al., 2016; Islam et al., 2018; Chen et al., 2019). However, the antitumor efficacy and the underlying molecular mechanisms of AD on human lung adenocarcinoma cells remains poorly understood. In this study, we demonstrated that AD exhibits a broad-spectrum proliferation inhibitory effect in lung cancer cells, and firstly reported that AD induced lung adenocarcinoma cell apoptosis via activating ATF4/Noxa axis. The present study provides a basis to clinically develop AD for the new era of chemotherapy.

MATERIALS AND METHODS

Cells and Reagents

Human lung adenocarcinoma cells (A549, H1299), human lung squamous cells (SK-MES-1), murine Lewis lung carcinoma cells (LLC), and normal human bronchial epithelial cells (BEAS-2B) were obtained from the American Type Culture Collection (Manassas, VA, United States). These cells were cultured in Dulbecco's modified Eagle's medium (DMEM, BasalMedia, Shanghai, China) which contains 10% fetal bovine serum (FBS, BasalMedia, Shanghai, China) and 1% penicillin–streptomycin solution (BasalMedia, Shanghai, China) at 37°C with 5% CO_2. Andrographolide (Sigma-Aldrich, Germany) was dissolved into a concentration of 100 mM with dimethyl sulfoxide (DMSO, Sigma-Aldrich, Germany) and stored at -20°C. Antibody against β-actin was obtained from HuaBio (Hangzhou, China); Antibodies against cleaved-PARP (c-PARP), PARP, cleaved-caspase-3 (c-Casp3), caspase3 (Casp3), ATF4, c-Myc, Noxa, Puma, Bid, Bim, Bik, Bax, and Bak were all obtained from Cell Signaling Technology (Beverly, MA, United States).

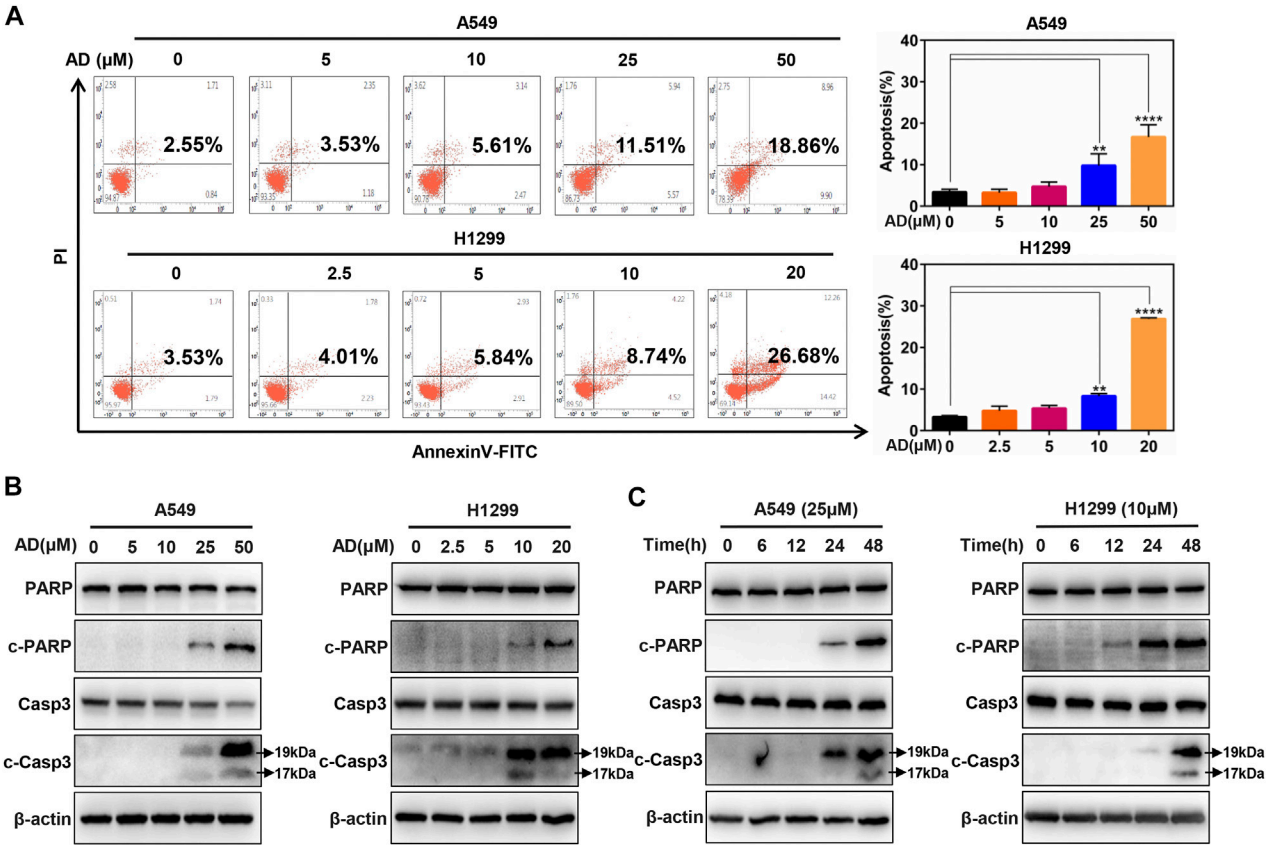

FIGURE 2 | Andrographolide triggered apoptosis in human lung adenocarcinoma cells **(A)** Cells were treated with 1‰ DMSO or indicated concentrations of AD for 24 h, then subjected to Annexin V-FITC/PI staining, followed by the flow cytometric analysis. **(B–C)** After being treated with 1‰ DMSO or AD at indicated concentrations and different times, cell protein was extracted and detected by Western blotting with antibodies against PARP, c-PARP, Casp3 and c-Casp3, and β-actin (** $p \leq 0.01$; **** $p \leq 0.0001$).

Cell Proliferation Assay

Cells in the exponential growth phase were seeded in ATPlite plates in triplicate, 2000 cells per well, cultured overnight, and treated with 1‰ DMSO or AD at indicated concentrations for 24 h and 48 h, followed by the ATPlite luminescence assay (BD Pharmingen, Franklin Lakes, New Jersey, United States).

Western Blotting

Cells were harvested and lysed in RIPA buffer (Beyotime, Shanghai, China). Protein concentrations were determined by the protein assay kit (Epizyme, Shanghai, China). Gel electrophoresis (SDS–PAGE) was used to separate the total proteins of the samples. Then, the proteins were transferred onto a polyvinylidene fluoride membrane (PVDF). 5% nonfat milk in TBST was used to block the PVDF membrane for 1 h at room temperature. The membranes with a primary antibody were co-incubated at 4°C and washed three times with TBST overnight, and then co-incubated with a secondary antibody at room temperature for 1 h. After then, washed three times with TBST and visualized with the ECL kit (Share Bio, Shanghai, China) and film (Tanon, Shanghai, China).

Real-Time Polymerase Chain Reaction Analyses (RT-PCR)

Ultrapure RNA kit (ComWin Biotech, Beijing, China) was used to isolate total RNA, and 1 μg total RNA was reversed to cDNA by using the PrimerScript reverse transcription reagent kit (Vazyme Biotech, Nanjing, China). Then, the cDNA was quantified with RT-PCR by using the Power SYBR Green PCR MasterMix (Vazyme Biotech, Nanjing, China) on the ABI 7500 thermocycler (Applied Biosystems, Foster City, CA, United States). The mRNA abundance of each sample was normalized to β-actin. Primers were designed and synthesized by BioSune (Shanghai, China). The sequences of the primers were as follows: human β-actin: forward 5′-CGTGCGTGACATTAAGGAGAAG-3′ and reverse 5′-AAGGAAGGCTGGAAGAGTGC-3′; human ATF4: forward 5′-ATGACCGAAATGAGCTTCCTG-3′ and reverse 5′-GCTGGAGAACCCATGAGGT-3′; human Noxa: forward 5′-ACCAAGCCGGATTTGCGATT-3′ and reverse 5′-ACTTGCACTTGTTCCTCGTGG-3′; and human

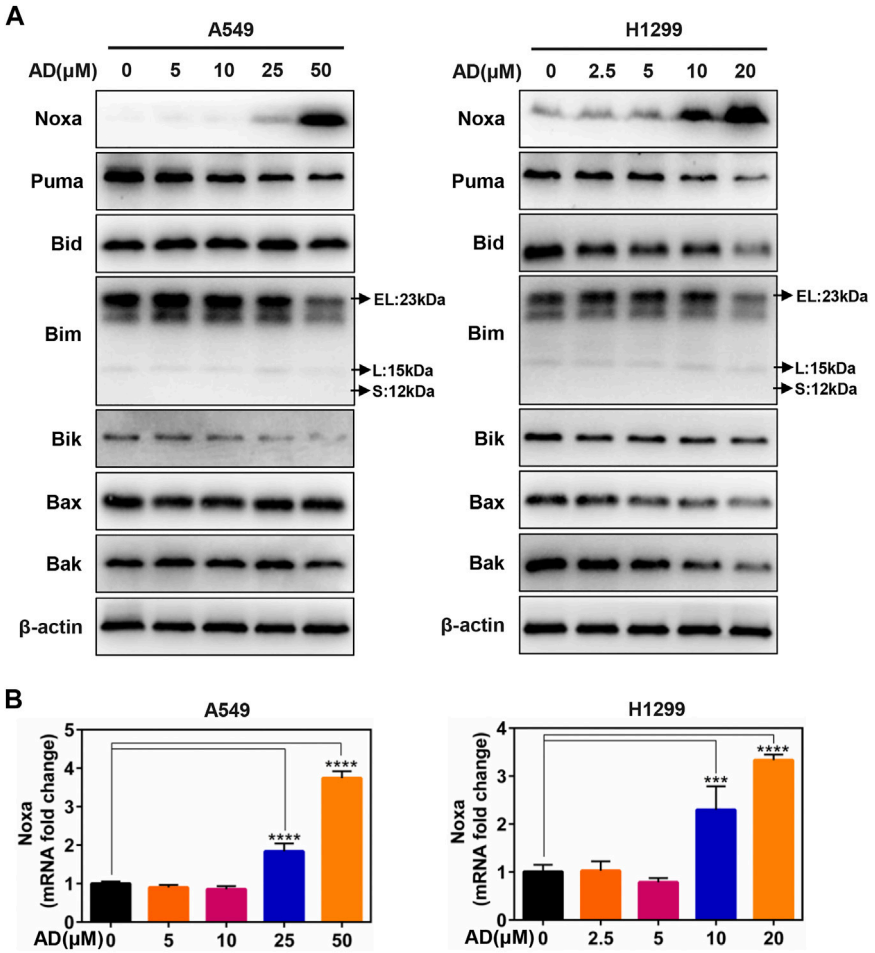

FIGURE 3 | The BH3-only protein Noxa mediated andrographolide-induced apoptosis. **(A)** Cells were treated with 1‰ DMSO or the indicated concentrations of AD for 24 h. Cell protein was extracted and detected by Western blotting with antibodies against Noxa, Puma, Bid, Bim, Bik, Bax, Bak, and β-actin. **(B)** The mRNA level of Noxa was quantified by RT-PCR (normalized to β-actin) (*** $p \leq 0.001$; **** $p \leq 0.0001$).

c-Myc: forward 5′-GGCTCCTGGCAAAAGGTCA-3′ and reverse 5′-CTGCGTAGTTGTGCTGATGT-3′.

Apoptosis Assay

Cells were harvested after treatment with different concentrations of AD for 24 h and then stained by using Annexin V-FITC/PI stain kit following the manufacturer's instructions (BD Pharmingen, New Jersey, United States). The stained cells were analyzed with flow cytometry (BD, New Jersey, United States).

Gene Silencing Using Small Interfering RNA

The siRNA oligonucleotides were transfected into cells by using Lipofectamine 2000. Briefly, Opti-MEM (Invitrogen) was used to incubate with siRNA and Lipofectamine 2000 separately for 5 min at room temperature and mixed for 20 min, and then the mixture together with the serum-free medium were applied to the cells (final concentration of siRNA is 20 nM). All siRNAs were synthesized by GenePharma (Shanghai, China). The sequences of the siRNA were as follows: negative control: 5′-UUCUCCGAA CGUGUCACGUTT-3′; siATF4: 5′-GCCUAGGUCUCUUAG AUGA-3′; siNoxa#1: 5′-GUAAUUAUUGACACAUUUC-3′ (Alves et al., 2006); and siNoxa#2: 5′-GGUGCACGUUUC AUCAAUUUG-3′ (Yao et al., 2014).

Statistical Analysis

Data were displayed as mean ± standard deviation. All data represented three independent experiments. Significant differences between groups were assessed by the two-tailed unpaired Student's t-test of GraphPad Prism software. Four levels of significance were used for all tests (*$p \leq 0.05$, **$p \leq 0.01$, ***$p \leq 0.001$, and ***$p \leq 0.0001$).

RESULTS

Andrographolide Inhibited the Proliferation of Lung Cancer Cells

The chemical structure of AD is shown in **Figure 1A**. To evaluate the inhibitory efficacy of AD on the proliferation of lung cancer cells, we determined the half-maximal inhibitory concentration

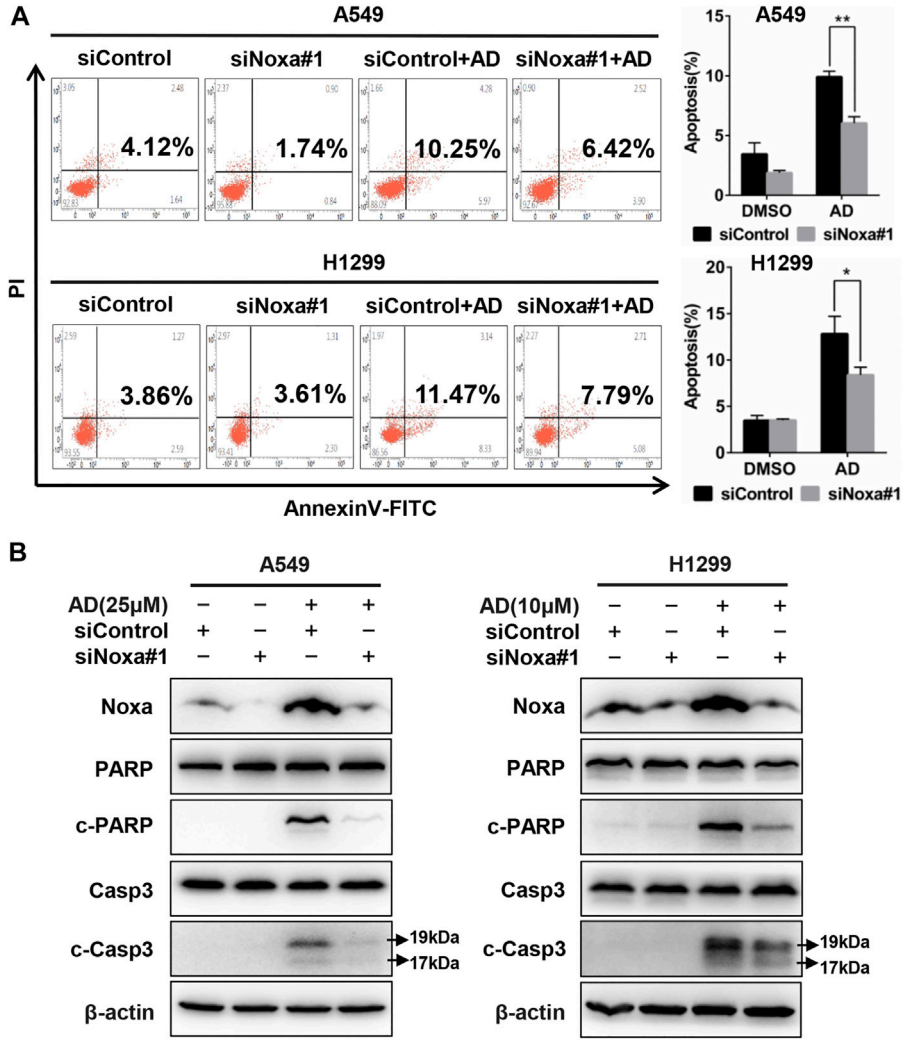

FIGURE 4 | Noxa knockdown significantly decreased andrographolide-induced apoptosis in human lung adenocarcinoma cells. **(A)** Cells were transfected with siControl or siNoxa#1 and treated with 1‰ DMSO and AD (A549 25 μM and H1299 10 μM) for 24 h. Apoptosis was determined and quantified with Annexin V-FITC/PI staining analysis. **(B)** Cell protein was extracted and detected by western blotting with antibodies against Noxa, PARP, c-PARP, Casp3, c-Casp3, and β-actin (* $p \leq 0.05$; ** $p \leq 0.01$).

IC_{50} of AD in five cell lines including squamous carcinoma cells (SK-MES-1), adenocarcinoma cells (A549, H1299), murine Lewis lung cancer cells (LLC), and normal human bronchial epithelial cells (BEAS-2B) at 48 h. As shown in **Figure 1B**, the IC_{50} values were approximately 8.72, 3.69, 10.99, 5.2, and 52.10 μM in A549, H1299, SK-MES-1, LLC, and BEAS-2B cells, respectively. The results indicated that AD has a broad-spectrum inhibitory effect on lung cancer cells but has a weaker inhibitory effect on the normal human bronchial epithelial cells.

Considering the morbidity and prognosis of lung adenocarcinoma, we next focused on lung adenocarcinoma cells to explore the antitumor property of AD. First, we selected four concentrations of AD for further studies according to the IC_{50} values. Then, we examined the inhibitory effect of these concentrations of AD on the proliferation of the two lung adenocarcinoma cells. As shown in **Figures 1C,D**, AD significantly suppressed the cell proliferation of the two lung adenocarcinoma cells in a dose- and time-dependent manner.

Andrographolide Triggered Apoptosis of Human Lung Adenocarcinoma Cells

To further investigate the underlying mechanisms of AD-induced cell growth inhibition, we determined cell apoptosis by Annexin V-FITC/PI stain and FACS in both A549 and H1299 cells after AD treatment for 24 h. As shown in **Figure 2A**, a significant dose-dependent increased apoptosis was detected in the two cells, especially in high concentration groups. Then, we examined c-PARP and c-Casp3 by immunoblotting to further confirm the induction of apoptosis by AD in A549 and H1299 cells. The results indicated that the expression levels of c-Casp3 and c-PARP were

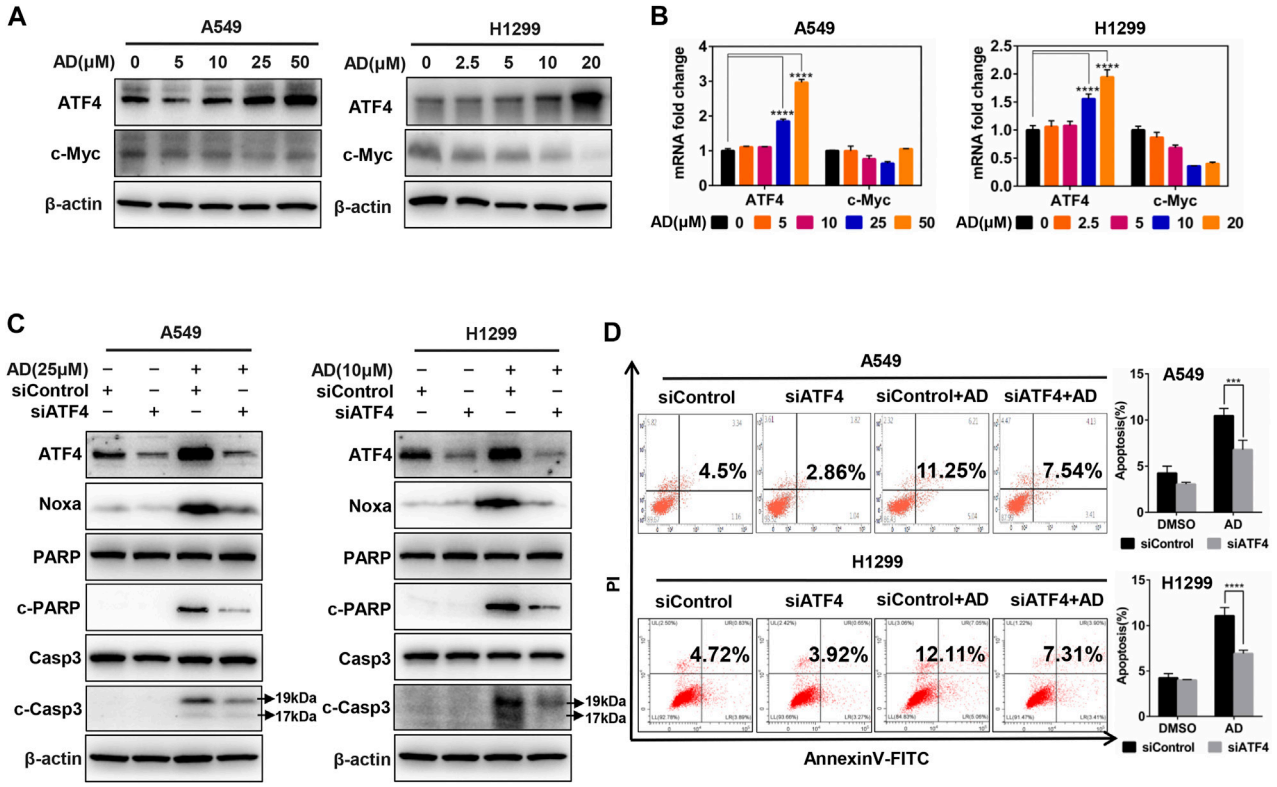

FIGURE 5 | Andrographolide induced apoptosis in human lung adenocarcinoma cells via ATF4/Noxa axis. **(A–B)** Cells were treated with 1‰ DMSO or indicated concentrations of AD for 24 h; cell protein was extracted and detected by western blotting with antibodies against ATF4 and c-Myc. The mRNA level of ATF4 and c-Myc was quantified with RT-PCR (normalized to β-actin). **(C–D)** Cells were transfected with siControl or siATF4, then, treated with 1‰ DMSO or AD (A549 25 μM, H1299 10 μM) for 24 h, cell protein was extracted and detected by western blotting with antibodies against ATF4, Noxa, PARP, c-PARP, Casp3, c-Casp3, and β-actin. Apoptosis was determined and quantified by AnnexinV-FITC/PI staining analysis (* $p \leq 0.05$; *** $p \leq 0.001$; **** $p \leq 0.0001$.).

greatly increased in a dose- and time-dependent manner (**Figures 2B,C**). These findings demonstrated that AD induced apoptosis of the human lung adenocarcinoma cells.

The BH3-Only Protein Noxa Was Upregulated by Andrographolide Treatment

Given that the role of the classical pro-apoptotic Bcl-2 family proteins in regulating apoptotic cell death, we next determined the expression of the pro-apoptotic proteins, including BH3-only proteins Puma, Bim, Bik, Bid, and Noxa, as well as their downstream pro-apoptotic proteins Bak and Bax in A549 and H1299 cells. These results indicated that only Noxa was significantly upregulated in the protein level in a dose-dependent manner (**Figure 3A**). Moreover, the mRNA level of Noxa was also substantially elevated by treatment of AD (**Figure 3B**). These findings indicated that Noxa was transcriptionally activated by AD treatment and suggested that Noxa plays a crucial role in AD-induced apoptosis.

Noxa Knockdown Inhibited Andrographolide-Induced Apoptosis

To confirm the role of Noxa in AD-induced apoptosis in A549 and H1299 cells, Noxa was knocked down by small interfering RNA (siRNA). As shown in **Figure 4A** and **supplementary Figure S1A**, Noxa knockdown significantly diminished AD-induced apoptosis as well as the expression levels of c-Casp3 and c-PARP (**Figure 4B** and **Supplementary Figure S1B**). These findings demonstrated that AD induced Noxa-dependent apoptosis of human lung adenocarcinoma cells.

Andrographolide-Induced Apoptosis in Human Lung Adenocarcinoma Cells via ATF4/Noxa Axis

Previous studies in our laboratory unveiled that ATF4 transcriptionally activated Noxa in esophageal squamous cell carcinoma cells after treated by small-molecule compound MLN4924 (Chen et al., 2016). In contrast, it was c-Myc but not ATF4 that transactivated Noxa to trigger cell apoptosis in head and neck squamous cell carcinoma cells after treated by MLN4924 (Zhang et al., 2019). To confirm the transcription factors responsible for Noxa induction upon AD treatment in both A549 and H1299 cells, we examined the protein and mRNA expression of c-Myc and ATF4. The results indicated that AD treatment strongly induced the upregulation of ATF4, but not c-Myc at both protein and mRNA levels (**Figures 5A,B**). Furthermore, ATF4 knockdown suppressed the transactivation

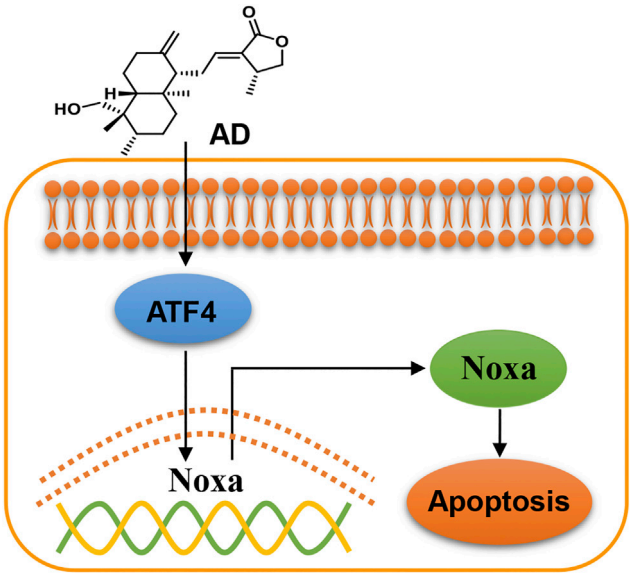

FIGURE 6 | Working model of andrographolide-induced ATF4/Noxa-dependent apoptosis. AD triggered human lung adenocarcinoma cells apoptosis by transcriptionally activating ATF4 and subsequently transactivating the pro-apoptotic BH3-only protein Noxa.

of Noxa as well as the cleavage of PARP and caspase 3 in AD-treated A549 and H1299 cells (**Figure 5C**). Consistently, the apoptotic population of AD-treated cells was significantly diminished in both two ATF4 knockdown cells (**Figure 5D**). Taken together, AD transcriptionally activated ATF4, which induced the transcriptional activation of the pro-apoptotic protein Noxa to trigger apoptosis in both A549 and H1299 cells.

DISCUSSION

In the present study, we found that AD exhibits a broad-spectrum inhibition of proliferation in lung cancer cells, and firstly demonstrated that AD activated the ATF4/Noxa axis to induce apoptosis of human lung adenocarcinoma cells (**Figure 6**). In recent years, emerging evidence has indicated that AD could exert an antitumor effect by inducing apoptosis of diverse cancer cells. Yang et al. reported that AD induced apoptosis of T-cell acute lymphoblastic leukemia cell (Jurkat) via inhibition of the PI3K/Akt pathway (Yang et al., 2016). Wu et al. reported that AD activated the LKB1/AMPK signal pathways and induced apoptosis of human nasopharyngeal carcinoma cells (C666–1) (Wu et al., 2018). Peng et al. also reported that AD induced apoptosis of nasopharyngeal carcinoma cells (HK1 and CNE-1) via inhibiting the NF-κB signal pathway (Peng et al., 2015). These findings collectively indicated that the mechanisms of AD-induced apoptosis may be cancer-type dependent.

While addressing the mechanisms of apoptosis induced by AD in human lung adenocarcinoma cells, we defined that the BH3-only protein Noxa mediated AD-induced apoptosis of human lung adenocarcinoma cells (A549 and H1299). BH3-only proteins Puma, Bim, Bik, Bid, Noxa, and their downstream proteins Bak and Bax all play critical roles in pro-apoptotic cell death (Gross et al., 1999; Cory et al., 2003; Breckenridge and Xue, 2004). It has been reported that some of the BH3-only proteins could mediate AD-induced cell apoptosis. Zhou et al. reported that AD promoted the cleavage of the BH3-only protein Bid to induce apoptosis of breast cancer cells (MDA-MB-231), cervical cancer cells (HeLa), and hepatoma cells (HepG2) (Zhou et al., 2006). Yang et al. reported that Bax and Bak are necessary for AD-induced apoptosis of lymphoma cells (Yang et al., 2010). In our study, we found that Noxa was significantly upregulated by AD in human lung adenocarcinoma cells, and Noxa knockdown significantly decreased AD-induced apoptosis. These results demonstrated that AD induced Noxa-dependent apoptosis of human lung adenocarcinoma cells.

The present study demonstrated that ATF4 transcriptionally activated Noxa in AD-treated lung adenocarcinoma cells. As a universal stress-responsive gene, ATF4 can be activated by several stimulations, such as oxidative stress, endoplasmic reticulum (ER) stress, and oxygen deprivation (Harding et al., 2003; Blais et al., 2004). A large number of studies indicated that activated ATF4 could induce cancer cell apoptosis for the oncotherapy (Jiang et al., 2013; Nunez-Vazquez et al., 2020; Xu et al., 2020). Zong et al. reported that radiation could upregulate ATF4 expression to induce cell apoptosis, and the overexpression of ATF4 could increase cell sensitivity to apoptosis in response to radiation (Zong et al., 2017). Sharma et al. found that cisplatin induced Noxa-dependent apoptosis through the upregulation of ATF4 in head and neck squamous cell carcinoma cells (Sharma et al., 2018). In this study, we found that both protein and mRNA levels of Noxa were upregulated after AD treatment, which suggested that Noxa was transcriptionally activated. Further studies showed that both the protein and mRNA levels of ATF4 were upregulated after AD treatment. Moreover, ATF4 knockdown inhibited the upregulation of Noxa as well as AD-induced apoptosis in human lung adenocarcinoma cells. Therefore, we confirmed that ATF4 transcriptionally activated Noxa in AD-induced apoptosis of human lung adenocarcinoma cells.

In summary, the present study firstly demonstrated that AD induced Noxa-dependent apoptosis by transactivating ATF4 in human lung cancer cells. These findings provided a scientific basis for developing AD as a promising candidate for the new era of chemotherapy.

DATA AVAILABILITY STATEMENT

The original contributions presented in the study are included in the article/**Supplementary Material**, and further inquiries can be directed to the corresponding author.

AUTHOR CONTRIBUTIONS

LJ designed and supervised the project. JZ, CL, and LZ carried out the experiments and drafted the manuscript, LJ finalized the

manuscript. YH, TX, and YZ performed statistical analyses. XC and RH coordinated the study over the entire time. All authors read and approved the final manuscript.

FUNDING

This work was supported by the National Natural Science Foundation of China (Grant Nos. 81625018, 81820108022, 82003297), Innovation Program of Shanghai Municipal Education Commission (2019-01-07-00-10-E00056), Program of Shanghai Academic/Technology Research Leader (18XD1403800), National Thirteenth Five-Year Science and Technology Major Special Project for New Drug and Development (2017ZX09304001), Special scientific research project of Postgraduate Innovative Training of Shanghai University of Traditional Chinese Medicine (Y2020004).

ACKNOWLEDGMENTS

We are thankful to all authorities of the National Natural Science Foundation of China, Innovation Program of Shanghai Municipal Education Commission, Program of Shanghai Academic/Technology Research Leader, National Thirteenth Five-Year Science and Technology Major Special Project for New Drug and Development, and Shanghai University of Traditional Chinese Medicine for their support.

SUPPLEMENTARY MATERIAL

The Supplementary Material for this article can be found online at: https://www.frontiersin.org/articles/10.3389/fphar.2021.680589/full#supplementary-material

REFERENCES

Albert, M.-C., Brinkmann, K., and Kashkar, H. (2014). Noxa and Cancer Therapy. *Mol. Cell Oncol.* 1 (1), e29906, doi:10.4161/mco.29906

Alves, N. L., Derks, I. A. M., Berk, E., Spijker, R., van Lier, R. A. W., and Eldering, E. (2006). The Noxa/Mcl-1 *Axis* Regulates Susceptibility to Apoptosis under Glucose Limitation in Dividing T Cells. *Immunity* 24 (6), 703–716. doi:10.1016/j.immuni.2006.03.018

Armstrong, J. L., Flockhart, R., Veal, G. J., Lovat, P. E., and Redfern, C. P. F. (2010). Regulation of Endoplasmic Reticulum Stress-Induced Cell Death by ATF4 in Neuroectodermal Tumor Cells. *J. Biol. Chem.* 285 (9), 6091–6100. doi:10.1074/jbc.M109.014092

Banerjee, M., Chattopadhyay, S., Choudhuri, T., Bera, R., Kumar, S., Chakraborty, B., et al. (2016). Cytotoxicity and Cell Cycle Arrest Induced by Andrographolide Lead to Programmed Cell Death of MDA-MB-231 Breast Cancer Cell Line. *J. Biomed. Sci.* 23, 40. doi:10.1186/s12929-016-0257-0

Blais, J. D., Filipenko, V., Bi, M., Harding, H. P., Ron, D., Koumenis, C., et al. (2004). Activating Transcription Factor 4 Is Translationally Regulated by Hypoxic Stress. *Mcb* 24 (17), 7469–7482. doi:10.1128/MCB.24.17.7469-7482.2004

Breckenridge, D. G., and Xue, D. (2004). Regulation of Mitochondrial Membrane Permeabilization by BCL-2 Family Proteins and Caspases. *Curr. Opin. Cel Biol.* 16 (6), 647–652. doi:10.1016/j.ceb.2004.09.009

Chen, P., Hu, T., Liang, Y., Li, P., Chen, X., Zhang, J., et al. (2016). Neddylation Inhibition Activates the Extrinsic Apoptosis Pathway through ATF4-CHOP-DR5 *Axis* in Human Esophageal *Cancer* Cells. *Clin. Cancer Res.* 22 (16), 4145–4157. doi:10.1158/1078-0432.Ccr-15-2254

Chen, Y.-P., Liu, Y.-W., Lee, D., Qiu, J. T., Lee, T.-Y., and Liu, S.-J. (2019). Biodegradable Andrographolide-Eluting Nanofibrous Membranes for the Treatment of Cervical Cancer. *Ijn* Vol. 14 421–429. doi:10.2147/ijn.S186714

Cory, S., Huang, D. C. S., and Adams, J. M. (2003). The Bcl-2 Family: Roles in Cell Survival and Oncogenesis. *Oncogene* 22 (53), 8590–8607. doi:10.1038/sj.onc.1207102

Denisenko, T. V., Budkevich, I. N., and Zhivotovsky, B. (2018). Cell Death-Based Treatment of Lung Adenocarcinoma. *Cell Death Dis* 9 (2), 117. doi:10.1038/s41419-017-0063-y

Efferth, T., Li, P. C. H., Konkimalla, V. S. B., and Kaina, B. (2007). From Traditional Chinese Medicine to Rational Cancer Therapy. *Trends Mol. Med.* 13 (8), 353–361. doi:10.1016/j.molmed.2007.07.001

Gerl, R., and Vaux, D. J. C. (2005). Apoptosis in the Development and Treatment of Cancer. *Carcinogenesis* 26 (2), 263–270. doi:10.1093/carcin/bgh283

Gross, A., McDonnell, J. M., and Korsmeyer, S. J. (1999). BCL-2 Family Members and the Mitochondria in Apoptosis. *Genes Develop.* 13 (15), 1899–1911. doi:10.1101/gad.13.15.1899

Guikema, J. E., Amiot, M., and Eldering, E. (2017). Exploiting the Pro-apoptotic Function of NOXA as a Therapeutic Modality in Cancer. *Expert Opin. Ther. Targets* 21 (8), 767–779. doi:10.1080/14728222.2017.1349754

Hanahan, D., and Weinberg, R. A. (2011). Hallmarks of Cancer: the Next Generation. *Cell* 144 (5), 646–674. doi:10.1016/j.cell.2011.02.013

Harding, H. P., Zhang, Y., Zeng, H., Novoa, I., Lu, P. D., Calfon, M., et al. (2003). An Integrated Stress Response Regulates Amino Acid Metabolism and Resistance to Oxidative Stress. *Mol. Cel* 11 (3), 619–633. doi:10.1016/s1097-2765(03)00105-9

Inoue, S., Riley, J., Gant, T. W., Dyer, M. J. S., and Cohen, G. M. (2007). Apoptosis Induced by Histone Deacetylase Inhibitors in Leukemic Cells Is Mediated by Bim and Noxa. *Leukemia* 21 (8), 1773–1782. doi:10.1038/sj.leu.2404760

Islam, M. T., Ali, E. S., Uddin, S. J., Islam, M. A., Shaw, S., Khan, I. N., et al. (2018). Andrographolide, a Diterpene Lactone from Andrographis Paniculata and its Therapeutic Promises in Cancer. *Cancer Lett.* 420, 129–145. doi:10.1016/j.canlet.2018.01.074

Jamal-Hanjani, M., Wilson, G., McGranahan, N., Birkbak, N., Watkins, T., Veeriah, S., et al. (2017). Tracking the Evolution of Non-small-cell Lung *Cancer*, *N. Engl. J. Med.*, 376(22), 2109–2121. doi:10.1056/NEJMoa1616288

Jiang, Q., Li, F., Shi, K., Wu, P., An, J., Yang, Y., et al. (2013). ATF4 Activation by the p38MAPK-eIF4E axis Mediates Apoptosis and Autophagy Induced by Selenite in Jurkat Cells. *FEBS Lett.* 587 (15), 2420–2429. doi:10.1016/j.febslet.2013.06.011

Kumar, D., Kumar, S., Gorain, M., Tomar, D., Patil, H. S., Radharani, N. N. V., et al. (2016). Notch1-MAPK Signaling *Axis* Regulates CD133+ *Cancer* Stem Cell-Mediated Melanoma Growth and Angiogenesis. *J. Invest. Dermatol.* 136 (12), 2462–2474. doi:10.1016/j.jid.2016.07.024

Lu, C.-L., Li, X., Zhou, H.-M., Zhang, C., Yang, Y.-Y., Feng, R.-L., et al. (2019). Randomised Controlled Trials of Traditional Chinese Medicine in Cancer Care Published in Chinese: an Overview. *The Lancet* 394, S26. doi:10.1016/s0140-6736(19)32362-1

Malhotra, V., and Perry, M. J. C. b. (2003). Classical Chemotherapy: Mechanisms, Toxicities and the Therapeutic Window, *Cancer Biol. Ther.* 2, S2–S4. doi:10.4161/cbt.199

Morsi, R. Z., Hage-Sleiman, R., Kobeissy, H., and Dbaibo, G. (2018). Noxa: Role in *Cancer* Pathogenesis and Treatment. *Ccdt* 18 (10), 914–928. doi:10.2174/1568009618666180308105048

Núñez-Vázquez, S., Sánchez-Vera, I., Saura-Esteller, J., Cosialls, A. M., Noisier, A. F. M., Albericio, F., et al. (2020). NOXA Upregulation by the Prohibitin-Binding Compound Fluorizoline Is Transcriptionally Regulated by Integrated Stress Response-Induced ATF3 and ATF4. *FEBS J.* 288(4), 1271–1285. doi:10.1111/febs.15480

Pérez-Galán, P., Roué, G., Villamor, N., Montserrat, E., and Colomer, D. J. B. (2006). The Proteasome Inhibitor Bortezomib Induces Apoptosis in Mantle-Cell Lymphoma through Generation of ROS and Noxa Activation Independent of P53 Status. *Blood*. 107(1), 257–264. doi:10.1182/blood-2005-05-2091

Peng, T., Hu, M., Wu, T., Zhang, C., Chen, Z., Huang, S., et al. (2015). Andrographolide Suppresses Proliferation of Nasopharyngeal Carcinoma

Cells via Attenuating NF-Kb Pathway, *Biomed. Res. Int.*, 2015, 735056. doi:10.1155/2015/735056

Rotow, J., and Bivona, T. G. (2017). Understanding and Targeting Resistance Mechanisms in NSCLC. *Nat. Rev. Cancer* 17 (11), 637–658. doi:10.1038/nrc.2017.84

Sharma, K., Vu, T. T., Cook, W., Naseri, M., Zhan, K., Nakajima, W., et al. (2018). p53-independent Noxa Induction by Cisplatin Is Regulated by ATF3/ATF4 in Head and Neck Squamous Cell Carcinoma Cells. *Mol. Oncol.* 12 (6), 788–798. doi:10.1002/1878-0261.12172

Shibue, T., Takeda, K., Oda, E., Tanaka, H., Murasawa, H., Takaoka, A., et al. (2003). Integral Role of Noxa in P53-Mediated Apoptotic Response. *Genes Develop.* 17 (18), 2233–2238. doi:10.1101/gad.1103603

Tang, J. L., Zhan, S. Y., and Ernst, E. (1999). Review of Randomized Controlled Trials of Traditional Chinese Medicine, *BMJ* 319(7203):160–161.doi:10.1136/bmj.319.7203.160

Thomas, A., Liu, S. V., Subramaniam, D. S., and Giaccone, G. (2015). Refining the Treatment of NSCLC According to Histological and Molecular Subtypes. *Nat. Rev. Clin. Oncol.* 12 (9), 511–526. doi:10.1038/nrclinonc.2015.90

Wu, B., Chen, X., Zhou, Y., Hu, P., Wu, D., Zheng, G., et al. (2018). Andrographolide Inhibits Proliferation and Induces Apoptosis of Nasopharyngeal Carcinoma Cell Line C666-1 through LKB1-AMPK-dependent Signaling Pathways. *Pharmazie* 73 (10), 594–597. doi:10.1691/ph.2018/8583

Xu, L., Jiao, J., Sun, X., Sang, W., Gao, X., Yang, P., et al. (2020). Cladribine Induces ATF4 Mediated Apoptosis and Synergizes with SAHA in Diffuse Large B-Cell Lymphoma Cells. *Int. J. Med. Sci.* 17 (10), 1375–1384. doi:10.7150/ijms.41793

Yang, S., Evens, A. M., Prachand, S., Singh, A. T. K., Bhalla, S., David, K., et al. (2010). Mitochondrial-Mediated Apoptosis in Lymphoma Cells by the Diterpenoid Lactone Andrographolide, the Active Component of Andrographis Paniculata. *Clin. Cancer Res.* 16 (19), 4755–4768. doi:10.1158/1078-0432.Ccr-10-0883

Yang, T., Yao, S., Zhang, X., and Guo, Y. (2016). Development, and therapyAndrographolide Inhibits Growth of Human T-Cell Acute Lymphoblastic Leukemia Jurkat Cells by Downregulation of PI3K/AKT and Upregulation of P38 MAPK Pathways. *Dddt* 10, 1389–1397. doi:10.2147/dddt.S94983

Yao, W.-T., Wu, J.-F., Yu, G.-Y., Wang, R., Wang, K., Li, L.-H., et al. (2014). Suppression of Tumor Angiogenesis by Targeting the Protein Neddylation Pathway. *Cel Death Dis* 5 (2), e1059. doi:10.1038/cddis.2014.21

Zhang, W., Liang, Y., Li, L., Wang, X., Yan, Z., Dong, C., et al. (2019). The Nedd8-activating Enzyme Inhibitor MLN 4924 (TAK -924/Pevonedistat) Induces Apoptosis via c-Myc-Noxa axis in Head and Neck Squamous Cell Carcinoma. *Cell Prolif* 52 (2), e12536, doi:10.1111/cpr.12536

Zhao, J., Yang, G., Liu, H., Wang, D., Song, X., and Chen, Y. (2002). Determination of Andrographolide, Deoxyandrographolide and Neoandrographolide in the Chinese Herb Andrographis Paniculata by Micellar Electrokinetic Capillary Chromatography. *Phytochem. Anal.* 13 (4), 222–227. doi:10.1002/pca.644

Zhou, J., Zhang, S., Choon-Nam, O., and Shen, H.-M. (2006). Critical Role of Pro-apoptotic Bcl-2 Family Members in Andrographolide-Induced Apoptosis in Human Cancer Cells. *Biochem. Pharmacol.* 72 (2), 132–144. doi:10.1016/j.bcp.2006.04.019

Zhu, H., Yang, W., He, L.-j., Ding, W.-j., Zheng, L., Liao, S.-d., et al. (2012). Upregulating Noxa by ER Stress, Celastrol Exerts Synergistic Anti-cancer Activity in Combination with ABT-737 in Human Hepatocellular Carcinoma Cells. *PLoS One* 7 (12), e52333, doi:10.1371/journal.pone.0052333

Zong, Y., Feng, S., Cheng, J., Yu, C., and Lu, G. (2017). Up-Regulated ATF4 Expression Increases Cell Sensitivity to Apoptosis in Response to Radiation. *Cell Physiol Biochem* 41 (2), 784–794. doi:10.1159/000458742

Conflict of Interest: RH was employed by Anticancer Inc.

The remaining authors declare that the research was conducted in the absence of any commercial or financial relationships that could be construed as a potential conflict of interest.

frontiers in Oncology

REVIEW
published: 21 June 2021
doi: 10.3389/fonc.2021.705903

Remodeling the Epigenetic Landscape of Cancer—Application Potential of Flavonoids in the Prevention and Treatment of Cancer

Weiyi Jiang[1†], *Tingting Xia*[1†], *Cun Liu*[1], *Jie Li*[1], *Wenfeng Zhang*[2] *and Changgang Sun*[3,4*]

[1] College of First Clinical Medicine, Shandong University of Traditional Chinese Medicine, Jinan, China, [2] Clinical Medical Colleges, Weifang Medical University, Weifang, China, [3] Department of Oncology, Weifang Traditional Chinese Hospital, Weifang, China, [4] Qingdao Academy of Chinese Medical Sciences, Shandong University of Traditional Chinese Medicine, Qingdao, China

OPEN ACCESS

Edited by:
Yuling Qiu,
Tianjin Medical University, China

Reviewed by:
Yu Cai,
Jinan University, China
Rong-Rong He, Jinan University, China

***Correspondence:**
Changgang Sun
scgdoctor@126.com

†These authors have contributed equally to this work

Specialty section:
This article was submitted to Pharmacology of Anti-Cancer Drugs, a section of the journal Frontiers in Oncology

Received: 06 May 2021
Accepted: 31 May 2021
Published: 21 June 2021

Citation:
Jiang W, Xia T, Liu C, Li J, Zhang W and Sun C (2021) Remodeling the Epigenetic Landscape of Cancer—Application Potential of Flavonoids in the Prevention and Treatment of Cancer. Front. Oncol. 11:705903. doi: 10.3389/fonc.2021.705903

Epigenetics, including DNA methylation, histone modification, and noncoding RNA regulation, are physiological regulatory changes that affect gene expression without modifying the DNA sequence. Although epigenetic disorders are considered a sign of cell carcinogenesis and malignant events that affect tumor progression and drug resistance, in view of the reversible nature of epigenetic modifications, clinicians believe that associated mechanisms can be a key target for cancer prevention and treatment. In contrast, epidemiological and preclinical studies indicated that the epigenome is constantly reprogrammed by intake of natural organic compounds and the environment, suggesting the possibility of utilizing natural compounds to influence epigenetics in cancer therapy. Flavonoids, although not synthesized in the human body, can be consumed daily and are common in medicinal plants, vegetables, fruits, and tea. Recently, numerous reports provided evidence for the regulation of cancer epigenetics by flavonoids. Considering their origin in natural and food sources, few side effects, and remarkable biological activity, the epigenetic antitumor effects of flavonoids warrant further investigation. In this article, we summarized and analyzed the multi-dimensional epigenetic effects of all 6 subtypes of flavonoids (including flavonols, flavones, isoflavones, flavanones, flavanols, and anthocyanidin) in different cancer types. Additionally, our report also provides new insights and a promising direction for future research and development of flavonoids in tumor prevention and treatment *via* epigenetic modification, in order to realize their potential as cancer therapeutic agents.

Keywords: flavonoids, natural compounds, phytochemicals, epigenetic, epigenome, cancer, HDAC, DNMT

INTRODUCTION

Cancer is a chronic consumptive disease that has not been overcome yet and has become a global health problem threatening human life (1, 2). Developments in the field of oncology suggest that cancer is regulated not only by genetics but also by epigenetic programming (3). First, epigenetic mechanisms can circumvent changes in the DNA sequence and directly target the expression of proto-oncogenes and tumor suppressor genes to induce carcinogenesis (4, 5). Second, epigenetic abnormalities occur in the early stage of carcinogenesis and precede mutations which also occur in somatic cells (6); therefore, such mechanisms have become a new therapeutic avenue to conquer tumors. More importantly, in the complex and multi-dimensional process of carcinogenesis, these mechanisms, which differ from genetics, are frequently bidirectional and reversible (7). And defects of epigenetics are largely a consequence of lifestyle and habits such as inadequate consumption of natural compounds, smoking, and drinking (8, 9), and they can also reverse abnormal epigenetic effects through proper intake of natural compounds (10, 11). These facts make epigenetics attractive for the development of new treatments.

Flavonoids are phytochemicals that are frequently consumed on a daily basis. Because of their remarkable biological activities, flavonoids have recently attracted scientific interest as they are beneficial to health and reduce the risk of disease (12, 13). In the field of cancer, evidence of cancer treatment effects of flavonoids through epigenetic pathways is continuously being investigated. For example, kaempferol, which occurs in grapefruit, broccoli, and other plants, can regulate the activity of histone deacetylase (HDAC) in various cancers (14). Epigallocatechin-3-gallate (EGCG) in tea can affect expression of DNA methyltransferases, HDACs, and noncoding RNAs in cancer cells (15–17). Key evidence such as this improves our understanding of the importance of diet for cancer prevention and suggests the potential of dietary flavonoids for epigenetic therapy against cancer.

Epigenetic mechanisms of cancer have been described in detail in previous studies (18, 19). Thus, we review the core mechanism of epigenetics and abnormal regulation in cancer to provide a clear groundwork. Recent research progress regarding anticancer efficacy of all types of flavonoids targeting epigenetic regulation pathways is reviewed here, and their potential for cancer prevention and treatment is elaborated to provide evidence for the anticancer effects of food and improve the understanding of respective epigenetic mechanisms to support the development of new treatment strategies and chemoprophylaxes.

EPIGENETICS AND CANCER

Epigenetics are heritable changes in gene expression without alterations in DNA sequences. There are numerous such phenomena, including DNA methylation, histone modification, genomic imprinting, maternal effects, and RNA editing (20). However, regarding physiological and pathological gene regulation of mammals, epigenetic effects predominantly refer to three aspects, i.e., DNA methylation, histone modification, and noncoding RNA regulation (21). Flavonoids also regulate cancer epigenetic abnormalities through these three aspects.

DNA Methylation

In the field of epigenetics, DNA methylation regulation is the most studied mechanism which can directly modify gene expression without changing genetic information and participates in various biological processes such as genomic stability, regulation of gene transcription, embryonic development, and tumorigenesis (22–24). DNA methylation modifications are common in human genomic DNA, covalently binding methyl groups to the fifth carbon in the cytosine group of CpG dinucleotides to form 5-methylcytosine. CpG dinucleotides are distributed inhomogeneously in the human genome and are more abundant in promoter regions of genes (25). Gene regions with a higher proportion of CpG are termed CpG islands and occur in promoters of more than 60% of genes (26). Hypermethylation of a promoter CpG island can inactivate the gene, whereas promoter CpG islands of transcriptionally active DNA sequences are typically not methylated (18). For example, even though the vast majority of CpG islands in developmental and differentiated tissues remain methylated, a small number of CpG islands are methylated in a tissue-specific manner to inhibit gene expression (27). In a few cases, DNA hypermethylation can lead to abnormal gene activation. This abnormal regulation has been described in detail in other reports (28), however, in-depth elaboration of this process is beyond the scope of this review.

DNA methylation requires catalysis by DNA methyltransferases (DNMTs) (29). Five types of DNMTs including DNMT1, DNMT3a, DNMT3b, DNMT2, and DNMT3L have been identified (30). The first three types are considered to exert methyltransferase activity: DNMT1 is mainly responsible for maintenance methylation (i.e., identifying the DNA strand that has been methylated and then methylating the complementary strand), while Dnmt3a and Dnmt3b are involved in *de novo* methylation to methylate unmethylated DNA double-strands (31). Abnormal DNA methylation leads to epigenetic imbalance which is an important mechanism underlying tumorigenesis (32). Compared with somatic cells, cancer cells are hypermethylated in the promoter regions of multiple cancer suppressor genes (e.g. MGMT, CdH1, E-cadherin, BRCA1) which is considered a common regulator of transcriptional silencing of tumor suppressor genes, while hypomethylation is observed in the whole genome of cancer cells and is associated with upregulated expression of proto-oncogenes (such as cyclinD2, PAX2, PAX2, and ABCB1) (33, 34). Most flavonoids exert strong effects on DNA methylation (**Figure 1**), and hesperidin and naringenin are candidate drugs that inhibit DNMTs.

Histone Modification

In addition to DNA methylation which occurs directly on gene sequences, the chromatin structure is also affected by histone modification which is associated with DNA replication, transcription, and repair through histone-DNA or histone-histone interaction (35). Histones are basic proteins of

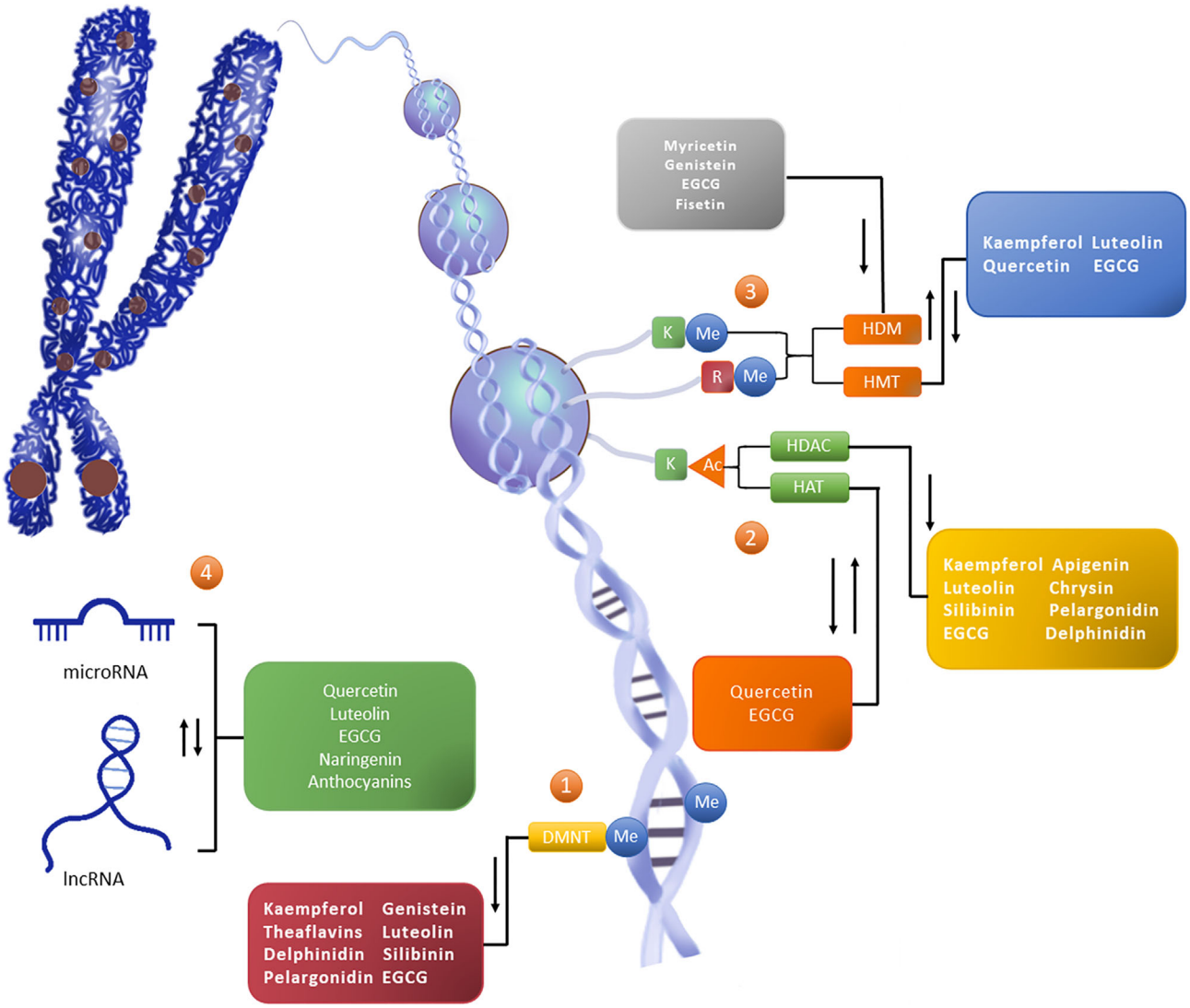

FIGURE 1 | Flavonoids reshape the epigenetic landscape of cancer. Flavonoids exert epigenetic anticancer activity by regulating the level of DNA methylation, histone modification, and the expression of noncoding RNA. The addition of epigenetic markers depends on writers (such as DNMT, HMT, and HAT), except for erasers (such as HDAC and HDM) which depend on readers (not marked in the figure). ①The level of CpG island methylation (Me) in the promoter region of the target gene is increased under the catalysis of DNMT, thus downregulating the activity of the gene. ②Histone modification occurs on lysine (K) and arginine (R) residues in the histone tail, in which K is the site of histone acetylation (Ac) modification. HAT promotes gene expression, while HDAC can reduce the level of histone acetylation to reduce gene activity. ③Histone methylation can occur in K and R. HMT and HDM catalyze epigenetic regulation, and their effects on gene activity vary with amino acid sites and methylation patterns. ④Noncoding RNAs are also an important part of epigenetic networks. Noncoding RNAs, represented by miRNA and lncRNA, can interact with DNA, mRNA, and proteins, and participate in gene expression processes such as chromosome modification, transcriptional interference, posttranscriptional modification, and translation regulation. In general, flavonoids can play the role of DNMTi, HDACi and HDMi, and can promote or inhibit the activity or expression of HAT,HMT and ncRNA.

eukaryotes that bind to chromosomal DNA. A histone octamer formed by two molecules of H2A and H2B and two molecules of H3 and H4, together with 147 base pairs of DNA form nucleosomes which participate in the formation of chromosomes (36). Histones in nucleosomes can undergo a variety of epigenetic regulation through the free N-terminal. According to the different modes of action, histone modification can be assigned to methylation, acetylation, phosphorylation, adenylation, ubiquitin, and ADP ribosylation (37). Acetylation and methylation are well-studied regulation modes (36, 38), which are also the main histone modifications mode of natural anti-tumor drug flavonoids (**Figure 1**).

Histone Acetylation

Histone acetylation is the best characterized histone modification and plays an important role in gene regulation, chromatin structure, and tumorigenesis (39–41). It is generally accepted that high acetylation activates and low acetylation inhibits gene expression (42–44). Histone acetylation is frequently modified on N-terminal lysine sites of H3 and H4 and is regulated by histone acetyltransferase (HAT) and HDAC (18, 45). There are three HAT families, i.e., the Gcn5-related N-acetyltransferase (GNAT) family which occurs in the nucleus and is associated with transcription; the MYST family, mainly comprising Ybf2-Sas3, Sas2, MOZ, and Tip60, which occur in the cytoplasm and participate in posttranslational modification; and the p300/cbp family which is responsible for transcription and posttranslational modification (46, 47). Based on structural characteristics and catalysis, HDACs are assigned to the following four categories – class I: HDAC1, 2, 3, and 8; class II: HDAC4, 5, 6, 7, 9, and 10; class III: sirtuins (SIRT1-7); and class IV: HDAC11. HDACs such as those of classes I, II, and IV show structural homology and require zinc ions to activate their catalytic effects, while sirtuins require NAD+ as a cofactor to exert catalysis (48).

Histone acetylation plays an important role in the development of cancer. HDAC and HAT can interact with proto-oncogenes and tumor suppressor genes and thereby interfere with the regulation of these genes during tumor cell proliferation, metastasis, and apoptosis (49, 50). For example, during promyelocytic leukemia, the mSin3-HDAC complex can deacetylate key genes and block transcription, leading to tumorigenesis. An imbalance in HAT activity can also lead to cancer. For example, p300/cbp can be reduced by the binding of viral oncoprotein (E1A), indicating the relationship between HAT and tumorigenesis.

Histone Methylation

Methylation is also involved in epigenetic regulation of histones. The N-terminal lysine and arginine residues of H3 and H4 are reversibly modified through catalysis of histone methyl invertase (HMT) and histone demethylase (HDM) (51). Histone methylation regulates the silencing and activation of gene transcription, and the specific biological behavior depends on the amino acid residue sites (different parts of lysine or arginine) and on the form of methylation (monomethylation, dimethylation, or trimethylation) (52). For example, methylation at lysine 9 (H3K9) of histone H3 leads to transcriptional inhibition, whereas trimethylation at lysine K4 (H3K4) and at K9 (H3K9) of histone H3 is responsible for transcriptional activation (53, 54). Imbalances in histone methylation and demethylation are closely associated with cancer. For example, MLL1 can cause H3K4 methylation, leading to acute lymphoblastic leukemia (55); LSD1 is both a classical oncogene and an active lysine demethylase(KDM) that removes the methyl group from H3K4 and H3K9 sites and is considered a therapeutic target for acute leukemia cases (56).

Regulation of Noncoding RNA

miRNA

The current understanding of miRNAs suggests that they are important epigenetic vectors and key factors in anticancer-targeting regulation by flavonoids. miRNAs, which comprise approximately 22 nucleotides, are single-stranded RNAs that are responsible for posttranscriptional silencing of target genes, thereby regulating cell proliferation, differentiation, migration, and other biological processes. As effectors of negative regulation of gene transcription, miRNAs participate in the expression of genetic information in two ways; first, perfect pairing of miRNA transcriptional sequences genes leads to degradation of the target mRNA and interrupts mRNA translation; second, miRNAs may inhibit the transcription process by binding to the incomplete complementary site of the 3'-untranslated region of mRNA. miRNAs can regulate 1/3 human gene and form a complex regulatory network with target genes. A given miRNA may correspond to multiple target genes, and a target gene may also be regulated by multiple miRNAs (57–59).

There is increasing evidence for the relationship between miRNAs and cancer. miRNA expression profiles can be used to distinguish normal tissue from cancerous tissue and to classify different types of cancer (60, 61). In addition, miRNAs play a role in carcinogenic and tumor-inhibitory signaling pathways, e.g., miRNAs of the miR-34 family act as a signal regulator in the p53 pathway, and miR-16 negatively regulates mitogenic signals and blocks the cell cycle. Interestingly, regulation of miRNAs in cancer is also affected by DNA methylation and histone modification, as discussed above. For example, hypermethylation of miR-9-1 was observed in breast cancer, and the MIR-17-92 cluster in hepatocellular carcinoma may be regulated by HDAC inhibitors (62, 63). Taken together, epigenetics is not an isolated complex of processes but a multilevel interrelated regulatory network, and miRNAs play an indispensable role in this regulatory mechanism.

lncRNA

Unlike miRNA, lncRNA, which is noncoding RNA exceeding 200 bp in length, is well-known for its regulatory effects on the cell cycle, cell differentiation, and epigenetic effects on biological processes (64, 65). Some recent studies examined epigenetic effects of lncRNAs. Their long chain structures enable lncRNAs to form complex secondary and tertiary structures which can bind to DNA, RNA, or proteins, reshape chromatin structures, and participate in transcriptional and posttranscriptional regulation (66–68). Although the specific functions of lncRNAs remain to be elucidated, their unregulated expression patterns have been shown to be related to diseases such as cancer. This type of long-chain RNA participates in malignant mechanisms such as proliferation, migration, and drug resistance and is of clinical importance regarding early diagnosis and prognosis of tumors (69). For example, lncRNA-p21 can induce apoptosis. Highly upregulated in liver cancer is considered a potential biomarker for breast cancer with liver metastasis. High expression of HOX antisense intergenic RNA in breast cancer is associated with invasiveness. lncRNAs have become one of the core targets of tumor research as they may be highly informative regarding cancer. lncRNA therapy can be an adequate tumor treatment option, and dietary phytochemicals such as flavonoids have been examined in the past few years to assess their therapeutic potential to regulate lncRNAs (**Figure 1**).

EPIGENETIC EFFECTS OF FLAVONOIDS DURING CANCER

Cancer is affected by interactions of genetics and epigenetics (1). Compared with the genome, the epigenome is often affected by acquired factors such as environment and diet (70, 71). To date, more than 4,000 flavonoids have been identified in plants, and these compounds are common in vegetables, fruits, and tea. The role of flavonoids in the treatment of diseases has been studied extensively (72–74). Prophylactic flavonoids can chemically reverse adverse epigenetic marking in cancer cells, which may inspire researchers to explore novel avenues of cancer prevention and early treatment (73).

Flavonoids, the largest group of secondary metabolites in the polyphenol family, are produced by plants where they provide flavor, color, and health effects (75, 76), and they have attracted research attention because of their effective antioxidant effects which may prevent environmental damage (73). **Table 1** shows different subtypes of flavonoids from dietary and medicinal plant sources. Flavonoids exert various pharmacological activities in mammals and have been commonly used in studies on various diseases (99, 100). In vivo and *in vitro* studies showed that these plant compounds exert beneficial effects such as antitumor, antibacterial, antiviral, liver-protective, anti-inflammatory, antipyretic, analgesic, antihypertensive, and anti-aging effects, in addition to neutralization of free radicals, improvement of immune functions, and beneficial effects on the cardiovascular system (101, 102).

Flavonoids share a particular molecular structure which is formed by the connection of two benzene rings with three carbon atoms, by which these compounds differ from other plant compounds (99, 100) (**Figure 2**). Flavonoids are assigned to six subcategories based on their structures (103). **Figure 3** describes the structural characteristics and representative compounds of the six flavonoid subgroups in detail. In the following sections, we revisit epigenetic cancer effects of flavonoids including flavonols (kaempferol, myricetin, and quercetin), flavones (diosmin, apigenin, luteolin, and chrysin), isoflavones (daidzein and genistein), flavanones (naringenin, naringin, hesperidin, phlorizin, taxifolin, and silibinin), flavanols (EGCG and theaflavins), and anthocyanidins (delphinidin and pelargonidin).

TABLE 1 | Dietary and plant sources of the different types of flavonoids.

Flavonoid class	Compound name	Dietary sources	Reference
Flavones	Apigenin	Achillea millefolium L	(77)
	Luteolin	Chrysanthemi Flos	(78)
	Tangeretin	Citrus Reticulata	(79)
	Diosmin	Black cardamom	(80)
	Chrysin	Propolis	(81)
Isoflavones	Daidzein	Soybeans	(82)
	Daidzein	Cyathulae Radix	(83)
	Daidzein	Sojae Semen Praeparatum	
	Genistein	Miso	(84)
	Genistein	Eucommiae Cortex	(83)
Flavonols	Kaempferol	Radix Bupleuri	(83)
	Kaempferol	Polygoni Avicularis Herba	(85)
	Kaempferol	Hippophae Fructus	(86)
	Kaempferol	Paeoniae Radix Alba	(83)
	Myricetin	Mori Fructus	(87)
	Myricetin	Hippophae Fructus	(88)
	Myricetin	Ginkgo Folium	(89)
	Myricetin	Red wine	(90)
	Myricetin	Black tea	(91)
	Quercetin	Hedyotis Diffusae Herba	(83)
	Quercetin	Radix Bupleuri	
	Quercetin	Toosendan Fructus	
	Quercetin	Slicing beans	(92)
	Quercetin	Broccoli	(93)
Flavanones	Naringenin	Grapefruit pulp	(94)
	Naringenin	Prunus yedoensis Mats	(95, 96)
	Hesperidin	Viticis Fructus	
	Hesperidin	Asteris Radix Et Rhizoma	
	Naringin	Grapefruit juice	
Flavanols	EGCG	Green tea	(97)
	EGCG	Ginkgo Semen	
	ECG	Black tea	
	EGC	Green tea	
Anthocyanidins	Delphinidin	blueberry	(98)
	Delphinidin	Ephedra Herba	(83)
	Pelargonidin	Fritillariae Thunbrgii Bulbus	
	Pelargonidin	Hippophae Fructus	
	Pelargonidin	Mori Cortex	

Flavonols

Kaempferol

Kaempferol, a flavonol compound, is derived from Zingiberaceae plants and commonly occurs in Ardisiae Japonicae Herba, Dysosmae Verspiellis Rhixoma Et Radix, Lobeliae Chinensis Herba, strawberries, grapefruit, grapes, broccoli, and other vegetables, fruits, and teas. Its physiological functions include antioxidation, prevention of cancer, inhibition of fat formation, protection of the nervous system and the heart, and antidiabetic and anti-allergy effects (104–106). Recent studies suggested that kaempferol intake is associated with reduced cancer incidence. In a study of epithelial ovarian cancer, the population with the highest intake of kaempferol had a 40% reduction in the incidence of ovarian cancer compared with the lowest fifth (107). In a cohort study, total flavonol intake was associated with reduced risk of pancreatic cancer, with kaempferol showing the highest reduction in cancer risk. In addition, total flavonol intake and kaempferol intake were negatively correlated with the risk of pancreatic cancer in smokers (108). Epidemiological investigations such as these demonstrated anticancer effects of kaempferol.

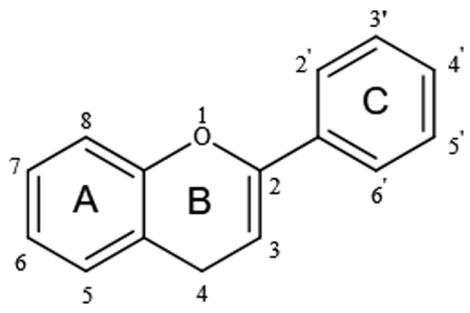

FIGURE 2 | Basic structure of flavonoids.

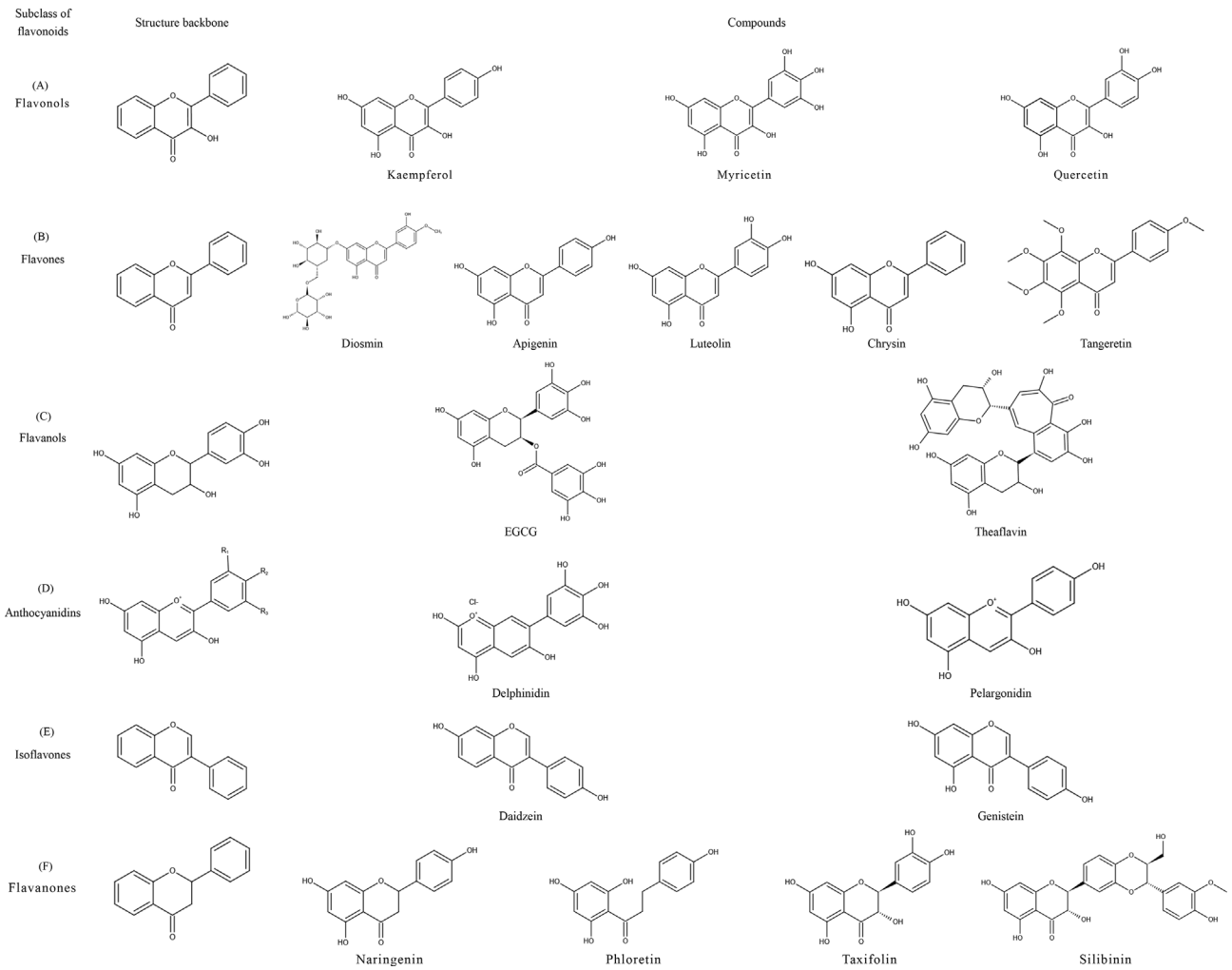

FIGURE 3 | Structural characteristics and representative compounds of six flavonoids subclasses. C6-C3-C6 shows the core structure of flavonoids with twobenzene rings linked to each other by three carbon atoms. After different modifications, flavonoids can occur in six subclasses with different characteristics: flavonols, flavones, isoflavones, flavanones, flavanols, and anthocyanidins; structures are shown in the figure. **(A)** Flavonols: contain 3-hydroxyl flavone analogs. **(B)** Flavones: the ketone of C4 in the C-ring is connected with C2-C3 by a double bond. **(C)** Flavanols: 3-hydroxy derivatives of flavanones; the hydroxyl is located at the third position of the C-ring. **(D)** Anthocyanidins: glavylium cation binding hydroxyl and/or methoxy groups at the R, R, and R sites. **(E)** Isoflavones: the B-ring is connected at C3 of the C-ring instead of C2. **(F)** Flavanones: contain flavone analogs with a C2-C3 single bond structure.

Part of the antitumor effect of kaempferol is due to its strong epigenetic effects such as targeting histone acetylation. In a previous study by Kim et al., kaempferol exerted the effect of an HDAC inhibitor (HDACi), inhibited expression of G9a, blocked the HDAC/G9a axis, and induced autophagy in gastric cancer cells (14). A different study also reported significant inhibitory effects of kaempferol on HDAC and found that kaempferol hyperacetylated histone complex H3 and inhibited the proliferation and survival of cancer cells in HCT-116 colon cancer cells and human hepatocellular carcinoma cell lines HepG2 and Hep3B (109).

Kaempferol is also thought to regulate DNA methylation. In HCT116, HT29, and YB5 colorectal cancer cell lines, kaempferol was found to bind to DNMT1, and it significantly downregulated DACT2 methylation, upregulated expression of this tumor suppressor gene, blocked the Wnt/β-catenin signaling pathway, and inhibited tumor cell proliferation and migration. This study also found that DACT2, regulated by kaempferol demethylation, reduced tumor load to some extent, indicating the potential of this compound for cancer therapy (110).

Myricetin

Exploring flavonols, numerous studies have shown that myricetin derived from myricanagi, Mori Fructus, ippophae Fructus, Ginkgo Folium, etc. has excellent nutritional value and biological activity, and plays a beneficial role regarding antitumor activity, prevention of cardiovascular diseases, lowering blood pressure, lowering blood lipid levels, and

reducing complications associated with diabetes and bacteriostasis (111–114). In recent years, with the rise of epigenetic therapy, an increasing number of epigenetic effects of myricetin has been revealed.

Lee et al. observed that several bioflavonoids can inhibit epigenetic regulation of SssI DNMT and DNMT1 in a concentration-dependent manner and reduce the level of DNA methylation. Compared with fisetin and quercetin, myricetin has a more prominent inhibitory ability on the two enzymes. Myricetin (20 μM) inhibited SssI DNMT-related methylation by up to 60%. When mediated by COMT, the IC_{50} value of myricetin inhibiting methylation of DNMT1 was 1.2 μM (115). This study reflects the epigenetic effects of flavonoids such as myricetin, particularly regarding inhibitory effects on DNMT.

Furthermore, epigenetic effects of myricetin nanoparticles have been reported. Silver nanoparticles(AgNPs) made from myricetin can promote oxidative stress responses and DNA damage and induce apoptosis in NIH3T3 mouse embryonic fibroblasts. Subsequent gene ontology analysis revealed that AgNPs promote nucleosome assembly and DNA methylation in the process of inducing apoptosis. A heat map showed that histones hist2h2ac and hist1h2ah of the necroptosis pathway were significantly upregulated after treatment with AgNPs (116). This study showed that this new material plays an important role in the epigenetic regulation of apoptosis, especially at DNA-methylation and histone levels.

JMJD3, a member of the Jmj-C HDM family, is considered a key factor in inflammation and tumorigenesis. Numerous recent studies showed that myricetin exerts significant inhibitory effects on JMJD3. Mallik et al. screened eight compounds, including ZINC15271426, from 65 myricetin analogs in the ZINC database using the molecular model method. They observed excellent docking affinity (all exceeding 9.0 kcal/mol), showing promising application prospects of these compounds as JMJD3 inhibitors (117). In addition, myricetin indirectly regulates deacetylation. Myricetin can activate HDAC SIRT1 to promote HIF-1α expression and inhibit cMyc and β-catenin (118).

Quercetin

Quercetin occurs in Hedyotis Diffusae Herba, Radix Bupleuri, Toosendan Fructus, onions, apples, hawthorn, etc. and naturally occurs in the form of glycosides. It is a commonly used natural flavonol which can neutralize free radicals and directly inhibits tumors; furthermore, it exerts biological activities such as anti-inflammatory, antibacterial, antiviral, immune-regulating, neuroprotective, anti-hypertensive, and hypolipidemic effects (119–121). Recent studies showed that quercetin modifies tumor epigenetics and can enhance the effects of epigenetic treatments when administered in combination with other drugs.

During synergistic action of quercetin and curcumin, prostate cancer cell lines PC3 and DU145 showed decreased DNMT activity and increased AR expression which induced apoptosis through the mitochondrial pathway. Compared with the single-drug group, combined administration was more effective and led to increased sensitivity of androgen-resistant prostate cancer cells to androgen receptor-induced apoptosis (122), suggesting the potential of quercetin and curcumin administration for prevention and treatment of prostate cancer.

Flavonoids quercetin and sodium butyrate can change histone acetylation modifications in cancer. Zheng et al. reported that curcumin and sodium butyrate can inhibit tumor cell growth in a dose-dependent manner. In the human esophageal cancer cell line Eca9706, both drugs can restrict cell growth, and combined administration produced stronger inhibitory effects on the proliferation of tumor cells. Western blotting showed that expression of NF-κBp65, HDAC1, and cyclin D1 was downregulated, whereas that of caspase-3 and p16INK4α was upregulated in treatments with quercetin, sodium butyrate, or a combination thereof. The authors also observed a trend of downregulation of HDAC1-IR and upregulation in E-cadherin-IR after combined treatment (123). This study suggests that quercetin and B, particularly in combination, can regulate abnormal epigenetic changes through the HDAC1-IR-NF-κB signaling axis and inhibit growth of the human esophageal cancer cell line Eca9706.

Wang et al. conducted a study on increased antitumor effects of quercetin due to combined administration with arctigenin. Quercetin and/or arctigenin were used to treat prostate cancer cell lines (androgen-dependent LAPC-4 and LNCaP), and compared with the controls and single-drug treatments, combined administration enhanced the pharmacological effects on anticancer cell proliferation. Combined administration of the two drugs also inhibited expression of AR and PI3K/Akt signaling pathways and that of various cancer-related miRNAs such as miR-21, miR-19b, and miR-148a, and it exerted stronger inhibitory effects on tumor cell migration than single-drug treatments (124). The combination of these two natural compounds may provide a new approach for the treatment and prevention of prostate cancer.

Using cell experiments and xenograft models, Pham et al. found that combination of quercetin with the epigenetic drug BET inhibitor JQ1 can enhance anticancer effects on pancreatic and thyroid cancer by inhibiting tumor cell proliferation and inhibit sphere-formation ability of tumor cells, which shows the effect of targeted therapy on tumor stem cells. In addition, knocking out HnRNPA1 can enhance the inhibiting effect of JQ1 on expression of survivin and the sphere-forming ability of cancer cells, which is consistent with the effects of quercetin (125). This shows that quercetin enhances the effects of BET inhibitor JQ1 by inhibiting expression of the hnRNPA1 gene, and combined administration may have promising application prospects for cancer patients, especially regarding patients with thyroid and pancreatic cancer.

Quercetin also showed broad-spectrum epigenetic activity when used in single-drug treatments in which miRNA regulation was most prominent, as confirmed in various forms of cancer. When carcinogenicity of hexavalent chromium Cr(VI) was reduced, long-term administration of BEAS-2B human bronchial epithelial cells Cr(VI) upregulated miRNA-21, downregulated programmed cell death 4 (PDCD4), promoted ROS expression, and induced cell malignancy. This process can be inhibited by quercetin. In a nude mouse model, the tumor

incidence in nude mice injected with Cr(VI) + quercetin BEAS-2B cells was significantly lower than that in the Cr(VI) group. Furthermore, after collecting tumors from nude mice and administering quercetin, promotion of miR-21 was associated with inhibition of PDCD4 (126). These results suggest that quercetin can regulate the miRNA-21-PDCD4 axis to inhibit malignant transformation of human bronchial epithelial cells induced by Cr(VI).

Moreover, quercetin inhibits the self-renewal and proliferation of AsPC1 human pancreatic cancer cells by regulating a variety of miRNAs. After cells were treated with quercetin for 12 h, changes in miRNA expression associated with Notch signaling and cell fate were analyzed, and 11 types of miRNAs including let-7c and miR-200b-3p were observed. miR-200b-3p was further examined and was shown to be a key factor controlling cell fate. Subsequent *in vitro* experiments showed that miR-200b-3p enhanced by quercetin inhibited the Notch signaling pathway, adjusted the transformation of the CSC division mode from symmetry to asymmetry, inhibited self-renewal and proliferation of CSCs, promoted cell differentiation, and reduced invasiveness (127).

Anticancer mechanisms of miRNAs regulated by quercetin have also been reported in hepatocellular carcinoma. In HepG2 hepatoma cells, quercetin promoted expression of miRNA-34a and mediated the p53/miR-34a/SIRT1 signaling mechanism to transmit apoptosis signals of cancer cells (128).

Quercetin plays a key role in inhibiting invasion and proliferation of breast cancer cells. The mechanism underlying the regulation of cancer cells is to promote expression of miR-146a, activate caspase-3 and Bax, and induce apoptosis through a mitochondrial-dependent pathway in human breast cancer cell lines MCF-7 and MDA-MB-231 to inhibit proliferation of tumor cells, inhibit expression of EGFR, and reduce invasiveness of tumor cells (129).

In osteosarcoma studies, quercetin enhanced the efficacy of cisplatin by regulating the miR-217-KRAS signaling axis. When human osteosarcoma 143 B cells were treated with quercetin and/or cisplatin, expression of KRAS was downregulated and miR-217 was upregulated, and a combined treatment significantly increased the expression of miRNA-217 (130). This also confirms previous reports which suggested that miR-217 targets KRAS in lung cancer cells to reverse cisplatin resistance (131).

Flavones

Diosmin

Diosmin is a well-known natural flavonoid used for the treatment of chronic venous insufficiency and varicose veins. Numerous recent studies showed that diosmin exerts various pharmacological activities including anti-inflammatory, antioxidative, antidiabetic, anticancer, antimicrobial, liver-protective, neuroprotective, cardiovascular-protective, kidney-protective, and retina-protective effects (132, 133).

Diosmin is effective against tumors on a genetic and epigenetic level. Epigenetic intervention effects of three flavonoids and their genotoxicity and apoptosis-inducing effects were assessed in DU145 prostate cancer cells. Naringin, diosmin, and hesperidin reduced the number of cancer cells and proliferation to varying degrees, and diosmin showed the strongest gene toxicity and considerable proapoptotic activity. This study also assessed changes in global DNA methylation, and diosmin downregulated the level of 5-methyl-20-deoxycytidine in DU145 cell lines and mediated DNA demethylation to regulate the epigenome of tumor cells (134).

Apigenin

Apigenin, which is common in medicinal plants, vegetables and fruits, including Menthae Herba, Radix Salviae, Codonopsis Radix, Chrysanthemi Flos, celery, onions, and oranges, is a kind of natural flavonoids with various pharmacological activities (135–137). It has been used in studies on many diseases because of its low toxicity and strong biological effects, and it has been reported to exert substantial anti-inflammation, antioxidation, antidiabetic, antitumor, antibacterial, and antiparasitic effects. Moreover, this compound can improve the symptoms of chronic diseases, such as depression, insomnia, amnesia, and Alzheimer's disease (138–140).

Tseng et al. reported that apigenin downregulated the expression of cyclins A, B, and CDK1 in the MB-231 breast cancer cell line in a time-dependent manner, and expression of CDKI $p21^{WAF1/CIP1}$ was also upregulated in a time-dependent manner. In addition, apigenin promotes acetylation of histone H3 and thus transcription of $p21^{WAF1/CIP1}$. A nude mouse model experiment using xenotransplantation also supported this conclusion (141). This study revealed for the first time the epigenetic targeting mechanisms and effects of apigenin on breast cancer.

Paredes-Gonzalez et al. evaluated epigenetic effects of apigenin in the prevention of skin cancer. Apigenin can inhibit expression of DNMT1, 3a, 3b, and HDAC in mouse skin epidermal JB6 P+ cells, demethylate 15 CpG sites, and silence Nrf2 to promote antioxidation and prevent skin cancer (142).

Apigenin can play the role of an HDACi in inducing apoptosis in prostate cancer cells. In prostate cancer cells and xenotransplantation models, apigenin decreases expression of apoptotic protein inhibitors such as XIAP, survivin, c-IAP1, and c-IAP2, inhibits HDAC1, upregulates acetylation of Ku70, destroys the Ku70-Bax interaction, and mediates apoptosis of prostate cancer cells by separating Bax and Ku70 (143). Similar anti-HDAC effects of apigenin were also reported by a different study on prostate cancer. Apigenin (20–40 μM) inhibited HDAC activity in human prostate cancer cell lines PC-3 and 22Rv1 and reduced expression of HDAC1 and 3. Histone acetylation was also increased by apigenin-mediated downregulation of HDAC, while the cell cycle regulatory protein p21/waf1 and apoptosis protein Bax were upregulated at the transcriptional level. As shown in a mouse model, bcl2 was downregulated and Bax was upregulated in animals treated with apigenin, and growth of transplanted tumors was inhibited (144).

Luteolin

Luteolin is a natural flavone extracted from plants and is commonly found in traditional Chinese herbal medicines such

as Lonicerae Japonicae Flos, Schizonepetae Herba, Chrysanthemi Flos and in vegetables such as broccoli, carrots, and celery. Luteolin exerts various pharmacological activities such as anti-inflammatory, anti-allergy, antitumor, anti-aging, antibacterial, antiviral, heart-protective, neuroprotective, and uric acid-reducing effects and is used to treat diabetes and Alzheimer's disease (145–147).

Selvi et al. confirmed that luteolin regulates epigenetics multidimensionally and inhibits growth of head and neck squamous cell carcinoma cells. Treatment of mice with luteolin inhibited p300 acetyltransferase, upregulated miR-195/215 and let7C, induced by p53, downregulated miR-135a, and significantly decreased tumor growth within four weeks (148).

Kanwal et al. found that flavonoids such as luteolin, apigenin, and chrysin can inhibit DNA methylation and trimethylation of lysine 27 on histone H3, and luteolin showed the strongest inhibitory effects on DNMT. Different concentrations of luteolin (10 μM and 20 μM) inhibited DNMT in a dose-dependent manner, and molecular docking showed that luteolin can interact with DNMT residues through six hydrogen bonds. Luteolin can inhibit H3K27me3 and downregulate the expression of EZH2 in human prostate cancer DU145 cells in a concentration-dependent manner (149).

Ganai et al. found that luteolin can stably bind to class-I HDAC isomers. Luteolin, as a natural product, may have better anticancer application prospects than synthetic HDACi's which are associated with more side effects (150).

Luteolin has been reported in many studies to be a regulator of epigenetic effects in various cancer signaling pathways. Zuo et al. found that luteolin can inhibit DNMTs and HDACs in HCT116 and HT29 colon cancer cells and promote Nrf2 demethylation and upregulate its expression, which activates the Nrf2/antioxidant responsive element(ARE) pathway and inhibits cancer cell proliferation (151). Their results show that luteolin positively regulates the epigenetic effects of anticancer signaling pathways. A study on the effects of luteolin on prostate cancer cells showed that it changed the acetylation state of the gene promoter histone, downregulated expression of 22 key genes of the cell cycle pathway such as cyclin A2 and cyclin E2, and upregulated expression of cyclin-dependent kinase inhibitor 1B (152).

Luteolin also alters histone H4 acetylation levels and regulates estrogen levels and cell proliferation in breast cancer cells. The estrogen signal pathway gene and the cell cycle pathway gene in MCF-7 breast cancer cells are regulated by this natural compound, and PLK-1 histone H4 acetylation modification which regulates the cell cycle is inhibited (153). This shows that luteolin regulates gene expression through epigenetic properties involving modified histone acetylation, which is consistent with the anti-estrogenic and cell proliferation activities of luteolin.

Luteolin, a natural inhibitor of EGFR tyrosine kinase, is also used in the development of targeted therapies. Markaverich et al. found that epigenetic regulation effects of luteolin on the epidermal growth factor signaling pathway may involve upregulation of c-Fos and p21, caused by histone H4 binding in PC-3 human prostate cancer cells (154).

Tangeretin

Similar to naringenin and diosmin, tangeretin is a phytochemical compound derived from citrus fruits, and it shows good antifungal, anti-inflammatory, antioxidant, and anticancer effects *in vivo* and *in vitro*. Tangeretin can inhibit tumor progression through various signaling pathways and epigenetic mechanisms (155–157).

Wei et al. examined antitumor and epigenetic activities of tangeretin (PMF1) and its derivative 4'-didemethyltangeretin (PMF2). In human prostate cancer LNCaP cells, both compounds inhibited cell growth, but PMF2 exerted stronger effects and less cytotoxicity to normal cells. PMF2 also induced apoptosis by increasing expression of proapoptotic proteins Bad and Bax, downregulating antiapoptotic proteins Bcl2, and activating caspase-3 and PARP. This study also confirmed epigenetic regulation of PMF2. PMF2 can demethylate the p21 promoter and inhibit expression of DNMT3B, HDAC1, HDAC2, and HDAC4\5\6. In addition, PMF2 can interact with DNMTs *in vitro*, which may lead to a decrease in DNMT catalytic activity (158).

Chrysin

Chrysin is a flavonoid extracted from *Artemisia mandshurica*, and it is also abundant in propolis, honey, and passion fruit. It exerts a wide range of pharmacological activities such as antioxidative, antitumor, antiviral, antihypertensive, antidiabetic, antibacterial, and anti-allergy effects. Due to its wide distribution in plants and low toxicity, it has become an important substrate for drug discovery (159).

Sun et al. examined anticancer effects of chrysin extracted from Chinese propolis. When breast cancer MDA-MB-231 cells were treated with chrysin, tumor cell growth and proliferation were inhibited. In a xenotransplantation model, oral administration of chrysin to immunodeficient mice reduced the size and weight of tumors. Concurrent enzyme activity analyses showed that chrysin, an HDACi, may inhibit HDAC8 activity. This study confirmed that chrysin has anti-HDAC8 activity and can inhibit chromatin remodeling in breast cancer cells to exert anticancer effects (160). Sun et al. proposed that the anti-HDAC activity of chrysin may be related to its anticancer effects (160), which was confirmed by other experiments (161).

For instance, the anti-melanoma activity of chrysin was found to be related to its anti-HDAC activity. After melanoma A375 cells were treated with chrysin, cell proliferation was inhibited, the cell cycle was blocked at the G1 phase, HDAC-2, 3, and 8 were downregulated at the translation level, and the degree of H3me2K9 methylation was decreased. In addition, chrysin upregulates expression of apoptosis-related protein p21 through protein methylation and hyperacetylation, which is considered an important factor leading to melanoma cell apoptosis (161).

TET1, which is involved in the demethylation of 5-methylcytosine, is a promising target for gastric cancer therapy, and chrysin can promote its expression to inhibit tumor progression. In gastric cancer MKN45 cells treated with chrysin, expression of TET1 and 5hmC increased, and the

increase in TET1 levels promoted apoptosis and inhibited migration and invasion of gastric cancer cells. Furthermore, a CRISPR/Cas9 system was used to knock out TET1 to promote tumor growth, which showed that TET1 expression is closely associated with tumor growth, thus chrysin is expected to become an effective target for this emerging gastric cancer (162).

Isoflavones

Daidzein and Genistein

Isoflavone is a flavonoid that mainly occurs in legumes. Due to similar characteristics regarding molecular structure and biological activities, isoflavones are also known as phytoestrogens. In addition to producing estrogens and antiestrogens, participating in lowering blood sugar, inhibiting obesity and type-2 diabetes, controlling inflammation, and protecting nerves, isoflavones can also be used to treat tumors related to hormone disorders, cardiovascular diseases, and human reproductive functions (163–166). The representative compounds are daidzein and genistein, which are often discussed together because of their similar origin and function.

It has been reported that isoflavones are epigenetic modulators of the Wnt pathway involved in tumorigenesis and epithelial mesenchymal transformation (EMT) intervention (167–169). In a study on colon cancer, genistein affected demethylation, upregulated the Wnt antagonist gene SFRP2, and inhibited Wnt signal transduction. Methylation-specific-PCR analysis showed that the demethylation degree of SFRP2 was up to 50% (168). In a different experiment involving the Wnt pathway, genistein led to demethylation of the CpG island of Wnt5a, a Wnt antagonist, and induction of re-expression of Wnt5a to inhibit proliferation of colon cancer cells (169); notably, these changes facilitated Wnt5a-associated demethylation regulation in early tumor cells, which may be a method for early intervention in colon cancer.

Epigenetic regulation of Wnt by isoflavones has also been demonstrated *in vitro*. Zhang et al. found that genistein included in the diet of rats can affect Wnt gene expression through DNA methylation regulation and histone modification and maintain normal Wnt signal transduction in rat colonic epithelium after exposure to the carcinogen azomethane (167), prompting the preventive effect of genistein supplementation through food intake on cancer.

The DNA methylation regulation activity of soybean isoflavones is an important mechanism for its anti-prostate cancer. Genistein and daidzein can down-regulate the methylation level of tumor suppressor gene promoter in human prostate cancer cells. When VARDI and his colleagues treated cancer cells with genistein and daidzein, EPHB2 and GSTP1 methylation was down-regulated, while BRCA1 methylation was not affected (170). Immunohistochemical results showed that the expression of BRCA1 and RASSF1A did not change, while the expression of GSTP1 and EPHB2 increased. In a different study on prostate cancer, daidzein and genistein inhibited cancer cell growth and promoted apoptosis by altering the methylation status of several genes involved in the NF-κB and p53 pathways in prostate cancer cells (171).

Genistein exerts a demethylation effect on tumor suppressor genes in esophageal squamous cell carcinoma cells. Approximately 2–20 μmol/L genistein inhibited DNMT, promoted activation of α-O6 methylguanine methyltransferase, and downregulated methylation of RARβ, p16INK4a and promoted their expression. Activity of DNMT was reduced in a dose-dependent manner with 20–50 μmol/L genistein, and HDAC activity was also inhibited by genistein (5–100 μmol/L) in a concentration-dependent manner. Additionally, the authors found that addition of 5-Aza-DCYD and trichostatin or SFN can enhance genistein effects through demethylation of tumor suppressor genes and inhibition of cell growth (172). However, the use of genistein alone or in combination with other drugs to reverse hypermethylation requires further research.

Flavanones

Naringenin

Naringenin is a common citrus flavonoid which mainly occurs in the peel of citrus fruits such as oranges, lemons, and grapefruit. It exerts pharmacological activities such as liver-protective, antioxidative, antiviral, cardiovascular-protective, kidney-protective, antidiabetic, and anticancer effects and can be used to treat sepsis (173–175).

Curti et al. examined the regulation of miRNA (miR-17-3p and miR-25-5p) by naringenin in the process of anti-inflammation and antioxidation treatments of human colon adenocarcinoma. When Caco-2 cells were treated with racemic and enantiomeric Naringenin at subtoxic concentrations, expression of miR-17-3p and miR-25-5p decreased. The decrease of miR-17-3p is accompanied by the up-regulation of the transcription levels of two antioxidant enzymes, glutathione peroxidase 2 and manganese superoxide dismutase, which are encoded by it. however, downregulated expression of miR-25-5p was not consistent with mRNA expression of tumor necrosis factor-α and interleukin-6, which are pro-inflammatory cytokines and Encoded by miR-25-5p (176). These results suggest that Naringenin can achieve antioxidant activity by targeting the epigenetic mechanism of miRNAs, even though anti-inflammatory effects may be mediated by other mechanisms.

Hesperidin

Hesperidin occurs in fruits of Rutaceae plants such as bergamot, orange, and lemon, and are also the important active components of some botanical drugs such as Schizonepetae Spica, Citri Fructus Retinervus, Citri Reticulatae Pericarpium Viride. Hesperidin regulate epigenetic processes and exert anti-inflammatory, antioxidant, anti-obesity, and cardiovascular and anticancer effects. Hesperidin significantly reduced the growth of liver nodules in rats with liver cancer induced by diethylnitrosamine and significantly ameliorated liver histological damage. In addition, cytotoxicity of Hesperidin to HL60 cells was dose-dependent, with an IC_{50} of 12.5 mM, and at this concentration, it produced the maximum value of LINE-1 sequence hypomethylation (47%). Hesperidin also downregulated methylation of ALUM2 repeats, and the highest hypomethylation level of 32% was observed at a concentration of

6 mM (177). This study suggests that hesperidin, an active demethylation drug, can play a significant role in the treatment of liver cancer.

Phlorizin

Phlorizin/phloridzin is a dihydrochalcone flavonoid that mainly occurs in Rubi Fructus, and fruits, leaves, and roots of apple trees, and it has been studied for many years to examine antioxidant, anti-inflammatory, and antitumor effects on mammalian cells (178).

Sandhya et al. found that in HepG2 human liver cancer cells, MDAMB human breast cancer cells, and THP-1 leukemia cells, phlorizin and its derivatives can significantly inhibit proliferation of tumor cells, and the antiproliferative activity of fatty esters of phloridzin (a phlorizin derivative) is similar to that of sorafenib and other chemotherapeutic drugs. Furthermore, Sandhya et al. explored the antitumor mechanism of several drugs and found that fatty esters of phloridzin can inhibit DNA topoisomerase IIa activity, downregulate growth factor receptors such as the antiapoptotic genes BCL2 and PDGFR, and block the cell cycle. In addition, a variety of HDACs (HDAC1, 4, 6, 7, and 11) are downregulated by phlorizin derivatives (179). This study suggests that the chemotherapeutic effect of this phlorizin derivative may be associated with downregulation of DNA topoisomerase IIa activity, cell cycle arrest, and epigenetic activity.

Taxifolin

Taxifolin, a natural flavonoid which is common in Cinnamomi Ramulus, Fructus Ligustri Lucidi, Viticis Fructus, milk thistle, larch, and other plants, shows cardiovascular-protective, antibacterial, and free-radical scavenging effects and has shown good anticancer activity through a variety of pathways *in vivo* and *in vitro (*180, 181). For example, in breast cancer cells, taxifolin can inhibit cell proliferation and migration by down-regulating β-catenin to promote EMT (182). Taxifolin has also been reported to inhibit cancer cell growth in scar cancer cells by inhibiting the PI3K/Akt/mTOR pathway (183).

Epigenetic effects of taxifolin have also been reported. After treatment with taxifolin, colony formation of mouse epidermal JB6 P+ cells was inhibited, and Nrf2, heme oxygenase-1, and NAD(P)H quinone oxidoreductase 1 were upregulated at transcriptional and translational levels. Bisulfite genome sequencing showed that methylation levels of the Nrf2 promoter were decreased by taxifolin, and expression of DNMT and DHAC were also reduced by taxifolin (184). This suggests that taxifolin can play a role in chemoprevention by promoting the expression of Nrf2 through an epigenetic pathway.

Silibinin

Silibinin, a representative flavanone compound, is a bioactive substance extracted from dried fruit of thistle which belongs to the family Compositae. It shows strong antioxidant functions and liver-protective, free-radical scavenging, and anti-aging, effects, among others, and it is commonly used in medicine, health care, food, and other applications.

Silibinin exerts considerable epigenetic effects and can be administered in combination with other epigenetic drugs. Mateen et al. reported that silibinin combined with an HDACi modified epigenetics and inhibited growth of non-small cell lung cancer. In vitro experiments showed that after administration of silibinin to tumor cells, acetylation of histones H3 and H4 was upregulated, accompanied by a decrease in HDAC activity, and expression of HDAC1, 2, and 3 were downregulated. After using several HDACi's and silibinin in combination, p21 acetylation was upregulated, cytotoxicity was increased, and cell cycle arrest and apoptosis were induced (185). In vivo experiments also revealed similar epigenetic effects of silibinin, and growth of transplanted tumors was inhibited. Similarly, in a different study on non-small cell lung cancer, silibinin combined with an HDACi or DNMTi restored E-cadherin expression and reduced tumor cell migration and invasion (186).

A previous study claimed that silibinin exerts substantial preclinical anticancer activity and that it is an epigenetic regulator of prostate cancer. When human prostate cancer cell lines DU145 and PC3 were treated with silibinin, expression of EZH2, SUZ12, and EED was downregulated, accompanied by an upregulation of H3K27me3 methylation. In addition, silibinin increased the activity of DNMT and suppressed the expression of HDAC1-2 (187). Silibinin also played an epigenetic targeting role in the process of antiproliferation of bladder cancer. Silibinin showed considerable cytotoxicity to bladder cancer cells with different TP53 statuses. In the highest grade tumors (TP53 mutation status is level 3), silibinin induces global DNA hypomethylation. In low-grade tumor cells (wild type TP53 gene), silibinin downregulated expression of HDAC and HAT (188).

Like many flavonoids, silibinin also regulates noncoding RNAs. In the exploration of anti-breast cancer, Silibinin has been found to induce apoptosis by regulating microRNA. When MCF-7 cells were treated with silibinin, decreased expression of miR-21 and miR-155 was detected, and apoptosis occurred in a dose- and time-dependent manner. Shengxin analysis was used to predict the potential targets of two kinds of microRNAs, caspase-9 and bid. PCR results showed that expression of caspase-9 and bid were increased, which was consistent with the results of the dry and wet experiments (189).

Flavanols

EGCG

Tea is the second most commonly consumed beverage in the world after water and is particularly common in Asia. Catechins are flavanols, and they are the main functional components of tea, comprising various monomer structures among which EGCG is most prominent due to its regulatory effects on many aspects of human physiological and pathological processes. EGCG has neurotrophic, anticancer, and antifibrotic pharmacological activities and plays an important role in inhibiting oxidation and inflammation (190–192). Epigenetic regulation of cancer by EGCG alone or in combination with other compounds was described in many recent studies.

Sheng et al. examined methylation regulation of EGCG in breast cancer. The tumor suppressor gene SCUBE2 is frequently methylated and silenced in breast cancer, while EGCG has been reported to regulate the levels of methylation in the promoter region of various tumor-related genes. In this study, MDA-MB-

231 and MCF-7 cell lines were treated with EGCG, and an MTT assay showed that growth of breast cancer cells was inhibited and the cell viability was significantly decreased; migration and invasion abilities of breast cancer cells were also inhibited. Regarding the underlying mechanism, EGCG reactivated SCUBE2 gene expression. Real-time PCR revealed that transcription of DNMT1, DNMT3a, and DNMT3b was downregulated, and the degree of DNA methylation was also reduced (15).

EGCG has been reported to reverse both DNA methylation and histone acetylation abnormalities to induce apoptosis in breast cancer cells and inhibit cancer development. When EGCG and sulforaphane (SFN) were used in a breast cancer-transformed cell system, cell viability decreased and apoptosis and cell cycle arrest were induced. EGCG decreased the activities of DNMT1 and HDAC1, and combined administration was more effective in regulating epigenetics. To further explore the regulation of epigenetic aberrations, histone H3 acetylation and DNA methylation levels were examined, and cotreatment with EGCG and SFN significantly promoted global acetylation of histone H3 in the breast cancer-transformed cell system. Cluster analysis and screening of methylation status using probes showed that the methylation status of tumor-related genes was changed to varying degrees. In addition, combined treatment inhibited oncogene Septin9 and promoted expression of the tumor suppressor gene DCBLD2. EGCG and/or SFN inhibited xenograft tumor growth in breast cancer mice, and the combined effect of the two drugs was stronger (193). This new dietary combination shows promising prospects for the prevention and treatment of breast cancer.

Deb et al. conducted experiments and proposed that green tea polyphenol (GTP) and its main active ingredient EGCG can remedy epigenetic disorders caused by abnormal expression of matrix metalloproteinase-3 (TIMP-3) in prostate cancer. GTP/EGCG decreased invasiveness and migration of prostate cancer cells and decreased the activity of matrix metalloproteinases (MMPs) such as MMP-2 and MMP-9. TIMP-3 was upregulated at a transcriptional and translational level, whereas acetylation of class-I HDAC, EZH2, and H3K9/18 and H3K27 trimethylation were downregulated; low expression of class-I HDAC and EZH2 was due to activation of TIMP-3. Deb et al. then used clinical samples for verification. After analyzing data of patients treated with EGCG, they found decreased expression of MMP-2, MMP-9, class-I HDAC, and EZH2, and TIMP-3 was upregulated, which was consistent with experimental results at a cellular level (16).

Zhao et al. reported that EGCG can regulate lncRNAs and miRNAs to reverse gastric cancer. When gastric cancer AGS and SGC7901 cell lines were treated with different doses of EGCG, growth of tumor cells was inhibited in a time- and dose-dependent manner. Bioinformatics showed that EGCG altered gene expression in gastric cancer cells and participated in the regulation of cell metastasis. Expression of LINC00511, which promotes tumor metastasis and proliferation, can be downregulated by EGCG, and miR-29b, as a downstream target of LINC00511, can be inhibited by this lncRNA, thus increasing expression of carcinogenesis-related KDM2A (a kind of KDM) (17). This study reflects epigenetic effects of EGCG on proliferation, metastasis, and invasion of gastric cancer, particularly regarding targeting of the LINC00511/miR-29b/KDM2A axis.

Multilevel epigenetic effects of EGCG on hematological tumors have also been examined. During acute promyelocytic leukemia (APL), GTP has been shown to inhibit cell proliferation and cause tumor cell apoptosis. Borutinskaitė et al. proposed that during the antitumor process, EGCG regulates expression of cell cycle-related genes, promotes expression of transcriptional regulatory protein families C/EBPα and C/EBPϵ, and upregulates PCAF and p27. RT-qPCR results showed that DNMT1, HDAC1, and HDAC2 were inhibited by EGCG, and G9A, which is related to H3K9me2 methylation, was also downregulated. Expression of genes related to PRC2 with HMT activity was inhibited at the protein level, and the binding effect of these genes with acetylated histone H4 and acetylated H3K14 is reduced, while in cell cycle-related genes such as C/EBPα and acetylated H3K14, the relationship between H4 and H4 has become closer (194). EGCG is not only used as a cell cycle blocker but also has an epigenetic remedy, and it has considerable potential for application in the treatment of APL.

Theaflavins

EGCG is a representative biologically active constituent of green tea, and theaflavins are natural flavonoids which are highly abundant in black tea where they are responsible for color and taste; moreover, these compounds are considered effective antioxidant and anticancer agents (195–197).In an enzyme inhibition test, theaflavins were identified as natural DNMT inhibitors. it inhibits DNMT1 by 65%, and the IC_{50} value of DNMT1 inhibition was 85.33 μM (198).

A different study found that theaflavins can reduce the activity of DNMT1 and DNMT3a and inhibit the proliferation of colon cancer cells HCT-116 and the progression of solid tumors induced by EAC in mice. The authors found that theaflavins can downregulate the activity of DNMT, both *in vivo* and *in vitro*. In addition, immunohistochemical analysis of mouse tumor tissues showed that theaflavins inhibited the expression of DNMT (199). This study demonstrates that theaflavins act as potential DNMT inhibitors in colorectal cancer.

Anthocyanidins

Anthocyanidins are natural water-soluble pigments belonging to the group of flavonols which are commonly found in plant petals and fruits. Because of their active biological activity and coloring function, they are commonly used in the production of food, drinks, and medicine. These flavonoids exert beneficial functions including vision-protective, antioxidative, antitumor, and anti-cardiovascular disease effects, and they can be used for preventing and treating type-2 diabetes and treating obesity (200–202). Due to the similarity of source and structure, different types of anthocyanidins show similar epigenetic effects in function.

In a report on the prevention of skin cancer, anthocyanidins were shown to modulate epigenetic activation of the NRF2-ARE

pathway and inhibit carcinogenesis in JB6 P+ cells. Kuo et al. treated JB6 P+ cells with the anthocyanidin delphinidin and found that ARE-driven luciferase activity was markedly upregulated, Nrf2 and its downstream antioxidant and carcinogenic detoxion-related genes were upregulated, and Nrf2-ARE was activated. Kuo et al. further investigated epigenetic activity of anthocyanidins during skin cancer. Delphinidin not only demethylates the Nrf2 promoter, but also inhibits expression of DNMTs and HDACs (203).

A different study on skin cancer study discussed the epigenetic regulation of Nrf2-ARE by pelargonidin, which is a commonly studied anthocyanidin. Similar to delphinidin, pelargonidin promoted activation of the Nrf2-ARE signaling pathway, upregulated expression of the Nrf2 target gene, demethylated the Nrf2 promoter at an epigenetic level, and inhibited expression of DNMT and HDAC (204).

The activity of anthocyanidins that target miRNAs has also been examined. Black raspberry anthocyanins (BRB) inhibit growth of human colon cancer cells by upregulating miR-24-1-5p. BRB upregulated the expression of miR-24-1-5p in a human colorectal cancer cell line and downregulated β-catenin in an AOM/DSS-induced mouse model. In addition, the authors used bioinformatics to predict β-catenin as a target gene of miR-24-1-5p and confirmed this using RT-qPCR and western blotting. The results showed that miR-24-1-5p inhibited the expression of β-catenin. In cell experiments, miR-24-1-5p regulated the downstream target genes of the Wnt/β-catenin signaling pathway, and cyclinD1, c-Myc, and CDK4 were downregulated at the transcriptional and translational level (205). This study suggests that miR-24-1-5p may act as a regulator of the Wnt/β-catenin signaling pathway to inhibit colorectal cancer, which is one of the possible mechanisms of anthocyanin anticancer effects through epigenetic pathways.

DISCUSSION

Epigenetics as a Link Between Flavonoids and Prevention and Treatment of Cancer

The epigenetic genome is affected by acquired factors, and natural compounds consumed by dietary and medicinal plants are involved in shaping the dynamic balance of epigenetic state (206, 207) (**Figure 4**). Natural compounds derived from natural medicines and foods which may act as epigenetic regulators to remedy adverse gene expression patterns have been accepted by the scientific community. Flavonoids are indispensable compounds in in human body, and their epigenetic effects may help counteract a variety of diseases.

Flavonoids show activity against various modifications in the multilevel epigenetic interaction network of cancer, from DNA histones to noncoding RNAs. Specifically, one kind of flavonoids can be involved in the remodeling of a variety of related enzymes or non-coding RNA in modifying one level of cancer epigenetic regulation. Also, one flavonoid compound can modify multi-level epigenetic network, playing a role in regulating DNA methylation, histone modification and regulating non-coding RNA, and at the same time up-regulate tumor suppressor genes and down-regulate oncogenes to interfere with the occurrence and progression of cancer (**Figure 1**). Remodeling of these epigenetic links eventually leads to the accumulation of changes in cell metabolism and self-renewal and ultimately results in the loss of tumor cell carcinogenicity (208–210).

Considering the heterogeneity of the population and the multi-target complexity of the epigenetic modification network, population-based clinical trials and observational studies have not yet shown sufficient clear links for flavonoids to target epigenetics. However, the success of *in vivo* and *in vitro* studies has fully demonstrated the driving force of flavonoids on epigenetics and has shown considerable therapeutic effects on different cancers (**Table 2**). This also encourages people to design more feasible solutions to search for the chain of evidence that these phytochemicals is effective in maintaining the human body's epigenetic balance and disease prevention.

Current Challenges for Flavonoid-Targeted Epigenetic Antitumor Research and Development

Research on flavonoids is inspired by their biological effects, including, but not limited to, antioxidation, free-radical scavenging, cell cycle regulation, anti-estrogens affects, protein tyrosine kinase inhibition, and epigenetic activity (211–214). Plant compounds may exert a plethora of effects (215), which

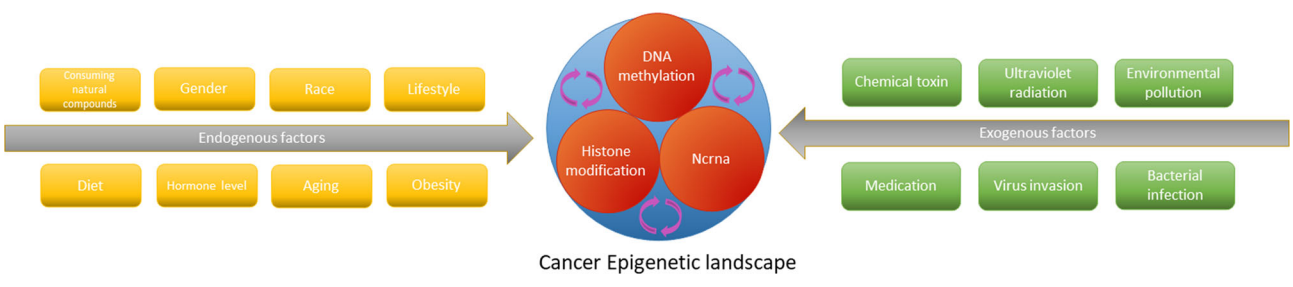

FIGURE 4 | The epigenetic cascade network mediated by endogenous and exogenous factors interferes with tumorigenesis and progression by affecting gene expression.

TABLE 2 | Epigenetic effects of flavonoids on different types of cancers *in vitro* and *in vivo*.

Flavonoid subtype	Phytochemical	Epigenetic modifications	Molecular targets	Regulation of cell phenotypes	Dose	In vitro model	In vivo model	Cancer species	References
Flavonols	Kaempferol	HDAC inhibitor G9a inhibitor	Down-regulation of P62; Up-regulation of p-JNK and CHOP	↑Autophagy	25,50,100 μM	AGS, SNU-216, NCI-N87, SNU-638, and MKN-74 cell lines		Gastric cancer	(14)
	Kaempferol	HDAC inhibitor		↓Cell viability ↓proliferation	5-100 μM	Hepg2,Hep3B cells		Liver cancer	(109)
	Kaempferol	HDAC inhibitor		↓Cell viability ↓proliferation	5-100 μM	HCT-116 cells		Colon cancer	(109)
	Kaempferol	DNMT1 inhibitor DNMT3b inhibitor DNMT3a inhibitor	Down-regulation of DACT2 and β-catenin	↓Proliferation ↓Migration	1.25-150 μM; 75 and 150 mg/kg	HCT116,HT29 and YB5 cell lines	Nude mice	Colorectal cancer	(110)
	Quercetin	Promotion of mir-146a expression	Activation of caspase-3 and Bax; Inhibition of EGFR expression	↑Apoptosis ↓Proliferation ↓Invasiveness of tumor cells	0,25,50,80 and 100 μm/ml; 10 mg/kg	MCF-7 and MDA-MB-231 cells	Athymic nude mice	Breast cancer	(129)
	Quercetin	Promotion of mir-217 expression	Down-regulation of kras	↓Viability	0, 5, 10, 50, and 100 μM	143B cells		Osteosarcoma	(130)
	Quercetin	Promotion of mir-200b-3p expression	Down-regulation of Notch signaling pathway	↑Asymmetric cell division ↓Self-renewal ↓Proliferation	50 μm	Aspc1 and PANC1 cells		Pancreatic cancer	(127)
	Quercetin	Promotion of mir-34a expression	Down-regulation of SIRT1; Up-regulation of p53 and p21	↑Apoptosis ↓Proliferation	31.25 μM	Hepg2 cells		Liver cancer	(128)
Flavones	Diosmin	DNA hypermethylation		↑Apoptosis ↓Proliferation	0,50,100,150,200 and 250 μM	DU145 cells		Prostate cancer	(134)
	Apigenin	HDAC inhibitor	Down-regulation of cyclin A, B and CDK1; Up-regulation of $p21^{waf1/CIP1}$	↓Proliferation ↓Cell cycle arrest	0, 10, 20 and 40 μM	MDA-MB-231 cells	Athymic nude mice	Breast cancer	(141)
	Apigenin	HDAC inhibitor	Decrease the expression of XIAP, survivin, c-IAP1 and c-IAP2; Disruption of Ku70–Bax interaction	↑Apoptosis ↑Cell cycle block ↓Cell survival rate	5–40 μM; 20,50 μg	PC-3 And DU145 cells	Athymic nude mice	Prostate cancer	(143)
	Apigenin	HDAC1 inhibitor HDAC3 inhibitor	Up-regulation of $p21^{waf1/CIP1}$ and bax in transcriptional levels	↑Growth Arrest ↑Apoptosis	20-40 μM; 20 and 50 μg	PC-3 and 22Rv1 cells	Athymic nude mice	Prostate cancer	(144)
	Luteolin	Inhibition of p300 acetyltransferase and histone acetylation; Up-regulation of mir-195/215,let7c; Down-regulation of mir-135a	Up-regulation of POFUT and DICER; Down-regulation of E2F2,DOK2	↑Cell cycle arrest ↓Cell migration	10μM and 25μM; 100 mg/kg	KB cells	Xenograft mice	Head and neck squamous cell carcinoma	(148)
	Luteolin	DNMT inhibitor HMT inhibitor Down-regulation of EZH2			10- μM,20- μM	DU145 cells		Prostate cancer	(149)

(Continued)

TABLE 2 | Continued

Flavonoid subtype	Phytochemical	Epigenetic modifications	Molecular targets	Regulation of cell phenotypes	Dose	In vitro model	In vivo model	Cancer species	References
	Luteolin	DNMT inhibitor HDAC inhibitor	Up-regulation of Nrf2,HO-1, and NQO1 expression	↓Cell proliferation ↓Cellular transformation	10- μM and 20- μM	HCT116 And HT29		Colon cancer	(151)
	Chrysin	HDAC8 inhibitor	Promoting p21 expression	↓Cell growth ↑Cell differentiation	10,20, and 40 μM; 45 or 90 mg/kg	MDA-MB-231 cells	Nude mice	Breast cancer	(160)
	Chrysin	HDAC2,3,8 inhibitor	Promoting STAT-1 and p21 expression	↓Cell proliferation ↑Cell cycle	40,120 μM	A375 cells		Melanoma	(161)
	Chrysin	Increase the expression of TET1 and 5hmc	Promoting the expression of BAX and inhibiting the expression of bcl2	↑Apoptosis ↓Cancer cell migration and invasion	0,10,20,40,80,160 μM; 20 mg/kg	MKN45 cells	Nude Mice Xenograft Model	Gastric cancer	(162)
Isoflavones	Genistein	Demethylation	Up-regulation of SFRP2, inhibition of Wnt signal transduction; Decreasing nuclear β-catenin and increasing phospho-β-catenin accumulation	↓Cell viability ↓Proliferation ↑Apoptosis	75 mmol/L	DLD-1 cells		Colon cancer	(168)
	Genistein	Decreasing of DNA methylation level	Up-regulation of WNT5a	↓Cell proliferation	75 μmol/l	SW1116 cells		Colon Cancer	(169)
	Genistein	DNA methylation regulation and histone modification	Down-regulation of Sfrp2,Sfrp5 and Wnt5a		140 mg/kg		Timed-pregnant Sprague-Dawley rats	Colon cancer	(167)
	Genistein	DNMT inhibitor	Up-regulation of RARβ And p16INK4a	↓Cell growth	2-100 μmol/L	KYSE 510, KYSE 150 cell lines		Esopharachaquest cell carcinoma	(172)
Flavanones	Hesperidin	Hypomethylation		↓Cell viability	0.78 to 25 mm;250,500,1000 ppm	HL60 Cell line	Pathogen-free male Sprague-Dawley rats	Liver cancer	(177)
	Silibinin	HDAC1,2,3 inhibitor		↓Migration ↓Invasion	3.75-12.5 μM	H1299 cells		Non-small cell lung cancer	(186)
	Silibinin	Improvement of total DNMT activity; Inhibition of the activity of HDAC1, 2	Down-regulation of EZH2,SUZ12 and EED		25–75 μg/ml	DU145 and PC3 cell lines		Prostate cancer	(187)
	Silibinin	Down-regulation of mir-21 and mir-155	Up-regulation of caspase-9 and bid	↓Proliferation ↑Apoptosis	0–300 μM	MCF-7 cells		Breast cancer	(189)
Flavanols	EGCG	DNMT1 inhibitor DNMT3a inhibitor DNMT3b inhibitor	Up-regulation of SCUBE2	↓Cell growth ↓Migration and invasion	0-100 μM	MDA-MB-231 and MCF-7 cell lines		Breast cancer	(15)
	EGCG	Regulation of LINC00511/mir-29b/KDM2A axis		↓Proliferation ↓Metastasis ↓Invasion	0-100 μM	AGS and SGC7901 cell lines		Gastric cancer	(17)
	EGCG	DNMT1 inhibitor HDAC1 inhibitor HDAC2 inhibitor G9a inhibitor	Up-regulation of C/EBPα,C/EBPϵ, PCAF and p27	↓Proliferation ↑Apoptosis	30, 40 μM	NB4 and HL-60 cells		APL	(194)

(Continued)

TABLE 2 | Continued

Flavonoid subtype	Phytochemical	Epigenetic modifications	Molecular targets	Regulation of cell phenotypes	Dose	In vitro model	In vivo model	Cancer species	References
	Theaflavins	DNMT1 inhibitor DNMT3a inhibitor		↓Cell Viability	0,25, 50,75, 100, 125, 150 μg/ml; 0.02 mg/kg,10 mg/kg	HCT-116 cells	Swiss albino mice	Colon cancer	(199)
Anthocyanidins	Delphinidin	Dnmts inhibitor Hdacs inhibitor	Up-regulation of Nrf2 and ARE	↓Cell carcinoma	0-100 μM	JB6 P+ cells		Skin cancer	(203)
	Pelargonidin	Dnmt inhibitor Hdac inhibitor	Up-regulation of Nrf2,NQO1 and HO-1	↓Cell deterioration	0-,10,30,50 μM	JB6 P+ cells		Skin cancer	(204)

may, however, harbor some disadvantages (216, 217). Flavonoids produce anticancer effects through various mechanisms, and unspecific action may be problematic for potential drug administration. This is also a clinically important consideration regarding the use of phytochemicals (213, 218). In addition, the hierarchical interaction and reversibility of the epigenetic network suggests that when flavonoids modulate epigenetic modifications in multiple dimensions, they may cause deviations in efficacy and expected results, This is also a problem faced by other epigenetic drugs in the application (219, 220). However, based on a large number of experimental studies, we believe that flavonoids have beneficial preclinical benefits of regulating cancer epigenetics. Their broad biological activities, however, should not be a reason to dismiss flavonoids from disease research and treatment; instead, the underlying mechanisms warrant further research to exploit the inherent therapeutic potential.

Even though clinical flavonoid research focusing on tumor epigenetics has made considerable progress recently, current evidence for clinical application is still insufficient (218). A series of problems such as insufficient bioavailability currently prevent clinical application of various plant products including flavonoids. Fortunately, the academic community has begun to tackle this problem and has provided effective solutions such as combined administration with other plant compounds or anticancer drugs to improve anticancer efficacy and nano-drug carrier system to improve the pharmacokinetic characteristics of flavonoids. In addition, considering that dosages used in cell culture and animal models may not be physiological and may thus not be transferable to humans, determining the most effective dosage of flavonoids is a crucial part of basic and clinical research to effectively and safely exploit epigenetic antitumor effects of flavonoids (221).

CONCLUSIONS AND FUTURE PROSPECTS

Dysfunctional epigenetics have been confirmed in various tumors in numerous studies. Flavonoids are important epigenetic regulators and are commonly consumed worldwide. In vivo and *in vitro* studies confirm that flavonoids can inhibit cancer by restoring dysfunctional epigenetics and intervening in DNA methylation, histone modification, and expression of noncoding RNA. Whether used alone or as an adjuvant therapy, flavonoids have shown significant efficacy. Despite many challenges, the application prospects of flavonoids are promising. Future research will provide further insights into the targeted epigenetic dimensional adjustment of flavonoids. More clinical trials are required to elucidate effects on cancer and the feasibility of clinical administration of flavonoids.

AUTHOR CONTRIBUTIONS

The research project was designed by WJ, TX, CL, and CS. WJ collected the literature, drew structures. WJ and TX wrote the

manuscript and checked the Tables and Figures as well as grammar of manuscript. CL, JL and WZ revised the manuscript. CS and WJ participated in and helped draft the manuscript. All authors contributed to the article and approved the submitted version.

FUNDING

This work was supported by the National Natural Science Foundation of China (grant number 81973677).

REFERENCES

1. Xu Z, Zeng S, Gong Z, Yan Y. Exosome-Based Immunotherapy: A Promising Approach for Cancer Treatment. *Mol Cancer* (2020) 19:160. doi: 10.1186/s12943-020-01278-3
2. Rashkin SR, Graff RE, Kachuri L, Thai KK, Alexeeff SE, Blatchins MA, et al. Pan-Cancer Study Detects Genetic Risk Variants and Shared Genetic Basis in Two Large Cohorts. *Nat Commun* (2020) 11:4423. doi: 10.1038/s41467-020-18246-6
3. Jones P, Ohtani H, Chakravarthy A, De Carvalho D. Epigenetic Therapy in Immune-Oncology. *Nat Rev Cancer* (2019) 19:151–61. doi: 10.1038/s41568-019-0109-9
4. Wooten M, Snedeker J, Nizami Z, Yang X, Ranjan R, Urban E, et al. Asymmetric Histone Inheritance Via Strand-Specific Incorporation and Biased Replication Fork Movement. *Nat Struct Mol Biol* (2019) 26:732–43. doi: 10.1038/s41594-019-0269-z
5. Abdelsamed HA, Zebley CC, Nguyen H, Rutishauser RL, Fan Y, Ghoneim HE, et al. Beta Cell-Specific CD8(+) T Cells Maintain Stem Cell Memory-Associated Epigenetic Programs During Type 1 Diabetes. *Nat Immunol* (2020) 21:578–87. doi: 10.1038/s41590-020-0633-5
6. Robertson KD, Wolffe AP. DNA Methylation in Health and Disease. *Nat Rev Genet* (2000) 1:11–9. doi: 10.1038/35049533
7. Hinohara K, Polyak K. Intratumoral Heterogeneity: More Than Just Mutations. *Trends Cell Biol* (2019) 29:569–79. doi: 10.1016/j.tcb.2019.03.003
8. Tidwell TR, Soreide K, Hagland HR. Aging, Metabolism, and Cancer Development: From Peto's Paradox to the Warburg Effect. *Aging Dis* (2017) 8:662–76. doi: 10.14336/AD.2017.0713
9. Tiffon C. The Impact of Nutrition and Environmental Epigenetics on Human Health and Disease. *Int J Mol Sci* (2018) 19. doi: 10.3390/ijms19113425
10. Rizzo HE, Escaname EN, Alana NB, Lavender E, Gelfond J, Fernandez R, et al. Maternal Diabetes and Obesity Influence the Fetal Epigenome in a Largely Hispanic Population. *Clin Epigenet* (2020) 12:34. doi: 10.1186/s13148-020-0824-9
11. Cheng Z, Zheng L, Almeida FA. Epigenetic Reprogramming in Metabolic Disorders: Nutritional Factors and Beyond. *J Nutr Biochem* (2018) 54:1–10. doi: 10.1016/j.jnutbio.2017.10.004
12. Bondonno NP, Dalgaard F, Kyro C, Murray K, Bondonno CP, Lewis JR, et al. Flavonoid Intake is Associated With Lower Mortality in the Danish Diet Cancer and Health Cohort. *Nat Commun* (2019) 10:3651. doi: 10.1038/s41467-019-11622-x
13. Shanmugam K, Ravindran S, Kurian GA, Rajesh M. Fisetin Confers Cardioprotection Against Myocardial Ischemia Reperfusion Injury by Suppressing Mitochondrial Oxidative Stress and Mitochondrial Dysfunction and Inhibiting Glycogen Synthase Kinase 3beta Activity. *Oxid Med Cell Longev* (2018) 2018:9173436. doi: 10.1155/2018/9173436
14. Kim TW, Lee SY, Kim M, Cheon C, Ko SG. Kaempferol Induces Autophagic Cell Death Via IRE1-JNK-CHOP Pathway and Inhibition of G9a in Gastric Cancer Cells. *Cell Death Dis* (2018) 9:875. doi: 10.1038/s41419-018-0930-1
15. Sheng J, Shi W, Guo H, Long W, Wang Y, Qi J, et al. The Inhibitory Effect of (-)-Epigallocatechin-3-Gallate on Breast Cancer Progression Via Reducing SCUBE2 Methylation and DNMT Activity. *Molecules* (2019) 24. doi: 10.3390/molecules24162899
16. Deb G, Shankar E, Thakur VS, Ponsky LE, Bodner DR, Fu P, et al. Green Tea-Induced Epigenetic Reactivation of Tissue Inhibitor of Matrix Metalloproteinase-3 Suppresses Prostate Cancer Progression Through Histone-Modifying Enzymes. *Mol Carcinog* (2019) 58:1194–207. doi: 10.1002/mc.23003
17. Zhao Y, Chen X, Jiang J, Wan X, Wang Y, Xu P. Epigallocatechin Gallate Reverses Gastric Cancer by Regulating the Long Noncoding RNA LINC00511/miR-29b/KDM2A Axis. *Biochim Biophys Acta Mol Basis Dis* (2020) 1866:165856. doi: 10.1016/j.bbadis.2020.165856
18. Bates SE. Epigenetic Therapies for Cancer. *N Engl J Med* (2020) 383:650–63. doi: 10.1056/NEJMra1805035
19. Jones PA, Issa JP, Baylin S. Targeting the Cancer Epigenome for Therapy. *Nat Rev Genet* (2016) 17:630–41. doi: 10.1038/nrg.2016.93
20. Feng X, Zhang Y, Zhang C, Lai X, Zhang Y, Wu J, et al. Nanomaterial-Mediated Autophagy: Coexisting Hazard and Health Benefits in Biomedicine. *Part Fibre Toxicol* (2020) 17:53. doi: 10.1186/s12989-020-00372-0
21. Jiang X, Liu Y, Ma L, Ji R, Qu Y, Xin Y, et al. Chemopreventive Activity of Sulforaphane. *Drug Des Devel Ther* (2018) 12:2905–13. doi: 10.2147/DDDT.S100534
22. Huh I, Wu X, Park T, Yi SV. Detecting Differential DNA Methylation From Sequencing of Bisulfite Converted DNA of Diverse Species. *Brief Bioinform* (2019) 20:33–46. doi: 10.1093/bib/bbx077
23. Peng Y, Shui L, Xie J, Liu S. Development and Validation of a Novel 15-CpG-Based Signature for Predicting Prognosis in Triple-Negative Breast Cancer. *J Cell Mol Med* (2020) 24:9378–87. doi: 10.1111/jcmm.15588
24. Zhang Y, Fukui N, Yahata M, Katsuragawa Y, Tashiro T, Ikegawa S, et al. Identification of DNA Methylation Changes Associated With Disease Progression in Subchondral Bone With Site-Matched Cartilage in Knee Osteoarthritis. *Sci Rep* (2016) 6:34460. doi: 10.1038/srep34460
25. Liu D, Meng X, Wu D, Qiu Z, Luo H. A Natural Isoquinoline Alkaloid With Antitumor Activity: Studies of the Biological Activities of Berberine. *Front Pharmacol* (2019) 10:9. doi: 10.3389/fphar.2019.00009
26. Sumei S, Xiangyun K, Fenrong C, Xueguang S, Sijun H, Bin B, et al. Hypermethylation of DHRS3 as a Novel Tumor Suppressor Involved in Tumor Growth and Prognosis in Gastric Cancer. *Front Cell Dev Biol* (2021) 9:624871. doi: 10.3389/fcell.2021.624871
27. Fu S, Wu H, Zhang H, Lian CG, Lu Q. DNA Methylation/Hydroxymethylation in Melanoma. *Oncotarget* (2017) 8:78163–73. doi: 10.18632/oncotarget.18293
28. Smith J, Sen S, Weeks RJ, Eccles MR, Chatterjee A. Promoter DNA Hypermethylation and Paradoxical Gene Activation. *Trends Cancer* (2020) 6:392–406. doi: 10.1016/j.trecan.2020.02.007
29. Koch A, Joosten SC, Feng Z, de Ruijter TC, Draht MX, Melotte V, et al. Analysis of DNA Methylation in Cancer: Location Revisited. *Nat Rev Clin Oncol* (2018) 15:459–66. doi: 10.1038/s41571-018-0004-4
30. Tzelepi V, Logotheti S, Efstathiou E, Troncoso P, Aparicio A, Sakellakis M, et al. Epigenetics and Prostate Cancer: Defining the Timing of DNA Methyltransferase Deregulation During Prostate Cancer Progression. *Pathology* (2020) 52:218–27. doi: 10.1016/j.pathol.2019.10.006
31. Zhang H, Lang Z, Zhu JK. Dynamics and Function of DNA Methylation in Plants. *Nat Rev Mol Cell Biol* (2018) 19:489–506. doi: 10.1038/s41580-018-0016-z
32. Reichard JF, Puga A. Effects of Arsenic Exposure on DNA Methylation and Epigenetic Gene Regulation. *Epigenomics* (2010) 2:87–104. doi: 10.2217/epi.09.45
33. Voisin S, Eynon N, Yan X, Bishop DJ. Exercise Training and DNA Methylation in Humans. *Acta Physiol (Oxf)* (2015) 213:39–59. doi: 10.1111/apha.12414
34. Ferreira HJ, Esteller M. CpG Islands in Cancer: Heads, Tails, and Sides. *Methods Mol Biol* (2018) 1766:49–80. doi: 10.1007/978-1-4939-7768-0_4
35. Esteller M. Cancer Epigenomics: DNA Methylomes and Histone-Modification Maps. *Nat Rev Genet* (2007) 8:286–98. doi: 10.1038/nrg2005
36. Lawrence M, Daujat S, Schneider R. Lateral Thinking: How Histone Modifications Regulate Gene Expression. *Trends Genet* (2016) 32:42–56. doi: 10.1016/j.tig.2015.10.007
37. Aebersold R, Mann M. Mass-Spectrometric Exploration of Proteome Structure and Function. *Nature* (2016) 537:347–55. doi: 10.1038/nature19949

38. Stoll S, Wang C, Qiu H. DNA Methylation and Histone Modification in Hypertension. *Int J Mol Sci* (2018) 19. doi: 10.3390/ijms19041174
39. Wysocka J, Milne TA, Allis CD. Taking LSD 1 to a New High. *Cell* (2005) 122:654–8. doi: 10.1016/j.cell.2005.08.022
40. Grunstein M. Histone Acetylation in Chromatin Structure and Transcription. *Nature* (1997) 389:349–52. doi: 10.1038/38664
41. Eckschlager T, Plch J, Stiborova M, Hrabeta J. Histone Deacetylase Inhibitors as Anticancer Drugs. *Int J Mol Sci* (2017) 18. doi: 10.3390/ijms18071414
42. Fozouni P, Ott M. How Cells Hush a Viral Invader. *Nature* (2018) 564:193–4. doi: 10.1038/d41586-018-07493-9
43. Salek Farrokhi A, Mohammadlou M, Abdollahi M, Eslami M, Yousefi B. Histone Deacetylase Modifications by Probiotics in Colorectal Cancer. *J Gastrointest Cancer* (2020) 51:754–64. doi: 10.1007/s12029-019-00338-2
44. Tong Q, Weaver MR, Kosmacek EA, O'Connor BP, Harmacek L, Venkataraman S, et al. MnTE-2-Pyp Reduces Prostate Cancer Growth and Metastasis by Suppressing P300 Activity and P300/HIF-1/CREB Binding to the Promoter Region of the PAI-1 Gene. *Free Radic Biol Med* (2016) 94:185–94. doi: 10.1016/j.freeradbiomed.2016.02.036
45. Chen K, Zhang F, Ding J, Liang Y, Zhan Z, Zhan Y, et al. Histone Methyltransferase SETDB1 Promotes the Progression of Colorectal Cancer by Inhibiting the Expression of TP53. *J Cancer* (2017) 8:3318–30. doi: 10.7150/jca.20482
46. Chen R, Zhang M, Zhou Y, Guo W, Yi M, Zhang Z, et al. The Application of Histone Deacetylases Inhibitors in Glioblastoma. *J Exp Clin Cancer Res* (2020) 39:138. doi: 10.1186/s13046-020-01643-6
47. Thiagarajan D, Vedantham S, Ananthakrishnan R, Schmidt AM, Ramasamy R. Mechanisms of Transcription Factor Acetylation and Consequences in Hearts. *Biochim Biophys Acta* (2016) 1862:2221–31. doi: 10.1016/j.bbadis.2016.08.011
48. Keppler BR, Archer TK. Chromatin-Modifying Enzymes as Therapeutic Targets–Part 1. *Expert Opin Ther Targets* (2008) 12:1301–12. doi: 10.1517/14728222.12.10.1301
49. Falkenberg KJ, Johnstone RW. Histone Deacetylases and Their Inhibitors in Cancer, Neurological Diseases and Immune Disorders. *Nat Rev Drug Discov* (2014) 13:673–91. doi: 10.1038/nrd4360
50. Trisciuoglio D, Di Martile M, Del Bufalo D. Emerging Role of Histone Acetyltransferase in Stem Cells and Cancer. *Stem Cells Int* (2018) 2018:8908751. doi: 10.1155/2018/8908751
51. Tie J, Zhang X, Fan D. Epigenetic Roles in the Malignant Transformation of Gastric Mucosal Cells. *Cell Mol Life Sci* (2016) 73:4599–610. doi: 10.1007/s00018-016-2308-9
52. Fu DG. Epigenetic Alterations in Gastric Cancer (Review). *Mol Med Rep* (2015) 12:3223–30. doi: 10.3892/mmr.2015.3816
53. Satomura S, Sakata Y, Omichi K, Ikenaka T. Alpha-Amylase Assay With Use of a Benzyl Derivative of P-Nitrophenyl Alpha-Maltopentaoside, BG5P. *Clin Chim Acta* (1988) 174:315–23. doi: 10.1016/0009-8981(88)90058-7
54. Kim S, Kaang BK. Epigenetic Regulation and Chromatin Remodeling in Learning and Memory. *Exp Mol Med* (2017) 49:e281. doi: 10.1038/emm.2016.140
55. Ono R, Taki T, Taketani T, Taniwaki M, Kobayashi H, Hayashi YLCX. Leukemia-Associated Protein With a CXXC Domain, is Fused to MLL in Acute Myeloid Leukemia With Trilineage Dysplasia Having t()(q22;q23). *Cancer Res* (2002) 62:4075–80. doi: 10.1016/S0165-4608(02)00534-4
56. Shi Y, Lan F, Matson C, Mulligan P, Whetstine JR, Cole PA, et al. Histone Demethylation Mediated by the Nuclear Amine Oxidase Homolog LSD1. *Cell* (2004) 119:941–53. doi: 10.1016/j.cell.2004.12.012
57. Chen X, Liang H, Zhang J, Zen K, Zhang CY. Secreted MicroRNAs: A New Form of Intercellular Communication. *Trends Cell Biol* (2012) 22:125–32. doi: 10.1016/j.tcb.2011.12.001
58. Mohr AM, Mott JL. Overview of microRNA Biology. *Semin Liver Dis* (2015) 35:3–11. doi: 10.1055/s-0034-1397344
59. Youn SW, Park KK. Small-Nucleic-Acid-Based Therapeutic Strategy Targeting the Transcription Factors Regulating the Vascular Inflammation, Remodeling and Fibrosis in Atherosclerosis. *Int J Mol Sci* (2015) 16:11804–33. doi: 10.3390/ijms160511804
60. Cantini L, Bertoli G, Cava C, Dubois T, Zinovyev A, Caselle M, et al. Identification of Microrna Clusters Cooperatively Acting on Epithelial to Mesenchymal Transition in Triple Negative Breast Cancer. *Nucleic Acids Res* (2019) 47:2205–15. doi: 10.1093/nar/gkz016
61. Elhamamsy AR, El Sharkawy MS, Zanaty AF, Mahrous MA, Mohamed AE, Abushaaban EA. Circulating miR-92a, miR-143 and miR-342 in Plasma are Novel Potential Biomarkers for Acute Myeloid Leukemia. *Int J Mol Cell Med* (2017) 6:77–86. doi: 10.22088/acadpub.BUMS.6.2.2
62. Toyota M, Suzuki H, Sasaki Y, Maruyama R, Imai K, Shinomura Y, et al. Epigenetic Silencing of microRNA-34b/c and B-cell Translocation Gene 4 is Associated With CpG Island Methylation in Colorectal Cancer. *Cancer Res* (2008) 68:4123–32. doi: 10.1158/0008-5472.CAN-08-0325
63. Yang H, Lan P, Hou Z, Guan Y, Zhang J, Xu W, et al. Histone Deacetylase Inhibitor SAHA Epigenetically Regulates miR-17-92 Cluster and MCM7 to Upregulate Mica Expression in Hepatoma. *Br J Cancer* (2015) 112:112–21. doi: 10.1038/bjc.2014.547
64. Xuan P, Jia L, Zhang T, Sheng N, Li X, Li J. LDAPred: A Method Based on Information Flow Propagation and a Convolutional Neural Network for the Prediction of Disease-Associated Lncrnas. *Int J Mol Sci* (2019) 20. doi: 10.3390/ijms20184458
65. Li Z, Lu M, Zhou Y, Xu L, Jiang Y, Liu Y, et al. Role of Long Non-Coding RNAs in the Chemoresistance of Gastric Cancer: A Systematic Review. *Onco Targets Ther* (2021) 14:503–18. doi: 10.2147/OTT.S294378
66. Chen Z, Zhang K, Qiu W, Luo Y, Pan Y, Li J, et al. Genome-Wide Identification of Long Noncoding RNAs and Their Competing Endogenous RNA Networks Involved in the Odontogenic Differentiation of Human Dental Pulp Stem Cells. *Stem Cell Res Ther* (2020) 11:114. doi: 10.1186/s13287-020-01622-w
67. Yoshioka H, Yoshiko Y. The Roles of Long Non-Protein-Coding RNAs in Osteo-Adipogenic Lineage Commitment. *Int J Mol Sci* (2017) 18. doi: 10.3390/ijms18061236
68. Xu X, Zhao Z, Li G. The Therapeutic Potential of MicroRNAs in Atrial Fibrillation. *Mediators Inflamm* (2020) 2020:3053520. doi: 10.1155/2020/3053520
69. Liao T, Qu N, Shi RL, Guo K, Ma B, Cao YM, et al. BRAF-Activated LncRNA Functions as a Tumor Suppressor in Papillary Thyroid Cancer. *Oncotarget* (2017) 8:238–47. doi: 10.18632/oncotarget.10825
70. Kussmann M, Morine MJ, Hager J, Sonderegger B, Kaput J. Perspective: A Systems Approach to Diabetes Research. *Front Genet* (2013) 4:205. doi: 10.3389/fgene.2013.00205
71. Link A, Balaguer F, Goel A. Cancer Chemoprevention by Dietary Polyphenols: Promising Role for Epigenetics. *Biochem Pharmacol* (2010) 80:1771–92. doi: 10.1016/j.bcp.2010.06.036
72. Vue B, Zhang S, Chen QH. Flavonoids With Therapeutic Potential in Prostate Cancer. *Anticancer Agents Med Chem* (2016) 16:1205–29. doi: 10.2174/1871520615666151008122622
73. Kopustinskiene DM, Jakstas V, Savickas A, Bernatoniene J. Flavonoids as Anticancer Agents. *Nutrients* (2020) 12. doi: 10.3390/nu12020457
74. Wen L, Jiang Y, Yang J, Zhao Y, Tian M, Yang B. Structure, Bioactivity, and Synthesis of Methylated Flavonoids. *Ann N Y Acad Sci* (2017) 1398:120–9. doi: 10.1111/nyas.13350
75. Liskova A, Samec M, Koklesova L, Samuel SM, Zhai K, Al-Ishaq RK, et al. Flavonoids Against the SARS-CoV-2 Induced Inflammatory Storm. *BioMed Pharmacother* (2021) 138:111430. doi: 10.1016/j.biopha.2021.111430
76. Gibellini L, Pinti M, Nasi M, Montagna JP, De Biasi S, Roat E, et al. Quercetin and Cancer Chemoprevention. *Evid Based Complement Alternat Med* (2011) 2011:591356. doi: 10.1093/ecam/neq053
77. Ayoobi F, Shamsizadeh A, Fatemi I, Vakilian A, Allahtavakoli M, Hassanshahi G, et al. Bio-Effectiveness of the Main Flavonoids of Achillea Millefolium in the Pathophysiology of Neurodegenerative Disorders- A Review. *Iran J Basic Med Sci* (2017) 20:604–12. doi: 10.22038/IJBMS.2017.8827
78. Fan LL, Zhang SS, Yao MX, Jiang Y, Su M, Wang XL, et al. [Changes in Chemical Compositions of Chrysanthemi Flos After Frying and Protective Effects on CCl_4-induced Acute Liver Injury in Mice]. *Zhongguo Zhong Yao Za Zhi* (2020) 45:3144–54. doi: 10.19540/j.cnki.cjcmm.20200424.303
79. Zheng G, Yang X, Chen B, Chao Y, Hu P, Cai Y, et al. Identification and Determination of Chemical Constituents of Citrus Reticulata Semen Through Ultra High Performance Liquid Chromatography Combined With Q Exactive Orbitrap Tandem Mass Spectrometry. *J Sep Sci* (2020) 43:438–51. doi: 10.1002/jssc.201900641

80. Feng Y, Dunshea FR, Suleria HAR. LC-ESI-QTOF/MS Characterization of Bioactive Compounds From Black Spices and Their Potential Antioxidant Activities. *J Food Sci Technol* (2020) 57:4671–87. doi: 10.1007/s13197-020-04504-4
81. Kurek-Gorecka A, Gorecki M, Rzepecka-Stojko A, Balwierz R, Stojko J. Bee Products in Dermatology and Skin Care. *Molecules* (2020) 25:556. doi: 10.3390/molecules25030556
82. Chan KKL, Siu MKY, Jiang YX, Wang JJ, Leung THY, Ngan HYS. Estrogen Receptor Modulators Genistein, Daidzein and ERB-041 Inhibit Cell Migration, Invasion, Proliferation and Sphere Formation Via Modulation of FAK and PI3K/AKT Signaling in Ovarian Cancer. *Cancer Cell Int* (2018) 18:65. doi: 10.1186/s12935-018-0559-2
83. Ru J, Li P, Wang J, Zhou W, Li B, Huang C, et al. TCMSP: A Database of Systems Pharmacology for Drug Discovery From Herbal Medicines. *J Cheminform* (2014) 6:13. doi: 10.1186/1758-2946-6-13
84. Dong JY, Kimura T, Ikehara S, Cui M, Kawanishi Y, Kimura T, et al. Soy Consumption and Incidence of Gestational Diabetes Mellitus: The Japan Environment and Children's Study. *Eur J Nutr* (2021) 60:897–904. doi: 10.1007/s00394-020-02294-1
85. Nugroho A, Kim EJ, Choi JS, Park HJ. Simultaneous Quantification and Peroxynitrite-Scavenging Activities of Flavonoids in Polygonum Aviculare L. Herb. *J Pharm BioMed Anal* (2014) 89:93–8. doi: 10.1016/j.jpba.2013.10.037
86. Wang W, Lin P, Ma L, Xu K, Lin X. Separation and Determination of Flavonoids in Three Traditional Chinese Medicines by Capillary Electrophoresis With Amperometric Detection. *J Sep Sci* (2016) 39:1357–62. doi: 10.1002/jssc.201501287
87. Huang G, Zeng Y, Wei L, Yao Y, Dai J, Liu G, et al. Comparative Transcriptome Analysis of Mulberry Reveals Anthocyanin Biosynthesis Mechanisms in Black (Morus Atropurpurea Roxb.) and White (Morus Alba L.) Fruit Genotypes. *BMC Plant Biol* (2020) 20:279. doi: 10.1186/s12870-020-02486-1
88. Jia Q, Zhang S, Zhang H, Yang X, Cui X, Su Z, et al. A Comparative Study on Polyphenolic Composition of Berries From the Tibetan Plateau by UPLC-Q-Orbitrap Ms System. *Chem Biodivers* (2020) 17:e2000033. doi: 10.1002/cbdv.202000033
89. Beck S, Stengel J. Mass Spectrometric Imaging of Flavonoid Glycosides and Biflavonoids in Ginkgo Biloba L. *Phytochemistry* (2016) 130:201–6. doi: 10.1016/j.phytochem.2016.05.005
90. Ditano-Vazquez P, Torres-Pena JD, Galeano-Valle F, Perez-Caballero AI, Demelo-Rodriguez P, Lopez-Miranda J, et al. The Fluid Aspect of the Mediterranean Diet in the Prevention and Management of Cardiovascular Disease and Diabetes: The Role of Polyphenol Content in Moderate Consumption of Wine and Olive Oil. *Nutrients* (2019) 11:2833. doi: 10.3390/nu11112833
91. Yang X, Ma Y, Li L. Beta-Glucosidase From Tartary Buckwheat Immobilization on Bifunctionalized Nano-Magnetic Iron Oxide and its Application in Tea Soup for Aroma and Flavonoid Aglycone Enhancement. *Food Funct* (2019) 10:5461–72. doi: 10.1039/c9fo00283a
92. Rassi CM, Lieberherr M, Chaumaz G, Pointillart A, Cournot G. Modulation of Osteoclastogenesis in Porcine Bone Marrow Cultures by Quercetin and Rutin. *Cell Tissue Res* (2005) 319:383–93. doi: 10.1007/s00441-004-1053-9
93. Duan Y, Eduardo Melo Santiago F, Rodrigues Dos Reis A, de Figueiredo MA, Zhou S, Thannhauser TW, et al. Genotypic Variation of Flavonols and Antioxidant Capacity in Broccoli. *Food Chem* (2021) 338:127997. doi: 10.1016/j.foodchem.2020.127997
94. Shin KC, Nam HK, Oh DK. Hydrolysis of Flavanone Glycosides by Beta-Glucosidase From Pyrococcus Furiosus and its Application to the Production of Flavanone Aglycones From Citrus Extracts. *J Agric Food Chem* (2013) 61:11532–40. doi: 10.1021/jf403332e
95. Justesen U, Knuthsen P, Leth T. Quantitative Analysis of Flavonols, Flavones, and Flavanones in Fruits, Vegetables and Beverages by High-Performance Liquid Chromatography With Photo-Diode Array and Mass Spectrometric Detection. *J Chromatogr A* (1998) 799:101–10. doi: 10.1016/s0021-9673(97)01061-3
96. Mouly PP, Arzouyan CR, Gaydou EM, Estienne JM. Differentiation of Citrus Juices by Factorial Discriminant Analysis Using Liquid Chromatography of Flavones Glycosides. *J Agric Food Chem* (1994) 42:70–9. doi: 10.1021/jf00037a011
97. Hollman PC, Arts IC. Flavonols, Flavones and Flavanols – Nature, Occurrence and Dietary Burden. *J Sci Food Agric* (2000) 80:1081–93. doi: 10.1002/(SICI)1097-0010(20000515)80:7<1081::AID-JSFA566>3.0.CO;2-G
98. Lee YM, Yoon Y, Yoon H, Park HM, Song S, Yeum KJ. Dietary Anthocyanins Against Obesity and Inflammation. *Nutrients* (2017) 9:1089. doi: 10.3390/nu9101089
99. Kozlowska A, Szostak-Wegierek D. Flavonoids–Food Sources and Health Benefits. *Rocz Panstw Zakl Hig* (2014) 65:79–85.
100. Kumar S, Pandey AK. Chemistry and Biological Activities of Flavonoids: An Overview. *ScientificWorldJournal* (2013) 2013:162750. doi: 10.1155/2013/162750
101. Santini A, Novellino E. Nutraceuticals in Hypercholesterolaemia: An Overview. *Br J Pharmacol* (2017) 174:1450–63. doi: 10.1111/bph.13636
102. Georgiev V, Ananga A, Tsolova V. Recent Advances and Uses of Grape Flavonoids as Nutraceuticals. *Nutrients* (2014) 6:391–415. doi: 10.3390/nu6010391
103. Jager AK, Saaby L. Flavonoids and the CNS. *Molecules* (2011) 16:1471–85. doi: 10.3390/molecules16021471
104. Imran M, Salehi B, Sharifi-Rad J, Aslam Gondal T, Saeed F, Imran A, et al. Kaempferol: A Key Emphasis to Its Anticancer Potential. *Molecules* (2019) 24. doi: 10.3390/molecules24122277
105. Devi KP, Malar DS, Nabavi SF, Sureda A, Xiao J, Nabavi SM, et al. Kaempferol and Inflammation: From Chemistry to Medicine. *Pharmacol Res* (2015) 99:1–10. doi: 10.1016/j.phrs.2015.05.002
106. Calderon-Montano JM, Burgos-Moron E, Perez-Guerrero C, Lopez-Lazaro M. A Review on the Dietary Flavonoid Kaempferol. *Mini Rev Med Chem* (2011) 11:298–344. doi: 10.2174/138955711795305335
107. Gates MA, Tworoger SS, Hecht JL, De Vivo I, Rosner B, Hankinson SE. A Prospective Study of Dietary Flavonoid Intake and Incidence of Epithelial Ovarian Cancer. *Int J Cancer* (2007) 121:2225–32. doi: 10.1002/ijc.22790
108. Nothlings U, Murphy SP, Wilkens LR, Henderson BE, Kolonel LN. Flavonols and Pancreatic Cancer Risk: The Multiethnic Cohort Study. *Am J Epidemiol* (2007) 166:924–31. doi: 10.1093/aje/kwm172
109. Berger A, Venturelli S, Kallnischkies M, Bocker A, Busch C, Weiland T, et al. Kaempferol, a New Nutrition-Derived Pan-Inhibitor of Human Histone Deacetylases. *J Nutr Biochem* (2013) 24:977–85. doi: 10.1016/j.jnutbio.2012.07.001
110. Lu L, Wang Y, Ou R, Feng Q, Ji L, Zheng H, et al. DACT2 Epigenetic Stimulator Exerts Dual Efficacy for Colorectal Cancer Prevention and Treatment. *Pharmacol Res* (2018) 129:318–28. doi: 10.1016/j.phrs.2017.11.032
111. Wang L, Wu H, Yang F, Dong W. The Protective Effects of Myricetin Against Cardiovascular Disease. *J Nutr Sci Vitaminol (Tokyo)* (2019) 65:470–6. doi: 10.3177/jnsv.65.470
112. Xie Y, Wang Y, Xiang W, Wang Q, Cao Y. Molecular Mechanisms of the Action of Myricetin in Cancer. *Mini Rev Med Chem* (2020) 20:123–33. doi: 10.2174/1389557519666191018112756
113. Jiang M, Zhu M, Wang L, Yu S. Anti-Tumor Effects and Associated Molecular Mechanisms of Myricetin. *BioMed Pharmacother* (2019) 120:109506. doi: 10.1016/j.biopha.2019.109506
114. Semwal DK, Semwal RB, Combrinck S, Viljoen A. Myricetin: A Dietary Molecule With Diverse Biological Activities. *Nutrients* (2016) 8:90. doi: 10.3390/nu8020090
115. Lee WJ, Shim JY, Zhu BT. Mechanisms for the Inhibition of DNA Methyltransferases by Tea Catechins and Bioflavonoids. *Mol Pharmacol* (2005) 68:1018–30. doi: 10.1124/mol.104.008367
116. Gurunathan S, Qasim M, Park C, Yoo H, Choi DY, Song H, et al. Cytotoxicity and Transcriptomic Analysis of Silver Nanoparticles in Mouse Embryonic Fibroblast Cells. *Int J Mol Sci* (2018) 19. doi: 10.3390/ijms19113618
117. Basu Mallik S, Pai A, Shenoy RR, Jayashree BS. Novel Flavonol Analogues as Potential Inhibitors of JMJD3 Histone Demethylase-a Study Based on Molecular Modelling. *J Mol Graph Model* (2017) 72:81–7. doi: 10.1016/j.jmgm.2016.12.002
118. Hong KS, Park JI, Kim MJ, Kim HB, Lee JW, Dao TT, et al. Involvement of SIRT1 in Hypoxic Down-Regulation of c-Myc and Beta-Catenin and Hypoxic Preconditioning Effect of Polyphenols. *Toxicol Appl Pharmacol* (2012) 259:210–8. doi: 10.1016/j.taap.2011.12.025
119. Andres S, Pevny S, Ziegenhagen R, Bakhiya N, Schafer B, Hirsch-Ernst KI, et al. Safety Aspects of the Use of Quercetin as a Dietary Supplement. *Mol Nutr Food Res* (2018) 62. doi: 10.1002/mnfr.201700447

120. Marunaka Y, Marunaka R, Sun H, Yamamoto T, Kanamura N, Inui T, et al. Actions of Quercetin, a Polyphenol, on Blood Pressure. *Molecules* (2017) 22. doi: 10.3390/molecules22020209
121. Patel RV, Mistry BM, Shinde SK, Syed R, Singh V, Shin HS. Therapeutic Potential of Quercetin as a Cardiovascular Agent. *Eur J Med Chem* (2018) 155:889–904. doi: 10.1016/j.ejmech.2018.06.053
122. Sharma V, Kumar L, Mohanty SK, Maikhuri JP, Rajender S, Gupta G. Sensitization of Androgen Refractory Prostate Cancer Cells to Anti-Androgens Through Re-Expression of Epigenetically Repressed Androgen Receptor - Synergistic Action of Quercetin and Curcumin. *Mol Cell Endocrinol* (2016) 431:12–23. doi: 10.1016/j.mce.2016.04.024
123. Zheng NG, Wang JL, Yang SL, Wu JL. Aberrant Epigenetic Alteration in Eca9706 Cells Modulated by Nanoliposomal Quercetin Combined With Butyrate Mediated Via epigenetic-NF-kappaB Signaling. *Asian Pac J Cancer Prev* (2014) 15:4539–43. doi: 10.7314/apjcp.2014.15.11.4539
124. Wang P, Phan T, Gordon D, Chung S, Henning SM, Vadgama JV. Arctigenin in Combination With Quercetin Synergistically Enhances the Antiproliferative Effect in Prostate Cancer Cells. *Mol Nutr Food Res* (2015) 59:250–61. doi: 10.1002/mnfr.201400558
125. Pham TND, Stempel S, Shields MA, Spaulding C, Kumar K, Bentrem DJ, et al. Quercetin Enhances the Anti-Tumor Effects of BET Inhibitors by Suppressing hnRNPA1. *Int J Mol Sci* (2019) 20. doi: 10.3390/ijms20174293
126. Pratheeshkumar P, Son YO, Divya SP, Wang L, Turcios L, Roy RV, et al. Quercetin Inhibits Cr(VI)-Induced Malignant Cell Transformation by Targeting miR-21-PDCD4 Signaling Pathway. *Oncotarget* (2017) 8:52118–31. doi: 10.18632/oncotarget.10130
127. Nwaeburu CC, Abukiwan A, Zhao Z, Herr I. Quercetin-Induced miR-200b-3p Regulates the Mode of Self-Renewing Divisions in Pancreatic Cancer. *Mol Cancer* (2017) 16:23. doi: 10.1186/s12943-017-0589-8
128. Lou G, Liu Y, Wu S, Xue J, Yang F, Fu H, et al. The p53/miR-34a/SIRT1 Positive Feedback Loop in Quercetin-Induced Apoptosis. *Cell Physiol Biochem* (2015) 35:2192–202. doi: 10.1159/000374024
129. Tao SF, He HF, Chen Q. Quercetin Inhibits Proliferation and Invasion Acts by Up-Regulating miR-146a in Human Breast Cancer Cells. *Mol Cell Biochem* (2015) 402:93–100. doi: 10.1007/s11010-014-2317-7
130. Zhang X, Guo Q, Chen J, Chen Z. Quercetin Enhances Cisplatin Sensitivity of Human Osteosarcoma Cells by Modulating microRNA-217-KRAS Axis. *Mol Cells* (2015) 38:638–42. doi: 10.14348/molcells.2015.0037
131. Guo J, Feng Z, Huang Z, Wang H, Lu W. MicroRNA-217 Functions as a Tumour Suppressor Gene and Correlates With Cell Resistance to Cisplatin in Lung Cancer. *Mol Cells* (2014) 37:664–71. doi: 10.14348/molcells.2014.0121
132. Zheng Y, Zhang R, Shi W, Li L, Liu H, Chen Z, et al. Metabolism and Pharmacological Activities of the Natural Health-Benefiting Compound Diosmin. *Food Funct* (2020) 11:8472–92. doi: 10.1039/d0fo01598a
133. Klimek-Szczykutowicz M, Szopa A, Ekiert H. Citrus Limon (Lemon) Phenomenon-A Review of the Chemistry, Pharmacological Properties, Applications in the Modern Pharmaceutical, Food, and Cosmetics Industries, and Biotechnological Studies. *Plants (Basel)* (2020) 9. doi: 10.3390/plants9010119
134. Lewinska A, Siwak J, Rzeszutek I, Wnuk M. Diosmin Induces Genotoxicity and Apoptosis in DU145 Prostate Cancer Cell Line. *Toxicol In Vitro* (2015) 29:417–25. doi: 10.1016/j.tiv.2014.12.005
135. Kasiri N, Rahmati M, Ahmadi L, Eskandari N. The Significant Impact of Apigenin on Different Aspects of Autoimmune Disease. *Inflammopharmacology* (2018) 26:1359–73. doi: 10.1007/s10787-018-0531-8
136. Salehi B, Venditti A, Sharifi-Rad M, Kregiel D, Sharifi-Rad J, Durazzo A, et al. The Therapeutic Potential of Apigenin. *Int J Mol Sci* (2019) 20. doi: 10.3390/ijms20061305
137. Wang M, Firrman J, Liu L, Yam K. A Review on Flavonoid Apigenin: Dietary Intake, ADME, Antimicrobial Effects, and Interactions With Human Gut Microbiota. *BioMed Res Int* (2019) 2019:7010467. doi: 10.1155/2019/7010467
138. Kowalczyk A, Bodalska A, Miranowicz M, Karlowicz-Bodalska K. Insights Into Novel Anticancer Applications for Apigenin. *Adv Clin Exp Med* (2017) 26:1143–6. doi: 10.17219/acem/41978
139. Tang D, Chen K, Huang L, Li J. Pharmacokinetic Properties and Drug Interactions of Apigenin, a Natural Flavone. *Expert Opin Drug Metab Toxicol* (2017) 13:323–30. doi: 10.1080/17425255.2017.1251903
140. Nabavi SM, Habtemariam S, Daglia M, Nabavi SF. Apigenin and Breast Cancers: From Chemistry to Medicine. *Anticancer Agents Med Chem* (2015) 15:728–35. doi: 10.2174/1871520615666150304120643
141. Tseng TH, Chien MH, Lin WL, Wen YC, Chow JM, Chen CK, et al. Inhibition of MDA-MB-231 Breast Cancer Cell Proliferation and Tumor Growth by Apigenin Through Induction of G2/M Arrest and Histone H3 Acetylation-Mediated p21(WAF1/CIP1) Expression. *Environ Toxicol* (2017) 32:434–44. doi: 10.1002/tox.22247
142. Paredes-Gonzalez X, Fuentes F, Su ZY, Kong AN. Apigenin Reactivates Nrf2 Anti-Oxidative Stress Signaling in Mouse Skin Epidermal JB6 P + Cells Through Epigenetics Modifications. *AAPS J* (2014) 16:727–35. doi: 10.1208/s12248-014-9613-8
143. Shukla S, Fu P, Gupta S. Apigenin Induces Apoptosis by Targeting Inhibitor of Apoptosis Proteins and Ku70-Bax Interaction in Prostate Cancer. *Apoptosis* (2014) 19:883–94. doi: 10.1007/s10495-014-0971-6
144. Pandey M, Kaur P, Shukla S, Abbas A, Fu P, Gupta S. Plant Flavone Apigenin Inhibits HDAC and Remodels Chromatin to Induce Growth Arrest and Apoptosis in Human Prostate Cancer Cells: In Vitro and In Vivo Study. *Mol Carcinog* (2012) 51:952–62. doi: 10.1002/mc.20866
145. Manzoor MF, Ahmad N, Ahmed Z, Siddique R, Zeng XA, Rahaman A, et al. Novel Extraction Techniques and Pharmaceutical Activities of Luteolin and its Derivatives. *J Food Biochem* (2019) 43:e12974. doi: 10.1111/jfbc.12974
146. Ali F, Siddique YH. Bioavailability and Pharmaco-therapeutic Potential of Luteolin in Overcoming Alzheimer's Disease. *CNS Neurol Disord Drug Targets* (2019) 18:352–65. doi: 10.2174/1871527318666190319141835
147. Pandurangan AK, Esa NM. Luteolin, a Bioflavonoid Inhibits Colorectal Cancer Through Modulation of Multiple Signaling Pathways: A Review. *Asian Pac J Cancer Prev* (2014) 15:5501–8. doi: 10.7314/apjcp.2014.15.14.5501
148. Selvi RB, Swaminathan A, Chatterjee S, Shanmugam MK, Li F, Ramakrishnan GB, et al. Inhibition of P300 Lysine Acetyltransferase Activity by Luteolin Reduces Tumor Growth in Head and Neck Squamous Cell Carcinoma (HNSCC) Xenograft Mouse Model. *Oncotarget* (2015) 6:43806–18. doi: 10.18632/oncotarget.6245
149. Kanwal R, Datt M, Liu X, Gupta S. Dietary Flavones as Dual Inhibitors of DNA Methyltransferases and Histone Methyltransferases. *PloS One* (2016) 11:e0162956. doi: 10.1371/journal.pone.0162956
150. Ganai SA, Farooq Z, Banday S, Altaf M. In Silico Approaches for Investigating the Binding Propensity of Apigenin and Luteolin Against Class I HDAC Isoforms. *Future Med Chem* (2018) 10:1925–45. doi: 10.4155/fmc-2018-0020
151. Zuo Q, Wu R, Xiao X, Yang C, Yang Y, Wang C, et al. The Dietary Flavone Luteolin Epigenetically Activates the Nrf2 Pathway and Blocks Cell Transformation in Human Colorectal Cancer HCT116 Cells. *J Cell Biochem* (2018) 119:9573–82. doi: 10.1002/jcb.27275
152. Shoulars K, Rodriguez MA, Thompson T, Markaverich BM. Regulation of Cell Cycle and RNA Transcription Genes Identified by Microarray Analysis of PC-3 Human Prostate Cancer Cells Treated With Luteolin. *J Steroid Biochem Mol Biol* (2010) 118:41–50. doi: 10.1016/j.jsbmb.2009.09.016
153. Markaverich BM, Shoulars K, Rodriguez MA. Luteolin Regulation of Estrogen Signaling and Cell Cycle Pathway Genes in MCF-7 Human Breast Cancer Cells. *Int J BioMed Sci* (2011) 7:101–11.
154. Markaverich BM, Vijjeswarapu M, Shoulars K, Rodriguez M. Luteolin and Gefitinib Regulation of EGF Signaling Pathway and Cell Cycle Pathway Genes in PC-3 Human Prostate Cancer Cells. *J Steroid Biochem Mol Biol* (2010) 122:219–31. doi: 10.1016/j.jsbmb.2010.06.006
155. Raza W, Luqman S, Meena A. Prospects of Tangeretin as a Modulator of Cancer Targets/Pathways. *Pharmacol Res* (2020) 161:105202. doi: 10.1016/j.phrs.2020.105202
156. Ashrafizadeh M, Ahmadi Z, Mohammadinejad R, Ghasemipour Afshar E. Tangeretin: A Mechanistic Review of its Pharmacological and Therapeutic Effects. *J Basic Clin Physiol Pharmacol* (2020) 31. doi: 10.1515/jbcpp-2019-0191
157. Braidy N, Behzad S, Habtemariam S, Ahmed T, Daglia M, Nabavi SM, et al. Neuroprotective Effects of Citrus Fruit-Derived Flavonoids, Nobiletin and Tangeretin in Alzheimer's and Parkinson's Disease. *CNS Neurol Disord Drug Targets* (2017) 16:387–97. doi: 10.2174/1871527316666170328113309
158. Wei GJ, Chao YH, Tung YC, Wu TY, Su ZY. A Tangeretin Derivative Inhibits the Growth of Human Prostate Cancer LNCap Cells by Epigenetically Restoring P21 Gene Expression and Inhibiting Cancer

Stem-like Cell Proliferation. *AAPS J* (2019) 21:86. doi: 10.1208/s12248-019-0345-7
159. Naz S, Imran M, Rauf A, Orhan IE, Shariati MA, Iahtisham Ul H, et al. Chrysin: Pharmacological and Therapeutic Properties. *Life Sci* (2019) 235:116797. doi: 10.1016/j.lfs.2019.116797
160. Sun LP, Chen AL, Hung HC, Chien YH, Huang JS, Huang CY, et al. Chrysin: A Histone Deacetylase 8 Inhibitor With Anticancer Activity and a Suitable Candidate for the Standardization of Chinese Propolis. *J Agric Food Chem* (2012) 60:11748–58. doi: 10.1021/jf303261r
161. Pal-Bhadra M, Ramaiah MJ, Reddy TL, Krishnan A, Pushpavalli SN, Babu KS, et al. Plant HDAC Inhibitor Chrysin Arrest Cell Growth and Induce p21WAF1 by Altering Chromatin of STAT Response Element in A375 Cells. *BMC Cancer* (2012) 12:180. doi: 10.1186/1471-2407-12-180
162. Zhong X, Liu D, Jiang Z, Li C, Chen L, Xia Y, et al. Chrysin Induced Cell Apoptosis and Inhibited Invasion Through Regulation of TET1 Expression in Gastric Cancer Cells. *Onco Targets Ther* (2020) 13:3277–87. doi: 10.2147/OTT.S246031
163. Krizova L, Dadakova K, Kasparovska J, Kasparovsky T. Isoflavones. *Molecules* (2019) 24. doi: 10.3390/molecules24061076
164. Zhang Q, Xie H, Chen D, Yu B, Huang Z, Zheng P, et al. Dietary Daidzein Supplementation During Pregnancy Facilitates Fetal Growth in Rats. *Mol Nutr Food Res* (2018) 62:e1800921. doi: 10.1002/mnfr.201800921
165. Das D, Sarkar S, Bordoloi J, Wann SB, Kalita J, Manna P. Daidzein, its Effects on Impaired Glucose and Lipid Metabolism and Vascular Inflammation Associated With Type 2 Diabetes. *Biofactors* (2018) 44:407–17. doi: 10.1002/biof.1439
166. Vitale DC, Piazza C, Melilli B, Drago F, Salomone S. Isoflavones: Estrogenic Activity, Biological Effect and Bioavailability. *Eur J Drug Metab Pharmacokinet* (2013) 38:15–25. doi: 10.1007/s13318-012-0112-y
167. Zhang Y, Li Q, Chen H. DNA Methylation and Histone Modifications of Wnt Genes by Genistein During Colon Cancer Development. *Carcinogenesis* (2013) 34:1756–63. doi: 10.1093/carcin/bgt129
168. Zhang Y, Chen H. Genistein Attenuates WNT Signaling by Up-Regulating sFRP2 in a Human Colon Cancer Cell Line. *Exp Biol Med (Maywood)* (2011) 236:714–22. doi: 10.1258/ebm.2011.010347
169. Wang Z, Chen H. Genistein Increases Gene Expression by Demethylation of WNT5a Promoter in Colon Cancer Cell Line SW1116. *Anticancer Res* (2010) 30:4537–45. doi: 10.1097/CAD.0b013e328340dc97
170. Vardi A, Bosviel R, Rabiau N, Adjakly M, Satih S, Dechelotte P, et al. Soy Phytoestrogens Modify DNA Methylation of GSTP1, RASSF1A, EPH2 and BRCA1 Promoter in Prostate Cancer Cells. *In Vivo* (2010) 24:393–400. doi: 10.1089/hum.2009.157
171. Karsli-Ceppioglu S, Ngollo M, Adjakly M, Dagdemir A, Judes G, Lebert A, et al. Genome-Wide DNA Methylation Modified by Soy Phytoestrogens: Role for Epigenetic Therapeutics in Prostate Cancer? *OMICS* (2015) 19:209–19. doi: 10.1089/omi.2014.0142
172. Fang MZ, Chen D, Sun Y, Jin Z, Christman JK, Yang CS. Reversal of Hypermethylation and Reactivation of P16INK4a, RARbeta, and MGMT Genes by Genistein and Other Isoflavones From Soy. *Clin Cancer Res* (2005) 11:7033–41. doi: 10.1158/1078-0432.CCR-05-0406
173. Zeng W, Jin L, Zhang F, Zhang C, Liang W. Naringenin as a Potential Immunomodulator in Therapeutics. *Pharmacol Res* (2018) 135:122–6. doi: 10.1016/j.phrs.2018.08.002
174. Hernandez-Aquino E, Muriel P. Beneficial Effects of Naringenin in Liver Diseases: Molecular Mechanisms. *World J Gastroenterol* (2018) 24:1679–707. doi: 10.3748/wjg.v24.i16.1679
175. Den Hartogh DJ, Tsiani E. Antidiabetic Properties of Naringenin: A Citrus Fruit Polyphenol. *Biomolecules* (2019) 9. doi: 10.3390/biom9030099
176. Curti V, Di Lorenzo A, Rossi D, Martino E, Capelli E, Collina S, et al. Enantioselective Modulatory Effects of Naringenin Enantiomers on the Expression Levels of miR-17-3p Involved in Endogenous Antioxidant Defenses. *Nutrients* (2017) 9. doi: 10.3390/nu9030215
177. Fernandez-Bedmar Z, Anter J, Alonso-Moraga A, Martin de Las Mulas J, Millan-Ruiz Y, Guil-Luna S. Demethylating and Anti-Hepatocarcinogenic Potential of Hesperidin, a Natural Polyphenol of Citrus Juices. *Mol Carcinog* (2017) 56:1653–62. doi: 10.1002/mc.22621
178. de Oliveira MR. Phloretin-Induced Cytoprotective Effects on Mammalian Cells: A Mechanistic View and Future Directions. *Biofactors* (2016) 42:13–40. doi: 10.1002/biof.1256
179. Nair SV, Ziaullah, Rupasinghe HP. Fatty Acid Esters of Phloridzin Induce Apoptosis of Human Liver Cancer Cells Through Altered Gene Expression. *PloS One* (2014) 9:e107149. doi: 10.1371/journal.pone.0107149
180. Sunil C, Xu B. An Insight Into the Health-Promoting Effects of Taxifolin (Dihydroquercetin). *Phytochemistry* (2019) 166:112066. doi: 10.1016/j.phytochem.2019.112066
181. Tanaka M, Saito S, Inoue T, Satoh-Asahara N, Ihara M. Novel Therapeutic Potentials of Taxifolin for Amyloid-beta-associated Neurodegenerative Diseases and Other Diseases: Recent Advances and Future Perspectives. *Int J Mol Sci* (2019) 20. doi: 10.3390/ijms20092139
182. Li J, Hu L, Zhou T, Gong X, Jiang R, Li H, et al. Taxifolin Inhibits Breast Cancer Cells Proliferation, Migration and Invasion by Promoting Mesenchymal to Epithelial Transition Via Beta-Catenin Signaling. *Life Sci* (2019) 232:116617. doi: 10.1016/j.lfs.2019.116617
183. Zhou W, Guo Z. Taxifolin Inhibits the Scar Cell Carcinoma Growth by Inducing Apoptosis, Cell Cycle Arrest and Suppression of PI3K/AKT/mTOR Pathway. *J BUON* (2019) 24:853–8.
184. Kuang H, Tang Z, Zhang C, Wang Z, Li W, Yang C, et al. Taxifolin Activates the Nrf2 Anti-Oxidative Stress Pathway in Mouse Skin Epidermal JB6 P+ Cells Through Epigenetic Modifications. *Int J Mol Sci* (2017) 18. doi: 10.3390/ijms18071546
185. Mateen S, Raina K, Jain AK, Agarwal C, Chan D, Agarwal R. Epigenetic Modifications and p21-Cyclin B1 Nexus in Anticancer Effect of Histone Deacetylase Inhibitors in Combination With Silibinin on Non-Small Cell Lung Cancer Cells. *Epigenetics* (2012) 7:1161–72. doi: 10.4161/epi.22070
186. Mateen S, Raina K, Agarwal C, Chan D, Agarwal R. Silibinin Synergizes With Histone Deacetylase and DNA Methyltransferase Inhibitors in Upregulating E-Cadherin Expression Together With Inhibition of Migration and Invasion of Human Non-Small Cell Lung Cancer Cells. *J Pharmacol Exp Ther* (2013) 345:206–14. doi: 10.1124/jpet.113.203471
187. Anestopoulos I, Sfakianos AP, Franco R, Chlichlia K, Panayiotidis MI, Kroll DJ, et al. A Novel Role of Silibinin as a Putative Epigenetic Modulator in Human Prostate Carcinoma. *Molecules* (2016) 22. doi: 10.3390/molecules22010062
188. Barros TMB, Lima APB, Almeida TC, da Silva GN. Inhibition of Urinary Bladder Cancer Cell Proliferation by Silibinin. *Environ Mol Mutagen* (2020) 61:445–55. doi: 10.1002/em.22363
189. Zadeh MM, Motamed N, Ranji N, Majidi M, Falahi F. Silibinin-Induced Apoptosis and Downregulation of MicroRNA-21 and MicroRNA-155 in MCF-7 Human Breast Cancer Cells. *J Breast Cancer* (2016) 19:45–52. doi: 10.4048/jbc.2016.19.1.45
190. Negri A, Naponelli V, Rizzi F, Bettuzzi S. Molecular Targets of Epigallocatechin-Gallate (EGCG): A Special Focus on Signal Transduction and Cancer. *Nutrients* (2018) 10. doi: 10.3390/nu10121936
191. Chu C, Deng J, Man Y, Qu Y. Green Tea Extracts Epigallocatechin-3-gallate for Different Treatments. *BioMed Res Int* (2017) 2017:5615647. doi: 10.1155/2017/5615647
192. Chakrawarti L, Agrawal R, Dang S, Gupta S, Gabrani R. Therapeutic Effects of EGCG: A Patent Review. *Expert Opin Ther Pat* (2016) 26:907–16. doi: 10.1080/13543776.2016.1203419
193. Li Y, Buckhaults P, Cui X, Tollefsbol TO. Combinatorial Epigenetic Mechanisms and Efficacy of Early Breast Cancer Inhibition by Nutritive Botanicals. *Epigenomics* (2016) 8:1019–37. doi: 10.2217/epi-2016-0024
194. Borutinskaite V, Virksaite A, Gudelyte G, Navakauskiene R. Green Tea Polyphenol EGCG Causes Anti-Cancerous Epigenetic Modulations in Acute Promyelocytic Leukemia Cells. *Leuk Lymphoma* (2018) 59:469–78. doi: 10.1080/10428194.2017.1339881
195. O'Neill EJ, Termini D, Albano A, Tsiani E. Anti-Cancer Properties of Theaflavins. *Molecules* (2021) 26. doi: 10.3390/molecules26040987
196. Takemoto M, Takemoto H. Synthesis of Theaflavins and Their Functions. *Molecules* (2018) 23. doi: 10.3390/molecules23040918
197. He HF. Research Progress on Theaflavins: Efficacy, Formation, and Preparation. *Food Nutr Res* (2017) 61:1344521. doi: 10.1080/16546628.2017.1344521
198. Juarez-Mercado KE, Prieto-Martinez FD, Sanchez-Cruz N, Pena-Castillo A, Prada-Gracia D, Medina-Franco JL. Expanding the Structural Diversity of DNA Methyltransferase Inhibitors. *Pharmaceuticals (Basel)* (2020) 14:17. doi: 10.3390/ph14010017

199. Bhattacharya R, Chatterjee R, Mandal AKA, Mukhopadhyay A, Basu S, Giri AK, et al. Theaflavin-Containing Black Tea Extract: A Potential DNA Methyltransferase Inhibitor in Human Colon Cancer Cells and Ehrlich Ascites Carcinoma-Induced Solid Tumors in Mice. *Nutr Cancer* (2020) 1–13. doi: 10.1080/01635581.2020.1828943
200. Nomi Y, Iwasaki-Kurashige K, Matsumoto H. Therapeutic Effects of Anthocyanins for Vision and Eye Health. *Molecules* (2019) 24:3311. doi: 10.3390/molecules24183311
201. Rozanska D, Regulska-Ilow B. The Significance of Anthocyanins in the Prevention and Treatment of Type 2 Diabetes. *Adv Clin Exp Med* (2018) 27:135–42. doi: 10.17219/acem/64983
202. Lin BW, Gong CC, Song HF, Cui YY. Effects of Anthocyanins on the Prevention and Treatment of Cancer. *Br J Pharmacol* (2017) 174:1226–43. doi: 10.1111/bph.13627
203. Kuo HD, Wu R, Li S, Yang AY, Kong AN. Anthocyanin Delphinidin Prevents Neoplastic Transformation of Mouse Skin JB6 P+ Cells: Epigenetic Re-activation of Nrf2-ARE Pathway. *AAPS J* (2019) 21:83. doi: 10.1208/s12248-019-0355-5
204. Li S, Li W, Wang C, Wu R, Yin R, Kuo HC, et al. Pelargonidin Reduces the TPA Induced Transformation of Mouse Epidermal Cells -Potential Involvement of Nrf2 Promoter Demethylation. *Chem Biol Interact* (2019) 309:108701. doi: 10.1016/j.cbi.2019.06.014
205. Zhang H, Guo J, Mao L, Li Q, Guo M, Mu T, et al. Up-Regulation of miR-24-1-5p is Involved in the Chemoprevention of Colorectal Cancer by Black Raspberry Anthocyanins. *Br J Nutr* (2019) 122:518–26. doi: 10.1017/S0007114518003136
206. Wang TH, Hsia SM, Shih YH, Shieh TM. Association of Smoking, Alcohol Use, and Betel Quid Chewing With Epigenetic Aberrations in Cancers. *Int J Mol Sci* (2017) 18:1210. doi: 10.3390/ijms18061210
207. Bjornsson HT, Sigurdsson MI, Fallin MD, Irizarry RA, Aspelund T, Cui H, et al. Intra-Individual Change Over Time in DNA Methylation With Familial Clustering. *JAMA* (2008) 299:2877–83. doi: 10.1001/jama.299.24.2877
208. Puthenveetil A, Dubey S. Metabolic Reprograming of Tumor-Associated Macrophages. *Ann Transl Med* (2020) 8:1030. doi: 10.21037/atm-20-2037
209. Yerinde C, Siegmund B, Glauben R, Weidinger C. Metabolic Control of Epigenetics and Its Role in CD8(+) T Cell Differentiation and Function. *Front Immunol* (2019) 10:2718. doi: 10.3389/fimmu.2019.02718
210. Shukla S, Meeran SM, Katiyar SK. Epigenetic Regulation by Selected Dietary Phytochemicals in Cancer Chemoprevention. *Cancer Lett* (2014) 355:9–17. doi: 10.1016/j.canlet.2014.09.017
211. Zheng YZ, Chen DF, Deng G, Guo R. The Substituent Effect on the Radical Scavenging Activity of Apigenin. *Molecules* (2018) 23:1989. doi: 10.3390/molecules23081989
212. Nagai S, Matsumoto C, Shibano M, Fujimori K. Suppression of Fatty Acid and Triglyceride Synthesis by the Flavonoid Orientin Through Decrease of C/EBPdelta Expression and Inhibition of PI3K/Akt-FOXO1 Signaling in Adipocytes. *Nutrients* (2018) 10:130. doi: 10.3390/nu10020130
213. Busch C, Burkard M, Leischner C, Lauer UM, Frank J, Venturelli S. Epigenetic Activities of Flavonoids in the Prevention and Treatment of Cancer. *Clin Epigenet* (2015) 7:64. doi: 10.1186/s13148-015-0095-z
214. Rossi M, Edefonti V, Parpinel M, Lagiou P, Franchi M, Ferraroni M, et al. Proanthocyanidins and Other Flavonoids in Relation to Endometrial Cancer Risk: A Case-Control Study in Italy. *Br J Cancer* (2013) 109:1914–20. doi: 10.1038/bjc.2013.447
215. Carrera AN, Grant MKO, Zordoky BN. CYP1B1 as a Therapeutic Target in Cardio-Oncology. *Clin Sci (Lond)* (2020) 134:2897–927. doi: 10.1042/CS20200310
216. Tse C, Warner A, Farook R, Cronin JG. Phytochemical Targeting of STAT3 Orchestrated Lipid Metabolism in Therapy-Resistant Cancers. *Biomolecules* (2020) 10:1118. doi: 10.3390/biom10081118
217. Zubair H, Azim S, Ahmad A, Khan MA, Patel GK, Singh S, et al. Cancer Chemoprevention by Phytochemicals: Nature's Healing Touch. *Molecules* (2017) 22:395. doi: 10.3390/molecules22030395
218. Vanden Berghe W. Epigenetic Impact of Dietary Polyphenols in Cancer Chemoprevention: Lifelong Remodeling of Our Epigenomes. *Pharmacol Res* (2012) 65:565–76. doi: 10.1016/j.phrs.2012.03.007
219. Mai A, Cheng D, Bedford MT, Valente S, Nebbioso A, Perrone A, et al. Epigenetic Multiple Ligands: Mixed Histone/Protein Methyltransferase, Acetyltransferase, and Class III Deacetylase (Sirtuin) Inhibitors. *J Med Chem* (2008) 51:2279–90. doi: 10.1021/jm701595q
220. Zheng YG, Wu J, Chen Z, Goodman M. Chemical Regulation of Epigenetic Modifications: Opportunities for New Cancer Therapy. *Med Res Rev* (2008) 28:645–87. doi: 10.1002/med.20120
221. George VC, Dellaire G, Rupasinghe HPV. Plant Flavonoids in Cancer Chemoprevention: Role in Genome Stability. *J Nutr Biochem* (2017) 45:1–14. doi: 10.1016/j.jnutbio.2016.11.007

Conflict of Interest: The authors declare that the research was conducted in the absence of any commercial or financial relationships that could be construed as a potential conflict of interest.

frontiers in Oncology

ORIGINAL RESEARCH
published: 02 August 2021
doi: 10.3389/fonc.2021.715673

Anticarin β Inhibits Human Glioma Progression by Suppressing Cancer Stemness *via* STAT3

Min Zhang[1,2], *Zhi Dai*[1], *Xudong Zhao*[1], *Gan Wang*[1*] and *Ren Lai*[1*]

[1] Key Laboratory of Animal Models and Human Disease Mechanisms, Chinese Academy of Sciences/Key Laboratory of Bioactive Peptides of Yunnan Province, Kunming Institute of Zoology - The Chinese University of Hong Kong (KIZ-CUHK) Joint Laboratory of Bioresources and Molecular Research in Common Diseases, National Resource Center for Non-Human Primates, Kunming Primate Research Center, and National Research Facility for Phenotypic & Genetic Analysis of Model Animals (Primate Facility), Kunming Institute of Zoology, Kunming, China, [2] Kunming College of Life Science, University of Chinese Academy of Sciences, Beijing, China

Glioma is the most common form of malignant brain cancer. It is very difficult to cure malignant glioma because of the presence of glioma stem cells, which are a barrier to cure, have high tumorigenesis, associated with drug resistance, and responsible for relapse by regulating stemness genes. In this study, our results demonstrated that anticarin β, a natural compound from *Antiaris toxicaria*, can effectively and selectively suppress proliferation and cause apoptosis in glioma cells, which has an IC_{50} that is 100 times lower than that in mouse normal neural stem cells. Importantly, cell sphere formation assay and real time-quantitative analysis reveal that anticarin β inhibits cancer stemness by modulating related stemness gene expression. Additionally, anticarin β induces DNA damage to regulate the oncogene expression of signal transducer and activator of transcription 3 (STAT3), Akt, mitogen-activated protein kinases (MAPKs), and eventually leading to apoptosis. Furthermore, anticarin β effectively inhibits glioma growth and prolongs the lifts pan of tumor-bearing mice without systemic toxicity in the orthotopic xenograft mice model. These results suggest that anticarin β is a promising candidate inhibitor for malignant glioma.

Keywords: natural product, glioma, apoptosis, DNA damage, stemness

OPEN ACCESS

Edited by:
Yuling Qiu,
Tianjin Medical University, China

Reviewed by:
Sze Kwan Lam,
The University of Hong Kong, Hong Kong, SAR China
Neethi Nandagopal,
Université de Montréal, Canada

****Correspondence:***
Ren Lai
rlai@mail.kiz.ac.cn
Gan Wang
wanggan@mail.kiz.ac.cn

Specialty section:
This article was submitted to Pharmacology of Anti-Cancer Drugs, a section of the journal Frontiers in Oncology

Received: *27 May 2021*
Accepted: *20 July 2021*
Published: *02 August 2021*

Citation:
Zhang M, Dai Z, Zhao X, Wang G and Lai R (2021) Anticarin β Inhibits Human Glioma Progression by Suppressing Cancer Stemness via STAT3. Front. Oncol. 11:715673. doi: 10.3389/fonc.2021.715673

INTRODUCTION

Glioma is the most common and lethal kind of brain tumor, accounting for about 50% of malignant brain tumors. The average survival time from diagnosis to death for glioma patients is less than 15 months, and the 5-year survival rate is about 4.7% (1–4). Subpopulations of cancer cells with high tumorigenic potential and unlimited self-renewal capacity, termed cancer stem cells, were found to have high stemness properties (5–7). It has been demonstrated that these stemness-high malignant cells have high tumorigenic potential, enhanced DNA repair capacity, and resistance to conventional chemotherapies and radiation. Moreover, standard chemotherapy and radiation have been found to induce stemness genes in cancer cells, converting stemness-low cancer cells to stemness-high cancer cells. These stemness cells are likely to survive after therapy and ultimately

lead to disease recurrence (7–13). Therefore, developing novel effective therapies for precise targeting stemness-high glioma is urgently needed.

Anticarin β is a natural product isolated from the bark of *Antiaris toxicaria*. Anticarin β is a coumarin derivative with a special structure that has been reported previously (14). The coumarins are an important class of heterocyclic compounds with diverse pharmacological activities and outstanding optical properties. Precious studies have demonstrated that coumarin and its derivatives have a variety of biological activities, including anti-inflammatory, antibacterial, antiviral, and anti-cancer activities which are associated with apoptosis (15–20).

In our study, anticarin β showed attractive bioactive properties to glioma *in vitro* and *in vivo* including selectively inhibit proliferatively and stemness, induce glioma apoptotic and DNA damage, suppress the growth of glioma on mice tumor model. Our finding suggested anticarin β is a potential inhibitor for human glioma.

MATERIALS AND METHODS

Purification and Characterization of Anticarin β

The powdered bark of *Antiaris toxicaria* was socked in EtOH and concentrated to give a crude extract after removal of the solvents. The crude extract was extracted successively with petroleum ether, dichloromethane, ethyl acetate, and n-butanol. The n-butanol phase extract exhibited a significant cytotoxic activity on glioma cells. We then performed column chromatography on the crude extract, using Macro-porous resin column, Medium Pressure Liquid Chromatography (MPLC), and High-Performance Liquid Chromatography (HPLC). The extract was divided into several peaks by C_{18} column according to absorbance at 365 nm (**Figure 1A**). Peak 15# (indicated by arrow) was further purified by a C_{18} reverse-phase (HPLC) (**Figure 1B**) column and identified by ESI-MS spectrum (**Figure 1C**), ^{1}H NMR spectrum (DMSO, **Figure 1D**), and ^{13}C DEPT NMR spectrum (DMSO, **Figure 1E**). The compound, anticarin β, is consistent with previous reports (14).

Cells and Culture

All human cell lines were obtained from the Conservation Genetics CAS Kunming Cell Bank (Kunming, Yunnan, China), which performs authentication on its cell lines. Human cell lines were cultured in DMEM/F12 supplemented with 10% heat-inactivated FBS, 100 U/mL penicillin, and 100 μg/mL streptomycin at 37˚C and 5% CO_2 in a humidified incubator.

Normal mouse neural stem cell line (mNSC) was obtained from Sigma-Aldrich (Darmstadt, Germany). Neural stem cells were cultured in glioma stem cell medium that consisted of DMEM/F12, 1 x B27, 50 ng/mL bFGF, and 50 ng/mL EGF supplemented with 100 U/mL penicillin and 100 μg/mL streptomycin. Culture dishes were pre-coated with 10 μg/mL laminin for 8 h at 37˚C in a humidified incubator before neural stem cells were seeded and maintained at 37˚C in a humidified incubator with 5% CO_2.

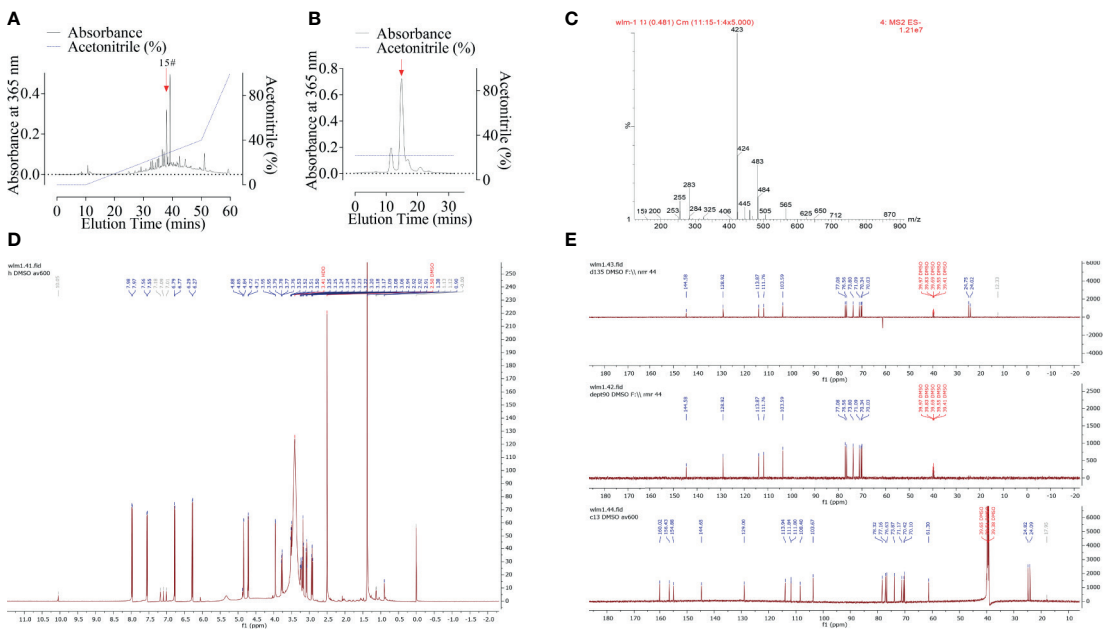

FIGURE 1 | Purification and characterization of anticarin β from *Antiaris toxicaria*. **(A)** Crude extract containing anticarin β was separated by a C_{18} column and absorbance at 365 nm was recorded. **(B)** Fractions containing anticarin β (indicated by arrow in A) was further purified by a C_{18} reverse phase (HPLC) column and the anticarin β was indicated by a red arrow. **(C–E)** Anticarin β was characterized by ESI-MS spectrum **(C)**, ^{1}H-NMR spectrum (DMSO, D), and ^{13}C DEPT NMR spectrum (DMSO, E).

Morphological Observation

The morphology of 10 μM anticarin β-treated cell lines (U87-MG, T98G, and mNSC) at 24 h after treatment was examined and images were observed by phase-contrast microscopy (magnification, 40x).

MTS Assay

A total of 2 x 10^4 cell lines (U87-MG, T98G, and mNSC) in 150 μl per well were seeded into 96-well plates and treated with 50 μl anticarin β at 10 μM, 5 μM, 2.5 μM, 1.25 μM, 625 nM, 312.5 nM, 156.25 nM, 78.125 nM, 39.0625 nM, respectively. Cells treated with the same volume of phosphate buffer saline (PBS, 0.01 M) were used as normal control. All groups of cells were incubated for 24 h at 37˚C with 5% CO_2 after treatment with anticarin β. MTS reagent was diluted 1:10 with fresh complete medium and added 100 μL per well. After incubating for 1 hour, the absorbance was measured at 490 nm. The inhibition of cells treated with anticarin β was compared with the control group and expressed as a percentage. The half-maximal inhibitory concentration (IC_{50}) was calculated using GraphPad Prism 6.0 (GraphPad Software).

Colony Formation Analysis

Human glioma cells, U87-MG and T98G, were plated in 6-well plates (100 cells each well) and incubated for 7 days with treatments of anticarin β (0.5 μM). The control groups were treated with the same volume of PBS. The cells were then fixed with 4% formaldehyde for 20 min and stained with 0.25% crystal violet for 15 min. The number of colonies, defined as > 50 cells/colony, was counted and quantified. The data were analyzed using ImageJ.

Cell Sphere Formation Assay

3.2% soft agar was made by 0.4 g low gelling agar, mixed with 13 mL water, and sterilized by high-pressure steam sterilization. Then, 3.2% soft agar was diluted to 0.8% with medium and plated 1 mL per well in a 6-well plate as the bottom layer of agar. After colling at room temperature, 2 x 10^4 cells were mixed with 0.8% soft agar to 0.4% and plated 1 mL per well in a 6-well plate, cooled, and added 1 mL medium each well. The plate was cultured in a humidified incubator at 37˚C with 5% CO_2 and the medium was supplemented every 3 days. After the clonal spheres had reached 20 μm, they were treated with 1 μM anticarin β or the same volume of PBS every 3 days. After two weeks, the clonal spheres were collected, washed, and fixed with 4% paraformaldehyde containing 0.005% crystal violet for 2 h at room temperature. Images were obtained and the clonal spheres were counted.

Transwell Migration and Invasion Assays

Cell migration and invasion abilities were detected *via* Transwell assay (8-μm filter). For the migration assay, 5 x 10^4 cells resuspended in 200 μL culture medium with treatments of anticarin β (0.5 μM) without FBS were inoculated into the top chambers, the control groups were treated with the same volume of PBS; the bottom chambers were supplemented with 500 μL medium supplemented with 10% FBS. After 48 h, the non-migrating cells were removed, and the cells migrating through the membrane were fixed with methanol for 30 min and stained with 0.1% crystal violet for 15 min. The migrating cells were counted and the data were analyzed using GraphPad Prism 6.0 (GraphPad Software). For the invasion assay, the same number of cells was seeded into the top chambers that were precoated with Matrigel solution (BD Diagnostics), and the following experimental steps were the same as the migration assay.

Cell Proliferation Assay

Cell proliferation assay was performed using EdU Cell Proliferation Kit with Alexa Fluor 594 (Beyotime, Shanghai, China) and following the protocol described by the manufacturer. Cells were seeded onto a 24-well plate with coverslips, with 1x10^5 cells/per well. Anticarin β (0.5 μM) was added and the control wells were treated with the same volume of PBS. Cells were treated for 12 h at 37˚C in a humidified incubator. Then, cells were treated with EdU (10 μM) for 2 h at 37˚C in a humidified incubator with 5% CO_2. Following incubation, the cells were fixed in 4% paraformaldehyde, permeabilized with 0.5% Triton X-100 in PBS containing 3% BSA (PBS - BSA) for 20 min. Then, the cells were immersed in Click reaction mixture for 30 min and in Hoechst 33324 (10 mg/mL; diluted 1:1,000 in PBS) for 10 min at room temperature protected from light. Before the observation, the cells were washed twice with PBS and mounted onto a glass slide. Images were obtained using a fluorescent microscope at the magnifications 20x.

Real Time-Quantitative Analysis

The total RNA extraction of cells was performed using Trizol reagent (Invitrogen; Thermo Fisher Scientific, Inc.). 1 μg of total RNA was reverse transcribed using FastKing gDNA Dispelling RT SuperMix (Tiangen Biotech). The action was carried out at 42℃ for 15 min and terminated by deactivation of the enzyme at 95℃ for 5 min. PCR was conducted using EvaGreen 2X qPCR MasterMix (ABM, BC, Canada) in StepOne™ Real-Time PCR System (ThermoFish Scientific, MA, USA) using the manufacturer's default settings for relative quantification of standard Ct. Baseline and threshold values were automatically detected using the StepOne™ Software v2.3 (ThermoFish Scientific, MA, USA) with default settings. Gene expression was calculated using the comparative ΔΔCT method with the housekeeping genes *GAPDH* for normalization. The primers used are provided as follows. *Oct4*: forward: 5'-TAG TCC CTT CGC AAG CCC T-3', Reverse: 5'-CGA GAA GGC GAA ATC CGA AG-3'; *Nanog*: forward: 5'-CAA TGG TGT GAC GCA GGG AT-3', Reverse: 5'-GGA CTG GAT GTT CTG GGT CTG-3'; *Klf4*: forward: 5'-ATG CTC ACC CCA CCT TCT TC-3', Reverse: 5'-TTC TCA CCT GTG TGG GTT CG-3'; *Sox2*: forward: 5'-ACC AGC GCA TGG ACA GTT AC-3', Reverse: 5'-CCG TTC ATG TAG GTC TGC GA-3'; *Stat3*: forward: 5'-ACC ATT GAC CTG CCG ATG TC-3', Reverse: 5'-TAG GCG CCT CAG TCG TAT CT-3'; *Cd133*: forward: 5'-AGT CGG AAA CTG GCA GAT AGC-3', Reverse: 5'-GGT AGT GTT GTA CTG GGC CAA T-3'; *GAPDH*: forward: 5'-GAA AGC CTG CCG GTG ACT AA-3', Reverse: 5'-GCA TCA CCC GGA GGA GAA AT-3'.

Neutral Comet Assay

DNA damage was assessed by single-cell gel electrophoresis assay under neutral conditions as described (21). Human glioma cell lines U87-MG treated with anticarin β (1 μM) for 12 hours were suspend at 2 x 10^5 cells/mL in PBS. Combine the cell suspension with 1% molten low melting point agarose and immediately pipette it onto a slide. After placing slides at 4°C for 10 min, immerse slides in lysis solution overnight. Then, slides were immersed in freshly Neutral electrophoresis solution (pH = 9.0) for 30 min. Electrophoresis was carried out at the rate of 1.0 V/cm for 45 min at 4°C. After electrophoresis, the slides were immersed with DNA precipitation solution for 30 min and ice-cold 70% ethanol for 30 min. Subsequently, the slides were dried at room temperature, and DNA was stained with 50 μL of SYBR Green I dye [MCE, 1:10,000 in Tris-EDTA buffer (pH 7.4)] for 15 min and immediately analyzed using a fluorescence microscope. Data were analyzed using CometScore (TriTek, Sumerduck, VA).

Apoptosis Assay

Apoptosis assay was performed using GreenNuc™ Caspase-3 Assay Kit for Live Cells (Beyotime, Shanghai, China) and fluorescent terminal deoxynucleotidyl transferase dUTP nick end labeling (TUNEL) assay for tissue sections.

For cells, human glioma cell lines U87-MG (1 x 10^5 cells/well) were plated in a 6 cm glass-bottom dish. Cells were treated with 1 μM anticarin β for 24 h. Each dish was incubated with 5 μM GreenNuc™ Caspase-3 Substrate and Hoechst 33324 (10 mg/mL; diluted 1:1,000 in PBS) for 30 min in dark at room temperature. Before observing, the dishes were washed with PBS. Images were obtained using a fluorescent microscope at the magnification of 20x and 40x.

For tissue sections, Sections were de-paraffinized and rehydrated by incubation in a xylene and ethanol gradient. Antigen retrieval was performed in sodium citrate buffer (pH 6.0) at 95°C for 5 min. Tunel assay was performed using TUNEL FITC Apoptosis Detection Kit (Vazyme, Nanjing, China) according to the manufacturer's protocol. The nuclei were counterstained with DAPI for 5 min. Images were obtained using a fluorescent microscope, and the staining was scored using ImageJ.

Western Blot Analysis

Human glioma cell lines U87-MG, treated with or without 1 μM anticarin β for a different time, and tumor tissues were collected and lysed in RIPA buffer (Sigma, St. Louis, MO), containing Protease Inhibitor Cocktail (MCE, Shanghai, China) and Phosphatase Inhibitor Cocktail II (MCE, Shanghai, China). Lysates were sonicated, clarified by centrifugation, and protein concentrations were measured using the BCA protein assay (Biosharp, Hefei, China). Proteins were separated on 10% acrylamide SDS–PAGE gels, transferred to PVDF membranes. After blocking, the membranes were incubated with primary antibodies at 4°C overnight and then incubated with secondary antibodies at room temperature for 1 h. The signal detection was performed using enhanced chemiluminescence ECL substrate (Bio-Rad, Hercules, USA). Band images were acquired using a LAS 4000 mini system (GE Healthcare, Little Chalfont, England). Each experiment was independently repeated in triplicate. The antibodies used as followed: Primary antibodies Phospho-p38 (Thr180/Tyr182) (4511, CST), p38 (8690, CST), phospho-Erk1/2 (Thr202/Tyr204) (9101, CST), Erk1/2 (4695, CST), phospho-JNK (Thr183/Tyr185) (9255, CST), JNK (9252, CST), phospho-Akt (Ser473) (4060, CST),Akt (pan)(4691, CST), p-STAT3 (Ser727) (9134, CST), STAT3 (12640, CST), E-cadherin (14472, CST), N-cadherin (13116, CST), β-catenin (8480, CST), vimentin (5741, CST), CD44 (5640, CST), Nanog (4903, CST), Sox2 (3579, CST), Oct4 (2840, CST), CD133 (64326, CST), Bcl-2 (15071, CST), Bax (89477, CST), clv-caspase3 (9661, CST), clv-PARP (5625, CST), GAPDH (97166, CST); secondary goat anti-mouse HRP-IgG (7076, CST) and goat anti-rabbit HRP-IgG (7074, CST) antibodies were used for immunoblotting.

Animal Experiment

Male NOD/SCID mice (5 weeks old, 15-18 g, N = 18) were purchased from Beijing Vital River Laboratory Animal Technology Company. Before the experiments, mice were performed to adapt to the environment for a week. A total of 18 male NOD/SCID mice were injected with 2 x 10^5 U87-MG cells in the right hippocampus. The injection position of each mouse was relatively consistent, and the injection depth was 3 mm. 3 days post-inject, the mice were randomly divided into three groups (6 mice per group). The intracranial administration of PBS or anticarin β (1 mg/kg) using Alzet Osmotic Pumps was started on animals each day, and the intragastric administration of temozolomide (TMZ, 50 mg/kg) was started on animals once. All mice were used *in vivo* research after death. The critical organs (heart, liver, spleen, lungs, and kidneys) and brains were harvested. The brain is divided into two parts according to the location of injection, and the tumor area was measured. Half of tissues were formalin-fixed, cut into small pieces, paraffin-embedded, sectioned, and stained with haematoxylin & eosin (H&E) or antibodies. The effect of anticarin β was evaluated on specimens in at least three different sections. Half of tissues were frozen at -80°C for other experiments.

Cell Detection

Flow cytometry was used to analyze the percentage of cancer stem cells in T98G and U87-MG. Tumor cells were collected, rinsed, and fixed in 4% polyoxymethylene for 30 min. Then, cells were incubated with anti-CD44 antibodies for 60 min at room temperature in the dark. After washing with PBS, cells were incubated with FITC-labled secondary antibodies for 60 min at room temperature in the dark. The cells were resuspended in PBS and analyzed using an LSRFortessa flow cytometer (BD, San Jose, CA, USA). The data were analyzed using FlowJo software (Beckman Coulter). Each experiment was carried out in triplicates.

Statistical Analysis

The quantitative data are represented as the mean ± s.d. of triplicate experiments. The difference between two groups was compared with Student's *t*-test. Ordinary one-way ANOVA with

multiple comparisons tests was used for examining differences among multiple groups. The overall survival of mice was analyzed by the Kaplan-Meier method and compared with the Log-rank test. All statistical analyses were performed using GraphPad Prism 6.0 (GraphPad Software), and p-values were calculated, significance is represented as follows, * ($P < 0.05$), ** ($P < 0.01$), and *** ($P < 0.001$).

RESULTS

Anticarin β Selectively Inhibits the Proliferation of Human Glioma Cells

A function-based purification strategy was guided the potential anti-glioma compound identification in *Antiaris toxicaria*. Anticarin β was purified and characterized (**Figure 1**). The structure of anticarin β was established as 4'-β-glucosyl-khellactone, angular dihydropyrano- coumarin, shown in **Figure 2A**. Then, the proliferation-inhibiting efficacy of anticarin β against human glioma cells (U87-MG and T98G) and normal mouse neural stem cells (mNSCs) was evaluated. Anticarin β effectively inhibited the proliferation of glioma cells with concentration-dependent manner and no significant cytotoxicity was observed in normal mouse neural stem cells (**Figure 2B**). Anticarin β effectively inhibits human glioma cells (U87-MG and T98G) with half-maximal inhibitory concentration (IC_{50}) ~1.01 ± 0.10 and 1.20 ± 0.11 μM at 24 h, respectively. For the mNSCs, the IC_{50} value was more than 500 μM. Furthermore, the colony formation assay was performed to determine the effect of anticarin β on cell proliferative potential of human glioma cells. The colonies formed after anticarin β treatment was reduced 25% in U87-MG and 35% in T98G compare with the control (**Figure 2C**). As shown in **Figure 2D**, EdU-positive proliferative cells decreased by more than 70% in cells treated with anticarin β compared with PBS group. Anticarin β had no significant inhibitory effect on proliferation in mNSCs (**Figure S1A**). This result indicated that anticarin β could suppress proliferation by reducing DNA synthesis. Additionally, transwell cell migration, matrigel invasion assay, and western blot analysis showed that the

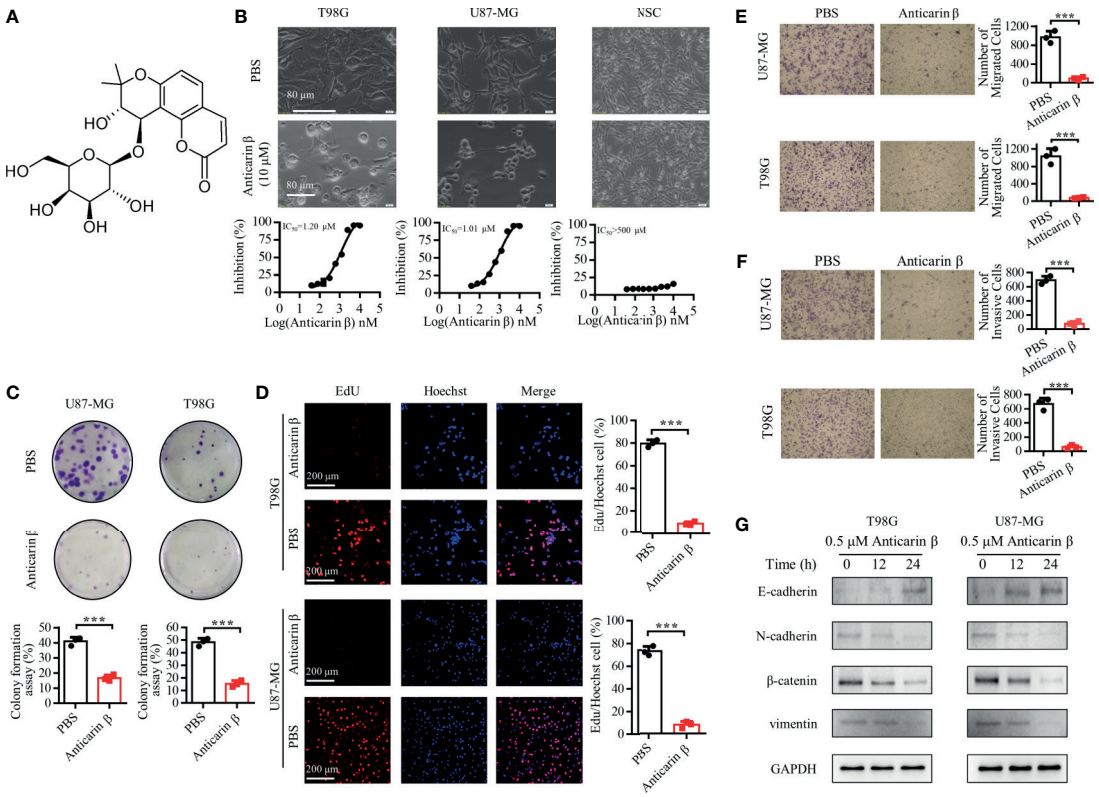

FIGURE 2 | Anticarin β inhibits the proliferation of human glioma cells. **(A)** The chemical structure of anticarin β. **(B)** Morphological changes and dose-dependent cytotoxicity on human glioma cell lines (U87-MG and T98G). Cells were treated with 0-10 μM anticarin β for 24h and then observed by phase-contrast microscopy. Cell viability was calculated using MTS analysis. **(C)** The colony formation results of U87-MG and T98G after treatments of anticarin β (0.5 μM) for 7 days were exhibited. **(D)** The number of proliferative cells labeled by EdU (red) and cell nucleus labeled by Hoechst 33324 (blue) was different between anticarin β (0.5 μM, 12 hours) and PBS group in U87-MG and T98G. Scale bar, 200 μm. **(E)** Migration and **(F)** invasion ability of human glioma cell lines U87-MG and T98G treated with anticarin β (0.5 μM) for 48 hours were measured with transwell migration assay and transwell invasion assay. **(G)** Western blotting analysis of E-cadherin, N-cadherin, β-catenin, vimentin in T98G and U87-MG treated with or without anticarin β (0.5 μM). Data are presented as mean ± s.d. of three independent experiments conducted in duplicate, ***$P < 0.001$ *versus* the control group.

treatment of anticarin β can suppress cell migration and invasion in both human glioma cell lines U87-MG and T98G compared to control (**Figures 2E–G**), and has no effects on migration and invasion in mNSC (**Figures S1B, C**). These results above illustrated that anticarin β selectively inhibit the human glioma cells and has no toxic to normal neural stem cells, suggesting anticarin β may targeting tumor-specific pathways.

Anticarin β Inhibits the Stemness of Human Glioma Cells

The stemness of cancer plays an essential role in tumorigenic, drug resistance, and relapse. The stem cells contain self-renewal capacity and give rise to the various cell lineages that comprise the tumor; they have been postulated as responsible for recurrence, and drug resistance of glioma (5). Thus, here we attempted to explore the effects of anticarin β on the stemness of glioma. CD44 have been identified as cancer stem cell markers for isolating and enriching cancer stem cells (22). Flow cytometric analysis showed that the high expression of CD44 in T98G and U87-MG. These results indicated that the high percentage of cancer stem cells in the T98G and U87-MG (**Figure S2A**). We examined whether anticarin β affects the self-renewal of glioma through cell sphere formation assay. U87-MG and T98G were treated with 1 μM anticarin β, clonal spheres were damaged, and the number of clonal spheres decreased dramatically compared with control (**Figure 3A**). Further, the expression of several stemness-associated factors and markers was examined in U87-MG with anticarin β (1 μM) for the different times by RT-qPCR analysis and Western Blotting analysis (**Figures 3B, C**). The treatment of U87-MG with anticarin β significantly decreased mRNA expression of many stemness factors and markers, including *Nanog, Oct4, Sox2, Cd133, and Stat3*. The protein expression of CD44, CD133, Nanog, Oct4, Sox2, and p-STAT3(Tyr705) was suppressed by anticarin β treatment for increasing time. Taken together, these results demonstrate that anticarin β destroy the self-renewal capacity of glioma cancer stem cells.

Anticarin β Induces Apoptosis and DNA Damage in Human Glioma Cells

In cancer therapies, DNA damage is a countermeasure to control cancer cell fate, death, or survival, to limit cancer progression. Upon DNA damage, cells initiate several response pathways to activate DNA repair or apoptosis (23). Previous experiments have shown that anticarin β can suppress DNA synthesis. For this reason, to further explore the mechanism of anticarin β's cytotoxicity, we performed Comet Assay to assess DNA damage. Anticarin β treatment could lead to obvious DNA damage (**Figure 4A**). Then, the caspase3 probe fluorescence analysis indicated that anticarin β (1 μM, 24 h) induced caspase-3 activation in human glioma cells and suppressing glioma cell growth (**Figure 4B**). This data indicated that anticarin β-induced cell death was, at least partly, associated with apoptosis induction.

To further explore the underlying molecular mechanism, western blot analysis was used to investigate signaling pathways. Akt, p38, extracellular-signal-regulated kinase (ERK), c-Jun N-terminal kinase (JNK), Bax, B-cell lymphoma-2 (Bcl-2), caspase3, and PARP both play important roles in regulating cancer cell proliferation and apoptosis (24, 25). Therefore, related proteins were examined in anticarin β-treated U87-MG cells by Western blotting (**Figures 4C, D**). Anticarin β treatment caused activation of p-p38 (Thr180/Tyr182), Bax, caspase3, and PARP. p-JNK (Thr183/Tyr18), and p-ERK1/2 (Thr202/Tyr204) were activated from 3 to 12 h then decreased. p-Akt (Ser473), and Bcl-2 was suppressed. These results elucidated that anticarin β inhibits cell growth and induces apoptosis in U87-MG cells *via* affecting Akt, MAPKs pathways, and apoptotic-related proteins.

Anticarin β Inhibits the Glioma Growth in Orthotopic Xenograft Mice Model

We next tested whether anticarin β can suppress glioma growth *in vivo* using an orthotopic xenograft NOD/SCID mice tumor model. Human glioma cell line U87-MG (2×10^5) was injected into the right hippocampus of mice. Mice were randomly divided into 3 groups (negative group (PBS), positive group (temozolomide, the most commonly used alkylating agent in glioma chemotherapy), and anticarin β group. Consistent with our *in vitro* results, anticarin β significantly suppressed the growth of glioma cells (**Figures 5A, B**). Mice weight has no significant change until ~23 days after glioma cell injected, and the survival of tumor-bearing mice has been prolonged in anticarin β group (**Figure 5C, D**). There was no obvious toxicity in the major organs of mice treated with anticarin β (**Figure S3A**). Tumor samples were collected, and western blot analysis showed that the expression of stemness-related proteins and apoptosis proteins *in vivo* was similar to that *in vitro*. In anticarin β-treated tumor tissues, CD44, CD133, Nanog, Oct4, Sox2, p-STAT3 were suppressed, and caspase3, PARP was activated (**Figure 5E**). Furthermore, Nanog and phosphorylated STAT3 in anticarin β-treated tumor tissues were decreased by immunofluorescent stain (**Figure 5F**). TUNEL staining confirmed a higher percentage of apoptotic cells in brain tumors treated with anticarin β than PBS (**Figure 5G**). Our data suggested that anticarin β block tumorigenesis, prolong overall survival duration, and has no obvious systemic toxicity *in vivo*, thus highlighting the potential of anticarin β to develop an inhibitor for glioma in the future.

DISCUSSION

The current standard therapeutic strategy for glioma is mainly relied on surgical treatment, followed by radiotherapy and chemotherapy. The limitations of surgical treatment make it impossible to completely remove tumors, and glioma cells are often tolerant to chemotherapy and radiotherapy. The prognosis for patients is still poor with a low five-year survival rate (1–4). Preciously, some novel strategies of therapy have been investigated. Many chemotherapeutic agents isolated from natural plants are served as the effective drug of cancer cells (13, 26–28).

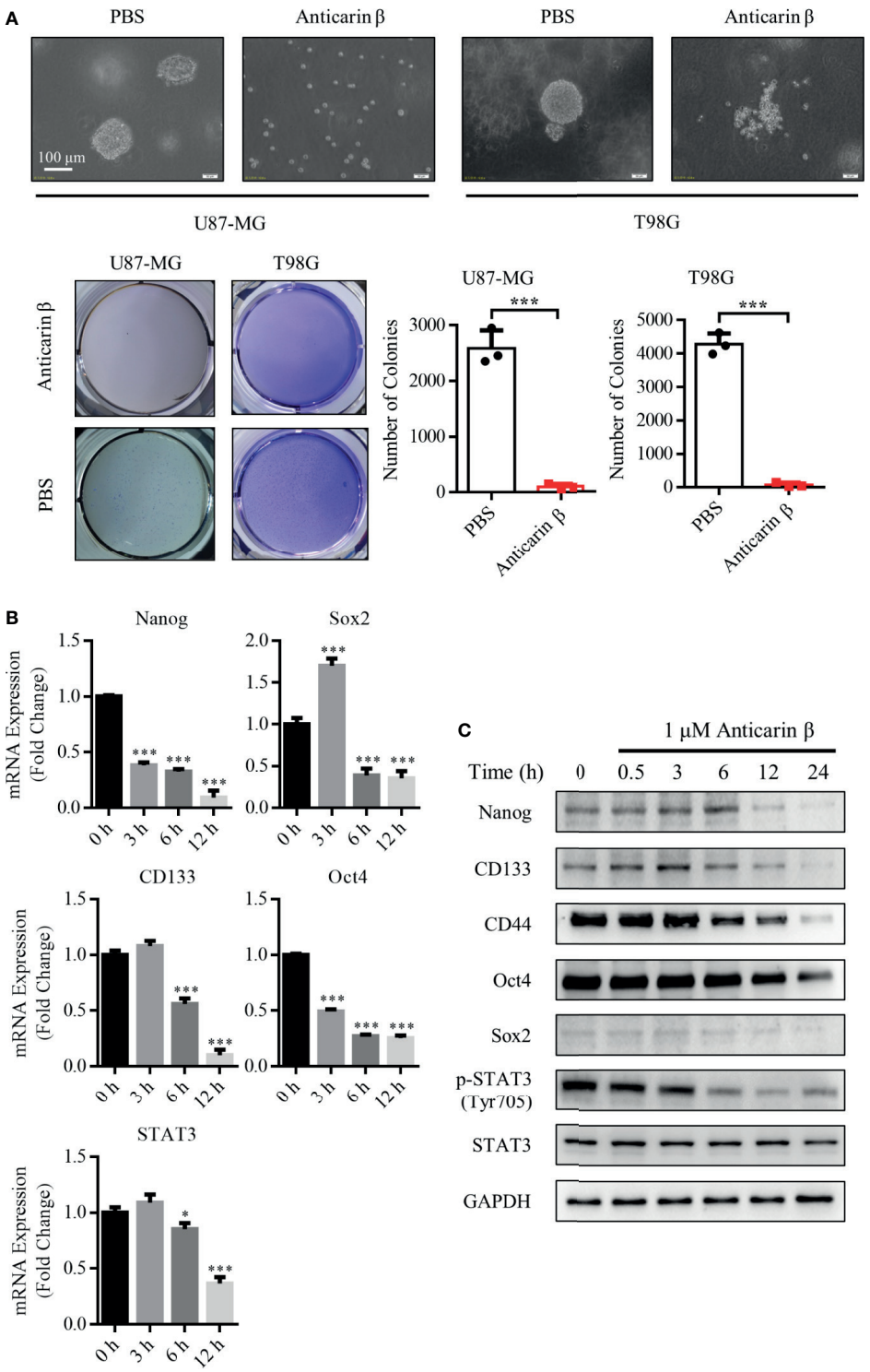

FIGURE 3 | Anticarin β inhibits the stemness of human glioma cells. **(A)** Human glioma cell lines U87-MG and T98G clonal sphere morphology were damaged following treatment with anticarin β (1 μM). Cells sphere formation was stained with 4% paraformaldehyde and 0.005% crystal violet for 2 hours. The quantitative data of the number of clonal spheres were shown. **(B)** The mRNA expression of the stemness-related genes was measured in U87-MG cells with anticarin β (1 μM) for different times using RT-qPCR analysis. **(C)** The expression of the stemness-related proteins and CD44 was detected by Western Blotting in U87-MG cells after treated with anticarin β (1 μM) for different times. Data are presented as mean ± s.d. of three independent experiments conducted in duplicate, $^{*}P < 0.05$ and $^{***}P < 0.001$ *versus* the control group.

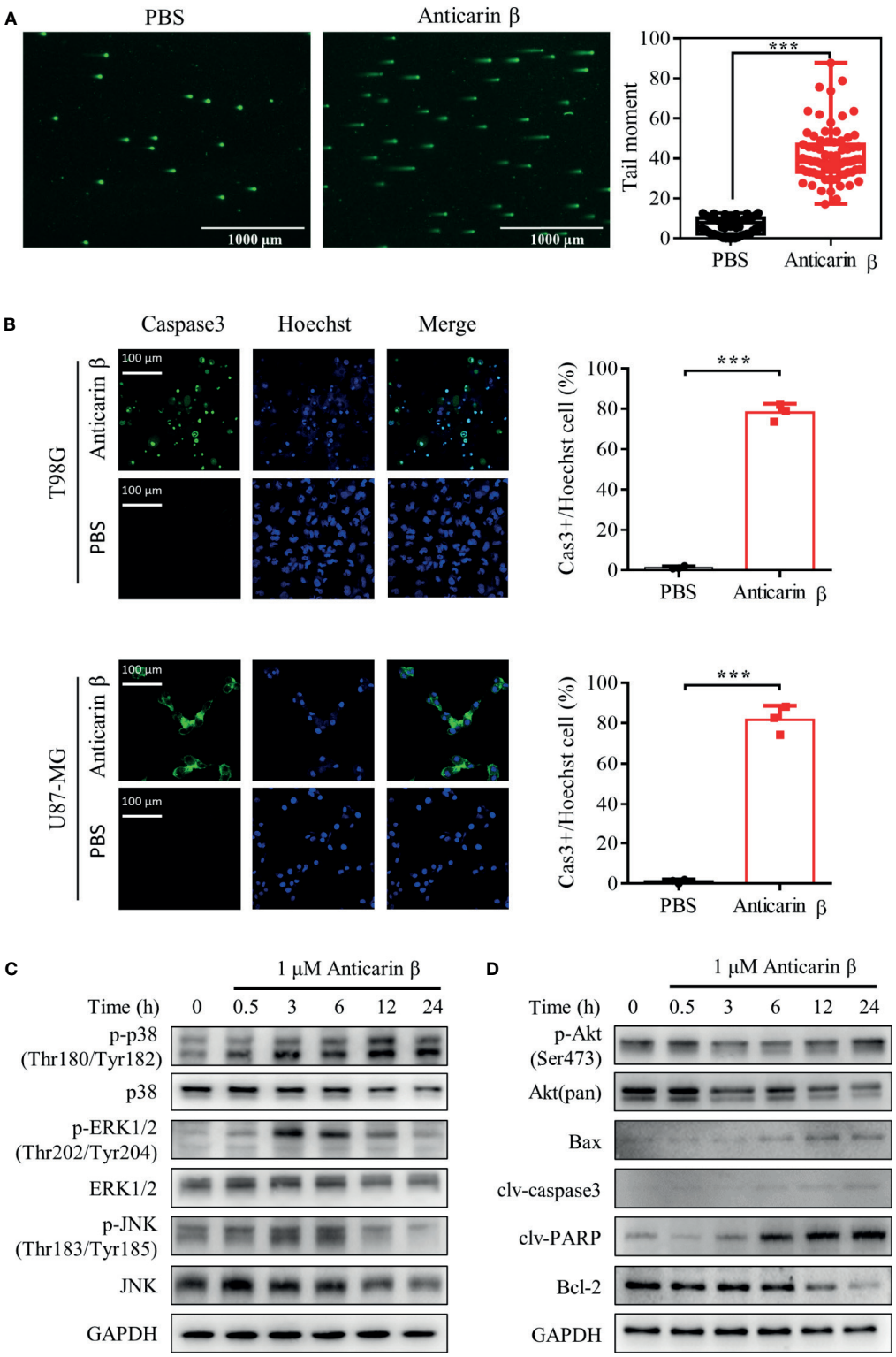

FIGURE 4 | Anticarin β induces apoptosis by DNA damage in human glioma cells. **(A)** The DNA damage in human glioma cell lines U87-MG treated with anticarin β (1 μM) for 12 hours was measured using the neutral comet assay. Scale bar, 1000 μm. **(B)** U87-MG and T98G cells were treated with anticarin β (1 μM) or PBS for 24 hours, followed by fluorescence analysis of caspase 3 probe (green) and Hoechst 33324 (blue). Scale bar, 100 μm. **(C, D)** Western blotting analysis showed the time-dependent effects of anticarin β (1 μM) in U87-MG cells on Akt, MAPKs signal pathways, and apoptotic-related proteins. Data are presented as mean ± s.d. of three independent experiments conducted in duplicate, ***$P < 0.001$ *versus* the control group.

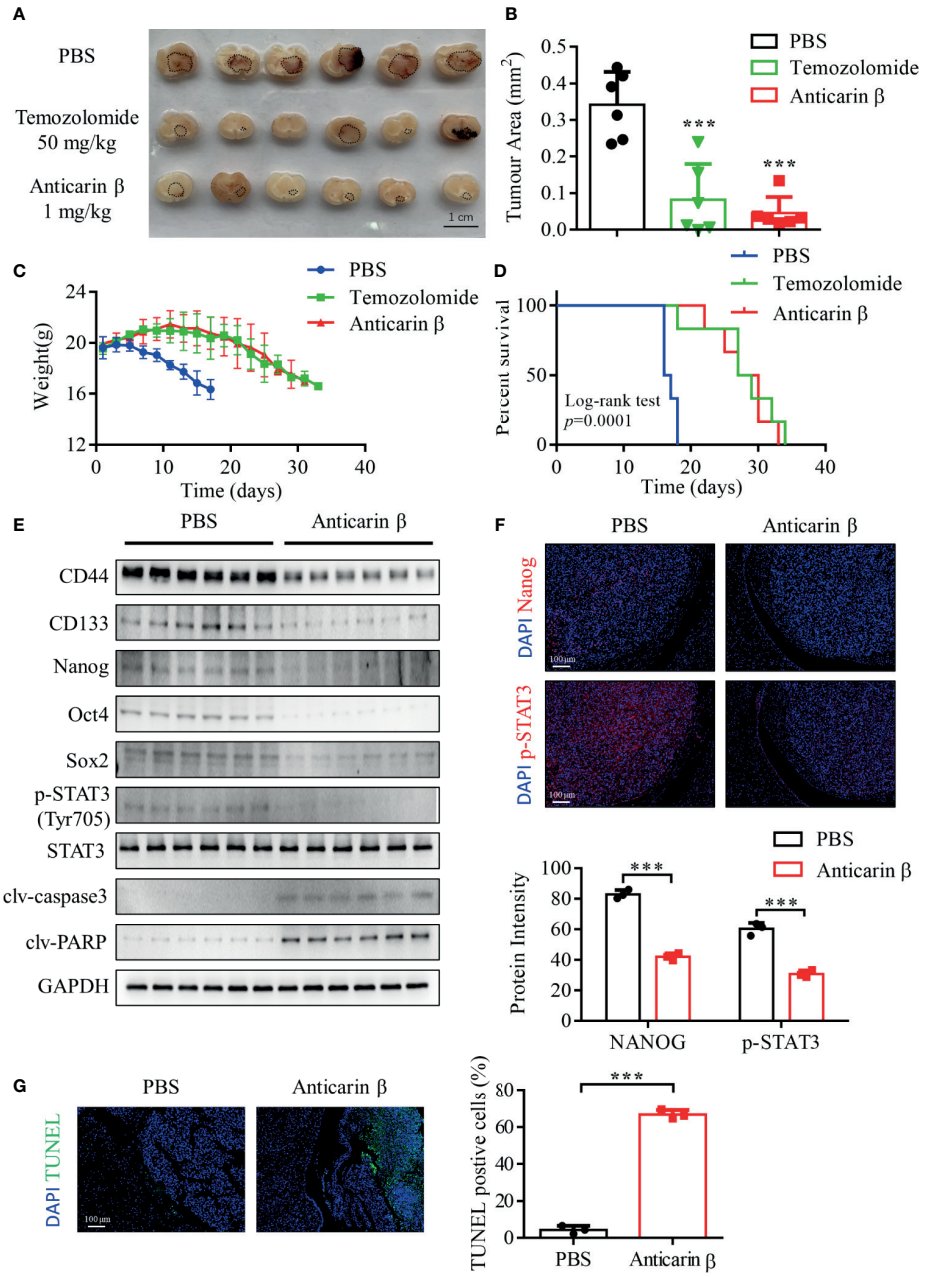

FIGURE 5 | Anticarin β inhibits the tumor growth of the human glioma orthotopic xenograft *in vivo*. U87-MG (2 x 10^5) cells were inoculated in the right hippocampus of NOD/SCID mice. 3 days post inject, the intracranial administration of PBS or anticarin β (1 mg/kg) using Alzet Osmotic Pumps was started on animals each day, and the intragastric administration of temozolomide (TMZ) (50 mg/kg) was started on animals once. All mice were used *in vivo* research after death. The tumor area was measured by brain sections, tumor areas are highlighted in black circles on the brain sections **(A, B)**, and the comparison of weight and Kaplan-Meier curves among each group is presented **(C, D)**. **(E)** Tumor samples were collected, and protein was extracted for western blot analysis. Stemness-related proteins and apoptosis proteins were detected, with GAPDH used as control. **(F)** Tumors were subjected to immunofluorescent stain and the level of Nanog and p-STAT3 was evaluated. Cells were stained for the DAPI (blue), Nanog (red), p-STAT3 (red). Scale bar, 100 μm. **(G)** Tumors were subjected to TUNEL assay and the percentage of TUNEL-positive cells were calculated. Data represent mean ± s.d. N = 6. ***$P < 0.001$ *versus* the Control group.

Anticarin β, a coumarin derivative isolated from the bark of *Antiaris toxicaria Lesch*, has been reported to have potential anticancer activities (14). However, the molecular mechanisms underlying anticarin β-mediated suppression of tumors remain poorly understood. In this study, we determined the anticancer effector and associated mechanisms of anticarin β on human glioma cell lines *in vitro*. With the concentrations used in our study, anticarin β effectively suppressed the proliferation of human

glioma cell lines (U87-MG and T98G) in a dose-dependent manner and showed no significant cytotoxicity to mouse neural stem cells. Additionally, our study indicated that anticarin β could suppress the migration, invasion, and proliferation of human glioma. *In vivo*, anticarin β had no obvious systemic toxicity, dramatically reduced tumor growth, and prolong overall survival duration. However, as for its specific adverse effects on mice, further study is still necessary for the future.

Stemness, initially defined by the expression of stem cell genes, is a property shared by embryonic stem cells and adult stem cells (7, 29). Glioma stem cell markers differentially expressed on glioma stem cells and functionally associated with the maintenance of glioma stem cells are ideal targets for glioma stem cells (6, 30). CD133, one of the earliest stem-cell surface markers, is essential for glioma stem cell maintenance and neurosphere formation. It is also an indicator of resistance to conventional therapy (31). CD44 is cancer stem cell marker and critical player in regulating self-renewal, tumor initiation, metastasis, and chemoradio-resistance (22). Some transcriptional factors with well-recognized functions in embryonic development, such as Nanog, Oct4, Sox2, STAT3, have been identified as oncogenic drivers which can affect the fate of glioma stem cells and regulation of glioma development (32). In addition to different gene expressions, stemness can be measured by a cell's ability to form spheres (33). In our study, we found that anticarin β inhibits clonal spheres forming in human glioma cells and reduces the expression of stemness-related markers, such as Nanog, Oct4, Sox2, CD133, STAT3, and CD44. Besides, anticarin β suppresses stemness-related protein expression in tumor model. These data indicated that anticarin β could inhibit cancer stemness by modulating the expression of several stemness-related genes.

Apoptosis is modulated by death receptors and death factors, to control cell proliferation and a reaction to cell injury. Tumorigenesis includes the occurrence of an imbalance between cell proliferation and apoptotic cell death, leading to the escape of apoptosis and over-proliferation. DNA damage can result in genomic instability, apoptosis, cell cycle checkpoint alteration, or postmitotic death (1, 34, 35). Signaling through MAPKs, Akt, STAT3 are known to play important role in various cell functions in gliomas, such as cell proliferation, angiogenesis, apoptosis, inflammation, oncogenesis, and differentiation (25, 36–43). Previous studies have shown that STAT3 promotes cell proliferation and inhibits apoptosis by increasing the expression of oncogenes, including survivin, c-Myc, Bcl-2 (44). The pro- or anti- apoptotic effects of MAPK activation depend on the duration of the signal. Persistent activation of JNK, p38, and ERK1/2 induce apoptosis (24, 25, 45, 46). In this study, our data demonstrated that anticarin β can induce DNA damage and apoptosis in human glioma cells. Western blotting results showed that anticarin β decreased the levels of Bcl-2, and increased the levels of Bax, clv-capase3, and clv-PARP, which indicated apoptosis-induced. Besides, anticarin β significantly decreased the phosphorylation levels of Akt, STAT3, and cause prolonged JNK, p38, ERK1/2 activation. These results demonstrated that the functional importance of the Akt, STAT3, and MAPKs pathways in anticarin β-induced DNA damage and apoptosis in human glioma cells.

In conclusion, our findings above suggested that anticarin β effectively and selectively suppress the growth, proliferation, and stemness of human glioma cells by inducing apoptosis and DNA damage, which likely through modulation of STAT3, Akt, MAPKs pathways, and apoptotic-related proteins. In the human glioma orthotopic xenograft models, administration of anticarin β exhibited obvious anti-cancer activity. Furthermore, anticarin β with low cytotoxicity has the potential to be a promising compound to prevent human glioma tumorigenesis. The anti-tumor effect of anticarin β against glioma could be combined with other FDA-approved DNA-damaging anti-cancer drugs in future studies.

DATA AVAILABILITY STATEMENT

The raw data supporting the conclusions of this article will be made available by the authors, without undue reservation. The original data is available at Mendeley Data (https://doi.org/10.17632/fhw7ff6gd3.1).

ETHICS STATEMENT

The animal study was reviewed and approved by Committee of Kunming Institute of Zoology, Chinese Academy of Sciences (authorization number: SMKX-2021-03-013).

AUTHOR CONTRIBUTIONS

Conception and design: MZ, GW, and RL. Development of methodology: MZ, XZ, GW, and RL. Acquisition of data (provided animals, provided facilities, etc.): MZ, ZD, GW, and RL. Analysis and interpretation of data (e.g., statistical analysis): MZ, DZ, and GW. Writing, review, and/or revision of the manuscript: MZ, GW, and RL. Administrative, technical, or material support (i.e., reporting or organizing data, constructing databases): MZ, GW, and RL. Study supervision: GW and RL. All authors contributed to the article and approved the submitted version.

FUNDING

This work was supported by funding from National Natural Science Foundation of China (81903666), Science and Technology Department of Yunnan Province (202101AT070301, 202002AA100007, and 2019ZF003).

SUPPLEMENTARY MATERIAL

The Supplementary Material for this article can be found online at: https://www.frontiersin.org/articles/10.3389/fonc.2021.715673/full#supplementary-material

REFERENCES

1. Guo Z, Guozhang H, Wang H, Li Z, Liu N. Ampelopsin Inhibits Human Glioma Through Inducing Apoptosis and Autophagy Dependent on ROS Generation and JNK Pathway. *BioMed Pharmacother* (2019) 116:108524. doi: 10.1016/j.biopha.2018.12.136
2. Kim JH, Bae Kim Y, Han JH, Cho KG, Kim SH, Sheen SS, et al. Pathologic Diagnosis of Recurrent Glioblastoma: Morphologic, Immunohistochemical, and Molecular Analysis of 20 Paired Cases. *Am J Surg Pathol* (2012) 36 (4):620–8. doi: 10.1097/PAS.0b013e318246040c
3. Liu Y, Shete S, Hosking F, Robertson L, Houlston R, Bondy M. Genetic Advances in Glioma: Susceptibility Genes and Networks. *Curr Opin Genet Dev* (2010) 20(3):239–44. doi: 10.1016/j.gde.2010.02.001
4. Janbazian L, Karamchandani J, Das S. Mouse Models of Glioblastoma: Lessons Learned and Questions to be Answered. *J Neurooncol* (2014) 118 (1):1–8. doi: 10.1007/s11060-014-1401-x
5. Li Y, Rogoff HA, Keates S, Gao Y, Murikipudi S, Mikule K, et al. Suppression of Cancer Relapse and Metastasis by Inhibiting Cancer Stemness. *Proc Natl Acad Sci U S A* (2015) 112(6):1839–44. doi: 10.1073/pnas.1424171112
6. Codrici E, Enciu AM, Popescu ID, Mihai S, Tanase C. Glioma Stem Cells and Their Microenvironments: Providers of Challenging Therapeutic Targets. *Stem Cells Int* (2016) 2016:5728438. doi: 10.1155/2016/5728438
7. Lathia JD, Mack SC, Mulkearns-Hubert EE, Valentim CL, Rich JN. Cancer Stem Cells in Glioblastoma. *Genes Dev* (2015) 29(12):1203–17. doi: 10.1101/gad.261982.115
8. Beier D, Schriefer B, Brawanski K, Hau P, Weis J, Schulz JB, et al. Efficacy of Clinically Relevant Temozolomide Dosing Schemes in Glioblastoma Cancer Stem Cell Lines. *J Neurooncol* (2012) 109(1):45–52. doi: 10.1007/s11060-012-0878-4
9. Chen J, Li Y, Yu TS, McKay RM, Burns DK, Kernie SG, et al. A Restricted Cell Population Propagates Glioblastoma Growth After Chemotherapy. *Nature* (2012) 488(7412):522–6. doi: 10.1038/nature11287
10. Lathia JD, Gallagher J, Myers JT, Li M, Vasanji A, McLendon RE, et al. Direct In Vivo Evidence for Tumor Propagation by Glioblastoma Cancer Stem Cells. *PloS One* (2011) 6(9):e24807. doi: 10.1371/journal.pone.0024807
11. Ma Q, Long W, Xing C, Chu J, Luo M, Wang HY, et al. Cancer Stem Cells and Immunosuppressive Microenvironment in Glioma. *Front Immunol* (2018) 9:2924. doi: 10.3389/fimmu.2018.02924
12. Bao S, Wu Q, McLendon RE, Hao Y, Shi Q, Hjelmeland AB, et al. Glioma Stem Cells Promote Radioresistance by Preferential Activation of the DNA Damage Response. *Nature* (2006) 444(7120):756–60. doi: 10.1038/nature05236
13. Chinese Glioma Cooperative Group (CGCG) and Chinese Glioma Atlas (CGGA). Chinese Glioma Molecular Guidelines. *Chin J Neurosurgery* (2014) 30(5):435–44. doi: 10.3760/cma.j.issn.1001-2346.2014.05.002
14. Shi LS, Kuo SC, Sun HD, Morris-Natschke SL, Lee KH, Wu TS. Cytotoxic Cardiac Glycosides and Coumarins From Antiaris Toxicaria. *Bioorg Med Chem* (2014) 22(6):1889–98. doi: 10.1016/j.bmc.2014.01.052
15. Cerqueira AFR, Almodovar VAS, Neves M, Tome AC. Coumarin-Tetrapyrrolic Macrocycle Conjugates: Synthesis and Applications. *Molecules* (2017) 22(6):994. doi: 10.3390/molecules22060994
16. Jia C, Zhang J, Yu L, Wang C, Yang Y, Rong X, et al. Antifungal Activity of Coumarin Against Candida Albicans Is Related to Apoptosis. *Front Cell Infect Microbiol* (2018) 8:445. doi: 10.3389/fcimb.2018.00445
17. Musa MA, Badisa VL, Latinwo LM, Patterson TA, Owens MA. Coumarin-Based Benzopyranone Derivatives Induced Apoptosis in Human Lung (A549) Cancer Cells. *Anticancer Res* (2012) 32(10):4271–6. doi: 10.1016/j.soc.2012.07.009
18. Mukherjee A, Ghosh S, Sarkar R, Samanta S, Ghosh S, Pal M, et al. Synthesis, Characterization and Unravelling the Molecular Interaction of New Bioactive 4-Hydroxycoumarin Derivative With Biopolymer: Insights From Spectroscopic and Theoretical Aspect. *J Photochem Photobiol B* (2018) 189:124–37. doi: 10.1016/j.jphotobiol.2018.10.003
19. Gaspar A, Matos MJ, Garrido J, Uriarte E, Borges F. Chromone: A Valid Scaffold in Medicinal Chemistry. *Chem Rev* (2014) 114(9):4960–92. doi: 10.1021/cr400265z
20. Yu H, Hou Z, Yang X, Mou Y, Guo C. Design, Synthesis, and Mechanism of Dihydroartemisinin(-)Coumarin Hybrids as Potential Anti-Neuroinflammatory Agents. *Molecules* (2019) 24(9):1672. doi: 10.3390/molecules24091672
21. Lu Y, Liu Y, Yang C. Evaluating In Vitro DNA Damage Using Comet Assay. *J Vis Exp* (2017) 128):56450. doi: 10.3791/56450
22. Yan Y, Zuo X, Wei D. Concise Review: Emerging Role of CD44 in Cancer Stem Cells: A Promising Biomarker and Therapeutic Target. *Stem Cells Transl Med* (2015) 4(9):1033–43. doi: 10.5966/sctm.2015-0048
23. Huang RX, Zhou PK. DNA Damage Response Signaling Pathways and Targets for Radiotherapy Sensitization in Cancer. *Signal Transduct Target Ther* (2020) 5(1):60. doi: 10.1038/s41392-020-0150-x
24. Ki YW, Park JH, Lee JE, Shin IC, Koh HC. JNK and P38 MAPK Regulate Oxidative Stress and the Inflammatory Response in Chlorpyrifos-Induced Apoptosis. *Toxicol Lett* (2013) 218(3):235–45. doi: 10.1016/j.toxlet.2013.02.003
25. Yue J, Lopez JM. Understanding MAPK Signaling Pathways in Apoptosis. *Int J Mol Sci* (2020) 21(7):2346. doi: 10.3390/ijms21072346
26. Huang YH, Sun Y, Huang FY, Li YN, Wang CC, Mei WL, et al. Toxicarioside O Induces Protective Autophagy in a Sirtuin-1-Dependent Manner in Colorectal Cancer Cells. *Oncotarget* (2017) 8(32):52783–91. doi: 10.18632/oncotarget.17189
27. Zhao HG, Zhou SL, Lin YY, Wang H, Dai HF, Huang FY. Autophagy Plays a Protective Role Against Apoptosis Induced by Toxicarioside N Via the Akt/mTOR Pathway in Human Gastric Cancer SGC-7901 Cells. *Arch Pharm Res* (2018) 41(10):986–94. doi: 10.1007/s12272-018-1049-8
28. Gezici S, Sekeroglu N. Current Perspectives in the Application of Medicinal Plants Against Cancer: Novel Therapeutic Agents. *Anticancer Agents Med Chem* (2019) 19(1):101–11. doi: 10.2174/1871520619666181224121004
29. Van Pham P. Stem Cells and Cancer Stem Cells. In: PV Pham, editor. *Breast Cancer Stem Cells & Therapy Resistance*. Cham: Springer International Publishing (2015). p. 5–24. doi: 10.1007/978-3-319-22020-8_2
30. Huang Z, Cheng L, Guryanova OA, Wu Q, Bao S. Cancer Stem Cells in Glioblastoma—Molecular Signaling and Therapeutic Targeting. *Protein Cell* (2010) 1(7):638–55. doi: 10.1007/s13238-010-0078-y
31. Brescia P, Ortensi B, Fornasari L, Levi D, Broggi G, Pelicci G. CD133 is Essential for Glioblastoma Stem Cell Maintenance. *Stem Cells* (2013) 31 (5):857–69. doi: 10.1002/stem.1317
32. Suva ML, Rheinbay E, Gillespie SM, Patel AP, Wakimoto H, Rabkin SD, et al. Reconstructing and Reprogramming the Tumor-Propagating Potential of Glioblastoma Stem-Like Cells. *Cell* (2014) 157(3):580–94. doi: 10.1016/j.cell.2014.02.030
33. Chen SF, Chang YC, Nieh S, Liu CL, Yang CY, Lin YS. Nonadhesive Culture System as a Model of Rapid Sphere Formation With Cancer Stem Cell Properties. *PloS One* (2012) 7(2):e31864. doi: 10.1371/journal.pone.0031864
34. Gourlay CW, Ayscough KR. The Actin Cytoskeleton: A Key Regulator of Apoptosis and Ageing? *Nat Rev Mol Cell Biol* (2005) 6(7):583–9. doi: 10.1038/nrm1682
35. Song W, Kwak HB, Lawler JM. Exercise Training Attenuates Age-Induced Changes in Apoptotic Signaling in Rat Skeletal Muscle. *Antioxid Redox Signal* (2006) 8(3-4):517–28. doi: 10.1089/ars.2006.8.517
36. Katanasaka Y, Kodera Y, Kitamura Y, Morimoto T, Tamura T, Koizumi F. Epidermal Growth Factor Receptor Variant Type III Markedly Accelerates Angiogenesis and Tumor Growth Via Inducing C-Myc Mediated Angiopoietin-Like 4 Expression in Malignant Glioma. *Mol Cancer* (2013) 12(1):31. doi: 10.1186/1476-4598-12-31
37. O'Neill LA, Hardie DG. Metabolism of Inflammation Limited by AMPK and Pseudo-Starvation. *Nature* (2013) 493(7432):346–55. doi: 10.1038/nature11862
38. Rodriguez EF, Scheithauer BW, Giannini C, Rynearson A, Cen L, Hoesley B, et al. PI3K/AKT Pathway Alterations Are Associated With Clinically Aggressive and Histologically Anaplastic Subsets of Pilocytic Astrocytoma. *Acta Neuropathol* (2011) 121(3):407–20. doi: 10.1007/s00401-010-0784-9
39. Xiang T, Jia Y, Sherris D, Li S, Wang H, Lu D, et al. Targeting the Akt/mTOR Pathway in Brca1-Deficient Cancers. *Oncogene* (2011) 30(21):2443–50. doi: 10.1038/onc.2010.603
40. Fathi N, Rashidi G, Khodadadi A, Shahi S, Sharifi S. STAT3 and Apoptosis Challenges in Cancer. *Int J Biol Macromol* (2018) 117:993–1001. doi: 10.1016/j.ijbiomac.2018.05.121
41. Fresno Vara JA, Casado E, de Castro J, Cejas P, Belda-Iniesta C, Gonzalez-Baron M. PI3K/Akt Signalling Pathway and Cancer. *Cancer Treat Rev* (2004) 30(2):193–204. doi: 10.1016/j.ctrv.2003.07.007

42. Guo YJ, Pan WW, Liu SB, Shen ZF, Xu Y, Hu LL. ERK/MAPK Signalling Pathway and Tumorigenesis. *Exp Ther Med* (2020) 19(3):1997–2007. doi: 10.3892/etm.2020.8454
43. Rezatabar S, Karimian A, Rameshknia V, Parsian H, Majidinia M, Kopi TA, et al. RAS/MAPK Signaling Functions in Oxidative Stress, DNA Damage Response and Cancer Progression. *J Cell Physiol* (2019) 234(9):14951–65. doi: 10.1002/jcp.28334
44. Qin JJ, Yan L, Zhang J, Zhang WD. STAT3 as a Potential Therapeutic Target in Triple Negative Breast Cancer: A Systematic Review. *J Exp Clin Cancer Res* (2019) 38(1):195. doi: 10.1186/s13046-019-1206-z
45. Ventura JJ, Hubner A, Zhang C, Flavell RA, Shokat KM, Davis RJ. Chemical Genetic Analysis of the Time Course of Signal Transduction by JNK. *Mol Cell* (2006) 21(5):701–10. doi: 10.1016/j.molcel.2006.01.018
46. Cagnol S, Chambard JC. ERK and Cell Death: Mechanisms of ERK-induced Cell Death–Apoptosis, Autophagy and Senescence. *FEBS J* (2010) 277(1):2–21. doi: 10.1111/j.1742-4658.2009.07366.x

Conflict of Interest: The authors declare that the research was conducted in the absence of any commercial or financial relationships that could be construed as a potential conflict of interest.

Publisher's Note: All claims expressed in this article are solely those of the authors and do not necessarily represent those of their affiliated organizations, or those of the publisher, the editors and the reviewers. Any product that may be evaluated in this article, or claim that may be made by its manufacturer, is not guaranteed or endorsed by the publisher.

frontiers in Pharmacology

ORIGINAL RESEARCH
published: 23 August 2021
doi: 10.3389/fphar.2021.746067

ACNPD: The Database for Elucidating the Relationships Between Natural Products, Compounds, Molecular Mechanisms, and Cancer Types

Xiaojie Tan[1,2,3†], *Jiahui Fu*[2†], *Zhaoxin Yuan*[1†], *Lingjuan Zhu*[1,2*] *and Leilei Fu*[1*]

[1]School of Life Science and Engineering, Southwest Jiaotong University, Chengdu, China, [2]Key Laboratory of Structure-Based Drug Design and Discovery of Ministry of Education, School of Traditional Chinese Materia Medica, Shenyang Pharmaceutical University, Shenyang, China, [3]MOE Key Laboratory of Protein Sciences, Beijing Advanced Innovation Center for Structural Biology, Beijing Frontier Research Center for Biological Structure, Department of Basic Medical Sciences, School of Medicine, Tsinghua University, Beijing, China

OPEN ACCESS

Edited by:
Haiyang Yu,
Tianjin University of Traditional Chinese Medicine, China

Reviewed by:
Xiaoxiao Huang,
Shenyang Pharmaceutical University, China
Xj He,
Guangdong Pharmaceutical University, China
Yan Shen,
Nanjing University, China

***Correspondence:**
Leilei Fu
leilei_fu@163.com
Lingjuan Zhu
zhulingjuanadele@163.com

[†]These authors have contributed equally to this work

Specialty section:
This article was submitted to Pharmacology of Anti-Cancer Drugs, a section of the journal Frontiers in Pharmacology

Received: 23 July 2021
Accepted: 10 August 2021
Published: 23 August 2021

Citation:
Tan X, Fu J, Yuan Z, Zhu L and Fu L (2021) ACNPD: The Database for Elucidating the Relationships Between Natural Products, Compounds, Molecular Mechanisms, and Cancer Types. Front. Pharmacol. 12:746067. doi: 10.3389/fphar.2021.746067

Objectives: Cancer is well-known as a collection of diseases of uncontrolled proliferation of cells caused by mutated genes which are generated by external or internal factors. As the mechanisms of cancer have been constantly revealed, including cell cycle, proliferation, apoptosis and so on, a series of new emerging anti-cancer drugs acting on each stage have also been developed. It is worth noting that natural products are one of the important sources for the development of anti-cancer drugs. To the best of our knowledge, there is not any database summarizing the relationships between natural products, compounds, molecular mechanisms, and cancer types.

Materials and methods: Based upon published literatures and other sources, we have constructed an anti-cancer natural product database (ACNPD) (http://www.acnpd-fu.com/). The database currently contains 521 compounds, which specifically refer to natural compounds derived from traditional Chinese medicine plants (derivatives are not considered herein). And, it includes 1,593 molecular mechanisms/signaling pathways, covering 10 common cancer types, such as breast cancer, lung cancer and cervical cancer.

Results: Integrating existing data sources, we have obtained a large amount of information on natural anti-cancer products, including herbal sources, regulatory targets and signaling pathways. ACNPD is a valuable online resource that illustrates the complex pharmacological relationship between natural products and human cancers.

Abbreviations: ACNPD, Anti-cancer natural product database; AP-1, activating protein-1; GRP78, Glucose regulated protein 78; HDAC, Histone deacetylase; IUPAC, International Union of Pure and Applied Chemistry chemical nomenclature; JNK, c-Jun N-terminal kinase; mTOR, mammalian target of rapamycin; MMP, matrix metalloprotein; MMP-9, Matrix metalloprotein 9; PI3K, phosphatidylinositol 3 kinase; ROS, Reactive oxygen species; STAT3, Signal Transducer and Activator of Transcription 3; TCGA, The Cancer Genome Atlas; TCM database, Traditional Chinese Medicine database; TCM, Traditional Chinese medicine; TCMSP, Traditional Chinese Medicine Systems Pharmacology database and Analysis Platform; TNF-α, Tumor necrosis factor-α; VPS34, vacuolar protein sorting 34.

Conclusion: In summary, ACNPD is crucial for better understanding of the relationships between traditional Chinese medicine (TCM) and cancer, which is not only conducive to expand the influence of TCM, but help to find more new anti-cancer drugs in the future.

Keywords: ACNPD, natural products, pharmacological mechanism, database, cancer

INTRODUCTION

Cancer, with the continuously increasing morbidity and mortality, is the second most deadly disease in the world, which seriously threaten people's life and health. (Fidler et al., 2017). At present, continuous proliferation, invasion and metastasis, angiogenesis and apoptosis resistance have been founded to be closely related to the occurrence and development of cancer (Hisano and Hla, 2019; Wimmer et al., 2020). For example, tumor metastasis is a common process in the development of malignant tumors, in which cancer cells undergo the invasion–metastasis cascade, including five main steps: leaving the primary lesion, passing through blood vessels, spreading through blood circulation and lymphatic circulation, or directly spreading through body cavity, continuing to proliferate and grow in other parts, and eventually forming colonization at a remote site of the body (Mittal, 2018). In this process, occurred autophagy and apoptosis inhibition may equip cancer cells with enhanced ability to divide and proliferate (Dower et al., 2018). In addition, abnormal metabolic and immune escape, as well as changes in the tumor microenvironment, are also considered to be crucial hallmarks of cancer (McGranahan et al., 2017; Counihan et al., 2018; Hinshaw and Shevde, 2019). Currently, many kinds of clinical treatments, including surgery, chemotherapy, radiotherapy, immunotherapy and gene therapy have been applied to treat cancer. (Fesnak et al., 2016; Chen and Mellman, 2017; Chen et al., 2019). However, the limited application scope and severe side effects restrain of above methods make the use of anticancer drugs crucial in treating cancer.

Notably, natural products (referring to natural compounds derived from Traditional Chinese Medicine (TCM) plants and derivatives are not considered herein) constitute an important source of anti-cancer drugs, and about 50% of the anti-cancer drugs currently in use are directly or indirectly derived from natural products, including flavonoids, alkaloids and terpenoids and others (Mondal et al., 2019; Deng et al., 2020; Kopustinskiene et al., 2020). Over the past two decades, a large number of natural anti-cancer products have been extracted, isolated and purified from Chinese herbal medicines. For example, paclitaxel, extracted from the bark of *Taxus chinensis*, is recognized as one of the most potent and broad-spectrum anti-cancer drugs especially for advanced, metastatic ovarian cancer, breast cancer, lung cancer (Abu Samaan et al., 2019; de Goeje et al., 2019; Zhu and Chen, 2019; Lau et al., 2020). Recently, accumulating evidences have shown that compounds derived from natural products could regulate various targets and signaling pathways and displayed great therapeutic potential in cancer. Curcumin, a polyphenolic compound mainly extracted from *Curcuma longa, Curcuma zedoaria and Acorus calamus* L., has been shown to induce autophagy through 5'AMP-activated protein kinase (AMPK) activation, resulting in the degradation of Akt, thereby inhibiting cell proliferation and migration of human breast cancer MDA-MB-231 cells (Guan et al., 2016). Additionally, curcumin induces apoptosis and autophagy in human non-small cell lung cancer A549 cells by inhibiting the phosphatidylinositol 3 kinase (PI3K)/Akt/mammalian target of rapamycin (mTOR) pathway (Liu et al., 2018). Berberine, an isoquinoline alkaloid, induces autophagic cell death in cancer cells by increasing the level of Glucose regulated protein 78 (GRP78) and enhancing its ability to bind to vacuolar protein sorting 34(VPS34) (La et al., 2017). Berberine also inhibits the epithelial mesenchymal transformation of mouse melanoma B16 cells through PI3K/Akt pathway (Kou et al., 2016). Moreover, ursolic acid, isolated from Spreng (bearberry), *Rhododendron hymenanthes* Makino, *Eriobotrya japonica*, etc., plays an anti-cancer role in human ovarian cancer cells through apoptosis induction, cell cycle arrest and down-regulation of PI3K/AKT pathway, which is mediated by reactive oxygen species (Ros) and matrix metalloprotein (MMP). Interestingly, monomer compounds isolated from natural products can also be used as lead compounds for the synthesis of anticancer drugs. Through structural modification, they eventually play an important role in the treatment of many malignant tumors such as breast cancer, cervical cancer and leukemia, and greatly promote the development of new candidate drugs. (Rodrigues et al., 2016; Spradlin et al., 2019; Wang et al., 2019; Patel et al., 2020).

Currently, a few traditional Chinese medicine web servers are available online to facilitate resource search, such as and Traditional Chinese Medicine database (TCM-database) and Traditional Chinese Medicine Systems Pharmacology database and Analysis Platform (TCMSP). However, few databases of natural anti-cancer products have been constructed, and the existing databases only constitute the framework of active ingredient-targets-disease, while no databases holds a systematic summary of the specific mechanism of natural products against cancer. (Zhang et al., 2019). Thus, we have constructed an online database, ACNPD, focusing on the information of compounds (referring to natural compounds derived from Traditional Chinese Medicine (TCM) plants) and their pharmacological mechanisms. ACNPD is expected to help deepen the understanding of the intricate molecular mechanism of natural products in treating cancer, with a view to providing new clues for the development of anticancer drugs.

MATERIALS AND METHODS

Data Collection and Integration

ACNPD is a collection of anti-cancer compounds in traditional Chinese herbal medicine, which can be divided into chemical and

TABLE 1 | Data source.

Data field	Data source	Amount of data
Natural compounds	ChemicalBook, PubMed, PubChem, SciFinder and Reaxys	521
Mechanisms	PubMed, SciFinder and Web of Science	1,593
Diseases	PubMed, SciFinder, TCGA, Text-mining and Web of Science	10

pharmacological parts, especially focusing on the anti-cancer molecular mechanism of natural products. Markedly, considering the variety and complexity of natural products, the pharmacological mechanisms of the compounds in the database are supported not only by systematic *in vivo* and *in vitro* studies, such as targets, signaling pathways, validation of animal models, etc., essential *in vitro* cytotoxicity tests are also included. These information and data come from the related network database and the text mining of the published articles. The names of natural products, IUPAC names, SMILES and CAS numbers were obtained primarily by PubChem (https://pubchem.ncbi.nlm.nih.gov/) and supplemented and verified by ChemicalBook (https://www.chemicalbook.com/) and Reaxys (http://new.reaxys.com). The TCMSP database (http://tcmspw.com/tcmsp.php), the Chemical composition database of natural products in China (pharmdata.ncmi.cn/cnpc/) are used to search and collect herbal sources of natural anticancer products. We retrieved and sorted the pharmacological information of the compounds from a series of databases such as PubMed, SciFinder and Web of Science, and finally integrated them into six categories: inhibition of proliferation, promotion of apoptosis, autophagy, necrosis, inhibition of invasion and molecular mechanism. In brief, ACNPD is a comprehensive, high-quality, freely available database of natural products against cancer (**Table 1**).

Web Server Generation

ACNPD builds Apache network server (version 2.4, The Apache Software Foundation, Wakefield, MA, United States) based on Linux operating system, PHP (Versions 7.1, Zend Technologies, Cupertino, CA, United States) scripting language for MySQL (version 5.1.48-log, Oracle Corporation, Redwood Shores, CA, United States). As the background system of ACNPD database, the system or software used is not only free and open source, but also has good stability and high security. The database interface is built on Web technology, Including CSS (Cascading Style Sheets), HTML (Hypertext Markup Language) and JavaScript (Oracle Corporation, Redwood Shores, CA, United States). Adopt Web server technology to develop and serve Web applications. Currently, the ACNPD database supports retrieval by all major Web browsers.

Web Server Construction and Structure

The integrated anti-cancer natural product data is composed of two main EXCEL tables, which are basic chemical information and pharmacological mechanism, respectively. Name, IUPAC Name, SMILES, CAS number, and Herb source of each compound are included in chemical information. The IUPAC Name is the Name of the International Union of Pure and Applied Chemistry, standardizing the names of all compounds in order to convert them into structural formulas corresponding to natural products. Importantly, information about pharmacological mechanism is the focus of our work, which is classified into six categories, including inhibition of proliferation, induction of apoptosis, autophagy, necrosis, inhibition of invasion. The above data and information are obtained from the network database and text retrieval, with guaranteed accuracy. Of note, the two datasheets can be interchanged by hyperlinking to meet different retrieval needs of users.

RESULTS

The Extracted Information of ACNPD

ACNPD brings together the chemical information and pharmacological mechanism of anti-cancer natural products to elucidate the intricate relationship between anticancer active compounds in herbs and cancers (**Figure 1**). Interestingly, we searched related literatures in PubMed, SciFinder and Web of science by text-mining, and classified the pharmacological contents in detail, focusing on the related target proteins and pathways. By contrast, given the large number of existing databases of compounds, such as PubChem, ChemicalBook and others, the chemical information of natural products in ACNPD provides only basic information, including the IUPAC Name, SMILES, CAS number, and herbal source. Hitherto, a wide variety of cancers have been uncovered. Focusing on the statistical data published by the World Health Organization's International Agency for Research on Cancer (IARC), considering morbidity and mortality, the final 10 cancer types were determined to be included in ACNPD, such as breast, cervical, ovarian, lung, gastric, liver, colorectal, prostate, leukemia, and melanoma. In addition, the 13 common cancers provided by The Cancer Genome Atlas (TCGA) database and the literature search results were also included as a reference condition (**Supplementary Table S1**) (**Figure 2**). Currently, the database contains 521 compounds and most of them show anti-cancer activity against a variety of cancers. For example, berberine, an alkaloid that isolated from herbs such as *Achyranthis Bidentatae radix*; *chelidonii herba*; *Coptidis Rhizoma*, etc., displays activity against 10 cancer cells mentioned above (Zhao et al., 2017; Mohammadlou et al., 2021). Studies have shown that berberine inhibits proliferation of colon cancer cells by inhibiting the Wnt/β-catenin signaling pathway (Wu et al., 2012). In another study, Berberine was found to inhibit TNF-α-induced matrix metalloprotein 9 (MMP-9) and cell invasion through inhibiting activating protein-1 (AP-1) in MDA-MB-231 human breast cancer cells (Kim et al., 2008). Additionally, 153 compounds such as Licoricidin, Limonin and Wogonin have been found to have anti-cancer effects by affecting the corresponding

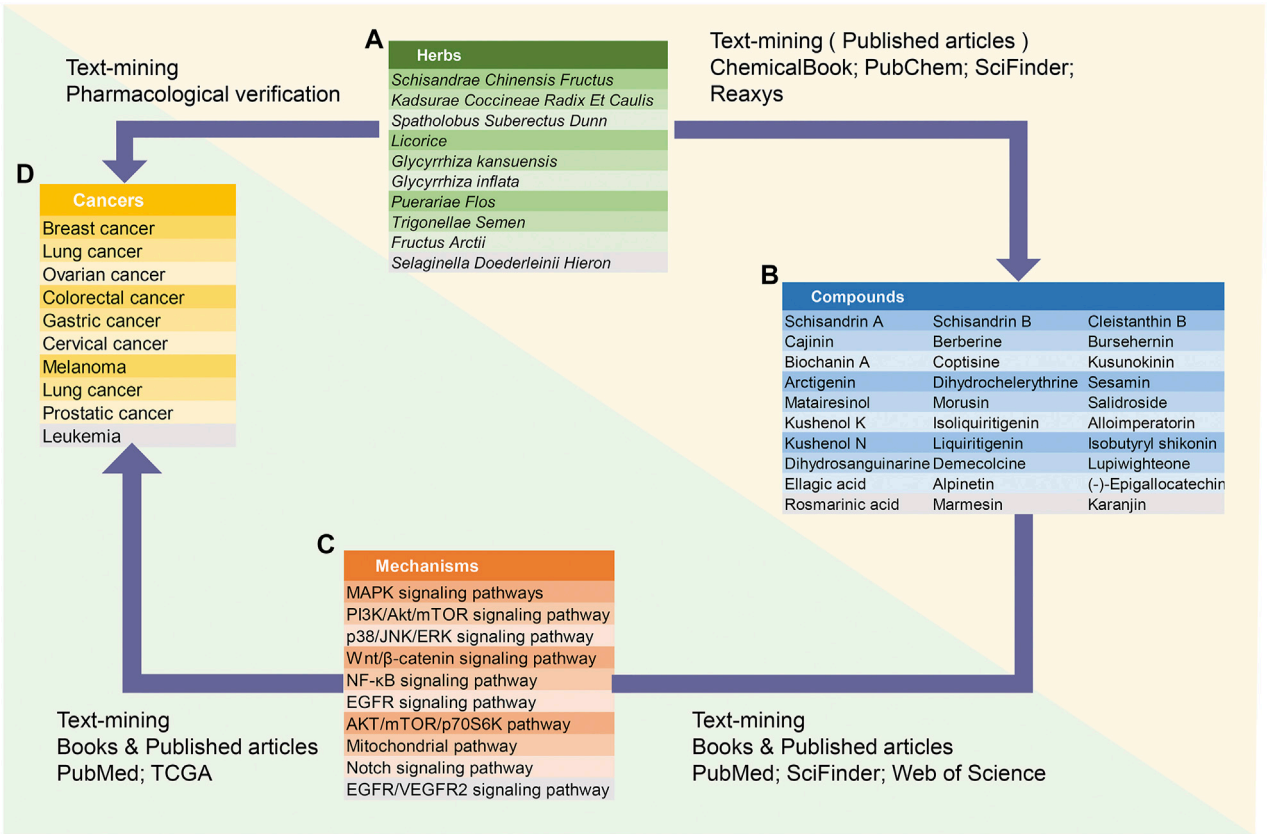

FIGURE 1 | Database structure. ACNPD is composed of compounds, traditional Chinese medicine sources, cancer types, and regulatory mechanisms. The relationship between the four key modules in ACNPD are described. Notably, the yellow triangle area represents the basic chemical information and the green triangle area represents the pharmacological mechanism contents.

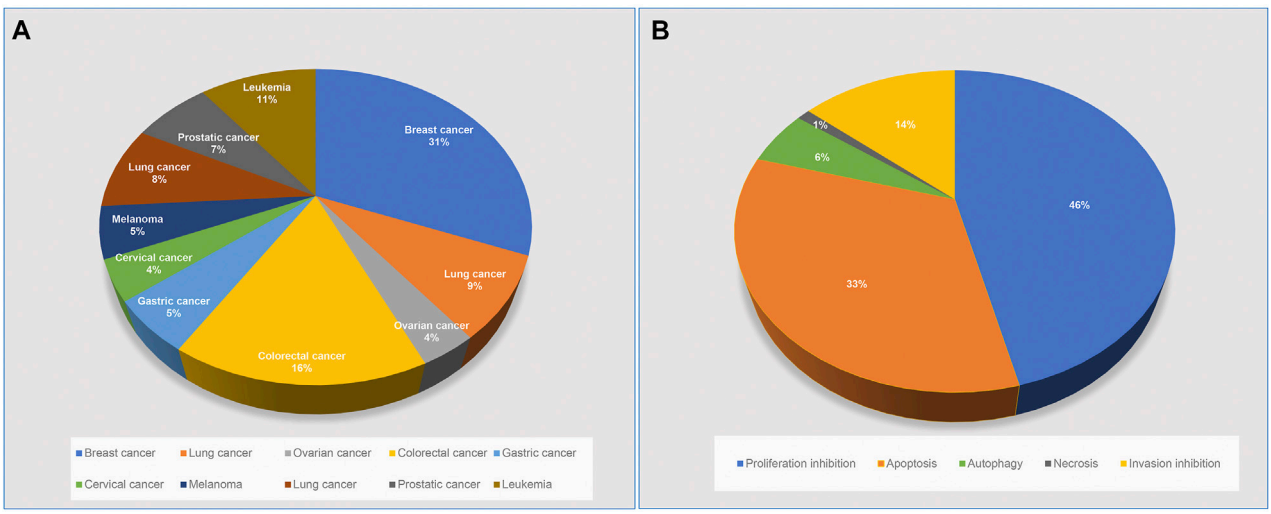

FIGURE 2 | Classification of compounds in the ACNPD. **(A)** Classified by cancer types: 521 compounds derived from natural products were involved in 10 cancer types and percentages, including: Breast, cervical, ovarian, lung, gastric, liver, colorectal, prostate, leukemia and melanoma. **(B)** Classified by pharmacological mechanisms: all compounds are classified into five groups according to text retrieval: proliferation inhibition, apoptosis, autophagy, necrosis, invasion inhibition. Note: Groups are marked with different colors. The percentage of compounds contained in each group is shown in the pie chart.

FIGURE 3 | Interface of ACNPD website. Users can search the database in two ways and query the detailed information through a link. For example, users can query not only by entering a cancer type name (such as Breast cancer) as a keyword, but also by entering the name of a compound from a natural product for field retrieval (e.g., arctigenin). **(A)** Query Home Page; **(B)** Breast cancer Search Result; **(C)** Search Result of Compound Arctigenin; **(D)** Submit Interface.

signaling pathways, mainly involving the Signal Transducer and Activator of Transcription 3 (STAT3) signaling pathway, PI3K/Akt/mTOR signaling, Wnt/β-catenin signaling pathway (Rasul et al., 2012; Ji et al., 2017; Chen et al., 2018). Compounds in ACNPD were subdivided into five categories according to different pharmacological mechanisms, among which 262 compound induced programmed cell death and 109 compound inhibited cell invasion.

Database Query

We built a friendly web interface that allows users to easily search across multiple browsers. Users can obtain the desired results through fuzzy search as follows: 1. Enter the type of cancer (currently limited to the 10 mentioned above), and the results page displays the relevant natural product items with the links to access the basic chemical information and pharmacological mechanism. For example, users can query 164 compounds with anti-breast cancer activity by entering breast cancer. Click the desired compound arbitrarily, and the corresponding database number, Herb source, pharmacological activity and other information will be displayed. 2. Users can use ACNPD to query the mechanism information of natural products. For example, by entering the name of a compound or CAS number, users can obtain the corresponding anticancer mechanism of this compound and intuitively know whether the natural product can inhibit proliferation, inhibit invasion, and

whether it is related to autophagy. The relevant content can be verified by the references we provide for more detailed information. (**Figure 3**).

DISCUSSION

Cancer, also known as malignant tumor, is characterized by cells with abnormal proliferation, which is caused by mutated genes generated by external and internal factors. Hitherto, malignant tumors have been threatening human health in modern society. Recently, with the continuous upgrading of tumor biology and the emergence of drug problems such as anti-cancer drug resistance in clinical use, it is urgent to develop novel anti-cancer drugs. Notably, natural products, with their potent anti-cancer effectiveness and abundant resources, have become the top priority of anti-cancer drug research and development.

Accumulating evidence has indicated that small-molecule compounds derived from natural plant products inhibit cell proliferation, metastasis, and invasion, regulate cell cycle, and induce cell apoptosis in various types of cancer through different targets and signaling pathways. For example, a large group of natural products, flavonoids, display pro-apoptosis effect, with Genistein, which acts on the p53 non-apoptotic pathway, and quercetin, which acts on the cytochrome C pathway. (Safarzadeh et al., 2014; George et al., 2018). Resveratrol inhibits the metastasis of cancer cells by down-regulating the expression of MMP-2, 9 by inhibiting the c-Jun N-terminal kinase (JNK) pathway (Bae et al., 2017). Quercetin, shikonin, and nobiletin are also demonstrated to inhibit cancer metastasis through suppressing MMP. (Jang et al., 2014). In addition, many compounds, including evodiamine, oridonin and jaceosidin, act on the PI3K/Akt pathway, which is a common inflammatory and cancer transformation pathway. Phosphorylation of its substrate GSK-3β can inhibit the translocation of Bax and the degradation of Bcl-2, leading to apoptosis inhibition of cancer cells (Mohan et al., 2016; Woo and Kwon, 2016). Arctigenin, a lignanolids isolated from *Arctium lappa* L. inhibits the angiogenesis through downregulating MMP-2, MMP-9 and heparinase (Lou et al., 2017). In recent years, emerging research suggested that the number and diversity of therapeutic targets in cancer far exceeds the oncogenes identified so far, expanding the understanding of cancer biology and corresponding therapeutic strategies (Hahn et al., 2021). In addition to traditional anti-cancer targets, natural products have also been found to act on several emerging targets, including targeted inhibition of histone deacetylase (HDAC), targeted inhibition of heat shock protein HSP90, targeted glycolysis, and others (Palermo et al., 2005; Yoon and Eom, 2016). Although natural products have unique anti-cancer properties, there is a lag in the construction of relevant mechanism databases, thus, the development of ACNPD has broad application prospects and far-reaching practical significance.

Importantly, ACNPD is an online webserver that provides users with the pharmacological mechanisms of natural anti-cancer products. The database contains 10 common cancer types, 521 compounds, 131 pharmacological pathways, including PI3K/Akt, STAT3, PI3K/Akt/mTOR, Wnt/β-catenin and other signaling pathways. The web interface allows users to query related information in a variety of ways, providing basic chemical information, such as IUPAC Name and CAS number, and detailed pharmacological mechanisms of natural compounds. Importantly, we divided the pharmacological effects in a more detailed way and provided the signaling pathways involved, which is a supplement to the previous database and helps users to obtain information quickly and intuitively. At present, ACNPD only contains 10 common cancer types with high incidence, and the number of compounds remains to be expanded. With the extraction and separation of more natural products and the in-depth study of their pharmacological mechanism, we will continue to expand the scope of cancer and add new natural compounds to update ACNPD.

In summary, we believe that ACNPD is a valuable database to fill the gaps between the therapeutic mechanism and natural anti-cancer products. The database is expected to help study the biological function and pharmacological activity of natural products in cancer, break the development bottleneck between natural anticancer compounds and modern anticancer drugs, and usher in a promising prospect for the innovative anticancer drugs.

DATA AVAILABILITY STATEMENT

The original contributions presented in the study are included in the article/**Supplementary Material**, further inquiries can be directed to the corresponding authors.

AUTHOR CONTRIBUTIONS

XT, JF contributed to conception, design, data interpretation, and drafting of manuscript; ZY contributed to data collection. LF, LZ gave guidance and support to the project. All authors contributed to the article and approved the submitted version.

FUNDING

This work was supported by Natural Science Foundation of China (Grant No. 31970374),Research Foundation for Administration of traditional Chinese Medicine of Sichuan Province (Grant No. 2020HJZX002), and Applied Basic Research Programs of Science and Technology Department of Sichuan Province (Grant No. 2020YJ0285).

ACKNOWLEDGMENTS

We are grateful to **Prof. Haoyang Cai** (Sichuan University) for his critical review on this manuscript.

SUPPLEMENTARY MATERIAL

The Supplementary Material for this article can be found online at: https://www.frontiersin.org/articles/10.3389/fphar.2021.746067/full#supplementary-material

REFERENCES

Abu Samaan, T. M., Samec, M., Liskova, A., Kubatka, P., and Büsselberg, D. (2019). Paclitaxel's Mechanistic and Clinical Effects on Breast Cancer. *Biomolecules* 9 (12). doi:10.3390/biom9120789

Bae, M. J., Karadeniz, F., Oh, J. H., Yu, G. H., Jang, M. S., Nam, K. H., et al. (2017). MMP-inhibitory Effects of Flavonoid Glycosides from Edible Medicinal Halophyte Limonium Tetragonum. *Evid. Based Complement. Alternat Med.* 2017, 6750274. doi:10.1155/2017/6750274

Chen, D. S., and Mellman, I. (2017). Elements of Cancer Immunity and the Cancer-Immune Set point. *Nature* 541 (7637), 321–330. doi:10.1038/nature21349

Chen, L., Wang, J., Wu, J., Zheng, Q., and Hu, J. (2018). Indirubin Suppresses Ovarian Cancer Cell Viabilities through the STAT3 Signaling Pathway. *Drug Des. Devel Ther.* 12, 3335–3342. doi:10.2147/DDDT.S174613

Chen, M., Mao, A., Xu, M., Weng, Q., Mao, J., and Ji, J. (2019). CRISPR-Cas9 for Cancer Therapy: Opportunities and Challenges. *Cancer Lett.* 447, 48–55. doi:10.1016/j.canlet.2019.01.017

Counihan, J. L., Grossman, E. A., and Nomura, D. K. (2018). Cancer Metabolism: Current Understanding and Therapies. *Chem. Rev.* 118 (14), 6893–6923. doi:10.1021/acs.chemrev.7b00775

de Goeje, P. L., Poncin, M., Bezemer, K., Kaijen-Lambers, M. E. H., Groen, H. J. M., Smit, E. F., et al. (2019). Induction of Peripheral Effector CD8 T-Cell Proliferation by Combination of Paclitaxel, Carboplatin, and Bevacizumab in Non-small Cell Lung Cancer Patients. *Clin. Cancer Res.* 25 (7), 2219–2227. doi:10.1158/1078-0432.CCR-18-2243

Deng, L. J., Qi, M., Li, N., Lei, Y. H., Zhang, D. M., and Chen, J. X. (2020). Natural Products and Their Derivatives: Promising Modulators of Tumor Immunotherapy. *J. Leukoc. Biol.* 108 (2), 493–508. doi:10.1002/JLB.3MR0320-444R

Dower, C. M., Wills, C. A., Frisch, S. M., and Wang, H. G. (2018). Mechanisms and Context Underlying the Role of Autophagy in Cancer Metastasis. *Autophagy* 14 (7), 1110–1128. doi:10.1080/15548627.2018.1450020

Fesnak, A. D., June, C. H., and Levine, B. L. (2016). Engineered T Cells: the Promise and Challenges of Cancer Immunotherapy. *Nat. Rev. Cancer* 16 (9), 566–581. doi:10.1038/nrc.2016.97

Fidler, M. M., Gupta, S., Soerjomataram, I., Ferlay, J., Steliarova-Foucher, E., and Bray, F. (2017). Cancer Incidence and Mortality Among Young Adults Aged 20-39 Years Worldwide in 2012: a Population-Based Study. *Lancet Oncol.* 18 (12), 1579–1589. doi:10.1016/S1470-2045(17)30677-0

George, A., Raji, I., Cinar, B., Kucuk, O., and Oyelere, A. K. (2018). Design, Synthesis, and Evaluation of the Antiproliferative Activity of Hydantoin-Derived Antiandrogen-Genistein Conjugates. *Bioorg. Med. Chem.* 26 (8), 1481–1487. doi:10.1016/j.bmc.2018.01.009

Guan, F., Ding, Y., Zhang, Y., Zhou, Y., Li, M., and Wang, C. (2016). Curcumin Suppresses Proliferation and Migration of MDA-MB-231 Breast Cancer Cells through Autophagy-dependent Akt Degradation. *PloS one* 11 (1), e0146553. doi:10.1371/journal.pone.0146553

Hahn, W. C., Bader, J. S., Braun, T. P., Califano, A., Clemons, P. A., Druker, B. J., et al. (2021). An Expanded Universe of Cancer Targets. *Cell* 184 (5), 1142–1155. doi:10.1016/j.cell.2021.02.020

Hinshaw, D. C., and Shevde, L. A. (2019). The Tumor Microenvironment Innately Modulates Cancer Progression. *Cancer Res.* 79 (18), 4557–4566. doi:10.1158/0008-5472.CAN-18-3962

Hisano, Y., and Hla, T. (2019). Bioactive Lysolipids in Cancer and Angiogenesis. *Pharmacol. Ther.* 193, 91–98. doi:10.1016/j.pharmthera.2018.07.006

Jang, S. Y., Lee, J. K., Jang, E. H., Jeong, S. Y., and Kim, J. H. (2014). Shikonin Blocks Migration and Invasion of Human Breast Cancer Cells through Inhibition of Matrix Metalloproteinase-9 Activation. *Oncol. Rep.* 31 (6), 2827–2833. doi:10.3892/or.2014.3159

Ji, S., Tang, S., Li, K., Li, Z., Liang, W., Qiao, X., et al. (2017). Licoricidin Inhibits the Growth of SW480 Human Colorectal Adenocarcinoma Cells *In Vitro* and *In Vivo* by Inducing Cycle Arrest, Apoptosis and Autophagy. *Toxicol. Appl. Pharmacol.* 326, 25–33. doi:10.1016/j.taap.2017.04.015

Kim, S., Choi, J. H., Kim, J. B., Nam, S. J., Yang, J. H., Kim, J. H., et al. (2008). Berberine Suppresses TNF-Alpha-Induced MMP-9 and Cell Invasion through Inhibition of AP-1 Activity in MDA-MB-231 Human Breast Cancer Cells. *Molecules* 13 (12), 2975–2985. doi:10.3390/molecules13122975

Kopustinskiene, D. M., Jakstas, V., Savickas, A., and Bernatoniene, J. (2020). Flavonoids as Anticancer Agents. *Nutrients* 12 (2). doi:10.3390/nu12020457

Kou, Y., Li, L., Li, H., Tan, Y., Li, B., Wang, K., et al. (2016). Berberine Suppressed Epithelial Mesenchymal Transition through Cross-Talk Regulation of PI3K/AKT and RARα/RARβ in Melanoma Cells. *Biochem. Biophys. Res. Commun.* 479 (2), 290–296. doi:10.1016/j.bbrc.2016.09.061

La, X., Zhang, L., Li, Z., Yang, P., and Wang, Y. (2017). Berberine-induced Autophagic Cell Death by Elevating GRP78 Levels in Cancer Cells. *Oncotarget* 8 (13), 20909–20924. doi:10.18632/oncotarget.14959

Lau, T. S., Chan, L. K. Y., Man, G. C. W., Wong, C. H., Lee, J. H. S., Yim, S. F., et al. (2020). Paclitaxel Induces Immunogenic Cell Death in Ovarian Cancer via TLR4/IKK2/SNARE-dependent Exocytosis. *Cancer Immunol. Res.* 8 (8), 1099–1111. doi:10.1158/2326-6066.CIR-19-0616

Liu, F., Gao, S., Yang, Y., Zhao, X., Fan, Y., Ma, W., et al. (2018). Antitumor Activity of Curcumin by Modulation of Apoptosis and Autophagy in Human Lung Cancer A549 Cells through Inhibiting PI3K/Akt/mTOR Pathway. *Oncol. Rep.* 39 (3), 1523–1531. doi:10.3892/or.2018.6188

Lou, C., Zhu, Z., Zhao, Y., Zhu, R., and Zhao, H. (2017). Arctigenin, a Lignan from Arctium Lappa L., Inhibits Metastasis of Human Breast Cancer Cells through the Downregulation of MMP-2/-9 and Heparanase in MDA-MB-231 Cells. *Oncol. Rep.* 37 (1), 179–184. doi:10.3892/or.2016.5269

McGranahan, N., Rosenthal, R., Hiley, C. T., Rowan, A. J., Watkins, T. B. K., Wilson, G. A., et al. (2017). Allele-Specific HLA Loss and Immune Escape in Lung Cancer Evolution. *Cell* 171 (6), 1259–e11. e1211. doi:10.1016/j.cell.2017.10.001

Mittal, V. (2018). Epithelial Mesenchymal Transition in Tumor Metastasis. *Annu. Rev. Pathol.* 13, 395–412. doi:10.1146/annurev-pathol-020117-043854

Mohammadlou, M., Abdollahi, M., Hemati, M., Baharlou, R., Doulabi, E. M., Pashaei, M., et al. (2021). Apoptotic Effect of Berberine via Bcl-2, ROR1, and Mir-21 in Patients with B-Chronic Lymphocytic Leukemia. *Phytother Res.* 35 (4), 2025–2033. doi:10.1002/ptr.6945

Mohan, V., Agarwal, R., and Singh, R. P. (2016). A Novel Alkaloid, Evodiamine Causes Nuclear Localization of Cytochrome-C and Induces Apoptosis Independent of P53 in Human Lung Cancer Cells. *Biochem. Biophys. Res. Commun.* 477 (4), 1065–1071. doi:10.1016/j.bbrc.2016.07.037

Mondal, A., Gandhi, A., Fimognari, C., Atanasov, A. G., and Bishayee, A. (2019). Alkaloids for Cancer Prevention and Therapy: Current Progress and Future Perspectives. *Eur. J. Pharmacol.* 858, 172472. doi:10.1016/j.ejphar.2019.172472

Palermo, C. M., Westlake, C. A., and Gasiewicz, T. A. (2005). Epigallocatechin Gallate Inhibits Aryl Hydrocarbon Receptor Gene Transcription through an Indirect Mechanism Involving Binding to a 90 kDa Heat Shock Protein. *Biochemistry* 44 (13), 5041–5052. doi:10.1021/bi047433p

Patel, S. S., Acharya, A., Ray, R. S., Agrawal, R., Raghuwanshi, R., and Jain, P. (2020). Cellular and Molecular Mechanisms of Curcumin in Prevention and Treatment of Disease. *Crit. Rev. Food Sci. Nutr.* 60 (6), 887–939. doi:10.1080/10408398.2018.1552244

Rasul, A., Yu, B., Khan, M., Zhang, K., Iqbal, F., Ma, T., et al. (2012). Magnolol, a Natural Compound, Induces Apoptosis of SGC-7901 Human Gastric Adenocarcinoma Cells via the Mitochondrial and PI3K/Akt Signaling Pathways. *Int. J. Oncol.* 40 (4), 1153–1161. doi:10.3892/ijo.2011.1277

Rodrigues, T., Sieglitz, F., and Bernardes, G. J. (2016). Natural Product Modulators of Transient Receptor Potential (TRP) Channels as Potential Anti-cancer Agents. *Chem. Soc. Rev.* 45 (22), 6130–6137. doi:10.1039/c5cs00916b

Safarzadeh, E., Sandoghchian Shotorbani, S., and Baradaran, B. (2014). Herbal Medicine as Inducers of Apoptosis in Cancer Treatment. *Adv. Pharm. Bull.* 4 (Suppl. 1), 421–427. doi:10.5681/apb.2014.062

Spradlin, J. N., Hu, X., Ward, C. C., Brittain, S. M., Jones, M. D., Ou, L., et al. (2019). Harnessing the Anti-cancer Natural Product Nimbolide for Targeted Protein Degradation. *Nat. Chem. Biol.* 15 (7), 747–755. doi:10.1038/s41589-019-0304-8

Wang, H. Y., Zhang, B., Zhou, J. N., Wang, D. X., Xu, Y. C., Zeng, Q., et al. (2019). Arsenic Trioxide Inhibits Liver Cancer Stem Cells and Metastasis by Targeting SRF/MCM7 Complex. *Cell Death Dis.* 10 (6), 453. doi:10.1038/s41419-019-1676-0

Wimmer, K., Sachet, M., and Oehler, R. (2020). Circulating Biomarkers of Cell Death. *Clin. Chim. Acta* 500, 87–97. doi:10.1016/j.cca.2019.10.003

Woo, S. M., and Kwon, T. K. (2016). Jaceosidin Induces Apoptosis through Bax Activation and Down-Regulation of Mcl-1 and C-FLIP Expression in Human

Renal Carcinoma Caki Cells. *Chem. Biol. Interact* 260, 168–175. doi:10.1016/j.cbi.2016.10.011

Wu, K., Yang, Q., Mu, Y., Zhou, L., Liu, Y., Zhou, Q., et al. (2012). Berberine Inhibits the Proliferation of colon Cancer Cells by Inactivating Wnt/β-Catenin Signaling. *Int. J. Oncol.* 41 (1), 292–298. doi:10.3892/ijo.2012.1423

Yoon, S., and Eom, G. H. (2016). HDAC and HDAC Inhibitor: From Cancer to Cardiovascular Diseases. *Chonnam Med. J.* 52 (1), 1–11. doi:10.4068/cmj.2016.52.1.1

Zhang, Y. F., Huang, Y., Ni, Y. H., and Xu, Z. M. (2019). Systematic Elucidation of the Mechanism of Geraniol via Network Pharmacology. *Drug Des. Devel Ther.* 13, 1069–1075. doi:10.2147/DDDT.S189088

Zhao, Y., Jing, Z., Lv, J., Zhang, Z., Lin, J., Cao, X., et al. (2017). Berberine Activates Caspase-9/cytochrome C-Mediated Apoptosis to Suppress Triple-Negative Breast Cancer Cells *In Vitro* and *In Vivo*. *Biomed. Pharmacother.* 95, 18–24. doi:10.1016/j.biopha.2017.08.045

Zhu, L., and Chen, L. (2019). Progress in Research on Paclitaxel and Tumor Immunotherapy. *Cell Mol. Biol. Lett.* 24, 40. doi:10.1186/s11658-019-0164-y

Conflict of Interest: The authors declare that the research was conducted in the absence of any commercial or financial relationships that could be construed as a potential conflict of interest.

Publisher's Note: All claims expressed in this article are solely those of the authors and do not necessarily represent those of their affiliated organizations, or those of the publisher, the editors and the reviewers. Any product that may be evaluated in this article, or claim that may be made by its manufacturer, is not guaranteed or endorsed by the publisher.

frontiers in Pharmacology

MINI REVIEW
published: 26 August 2021
doi: 10.3389/fphar.2021.748149

Targeting Autophagy with Natural Compounds in Cancer: A Renewed Perspective from Molecular Mechanisms to Targeted Therapy

Qiang Xie[1†], Yi Chen[2†], Huidan Tan[3], Bo Liu[3], Ling-Li Zheng[4]* and Yandong Mu[1]**

[1]Department of Stomatology, Sichuan Provincial People's Hospital, University of Electronic Science and Technology of China, Chengdu, China, [2]Department of Stomatology, Zigong First People's Hospital, Zigong, China, [3]Department of Gastrointestinal Surgery, State Key Laboratory of Biotherapy and Cancer Center, West China Hospital, Sichuan University, Chengdu, China, [4]Department of Pharmacy, The First Affiliated Hospital of Chengdu Medical College, Chengdu, China

OPEN ACCESS

Edited by:
Lu Chen,
Tianjin University of Traditional Chinese Medicine, China

Reviewed by:
Yan Shen,
Nanjing University, China
XJ He,
Guangdong Pharmaceutical University, China

***Correspondence:**
Bo Liu
liubo2400@163.com
Ling-Li Zheng
zhenglingli@cmc.edu.cn
Yandong Mu
muyd@uestc.edu.cn

†These authors have contributed equally to this work

Specialty section:
This article was submitted to Pharmacology of Anti-Cancer Drugs, a section of the journal Frontiers in Pharmacology

Received: 27 July 2021
Accepted: 16 August 2021
Published: 26 August 2021

Citation:
Xie Q, Chen Y, Tan H, Liu B, Zheng L-L and Mu Y (2021) Targeting Autophagy with Natural Compounds in Cancer: A Renewed Perspective from Molecular Mechanisms to Targeted Therapy. Front. Pharmacol. 12:748149. doi: 10.3389/fphar.2021.748149

Natural products are well-characterized to have pharmacological or biological activities that can be of therapeutic benefits for cancer therapy, which also provide an important source of inspiration for discovery of potential novel small-molecule drugs. In the past three decades, accumulating evidence has revealed that natural products can modulate a series of key autophagic signaling pathways and display therapeutic effects in different types of human cancers. In this review, we focus on summarizing some representative natural active compounds, mainly including curcumin, resveratrol, paclitaxel, Bufalin, and Ursolic acid that may ultimately trigger cancer cell death through the regulation of some key autophagic signaling pathways, such as RAS-RAF-MEK-ERK, PI3K-AKT-mTOR, AMPK, ULK1, Beclin-1, Atg5 and p53. Taken together, these inspiring findings would shed light on exploiting more natural compounds as candidate small-molecule drugs, by targeting the crucial pathways of autophagy for the future cancer therapy.

Keywords: autophagy, natural compound, pathway, cancer therapy, small-molecule drug

INTRODUCTION

The term of autophagy was first reported in 1963 (Yang and Klionsky, 2010), with gradually understanding that autophagy plays a role in the regulation of human life activities. Autophagy, through its conservative mechanism, decomposes macromolecules and provides a lot of nutrients, so it plays an irreplaceable role in regulating metabolism and cell growth (Yan et al., 2019). Importantly, autophagy has dual effect on cancers, which may protect cancer cells from extreme nutrient conditions, while it also causes destruction of energy homeostasis and kill cancer cells (Chen et al., 2021). In physiological state, autophagy maintains cell homeostasis by degrading and removing damaged or dead organelles, misfolded proteins and other substances, while abnormal autophagy

Abbreviations: Ambra-1, Activating molecule in Beclin-1-regulated autophagy; AMPK, AMP-activated protein kinase; Atg, Autophagy related genes; Bcl-2, B cell lymphoma/leukemia-2; Bif-1, Bax-interacting factor-1; BRAFV600E, BRAF position 600; CML, Chronic myeloid leukemia; EIF4EBPs, EIF-4E binding proteins; FoxO, Forkhead box O; GEMMs, Genetically engineered mouse tumor models; HDAC, Histone deacetylase; HO-1, Heme oxygenase 1; JNK, c-Jun N-terminal kinase; KRAS, Kirsten rat sarcoma viral oncogene; LEC, Lymphatic endothelial cell; mTOR, mammalian target of rapamycin; p53, protein 53; PI3K, Phosphoinositide 3-kinase; QCT, Quercetin; ROS, Reactive oxygen species; SIMI, Stromal interaction molecule 1; SIRT1, Sirtuin-1; SIRT2, Sirtuin-2; TMZ, Temozolomide; UA, Ursolic acid; VPS34, Vacuolar protein sorting 34.

will break the original balance of cells, and even play a key role in the occurrence and development of cancer (Byun et al., 2017). Herein, a deep understanding of the biological relationship between autophagy and cancer is critical to explore potential targets for cancer treatment and provide new clues for anti-cancer drug development.

As we all know, natural compounds (refer to the small and large molecules extracted and separated from natural products) come from a variety of sources, including plants, animals, and even microbes. For example, curcumin, a diketone compound extracted from the rhizomes of some plants in the family Zingiberaceae and Araceae, and oridonin is a bioactive diterpenoid compound isolated from *Rabdosia* (Iabtea). In addition, there is a secretion from the animal toad - Bufalin. Accumulating evidences have shown that natural compounds play an important role in the treatment of cancer, including inhibiting cancer cell proliferation and inducing apoptosis, as well as inhibiting cancer cell metastasis and angiogenesis (Liu et al., 2019a; Sun et al., 2019; Liu et al., 2020; Kang et al., 2021). More interestingly, in the treatment of tumors, multiple natural compounds are reported to exert therapeutic effect by targeting autophagy (Towers et al., 2020). For example, Resveratrol has been shown to induce protective autophagy and exert anticancer activity in non-small cell lung cancer by inhibiting Akt/mTOR and activating the P38-MAPK pathway (Wang et al., 2018b). Additionally, the antitumor bioactivity of curcumin is achieved by inhibiting PI3K/Akt/mTOR pathway and inducing apoptosis and autophagy of human lung cancer A549 cells (Liu F. et al., 2018).

In different types of tumors, natural compounds induce or inhibit autophagy and thus suppress tumor growth through a variety of different mechanisms of action. Notably, the exact mode of autophagy modulated by natural compounds derived from Mother Nature is highly complex, it needs to be further studied and explored deeply. Therefore, we write this review to clarify the complex biological relationship between natural compounds, autophagy, and cancer, in order to provide new ideas for the development of anticancer drugs.

AUTOPHAGIC PROCESS

Autophagy is a continuous process of dynamic development, mainly including the initial stage, extension stage and mature degradation stage of autophagosome, a bilayer membrane structure which fuses into lysosome, and further form autophagolysosomes to degrade the material encapsulated in it and release it for reuse. The autophagic process is regulated by many factors, and more than 40 autophagy related genes (ATG) and corresponding proteins have been found to participate in autophagy regulation (Chou et al., 2021; Ferreira et al., 2021).

Different from the lower autophagy level under normal physiological conditions, when cells undergo starvations, autophagy may produce intermediate nutrients for cells survival, which was exploit by cancer cells to establish chemoresistance and adapt nutrient depletion. On the contrary, some mutations of oncogenes and epigenic modifications occurring in cancer may negatively regulate autophagic level and suppress carcinogenesis, representing a tumor-suppressive role of autophagy (Morselli et al., 2009; Arroyo et al., 2014). Therefore, autophagy has the dual effects in the promotion and inhibition of cancer with cytotoxic and cytoprotective effects on tumor cells.

The Janus Role of Autophagy in Cancer

Autophagy could promote tumor progression under low-oxygen and low-nutrient conditions. Meanwhile, autophagy may exert a tumor suppressor effect through a variety of mechanisms, so the role of autophagy in cancer development appears to be paradoxical and complex. Depending on different environments, such as tumor type, stage and stress type, autophagy regulates pro-survival or pro-death signaling pathways in cancers (Singh et al., 2018).

At the molecular level, the occurrence and development of tumors involve numerous signaling pathways, and the signaling pathways of autophagy are still emerging, mainly involving protein 53 (p53), B cell lymphoma/leukemia-2 (Bcl-2), Akt, Bax-interacting factor-1 (Bif-1), Ras, mammalian rapamycin target (mTOR) and phosphoinositide 3-kinase (PI3K) I (Khandia et al., 2019). Moreover, these signaling pathways are often associated with each other, and can be integrated into the tumor regulatory network of autophagy related proteins, which ultimately affect the fate of tumor cells (Morselli et al., 2009).

Tumor Suppressive Role of Autophagy

At present, it is generally believed that autophagy that appears in the early stage of tumorigenesis has an inhibitory effect. Spontaneous tumors are found in Beclin-1 ± mouse, indicating that defective autophagy may promote tumorigenesis. In addition, research on Beclin-1, which is a common haploin-sufficient tumor suppressor missing in ovarian, breast and prostate cancers, establishes the first direct functional connection between cancer and autophagy and supports the theory that autophagy can inhibit the formation of initial tumors. In addition, deletions of other several Atg genes besides Beclin-1 have also been found to promote tumorigenesis. For example, systematic deletion of liver-specific Atg7 and Atg5 in mice will lead to an enhancement in the formation rate of liver tumors. These researches on the effect of defective autophagy on cancers using Atgs gene deletion mice support that autophagy suppresses tumor formation in the early stage. In addition, allelic deletion of Beclin-1–interacting proteins, such as Bif-1 and UVRAG also occurs in various cancers, and changes in the expression of them can increase the incidence of spontaneous cancer by altering the autophagy pathway. Beclin-1 synergistically activates lipid kinase vacuolar protein sorting 34 (Vps34) with activating molecule in Beclin-1-regulated autophagy (Ambra-1), Bif-1 and UVRAG to induce autophagy (Brech et al., 2009). However, in the lysosomal degradation pathway of autophagy, it can inhibit tumor function.

Forkhead box O (FOXO) is a key autophagy regulator that regulates cell proliferation and apoptosis by activating autophagy activity. FOXO1 regulated cell death may be related to tumor inhibitory activity (Zhao et al., 2010; Ling et al., 2011). The

expression of tumor suppressor FOXO3a is usually down regulated in cancer (Liu Y. et al., 2018). Activated FOXO3a may induce autophagy *via* enhancing the transcription of autophagic regulators including BNIP3 and LC3, while mTORC2 blocks the activation of FOXO3a by activating Akt (Ni et al., 2013). Therefore, FOXO3a is a key molecule connecting autophagy and cancer, and its expression may be regulated by autophagy-related signaling pathways, and therefore it is hopeful that it will become a therapeutic target for cancer.

Sirtuin-1 (SIRT1), as a NAD^+-dependent deacetylase, mainly regulates the deacetylation of FoxO (Wang and Tong, 2009; Kim et al., 2012; Hu et al., 2017). Under stress conditions, the complex of FOXO1 and sirtuin-2 (SIRT2) was dissociated and then acetylated and acetylated FOXO1 is balanced by histone acetylase and histone deacetylase (HDAC). FOXO1-Atg7 complex affects the autophagy process and eventually leads to cell death.

Oncogenic Role of Autophagy

When exposed to the two induction conditions of either hypoxia or nutrient deficiency, damaged organelles and unnecessary proteins can be decomposed by autophagy, and thereby promoting the viability of cancer cells, which indicates that autophagy can promote tumor growth and progression. In addition, in some cases, autophagy can be activated through some carcinogenic pathways. For example, oncogene pathways such as mTOR, Akt, PI3KCI, Bcl-X_L, Bcl-2, BCR-ABL, and Ras play an irreplaceable role in determining the survival of cancer cells. In pancreatic colorectal tumors with high RAS (rat sarcoma) gene mutation frequency, the level of autophagy is observed to be correlatively high, where the increase of autophagy helps to maintain the proliferation of cancer cells. The dependence of tumor growth on autophagy similar to that of RAS-driven cancers has also been observed in lung cancer, which was due to the substitution drive of valine to glutamate at BRAF position 600 (BRAFV600E). Of note, the activation of some oncogenes such as kirsten rat sarcoma viral oncogene (KRAS) or the deletion of tumor suppressor genes such as p53 have been used to form spontaneous tumors to establish genetically engineered mouse tumor models (GEMMs).

Sustained Ras-Raf-MAPK may be necessary to maintain tumor survival through autophagy. Importantly, mTOR is the main negative regulator of tumor cell autophagy, which can be activated by Ras-Raf-1-MEK1/2-ERK1/2 and PI3KCI-Akt signaling pathways, while inhibited by kinase B1 (LKB1)-AMP-activated protein kinase (AMPK) pathway (Wang et al., 2011). mTOR pathway regulates autophagy through two mechanisms. MTORC1 acts on EIF-4E Binding Proteins (EIF4EBPs) and S6K1 through signal transduction pathway, which may start the transcription and translation of related genes and regulate autophagy (Wang and Zhang, 2019). mTOR kinase may also act directly on Atg and regulate autophagy (Petherick et al., 2015). As a negative regulator of translation that can be phosphorylated by mTORC1, 4E-BP1 is inactivated and separated from eIF-4E after phosphorylation, so as to activate eIF-4E. EIF-4E can affect cancer progression by regulating the translation of a variety of proteins including RAS and cyclin D-MYC, which are closely related to the proliferation, cell cycle regulation and growth of cancer cells. (Huang et al., 2019; Joseph et al., 2019). In addition, BCR-ABL may function as a key factor to stimulate mTOR transcription in chronic myeloid leukemia (CML) through PI3KCI-Akt-FOXO signaling (Kang et al., 2011).

NATURAL COMPOUNDS AS AUTOPHAGIC MODULATORS IN CANCER

Based on the duality of autophagy in tumor cells, the current development and research of autophagy regulatory drugs mainly includes autophagy inducers and autophagy inhibitors. This section focuses on several representative natural compounds including Curcumin, Paclitaxel, Resveratrol, Bufalin and Ursolic acid, and summarize the autophagy-regulating mechanisms of other compounds (**Supplementary Table 1**).

Curcumin

Curcumin is a chemical component extracted from the rhizomes of some plants of Zingiberaceae and Araceae. Many preclinical studies *in vitro* and *in vivo* have proved that curcumin is safe and effectual in a variety of cancers. In recent years, curcumin was found to regulate autophagy, active apoptosis and inhibit the proliferation of tumor cells. (Li et al., 2020). The autophagy-related molecules such as Beclin-1, mTOR, ERK1/2, P53, play important roles in the initiation of autophagy (White, 2016; Xu et al., 2018; Shi et al., 2019). In human ovarian cells, lung cancer cells and human melanoma cells, curcumin inhibits the Akt/mTOR/p70S6K pathway to induce protective autophagy (Zhao et al., 2016; Liu et al., 2019b; Zhang et al., 2019). Curcumin is also found to activate the ERK1/2 pathway and inhibit the Akt/mTOR/p70S6K pathway and activate the ERK1/2 pathway to induce autophagy in malignant glioma cells (Aoki et al., 2007). Moreover, curcumin stimulates the p38 MAPK and phosphorylation of ERK1/2 in malignant mesothelioma cells (Masuelli et al., 2017). In SiHa cells and HCT116 cells, curcumin is found to upregulate p53 and Beclin-1 and induce reactive oxygen species (ROS) in activation of autophagy (Lee et al., 2011; Wang T. et al., 2020). Besides that, curcumin exerts its antitumor action inhibiting Bcl-2 and elevating the expression of Bax, p53, pro-caspases 3, 8, and 9 (Kuttan et al., 2007). YAP and P62 are observed to be reduced and LC3-Ⅱis enhanced with the treatment of curcumin in HCT116 and SW620. The results reveal that curcumin promotes autophagy and inhibits the proliferation of colon cancer cells (Zhu et al., 2018). Recently, studies have suggested that curcumin can modulate the expression of miRNAs, which induce apoptosis and suppress tumorigenesis and metastasis (Norouzi et al., 2018). Also, in human prostate cancer, curcumin could sensitize them to radiation by autophagy inhibition through miR-143 mediated pathway (Liu et al., 2017). Additionally, curcumin downregulates Bcl-xL by interfering with the PI3K/Akt and NF-κB signal pathways, as well as inducing the mitochondrial dysfunction together with caspase-3 activation (Liu et al., 2007) (**Figure 1A**).

Resveratrol

Resveratrol, a constituent of red wine, is reported to exert therapeutic potential on various tumors, whose mechanism is closely associated with the regulation of autophagy (Fremont, 2000; Baur and Sinclair, 2006; Deng et al., 2019). Resveratrol was reported to induce autophagy

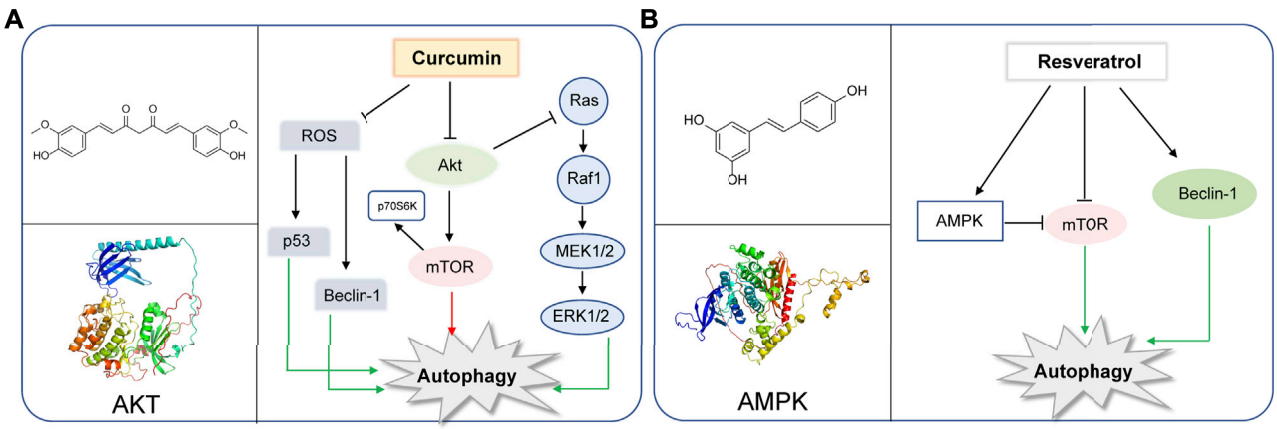

FIGURE 1 | Representative natural compounds targeting autophagic pathways in cancer **(A)** Curcumin **(B)** Resveratrol.

by direct inhibition of mTOR-ULK1 pathway in an ATP-competitive way, and can kill MCF7 cells which are mTOR inhibitor sensitive, displaying anti-cancer potential (Park et al., 2016). Resveratrol may induce autophagic cell death by activating c-Jun N-terminal kinase (JNK) pathway, as well as inducing AMPK pathway and ultimately leading to inhibition of mTOR pathway (Puissant et al., 2010).Resveratrol was reported to trigger autophagy through suppressing Akt/mTOR and inducing p38-MAPK pathways in human non-small-cell lung cancer cells A549 and H1299, thereby hindering cancer cell proliferation (Wang et al., 2018b). Additionally, resveratrol evokes autophagic cell death in a stromal interaction molecule 1 (SIMI)-dependent way, while involving the downregulation of mTOR pathway in human prostate cancer cells PC3 and DU145 (Selvaraj et al., 2016). When combined with quercetin (QCT), resveratrol reduced the QCT-induced autophagy through AMPK phosphorylation and heme oxygenase 1 (HO-1) downregulation, sensitizing the therapeutic effect of QCT (Tomas-Hernandez et al., 2018). Notably, resveratrol was recently used as supplement drug for chemotherapeutic anti-cancer drugs such as temozolomide (TMZ) to enhance the therapeutic effect (Lin et al., 2012). In gliomas, resveratrol suppressed cytoprotective autophagy which is triggered by TMZ treatment through inhibiting the ROS/ERK pathway, thus enhancing the efficacy of TMZ. Moreover, combined treatment of resveratrol and TMZ may significantly reduce the tumor volume through suppressing the ROS/ERK pathway than either TMZ or resveratrol alone, suggesting the synergistic effect of these two drugs (Lin et al., 2012). In cisplatin-resistant human oral cancer CAR cells, resveratrol activates autophagy *via* regulating AMPK and Akt/mTOR pathways, by phosphorylating AMPKα on Thr172 and AMPKα and dephosphorylating Akt on Ser473 and mTOR on Ser2448, and ultimately inhibits CAR cell viability (Chang et al., 2017) (**Figure 1B**).

Paclitaxel

Paclitaxel is known as a plant alkaloid extracted from the dry root, branches, leaves, and bark of the Taxus (Wessely et al., 2006). Nowadays, paclitaxel has been a first-line drug for plenty of cancers, and greatly help improve patient survival in lung, ovarian and breast cancer (Yu et al., 2015). In a study, paclitaxel could be applied for metastatic or locally advanced breast cancer by inducing autophagy in lymphatic endothelial cell (LEC). This process was independent from lymph node lymphangiogenesis because paclitaxel can only strongly inhibit lymphangiogenesis in combination with autophagy inhibitors such as chloroquine (Zamora et al., 2019). Moreover, paclitaxel treatment can induce autophagy by increasing expression levels of Atg5 and Beclin-1, which are essential to autophagy initiation in the A549 cells (Xi et al., 2011). In breast cancer, paclitaxel could induce early autophagy and is associated with apoptosis (Notte et al., 2013). Interestingly, paclitaxel exerts the same function in cervical cancer (Zou et al., 2018). Hitherto, paclitaxel has been shown to induce autophagy in BGC823 gastric cancer cell line, thus playing an anticancer role in inhibiting cell proliferation (Yu et al., 2017). In addition, multidrug resistance is a great challenge for paclitaxel to exert effect on cancers (Wang et al., 2018a). While, it was found that esomeprazole could overcome drug resistance of paclitaxel and enhance its anticancer effects by inducing autophagy in A549/Taxol cells (Bai et al., 2021). In a randomized phase II preoperative study, combination of autophagy inhibitor hydroxychloroquine and gemcitabine and nab-paclitaxel could exert autophagy inhibition in pancreatic cancer patients (Zeh et al., 2020) (**Figure 2A**).

Bufalin

Bufalin was found to be a cardiac steroid derived from posterior auricular glands and the skin of *Bufo gargarizans*. As an active ingredient in traditional Chinese medicine, Bufalin has been shown to be biologically active against various cancers (Zhang et al., 1992; Lee et al., 2017; Wu et al., 2017; Yang et al., 2018). Bufalin has been reported to inhibit glycolysis-induced ovarian cancer cell growth and proliferation *via* the suppression of Integrin β2/FAK signaling pathway (Li H. et al., 2018). In addition, bufalin could induce cell death through reactive oxygen species mediated RIP1/RIP3/PARP-1 pathway, thus exerting pharmacological activity to inhibit the development of human breast cancer (Li Y. et al., 2018). Notably, autophagy plays an important role in Bufalin's anti-tumor biological function, and it induces autophagy-mediated cell death through ROS production and JNK activation in colon cancer (Xie et al., 2011). In recent years, Bufalin has also been shown to induce autophagy in

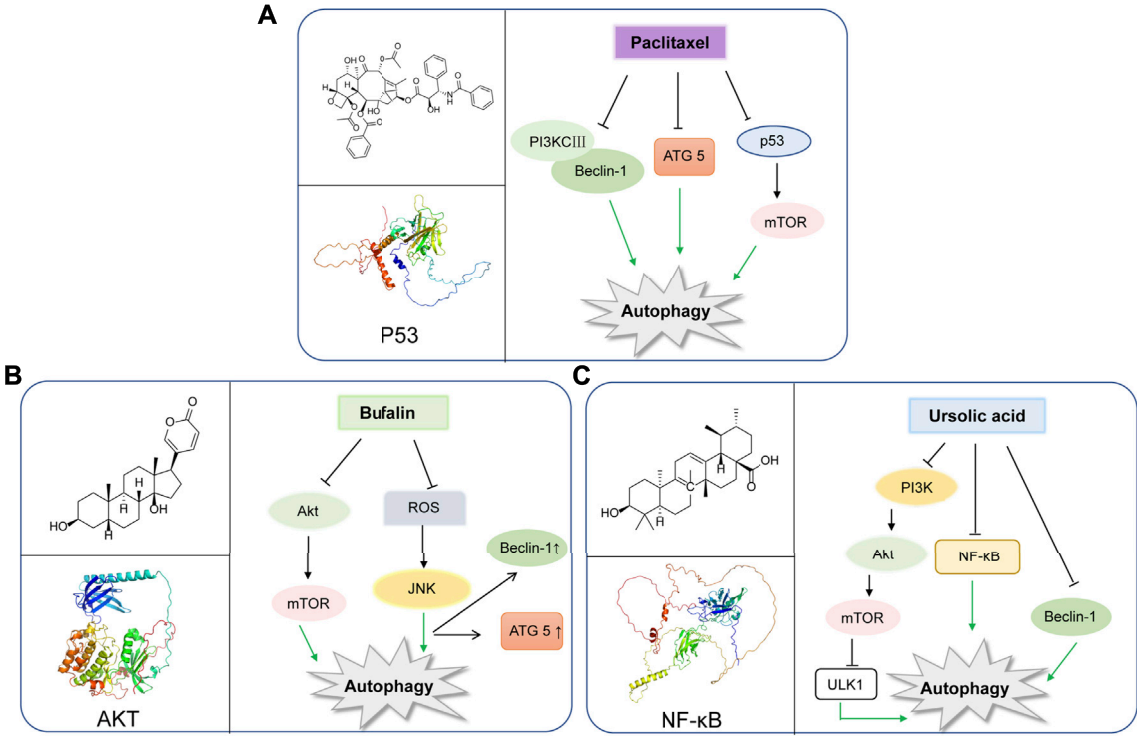

FIGURE 2 | Representative natural compounds targeting autophagic pathways in cancer **(A)** Paclitaxel **(B)** Bufalin **(C)** Ursolic acid.

gastric cancer MGC803 cells through Akt/mTOR/P70S6K and ERK signaling pathways. It is worth mentioning that Cbl-b mediated inhibition of mTOR and activation of ERK1/2 may play key roles. (Qi et al., 2019). Bufalin and JNK pathway induced autophagy, which was closely related to down-regulation of Bid and BCL-2, and up-regulation of MAPK, TNF, ATG8 Beclin-1 (Hsu et al., 2013). Moreover, Bufalin also activated autophagy in HepG2 cells, enhancing LC3-I to LC3-II transformation and Beclin-1 expression, and decreasing mTOR signal activation and p62 expression. Intriguingly, inhibition of autophagy by selective inhibitor 3-MA decreased the rate of apoptosis of HepG2 cells treated with Bufalin, which indicated that Bufalin-induced autophagy could promote apoptosis (Miao et al., 2013). Interestingly, Bufalin not only induces apoptosis through autophagy, it also plays a crucial role in anti-metastasis and anti-invasion. Bufalin has been found to inhibit the metastasis and invasion of hepatoma cells *via* PI3K/Akt/mTOR signaling pathway (Sheng et al., 2021) (**Figure 2B**).

Ursolic Acid

Ursolic acid (UA) is well-known as a triterpenoid compound enriched in various plants, which has been widely reported to exhibit its antitumor activity by modulating autophagy in different types of cancers. And, it can inhibit breast cancer cell proliferation through the PI3K-Akt and NF-κB pathways, leading to autophagy and apoptosis (Luo et al., 2017). In addition, UA can also promote cytotoxic autophagy and apoptosis, associated with AMPK and ERK1/2 signaling pathways by targeting glycolysis in different types of breast cancer cells (Lewinska et al., 2017). Additionally, UA also shows the inhibition of cell migration and induces JNK-dependent lysosomal associated cancer cell death, which is similar to autophagy in glioblastoma multiforme cells (Conway et al., 2021). Moreover, UA modulates autophagy and apoptosis in oral cancer cells through the Akt-mTOR and NF-κB pathways (Lin et al., 2019). Interestingly, UA induces mitophagy *via* the Akt-mTOR signaling pathway and is dependent on PINK1 in A549 human lung cancer cells. And, UA induces a Reactive Oxygen Species production by regulating p62 and Nrf2. (Castrejon-Jimenez et al., 2019). Similarly, UA is also reported to inhibit metastasis of esophageal cancer cells by ROS-mediated autophagy (Lee et al., 2020). Additionally, UA induces apoptosis and inhibits autophagy progression, leading to PC-12 cell death (Jung et al., 2018). Also, UA can inhibit pigmentation by activating B16F1 cell melanosomal autophagy (Park et al., 2020). More importantly, autophagy (cytoprotective autophagy) inhibition has been recently reported to enhance the anti-tumor effects of UA on lung cancer cells by the mTOR (Wang M. et al., 2020). More importantly, in gemcitabine-resistant human pancreatic cancer cells, UA has been shown to induce apoptosis, autophagy, and chemosensitivity (Lin et al., 2020). Combined use of Zoledronic acid can augment UA-induced apoptosis *via* enhancing oxidative stress and autophagy in osteosarcoma cells, indicating a potential combination therapeutic strategy for UA (Wu et al., 2016). Taken together, the above-mentioned findings may elucidate the potential underlying molecular mechanisms of UA and provide a novel therapeutic strategy to improve cancer treatment. (**Figure 2C**).

OTHER NATURAL COMPOUNDS TARGETING AUTOPHAGY IN CANCER

In addition to the above five compounds, other natural compounds have also been reported in recent years to regulate autophagy and induce cancer cell death. Genistein could promote cancer cell death through autophagic activation by inhibiting Akt in the treatment of many tumor types (Gossner et al., 2007). Additionally, fixetine can regulate autophagy by acting as an inhibitor of PI3K/Akt/mTOR pathway in human NSCLC cells and prostate cancer (Sun et al., 2018). Angelica sinensis is psoralen, derived from Angelica sinensis polymorph, which has been proved to regulate autophagy and apoptosis (Rahman et al., 2016; Wang et al., 2019) Angelicin increases autophagic proteins including Atg3, 7 and Atg12-5 through the phosphorylation of mTOR (Wang et al., 2019; Uddin et al., 2020). In addition, Camptothecin, vincristine, podophyllotoxin, Betulinic acid and other Changchun herbs can trigger autophagy in multiple myeloma cells, breast cancer cells, colon cancer cells and other different types of tumors (Deng et al., 2019; Chen et al., 2021; Pang et al., 2021).

THERAPEUTIC POTENTIAL OF NATURAL COMPOUNDS IN CANCER

As we have known, autophagy plays a dual role in cancer. Natural compound could promote or inhibit autophagy to treat cancer cell. In the past decades, numerous natural compounds have been studied their function on cancer treatment by targeting autophagy. Some key regulators of autophagy, such as mTOR, Beclin-1, p53, Akt, ERK, NF-κB and reactive oxygen species (ROS) have been the target for natural compounds to modulate cancer development and exhibit therapeutic effects against various cancers. For example, regulation of PI3K/Akt/mTOR signaling is a classic pathway involved in autophagy regulation, thus G-protein-coupled receptor antagonists, PI3K inhibitors, Akt inhibitors and mTOR inhibitors can inhibit this signaling pathway and induce autophagy in cancer therapy. In addition, it has been reported that Beclin-1 plays a key role as an essential gene for autophagic vesicle formation, therefore these compounds also regulating Beclin-1 in autophagic cell death. Meanwhile, Bcl-2 and Bcl-xL may inhibit autophagy activation by binding to Beclin-1. Thus, natural compounds, such as gossypol, potently bind to Bcl-2 and Bcl-xL and release Beclin-1 to preferentially inducing autophagy. Of note, a series of natural compounds have also shown strong anti-tumor efficacy by directly targeting ROS production through multiple signaling pathways involved in the interaction of ROS and autophagy. All above, increasing autophagy pathways of natural compounds have been discovered and show anti-tumor effect by regulating these signaling. Therefore, natural compounds have a great clinical prospect in cancer therapy by regulation of autophagy. With the discovery of more new natural products, it will provide opportunities for the discovery of new anticancer drugs.

CONCLUDING REMARKS

Hitherto, autophagy has been widely considered to have a dual role in tumorigenesis, in which defective autophagy may facilitate cancer development whereas cytoprotective autophagy helps cancer cell escape stress including starvation and hypoxia and ultimately promote the progression of cancer. Growing numbers of natural compounds have been reported to modulate multiple signal pathways associated with autophagy, such as Ras-Raf-MEK-ERK, PI3K-Akt-mTOR and AMPK, thus exerting therapeutic effect on different cancers. Notably, natural compounds are multiple-targets and less toxic, and represent promising candidates for treating cancer. In this review, we focus on five widely-investigated compounds in regulating autophagy, namely curcumin, resveratrol, paclitaxel, Bufalin, and Ursolic acid, and summarize their corresponding molecular mechanism of regulating autophagy. However, plenty of studies on these natural compounds only investigate their anti-cancer effects *in vitro*, lacking experimental data of *in vivo* studies. However, with the further research, animal model validation and other methods will effectively solve these problems, and greatly promote the study of natural compounds pharmacological mechanism.

Interestingly, most of these natural compounds not only regulate autophagy, but also have effects on apoptosis, so they can be good candidates to target the Regulated Cell Death (RCD) network, which is a hot and promising researching field. Moreover, due to their modulative role of autophagy, they exhibit good property to supplement classical chemotherapy drugs and help to overcome drug resistance. Also, combination of natural compounds is benefit to reduce the effective dose and enhance efficacy, representing a future research direction. In summary, our review on natural compounds targeting autophagy in cancer therapy may shed new light on exploiting more natural compounds and provide clues for developments of anti-cancer drugs.

AUTHOR CONTRIBUTIONS

YM, L-LZ and BL conceived, formatted, revised extensively, and submitted this manuscript. QX and YC wrote the manuscript. QX and HT searched and archived the literature.

FUNDING

This work was supported by the Department of Science and Technology of Sichuan Province (Grant No. 2021YFS0009), Chinese National Natural Science Foundation (Grant No. 82071168), and Research Foundation for Administration of traditional Chinese Medicine of Sichuan Province (2020HJZX002).

SUPPLEMENTARY MATERIAL

The Supplementary Material for this article can be found online at: https://www.frontiersin.org/articles/10.3389/fphar.2021.748149/full#supplementary-material

REFERENCES

Aoki, H., Takada, Y., Kondo, S., Sawaya, R., Aggarwal, B. B., and Kondo, Y. (2007). Evidence that Curcumin Suppresses the Growth of Malignant Gliomas *In Vitro* and *In Vivo* through Induction of Autophagy: Role of Akt and Extracellular Signal-Regulated Kinase Signaling Pathways. *Mol. Pharmacol.* 72 (1), 29–39. doi:10.1124/mol.106.033167

Arroyo, D. S., Gaviglio, E. A., Peralta Ramos, J. M., Bussi, C., Rodriguez-Galan, M. C., and Iribarren, P. (2014). Autophagy in Inflammation, Infection, Neurodegeneration and Cancer. *Int. Immunopharmacol* 18 (1), 55–65. doi:10.1016/j.intimp.2013.11.001

Bai, Z., Ding, N., Ge, J., Wang, Y., Wang, L., Wu, N., et al. (2021). Esomeprazole Overcomes Paclitaxel-Resistance and Enhances Anticancer Effects of Paclitaxel by Inducing Autophagy in A549/Taxol Cells. *Cell Biol. Int.* 45 (1), 177–187. doi:10.1002/cbin.11481

Baur, J. A., and Sinclair, D. A. (2006). Therapeutic Potential of Resveratrol: the *In Vivo* Evidence. *Nat. Rev. Drug Discov.* 5 (6), 493–506. doi:10.1038/nrd2060

Brech, A., Ahlquist, T., Lothe, R. A., and Stenmark, H. (2009). Autophagy in Tumour Suppression and Promotion. *Mol. Oncol.* 3 (4), 366–375. doi:10.1016/j.molonc.2009.05.007

Byun, S., Lee, E., and Lee, K. W. (2017). Therapeutic Implications of Autophagy Inducers in Immunological Disorders, Infection, and Cancer. *Int. J. Mol. Sci.* 18 (9). doi:10.3390/ijms18091959

Castrejón-Jiménez, N. S., Leyva-Paredes, K., Baltierra-Uribe, S. L., Castillo-Cruz, J., Campillo-Navarro, M., Hernández-Pérez, A. D., et al. (2019). Ursolic and Oleanolic Acids Induce Mitophagy in A549 Human Lung Cancer Cells. *Molecules* 24 (19). doi:10.3390/molecules24193444

Chang, C. H., Lee, C. Y., Lu, C. C., Tsai, F. J., Hsu, Y. M., Tsao, J. W., et al. (2017). Resveratrol-induced Autophagy and Apoptosis in Cisplatin-Resistant Human Oral Cancer CAR Cells: A Key Role of AMPK and Akt/mTOR Signaling. *Int. J. Oncol.* 50 (3), 873–882. doi:10.3892/ijo.2017.3866

Chen, C., Gao, H., and Su, X. (2021). Autophagy-related Signaling Pathways Are Involved in Cancer (Review). *Exp. Ther. Med.* 22 (1), 710. doi:10.3892/etm.2021.10142

Chou, H. Y., Liu, L. H., Chen, C. Y., Lin, I. F., Ali, D., Yueh-Luen Lee, A., et al. (2021). Bifunctional Mechanisms of Autophagy and Apoptosis Regulations in Melanoma from Bacillus Subtilis Natto Fermentation Extract. *Food Chem. Toxicol.* 150, 112020. doi:10.1016/j.fct.2021.112020

Conway, G. E., Zizyte, D., Mondala, J. R. M., He, Z., Lynam, L., Lecourt, M., et al. (2021). Ursolic Acid Inhibits Collective Cell Migration and Promotes JNK-dependent Lysosomal Associated Cell Death in Glioblastoma Multiforme Cells. *Pharmaceuticals (Basel)* 14 (2). doi:10.3390/ph14020091

Deng, S., Shanmugam, M. K., Kumar, A. P., Yap, C. T., Sethi, G., and Bishayee, A. (2019). Targeting Autophagy Using Natural Compounds for Cancer Prevention and Therapy. *Cancer* 125 (8), 1228–1246. doi:10.1002/cncr.31978

Ferreira, P. M. P., Sousa, R. W. R., Ferreira, J. R. O., Militão, G. C. G., and Bezerra, D. P. (2021). Chloroquine and Hydroxychloroquine in Antitumor Therapies Based on Autophagy-Related Mechanisms. *Pharmacol. Res.* 168, 105582. doi:10.1016/j.phrs.2021.105582

Frémont, L. (2000). Biological Effects of Resveratrol. *Life Sci.* 66 (8), 663–673. doi:10.1016/s0024-3205(99)00410-5

Gossner, G., Choi, M., Tan, L., Fogoros, S., Griffith, K. A., Kuenker, M., et al. (2007). Genistein-induced Apoptosis and Autophagocytosis in Ovarian Cancer Cells. *Gynecol. Oncol.* 105 (1), 23–30. doi:10.1016/j.ygyno.2006.11.009

Hsu, C. M., Tsai, Y., Wan, L., and Tsai, F. J. (2013). Bufalin Induces G2/M Phase Arrest and Triggers Autophagy *via* the TNF, JNK, BECN-1 and ATG8 Pathway in Human Hepatoma Cells. *Int. J. Oncol.* 43 (1), 338–348. doi:10.3892/ijo.2013.1942

Hu, Q., Wang, G., Peng, J., Qian, G., Jiang, W., Xie, C., et al. (20172017 37819). Knockdown of SIRT1 Suppresses Bladder Cancer Cell Proliferation and Migration and Induces Cell Cycle Arrest and Antioxidant Response through FOXO3a-Mediated Pathways. *Biomed. Res. Int.* 2017, 1–14. doi:10.1155/2017/3781904

Huang, C. I., Wang, C. C., Tai, T. S., Hwang, T. Z., Yang, C. C., Hsu, C. M., et al. (2019). eIF4E and 4EBP1 Are Prognostic Markers of Head and Neck Squamous Cell Carcinoma Recurrence after Definitive Surgery and Adjuvant Radiotherapy. *PLoS One* 14 (11), e0225537. doi:10.1371/journal.pone.0225537

Joseph, B., Kumar, R. V., Champaka, G., Shenoy, A., Sabitha, K. S., Lokesh, V., et al. (2019). Biological Tailoring of Adjuvant Radiotherapy in Head and Neck and Oral Malignancies - the Potential Role of P53 and eIF4E as Predictive Parameters. *Indian J. Cancer* 56 (4), 330–334. doi:10.4103/ijc.IJC_56_18

Jung, J., Seo, J., Kim, J., and Kim, J. H. (2018). Ursolic Acid Causes Cell Death in PC-12 Cells by Inducing Apoptosis and Impairing Autophagy. *Anticancer Res.* 38 (2), 847–853. doi:10.21873/anticanres.12293

Kang, D. Y., Sp, N., Lee, J. M., and Jang, K. J. (2021). Antitumor Effects of Ursolic Acid through Mediating the Inhibition of STAT3/PD-L1 Signaling in Non-small Cell Lung Cancer Cells. *Biomedicines* 9 (3). doi:10.3390/biomedicines9030297

Kang, R., Zeh, H. J., Lotze, M. T., and Tang, D. (2011). The Beclin 1 Network Regulates Autophagy and Apoptosis. *Cell Death Differ* 18 (4), 571–580. doi:10.1038/cdd.2010.191

Khandia, R., Dadar, M., Munjal, A., Dhama, K., Karthik, K., Tiwari, R., et al. (2019). A Comprehensive Review of Autophagy and its Various Roles in Infectious, Non-infectious, and Lifestyle Diseases: Current Knowledge and Prospects for Disease Prevention, Novel Drug Design, and Therapy. *Cells* 8 (7). doi:10.3390/cells8070674

Kim, M., Chung, H., Yoon, C., Lee, E., Kim, T., Kim, T., et al. (2012). Increase of INS-1 Cell Apoptosis under Glucose Fluctuation and the Involvement of FOXO-SIRT Pathway. *Diabetes Res. Clin. Pract.* 98 (1), 132–139. doi:10.1016/j.diabres.2012.04.013

Kuttan, G., Kumar, K. B., Guruvayoorappan, C., and Kuttan, R. (2007). Antitumor, Anti-invasion, and Antimetastatic Effects of Curcumin. *Adv. Exp. Med. Biol.* 595, 173–184. doi:10.1007/978-0-387-46401-5_6

Lee, C. H., Shih, Y. L., Lee, M. H., Au, M. K., Chen, Y. L., Lu, H. F., et al. (2017). Bufalin Induces Apoptosis of Human Osteosarcoma U-2 OS Cells through Endoplasmic Reticulum Stress, Caspase- and Mitochondria-dependent Signaling Pathways. *Molecules* 22 (3). doi:10.3390/molecules22030437

Lee, N. R., Meng, R. Y., Rah, S. Y., Jin, H., Ray, N., Kim, S. H., et al. (2020). Reactive Oxygen Species-Mediated Autophagy by Ursolic Acid Inhibits Growth and Metastasis of Esophageal Cancer Cells. *Int. J. Mol. Sci.* 21 (24). doi:10.3390/ijms21249409

Lee, Y. J., Kim, N. Y., Suh, Y. A., and Lee, C. (2011). Involvement of ROS in Curcumin-Induced Autophagic Cell Death. *Korean J. Physiol. Pharmacol.* 15 (1), 1–7. doi:10.4196/kjpp.2011.15.1.1

Lewinska, A., Adamczyk-Grochala, J., Kwasniewicz, E., Deregowska, A., and Wnuk, M. (2017). Ursolic Acid-Mediated Changes in Glycolytic Pathway Promote Cytotoxic Autophagy and Apoptosis in Phenotypically Different Breast Cancer Cells. *Apoptosis* 22 (6), 800–815. doi:10.1007/s10495-017-1353-7

Li, H., Hu, S., Pang, Y., Li, M., Chen, L., Liu, F., et al. (2018a). Bufalin Inhibits Glycolysis-Induced Cell Growth and Proliferation through the Suppression of Integrin β2/FAK Signaling Pathway in Ovarian Cancer. *Am. J. Cancer Res.* 8 (7), 1288–1296.

Li, X., He, S., and Ma, B. (2020). Autophagy and Autophagy-Related Proteins in Cancer. *Mol. Cancer* 19 (1), 12. doi:10.1186/s12943-020-1138-4

Li, Y., Tian, X., Liu, X., and Gong, P. (2018b). Bufalin Inhibits Human Breast Cancer Tumorigenesis by Inducing Cell Death through the ROS-Mediated RIP1/RIP3/PARP-1 Pathways. *Carcinogenesis* 39 (5), 700–707. doi:10.1093/carcin/bgy039

Lin, C. J., Lee, C. C., Shih, Y. L., Lin, T. Y., Wang, S. H., Lin, Y. F., et al. (2012). Resveratrol Enhances the Therapeutic Effect of Temozolomide against Malignant Glioma *In Vitro* and *In Vivo* by Inhibiting Autophagy. *Free Radic. Biol. Med.* 52 (2), 377–391. doi:10.1016/j.freeradbiomed.2011.10.487

Lin, C. W., Chin, H. K., Lee, S. L., Chiu, C. F., Chung, J. G., Lin, Z. Y., et al. (2019). Ursolic Acid Induces Apoptosis and Autophagy in Oral Cancer Cells. *Environ. Toxicol.* 34 (9), 983–991. doi:10.1002/tox.22769

Lin, J. H., Chen, S. Y., Lu, C. C., Lin, J. A., and Yen, G. C. (2020). Ursolic Acid Promotes Apoptosis, Autophagy, and Chemosensitivity in Gemcitabine-Resistant Human Pancreatic Cancer Cells. *Phytother Res.* 34 (8), 2053–2066. doi:10.1002/ptr.6669

Ling, L. U., Tan, K. B., Lin, H., and Chiu, G. N. (2011). The Role of Reactive Oxygen Species and Autophagy in Safingol-Induced Cell Death. *Cell Death Dis.* 2, e129. doi:10.1038/cddis.2011.12

Liu, E., Wu, J., Cao, W., Zhang, J., Liu, W., Jiang, X., et al. (2007). Curcumin Induces G2/M Cell Cycle Arrest in a P53-dependent Manner and Upregulates

ING4 Expression in Human Glioma. *J. Neurooncol.* 85 (3), 263–270. doi:10.1007/s11060-007-9421-4

Liu, F., Gao, S., Yang, Y., Zhao, X., Fan, Y., Ma, W., et al. (2018a). Antitumor Activity of Curcumin by Modulation of Apoptosis and Autophagy in Human Lung Cancer A549 Cells through Inhibiting PI3K/Akt/mTOR Pathway. *Oncol. Rep.* 39 (3), 1523–1531. doi:10.3892/or.2018.6188

Liu, H., Shen, M., Zhao, D., Ru, Y., Ding, C., et al. (2019a). The Effect of Triptolide-Loaded Exosomes on the Proliferation and Apoptosis of Human Ovarian Cancer SKOV3 Cells. *Biomed. Res. Int.* 2019, 1–14. doi:10.1155/2019/2595801

Liu, J., Li, M., Wang, Y., and Luo, J. (2017). Curcumin Sensitizes Prostate Cancer Cells to Radiation Partly *via* Epigenetic Activation of miR-143 and miR-143 Mediated Autophagy Inhibition. *J. Drug Target.* 25 (7), 645–652. doi:10.1080/1061186X.2017.1315686

Liu, L. D., Pang, Y. X., Zhao, X. R., Li, R., Jin, C. J., Xue, J., et al. (2019b). Curcumin Induces Apoptotic Cell Death and Protective Autophagy by Inhibiting AKT/mTOR/p70S6K Pathway in Human Ovarian Cancer Cells. *Arch. Gynecol. Obstet.* 299 (6), 1627–1639. doi:10.1007/s00404-019-05058-3

Liu, Y., Ao, X., Ding, W., Ponnusamy, M., Wu, W., Hao, X., et al. (2018b). Critical Role of FOXO3a in Carcinogenesis. *Mol. Cancer* 17 (1), 104. doi:10.1186/s12943-018-0856-3

Liu, Y., Hua, W., Li, Y., Xian, X., Zhao, Z., Liu, C., et al. (2020). Berberine Suppresses colon Cancer Cell Proliferation by Inhibiting the SCAP/SREBP-1 Signaling Pathway-Mediated Lipogenesis. *Biochem. Pharmacol.* 174, 113776. doi:10.1016/j.bcp.2019.113776

Luo, J., Hu, Y. L., and Wang, H. (2017). Ursolic Acid Inhibits Breast Cancer Growth by Inhibiting Proliferation, Inducing Autophagy and Apoptosis, and Suppressing Inflammatory Responses *via* the PI3K/AKT and NF-Kb Signaling Pathways *In Vitro*. *Exp. Ther. Med.* 14 (4), 3623–3631. doi:10.3892/etm.2017.4965

Masuelli, L., Benvenuto, M., Di Stefano, E., Mattera, R., Fantini, M., De Feudis, G., et al. (2017). Curcumin Blocks Autophagy and Activates Apoptosis of Malignant Mesothelioma Cell Lines and Increases the Survival of Mice Intraperitoneally Transplanted with a Malignant Mesothelioma Cell Line. *Oncotarget* 8 (21), 34405–34422. doi:10.18632/oncotarget.14907

Miao, Q., Bi, L. L., Li, X., Miao, S., Zhang, J., Zhang, S., et al. (2013). Anticancer Effects of Bufalin on Human Hepatocellular Carcinoma HepG2 Cells: Roles of Apoptosis and Autophagy. *Int. J. Mol. Sci.* 14 (1), 1370–1382. doi:10.3390/ijms14011370

Morselli, E., Galluzzi, L., Kepp, O., Vicencio, J. M., Criollo, A., Maiuri, M. C., et al. (2009). Anti- and Pro-tumor Functions of Autophagy. *Biochim. Biophys. Acta* 1793 (9), 1524–1532. doi:10.1016/j.bbamcr.2009.01.006

Ni, H. M., Du, K., You, M., and Ding, W. X. (2013). Critical Role of FoxO3a in Alcohol-Induced Autophagy and Hepatotoxicity. *Am. J. Pathol.* 183 (6), 1815–1825. doi:10.1016/j.ajpath.2013.08.011

Norouzi, S., Majeed, M., Pirro, M., Generali, D., and Sahebkar, A. (2018). Curcumin as an Adjunct Therapy and microRNA Modulator in Breast Cancer. *Curr. Pharm. Des.* 24 (2), 171–177. doi:10.2174/1381612824666171129203506

Notte, A., Ninane, N., Arnould, T., and Michiels, C. (2013). Hypoxia Counteracts Taxol-Induced Apoptosis in MDA-MB-231 Breast Cancer Cells: Role of Autophagy and JNK Activation. *Cel Death Dis.* 4, e638. doi:10.1038/cddis.2013.167

Pang, X., Zhang, X., Jiang, Y., Su, Q., Li, Q., and Li, Z. (2021). Autophagy: Mechanisms and Therapeutic Potential of Flavonoids in Cancer. *Biomolecules* 11 (2). doi:10.3390/biom11020135

Park, D., Jeong, H., Lee, M. N., Koh, A., Kwon, O., Yang, Y. R., et al. (2016). Resveratrol Induces Autophagy by Directly Inhibiting mTOR through ATP Competition. *Sci. Rep.* 6, 21772. doi:10.1038/srep21772

Park, H. J., Jo, D. S., Choi, D. S., Bae, J. E., Park, N. Y., Kim, J. B., et al. (2020). Ursolic Acid Inhibits Pigmentation by Increasing Melanosomal Autophagy in B16F1 Cells. *Biochem. Biophys. Res. Commun.* 531 (2), 209–214. doi:10.1016/j.bbrc.2020.07.125

Petherick, K. J., Conway, O. J., Mpamhanga, C., Osborne, S. A., Kamal, A., Saxty, B., et al. (2015). Pharmacological Inhibition of ULK1 Kinase Blocks Mammalian Target of Rapamycin (mTOR)-dependent Autophagy. *J. Biol. Chem.* 290 (48), 11376–11383. doi:10.1074/jbc.A114.62777810.1074/jbc.C114.627778

Puissant, A., Robert, G., Fenouille, N., Luciano, F., Cassuto, J. P., Raynaud, S., et al. (2010). Resveratrol Promotes Autophagic Cell Death in Chronic Myelogenous Leukemia Cells *via* JNK-Mediated p62/SQSTM1 Expression and AMPK Activation. *Cancer Res.* 70 (3), 1042–1052. doi:10.1158/0008-5472.CAN-09-3537

Qi, H. Y., Qu, X. J., Liu, J., Hou, K. Z., Fan, Y. B., Che, X. F., et al. (2019). Bufalin Induces Protective Autophagy by Cbl-B Regulating mTOR and ERK Signaling Pathways in Gastric Cancer Cells. *Cel Biol. Int.* 43 (1), 33–43. doi:10.1002/cbin.11076

Rahman, M. A., Bishayee, K., and Huh, S. O. (2016). Angelica Polymorpha Maxim Induces Apoptosis of Human SH-Sy5y Neuroblastoma Cells by Regulating an Intrinsic Caspase Pathway. *Mol. Cell* 39 (2), 119–128. doi:10.14348/molcells.2016.2232

Selvaraj, S., Sun, Y., Sukumaran, P., and Singh, B. B. (2016). Resveratrol Activates Autophagic Cell Death in Prostate Cancer Cells *via* Downregulation of STIM1 and the mTOR Pathway. *Mol. Carcinog* 55 (5), 818–831. doi:10.1002/mc.22324

Sheng, X., Zhu, P., Zhao, Y., Zhang, J., Li, H., Zhao, H., et al. (2021). Effect of PI3K/AKT/mTOR Signaling Pathway on Regulating and Controlling the Anti-invasion and Metastasis of Hepatoma Cells by Bufalin. *Recent Pat Anticancer Drug Discov.* 16 (1), 54–65. doi:10.2174/1574892816666210201120324

Shi, B., Ma, M., Zheng, Y., Pan, Y., and Lin, X. (2019). mTOR and Beclin1: Two Key Autophagy-Related Molecules and Their Roles in Myocardial Ischemia/reperfusion Injury. *J. Cel Physiol.* 234 (8), 12562–12568. doi:10.1002/jcp.28125

Singh, S. S., Vats, S., Chia, A. Y., Tan, T. Z., Deng, S., Ong, M. S., et al. (2018). Dual Role of Autophagy in Hallmarks of Cancer. *Oncogene* 37 (9), 1142–1158. doi:10.1038/s41388-017-0046-6

Sun, X., Ma, X., Li, Q., Yang, Y., Xu, X., Sun, J., et al. (2018). Anti-cancer E-ffects of F-isetin on M-ammary C-arcinoma C-ells *via* R-egulation of the PI3K/Akt/mTOR P-athway: In vitro and I-n vivo S-tudies. *Int. J. Mol. Med.* 42 (2), 811–820. doi:10.3892/ijmm.2018.3654

Sun, Y., Zhou, Q. M., Lu, Y. Y., Zhang, H., Chen, Q. L., Zhao, M., et al. (2019). Resveratrol Inhibits the Migration and Metastasis of MDA-MB-231 Human Breast Cancer by Reversing TGF-B1-Induced Epithelial-Mesenchymal Transition. *Molecules* 24 (6). doi:10.3390/molecules24061131

Tomas-Hernández, S., Blanco, J., Rojas, C., Roca-Martínez, J., Ojeda-Montes, M. J., Beltrán-Debón, R., et al. (2018). Resveratrol Potently Counteracts Quercetin Starvation-Induced Autophagy and Sensitizes HepG2 Cancer Cells to Apoptosis. *Mol. Nutr. Food Res.* 62 (5). doi:10.1002/mnfr.201700610

Towers, C. G., Wodetzki, D., and Thorburn, A. (2020). Autophagy and Cancer: Modulation of Cell Death Pathways and Cancer Cell Adaptations. *J. Cel Biol.* 219 (1). doi:10.1083/jcb.201909033

Uddin, M. S., Rahman, M. A., Kabir, M. T., Behl, T., Mathew, B., Perveen, A., et al. (2020). Multifarious Roles of mTOR Signaling in Cognitive Aging and Cerebrovascular Dysfunction of Alzheimer's Disease. *IUBMB Life* 72 (9), 1843–1855. doi:10.1002/iub.2324

Wang, F., and Tong, Q. (2009). SIRT2 Suppresses Adipocyte Differentiation by Deacetylating FOXO1 and Enhancing FOXO1's Repressive Interaction with PPARgamma. *Mol. Biol. Cel* 20 (3), 801–808. doi:10.1091/mbc.E08-06-0647

Wang, J., Garbutt, C., Ma, H., Gao, P., Hornicek, F. J., Kan, Q., et al. (2018a). Expression and Role of Autophagy-Associated P62 (SQSTM1) in Multidrug Resistant Ovarian Cancer. *Gynecol. Oncol.* 150 (1), 143–150. doi:10.1016/j.ygyno.2018.04.557

Wang, J., Li, J., Cao, N., Li, Z., Han, J., and Li, L. (2018b). Resveratrol, an Activator of SIRT1, Induces Protective Autophagy in Non-small-cell Lung Cancer *via* Inhibiting Akt/mTOR and Activating P38-MAPK. *Onco Targets Ther.* 11, 7777–7786. doi:10.2147/OTT.S159095

Wang, M., Yu, H., Wu, R., Chen, Z. Y., Hu, Q., Zhang, Y. F., et al. (2020a). Autophagy Inhibition Enhances the Inhibitory Effects of Ursolic Acid on Lung Cancer Cells. *Int. J. Mol. Med.* 46 (5), 1816–1826. doi:10.3892/ijmm.2020.4714

Wang, S. Y., Yu, Q. J., Zhang, R. D., and Liu, B. (2011). Core Signaling Pathways of Survival/death in Autophagy-Related Cancer Networks. *Int. J. Biochem. Cel Biol.* 43 (9), 1263–1266. doi:10.1016/j.biocel.2011.05.010

Wang, T., Wu, X., Al Rudaisat, M., Song, Y., and Cheng, H. (2020b). Curcumin Induces G2/M Arrest and Triggers Autophagy, ROS Generation and Cell Senescence in Cervical Cancer Cells. *J. Cancer* 11 (22), 6704–6715. doi:10.7150/jca.45176

Wang, Y., Chen, Y., Chen, X., Liang, Y., Yang, D., Dong, J., et al. (2019). Angelicin Inhibits the Malignant Behaviours of Human Cervical Cancer Potentially *via*

Inhibiting Autophagy. *Exp. Ther. Med.* 18 (5), 3365–3374. doi:10.3892/etm.2019.7985

Wang, Y., and Zhang, H. (2019). Regulation of Autophagy by mTOR Signaling Pathway. *Adv. Exp. Med. Biol.* 1206, 67–83. doi:10.1007/978-981-15-0602-4_3

Wessely, R., Schömig, A., and Kastrati, A. (2006). Sirolimus and Paclitaxel on Polymer-Based Drug-Eluting Stents: Similar but Different. *J. Am. Coll. Cardiol.* 47 (4), 708–714. doi:10.1016/j.jacc.2005.09.047

White, E. (2016). Autophagy and P53. *Cold Spring Harb Perspect. Med.* 6 (4), a026120. doi:10.1101/cshperspect.a026120

Wu, C. C., Huang, Y. F., Hsieh, C. P., Chueh, P. J., and Chen, Y. L. (2016). Combined Use of Zoledronic Acid Augments Ursolic Acid-Induced Apoptosis in Human Osteosarcoma Cells through Enhanced Oxidative Stress and Autophagy. *Molecules* 21 (12). doi:10.3390/molecules21121640

Wu, S. H., Bau, D. T., Hsiao, Y. T., Lu, K. W., Hsia, T. C., Lien, J. C., et al. (2017). Bufalin Induces Apoptosis *In Vitro* and Has Antitumor Activity against Human Lung Cancer Xenografts *In Vivo*. *Environ. Toxicol.* 32 (4), 1305–1317. doi:10.1002/tox.22325

Xi, G., Hu, X., Wu, B., Jiang, H., Young, C. Y., Pang, Y., et al. (2011). Autophagy Inhibition Promotes Paclitaxel-Induced Apoptosis in Cancer Cells. *Cancer Lett.* 307 (2), 141–148. doi:10.1016/j.canlet.2011.03.026

Xie, C. M., Chan, W. Y., Yu, S., Zhao, J., and Cheng, C. H. (2011). Bufalin Induces Autophagy-Mediated Cell Death in Human colon Cancer Cells through Reactive Oxygen Species Generation and JNK Activation. *Free Radic. Biol. Med.* 51 (7), 1365–1375. doi:10.1016/j.freeradbiomed.2011.06.016

Xu, X., Zhi, T., Chao, H., Jiang, K., Liu, Y., Bao, Z., et al. (2018). Corrigendum to "ERK1/2/mTOR/Stat3 Pathway-Mediated Autophagy Alleviates Traumatic Brain Injury-Induced Acute Lung Injury" [Biochim. Biophys. Acta 1864/5PA(2018) 1663-1674]. *Biochim. Biophys. Acta Mol. Basis Dis.* 1864 (5 Pt A), 2214–1674. doi:10.1016/j.bbadis.2018.02.01110.1016/j.bbadis.2018.04.003

Yan, X., Zhou, R., and Ma, Z. (2019). Autophagy-Cell Survival and Death. *Adv. Exp. Med. Biol.* 1206, 667–696. doi:10.1007/978-981-15-0602-4_29

Yang, Z., and Klionsky, D. J. (2010). Eaten Alive: a History of Macroautophagy. *Nat. Cel Biol.* 12 (9), 814–822. doi:10.1038/ncb0910-814

Yang, Z., Tao, Y., Xu, X., Cai, F., Yu, Y., and Ma, L. (2018). Bufalin Inhibits Cell Proliferation and Migration of Hepatocellular Carcinoma Cells *via* APOBEC3F Induced Intestinal Immune Network for IgA Production Signaling Pathway. *Biochem. Biophys. Res. Commun.* 503 (3), 2124–2131. doi:10.1016/j.bbrc.2018.07.169

Yu, Y., Gaillard, S., Phillip, J. M., Huang, T. C., Pinto, S. M., Tessarollo, N. G., et al. (2015). Inhibition of Spleen Tyrosine Kinase Potentiates Paclitaxel-Induced Cytotoxicity in Ovarian Cancer Cells by Stabilizing Microtubules. *Cancer Cell* 28 (1), 82–96. doi:10.1016/j.ccell.2015.05.009

Yu, Y. F., Hu, P. C., Wang, Y., Xu, X. L., Rushworth, G. M., Zhang, Z., et al. (2017). Paclitaxel Induces Autophagy in Gastric Cancer BGC823 Cells. *Ultrastruct. Pathol.* 41 (4), 284–290. doi:10.1080/01913123.2017.1334019

Zamora, A., Alves, M., Chollet, C., Therville, N., Fougeray, T., Tatin, F., et al. (2019). Paclitaxel Induces Lymphatic Endothelial Cells Autophagy to Promote Metastasis. *Cel Death Dis.* 10 (12), 956. doi:10.1038/s41419-019-2181-1

Zeh, H. J., Bahary, N., Boone, B. A., Singhi, A. D., Miller-Ocuin, J. L., Normolle, D. P., et al. (2020). A Randomized Phase II Preoperative Study of Autophagy Inhibition with High-Dose Hydroxychloroquine and Gemcitabine/Nab-Paclitaxel in Pancreatic Cancer Patients. *Clin. Cancer Res.* 26 (13), 3126–3134. doi:10.1158/1078-0432.CCR-19-4042

Zhang, L., Nakaya, K., Yoshida, T., and Kuroiwa, Y. (1992). Induction by Bufalin of Differentiation of Human Leukemia Cells HL60, U937, and ML1 toward Macrophage/monocyte-like Cells and its Potent Synergistic Effect on the Differentiation of Human Leukemia Cells in Combination with Other Inducers. *Cancer Res.* 52 (17), 4634–4641.

Zhang, Q., Qiao, H., Wu, D., Lu, H., Liu, L., Sang, X., et al. (2019). Curcumin Potentiates the Galbanic Acid-Induced Anti-tumor Effect in Non-small Cell Lung Cancer Cells through Inhibiting Akt/mTOR Signaling Pathway. *Life Sci.* 239, 117044. doi:10.1016/j.lfs.2019.117044

Zhao, G., Han, X., Zheng, S., Li, Z., Sha, Y., Ni, J., et al. (2016). Curcumin Induces Autophagy, Inhibits Proliferation and Invasion by Downregulating AKT/mTOR Signaling Pathway in Human Melanoma Cells. *Oncol. Rep.* 35 (2), 1065–1074. doi:10.3892/or.2015.4413

Zhao, Y., Wang, L., Yang, J., Zhang, P., Ma, K., Zhou, J., et al. (2010). Anti-neoplastic Activity of the Cytosolic FoxO1 Results from Autophagic Cell Death. *Autophagy* 6 (7), 988–990. doi:10.4161/auto.6.7.13289

Zhu, J., Zhao, B., Xiong, P., Wang, C., Zhang, J., Tian, X., et al. (2018). Curcumin Induces Autophagy *via* Inhibition of Yes-Associated Protein (YAP) in Human Colon Cancer Cells. *Med. Sci. Monit.* 24, 7035–7042. doi:10.12659/MSM.910650

Zou, S. H., Du, X., Lin, H., Wang, P. C., and Li, M. (2018). Paclitaxel Inhibits the Progression of Cervical Cancer by Inhibiting Autophagy *via* lncRNARP11-381N20.2. *Eur. Rev. Med. Pharmacol. Sci.* 22 (10), 3010–3017. doi:10.26355/eurrev_201805_15058

Conflict of Interest: The authors declare that the research was conducted in the absence of any commercial or financial relationships that could be construed as a potential conflict of interest.

Publisher's Note: All claims expressed in this article are solely those of the authors and do not necessarily represent those of their affiliated organizations, or those of the publisher, the editors and the reviewers. Any product that may be evaluated in this article, or claim that may be made by its manufacturer, is not guaranteed or endorsed by the publisher.

frontiers in Oncology

ORIGINAL RESEARCH
published: 26 August 2021
doi: 10.3389/fonc.2021.731522

Exploration of the Potential Mechanism of Tao Hong Si Wu Decoction for the Treatment of Breast Cancer Based on Network Pharmacology and *In Vitro* Experimental Verification

Shi Huang[1,2†], Yan Chen[1,2†], Lingyu Pan[1], Changyi Fei[2], Ni Wang[2], Furui Chu[2], Daiyin Peng[2], Xianchun Duan[1] and Yongzhong Wang[1*]*

[1] The First Affiliated Hospital of Anhui University of Chinese Medicinee, Hefei, China, [2] College of Pharmacy, Anhui University of Chinese Medicine, Hefei, China

Background: Tao Hong Si Wu Decoction (THSWD) is a well-known traditional Chinese medicine used clinically alone or combined with drugs to treat breast cancer. However, there has been no study to date on the underlying mechanisms of its therapeutic effects.

Objectives: To explore the potential mechanism of THSWD for the treatment of breast cancer using network pharmacology and experimental research.

Methods: The active ingredients of THSWD were screened according to Lipinski's rule of five based on the 107 ingredients of THSWD identified by UPLC-Q-TOF-MS^E. The targets of THSWD and breast cancer from multiple databases were collected, and a Compound-Target-Pathway network based on protein-protein interaction (PPI) was constructed. Gene ontology (GO) analysis and KEGG pathway analysis were performed *via* the DAVID server. Molecular docking studies verified the selected key ingredients and key targets. The results of network pharmacology were verified by *in vitro* experiments. Including the effects of THSWD drug-containing rat serum (THSWD serum) on cell proliferation, and on the targets HRAS, MAPK1, AKT1, GRB2, and MAPK14 were assayed by RT-qPCR and Western blot assays.

Results: In total, 27 active ingredients including 8 core components, were obtained from 107 ingredients and 218 THSWD target genes for the treatment of breast cancer were identified. THSWD is active in the treatment of breast cancer by targeting Ras, FoxO, PI3K-Akt and other signaling pathways. MCF-7 and MDA-MB-231 cell proliferation was inhibited by THSWD serum in a time and concentration dependent manner. THSWD could regulated the RNA and protein expression of core targets HRAS, MAPK1, AKT1, GRB2, and MAPK14 for treatment of breast cancer.

OPEN ACCESS

Edited by:
Haiyang Yu,
Tianjin University of Traditional Chinese Medicine, China

Reviewed by:
Ming Niu,
Fifth Medical Center of Chinese PLA General Hospital, China
Jiao Liu,
Hebei University of Chinese Medicine, China
Yuanjia Hu,
University of Macau, China

****Correspondence:***
Xianchun Duan
ahtcmdxc@163.com
Yongzhong Wang
wyzhmail@163.com

†These authors have contributed equally to this work

Specialty section:
This article was submitted to Pharmacology of Anti-Cancer Drugs, a section of the journal Frontiers in Oncology

Received: *27 June 2021*
Accepted: *09 August 2021*
Published: *26 August 2021*

Citation:
Huang S, Chen Y, Pan L, Fei C, Wang N, Chu F, Peng D, Duan X and Wang Y (2021) Exploration of the Potential Mechanism of Tao Hong Si Wu Decoction for the Treatment of Breast Cancer Based on Network Pharmacology and In Vitro Experimental Verification. Front. Oncol. 11:731522. doi: 10.3389/fonc.2021.731522

Conclusion: The results of network pharmacology study showed that THSWD is active against breast cancer by intervening with multiple targets and pathways. Luteolin, kaempferol, senkyunolide E, and other 8 compounds may be the core active ingredients of THSWD in the treatment of breast cancer. THSWD treatment of breast cancer may be related to targeting Ras, FoxO, PI3K-Akt, and other signal pathways associated with the core targets HRAS, MAPK1, AKT1, GRB2, and MAPK14.

Keywords: Taohong Siwu Decoction (THSWD), network pharmacology, breast cancer, traditional Chinese medicine, target identification

INTRODUCTION

The latest data from the International Agency for Research on Cancer (IARC) survey showed that Female breast cancer has surpassed lung cancer as the most commonly diagnosed cancer, with an estimated 2.3 million new cases (11.7%) in 2018 (1). Epidemiological data across Chinese cancer centers in 2019 showed that the incidence and mortality rates of breast cancer were first and fifth among female malignant tumors, respectively, and both rates have shown a rising trend. Breast cancer has become a serious disease that threatens the health of women in China and women across the world. At present, the most common clinical treatment interventions are surgical resection, radiotherapy, and chemotherapy, but surgical resection does not improve prognosis, while long-term radiotherapy and chemotherapy can cause serious side effects. Studies have shown that the combined treatment with traditional Chinese medicine (TCM) can improve the quality of life of breast cancer patients (2). Therefore, it is of great significance to search for the TCM treatment of breast cancer and to explore the prevention and treatment of breast cancer.

Tao Hong Si Wu Decoction (THSWD) was documented in "The Golden Mirror of Medicine" compiled by Wu Qian in the Qing Dynasty. It consists of six species of medicinal herbs: Prunus persica (L.) Batsch (Taoren, TR), Carthamustinctorius L. (Honghua, HH), Angelica sinensis (Oliv.) Diels (Danggui, DG), Ligusticum chuanxiong Hort (Chuanxiong, CX), Paeoniae Radix Alba (Baishao, BS), and Rehmannia glutinosa (Gaertn.) DC (Shudi, SD). THSWD eliminates blood stasis and promotes blood circulation and nourishment (3). Xia using network pharmacology and *in vivo* experiments, found that THSWD plays a therapeutic role in postpartum blood stasis by regulating oxidative stress through the mitochondria (4). THSWD promotes angiogenesis after cerebral ischemia in rats through activation of platelets (5). Further, THSWD may inhibit tumor angiogenesis in breast cancer patients by decreasing microvessel density (MVD) and vascular endothelial growth factor-A (VEGF-A) expression (6). Clinically, it is often added or subtracted on the basis of this prescription to treat cerebrovascular, gynecological cardiovascular and others, DG and CX have good therapeutic effects on gynecological conditions, especially breast diseases. Our group previously combined UPLC-Q-TOF-MS^E technology to investigate the therapeutic effects of THSWD on breast cancer in a murine model and revealed its beneficial effects were closely related to apoptosis (7). However, research on the mechanism by which THSWD functions is still not fully clear, therefore, it is of great theoretical value and research significance to further explore the mechanism of action of THSWD in the treatment of breast cancer. Network pharmacology is an emerging discipline that combines pharmacology, computer science, and information networking on the basis of systems biology (8). Through network pharmacology, data on ingredients, diseases, and their related targets are often gathered through existing online databases, and visualization software is then used to systematically analyze TCMs by constructing an "ingredient-target-pathway" network, so as to define the drug intervention and the treatment effects on different diseases (9). The systematic nature of network pharmacology is consistent with the holistic view and syndrome differentiation theory of TCM has been widely applied to the study of TCM to generate new research data, methods and results (10–12). Based on this approach, we used network databases to construct an "ingredient-target" network, a PPI network for enrichment analysis. Next, we used molecular docking studies to further investigate the mechanisms through which THSWD exerts its therapeutic effects and these were accompanied by *in vitro* cell experiments, to provide a basis for its clinical application in breast cancer.

MATERIALS AND METHODS

Network Pharmacology Study

Screening of Active Ingredients of THSWD

The *in vitro* chemical composition of THSWD was determined by ultraperformance liquid chromatography quadrupole time of flight mass spectrometry (UPLC-Q-TOF-MS^E) (7), and compounds were selected according to the Lipinski's rule of five (13)— MWT ≤ 500, H-bond donors ≤ 5, H-bond acceptors ≤ 10, and logP ≤ 5—to select the most likely active ingredients. Moreover, several active ingredients with relative high content or excellent bioactivity, which did not satisfy these criteria, were also manually supplemented as candidate compounds for further analysis (14).

Compound-Related Targets Prediction

The mol2 file or SDF file of the active ingredient was downloaded using the zinc website (zinc.docking.org) and PubChem website (pubchem.ncbi.nlm.nih.gov) and was uploaded to the

PharmMapper database (www.lilab-ecust.cn/pharmmapper) and "Homo sapiens" was selected for the prediction results.

Breast Cancer-Related Targets Prediction

The terms for "breast cancer", for breast cancer targets and the OMIM database (http://omim.org) and the Genecards database (http://www.genecards.org) search.

Intersection of Compound Targets and Breast Cancer Targets

After obtaining the targets related to THSWD and targets of breast cancer, overlapping targets were selected. The overlapping targets are the possible targets for THSWD to exert therapeutic effects on breast cancer, which can improve the accuracy of screening targets and increase the credibility of the results. Using the "Compounds-targets" network of Cytoscape 3.7.1 software, the ingredients and intersection targets are nodes in the network, and the edges represent connections between ingredients and their active targets. The network was topologically analyzed using the "network analyzer" function of the software. The key compounds of THSWD for breast cancer treatment were screened based on the analysis results.

Establishment of the Protein-Protein Interaction Network

Common targets were uploaded to the STRING database (https://www.string-db.org/) to construct a protein-protein interaction (PPI) network. Protein species were set as human origin, and minimum required interaction score was set as the "highest confidence (0.900)" while concealing free points, to obtain the PPI network. The PPI network data were input into Cytoscape 3.7.1 software, and the PPI network was analyzed using the "network analyzer" function, with nodes whose degree and betweenness centrality values were greater than those of mean values as the key targets. In the network, node means compound or target, high degree indicates greater probability that the compound or target is exerting its effect.

Gene Ontology and Pathway Enrichment Analysis

Gene Ontology (GO) functional enrichment and KEGG pathway enrichment were performed using the David database (https://david.ncifcrf.gov/), in which the GO analysis included 3 components: Biological Process (BP), Cellular Component (CC), Molecular Function (MF), and the False Discovery Rate (FDR) values were set to obtain GO and KEGG enrichment results, we used the cluster profiler R package to perform GO analysis and KEGG analysis for the potential targets of THSWD in the treatment of breast cancer.

Molecular Docking Validation of Key Components and Key Targets

The top three key compounds from the results of item "2.1.4" were output as mol2 format files in TCMSP database (https://tcmspw.com/tcmsp.php), and the top three key targets in the PPI network, in the PDB database (http://www.rcsb.org) were used to define the molecular structures. Molecular docking of key active ingredients with key targets was performed using Autodock VINA software, binding energies were evaluated as evaluation indexes, and PyMOL software was used to present the results.

In Vitro Experiments

Chemicals and Reagents

Prunus persica (L.) Batsch (Taoren, TR, batch number: 17033101), Carthamus tinctorius L. (Honghua, HH, batch number: 17041401), Angelica sinensis (Oliv.) Diels (Danggui, DG, batch number: 16070501), Conioselinum anthriscoides 'Chuanxiong' (syn. Ligusticum chuanxiong Hort) (Chuanxiong, CX, batch number: 17061601), Paeoniae lactiflora Pall. (Baishao, BS, batch number: 17050301), and Rehmannia glutinosa (Gaertn.) DC (Shudi, SD, batch number: 17042501) were purchased from Anqing Huashi Chinese Herbal Medicine Co. Ltd. (Anqing, China). All TCM materials were qualified by Professor Huasheng Peng (hspeng@126.com). For cell culture studies, Dulbecco's modified Eagle's medium (DMEM) was purchased from Gibco and fetal bovine serum (FBS) were purchased from Gemini(Shanghai China).

Sample Preparation

The herbs TR, HH, DG, SD, CX, and BS (3:2:3:4:2:3) were soaked then decocted twice with 10 volumes of 75% ethanol for 2 h and 8 volumes of 75% ethanol for 1.5 h. The extraction solutions were then filtered and combined. The filtrates were concentrated to 18 g/kg.

Animals

Healthy male adult Sprague-Dawley (SD) rats weighing 200 ± 20 g and aged 63–70 days were purchased from Shandong Experimental Animal Center (permit number: scxk-2019000). After adaptive feeding for 7 days, 25 rats each were randomly assigned to the rat serum control group and THSWD serum groups using a random numbers table.

THSWD Serum

Rats were administered the THSWD solution (9.0g/kg) intragastrically by gavage once daily for 7 days. Rats in the blank group were given saline. Blood samples were obtained from the aorta 1 h after the last gavage, all rats were anesthetized by intraperitoneal injection of chloral hydrate (350 mg-kg^{-1}) and sacrificed by cervical vertebrae dislocation. The serum was separated from the blood. Subsequently, the serum was put in water bath 56°C for 30 min to be inactivated, after which the bacteria were eliminated by filtering through a 0.22-μm filter and stored at -20°C until use. All experiments were subject to approval by the Committee on the Ethics of Animal Experiments of Anhui University of Chinese medicine (Permit Number: AHUCM-Rats-2021023).

Cell Culture

Human breast cancer MCF-7 (Cat: 100137) and MDA-MB-231 (Cat: 339911) cell lines were obtained from Beina Biology (Beijing China), maintained in RPMI 1640 media supplemented with 10% FBS and 1% penicillin/streptomycin, then incubated in a humidified atmosphere at 37°C with 5% CO_2.

The media was changed daily and logarithmic growth cells were recorded for the experiment.

Cell Proliferation Assay

We seeded MCF-7 and MDA-MB-231 cells in a 96-well plate. The results of network pharmacology show that THSWD exerted therapeutic closely to Ras related Signaling pathways. GRB2, AKT1, MAPK1 and MAPK14 were located up/downstream of ras pathway. Lonafarnib (SCH-66336), is a potent and orally active farnesyl transferase (FTase) inhibitor that has shown anticancer activity. Lonafarnib inhibits the activities of H-RAS, K-RAS and N-RAS. The experimental conditions were divided into the blank control, negative control group, different concentrations of THSWD serum, and different concentrations of the inhibitor lonafarnib. Cells were incubated for 24 h, 48 h, and 72 h with the different concentrations of THSWD serum (1.25%, 2.5%, 5%, 10%, 20%, 40%, 50%), and different concentrations of the inhibitor Lonafarnib (1, 2.5, 5, 10, 20, 25, 30 μM). CCK-8 was added to each well, and cells were incubated for 2 h, and then the optical density at 450 (OD450) of each well was detected by enzymatic-reader (BioRad 680). There were six replicates for each treatment.

RNA Isolation and Real-Time Quantitative Polymerase Chain Reaction

Total RNA was extracted with Trizol solution following the manufacturer's instructions. cDNA was synthesized with a first strand cDNA synthesis kit. SYBR Green qPCR SuperMix was used for real-time quantitative polymerase chain reaction (qRT-PCR). The reaction conditions were 50°C 2 min; 95°C 2 min; 95°C 15 s, and 60°C 32 s, for 40 cycles; melting curve analysis was at 60°C–95°C. Each sample was assayed three times by qRT-PCR (Biorad IQ5). Relative mRNA expression was normalized to the corresponding β-actin expression and analyzed by the $2^{-\triangle\triangle Ct}$ method. The nucleotide sequences of the primer pairs used for Quantitative gene expression are provided in **Table 1**.

Western Blotting

RIPA lysate buffer (Beyotime Biotechnology, P0013B) containing 1% PMSF was used to extract the total proteins from cells, after SDS-PAGE, the target protein range was mapped according to a marker size position. The separated proteins were then transferred to nitrocellulose filter membranes. The membrane was blocked overnight at 4°C in TBS-Tween 20 (TBST) buffer containing 5% skimmed milk powder. The HRP-labeled secondary antibody was used after washing membranes in TBST and was incubated with secondary antibodies for 1.5 hour at room temperature. Finally, the protein bands were imaged using an enhanced chemiluminescence system (P90720, Millipore).

TABLE 1 | The nucleotide sequences of the primer pairs used for Quantitative gene expression.

Gene name	Forward and Reverse Primer (5'to3')	Amplicon length
HRAS-F	5'-TGCCATCAACAACACCAAG-3'	143
HRAS-R	5'-CCTGCCGAGATTCCACA-3'	
MAPK1-F	5'-CCAGAGCAAGTCCTCCAG-3'	130
MAPK1-R	5'-GGCACCAACAGTACAAAGC-3'	
AKT1-F	5'-AAGCCCCAGGTCACGTC-3'	116
AKT1-R	5'-TCGCTGTCCACACACTCC-3'	
GRB2-F	5'-CTGGAGCGTTTGCTGTG-3'	131
GRB2-R	5'-CCAGGTGTAGAATGCCAGA-3'	
MAPK14-F	5'-CACAGGGCCACCTTCTT-3'	100
MAPK14-R	5'-GCACCTCCCAGATTGTCTT-3'	
beta-Actin-F	5'-TCTCCCAAGTCCACACAGG-3'	127
beta-Actin-R	5'-GGCACGAAGGCTCATCA-3'	

Statistical Analysis

SPSS 23.0 software was used for statistical analysis. The results were expressed as mean ± standard deviation (x ± sd). Multiple groups of independent data were compared using single factor analysis of variance. Pairwise comparisons between multiple groups were performed using t-test. *P*-values were calculated to show statistically significant differences. $P < 0.05$ was considered statistically significant.

RESULTS

THSWD Active Ingredients

Of the 107 ingredients of the THSWD, 27 active ingredients were screened *in vitro* using the Lipinski's rule of five (shown in **Table 2**), including 3 from Taoren, 8 from Honghua, 6 from Danggui, 2 from Shudi, 4 from Baishao, and 10 from Chuanxiong. Among these, there were 5 common components between Danggui and Chuanxiong, 2 common components between Baishao and Honghua, and 1 common component between Shudi, Baishao and Honghua.

Common Targets of THSWD and Breast Cancer

Integration of the targets of the ingredients in the PharmMapper database produced 5757 gene targets. After removing duplicates, a total of 461 relevant human genes were obtained. In OMIM and Genecard databases, 3264 repetitive breast cancer-related targets were obtained, the 461 targets predicted with the active ingredients of THSWD were intersected using a Venn diagram, resulting in 218 intersection targets, which were potential active targets of THSWD acting on breast cancer (**Figure 1**).

"Components-Targets" Network Analysis

Twenty-seven active components and 218 common targets were imported into Cytocsape 3.7.1 software to construct the "Components-targets" network. There were 245 nodes (27 active ingredients and 218 targets) and 2855 edges in the network, shown in **Figure 2**. The network analyzer results showed, the average degree of node was 105.74, the average betweenness centrality was 0.034, the average closeness centrality was 0.511, and there were 11 compound nodes whose values all exceeded the average value (shown in **Table 3**), it is speculated that these compounds may be key compounds for THSWD to exert therapeutic effects against breast cancer.

PPI Network Analysis

In total, 102 nodes and 301 edges were included in the PPI network, indicating that 102 targets could interact with each

TABLE 2 | Active components of THSWD.

ID	Active Component	MW	nOHNH	nON	miLog P	Source
MOL001320	Amygdalin	457.48	7	12	-2.30	T
MOL001321	Mandelonitrile	133.16	1	2	1.20	T
MOL000771	P-Hydroxycinnamic acid	164.17	2	3	1.64	T
MOL002690	Hydroxysafflor-yellow-A	612.59	12	16	-4.45	H
MOL000340	3-Phenylpropionic acid	150.19	1	2	1.93	H
MOL002737	Scutellarein	342.34	0	6	3.10	H
MOL000006	Luteolin	286.25	4	6	2.07	H
MOL000415	Rutin	610.57	10	16	-1.45	H
MOL004474	4-Ethylphenol	122.18	1	1	2.51	H
MOL000414	Caffeic acid	180.17	3	4	1.37	D
MOL001456	Citric acid	192.14	4	7	-1.39	D
MOL010858	Tianshic acid	330.52	4	5	3.67	D
MOL002111	Butylidenephthalide	188.24	0	2	3.00	D C
MOL002143	Senkyunolide C	204.24	1	3	2.74	D C
MOL002146	Senkyunolide F	206.26	1	3	1.84	D C
—	Jionoside B1	814.78				S
MOL000360	Ferulic acid	194.20	2	4	1.62	S B H
MOL001935	paeonilactone B	196.22	1	4	-0.10	B
MOL000422	Kaempferol	286.25	4	6	1.77	B H
MOL000513	Gallic acid	170.13	4	5	0.63	B H
MOL011782	Ligustilide	190.26	0	2	2.94	C
MOL002208	Senkyunolide A	192.28	0	2	3.19	C
MOL002209	Senkyunolide G	208.28	1	3	2.54	C
MOL000114	Vanillic acid	168.16	2	4	1.15	C
MOL002181	4-Hydroxy-3-Butylphthalide	206.26	1	3	2.99	C
MOL002049	Ferulaldehyde	178.20	1	3	1.67	C D
MOL011786	Senkyunolide E	204.24	1	3	1.90	C D

other, resulting in a total of 301 interactions, shown in **Figure 3**. The network analyzer results showed, the average degree of nodes was 5.902, the average betweenness centrality was 0.022, and the average closeness centrality was 0.367; there were 14 compound nodes whose values all exceeded the average value, It was visualized and displayed by Cytoscape software, in which, node size represented the size of degree value, and the larger the node, the greater the corresponding degree value, and the higher

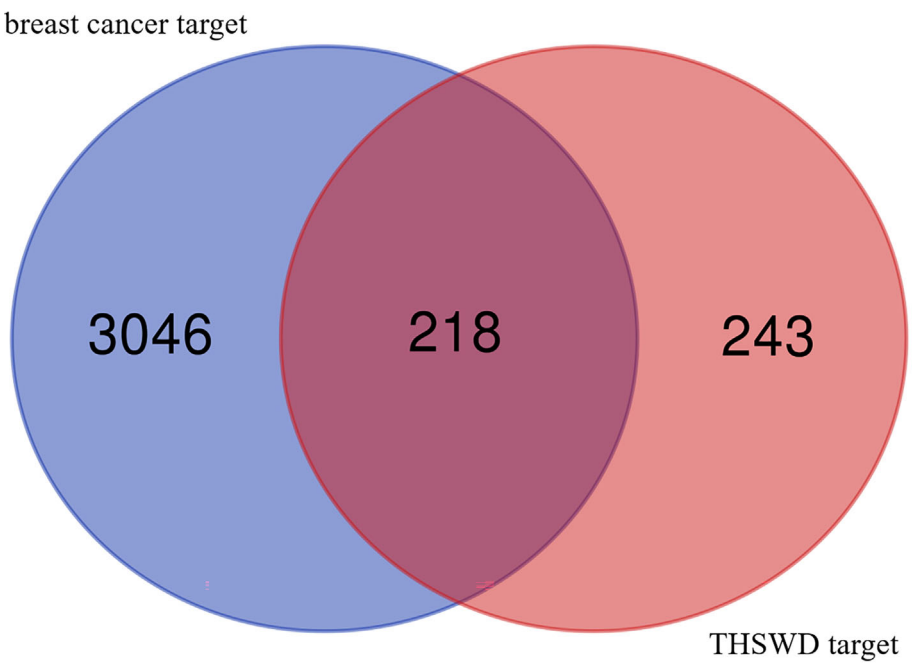

FIGURE 1 | Venn diagram of component target and disease target.

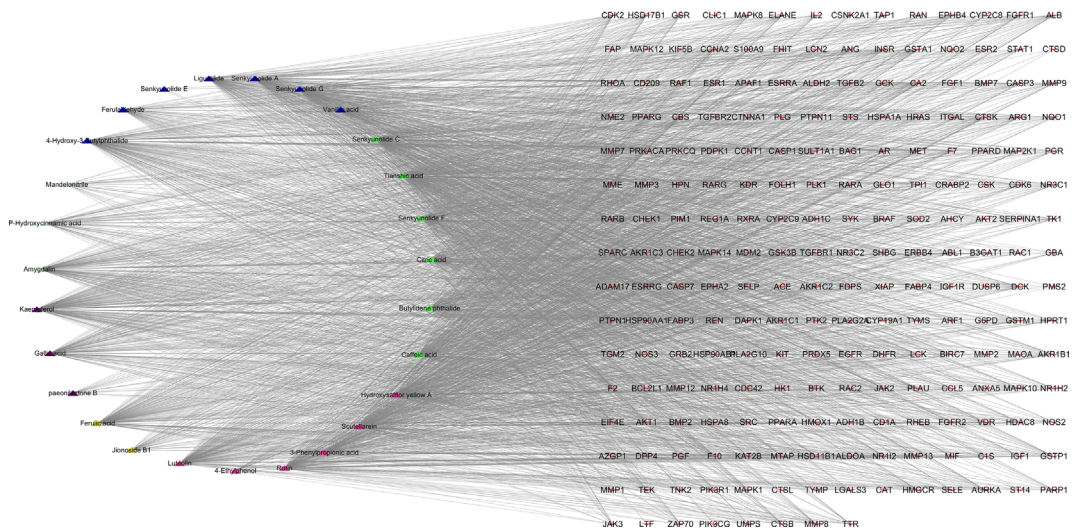

FIGURE 2 | "Components-targets" interaction network.

the degree of interaction association of this protein with others, We speculated that these targets were be the key targets for THSWD for the treatment of breast cancer (**Figure 4**).

GO Function Enrichment Analysis

To explore the dynamic activity of THSWD in breast cancer, we used the DAVID database to enrich the GO bioprocesses of 218 common targets; FDR and P-values <0.01 were used for filtering. The results of the GO enrichment analysis contained 62 BPs involved in negative regulation of apoptotic processes, protein autophosphorylation, steroid hormone-mediated signaling pathways, and peptidyl-tyrosine autophosphorylation; 32 MF involved protein tyrosine kinase activity, steroid hormone receptor activity, and ATP binding; 16 CC involved cytosol, extracellular space, and extracellular exosomes. The top 10 related entries for BP, MF, and CC are shown in bubble plots using the cluster profiler R package (**Figure 5**).

KEGG Analysis

The KEGG pathway enrichment function of pathways module in David database was used to explore the function of 218 potential gene targets in signaling pathways involved in the treatment of breast cancer by THSWD. KEGG enrichment analysis showed a total of 54 pathways with significant differences (FDR<0.01, P<0.01). The top 10 pathways are visually represented in a bubble plot in **Figure 6**. KEGG enrichment results indicated that THSWD might exert therapeutic effects by participating in the regulation of RAS, FOXO, PI3K/Akt, and other signaling pathways.

THSWD-Prescription Composition-Active Ingredients-Targets-Pathway

Based on the KEGG pathway enrichment results, the top 10 ranked signaling pathways that were identified to be closely related to breast cancer were combined with information of the THSWD active ingredients and intersection targets with breast cancer to construct a "THSWD-prescription composition-active ingredients-targets-pathway" network (**Figure 7**). This plot intuitively indicates that the processes of THSWD for the treatment of breast cancer involve multiple active ingredients, targets, and pathways.

TABLE 3 | Basic information of hub compounds of Tao-Hong-Si-Wu Decoction in the treatment of breast cancer.

Compound	Degree	Betweenness Centrality	Closeness Centrality
Senkyunolide E	166	0.11965001	0.65498652
Kaempferol	158	0.06122716	0.62790698
Luteolin	157	0.05458365	0.62467866
Rutin	152	0.07629322	0.60902256
Scutellarein	151	0.05224282	0.60598504
Senkyunolide C	148	0.07755585	0.5970516
Hydroxysafflor yellow A	148	0.05995414	0.5970516
4-Hydroxy-3-Butylphthalide	147	0.05197661	0.59413203
Senkyunolide G	146	0.04863749	0.59124088
Ferulic acid	134	0.04116615	0.55862069
Senkyunolide A	128	0.03593588	0.54362416

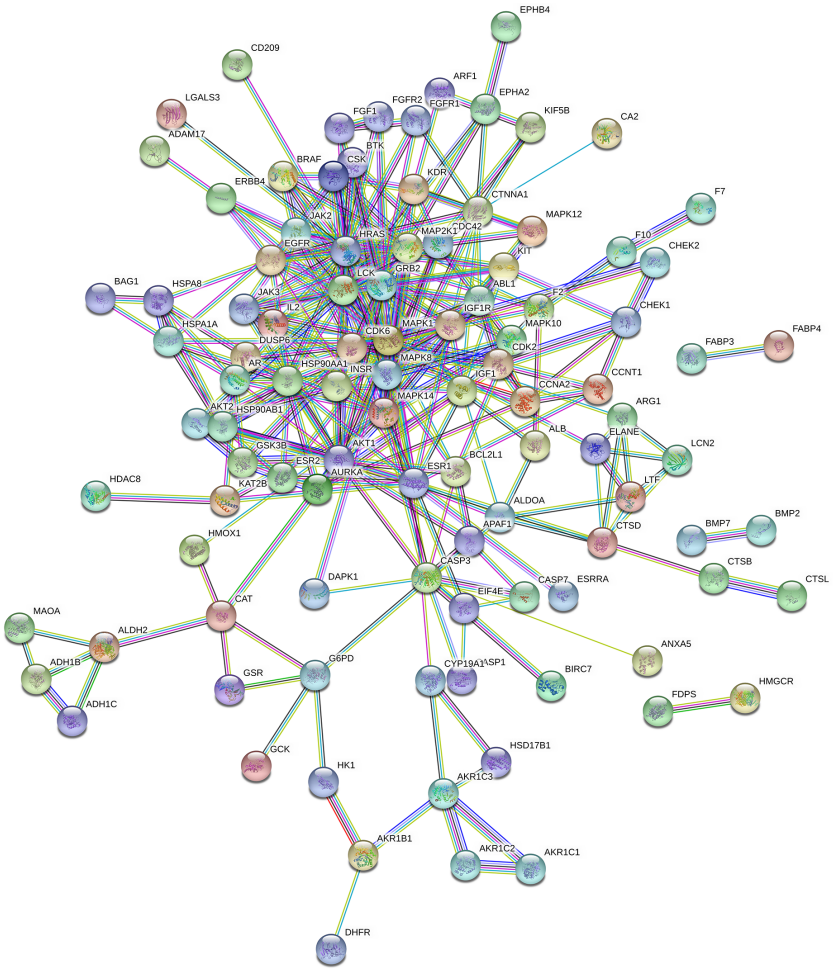

FIGURE 3 | PPI network of THSWD in treating potential targets of breast cancer.

Molecular Docking Results

The top 3 ingredients selected from 11 key ingredients with the corresponding top 5 of 14 key targets were subjected to molecular docking, and the results are shown in **Table 4**, and the partial docking conformations are shown in **Figure 8**. Different ligand molecules have greater affinity for the receptor protein through hydrogen bonding. The molecular docking results demonstrated that the key active ingredients of THSWD could tightly bind to the relevant targets, confirming the ingredient target prediction results. The binding energies between key components and corresponding target proteins did not exceed -4.5 kcal/mol, which indicated that the key components of THSWD had good binding ability to the corresponding target proteins. Most of the docked targets were distributed in pathways involving cancer, such as Ras, FoxO, PI3K-Akt, and other signaling pathways, thus demonstrating that the active ingredients of THSWD could have an impact on the occurrence and development of breast cancer by acting on the related targets and their corresponding signaling pathways.

In Vitro Experiments

THSWD Serum and Inhibitor Lonafarnib Effects on Breast Cancer Cell Proliferation

The OD450 values and inhibition rate of cells in each group were calculated by treating the cells with different concentrations of THSWD serum and the inhibitor lonafarnib. The lgIC50=Xm-I(P-(3-Pm-Pn)/4). In MCF-7 cells, the IC50 dose of THSWD was determined to be 21.7% for 48 h, while for the inhibitor Lonafarnib the IC50 was 20.9 μM for 48 h. In MDA-MB-231 cells, the IC50 dose of THSWD was 19.5% for 48 h, while for the inhibitor lonafarnib the IC50 was 19.9 μM for 48 h (**Figure 9**).

Effects of THSWD Serum on the mRNA Expression of HRAS, MAPK1, AKT1, GRB2, and MAPK14 in Breast Cancer Cells

The network pharmacology results identified potential key targets and pathways of THSWD active against breast cancer. To verify the reliability of the network pharmacology prediction

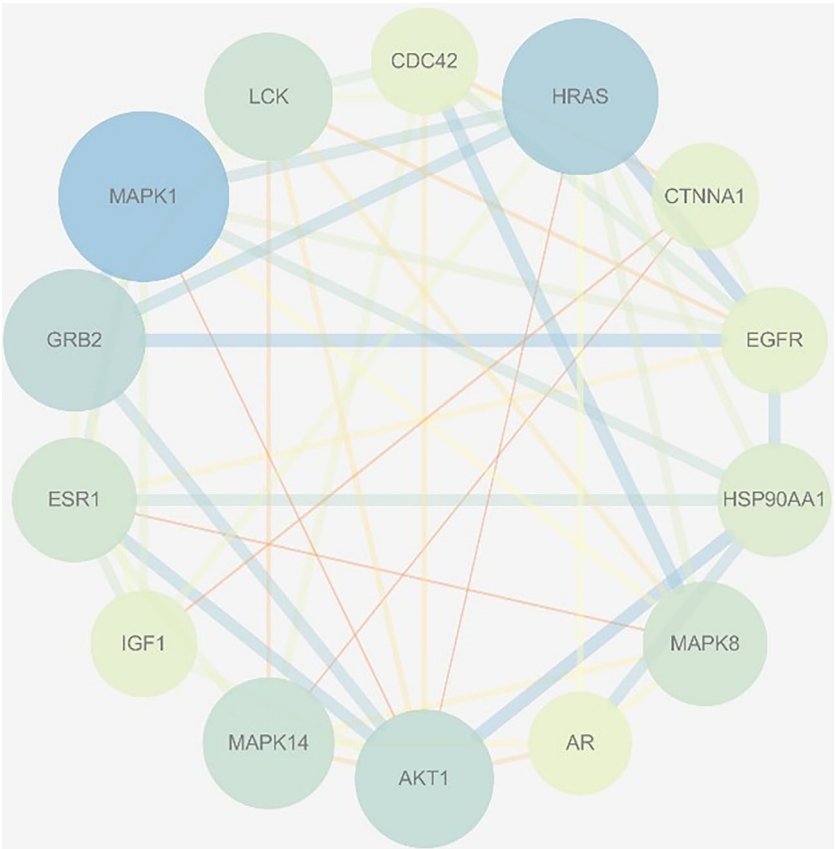

FIGURE 4 | Selected 14 core targets.

results, mRNA levels of these key genes (HRAS, MAPK1, AKT1, GRB2, and MAPK14) were assessed by qRT-PCR in MCF-7 and MDA-MB-231. As shown in **Figure 10**, 48 h after the cell lines in each group were treated, the mRNA levels of HRAS, MAPK1, AKT1, GRB2, and MAPK14 were significantly down-regulated in THSWD serum and inhibitor-treated groups compared with controls and normal serum groups, respectively ($P<0.01$). The results suggested that THSWD serum and inhibitor could inhibit HRAS, MAPK1, AKT1, GRB2, and MAPK14 transcript levels.

Effects of THSWD Serum on Protein Expression of HRAS, MAPK1, AKT1, GRB2, and MAPK14 in Breast Cancer Cells

Western blotting analysis was used to examine the expression of HRAS, MAPK1, AKT1, GRB2, and MAPK14 proteins in MCF-7 and MDA-MB-231. As shown in **Figure 11**, based on triplicate experiments, the levels of HRAS, MAPK1, AKT1, GRB2, and MAPK14 were slightly decreased in THSWD serum compared to the controls and the normal serum group. The results showed that THSWD could down-regulate the protein levels of HRAS, MAPK1, AKT1, GRB2, and MAPK14 in MCF-7 and MDA-MB-231 cells.

DISCUSSION

Surgical resection, radiotherapy, and chemotherapy are the three most common therapies for clinical breast cancer treatment; however, surgical resection cannot improve prognosis, and long-term radiotherapy and chemoradiotherapy can cause severe toxic effects. THSWD is a combination of the classic prescription Siwu Decoction plus Prunus persica (L.) Batsch and Carthamus tinctorius L. THSWD can comprehensively exert it drug activity using multiple mechanisms. It is currently used clinically as an adjunctive treatment of diseases such as breast cancer and has good efficacy for improving the hypercoagulable state of blood and preventing thrombosis in cancer patients (15). In this study, in order to explore the therapeutic mechanism of THSWD in breast cancer, network pharmacology was used to explore the key pharmacodynamic agents and target pathways of THSWD activities for breast cancer treatment by constructing "ingredients-targets," "ingredients-targets-pathway" and other networks; PPI, GO functional enrichment, KEGG pathway enrichment and molecular docking of key active ingredients and key targets were performed.

In total, 27 active ingredients and 218 common targets were used to construct the "ingredient-target" network. The results

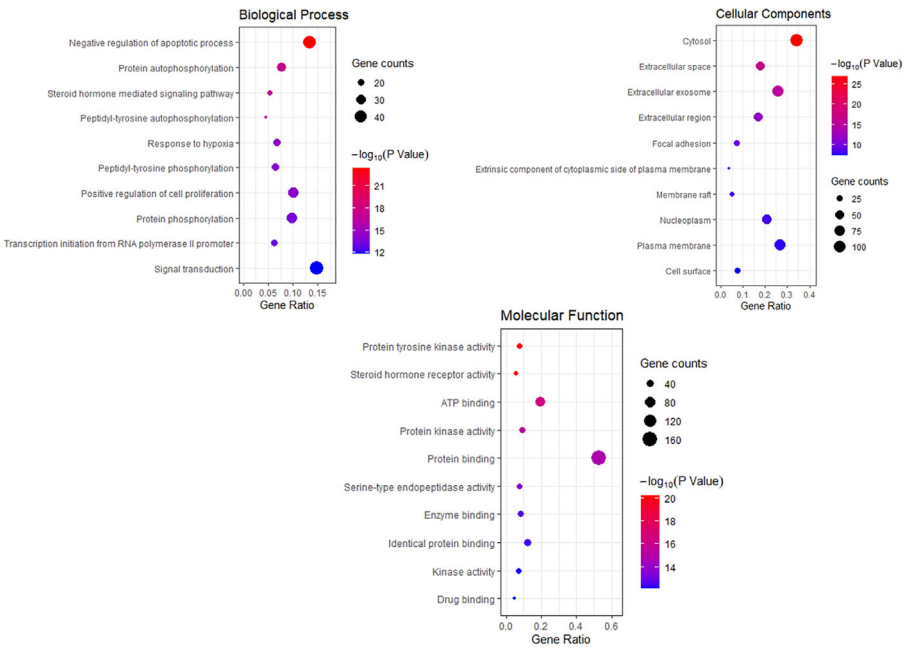

FIGURE 5 | Bubble Diagram of GO function enrichment of potential targets from the THSWD for Treatment of breast cancer. The larger the number of enriched targets, the larger the dots; the larger the P value, the bluer the dot color.

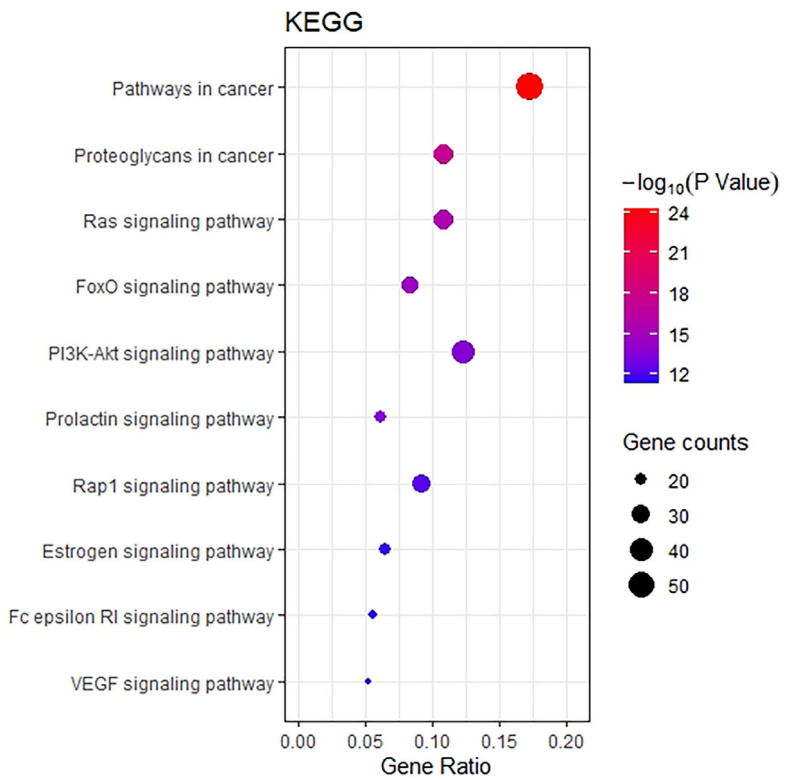

FIGURE 6 | Bubble Diagram of KEGG enrichment of potential targets from the THSWD for treatment of breast cancer. The larger the number of enriched targets, the larger the dots; the larger the P value, the bluer the dot color.

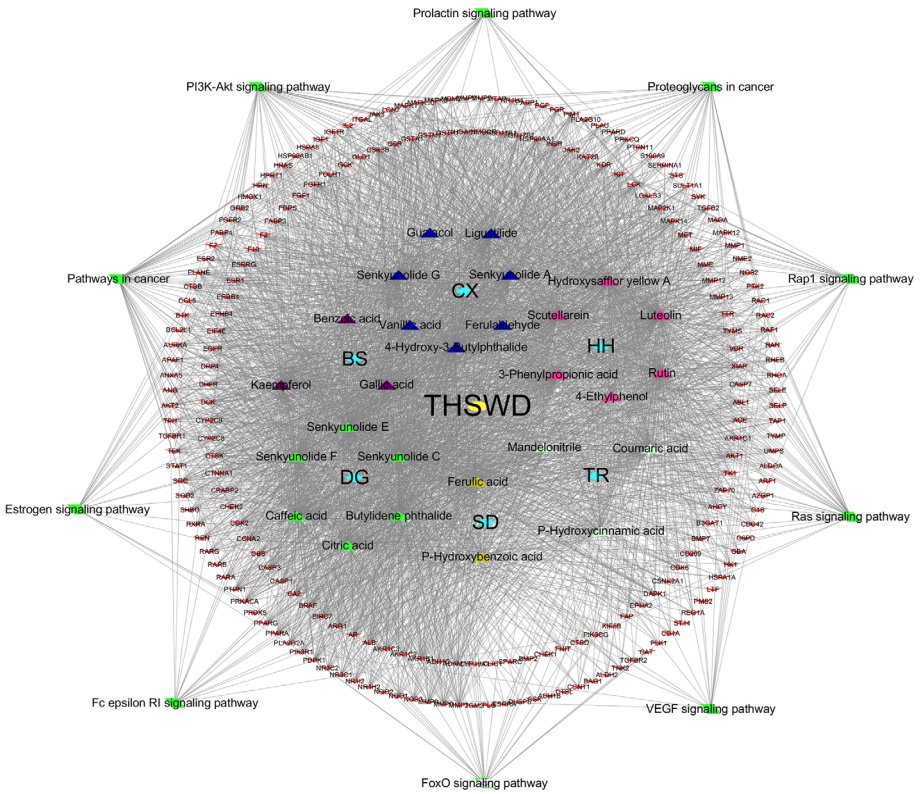

FIGURE 7 | "THSWD-prescription composition-active ingredients-targets-pathways". The yellow diamond represent THSWD, the cyan diamond represent medicinal herbs, the triangle represent the components, the red v-shaped represent the intersection targets, and the green diamond represent the signal paths.

indicated that 11 compounds including luteolin, kaempferol, and senkyunolide E might be the key ingredients in THSWD able to exert therapeutic effects against breast cancer. Luteolin is a natural flavonoid, significantly inhibited proliferation and suppressed the expression of p-STAT3, p-EGFR, p-Akt, and p-Erk1/2 in EGF-treated MCF-7 breast cancer cells (16), it also inhibited proliferation and Notch signaling-associated protein expression and regulated miRNAs in MDA-MB-231 human breast cancer cells (17). Found that combination treatment with luteolin and celecoxib in MCF-7 and MCF7/HER18 cells disturbed cell progression through the G1 phase, enhanced the expression of death receptors (such as DR5), and activated the caspase cascade. Instead, luteolin could increase Bax expression by inhibiting Bcl-2 expression, enhancing mitochondrial membrane potential collapse, and cytochrome c release (18). In MCF-7 breast cancer cells treated with 12-O-tetradecanoylphorbol-13-acetate (TPA), luteolin suppressed the expression of interleukin 8 (IL-8) and the activation of matrix metalloproteinase 9 (MMP-9), which play important roles in breast cancer proliferation. Luteolin inhibits mRNA expression by inhibiting the mitogen activated protein kinase (MAPK) signaling pathway and down regulating the AP-1 and NF-κB. In addition, luteolin inhibited TPA-induced ERK1/2 phosphorylation, and inhibited the ERK1/2 pathway following IL-8 and MMP-9 expression (19). Kaempferol is a natural flavonoid widely distributed in nature. Modern pharmacological studies have revealed that kaempferol has anti-tumor, anti-oxidant, and anti-inflammatory effects (20), and exhibits suppressive effects on a variety of tumors, including gastric (21), esophageal (22), and breast cancers (23). Kaempferol treatment of MDA-MB-231 cells for 48 h resulted in a significant decrease in the number of cells in the G1 phase, from 85.48% to 51.35%, and a significant increase in the number of cells in the G2 phase, from 9.27% to 37.5%, indicating that kaempferol contributes to the induction of G2/M arrest, and can also induce apoptosis and DNA damage in MDA-MB-231 cells. Senkyunolide E belongs to the phthalides class of compounds

TABLE 4 | Molecular docking results.

Molecule Name	Target Name	Docking score (kcal/mol)
Kaempferol	AKT1	-5.8
Kaempferol	HRAS	-5.4
Kaempferol	MAPK14	-7.6
Luteolin	AKT1	-6.1
Luteolin	HRAS	-5.9
Luteolin	MAPK1	-6.7
Luteolin	MAPK14	-8.0
Senkyunolide E	AKT1	-4.9
Senkyunolide E	MAPK1	-5.3
Senkyunolide E	MAPK14	-7.5

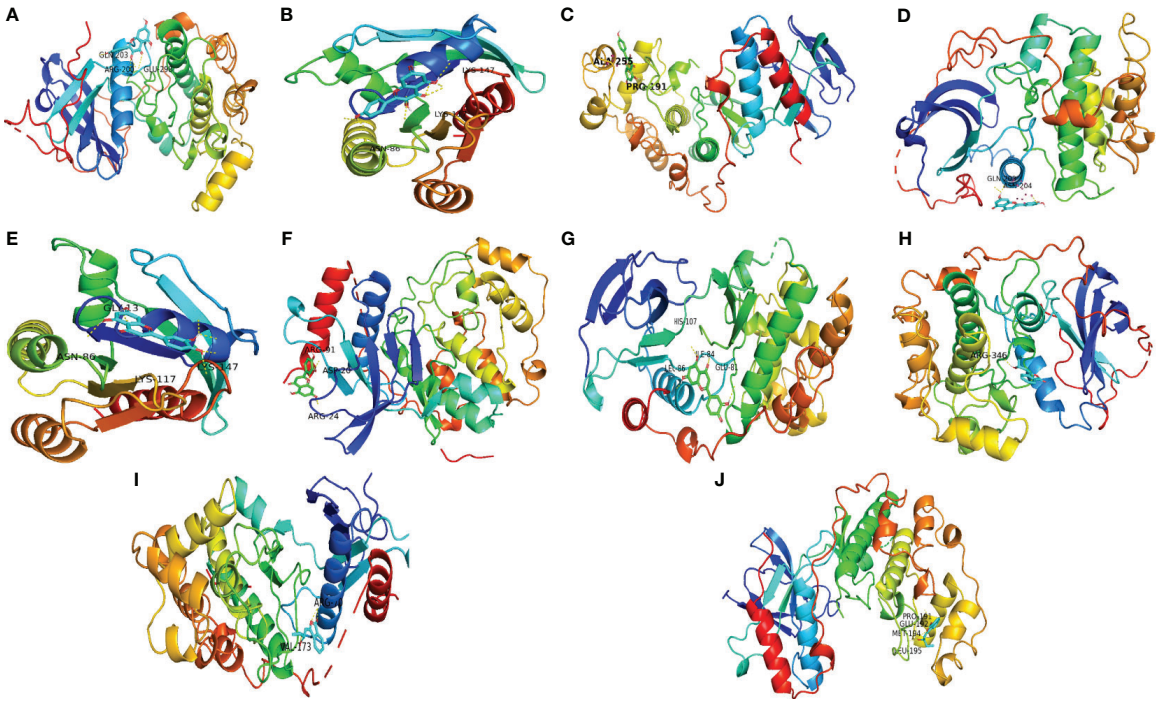

FIGURE 8 | Schematic diagram of docking results. **(A)** Kaempferol-AKT1; **(B)** Kaempferol-HRAS; **(C)** Kaempferol-MAPK14; **(D)** Luteolin-AKT1; **(E)** Luteolin-HRAS; **(F)** Luteolin-MAPK1; **(G)** Luteolin-MAPK14; **(H)** Senkyunolide E-AKT1; **(I)** Senkyunolide E-MAPK1; **(J)** Senkyunolide E-MAPK14 ARG, arginine; GLN, glutamine; LYS, lysine; GLY, glycine; ASP, aspartic acid; HIS, histidine; LEU, leucine; GLU, glutamic acid; VAL, valine; ALA, alanine; PRO, proline; ILE, isoleucine.

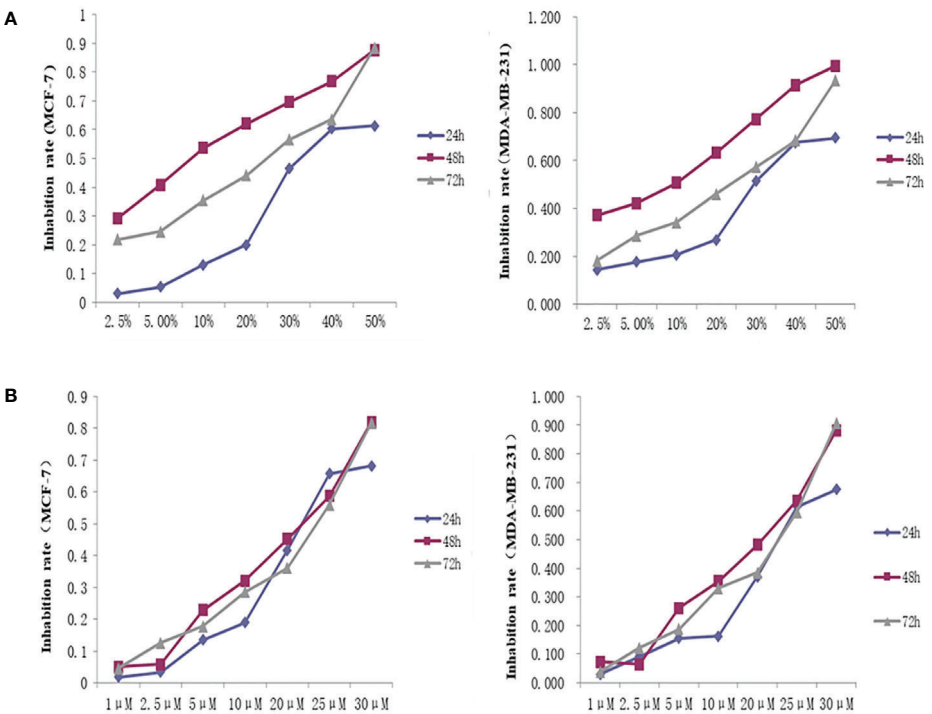

FIGURE 9 | Inhibition curve of different concentrations of THSWD serum and inhibitor Lonafarnib on MCF-7, MDA-MB-231 cells. **(A)** THSWD serum **(B)** inhibitor Lonafarnib.

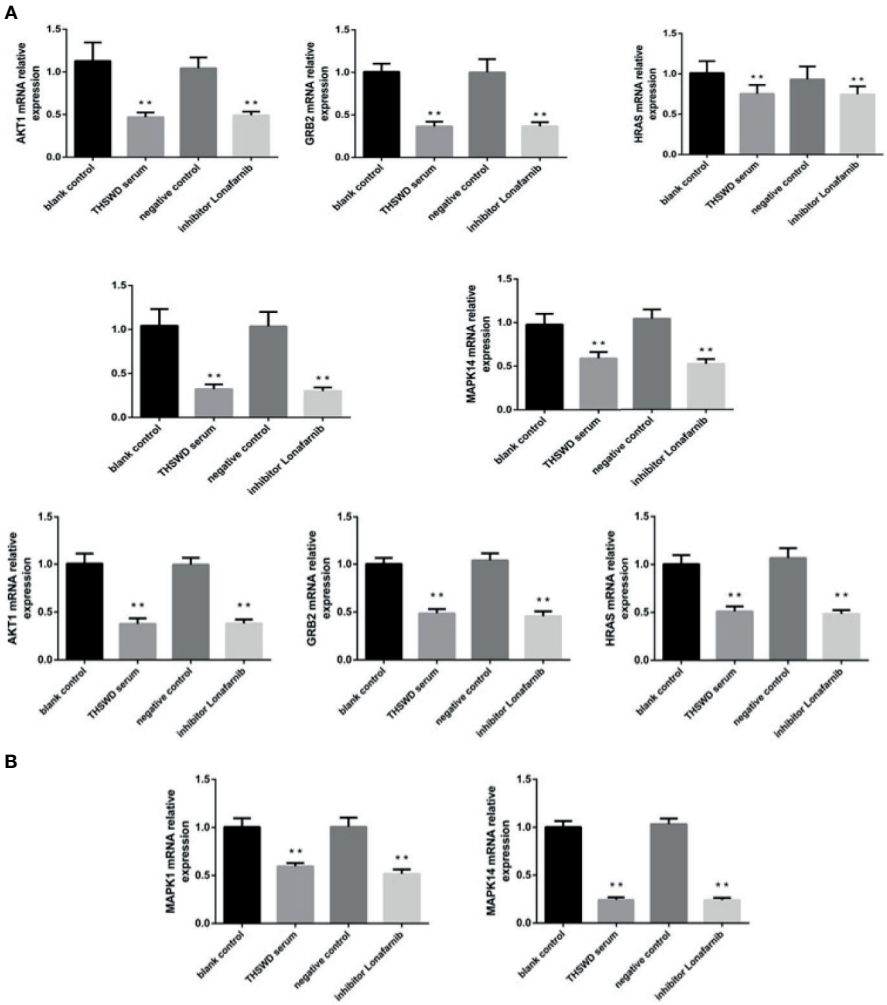

FIGURE 10 | The expression of breast cancer-related genes in MCF-7 and MDA-MB-231 cells after treatment with THSWD **(A)** MDA-MB-231 **(B)** MCF-7. **P < 0.01 compared with blank control group.

with anti-inflammatory efficacy (24) and is speculated to be associated with modulating the tumor microenvironment.

KEGG pathway enrichment results indicated that THSWD might exert its therapeutic effects on breast cancer by regulating Ras, FoxO, and PI3K-Akt signaling pathways, which have been confirmed to be involved in breast carcinogenesis. Of these, the Ras pathway is the most significant pathway, Ras oncogenes are the most common oncogenes in human cancer, members of this superfamily of GTPases (KRAS, NRAS, and HRAS), which encode four highly conserved Ras proteins sharing 85% homology. Ras protein activity is regulated by binding to GTP or GDP and involves three main downstream signaling pathways: Ras/Raf/ERK, Ras/PI3K/AKT, and Ral-GEF (25). Based on the enrichment results, THSWD exerted its therapeutic effects mostly *via* Ras/Raf/ERK, Ras/PI3K/AKT, while both pathways were closely related to cell apoptosis and proliferation (26, 27).

The Ras-MAPK signaling pathway is involved in a variety of human tumors and development processes. MAPK signaling follows a tertiary enzymatic cascade, the Ras-Raf-MEK-MAPK pathway. Four subfamilies have been identified in the MAPK pathway, of which the extracellular signal regulated protein kinase (ERK) is the most studied. The main mechanism currently recognized for the Ras-MAPK/ERK signaling pathway is that this pathway, once aberrantly activated, auto mutation activation and sustained activation by upstream signaling, further activates downstream proteins, leading to cell proliferation, vascularization, apoptosis inhibition, tissue invasion, and ultimately promotes tumor development. The Ras-MAPK pathway can also act as a tumor suppressor by inducing cell senescence and apoptosis, and as a MAPK subfamily, active ERK is abnormally elevated in breast cancer cells during development and progression (28), aberrant ERK activation leads to proliferation and apoptosis inhibition in breast cancer (29).

Through *in vitro* experiments, using THSWD serum as an intervention, we selected two types of breast cancer cell lines,

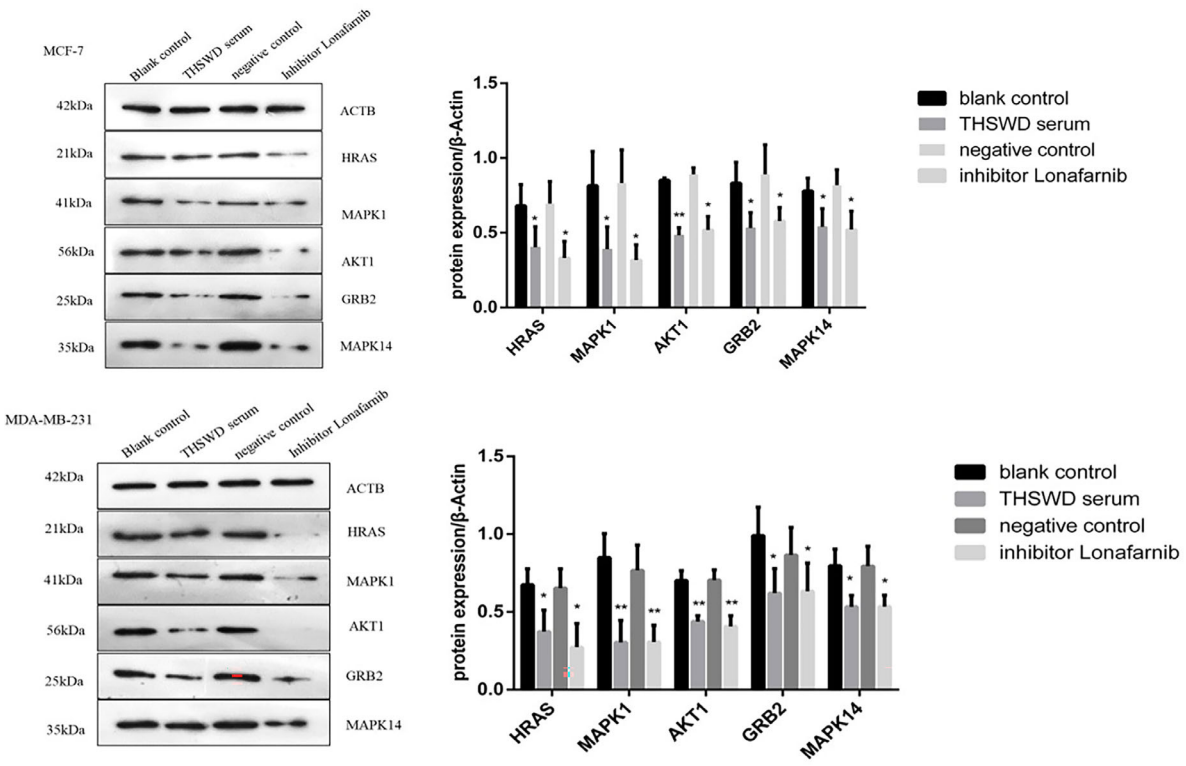

FIGURE 11 | Effect of serum containing THSWD on the protein expression of HRAS, MAPK1, AKT1, GRB2 and MAPK14 in MCF-7 and MDA-MB-231 cells. *P < 0.05, **P < 0.01 compared with blank control group.

MCF-7 and MDA-MB-231, to conduct CCK-8 experiments, and found that THSWD exerted inhibitory effects on the proliferation of breast cancer cells, and the optimal concentration of THSWD serum was approximately 20%. Western blotting and PCR experiments proved THSWD induced down-regulation of HRAS, MAPK1, AKT1, GRB2, and MAPK14 protein and mRNA levels in two types of cell lines. These targets were the top five targets identified in the previous PPI network analysis, MAPK is mitogen activated protein kinases, a family of serine/threonine protein kinases, that are important transmitters of signals from the cell surface to the interior of the nucleus, and can transduce extracellular signals into the nucleus, through cascades that phosphorylate and activate downstream transcription factors, to regulate gene expression, and ultimately participate in various physiological processes, such as cell invasion, differentiation, proliferation, and apoptosis (30). MAPK1 is phosphorylated by upstream kinases and upon activation, it translocates to the nucleus of stimulated cells where it phosphorylates nuclear targets. MAPK1 has been shown to be involved in processes such as autophagy, lipid metabolism, proliferation, migration, and invasion (31, 32), HRAS belongs to the RAS family of small GTPases and is a frequently mutated oncogene in cancer, HRAS regulates a complex signal transduction network, including the RAF-MEK-ERK cascade, VEGF-PI3K-AKT pathway and Raf-1 signaling to promote cancer cell proliferation, migration, angiogenesis, and autophagy (33).

Thus, our findings show that THSWD regulates breast cancer in many ways through active ingredients and targets. THSWD can suppress breast cancer cell proliferation. Therefore, these results provide a valuable theoretical basis for THSWD as a potential drug for the treatment of breast cancer.

CONCLUSIONS

In the present study, the network pharmacology approach was adopted for the first time to explore the underlying mechanism of THSWD on breast cancer. Studies on the MCF-7 and MDA-MB-231 cells showed that THSWD had significant anti-cancer activities. By network pharmacology analysis, the results demonstrated that the anti-cancer mechanism of THSWD might be through modulation of the Ras, FoxO, and PI3K-Akt signaling pathways. THSWD serum regulated the expression of cancer-related genes and proteins. It induced apoptosis, and inhibited cell proliferation of MCF-7 and MDA-MB-231 cells. The anti-cancer effect of THSWD might by achieved *via* the down-regulation of MAPK1, HRAS, GRB2, AKT1, and MAPK14. Our study demonstrated the reliability of the network pharmacology method, as well as revealed the anti-cancer effect and potential mechanisms of action of THSWD.

DATA AVAILABILITY STATEMENT

The datasets presented in this study can be found in online repositories. The names of the repository/repositories and accession number(s) can be found in the article/supplementary material.

ETHICS STATEMENT

The animal study was reviewed and approved by The Committee on the Ethics of Animal Experiments of Anhui University of Chinese medicine (Permit Number: AHUCM-Rats-2021023).

AUTHOR CONTRIBUTIONS

SH and YC contributed equally to this work. SH and YC conceived and designed the study. SH, LP, CF, NW, and FC performed the *in vitro* experiments. SH and YC wrote the manuscript. YW and XC provided ideas for the experimental design and modified the manuscripts to ensure the integrity of the entire experimental design. All authors contributed to the article and approved the submitted version.

FUNDING

This research was supported by the National Natural Science Fund Regional Innovation and Development Joint Fund Project (No.U19A2009), National Natural Science Foundation of China (Grant No. 82074059), Anhui University Collaborative Innovation Project (GXXT-2019-043), the Anhui Provincial College Natural Science Research Key Project (No. KJ2019A0466), Excellent and Top Talents Program in Colleges and Universities (No. gxyq2019034), Anhui Provincial Key Laboratory of Traditional Chinese Medicine Compounds (2019AKLCMF03), and the Natural Science Research Project of Colleges and Universities in Anhui Province (2019fyyb038).

REFERENCES

1. Sung H, Ferlay J, Siegel RL, Laversanne M, Soerjomataram I, Jemal A, et al. Erratum: Global Cancer Statistics 2018: GLOBOCAN Estimates of Incidence and Mortality Worldwide for 36 Cancers in 185 Countries. *CA Cancer J Clin* (2020) 70(4):313. doi: 10.3322/caac.21609
2. Kim W, Lee B, Le W, Min B, Ba K, Le S, et al. Traditional Herbal Medicine as Adjunctive Therapy for Breast Cancer: A Systematic Review. *Complement Ther Med* (2015) 23(4):626–32. doi: 10.1016/j.ctim.2015.03.011
3. Liu L, Duan J, Su S, Liu P, Tang Y, Qian D. Siwu Series Decoctions for Treating Primary Dysmenorrea of Gynecology Blood Stasis Syndrome–Research Progress of Taohong Siwu Decoction. *Chin J Chin Mater Med* (2015) 40(05):814–21. doi: 10.4268/cjcmm20150508
4. Xia W, Hu S, Wang M, Xu F, Han L, Peng D. Exploration of the Potential Mechanism of the Tao Hong Si Wu Decoction for the Treatment of Postpartum Blood Stasis Based on Network Pharmacology and *In Vivo* Experimental Verification. *J Ethnopharmacol* (2021) 268:113641. doi: 10.1016/j.jep.2020.113641
5. Duan X, Han L, Peng D, Chen W, Peng C, Xiao L, et al. High Throughput mRNA Sequencing Reveals Potential Therapeutic Targets of Tao-Hong-Si-Wu Decoction in Experimental Middle Cerebral Artery Occlusion. *Front Pharmacol* (2018) 9:1570. doi: 10.3389/fphar.2018.01570
6. Yang H, Tong C, Chu A, Xie D. Effect of Tao Hong Siwu Decoction on Angiogenesis in Patients With Breast Cancer. *J Guangzhou Univ Tradit Med* (2012) 29(06):623–6. doi: 10.13359/j.cnki.gzxbtcm.2012.06.028
7. Duan X, Pan L, Bao Q, Peng D. UPLC-Q-TOF-MS Study of the Mechanism of THSWD for Breast Cancer Treatment. *Front Pharmacol* (2019) 10:1625. doi: 10.3389/fphar.2019.01625
8. Luo T, Lu Y, Yan S, Xiao X, Rong X, Guo J. Network Pharmacology in Research of Chinese Medicine Formula: Methodology, Application and Prospective. *Chin J Integr Med* (2020) 26(1):72–80. doi: 10.1007/s11655-019-3064-0
9. Zhang R, Zhu X, Bai H, Ning K. Network Pharmacology Databases for Traditional Chinese Medicine: Review and Assessment. *Front Pharmacol* (2019) 10:123. doi: 10.3389/fphar.2019.00123
10. He D, Huang J, Zhang Z, Du Q, Peng W, Yu R, et al. A Network Pharmacology-Based Strategy For Predicting Active Ingredients And Potential Targets Of LiuWei DiHuang Pill In Treating Type 2 Diabetes Mellitus. *Drug Des Devel Ther* (2019) 13:3989–4005. doi: 10.2147/dddt.S216644
11. Lin H, Wang X, Wang L, Dong H, Huang P, Cai Q, et al. Identified the Synergistic Mechanism of Drynariae Rhizoma for Treating Fracture Based on Network Pharmacology. *Evid Based Complement Alternat Med* (2019) 2019:7342635. doi: 10.1155/2019/7342635
12. Ma X, Yu M, Hao C, Yang W. Identifying Synergistic Mechanisms of Multiple Ingredients in Shuangbai Tablets Against Proteinuria by Virtual Screening and a Network Pharmacology Approach. *Evid Based Complement Alternat Med* (2020) 2020:1027271. doi: 10.1155/2020/1027271
13. Lipinski C. Lead-And Drug-Like Compounds: The Rule-of-Five Revolution. *Drug Discov Today Technol* (2004) 1(4):337–41. doi: 10.1016/j.ddtec.2004.11.007
14. Jiang Z, Wang L, Pang H, Guo Y, Xiao P, Chu C, et al. Rapid Profiling of Alkaloid Analogues in Sinomenii Caulis by an Integrated Characterization Strategy and Quantitative Analysis. *J Pharm BioMed Anal* (2019) 174:376–85. doi: 10.1016/j.jpba.2019.06.011
15. Fu S, He Y, Wang N, Xie Y. Effects of Taohong Siwu Decoction on Protein Expressions of Bcl-2, Bax and Ki-67 in Invasive Breast Cancer. *Acta Chin Med Pharm* (2018) 46(04):89–92. doi: 10.19664/j.cnki.1002-2392.180124
16. Wruck CJ, Claussen M, Fuhrmann G, Romer L, Schulz A, Pufe T, et al. Luteolin Protects Rat PC12 and C6 Cells Against MPP+Induced Toxicity Via an ERK Dependent Keap1-Nrf2-ARE Pathway. *J Neural Transm Suppl* (2007) (72):57–67. doi: 10.1007/978-3-211-73574-9_9
17. Blancas-Benitez F, Mercado-Mercado G, Quirós-Sauceda A, Montalvo-González E, González-Aguilar G, Sáyago-Ayerdi S. Bioaccessibility of Polyphenols Associated With Dietary Fiber and *In Vitro* Kinetics Release of Polyphenols in Mexican 'Ataulfo' Mango (Mangifera Indica L.) by-Products. *Food Funct* (2015) 6(3):859–68. doi: 10.1039/c4fo00982g
18. Sui J, Xie K, Xie M. Inhibitory Effect of Luteolin on the Proliferation of Human Breast Cancer Cell Lines Induced by Epidermal Growth Factor. *Sheng Li Xue Bao* (2016) 68(1):27–34. doi: 10.13294/j.aps.2016.0005
19. Jeon Y, Ahn Y, Chung W, Choi H, Suh Y. Synergistic Effect Between Celecoxib and Luteolin is Dependent on Estrogen Receptor in Human Breast Cancer Cells. *Tumour Biol* (2015) 36(8):6349–59. doi: 10.1007/s13277-015-3322-5
20. Choi J, Kim J, Lee H, Pak J, Shim B, Kim S. Reactive Oxygen Species and P53 Mediated Activation of P38 and Caspases is Critically Involved in Kaempferol Induced Apoptosis in Colorectal Cancer Cells. *J Agric Food Chem* (2018) 66 (38):9960–7. doi: 10.1021/acs.jafc.8b02656
21. Kim T, Lee S, Kim M, Cheon C, Ko S. Kaempferol Induces Autophagic Cell Death *via* IRE1-JNK-CHOP Pathway and Inhibition of G9a in Gastric Cancer Cells. *Cell Death Dis* (2018) 9(9):875. doi: 10.1038/s41419-018-0930-1
22. Yao S, Wang X, Li C, Zhao T, Jin H, Fang W. Kaempferol Inhibits Cell Proliferation and Glycolysis in Esophagus Squamous Cell Carcinoma *via* Targeting EGFR Signaling Pathway. *Tumour Biol* (2016) 37(8):10247–56. doi: 10.1007/s13277-016-4912-6

23. Zhu L, Xue L. Kaempferol Suppresses Proliferation and Induces Cell Cycle Arrest, Apoptosis, and DNA Damage in Breast Cancer Cells. *Oncol Res* (2019) 27(6):629–34. doi: 10.3727/096504018x15228018559434
24. Ma N, Fan S, Li X, Yang Z, Lin M, Wang H, et al. Screening of Anti-Inflammatory Substances of Chuanxiong R Hizoma and Analysis of Its Mechanism. *Chin J Exp Tradit Med Formulae* (2018) 24(18):140–6. doi: 10.13422/j.cnki.syfjx.20181701
25. Shan X, Zhang J, Li Y, Liu Y. Progress on Correlation Between Mfn2 and R as-MAPK Signal Pathway in Breast Cancer. *Chin Clin Oncol* (2014) 19(04):371–4.
26. Muthuswami M, Ramesh V, Banerjee S, Viveka Thangaraj S, Periasamy J, Bhaskar Rao D, et al. Breast Tumors With Elevated Expression of 1q Candidate Genes Confer Poor Clinical Outcome and Sensitivity to Ras/PI3K Inhibition. *PloS One* (2013) 8(10):e77553. doi: 10.1371/journal.pone.0077553
27. Gao J, Liu X, Yang F, Liu T, Yan Q, Yang X. By Inhibiting Ras/Raf/ERK and MMP-9, Knockdown of EpCAM Inhibits Breast Cancer Cell Growth and Metastasis. *Oncotarget* (2015) 6(29):27187–98. doi: 10.18632/oncotarget.4551
28. Zafrakas M, Papasozomenou P, Emmanouilides C. Sorafenib in Breast Cancer Treatment: A Systematic Review and Overview of Clinical Trials. *World J Clin Oncol* (2016) 7(4):331–6. doi: 10.5306/wjco.v7.i4.331
29. Yan K, Zhang C, Feng J, Hou L, Yan L, Zhou Z, et al. Induction of G1 Cell Cycle Arrest and Apoptosis by Berberine in Bladder Cancer Cells. *Eur J Pharmacol* (2011) 661(1-3):1–7. doi: 10.1016/j.ejphar.2011.04.021
30. Koul H, Pal M, Koul S. Role of P38 MAP Kinase Signal Transduction in Solid Tumors. *Genes Cancer* (2013) 4(9-10):342–59. doi: 10.1177/1947601913507951
31. Tang Y, Huang H, Guo H, Meng M, Long X. HOTAIR Interacting With MAPK1 Regulates Ovarian Cancer Skov3 Cell Proliferation, Migration, and Invasion. *Med Sci Monit* (2015) 21:1856–63. doi: 10.12659/msm.893528
32. Xiao Y, Liu H, Yu J, Zhao Z, Xiao F, Xia T, et al. MAPK1/3 Regulate Hepatic Lipid Metabolism *via* ATG7-Dependent Autophagy. *Autophagy* (2016) 12(3):592–3. doi: 10.1080/15548627.2015.1135282
33. Wu X, Liu W, Wu Z, Chen C, Liu J, Wu G, et al. Identification of HRAS as Cancer-Promoting Gene in Gastric Carcinoma Cell Aggressiveness. *Am J Cancer Res* (2016) 6(9):1935–48.

Conflict of Interest: The authors declare that the research was conducted in the absence of any commercial or financial relationships that could be construed as a potential conflict of interest.

Publisher's Note: All claims expressed in this article are solely those of the authors and do not necessarily represent those of their affiliated organizations, or those of the publisher, the editors and the reviewers. Any product that may be evaluated in this article, or claim that may be made by its manufacturer, is not guaranteed or endorsed by the publisher.

frontiers in Oncology

REVIEW
published: 31 August 2021
doi: 10.3389/fonc.2021.739191

Non-Small Cell Lung Cancer: Challenge and Improvement of Immune Drug Resistance

Fanming Kong[1,2*†], *Ziwei Wang*[1,2†], *Dongying Liao*[1,2], *Jinhui Zuo*[1,2], *Hongxia Xie*[1,2], *Xiaojiang Li*[1,2] *and Yingjie Jia*[1,2]

[1] Department of Oncology, First Teaching Hospital of Tianjin University of Traditional Chinese Medicine, Tianjin, China,
[2] National Clinical Research Center for Chinese Medicine Acupuncture and Moxibustion, Tianjin, China

Lung cancer is the leading cause of cancer deaths in the world. At present, immunotherapy has made a great breakthrough in lung cancer treatment. A variety of immune checkpoint inhibitors have been applied into clinical practice, including antibodies targeting the programmed cell death-1, programmed cell death-ligand 1, and cytotoxic T-lymphocyte antigen 4. However, in the actual clinical process, about 30%–50% of patients still do not receive long-term benefits. Abnormal antigen presentation, functional gene mutation, tumor microenvironment, and other factors can lead to primary or secondary resistance. In this paper, we reviewed the immune mechanism of immune checkpoint inhibitor resistance, various combination strategies, and prediction of biomarkers to overcome resistance in order to accurately screen out the advantageous population, expand the beneficiary population, and enable precise and individualized medicine.

Keywords: non-small cell lung cancer, immunotherapy, drug resistance, strategy, biomarkers

OPEN ACCESS

Edited by:
Yuling Qiu,
Tianjin Medical University, China

Reviewed by:
Dongying Tian,
Beijing Cancer Hospital, China
Peijun Lin,
Cornell University, United States

****Correspondence:***
Fanming Kong
kongfanming08@163.com

†These authors have contributed equally to this work

Specialty section:
This article was submitted to Pharmacology of Anti-Cancer Drugs, a section of the journal Frontiers in Oncology

Received: *10 July 2021*
Accepted: *30 July 2021*
Published: *31 August 2021*

Citation:
Kong F, Wang Z, Liao D, Zuo J, Xie H, Li X and Jia Y (2021) Non-Small Cell Lung Cancer: Challenge and Improvement of Immune Drug Resistance. Front. Oncol. 11:739191. doi: 10.3389/fonc.2021.739191

BACKGROUND

This article provides an update on the global cancer burden using the GLOBOCAN 2020 estimates of cancer incidence and mortality produced by the International Agency for Research on Cancer. Worldwide, an estimated 19.3 million new cancer cases and almost 10.0 million cancer deaths occurred in 2020. Lung cancer is one of the most commonly diagnosed cancers after breast cancer, with an estimated 2.3 million (11.7%) new cases and 1.8 million (18%) deaths in 2020. Lung cancer has not only become the leading cause of cancer death. It is also the leading burden on global health care (1). Through the traditional treatment methods [radiotherapy (RT), chemotherapy, targeting], lung cancer patients have little benefit. Recently, immune checkpoint inhibitors (ICIs) have become the most promising treatment for several kinds of cancer, especially in lung cancer. Nivolumab, pembrolizumab, and atezolizumab have been approved by the Food and Drug Administration (FDA). However, as clinical use becomes more widespread, approximately 30%–50% of patients receiving first-line ICIs experience temporary or no benefit. Immune drugs can also be divided into endogenous and exogenous drug resistance. Endogenous drug resistance refers to drug resistance caused by changes in tumor cells themselves, such as abnormal antigen presentation, functional gene mutation and inactivation, reduced immunogenicity, and tumor microenvironment. Exogenous drug resistance refers to external factors that affect all processes of T-cell activation. Therefore, in the current era of precision medicine, it is an urgent problem to clarify the mechanism

of drug resistance and screen the beneficiaries. In this review, the known mechanisms of immune resistance and potential therapeutic strategies to reverse immune resistance and to predict poor prognosis are reviewed.

DRUG RESISTANCE MECHANISM

Abnormal Antigen Presentation

The activation of T cells requires two signals. The first signal is the T-cell receptor (TCR) signal formed by the combination of TCR and peptide-major histocompatibility complex (MHC) molecules, but this signal is not enough to activate resting T cells. Only in the case of the second costimulatory signal provided by CD28 and its receptor, T-cell activation-related RNA and proteins will be synthesized, the key cytokine interleukin (IL)-2 will be secreted, and cells will enter from G0 phase to G1 phase. Therefore, it is the costimulatory signal and TCR signal that complete the activation of T cells. Studies have shown that B2M, as an important part of human leukocyte antigen (HLA)-I molecules, participates in the folding and transport of MHC-I molecules and plays an important role in the processing and presentation of tumor antigens. B2M mutation can lead to impaired expression of MHC-I molecules on the surface of antigen-presenting cells (APCs) and then lead to impaired antigen presentation, resulting in immunotherapy resistance (2). In addition, negative costimulatory molecules such as cytotoxic T-lymphocyte antigen 4 (CTLA-4) and programmed cell death-1 (PD-1) and their ligands CD80, CD86, PD-L1, and PD-L2 can prevent the body from producing second signals, resulting in downregulation or termination of T-cell activation (3).

Immune Cells: Tumor-Associated Macrophages, Myeloid-Derived Suppressor Cells, Regulatory T Cells

A large number of studies have shown that immune cells play a key role in tumor progression and inflammation. First, tumor-associated macrophages (TAMs) showed significant plasticity toward environmental cues (4, 5). In the early stage of the tumor, TAMS mainly showed M1 phenotype, while in the late stage, TAMS mostly belonged to M2 phenotype (6). M1 macrophages are pro-inflammatory cells, but they have an antitumor effect, which is related to the cytotoxicity and immunostimulatory function to cancer cells. M2 macrophages expressing anti-inflammatory cytokines such as IL-10, C-C motif chemokine ligand 22 (CCL22), and CCL18 can reduce inflammatory response but can promote tumors due to immunosuppression and angiogenesis induction (4, 7, 8). In tumors, microenvironment, such as hypoxia, nitric oxide (NO), can promote TAMs to M2 polarization. In addition, macrophage colony-stimulating factor (M-CSF) produced by tumor cells can also promote the polarization of TAMs to M2, resulting in tumor escape. The main secretion of M2 suppresses cytokines IL-10 and transforming growth factor-β (TGF-β), and the presence of antigen is weak, which inhibits T-cell activation and contributes to tumor immunity (7, 8).

Second, regulatory T (Treg) cells exert their immunosuppressive function through a variety of mechanisms. The high expression of IL-2 receptor on the surface of Treg cells can neutralize IL-2 to limit the proliferation and activation of T cells and produce inhibitory cytokines (TGF-β, IL-10, and IL-35) and cytotoxic substances (perforin and granulase) to inhibit and kill the excitation of effector T cells (9). CTLA-4 expressed by Treg cells binds to CD80/86 to impair APC maturation and inhibit T-cell proliferation, such as dendritic cells (DCs) (10). In addition, Treg cells had low expression of Nrf2, which is a key transcription factor of antioxidant reaction. Oxidative stress can induce apoptosis of Treg cells and release a large number of ATP, which is metabolized into adenosine by CD39 and CD73, which are highly expressed in Treg cells. Adenosine binds to A2A receptor (A2AR) to inhibit effector T cells (9, 11).

Last, myeloid-derived suppressor cells (MDSCs) can promote tumor growth through immunological inhibition and non-immunological inhibition, in which immunosuppressive mediator ARG1 and inducible NO synthase (INOS) can decompose L-arginine into 1-ornithine and urea, NO and nitrite, an important mediator of the IL-2 pathway, resulting in T-cell expression incompetence (12, 13). MDSC also expressed a high level of indoleamine 2mine3-dioxygenase (IDO), which can degrade 1-tryptophan to N-formylcanine, inhibit the proliferation and activation of T cells and NK cells, and promote CD4+ T cells to differentiate into Treg (14, 15). In addition, MDSC secretes immunosuppressive cytokines and growth factors (TGF-β and IL-10) to reduce the antitumor activity of effector T cells, recruit Treg cells, and increase reactive oxygen species (ROS) and NO in the microenvironment to inhibit the antitumor activity of natural killer (NK) cells and effector T cells (7, 16–18). The latest research shows that MDSCs can exert an immunosuppressive effect by upregulating PD-L1 (19). In addition, MDSCs can also promote tumor progression through non-immunological mechanisms (20). MDSCs can produce a large number of matrix metalloproteinases (MMPs), especially MMP9, to promote the infiltration of metastatic cells (21) and secrete high levels of vascular endothelial growth factor (VEGF) and basic fibroblast growth factor (bFGF) to promote angiogenesis (22). To sum up, MDSCs play an important role in the occurrence and development of tumors.

Tumor Endothelial Cells

Solid tumors tend to secrete a variety of pro-angiogenic factors, such as VEGF, hepatocyte growth factor, and platelet-derived growth factor. In 1971, Folkman (23) proposed that tumor growth was angiogenesis dependent, with further research. From 1983 to 1989, Senger et al. (24) proposed vascular permeability factor (VPF)/VEGF and Ferrara et al. (25) established the important position of VEGF until Terman isolated and purified VEGFR2 in the 1990s. These results fully indicate that VEGF (VEGFR2) plays an important role in the process of tumor growth, recurrence, and metastasis. VEGF/VEGFR is expressed in most tumors, including non-small cell

lung cancer (NSCLC), and it has been found to increase the risk of tumor recurrence, metastasis, and death. Angiogenic factors are continuously secreted in the tumor microenvironment, resulting in abnormal angiogenesis. On the one hand, neovascularization usually lacks some adhesion molecules, and the downregulation of adhesion molecules leads to T-cell extravasation (26). At the same time, circulating VEGF hinders the maturation and function of DCs and helps tumors escape immune surveillance. On the other hand, neovascularization cannot offset the increase in oxygen consumption, so the hypoxia environment will directly damage the function of tumor-infiltrating lymphocyte (TIL). In addition, on the one hand, hypoxia can upregulate the inhibitory signals of antitumor immune response, such as PD-L1, IDO, IL-6, and IL-10 (27).

On the other hand, hypoxia induces upregulation of chemokine expression, which makes Treg cells reenter the tumor (28, 29). In addition, hypoxia can also promote the polarization of TAM to M2-like phenotype of TAMs (30). To sum up, angiogenesis can participate in tumor growth and immune escape through a variety of ways.

Functional Gene Mutation and Inactivation

PTEN gene plays an important role in maintaining cell proliferation, differentiation, and apoptosis. PTEN can inhibit phosphoinositide 3-kinase (PI3K) pathway, which plays a regulatory role in some key cell processes such as tumor survival and proliferation. On the other hand, the lack of PTEN expression can activate the PI3K–AKT pathway, thus reducing the infiltration of lymphoid T cells and reduce the tumor killing effect of effector T cells (31). Similar to Janus kinase (JAK), it plays an important role in cytokine signal transduction. The JAK protein tyrosine kinase family consists of four members: tyrosine kinase (TYK)2, JAK1, JAK2, and JAK3. Patients with JAK1/2 gene mutations may be resistant to primary immunotherapy (32). Although JAK2 mutant tumor cells can produce interferon (IFN)-γ, the JAK2–signal transducer and activator of transcription _(STAT) signal pathway cannot be activated by IFN-γ and cannot upregulate the expression of PD-L1, which leads to the weak killing effect of IFN on JAK2 mutant tumor cells. However, the mutant cells of JAK1 were not sensitive to all kinds of effects of IFN. The above results suggest that the mutant tumor cells of the JAK1/JAK2 gene are not sensitive to the killing effect of IFN, and the expression level of PD-L1 is low, which makes the mutated tumor cells resistant to ICIs (33).

RAISING DRUG RESISTANCE

Combined Application With Chemotherapy

Immune combined chemotherapy can not only increase the cross-presentation of antigens by dendritic cells (34) but also weaken the immunosuppressive components of the tumor microenvironment (35), such as Treg cells, MDSCs, immunosuppressive cytokines, etc., and then increase toxic lymphocytes and the ratio of Treg cells (36). In 2019, the American Society of Clinical Oncology (ASCO) published a three-phase clinical trial KEYNOTE-189 to evaluate the efficacy of NSCLC first-line treatment for advanced non-squamous NSCLC: pablizumab combined with chemotherapy compared with chemotherapy alone. The results showed that the immune combined chemotherapy group could significantly double the levels of overall survival time (OS), progression-free survival (PFS), and PFS2 [mean OS (mOS): 22.0 *vs*. 10.7 months, hazard ratio (HR): 0.56, 95% confidence interval (CI): 0.45–0.70; mean PFS (mPFS): 9.0 *vs*. 4.9 months, HR: 0.48, 95% CI: 0.40–0.58; and mPFS2: 17.0 *vs*. 9.0 months, HR: 0.49, 95% CI: 0.40–0.59]. From the safety analysis, the incidence of treatment-related select adverse events (AEs) of any grade in the combination chemotherapy group and the simple chemotherapy group was 26.4% *vs*. 12.9%. The grade 3–5 treatment-related select AEs were 10.9% *vs*. 4.5%. It further confirmed the safety and efficacy of this first-line chemotherapy regimen combined with pablizumab in the treatment of non-squamous NSCLC (37). In addition, KEYNOTE407 3-year follow-up data were released at this year's European Lung Cancer Congress (ELCC) to evaluate the efficacy of immunotherapy combined with chemotherapy and chemotherapy alone. Studies have shown that immunotherapy combined with chemotherapy provides more lasting benefits to patients than chemotherapy (mOS: 17.1 *vs*. 11.6 months, HR: 0.71, 95% CI: 0.58–0.88; mPFS: 8.0 *vs*. 5.1 months, HR: 0.57, 95% CI: 0.47–0.69; mPFS2: 13.8 *vs*. 9.1 months, HR: 0.59, 95% CI: 0.49–0.72). Three-year follow-up data showed that OS: 29.7% *vs*. 18.2%, PFS: 16.1% *vs*. 6.5%; in terms of safety, the two groups of 3 and above treatment related adverse reactions were 74.8% *vs*. 70.0% (38). In the latest Camel-sq study released by the ELCC in 2021, carrizumab combined with carboplatin and paclitaxel combined with carboplatin chemotherapy regimen in the treatment of advanced non-small cell lung squamous cell carcinoma, objective response rate (ORR) and PFS were significantly prolonged (ORR: 64.8% *vs*. 36.7%, PFS: 8.5 *vs*. 4.9 months) (39).

Combined Radiotherapy With Immunotherapy

Preclinical evidence points to RT as a priming event for immunotherapy. By modulating the host's immune system, RT can render tumor cells more susceptible to T cell-mediated attack. RT promotes the release of tumor neoantigens from dying tumor cells, enhances MHC-I expression, and upregulates chemokines, cell adhesion molecules, and other immunomodulatory cell surface molecules, thereby potentiating an antitumor immune response by triggering immunogenic cell death (40). Just as the PACIFIC trial evaluated the efficacy of durvalumab consolidation therapy in patients with NSCLC after simultaneous RT and chemotherapy, the results showed that the mPFS was 16.9 *vs*. 5.6 months (HR: 0.55, 95% CI: 0.45–0.68), and the mOS was 47.5 *vs*. 28.1 months (HR: 0.55, 95% CI: 0.45–0.68) (41). In addition, a retrospective study at the 2020 ASCO conference showed that local treatment can significantly improve survival benefits (42). After immune resistance, local therapy combined with immunotherapy can reverse drug resistance to some extent, providing new treatment ideas for patients with immune drug resistance.

Combined With Targeted Drugs

Anti-angiogenic therapy can change the function of tumor vascular endothelial cells to regulate immunosuppression and reduce the inhibitory effect of VEGF on DC migration and immune function (43, 44). Studies have shown that CTLA-4 or PD-1 inhibitors can reduce tumor vascular density, improve vascular perfusion, relieve hypoxia of tumor tissue, normalize blood vessels, and reduce the immunosuppressive effect of Treg, TAMS, and MDSCs (44–46). Therefore, the combination of immunosuppressive and anti-angiogenic drugs may play a synergistic role. As the latest results of the IMpower150 trial were presented at the American Association for Cancer Research (AACR) 2020 meeting of the AACR, the mOS of ABCP (atezolizumab+carboplatin+paclitaxel+bevacizumab) *vs*. BCP (carboplatin+paclitaxel+bevacizumab) was 19.5 *vs*. 14.7 months (HR: 0.80, 95% CI: 0.67-0.95), the mPFS was 8.4 *vs*. 6.8 months, and the ORR was 63.5% *vs*. 48.0%, mOS was 29.4% *vs*. 18.1%, respectively. In the liver metastasis subgroup, the mOS of ABCP *vs*. BCP was 13.2 *vs*. 9.1 months, and the PFS was 8.2 *vs*. 5.4 months. From the data survey, it can be seen that compared with BCP, ABCP can significantly improve the PFS and OS of patients (47, 48). From the above trial results, for epidermal growth factor receptor (EGFR) and anaplastic lymphoma kinase (ALK) mutant population, the combination of four drugs can bring significant survival benefits to patients with advanced NSCLC (49).

The Phase I/II KRYSTAL-1 test (NCT03785249) included patients with KRASG12C mutation-positive, unresectable, or metastatic NSCLC. After adagrasib monotherapy, the results showed that in patients with NSCLC, the overall remission rate of adagrasib treatment reached 45% and the disease control rate (DCR) reached 96%, and for NSCLC patients with STK11 mutation, the overall remission rate reached 64%. In terms of safety, the most common AEs of adagrasib treatment included nausea (54%), diarrhea (51%), vomiting (35%), and fatigue (32%) (50, 51). The researchers indicated that they plan to verify the efficacy of adagrasib in combination with other drugs or treatments in future trials, such as pembrolizumab, Keytruda (52). The Phase II KRYSTAL-7 trial (NCT04613596) of adagrasib combined with pimumab is under preparation, and the results are worth looking forward to. And now there are more and more data supporting the combination of immunotherapy and other targeted treatments.

COMBINED APPLICATION OF DOUBLE IMMUNITY

PD-1 is highly expressed on T cells and interacts with its ligands PD-L1 and PD-L2 to inhibit T-cell activation and proliferation (53). CTLA-4 can reduce T-cell activity to maintain immune tolerance and homeostasis (54). The two interact to enhance the efficacy of immunotherapy. For example, in patients with advanced melanoma, the results showed that the ORR and PFS of double immunotherapy were higher than those of single-drug immunotherapy (55, 56). The Checkmate-227 test was used to evaluate the efficacy of dual immunotherapy and chemotherapy alone in the treatment of advanced NSCLC. The study showed that the OS and duration of response (DOR) of patients with PD-L1 ≥1% and PD-L1 <1% were significantly longer than those in the chemotherapy group (PD-L1-positive patients: mOS was 17.1 *vs*. 14.9 months, ORR value was 31.9% *vs*. 30%; mOS was 17.2 *vs*. 12.2 months, ORR value was 27.3% *vs*. 23.1%) (57, 58). In addition, like the Checkmate-227 study, the Checkmate-9LA trial, presented at the 2020 World Conference on Lung Cancer (WCLC), aims to evaluate the efficacy of chemotherapy alone or navulizumab combined with two cycles of chemotherapy in the treatment of metastatic NSCLC in Asian populations. The results showed that no matter what the expression of PD-L1 was, the combination of immunotherapy and chemotherapy could improve the expression of OS, without considering the expression of PD-L1. According to the expression analysis of PD-L1, the risk of death of patients with PD-L1 <1% (HR: 0.62, 95% CI: 0.45~0.85) and PD-L1 ≥1% (HR: 0.64, 95% CI: 0.5~0.82) decreased by 38% *vs*. 36% (HR: 0.64, 95% CI: 0.5~0.82) (59, 60). In addition, for the study of immune checkpoints, some new checkpoints have been explored, such as T-cell immunoreceptor with immunoglobulin (Ig) and ITIM domains (TIGIT), IDO, and lymphocyte activation gene (LAG)-3. Among the many new combinations and new targets, T-cell immune receptor (TIGIT) inhibitors carrying Ig and ITIM domains have attracted particular attention. A phase II study of atrizumab combined with TIGIT inhibitor tiragolumab *vs*. placebo combined with atrizumab was released at the 2020 ASCO Congress (61). The main characters were ORR and PFS. The results showed that for people with PDL1 >50%, tiragolumab+atrizumab significantly increased ORR and PFS time in the intention-to-treat (ITT) population compared with those in the control group, but for 1% ~49% of PD-L1, the benefit of ORR and PFS time was limited. This study is still under further study, and the results are worth looking forward to.

DISCUSSION

Although the research ideas of immunotherapy drug resistance emerge endlessly, there are also some problems that cannot be ignored in the clinical trials of reversing immune drug resistance. In recent years, with the rapid development of medicine, we advocate "individualized medical treatment" and "precision treatment" in the field of oncology. Biomarkers have important clinical significance for the discovery, treatment, and prognosis of tumors. At present, PD-L1 is the most commonly used marker for predicting the efficacy of immunotherapy, but it still has some limitations and cannot be used as a routine marker in the clinic. Other related studies have shown that tumor mutation load, TILs, and microsatellite instability are important biomarkers to predict the efficacy of immunotherapy.

According to the retrospective analysis of CHECKMate-026 and the survival data of CHECKMate-227, the efficacy of immunotherapy in patients with high tumor mutation burden (TMB) was significantly better than that of chemotherapy (57, 62). In 2019, the National Comprehensive Cancer Network

TABLE 1 | Data on the results of trials related to non-small cell lung cancer.

Study (NCT-number)	Trial group	Trial design	Primary end points	Secondary end point	Adverse reactions greater than or equal to grade 3
Impower150 (46, 47), (NCT02366143)	Previously untreated non-squamous NSCLC patients without EGFR/ALK aberrations	Atezolizumab+Carboplatin+Paclitaxel+ Bevacizumab (ABCP); Atezolizumab+ Carboplatin+Paclitaxel (ACP); Carboplatin+ Paclitaxel+ Bevacizumab (BCP)	PFS (Teff-high WT): NR* OS (ITT-WT): median, ACP *vs*. BCP = 19.0 *vs*. 14.7 months median, ABCP *vs*. BCP = 19.5 *vs*. 14.7 months ABCP group is of great significance to liver metastasis and EGFR mutation	ORR: NR* DOR: NR*	Gr 3–4 treatment-related AEs occurred in 43%, 57%, and 49% of patients in ABCP, ACP, and BCP, respectively.
Keynote189 (36), (NCT02578680)	Patients with advanced non-squamous (NSCLC) without an EGFR/ALK alteration	Pembrolizuab+Chemotherapy; Placebo+ Chemotherapy	OS: median, 22.0 *vs*. 10.7 months PFS: median, 9.0 *vs*. 4.9 months	ORR: 48.3% *vs*. 19.9% DOR: median,12.4 *vs*. 7.1 PFS2: median,17.0 *vs*. 9.0 months	Gr 3–5 immune-mediated adverse reactions and infusion-related reactions occurred in 10.9% and 4.5%, respectively
Keynote407 (37), (NCT02775435)	Patients with previously untreated metastatic squamous NSCLC	Pembrolizuab+Chemotherapy; Placebo+ Chemotherapy	OS: median, 17.2 *vs*. 11.6 months PFS: median, 8.0 *vs*. 5.1 months	ORR: 62.6% *vs*. 38.4% DOR: 8.8 *vs*. 4.9months PFS2: 13.8 *vs*. 9.1months	Gr 3–5 treatment-related AEs occurred in 74.1% *vs*. 69.6%
PACIFIC (40), (NCT02125461)	Patients with unresectable stage III NSCLC without progression after chemoradiotherapy	Durvalumab+Chemotherapy; Placebo+ Chemotherapy	OS: median, 47.5 *vs*. 28.1 months PFS: median, 16.9 *vs*. 5.6 months	NR*	NR*
Checkmate-227 (56, 57), (NCT02477826)	Patients with unresectable stage III NSCLC without progression	Nivolumab+Ipilimumab; Chemotherapy	OS: (PD-L1 ≥1%): median, 17.1*vs*. 14.9 months (PD-L1 ≥50%): median, 21.2 *vs*. 14.0 months (PD-L1 <1%): median, 17.2 *vs*. 12.2 months	DOR: (PD-L1 ≥1%): 23.2 *vs*. 6.7 months; (PD-L1 ≥50%): 31.8 *vs*. 5.8 months; (PD-L1 <1%): 18.0 *vs*. 4.8 months	Gr 3–4 treatment-related AEs occurred in 33% *vs*. 36%
Checkmate-9LA (58, 59), (NCT03215706)	Patients with treatment-naive, histologically confirmed stage IV or recurrent NSCLC without an EGFR/ALK alteration	Nivolumab+Ipilimumab+Chemotherapy; Chemotherapy	OS: median, 15.8 *vs*. 11.0 months PFS: median, 6.7 *vs*. 5.3 months	ORR: 38% *vs*. 25.4% DOR: 13.0 *vs*. 5.6 months	Gr 3–5 treatment-related AEs occurred in 47% *vs*. 38% (The incidence of blood toxicity was higher in the chemotherapy group than in the chemotherapy group)
Checkmate-026 (61), (NCT02041533)	Patients with untreated stage IV or recurrent NSCLC and a PD-L1 tumor-expression level of 1% or more	Nivolumab; Chemotherapy	PFS (PD-L1 ≥5%): median, 4.2 *vs*. 5.9 months	OS: 14.4 *vs*. 13.2 months	Gr 3 treatment-related AEs occurred in 71% *vs*. 92%; Gr 4 treatment-related AEs occurred in 18% *vs*. 51%
Camel-sq (38), (NCT03668496)	Chinese patients with advanced non-squamous NSCLC and negative EGFR/ALK mutation	Camrelizumab+Chemotherapy; Placebo+ Chemotherapy	OS: median, NR* *vs*. 14.5 months PFS: median, 8.5 *vs*. 4.9 months	ORR: 64.8% *vs*. 36.7% DOR: median, 13.1 *vs*. 4.4 months	Gr 3-5 treatment-related AEs occurred in 73.6% *vs*. 73.6%

**There is no report in the recently updated data of the trial.*

(NCCN) guidelines recommended TMB as one of the indicators to evaluate the efficacy of immunotherapy for NSCLC. At the AACR 2019 meeting, Wang et al. (63) reported the latest research results on the blood-based tumor mutant (bTMB) and realized bTMB's effective prediction of PFS, especially OS, by redefining bTMB. However, due to the influence of different critical values, different sampling time, tumor heterogeneity, and other factors, TMB may still be a biomarker for clinical reference, and the selection of its effective threshold and the feasibility of detection need to be further verified by clinical data. Also at the ASCO conference in 2019, Johns Hopkins and Memorial Sloan Kettering Cancer Celter (MSKCC) published the results of trials on patients with NSCLC who received nivolumab before operation, suggesting that circulating tumor DNA (CtDNA) clearance and peripheral blood T-cell expansion can be used as biomarkers to predict recurrence and treatment efficacy (64). The WCLC in 2021 also reported on CtDNA. In addition, new biomarkers are being discovered. For example, a retrospective trial was conducted in Japan to evaluate the efficacy of nivumab or pembrolizumab in patients with advanced NSCLC with positive antibodies (rheumatoid factor, antinuclear antibodies, thyroid antibodies) before selection. The results showed that the ORR, DCR, and PFS of antibody-positive patients were significantly better than those of non-antibody-positive patients. Although the sample size included in this study is relatively small, its research is worthy of further study (65).

At present, with the further study of biomarkers, some studies also have found that Tumor Protein p53 (TP53) or Kirsten Rat Sarcoma Viral Oncogene Homolog (KRAS) gene mutations can increase the expression of PD-L1 and CD8+ T-cell infiltration; when both mutations are present, the expression of PD-L1 will be more significant, the tumor mutation load is often high, and the clinical benefits of pembrolizumab therapy are often better. Therefore, KRAS or TP53 mutations combined with PD-L1 or CD8+ T cells may be of better predictive value (66).

CONCLUSION

There is still a certain problem of drug resistance in the clinical application of immunotherapy for NSCLC, although the combination of drugs can expand the effect of immunotherapy and improve immune drug resistance. However, based on these results, there are still several important problems to be solved: how to accurately grasp the dose and time sequence of the combination, and the choice of the dominant population is the key to improving the efficacy of drugs. The development of immunotherapy is a great breakthrough in tumor therapy and the cornerstone of advanced NSCLC therapy. In the future, looking for biomarkers to predict the efficacy of immunotherapy can make immunotherapy individualized and accurate. The research and development of new drugs will further improve the prognosis of patients with lung cancer (**Table 1**).

AUTHOR CONTRIBUTIONS

FK and ZW contributed equally to this work. Other authors offer advice. All authors contributed to the article and approved the submitted version.

FUNDING

This work is supported by the National Natural Science Foundation of China (No. 81403220 and No. 81904151), Tianjin Health and family planning-high level talent selection and training project, Tianjin Science and Technology Plan Projects (No. 17ZXMFSY00190), and Tianjin Traditional Chinese Medicine Research Project, Tianjin health and family planning commission (No. 2017003).

REFERENCES

1. Sung H, Ferlay J, Siegel RL, Laversanne M, Soerjomataram I, Jemal A, et al. Global Cancer Statistics 2020: GLOBOCAN Estimates of Incidence and Mortality Worldwide for 36 Cancers in 185 Countries. *CA Cancer J Clin* (2021) 71(3):209–49. doi: 10.3322/caac.21660
2. Nowicki TS, Hu-Lieskovan S, Ribas A. Mechanisms of Resistance to PD-1 and PD-L1 Blockade. *Cancer J* (2018) 24(1):47–53. doi: 10.1097/PPO.0000000000000303
3. Xu W, Hiếu T, Malarkannan S, Wang L. The Structure, Expression, and Multifaceted Role of Immune-Checkpoint Protein VISTA as a Critical Regulator of Anti-Tumor Immunity, Autoimmunity, and Inflammation. *Cell Mol Immunol* (2018) 15(5):438–46. doi: 10.1038/cmi.2017.148
4. Delprat V, Tellier C, Demazy C, Raes M, Feron O, Michiels C. Cycling Hypoxia Promotes a Pro-Inflammatory Phenotype in Macrophages *via* JNK/p65 Signaling Pathway. *Sci Rep* (2020) 10(1):882. doi: 10.1038/s41598-020-57677-5
5. Palmieri EM, Gonzalez-Cotto M, Baseler WA, Davies LC, Ghesquière B, Maio N, et al. Nitric Oxide Orchestrates Metabolic Rewiring in M1 Macrophages by Targeting Aconitase 2 and Pyruvate Dehydrogenase. *Nat Commun* (2020) 11(1):698. doi: 10.1038/s41467-020-14433-7
6. Singhal S, Stadanlick J, Annunziata MJ, Rao AS, Bhojnagarwala PS, O'Brien S, et al. Human Tumor-Associated Monocytes/Macrophages and Their Regulation of T Cell Responses in Early-Stage Lung Cancer. *Sci Transl Med* (2019) 11(479). doi: 10.1126/scitranslmed.aat1500
7. Veglia F, Perego M, Gabrilovich D. Myeloid-Derived Suppressor Cells Coming of Age. *Nat Immunol* (2018) 19(2):108–19. doi: 10.1038/s41590-017-0022-x
8. Motallebnezhad M, Jadidi-Niaragh F, Qamsari ES, Bagheri S, Gharibi T, Yousefi M. The Immunobiology of Myeloid-Derived Suppressor Cells in Cancer. *Tumour Biol* (2016) 37(2):1387–406. doi: 10.1007/s13277-015-4477-9
9. Ohue Y, Nishikawa H, Regulatory T. (Treg) Cells in Cancer: Can Treg Cells be a New Therapeutic Target? *Cancer Sci* (2019) 110(7):2080–9. doi: 10.1111/cas.14069
10. Walker LS, Sansom DM. The Emerging Role of CTLA4 as a Cell-Extrinsic Regulator of T Cell Responses. *Nat Rev Immunol* (2011) 11(12):852–63. doi: 10.1038/nri3108
11. Maj T, Wang W, Crespo J, Zhang H, Wang W, Wei S, et al. Oxidative Stress Controls Regulatory T Cell Apoptosis and Suppressor Activity and PD-L1-Blockade Resistance in Tumor. *Nat Immunol* (2017) 18(12):1332–41. doi: 10.1038/ni.3868
12. Kowanetz M, Wu X, Lee J, Tan M, Hagenbeek T, Qu X, et al. ranulocyte-Colony Stimulating Factor Promotes Lung Metastasis Through Mobilization of Ly6G+Ly6C+ Granulocytes. *Proc Natl Acad Sci USA* (2010) 107(50):21248–55. doi: 10.1073/pnas.1015855107

13. Yen BL, Yen ML, Hsu PJ, Liu KJ, Wang CJ, Bai CH, et al. Multipotent Human Mesenchymal Stromal Cells Mediate Expansion of Myeloid-Derived Suppressor Cells *via* Hepatocyte Growth Factor/C-Met and STAT3. *Stem Cell Rep* (2013) 1(2):139–51. doi: 10.1016/j.stemcr.2013.06.006
14. Hu X, Li B, Li X, Zhao X, Wan L, Lin G, et al. Transmembrane TNF-α Promotes Suppressive Activities of Myeloid-Derived Suppressor Cells *via* TNFR2. *J Immunol* (2014) 192(3):1320–31. doi: 10.4049/jimmunol.1203195
15. Highfill SL, Rodriguez PC, Zhou Q, Goetz CA, Koehn BH, Veenstra R, et al. Bone Marrow Myeloid-Derived Suppressor Cells (MDSCs) Inhibit Graft-*Versus*-Host Disease (GVHD) *via* an Arginase-1-Dependent Mechanism That is Up-Regulated by Interleukin-13. *Blood* (2010) 116(25):5738–47. doi: 10.1182/blood-2010-06-287839
16. Prima V, Kaliberova LN, Kaliberov S, Curiel DT, Kusmartsev S. COX2/mPGES1/PGE2 Pathway Regulates PD-L1 Expression in Tumor-Associated Macrophages and Myeloid-Derived Suppressor Cells. *Proc Natl Acad Sci USA* (2017) 114 (5):1117–22. doi: 10.1073/pnas.1612920114
17. Li L, Wang L, Li J, Fan Z, Yang L, Zhang Z, et al. Metformin-Induced Reduction of CD39 and CD73 Blocks Myeloid-Derived Suppressor Cell Activity in Patients With Ovarian Cancer. *Cancer Res* (2018) 78(7):1779–91. doi: 10.1158/0008-5472.CAN-17-2460
18. Li J, Wang L, Chen X, Li L, Li Y, Ping Y, et al. CD39/CD73 Upregulation on Myeloid-Derived Suppressor Cells *via* TGF-β-mTOR-HIF-1 Signaling in Patients With non-Small Cell Lung Cancer. *Oncoimmunology* (2017) 6(6):e1320011. doi: 10.1080/2162402X.2017.1320011
19. Berger KN, Pu JJ. PD-1 Pathway and its Clinical Application: A 20year Journey After Discovery of the Complete Human PD-1 Gene. *Gene* (2018) 638:20–5. doi: 10.1016/j.gene.2017.09.050
20. Safarzadeh E, Orangi M, Mohammadi H, Babaie F, Baradaran B. Myeloid-Derived Suppressor Cells: Important Contributors to Tumor Progression and Metastasis. *J Cell Physiol* (2018) 233(4):3024–36. doi: 10.1002/jcp.26075
21. Jacob A, Prekeris R. The Regulation of MMP Targeting to Invadopodia During Cancer Metastasis. *Front Cell Dev Biol* (2015) 3:4. doi: 10.3389/fcell.2015.00004
22. Shen P, Wang A, He M, Wang Q, Zheng S. Increased Circulating Lin(-/Low) CD33(+) HLA-DR(-) Myeloid-Derived Suppressor Cells in Hepatocellular Carcinoma Patients. *Hepatol Res* (2014) 44(6):639–50. doi: 10.1111/hepr.12167
23. Folkman J. Endogenous Angiogenesis Inhibitors. *Apmis* (2004) 112(7-8):496–507. doi: 10.1111/j.1600-0463.2004.apm11207-0809.x
24. Senger DR, Galli SJ, Dvorak AM, Perruzzi CA, Harvey VS, Dvorak HF. Tumor Cells Secrete a Vascular Permeability Factor that Promotes Accumulation of Ascites Fluid. *Science* (1983) 219(4587):983–5. doi: 10.1126/science.6823562
25. Ferrara N, Henzel WJ. Pituitary Follicular Cells Secrete a Novel Heparin-Binding Growth Factor Specific for Vascular Endothelial Cells. *Biochem Biophys Res Commun* (1989) 161(2):851–8. doi: 10.1016/0006-291x(89)92678-8
26. Valach J, Fík Z, Strnad H, Chovanec M, Plzák J, Cada Z, et al. Smooth Muscle Actin-Expressing Stromal Fibroblasts in Head and Neck Squamous Cell Carcinoma: Increased Expression of Galectin-1 and Induction of Poor Prognosis Factors. *Int J Cancer* (2012) 131(11):2499–508. doi: 10.1002/ijc.27550
27. Reck M, Garassino MC, Imbimbo M, Shepherd FA, Socinski MA, Shih JY, et al. Antiangiogenic Therapy for Patients With Aggressive or Refractory Advanced Non-Small Cell Lung Cancer in the Second-Line Setting. *Lung Cancer* (2018) 120:62–9. doi: 10.1016/j.lungcan.2018.03.025
28. Curiel TJ, Coukos G, Zou L, Alvarez X, Cheng P, Mottram P, et al. Specific Recruitment of Regulatory T Cells in Ovarian Carcinoma Fosters Immune Privilege and Predicts Reduced Survival. *Nat Med* (2004) 10(9):942–9. doi: 10.1038/nm1093
29. Facciabene A, Hagemann IS, Balint K, Barchetti A, Wang L-P, Gimotty PA, et al. Tumour Hypoxia Promotes Tolerance and Angiogenesis *via* CCL28 and T(reg) Cells. *Nature* (2011) 475(7355):226–30. doi: 10.1038/nature10169
30. Movahedi K, Laoui D, Gysemans C, Baeten M, Stangé G, Van den Bossche J, et al. Different Tumor Microenvironments Contain Functionally Distinct Subsets of Macrophages Derived From Ly6C(high) Monocytes. *Cancer Res* (2010) 70(14):5728–39. doi: 10.1158/0008-5472.CAN-09-4672
31. Bucheit AD, Chen G, Siroy A, Tetzlaff M, Broaddus R, Milton D, et al. Complete Loss of PTEN Protein Expression Correlates With Shorter Time to Brain Metastasis and Survival in Stage IIIB/C Melanoma Patients With BRAFV600 Mutations. *Clin Cancer Res* (2014) 20(21):5527–36. doi: 10.1158/1078-0432.CCR-14-1027
32. Shin DS, Zaretsky JM, Escuin-Ordinas H, Garcia-Diaz A, Hu-Lieskovan S, Kalbasi A, et al. Primary Resistance to PD-1 Blockade Mediated by JAK1/2 Mutations. *Cancer Discovery* (2017) 7(2):188–201. doi: 10.1158/2159-8290.CD-16-1223
33. Zaretsky JM, Garcia-Diaz A, Shin DS, Escuin-Ordinas H, Hugo W, Hu-Lieskovan S, et al. Mutations Associated With Acquired Resistance to PD-1 Blockade in Melanoma. *N Engl J Med* (2016) 375(9):819–29. doi: 10.1056/NEJMoa1604958
34. Bracci L, Schiavoni G, Sistigu A, Belardelli F. Immune-Based Mechanisms of Cytotoxic Chemotherapy: Implications for the Design of Novel and Rationale-Based Combined Treatments Against Cancer. *Cell Death Differ* (2014) 21 (1):15–25. doi: 10.1038/cdd.2013.67
35. Wang Z, Till B, Gao Q. Chemotherapeutic Agent-Mediated Elimination of Myeloid-Derived Suppressor Cells. *Oncoimmunology* (2017) 6(7):e1331807. doi: 10.1080/2162402X.2017.1331807
36. Roselli M, Cereda V, di Bari MG, Formica V, Spila A, Jochems C, et al. Effects of Conventional Therapeutic Interventions on the Number and Function of Regulatory T Cells. *Oncoimmunology* (2013) 2(10):e27025. doi: 10.4161/onci.27025
37. Gadgeel S, Rodríguez-Abreu D, Speranza G, Esteban E, Felip E, Dómine M, et al. Updated Analysis From KEYNOTE-189: Pembrolizumab or Placebo Plus Pemetrexed and Platinum for Previously Untreated Metastatic Nonsquamous Non-Small-Cell Lung Cancer. *J Clin Oncol* (2020) 38 (14):1505–17. doi: 10.1200/jco.19.03136
38. Paz-Ares L, Luft A, Vicente D, Tafreshi A, Gümüş M, Mazières J, et al. Pembrolizumab Plus Chemotherapy for Squamous Non-Small-Cell Lung Cancer. *N Engl J Med* (2018) 379(21):2040–51. doi: 10.1056/NEJMoa1810865
39. Zhou C, Ren S, Chen J, Xu X, Cheng Y, Chen G, et al. 96o Camrelizumab or Placebo Plus Carboplatin and Paclitaxel as First-Line Treatment for Advanced Squamous NSCLC (CameL-Sq): A Randomized, Double-Blind, Multicenter, Phase III Trial. *J Thoracic Oncol* (2021) 16(4S). doi: 10.1016/S1556-0864(21)01938-9
40. Ko EC, Raben D, Formenti SC. The Integration of Radiotherapy With Immunotherapy for the Treatment of Non-Small Cell Lung Cancer. *Clin Cancer Res* (2018) 24(23):5792–806. doi: 10.1158/1078-0432.CCR-17-3620
41. Faivre-Finn C, Vicente D, Kurata T, Planchard D, Paz-Ares L, Vansteenkiste JF, et al. Four-Year Survival With Durvalumab After Chemoradiotherapy in Stage III NSCLC—an Update From the PACIFIC Trial. *J Thoracic Oncol* (2021) 16(5):860–7. doi: 10.1016/j.jtho.2020.12.015
42. Ranjan P, Atish M MVV, Ravi S, Erminia M. Acquired Resistance to PD-1/PD-L1 Blockade in Lung Cancer: Mechanisms and Patterns of Failure. *Cancers* (2020) 12(12). doi: 10.3390/cancers12123851
43. Long J, Hu Z, Xue H, Wang Y, Chen J, Tang F, et al. Vascular Endothelial Growth Factor (VEGF) Impairs the Motility and Immune Function of Human Mature Dendritic Cells Through the VEGF Receptor 2-RhoA-Cofilin1 Pathway. *Cancer Sci* (2019) 110(8):2357–67. doi: 10.1111/cas.14091
44. Tian L, Goldstein A, Wang H, Ching Lo H, Sun Kim I, Welte T, et al. Mutual Regulation of Tumour Vessel Normalization and Immunostimulatory Reprogramming. *Nature* (2017) 544(7649):250–4. doi: 10.1038/nature21724
45. Huang Y, Yuan J, Righi E, Kamoun WS, Ancukiewicz M, Nezivar J, et al. Vascular Normalizing Doses of Antiangiogenic Treatment Reprogram the Immunosuppressive Tumor Microenvironment and Enhance Immunotherapy. *Proc Natl Acad Sci USA* (2012) 109(43):17561–6. doi: 10.1073/pnas.1215397109
46. Gray JE, Villegas A, Daniel D, Vicente D, Murakami S, Hui R, et al. Three-Year Overall Survival With Durvalumab After Chemoradiotherapy in Stage III NSCLC-Update From PACIFIC. *J Thorac Oncol* (2020) 15(2):288–93. doi: 10.1016/j.jtho.2019.10.002
47. Fukumura D, Kloepper J, Amoozgar Z, Duda DG, Jain RK. Enhancing Cancer Immunotherapy Using Antiangiogenics: Opportunities and Challenges. *Nat Rev Clin Oncol* (2018) 15(5):325–40. doi: 10.1038/nrclinonc.2018.29
48. Reck M, Mok TSK, Nishio M, Jotte RM, Cappuzzo F, Orlandi F, et al. Atezolizumab Plus Bevacizumab and Chemotherapy in Non-Small-Cell Lung Cancer (IMpower150): Key Subgroup Analyses of Patients With EGFR Mutations or Baseline Liver Metastases in a Randomised, Open-Label Phase

3 Trial. *Lancet Respir Med* (2019) 7(5):387–401. doi: 10.1016/S2213-2600(19)30084-0
49. Socinski MA, Jotte RM, Cappuzzo F, Orlandi F, Stroyakovskiy D, Nogami N, et al. Atezolizumab for First-Line Treatment of Metastatic Nonsquamous NSCLC. *N Engl J Med* (2018) 378(24):2288–301. doi: 10.1056/NEJMoa1716948
50. Another KRAS Inhibitor Holds Its Own. *Cancer Discov* (2020) 10(12):Of2. doi: 10.1158/2159-8290.CD-NB2020-098
51. Jänne PA, Rybkin II, Spira AI, Riely GJ, Papadopoulos KP, Sabari JK, et al. KRYSTAL-1: Activity and Safety of Adagrasib (MRTX849) in Advanced/Metastatic Non–Small-Cell Lung Cancer (NSCLC) Harboring KRAS G12C Mutation. *Eur J Cancer* (2020) 138:S1–2. doi: 10.1016/S0959-8049(20)31076-5
52. Hong DS, Fakih MG, Strickler JH, Desai J, Durm GA, Shapiro GI, et al. KRAS (G12C) Inhibition With Sotorasib in Advanced Solid Tumors. *N Engl J Med* (2020) 383(13):1207–17. doi: 10.1056/NEJMoa1917239
53. Weber JS, D'Angelo SP, Minor D, Hodi FS, Gutzmer R, Neyns B, et al. Nivolumab *Versus* Chemotherapy in Patients With Advanced Melanoma Who Progressed After Anti-CTLA-4 Treatment (CheckMate 037): A Randomised, Controlled, Open-Label, Phase 3 Trial. *Lancet Oncol* (2015) 16(4):375–84. doi: 10.1016/S1470-2045(15)70076-8
54. Blank CU, Enk A. Therapeutic Use of Anti-CTLA-4 Antibodies. *Int Immunol* (2015) 27(1):3–10. doi: 10.1093/intimm/dxu076
55. Robert C, Schachter J, Long GV, Arance A, Grob JJ, Mortier L, et al. Pembrolizumab *Versus* Ipilimumab in Advanced Melanoma. *N Engl J Med* (2015) 372(26):2521–32. doi: 10.1056/NEJMoa1503093
56. Larkin J, Chiarion-Sileni V, Gonzalez R, Grob JJ, Rutkowski P, Lao CD, et al. Five-Year Survival With Combined Nivolumab and Ipilimumab in Advanced Melanoma. *N Engl J Med* (2019) 381(16):1535–46. doi: 10.1056/NEJMoa1910836
57. Reck M, Schenker M, Lee KH, Provencio M, Nishio M, Lesniewski-Kmak K, et al. Nivolumab Plus Ipilimumab *Versus* Chemotherapy as First-Line Treatment in Advanced Non-Small-Cell Lung Cancer With High Tumour Mutational Burden: Patient-Reported Outcomes Results From the Randomised, Open-Label, Phase III CheckMate 227 Trial. *Eur J Cancer* (2019) 116:137–47. doi: 10.1016/j.ejca.2019.05.008
58. Hellmann MD, Paz-Ares L, Bernabe Caro R, Zurawski B, Kim SW, Carcereny Costa E, et al. Nivolumab Plus Ipilimumab in Advanced Non-Small-Cell Lung Cancer. *N Engl J Med* (2019) 381(21):2020–31. doi: 10.1056/NEJMoa1910231
59. John T, Sakai H, Ikeda S, Cheng Y, Kasahara K, Sato Y, et al. 1311p First-Line (1L) Nivolumab (NIVO) + Ipilimumab (IPI) + Chemotherapy (Chemo) in Asian Patients (Pts) With Advanced non-Small Cell Lung Cancer (NSCLC) From CheckMate 9la. *Ann Oncol* (2020) 31:S847–8. doi: 10.1016/j.annonc.2020.08.1625
60. Reck M, Ciuleanu T-E, Dols MC, Schenker M, Zurawski B, Menezes J, et al. Nivolumab (NIVO) + Ipilimumab (IPI) + 2 Cycles of Platinum-Doublet Chemotherapy (Chemo) *vs* 4 Cycles Chemo as First-Line (1L) Treatment (Tx) for Stage IV/recurrent Non-Small Cell Lung Cancer (NSCLC): CheckMate 9la. *J Clin Oncol* (2020) 38(15_suppl):9501–1. doi: 10.1200/JCO.2020.38.15_suppl.9501
61. Rodriguez-Abreu D, Johnson ML, Hussein MA, Cobo M, Patel AJ, Secen NM, et al. Primary Analysis of a Randomized, Double-Blind, Phase II Study of the Anti-TIGIT Antibody Tiragolumab (Tira) Plus Atezolizumab (Atezo) *Versus* Placebo Plus Atezo as First-Line (1L) Treatment in Patients With PD-L1-Selected NSCLC (CITYSCAPE). *J Clin Oncol* (2020) 38(15_suppl):9503–3. doi: 10.1200/JCO.2020.38.15_suppl.9503
62. Carbone DP, Reck M, Paz-Ares L, Creelan B, Horn L, Steins M, et al. First-Line Nivolumab in Stage IV or Recurrent Non-Small-Cell Lung Cancer. *N Engl J Med* (2017) 376(25):2415–26. doi: 10.1056/NEJMoa1613493
63. Wang Z, Duan J, Cai S, Han M, Dong H, Zhao J, et al. Assessment of Blood Tumor Mutational Burden as a Potential Biomarker for Immunotherapy in Patients With Non-Small Cell Lung Cancer With Use of a Next-Generation Sequencing Cancer Gene Panel. *JAMA Oncol* (2019) 5(5):696–702. doi: 10.1001/jamaoncol.2018.7098
64. Cascone T, William WN, Weissferdt A, Lin HY, Leung CH, Carter BW, et al. Neoadjuvant Nivolumab (N) or Nivolumab Plus Ipilimumab (NI) for Resectable Non-Small Cell Lung Cancer (NSCLC): Clinical and Correlative Results From the NEOSTAR Study. *J Clin Oncol* (2019) 37(15_suppl):8504–4. doi: 10.1200/JCO.2019.37.15_suppl.8504
65. Toi Y, Sugawara S, Sugisaka J, Ono H, Kawashima Y, Aiba T, et al. Profiling Preexisting Antibodies in Patients Treated With Anti-PD-1 Therapy for Advanced Non-Small Cell Lung Cancer. *JAMA Oncol* (2019) 5(3):376–83. doi: 10.1001/jamaoncol.2018.5860
66. Dong ZY, Zhong WZ, Zhang XC, Su J, Xie Z, Liu SY, et al. Potential Predictive Value of TP53 and KRAS Mutation Status for Response to PD-1 Blockade Immunotherapy in Lung Adenocarcinoma. *Clin Cancer Res* (2017) 23(12):3012–24. doi: 10.1016/j.jtho.2016.11.504

Conflict of Interest: The authors declare that the research was conducted in the absence of any commercial or financial relationships that could be construed as a potential conflict of interest.

Publisher's Note: All claims expressed in this article are solely those of the authors and do not necessarily represent those of their affiliated organizations, or those of the publisher, the editors and the reviewers. Any product that may be evaluated in this article, or claim that may be made by its manufacturer, is not guaranteed or endorsed by the publisher.

frontiers in Pharmacology

SYSTEMATIC REVIEW
published: 13 September 2021
doi: 10.3389/fphar.2021.739843

Kanglaite Combined With Epidermal Growth Factor Receptor-Tyrosine Kinase Inhibitor Therapy for Stage III/IV Non-Small Cell Lung Cancer: A PRISMA-Compliant Meta-Analysis

Fanming Kong[1,2†], *Chaoran Wang*[1,2,3†], *Xiaojiang Li*[1,2] *and Yingjie Jia*[1,2*]

[1]Department of Oncology, First Teaching Hospital of Tianjin University of Traditional Chinese Medicine, Tianjin, China, [2]National Clinical Research Center for Chinese Medicine Acupuncture and Moxibustion, Tianjin, China, [3]Graduate School, Tianjin University of Traditional Chinese Medicine, Tianjin, China

Objective: Kanglaite(KLT), a type of Chinese medicine preparation, is considered as an adjuvant therapeutic option for malignant cancer treatment. This study aimed to systematically investigate the efficacy and safety of the combination of KLT and epidermal growth factor receptor-tyrosine kinase inhibitor (EGFR-TKI) for the treatment of stage III/IV non-small cell lung cancer.

Methods: Randomized controlled trials (RCTs) that compared KLT plus EGFR-TKI with EGFR-TKI alone for the treatment of stage III/IV non-small cell lung cancer were reviewed. Literature searches (up to July 10, 2021) were performed on PubMed, Web of Science, Cochrane Library, Embase, ClinicalTrials.gov, China National Knowledge Infrastructure (CNKI), Wanfang Database, and the Chinese Scientific Journal Database. Two researchers independently assessed the risk of bias with the tool of Cochrane Collaboration. RevMan 5.3.0 was used in the analysis of the included trial data.

Results: 12 RCTs recruiting 1,046 patients with stage III/IV NSCLC were included. Results showed that compared with EGFR-TKI alone, KLT plus EGFR-TKI significantly increased the disease control rate (DCR) (odds ratio [OR]=3.26; 95% confidence interval [CI]:2.22–4.77; $p < 0.00001$), the objective response rate (ORR) (OR=2.59; 95% CI:1.87–3.58; $p < 0.00001$) and Karnofsky performance status (KPS) (OR = 2.76; 95% CI:1.73–4.39; $p < 0.00001$). Furthermore, patient immunity was enhanced with KLT plus EGFR-TKI. The combined treatment increased the percentage of CD4 + T cells (weighted mean difference [WMD]= 5.36; 95% CI:3.60–7.13; $p < 0.00001$),the CD4+/CD8 + ratio (WMD = 0.18; 95% CI: 0.08–0.27; $p = 0.004$), and percentage of NK cells (WMD=4.84; 95% CI: 3.66–6.02; $p < 0.00001$).With regard to drug toxicity, the occurrence rate of nausea and vomiting was significantly reduced by KLT plus EGFR-TKI (OR=0.37; 95% CI: 0.16–0.86; $p = 0.02$).

Conclusion: KLT plus EGFR-TKI was effective in treating stage III/IV non-small cell lung cancer. Thus, its application in these patients is worth promoting. Additional double-blind, well-designed and multicenter RCTs are required to confirm the efficacy and safety of this treatment.

Keywords: EGFR-TKI, kanglaite, NSCLC, meta-analysis, stage III/IV

OPEN ACCESS

Edited by:
Yuling Qiu,
Tianjin Medical University, China

Reviewed by:
Hamed Barabadi,
Shahid Beheshti University of Medical Sciences, Iran
Jung-Mao Hsu,
China Medical University, Taiwan

***Correspondence:**
Yingjie Jia
jiayingjie1616@sina.com

†These authors have contributed equally to this work

Specialty section:
This article was submitted to Pharmacology of Anti-Cancer Drugs, a section of the journal Frontiers in Pharmacology

Received: *12 July 2021*
Accepted: *02 September 2021*
Published: *13 September 2021*

Citation:
Kong F, Wang C, Li X and Jia Y (2021) Kanglaite Combined With Epidermal Growth Factor Receptor-Tyrosine Kinase Inhibitor Therapy for Stage III/IV Non-Small Cell Lung Cancer: A PRISMA-Compliant Meta-Analysis. Front. Pharmacol. 12:739843. doi: 10.3389/fphar.2021.739843

INTRODUCTION

Lung cancer remains the leading cause of cancer-related death worldwide (Sung et al., 2021). Despite the recent remarkable progress in screening, diagnosis, and treatment. 57% of patients with lung cancer are diagnosed at an advanced or metastatic stage, during which the 5-years relative survival rate is only 5% (Richards et al., 2017). Epidermal growth factor receptor-tyrosine kinase inhibitors (EGFR-TKIs) have improved clinical benefits for patients with metastatic non-small cell lung cancer (NSCLC) patients (Rosell et al., 2012). The National Comprehensive Cancer Network NSCLC Panel recommends identification of EGFR mutations for all patients with adenocarcinoma. EGFR-TKI combined with chemotherapy improved progression free survival (PFS) in untreated advanced NSCLC patients with EGFR mutation (Hosomi et al., 2020). However, the undesirable effects of EGFR-TKIs adversely affect the quality of life and treatment compliance of patients (Shah and Shah, 2019). Of patients with EGFR-mutated NSCLC, 20–40% experience primary resistance to first or second-generation EGFR-TKIs, which is attributed to genetic alterations (Wang et al., 2016). Moreover, some patients do not show a good initial clinical response. Therefore, a EGFR-TKI-based combination treatment regimen may be more beneficial.

Traditional Chinese medicine (TCM) has been widely used as an adjuvant therapeutic option for cancer treatment (Xiang et al., 2019; Liu S.-H. et al., 2021). High-level clinical studies of TCM injection in cancer care has gradually increased (Yang et al., 2021). Kanglaite injection had been approved by the Chinese State Food and Drug Administration (SFDA) for the treatment of various malignant tumors. KLT is extracted and isolated from coix seeds (Coix lacryma-jobi). A few clinical studies on KLT for patients with solid tumor have been approved in the United States. KLT is the first TCM to be approved by the US Food and Drug Administration (FDA). The clinical mechanisms of KLT for NSCLC are related to the promotion of cancer cell apoptosis, inhibition of migration and proliferation and improvement of the immunity (Pan et al., 2012; Lu et al., 2013; Luo et al., 2017; Duan, 2018; Wu et al., 2018).

In previous studies, KLT injection combined with platinum-based chemotherapy showed significantly higher efficacy in the treatment of stage III/IV NSCLC (Hailang et al., 2020a; Li et al., 2020; Ni et al., 2021). With the widespread application of EGFR-TKI, the number of published clinical studies on KLT combined with EGFR-TKI has been increasing. On the basis of previous clinical studies, we performed a PRISMA-compliant meta-analysis of KLT combined with EGFR-TKI in patients with stage III/IV NSCLC (**Figure 1**) to assess the clinical efficacy, quality of life, immune function (including percentages of $CD3^+$, $CD4^+$, NK cells and the CD4+/CD8+ratio) and adverse events. This work was conducted to provide comprehensive evidence for further studies and explore the clinical outcome of combination therapy with KLT and EGFR-TKI.

MATERIALS AND METHODS

We performed this meta-analysis following the Preferred Reporting Items for Systematic Reviews and Meta-Analyses (PRISMA) guidelines and Cochrane Handbook. The data were obtained from published trials. As this study does not involve animal and patient experiments, the ethical approval was not required.

Literature Source and Search Strategy

A comprehensive literature search was conducted by two independent researchers (FM Kong and CR Wang). Published studies were retrieved from eight databases including PubMed, Web of Science, Cochrane Library, Embase, ClinicalTrials.gov, the China National Knowledge Infrastructure (CNKI), Wanfang Database and the Chinese Scientific Journal Database. The last search date was July 10, 2021. In addition, we searched the relevant systematic reviews and meta-analyses to find the potential studies that may have been missed in the online searches.

The following search terms were used: "Lung Cancer" or "Non small cell lung cancer" or "NSCLC" or "Lung Carcinoma"or "Carcinoma of the lung" and "Kanglaite" and "Gefitinib" or "Erlotinib" or "Icotinib" or "Afatinib" or "Dacomitinib" or "Osimertinib" or "EGFR-TKI". No language limits were applied.

Types of Studies and Selection Criteria

All RCTs that compared KLT plus EGFR-TKI with EGFR-TKI alone were selected and assessed for inclusion in the study.

The inclusion criteria were as follows:

1) Randomized controlled trials (RCTs).
2) Patients with stage III/IV NSCLC confirmed by cytology or pathology.
3) Studies that included >30 patients with NSCLC.
4) Studies that compared the clinical outcomes of EGFR-TKI plus KLT adjuvant therapy (experimental group) with those of EGFR-TKI alone (control group).
5) The EGFR-TKIs included Gefitinib, Icotinib, Erlotinib, Afatinib, Dacomitinib, and Osimertinib.

The exclusion criteria were as follows:

1) Neither RCT nor "random"was mentioned.
2) Articles without sufficient data available.
3) Duplication of previous publications.
4) Case studies, review papers, comments, and conference abstracts.

Data Extraction and Quality Assessment

Data were independently extracted by two reviewers (FM Kong and CR Wang) according to the above inclusion and exclusion criteria; any disagreement was adjudicated by a third reviewer (XJ Li).

The following data were extracted:

1) The first author's name
2) Year of publication
3) Study location
4) Tumor stage
5) Number of cases
6) Age of the patients
7) Gender of the patients
8) Therapeutic regimens

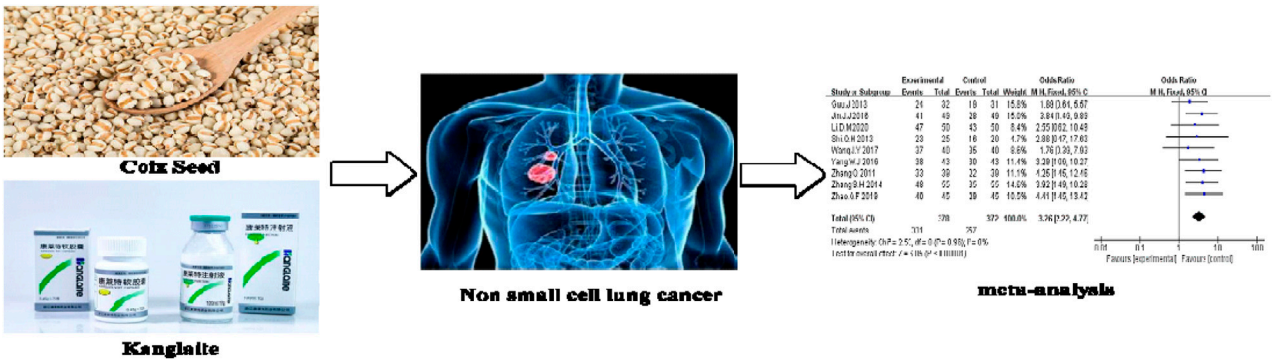

FIGURE 1 | Work flow of the present study.

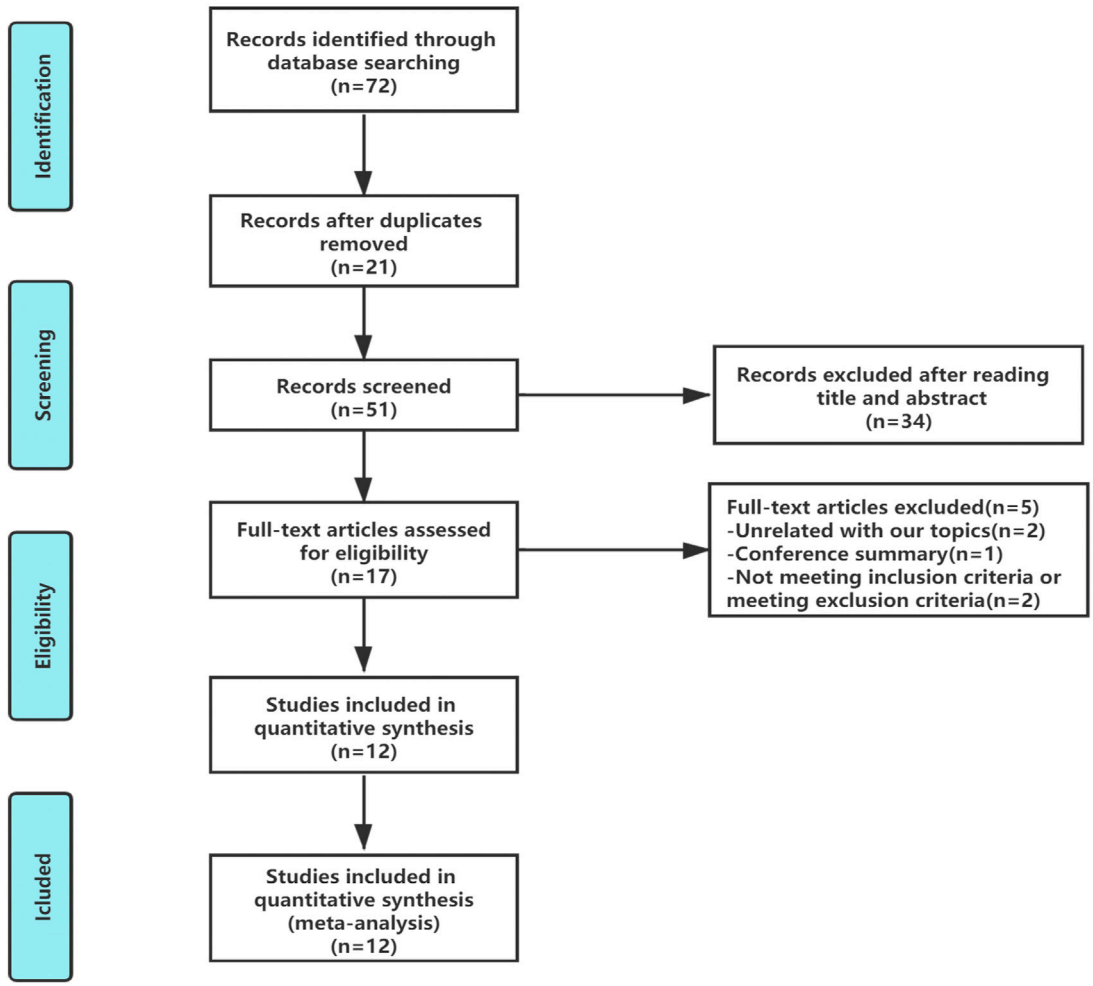

FIGURE 2 | Flow diagram showing study selection for the meta-analysis.

9) Main outcomes

Outcome Definition

The clinical responses assessed included treatment efficacy, performance status, immune function, and adverse events. Treatment efficacy was evaluated in terms of the disease control rate (DCR), objective response rate (ORR), Karnofsky performance status (KPS), immune function indicators (percentages of $CD3^+$, $CD4^+$, NK cells and the CD4+/CD8+ratio) and adverse events including rash, nausea and vomiting, diarrhea, and liver injury.

TABLE 1 | Clinical information from the eligible trials included in the meta-analysis.

Included studies	TNM stage	Patients Exp/Con	Therapeutic regimen		Dosage of kanglaite (daily)	Dose of EGFR-TKI (daily) (mg)	Duration	Outcomes measure
			Experimental	Control				
Ning.J.L (2015)	IIIB-IV	93/93	Con + KLT[a]	Gefitinib	200 ml	250	8 weeks	IF
Zhang.S.H (2014)	III-IV	55/55	Con + KLT[a]	Gefitinib	200 ml	250	9 weeks	DCR ORR KPS AE
Li.D.M (2020)	IIIB-IV	50/50	Con + KLT[b]	Gefitinib	2.7 g Qid	250	Not provide	DCR ORR AE
Wang.J.Y (2017)	IIIB-IV	40/40	Con + KLT[b]	Gefitinib	2.7 g Qid	250	60 d	DCR ORR AE
Zeng.H.X (2014)	IIIB-IV	23/23	Con + KLT[a]	Gefitinib	200 ml	250	6 weeks	IF AE KPS
Yang.L (2016)	III-IV	32/32	Con + KLT[a]	Gefitinib	200 ml	250	6 weeks	IF
Yang.W.J (2016)	IIIB-IV	43/43	Con + KLT[a]	Icotinib	200 ml	375	9 weeks	DCR ORR KPS IF AE
Guo.J (2013)	IIIB-IV	32/31	Con + KLT[a]	Erlotinib	200 ml	150	9 weeks	DCR ORR IF AE
Jin.J.J (2016)	III-IV	49/49	Con + KLT[a]	Gefitinib	200 ml	250	3 weeks	DCR ORR IF AE
Zhang.Q (2011)	III-IV	39/39	Con + KLT[a]	Gefitinib	100 ml	250	9 weeks	DCR ORR KPS AE
Zhao.Q.F (2019)	III-IV	45/45	Con + KLT[a]	Gefitinib	200 ml	251	3 weeks	DCR ORR IF AE
Shi.Q.H (2013)	IIIB-IV	25/20	Con + KLT[a]	Gefitinib	100 ml	250	60 d	DCR ORR KPS

Con, control group; Exp, experimental group; DCR, disease control rate; ORR, objective response rate; KPS, Karnofsky performance status; IF, Immune function; AE, adverse event.
[a]*Kanglaite injection.*
[b]*Kanglaite capsule.*

TABLE 2 | Subgroup analyses of DCR and ORR between the experimental and control group.

Parameter	Factors at study	Experimental Patients(n)	Control Patients(n)	Analysis method	I^2	Odds ratio (OR)	95%CI	*p*-value
DCR	**Sample size**							
	≥80	282	282	Fixed	0	3.44	2.17–5.44	< 0.00001
	< 80	96	90	Fixed	0	2.87	1.43–5.74	0.003
	Form of KLT							
	Injection	288	282	Fixed	0	3.48	2.31–5.46	< 0.00001
	Capsule	90	90	Fixed	0	2.15	0.77–6.01	0.14
	Duration							
	3 W	94	94	Fixed	0	1.42	1.19–1.70	0.0001
	9 W	169	168	Fixed	0	1.34	1.18–1.53	< 0.00001
ORR	**Sample size**							
	≥80	282	282	Fixed	0	2.96	2.01–4.37	< 0.00001
	< 80	96	90	Fixed	0	1.89	1.04–3.42	0.04
	Form of KLT							
	Injection	288	282	Fixed	0	2.54	1.80–3.58	< 0.00001
	Capsule	90	90	Fixed	0	3.03	1.13–8.14	0.003
	Duration							
	3 W	94	94	Fixed	0	3.32	1.79–6.15	0.0001
	9 W	169	168	Fixed	0	2.29	1.47–3.57	0.0002

Risk of Bias Assessment

Two researchers (XJ Li and YJ Jia) independently assessed the risk of bias with the tool of Cochrane Collaboration (Higgins et al., 2011). The Cochrane Collaboration contained the following assessment tools: random sequence generation; allocation concealment; blinding of participants, and personnel; blinding of outcome assessment; incomplete data; selective reporting and other bias. Each study was classified as"low risk of bias","unclear risk of bias"or"high risk of bias". Any disagreement was settled through the third researcher (FM Kong).

Statistical Analysis

Statistical analysis was performed with the RevMan 5.3 software (Nordic Cochran Centre, Copenhagen, Denmark) software. Treatment effects were mainly represented by odds ratio (OR), and continuous data were shown as the weighted mean difference (WMD) with a 95% confidence intervals (CI). p value < 0.05 was considered statistically significant. Heterogeneity among the studies was assessed by Cochran's Q test; I^2 < 50% or p > 0.1 indicated a lack of heterogeneity among the studies. When the level of heterogeneity was small (I^2< 50%), a fixed-effects model was applied for estimation; otherwise, a random-effects model was selected.

RESULTS

Search Results

In total, 72 articles were initially identified. Of these articles, 21 papers were excluded because they were duplicates. After the title

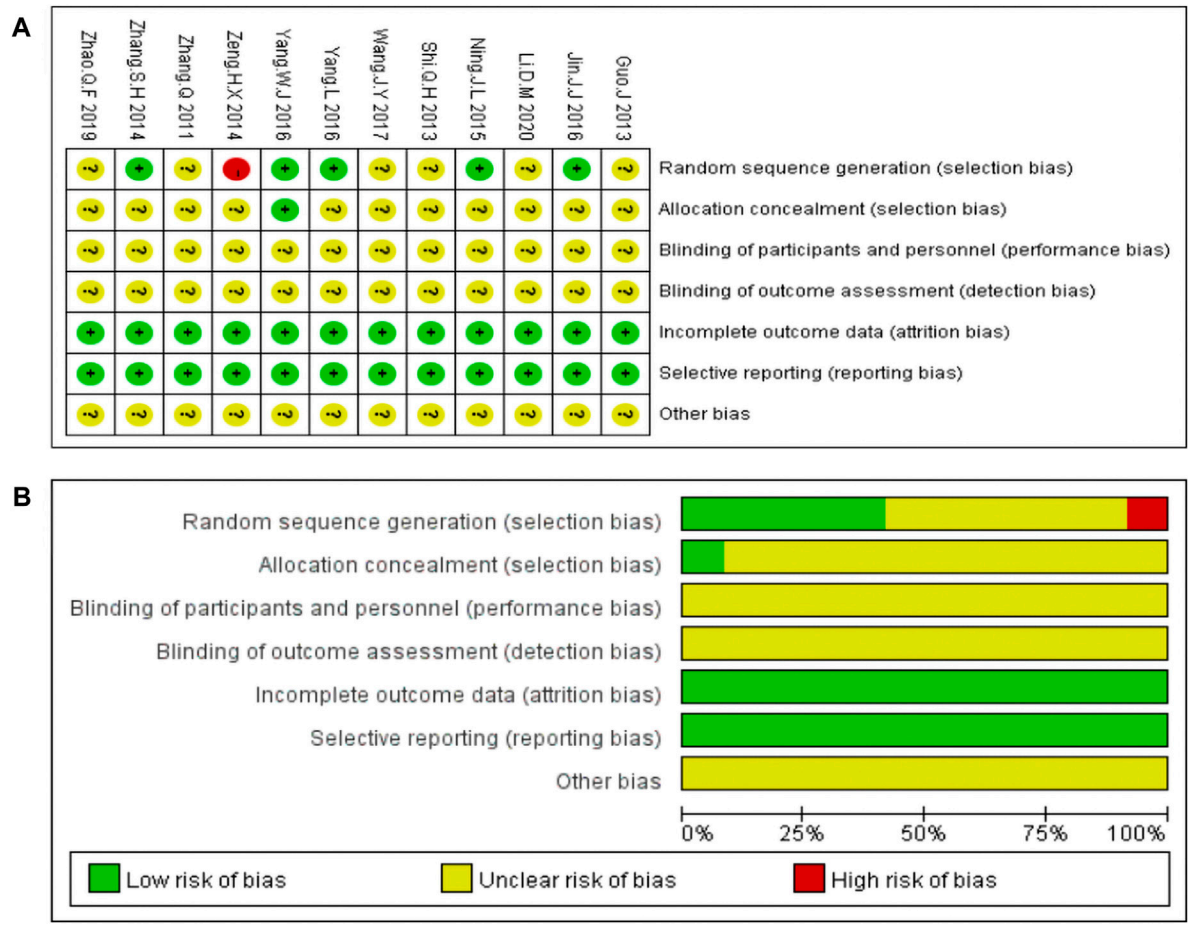

FIGURE 3 | Risk of bias of the included studies **(A)** Risk of bias graph **(B)** Risk of bias summary.

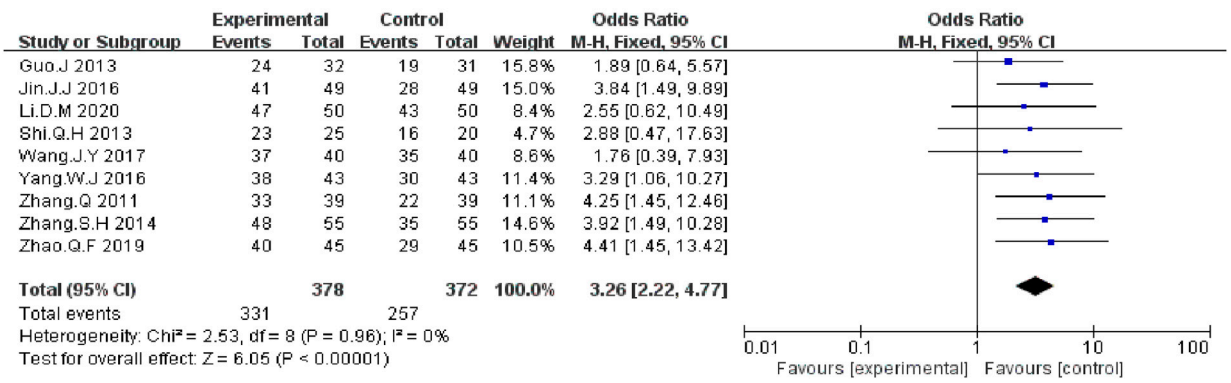

FIGURE 4 | Forest plot of DCR in patients treated with KLT + EGFR-TKI and EGFR-TKI alone.

and abstract review, 34 articles were further excluded. After a detailed assessment of the full text articles, those unrelated with our topics ($n = 2$), conference summary ($n = 1$), and those that did not meeting the inclusion criteria or exclusion criteria ($n = 2$) were also excluded. Ultimately, 12 trials involving a total of 1,046 patients were included in this analysis (**Figure 2**).

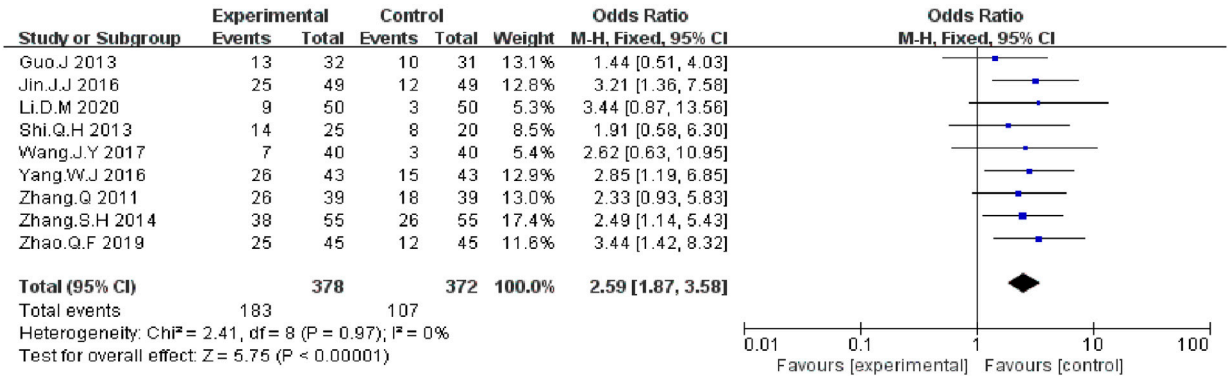

FIGURE 5 | Forest plot of ORR in patients treated with KLT + EGFR-TKI and EGFR-TKI alone.

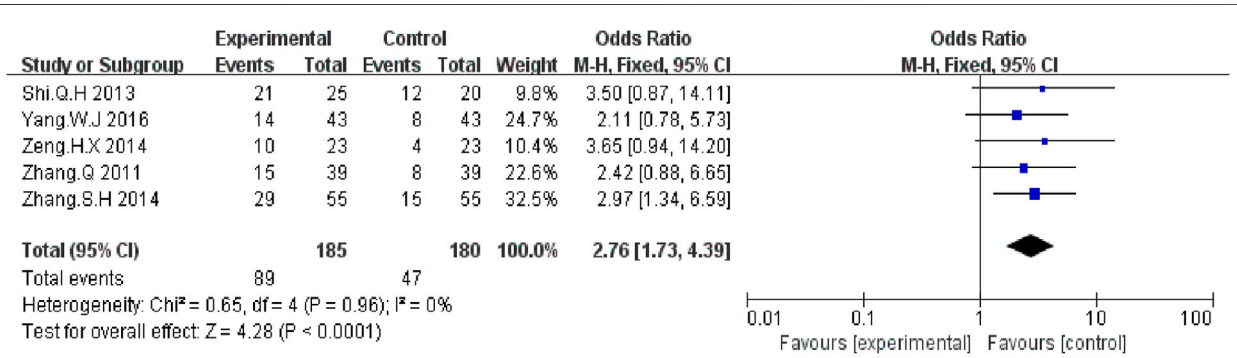

FIGURE 6 | Forest plot of KPS improvement in patients treated with KLT + EGFR-TKI and EGFR-TKI alone.

Characteristics of Included Studies

Table 1 summarizes the basic characteristics of the 12 RCTs. All the studies were conducted in different medical centers in China (Zhang and Yuan, 2011; Guo and Wang, 2013; Shi and Chen, 2013; Zeng et al., 2014; Zhang and Zhou, 2014; Ning et al., 2015; Jin et al., 2016; Yang, 2016; Yang et al., 2016; Wang et al., 2017; Zhao et al., 2019; Li, 2020). A total of 1,046 patients were recruited, of which 526 patients with stage III/IV NSCLC were treated with EGFR-TKI in combination with KLT, while 520 patients were treated with EGFR-TKI alone, with a sample size of 46–186 in each trial. The course of treatment lasted from 3 to 9 weeks. The control group received EGFR-TKIs, including gefitinib (Zhang and Yuan, 2011; Shi and Chen, 2013; Zeng et al., 2014; Zhang and Zhou, 2014; Ning et al., 2015; Jin et al., 2016; Yang et al., 2016; Wang et al., 2017; Zhao et al., 2019; Li, 2020), Icotinib (Yang, 2016) and Erlotinib (Guo and Wang, 2013). The patients in the experimental group received EGFR-TKI in combination with KLT, including KLT injections (Zhang and Yuan, 2011; Guo and Wang, 2013; Shi and Chen, 2013; Zeng et al., 2014; Zhang and Zhou, 2014; Ning et al., 2015; Jin et al., 2016; Yang, 2016; Yang et al., 2016; Zhao et al., 2019) and KLT capsules (Wang et al., 2017; Li, 2020). Patient characteristics are shown in **Table 1**.

Risk of Bias Assessment

The bias risk analysis performed using the Cochrane Collaboration tool revealed bias in all the included studies. "Random" or "randomized" or "randomization" was mentioned in 11 studies, except for one study (Zeng et al., 2014). Only one study reported allocation concealment (Yang, 2016). All the included studies reported detailed outcome data. None of the 12studies provided blinding of the outcome data, clear descriptions of selective and other biases. Risk of bias assessment are shown in **Figure 3**.

Outcomes Measures

Disease Control Rate and Objective Response Rate

We extracted the data on DCR and ORR data from nine included RCTs report (Zhang and Yuan, 2011; Guo and Wang, 2013; Shi and Chen, 2013; Zhang and Zhou, 2014; Jin et al., 2016; Yang, 2016; Wang et al., 2017; Zhao et al., 2019; Li, 2020). The meta-analysis data showed that, compared with EGFR-TKI alone, KLT plus EGFR-TKI significantly improved DCR (OR = 3.26; 95% CI:2.22–4.77; $p < 0.00001$) (**Figure 4**) and ORR (OR: 2.59; 95% CI: 1.87–3.58; $p < 0.00001$) (**Figure 5**). Statistical homogeneity was observed for both outcomes ($I^2 = 0\%$).

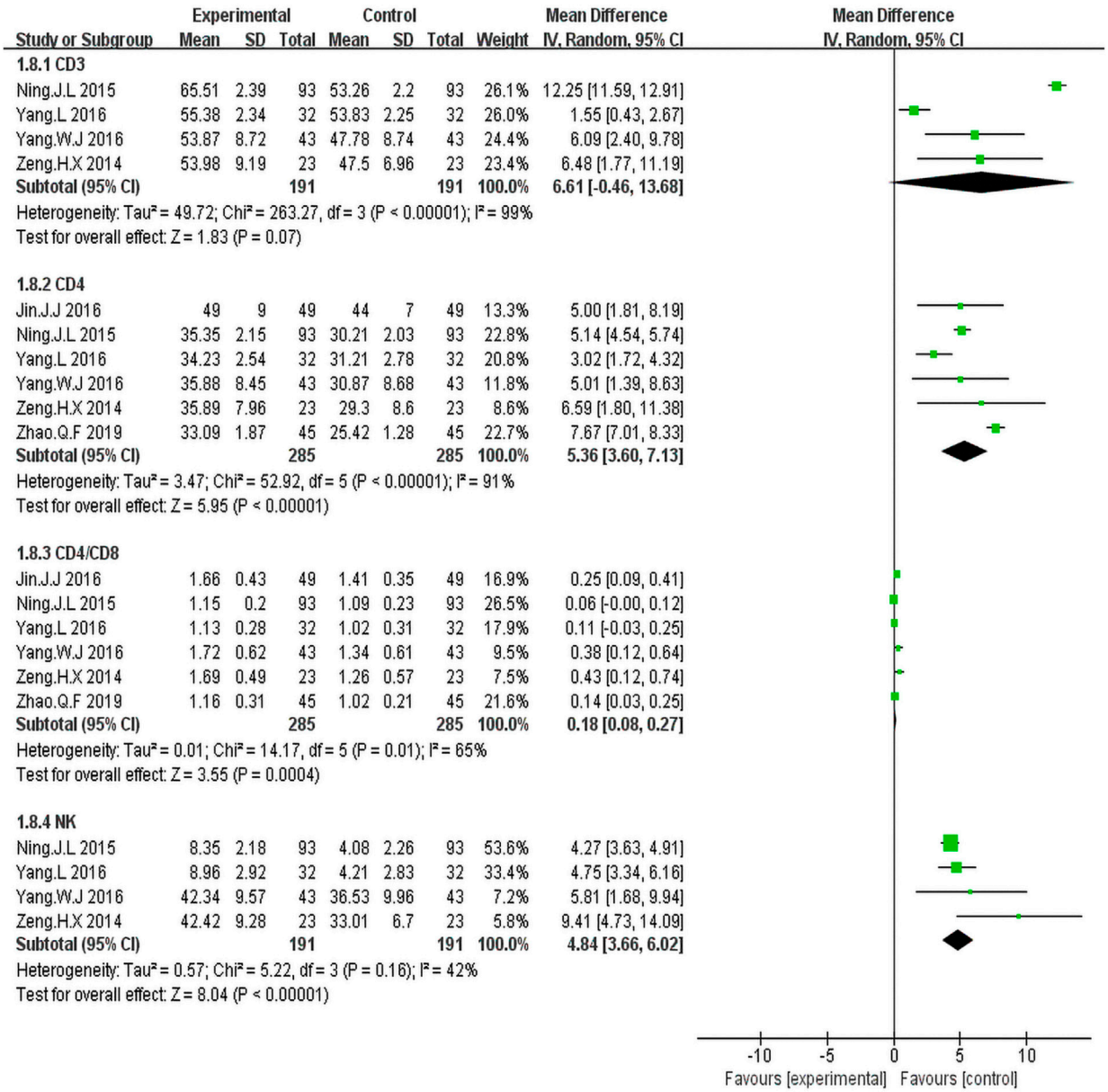

FIGURE 7 | Forest plot of Immune function in patients treated with KLT + EGFR-TKI and EGFR-TKI alone.

Karnofsky Performance Status

Five trials (Zhang and Yuan, 2011; Shi and Chen, 2013; Zeng et al., 2014; Zhang and Zhou, 2014; Yang, 2016) with a total of 750 patients reported improvement in KPS improvement. According to the results, the KPS was significantly higher in the KLT plus EGFR-TKI group than the control group (OR = 2.76, 95% CI: 1.73–4.39; $p < 0.00001$) (**Figure 6**). A fixed-effect model was used due to the heterogeneity ($I^2 = 0\%$).

Immune Function

Four trials (Zeng et al., 2014; Ning et al., 2015; Yang, 2016; Yang et al., 2016) including 382 patients reported percentages of $CD3^+$ cells. Statistical heterogeneity was observed ($I^2 = 99\%$, $p < 0.00001$); Hence, the random effect model was employed. The results showed that the percentage of $CD3^+$ cells was similar between the KLT plus EGFR-TKI group and control group (WMD = 6.61; 95% CI: 0.46 to 13.68; $p = 0.07$) (**Figure 7**).

Six trials (Zeng et al., 2014; Ning et al., 2015; Jin et al., 2016; Yang, 2016; Yang et al., 2016; Zhao et al., 2019) including 570 patients reported percentage of CD4+cells and the CD4+/CD8+ratio.There was statistical heterogeneity. The random effect model was employed for the analysis. The results illustrated that KLT plus EGFR-TKI group had an advantage

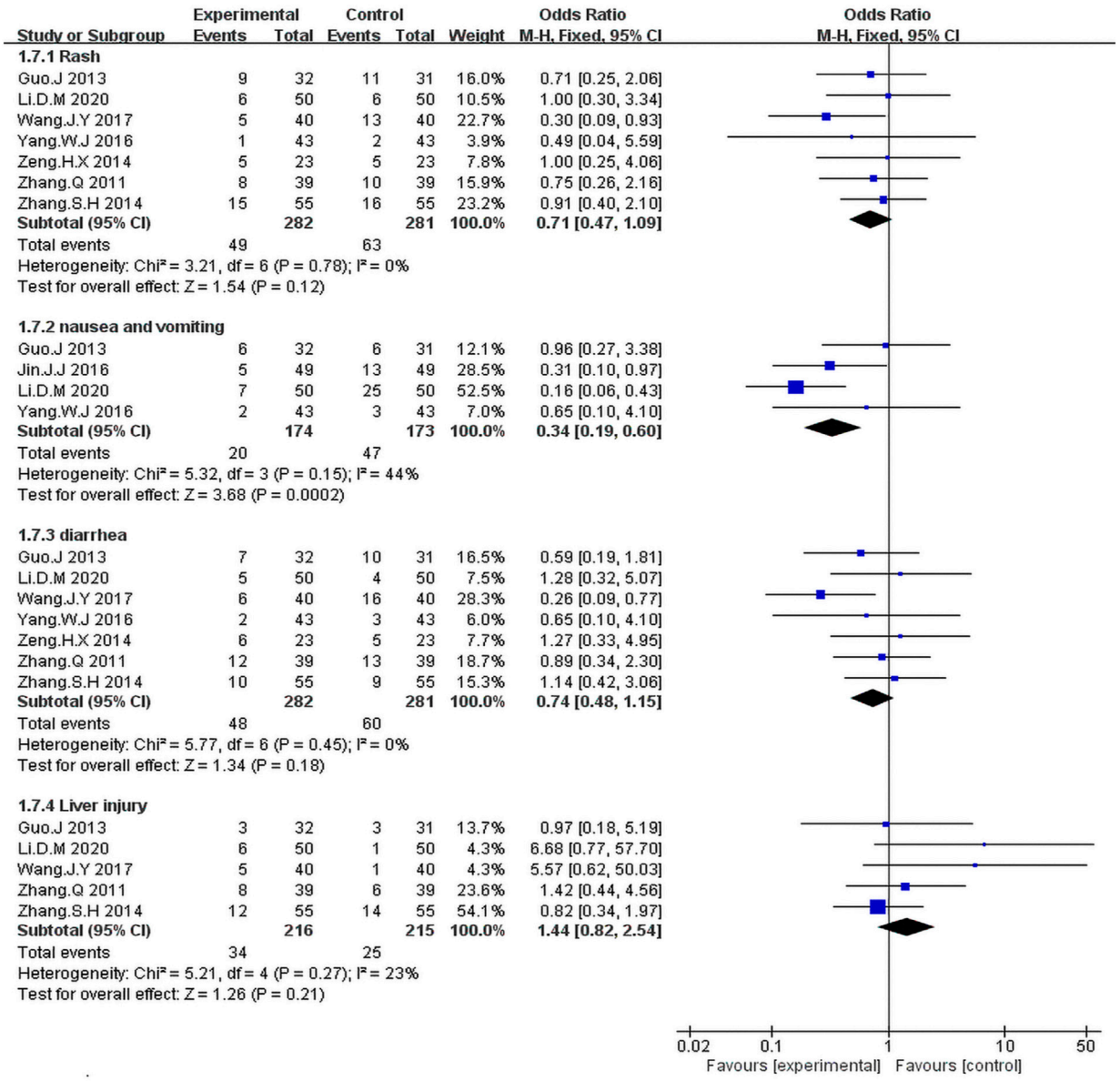

FIGURE 8 | Forest plot of adverse events in the patients treated with EGFR-TKI + KLT and EGFR-TKI alone.

TABLE 3 | Main Anticancer Mechanism of Coix seed in treatment of lung cancer.

Pharmacological effects	Types	Main anticancer mechanism	Fraction
Promotes tumor cell apoptosis	NSCL A549 cells	Mechanism of the intrinsic mitochondrial pathway (Lu et al., 2013)	Polysaccharide
Improves the immunity	Lewis lung carcinoma	Regulates the expression of NF-κB/IκB, increases IL-2 (Pan et al., 2012)	Coix seed extract
	Lewis lung carcinoma	Decreases the TAM levels and improves hypoxia status (Duan, 2018)	Coix seed extract
Inhibits migration and invasion	NSCL A549 cells	Inhibits JAK2/STAT3 signaling pathway (Wang and Wang, 2019)	Coix seed extract
	NSCL A549 cells	Downregulates the S100A4 (Luo et al., 2017)	Polysaccharide
Inhibits proliferation	Serum sample	Reduces the expressions of miRNA-21 (Wu et al., 2018)	Coix seed extract

of increased percentage of CD4+cells (WMD = 5.36; 95%CI: 3.60–7.13; $p < 0.00001$; $I^2 = 91\%$) and the CD4+/CD8+ ratio (WMD = 0.18; 95% CI: 0.08–0.27; $p = 0.004$; $I^2 = 65\%$) (**Figure 7**).

Four trials (Zeng et al., 2014; Ning et al., 2015; Yang, 2016; Yang et al., 2016) including 382 patients reported percentage of NK cells. The results showed that the KLT plus EGFR-TKI group

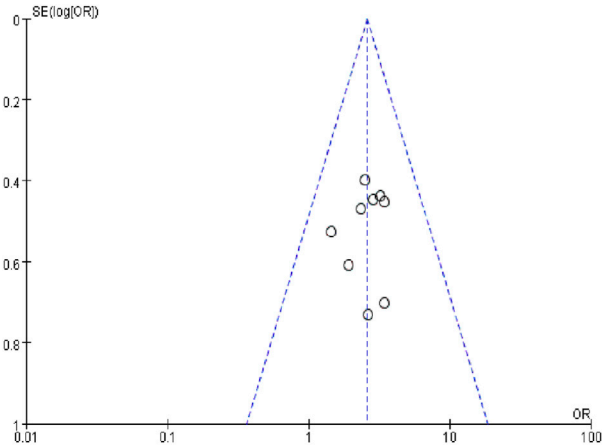

FIGURE 9 | Funnel plot of publication bias.

had an advantage of increased NK cells (WMD = 4.84; 95% CI: 3.66–6.02; $p < 0.00001$; $I^2 = 42\%$) (**Figure 7**).

Adverse Event

The fixed-effects meta-analysis revealed a significantly lower occurrence rate of nausea and vomiting in the KLT plus EGFR-TKI group than in the control group (OR = 0.37; 95% CI:0.16–0.86; $p = 0.02$; $I^2 = 44\%$) (**Figure 8**).

We identified seven studies (Zhang and Yuan, 2011; Guo and Wang, 2013; Zeng et al., 2014; Zhang and Zhou, 2014; Yang, 2016; Yang et al., 2016; Wang et al., 2017) including 563 patients with rash and diarrhea. The Fixed-effects model revealed that the KLT plus EGFR-TKI group showed no significant differences in the occurrence rates of rash (OR = 0.71; 95% CI:0.47–1.09; $p = 0.12$; $I^2 = 0\%$) and diarrhea (OR = 0.74; 95% CI:0.48–1.15; $p = 0.18$; $I^2 = 0\%$) compared with the control group (**Figure 8**).

As can be seen in **Figure 8**, five studies (Zhang and Yuan, 2011; Guo and Wang, 2013; Zhang and Zhou, 2014; Wang et al., 2017; Li, 2020) including 431 patients reported the incidence of liver injury. The meta-analysis revealed that the combination treatment with KLT plus EGFR-TKI did not significantly reduce the risk of liver injury risk when compared with the EGFR-TKI alone (OR = 1.44; 95% CI: 0.82–2.54; $p = 0.21$; $I^2 = 23\%$).

Sensitivity Analysis

We performed a subgroup analysis to examine the source of the heterogeneities in ORR and DCR with regard to sample size, form of KLT, duration of therapy. As shown in **Table 2**, there were no significant differences between sample size, form of KLT, and therapy duration. Moreover, in terms of DCR index, KLT injection plus EGFR-TKI was found to be more effective than KLT capsule plus EGFR-TKI.

Publication Bias

A funnel plot of the nine studies that reported ORR data was used to assess publication bias (**Figure 9**). The funnel plot was asymmetrical, indicating the existence of publication bias.

DISCUSSION

Clinically, KLT has synergistic effects with radiotherapy and chemotherapy, it has been used in the adjuvant treatment of various tumors such as lung cancer (Hailang et al., 2020a; Li et al., 2020), breast Cancer (Liu S. et al., 2021), hepatocellular carcinoma (Liu et al., 2019; Dou et al., 2020)and colorectal cancer (Mao et al., 2020). The main effects targeted the improvements of clinical efficacy, performance status, KPS score, immune function and the reduction of the side effects of radiotherapy and chemotherapy. In advanced NSCLC, KLT injection combined with platinum-based chemotherapy showed significantly higher efficacy (Wen et al., 2020). EGFR-TKIs have proved effective as first-or second-line therapy for advanced NSCLC. Although the achieved efficacy is significant, most patients acquire resistance to the EGFR-TKIs, which limits the benefits of this treatment. Chinese herbal extracts play a role in overcoming EGFR-TKI resistance in NSCLC (Lee et al., 2021). TCM combined with EGFR-TKI treatment prolonged progression-free survival (PFS) in patients with NSCLC who were harboring EGFR mutations and caused no adverse effects (Jiao et al., 2019; Tang et al., 2019). TCMs have better effects on ORR than EGFR-TKI alone in the treatment of NSCLC (Sui et al., 2020). A systematic review revealed that combination of KLT injection with gefitinib may enhance the therapeutic effectiveness for the patients with NSCLC (Hailang et al., 2020b). However, this study only included seven RCTs up to 2016. The meta-analysis did not include other EGFR-TKIs and different forms of KLT. In recent years, the number of published clinical studies on KLT combined with EGFR-TKI has been increasing. Based on this, we comprehensively searched the literature (up to July 10, 2021) for studies that included icotinib, erlotinib and the capsule form of KLT to systematically evaluate the efficacy and safety of the treatment for stage III/IV non-small cell lung cancer. DCR is regarded as one of the best indicators for predicting OS and PFS (Claret et al., 2014). Our study included DCR as the main outcome indicator. Compared with previous studies, we followed the PRISMA guidelines and additionally performed a subgroup analysis, risk-of-bias assessment, and publication bias analysis for a more comprehensive research.

The meta-analysis was performed with 12 RCTs to evaluate the clinical efficacy of the addition of KLT to EGFR-TKI. The study results showed that compared with EGFR-TKI alone, the combination of KLT and EGFR-TKI significantly improved DCR, ORR, KPS and immune function. The percentages of $CD4^+$ cells, NK cells and the CD4+/CD8+ratio were significantly increased when KLT was administered, indicating that the immune function of NSCLC patients was improved. Previous studies have shown that KLT has pronounced immunostimulatory activities in C57BL/6 mice (Pan et al., 2012). KLT in combination with chemotherapy influences the peripheral blood T lymphocyte subsets and blood immunoglobulins in patients with advanced NSCLC (Wen et al., 2020). In the subgroup analysis, no significant differences in ORR and DCR were found between sample size, form of KLT, and therapy duration. This suggests that the dosage form of KLT should be chosen depending on the patient's condition. Moreover, in terms

of DCR index, KLT injection plus EGFR-TKI was found to be more effective than KLT capsule plus EGFR-TKI. The subgroup analysis revealed that even with the increased treatment duration (from 3 to 9 weeks), DCR was not improved, indicating that 3 weeks of KLT therapy might be an optimal choice. All these results indicate that the addition of KLT might enhance the curative effects of treatment for stage III/IV non-small cell lung cancer.

Although the combination of KLT and gefitinib has shown better clinical efficacy, the synergistic mechanisms are currently unclear. Previous basic experiments showed that the clinical mechanisms of action of KLT for lung cancer are related to the promotion of cancer cell apoptosis (Lu et al., 2013), improvement of the immunity (Pan et al., 2012; Duan, 2018), inhibition of migration and invasion (Luo et al., 2017; Wang and Wang, 2019) and inhibition of proliferation (Wu et al., 2018). (**Table 3**). KLT combined with Gefitinib can reduce the number of angiogenesis in Lewis lung cancer tissues. The vascular endothelial growth factor-kinase domain receptor (VEGF-KDR) pathway may be one of the mechanisms to inhibit tumor angiogenesis. This may be one of the reasons for the synergistic effect in the treatment of lung cancer (Shen et al., 2013). The combination of KLT and gefitinib can induce cell apoptosis significantly. KLT may increase the sensitivity of the human lung adenocarcinoma cell line A549 to gefitinib, (Zhao et al., 2015). At present, the synergistic mechanism of KLT and EGFR-TKI is still unclear, and more experimental data are needed to clarify this.

There were some limitations in this study. First, all the trials were published in China, which is a source of selection bias. Only one study on KLT treatment for lung cancer in the United States is registered at ClinicalTrials.gov (NCT01640730). Second, the studies included in this meta-analysis used an"A + B vs. B"design, without a rigorous control for placebo effect. Third, none of the trials reported the OS and PFS rates. Whether KLT plus EGFR-TKI improve the OS and PFS for NSCLC remains unclear. Fourth, only first-generation EGFR-TKIs were used in the studies included in this meta-analysis. No relevant clinical study has used KLT combined with afatinib or osimertinib. Furthermore, our current study has not been registered, and bias may have been present. Future trials are needed to ensure that the reporting follows the consolidated standards for reporting trials guidelines. Additional double-blind, well-designed and multicenter RCTs are required to confirm the efficacy and safety of this combination treatment.

CONCLUSION

The results of this study indicate that treatment with KLT combined with EGFR-TKI is more effective than EGFR-TKI alone in the treatment for stage III/IV non-small cell lung cancer patients. KLT can be used as a complementary therapy for NSCLC. However, the low quality of some of the included publications increased the risk of bias, which, to some extent, affected the reliability of the research. The clinical efficacy of KLT-mediated adjuvant therapy for stage III/IV non-small cell lung cancer requires verification in methodologically rigorous trials.

DATA AVAILABILITY STATEMENT

The original contributions presented in the study are included in the article/supplementary material, further inquiries can be directed to the corresponding author.

AUTHOR CONTRIBUTIONS

FK and XL initiated this study. FK and CW performed study selection, data extraction, and data analysis. The article was drafted by YJ and revised by XL. All authors contributed to the article and approved the submitted version.

FUNDING

This study was funded by the National Natural Science Foundation of China (No. 81403220 and No. 81904151), Tianjin Health and family planning-high level talent selection and training project, Tianjin Science and Technology Plan Projects (No. 17ZXMFSY00190), and Tianjin Traditional Chinese Medicine Research Project, Tianjin health and family planning commission (No. 2017003).

REFERENCES

Claret, L., Gupta, M., Han, K., Joshi, A., Sarapa, N., He, J., et al. (2014). Prediction of Overall Survival or Progression Free Survival by Disease Control Rate at Week 8 Is Independent of Ethnicity: Western versus Chinese Patients with First-Line Non-small Cell Lung Cancer Treated with Chemotherapy with or without Bevacizumab. *J. Clin. Pharmacol.* 54(3), 253–257. doi:10.1002/jcph.191

Dou, D., Zhang, Z. Y., Wu, Z. Y., Qiu, X. D., and Zhong, X. G. (2020). Aidi Injection, Compound Kushen Injection, or Kanglaite Injection: Which Is the Best Partner with Systemic Chemotherapy for Patients with HCC? A Network Meta-Analysis. *Evid. Based Complement. Alternat Med.* 2020, 5497041. doi:10.1155/2020/5497041

Duan, G. C. (2018). The Effects of Combination of Coix Seed Extract and Cisplatin on TAM and Expression of HIF-1α *In Vivo* in Lewis Lung Carcinoma. *Iran. J. Public Health*. 47(6), 838–843.

Guo, J., and Wang, N. (2013). Observation of Kanglaite Injection Combined with Erlotinib in the Treatment of Advanced Non-small Cell Lung Cancer. *Hebei Med. J.* 35(05), 685–686. doi: doi:10.3969/j.issn.1002-7386.2013.05.021

Hailang, H., Jiping, Z., Ailing, C., and Xianmei, Z. (2020b). The Effect of Kanglaite Injection in Combination with Gefitinib versus Gefitinib Alone in Patients with Nonsmall Cell Lung Cancer: A Meta-Analysis. *J. Cancer Res. Ther.* 16(4), 745, 751. doi:10.4103/jcrt.JCRT_1213_16

Higgins, J. P., Altman, D. G., Gøtzsche, P. C., Jüni, P., Moher, D., Oxman, A. D., Savovic, J., Schulz, K. F., Weeks, L., and Sterne, J. A. (2011). The Cochrane Collaboration's Tool for Assessing Risk of Bias in Randomised Trials. *BMJ.* 343(oct18 2), d5928. doi:10.1136/bmj.d5928

Hosomi, Y., Morita, S., Sugawara, S., Kato, T., Fukuhara, T., Gemma, A., et al. (2020). Gefitinib Alone versus Gefitinib Plus Chemotherapy for Non-small-cell Lung Cancer with Mutated Epidermal Growth Factor Receptor: NEJ009 Study. *J. Clin. Oncol.* 38(2), 115–123. doi:10.1200/JCO.19.01488

Huang, X., Wang, J., Lin, W., Zhang, N., Du, J., Long, Z., et al. (2020a). Kanglaite Injection Plus Platinum-Based Chemotherapy for Stage III/IV Non-small Cell

Lung Cancer: A Meta-Analysis of 27 RCTs. *Phytomedicine.* 67, 153154. doi:10.1016/j.phymed.2019.153154

Jiao, L., Xu, J., Sun, J., Chen, Z., Gong, Y., Bi, L., et al. (2019). Chinese Herbal Medicine Combined with EGFR-TKI in EGFR Mutation-Positive Advanced Pulmonary Adenocarcinoma (CATLA): A Multicenter, Randomized, Double-Blind, Placebo-Controlled Trial. *Front. Pharmacol.* 10, 732. doi:10.3389/fphar.2019.00732

Jin, J. J., Hu, Q. L., and Tao, Q (2016). Effects of Kanglaite Injection Combined with Gefitinib on Inflammatory Factors and Immune Function with Advanced Lung Cancer. *Chin. J. Biochem. Pharmaceuticals.* 36(12), 147–150.

Lee, H. Y. J., Meng, M., Liu, Y., Su, T., and Kwan, H. Y. (2021). Medicinal Herbs and Bioactive Compounds Overcome the Drug Resistance to Epidermal Growth Factor Receptor Inhibitors in Non-small Cell Lung Cancer. *Oncol. Lett.* 22(3), 646. doi: doi:10.3892/ol.2021.12907

Li, D. M. (2020). Evaluation of the Clinical Effect of Gefitinib Tablets Combined with Kanglaite Capsules in the Treatment of Stage IIIB/IV Non-small Cell Lung Cancer. *Chin. J. Mod. Drug Appl.* 14(05), 132–134. doi:10.14164/j.cnki.cn11-5581/r.2020.05.060

Li, J., Li, H. Z., Zhu, G. H., Gao, R. K., Zhang, Y., Hou, W., et al. (2020). Efficacy and Safety of Kanglaite Injection Combined with First-Line Platinum-Based Chemotherapy in Patients with Advanced NSCLC: a Systematic Review and Meta-Analysis of 32 RCTs. *Ann. Palliat. Med.* 9(4), 1518–1535. doi:10.21037/apm-20-616

Liu, J., Liu, X., Ma, J., Li, K., and Xu, C. (2019). The Clinical Efficacy and Safety of Kanglaite Adjuvant Therapy in the Treatment of Advanced Hepatocellular Carcinoma: A PRISMA-Compliant Meta-Analysis. *Biosci. Rep.* 39(11). doi:10.1042/BSR20193319

Liu, S.-H., Chen, P.-S., Huang, C.-C., Hung, Y.-T., Lee, M.-Y., Lin, W.-H., Lin, Y.-C., and Lee, A. Y.-L. (2021a). Unlocking the Mystery of the Therapeutic Effects of Chinese Medicine on Cancer. *Front. Pharmacol.* 11. doi:10.3389/fphar.2020.601785

Liu, S., Wang, H., Wang, M., Hu, X., Yang, W., Jin, R., et al. (2021b). Comparative Efficacy and Safety of Chinese Herbal Injections Combined with Cyclophosphamide and 5-Fluorouracil Chemotherapies in Treatment of Breast Cancer: A Bayesian Network Meta-Analysis. *Front. Pharmacol.* 11. doi:10.3389/fphar.2020.572396

Lu, X., Liu, W., Wu, J., Li, M., Wang, J., Wu, J., et al. (2013). A Polysaccharide Fraction of Adlay Seed (Coixlachryma-Jobi L.) Induces Apoptosis in Human Non-small Cell Lung Cancer A549 Cells. *Biochem. Biophys. Res. Commun.* 430(2), 846–851. doi:10.1016/j.bbrc.2012.11.058

Luo, C., Wang, X., An, C., Hwang, C. F., Miao, W., Yang, L., et al. (2017). Molecular Inhibition Mechanisms of Cell Migration and Invasion by Coix Polysaccharides in A549 NSCLC Cells via Targeting S100A4. *Mol. Med. Rep.* 15(1), 309–316. doi: doi:10.3892/mmr.2016.5985

Mao, W., Fan, Y., Cheng, C., Yuan, X., Lan, T., Mao, K., et al. (2020). Efficacy and Safety of Kanglaite Injection Combined with Chemotherapy for Colorectal Cancer: A Protocol for Systematic Review and Meta-Analysis. *Medicine (Baltimore).* 99(39), e22357. doi:10.1097/MD.0000000000022357

Ni, M., Wang, H., Wang, M., Zhou, W., Zhang, J., Wu, J., et al. (2020). Investigation on the Efficiency of Chinese Herbal Injections for Treating Non-small Cell Lung Cancer with Vinorelbine and Cisplatin Based on Multidimensional Bayesian Network Meta-Analysis. *Front. Pharmacol.* 11, 631170. doi: doi:10.3389/fphar.2020.631170

Ning, J. L., Zhu, F. Q., and Gao, Y. C. (2015). Effect of Gefitinib Combined with KLT Nepalese on the Function and Quality of Life of Non-small Cell Lung Cancer Patients. *MODERN ONCOLOGY.* 23(14), 1976–1979. doi:10.3969/j.issn.1672-4992.2015.14.11

Pan, P., Wu, Y., Guo, Z. Y., Wang, R., Wang, Y. J., and Yuan, Y. F. (2012). Antitumor Activity and Immunomodulatory Effects of the Intraperitoneal Administration of Kanglaite *In Vivo* in Lewis Lung Carcinoma. *J. Ethnopharmacol.* 143(2), 680–685. doi: doi:10.1016/j.jep.2012.07.025

Richards, T. B., Henley, S. J., Puckett, M. C., Weir, H. K., Huang, B., Tucker, T. C., et al. (2017). Lung Cancer Survival in the United States by Race and Stage (2001-2009): Findings from the CONCORD-2 Study. *Cancer* 123, 5079–5099. doi: doi:10.1002/cncr.31029

Rosell, R., Carcereny, E., Gervais, R., Vergnenegre, A., Massuti, B., Felip, E., et al. (2012). Erlotinib versus Standard Chemotherapy as First-Line Treatment for European Patients with Advanced EGFR Mutation-Positive Non-small-cell Lung Cancer (EURTAC): a Multicentre, Open-Label, Randomised Phase 3 Trial. *Lancet Oncol.* 13(3), 239–246. doi:10.1016/S1470-2045(11)70393-X

Shah, R. R., and Shah, D. R. (2019). Safety and Tolerability of Epidermal Growth Factor Receptor (EGFR) Tyrosine Kinase Inhibitors in Oncology. *Drug Saf.* 42(2), 181–198. doi:10.1007/s40264-018-0772-x

Shen, F. Q., Wei, S. J., Hong, L., Wang, J. Y., Zhao, N., and Zhang, F. (2013). The Effect of Kanglaite Injection in Combination with Gefitinib on Angiogenesis in Mice with Lewis Lung Cancer. *TUMOR.* 33(12), 1047–1053. doi:10.3781/j.issn.1000-7431.2013.12.003

Shi, Q. H., and Chen, G. F. (2013). Clinical Observation of Kanglaite InJection Combined with Gefitinib in the Treatment of Non-small Cell Lung Cancer with EGFR Positive in Medium or Late Stage. *Chin. Manipulation Rehabil. Med.* 4(4), 76–78.

Sui, X., Zhang, M., Han, X., Zhang, R., Chen, L., Liu, Y., et al. (2020). Combination of Traditional Chinese Medicine and Epidermal Growth Factor Receptor Tyrosine Kinase Inhibitors in the Treatment of Non-small Cell Lung Cancer: A Systematic Review and Meta-Analysis. *Medicine (Baltimore).* 99(32), e20683. doi:10.1097/MD.0000000000020683

Sung, H., Ferlay, J., Siegel, R. L., Laversanne, M., Soerjomataram, I., Jemal, A., et al. (2021). Global Cancer Statistics 2020: GLOBOCAN Estimates of Incidence and Mortality Worldwide for 36 Cancers in 185 Countries. *CA CANCER J. CLIN.* 71(3), 209–249. doi:10.3322/caac.21660

Tang, M., Wang, S., Zhao, B., Wang, W., Zhu, Y., Hu, L., et al. (2019). Traditional Chinese Medicine Prolongs Progression-free Survival and Enhances Therapeutic Effects in Epidermal Growth Factor Receptor Tyrosine Kinase Inhibitor (EGFR-TKI)Treated Non-small-cell Lung Cancer (NSCLC) Patients Harboring EGFR Mutations. *Med. Sci. Monit.* 25, 8430–8437. doi:10.12659/MSM.917251

Wang, G., and Wang, F. (2019). Effects of Kanglaite and Erlotinib Combination on Proliferation and Invasion and JAK2/STAT3 Signaling Pathway of Lung Cancer A549 Cells. *J. Zhengzhou Univ.* 54(03), 418–422. doi:10.13705/j.issn.1671-6825.2018.05.042

Wang, J., Wang, B., Chu, H., and Yao, Y. (2016). Intrinsic Resistance to EGFR Tyrosine Kinase Inhibitors in Advanced Non-small-cell Lung Cancer with Activating EGFR Mutations. *Onco Targets Ther.*, 9., 3711, 26. doi:10.2147/OTT.S106399

Wang, J. Y., Wei, S. J., Hong, L., Zhang, F., Liu, C. Y., and Kong, Y. (2017). Clinical Trial of Gefitinib Tablets Combined with Kanglaite Capsules in the Treatmentof Stage IIIB/IV Non-small Cell Lung Cancer. *Chin. J. Clin. Pharmaco* 33(17), 1631–1633.

Wen, J., Yang, T., Wang, J., Ma, X., Tong, Y., and Zhao, Y. (2020). Kanglaite Injection Combined with Chemotherapy versus Chemotherapy Alone for the Improvement of Clinical Efficacy and Immune Function in Patients with Advanced Non-small-cell Lung Cancer: A Systematic Review and Meta-Analysis. *Evid. Based Complement. Alternat Med.* 2020, 8586596. doi:10.1155/2020/8586596

Wu, Y., Zhang, J., Hong, Y., and Wang, X. (2018). Effects of Kanglaite Injection on Serum miRNA-21 in Patients with Advanced Lung Cancer. *Med. Sci. Monit.* 24, 2901–2906. doi: doi:10.12659/MSM.909719

Xiang, Y., Guo, Z., Zhu, P., Chen, J., and Huang, Y. (2019). Traditional Chinese Medicine as a Cancer Treatment: Modern Perspectives of Ancient but Advanced Science. *Cancer Med.* 8(5), 1958–1975. doi: doi:10.1002/cam4.2108

Yang, L., Tian, Y., Yang, H., Zhang, L., and Jin, R. (2016). Influence of Kanglaite Combined with Gefitinib on Immune Function and Quality of Life of Patients with Advanced Non-small Cell Lung Cancer. *Prog. Mod. Biomed.* 16(19), 3728–3730+3775. doi:10.13241/j.cnki.pmb.2016.19.033

Yang, M., Zhu, S.-j., Shen, C., Zhai, R., Li, D.-d., and Fang, M. (2021). Clinical Application of Chinese Herbal Injection for Cancer Care: Evidence-Mapping of the Systematic Reviews, Meta-Analyses, and Randomized Controlled Trials. *Front. Pharmacol.* 12. doi:10.3389/fphar.2021.666368

Yang, W. J. (2016). Clinical Study on Kanglaite Injection Combined with Icotinib in Treatment of Non-small Cell Lung Cancer. *Drugs & Clinic.* 31(12), 1984–1987. doi: doi:10.7501/j.issn.1674-5515.2016.12.027

Zeng, X. H., Zeng, C. S., Liu, L. B., Huang, Z. C., Guo, S. J., and Xu, Q. Y. (2014). Influence of Kanglaite Plus Gefitinib on Immune Function and Quality of Life in Patients with Advanced Non-small-cell Lung Cancer. *J. Chin. Pract. Diagn. Ther.* 28(09), 930–931.

Zhang, Q., and Yuan, H. (2011). Clinical Observation on 78 Cases of Kanglaite Injection Combined with Gefitinib in the Treatment of Advanced Non-small Cell Lung Cancer. *Tumor.* 31(01), 89–90. doi:10.3781/j.issn.1000-7431.2011.01.019

Zhang, S. H., and Zhou, L. X. (2014). Clinical Efficacy of Gefitinib Combined with LT in Treatment of Advanced Non-small Cell Lung Cancer. *MODERN ONCOLOGY*. 22(12), 2857–2859. doi:10.3969/j.issn.1672-4992.2014.12.26

Zhao, N., Wei, S. J., Hong, L., Wang, J. Y., Shen, F. Q., and Zhang, F. (2015). Effects of Kanglaite Injection on the Apoptosis Induced by Gefitinib in Lung Adenocarcinoma A549 Cell Line. *Chin. Clin. Oncol.* 20(01), 1–7.

Zhao, Q. F., Shen, H. R., and Zhang, Y. W. (2019). Effects of Gefitinib Combined with Kanglaite Injection on Advanced Lung Cancer in Older Patients. *Int. J. Geriatr.* 40(5), 257–260. doi:10.3969/j.issn.1674-7593.2019.05.001

Conflict of Interest: The authors declare that the research was conducted in the absence of any commercial or financial relationships that could be construed as a potential conflict of interest.

Publisher's Note: All claims expressed in this article are solely those of the authors and do not necessarily represent those of their affiliated organizations, or those of the publisher, the editors and the reviewers. Any product that may be evaluated in this article, or claim that may be made by its manufacturer, is not guaranteed or endorsed by the publisher.

frontiers in Oncology

REVIEW
published: 20 September 2021
doi: 10.3389/fonc.2021.733369

Potential of Steroidal Alkaloids in Cancer: Perspective Insight Into Structure–Activity Relationships

Ying Huang[1†], Gen Li[2†], Chong Hong[1], Xia Zheng[3], Haiyang Yu[4] and Yan Zhang[1*]*

[1] Key Laboratory of Computational Chemistry-Based Natural Antitumor Drug Research & Development, Liaoning Province, School of Traditional Chinese Materia Medica, Shenyang Pharmaceutical University, Shenyang, China, [2] School of Chinese Materia Medica, Tianjin University of Traditional Chinese Medicine, Tianjin, China, [3] The Second Affiliated Hospital of Liaoning University of Traditional Chinese Medicine, Shenyang, China, [4] State Key Laboratory of Component-Based Chinese Medicine, Tianjin University of Traditional Chinese Medicine, Tianjin, China

OPEN ACCESS

Edited by:
Simona Rapposelli, University of Pisa, Italy

Reviewed by:
Iti Gupta, Indian Institute of Technology Gandhinagar, India
Ahm Khurshid Alam, University of Rajshahi, Bangladesh

***Correspondence:**
Yan Zhang
zhangyan_929@yeah.net
Haiyang Yu
hyyu@tjutcm.edu.cn

[†]These authors have contributed equally to this work and share first authorship

Specialty section:
This article was submitted to Pharmacology of Anti-Cancer Drugs, a section of the journal Frontiers in Oncology

Received: *30 June 2021*
Accepted: *12 August 2021*
Published: *20 September 2021*

Citation:
Huang Y, Li G, Hong C, Zheng X, Yu H and Zhang Y (2021) Potential of Steroidal Alkaloids in Cancer: Perspective Insight Into Structure–Activity Relationships. Front. Oncol. 11:733369. doi: 10.3389/fonc.2021.733369

Steroidal alkaloids contain both steroidal and alkaloid properties in terms of chemical properties and pharmacological activities. Due to outstanding biological activities such as alkaloids and similar pharmacological effects to other steroids, steroidal alkaloids have received special attention in anticancer activity recently. Substituted groups in chemical structure play markedly important roles in biological activities. Therefore, the effective way to obtain lead compounds quickly is structural modification, which is guided by structure–activity relationships (SARs). This review presents the SAR of steroidal alkaloids and anticancer, including pregnane alkaloids, cyclopregnane alkaloids, cholestane alkaloids, C-nor-D-homosteroidal alkaloids, and bis-steroidal pyrazine. A summary of SAR can powerfully help to design and synthesize more lead compounds.

Keywords: steroidal alkaloids, structure–activity relationships, anticancer, drug design, medicinal potential

INTRODUCTION

Steroidal alkaloids as one large and important class of alkaloids are mainly found in various plants from Solanaceae, Buxaceae, Apocynaceae, and Liliaceae, marine invertebrates, and amphibians (**Figure 1**) (1–3). According to the carbon skeleton, they can be divided into five types: pregnane alkaloids, cyclopregnane alkaloids, cholestane alkaloids, C-nor-D-homosteroidal alkaloids, and bis-steroidal pyrazine (2).

Steroidal alkaloids are nitrogen-containing derivatives of natural steroids, having the basic steroidal skeleton and a nitrogen atom, which contain both steroidal and alkaloid properties in terms of chemical properties and pharmacological activities (4). Therefore, they have significantly outstanding biological activities as alkaloids and similar pharmacological effects to other steroids (4). Previous pharmacological studies have shown that steroidal alkaloids own a variety of pharmacological activities, such as anticancer, anti-inflammatory, antimicrobial, and analgesic (1, 5).

Cancer is considered as one of the most threatening diseases worldwide (6). Currently, the treatments used to treat cancer include four main strategies: chemotherapy, radiotherapy, surgery, and immunotherapy (7, 8). The anticancer natural products include alkaloids (vinblastine, camptothecin), terpenoids (farnesol, geraniol, paclitaxel), anthranilic acid derivatives (tranilast),

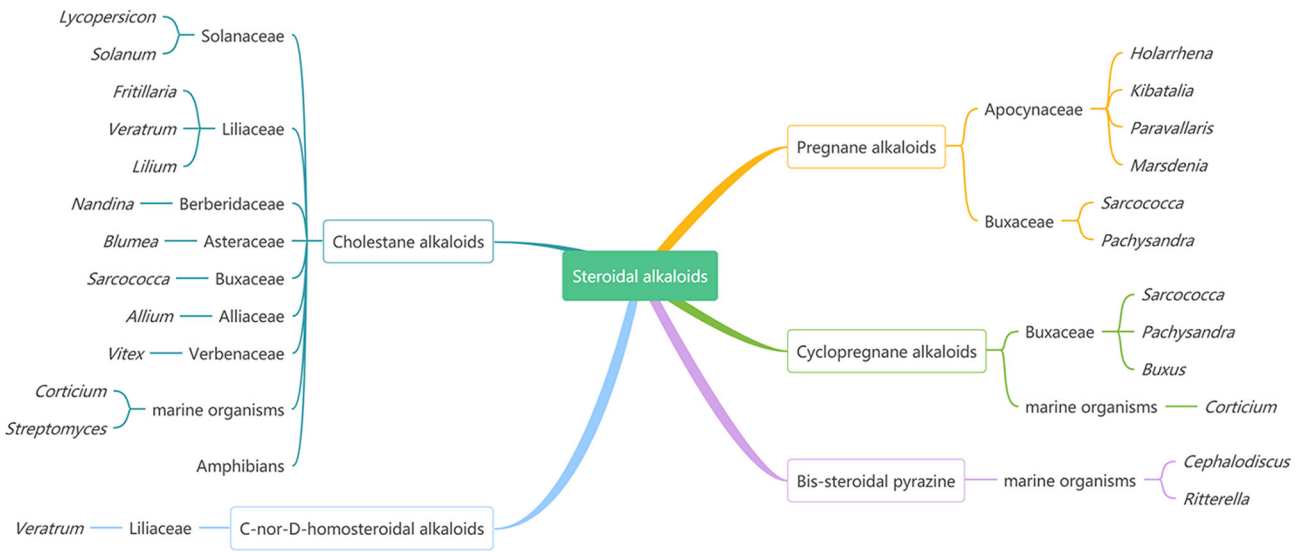

FIGURE 1 | The Main Sources of Steroidal Alkaloids.

polyphenolic compounds (gossypol), lignans (podophyllotoxin), and so on (9). Among these, alkaloids and their analogues account for almost the majority of clinical anticancer drugs (10).

Due to the particularity of the structure and potent activities, steroidal alkaloids have received more and more attention for the treatment of cancer in recent years. There are many drugs developed into clinical treatment drugs. At present, most discoveries of new drugs are based on structural modifications through structure–activity relationships. For instance, the hydrochloride of solanamine is used as an antineoplastic drug for preclinical study. Cyclopamine has completed phase I clinical trial as a potential antitumor drug by companies Curis and Genentech (11).

Steroidal alkaloids are important and potential bioactive agents, having a promising feature in the treatment of cancer. More exploitation of new drugs is based on structural modification referring to SAR. Therefore, it is necessary to systematically summarize the structure–activity relationships of steroid alkaloids to design and synthesize potent anticancer drugs.

In this review, any search (including literature and PhD and MSc dissertations) published before 1950 and up to 2020 was performed in the following databases: Web of Science, Science Direct, Scifinder, and the China National Knowledge Infrastructure (CNKI). "Steroidal alkaloids" and "anticancer" were used as keywords in literature searches, and 881 references were obtained in total, of which 189 references meet the requirements. Through these literatures, we summarized the structure–activity relationships of steroid alkaloids in anticancer.

This review focuses on the extensive structure–activity relationships of steroidal alkaloids in the area of anticancer activity. From different carbon skeleton points of view, the differences of activity caused by structural changes were discussed. This review will provide a reference for the discovery of steroidal alkaloid as anticancer drugs.

PREGNANE ALKALOIDS

Pregnane alkaloids are also called C-21 steroidal alkaloids, which are mainly found in the *Holarrhena, Kibatalia, Paravallaris*, and *Marsdenia* genera of Apocynaceae as well as the *Sarcococca* and *Pachysandra* genera of the Buxaceae. Due to their good anticancer activity, pregnane alkaloids have been reported in many literatures, patents, and graduation papers. Based on previous studies, preliminary SAR about the cytotoxic activity of pregnane alkaloids was affected by substituents at C-3, 5, 6, 7, 15, 16, 17, and 21. The schematic diagram of structure–activity relationships of pregnane alkaloids is shown in **Figure 2**.

The substituted forms of C-16 and 17 in pregnane alkaloids are of great importance for the anticancer activity. Huo et al. isolated hookerianine A (1), hookerianine B (2), sarcorucinine G (3), and epipachysamine D (4) from *Sarcococca hookeriana* Baill and evaluated the above three compounds in SW480, SMMC-7721, PC3, MCF-7, and K562 cell lines. Compared to epipachysamine D (4), sarcorucinine G (3) with C-16, C-17 double bond presented better cytotoxicity (**Figure S1**). And hookerianine B (2) with the epoxy group at C-16 and C-17 was stronger than epipachysamine D (4) on cytotoxicity (12). Qin et al. synthesized novel pregn-17(20)-en-3-amine derivatives and performed derivatives of chemotaxis assay against human breast cancer cells (**Table S1**). Although the results demonstrated that the derivatives had no cytotoxicity on MDA-MB-231 cells, some of them displayed strong inhibitory effects against migration such as 5a, 5c, 8e, 8f, 9a, 9g, 10a, and 10f (**Figure S1**). Among these, 10f (IC_{50} value = 0.03 μM) showed the best potency. A majority of C-16 hydroxyl derivatives (7a, 7c-e, 8b, and 8g) presented strong toxicity. A minority of C-16 carbonyl derivatives (10b-c and 9e) presented the toxicity. The derivatives without the substituted group at the C-16 position showed no

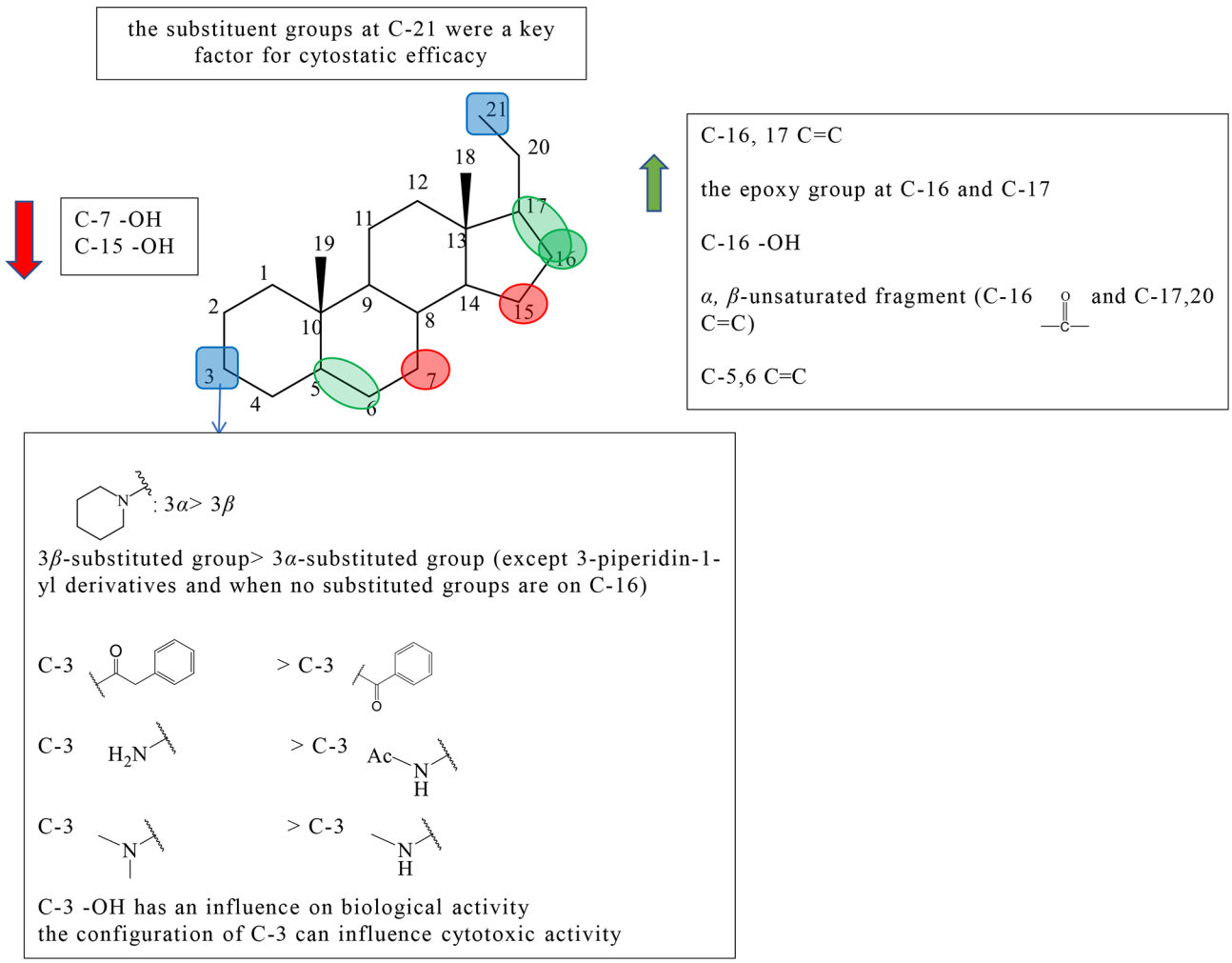

FIGURE 2 | Summary of Structure-activity Relationship of Pregnane Alkaloids.

toxicity, except 5a and 5c (IC_{50} value < 1 μM). The activities of these C-16 carbonyl derivatives including 9a, 9g, 10a, and 10f were better than other two kinds of derivatives, which indicated that α, β-unsaturated fragment in ring D might be key for activities. It was worth noting that, except for 3-piperidin-1-yl derivatives, the activities of 3β-substituted derivatives were better than 3α-substituted derivatives among the derivatives without the substituted group on C-16 (5a-e, 5g *vs* 6a-e, 6g), but it did not appear the same phenomenon among C-16 carbonyl derivatives (13).

The earlier conclusion has been proved that the presence of a 5,6-double bond played an important role in an antiproliferative effect. Compounds 11–13 (the synthetic analogs of solanidine) researched by Minorics et al. showed the effective inhibitory effects against HL-60 cell lines, which verified the earlier conclusion (14). Badmus et al. isolated holamine (14) and funtumine (15) from *Holarrhena floribunda* and tested for their inhibited proliferation against MCF-7, HeLa, HT-29, and KMST-6 (**Figure S1**). Holamine (14) displayed cytotoxic effects on HL-60 and P-388, while funtumine (15) exhibited no cytotoxicity. Therefore, it was speculated that the presence of 5,6-double bond can strengthen cytotoxicity. However, this SAR showed a little effect on the cytotoxic activity against HT-29, HeLa, MCF-7, and KMST-6 cell lines (15).

C-3 is one of the most important positions of the substituent group to affect the activity; the relative configuration of C-3 is also the influential factor. Pregn-17(20)-en-3-amine derivatives by Qin et al. showed results that for compounds with no substituent at C-16, except for 3-piperidine-1-yl derivatives, the activity of 3β-substituted derivatives was better than that of 3α-substituted derivatives (5a *vs* 6a, 5b *vs* 6b, 5c *vs* 6c, 5d *vs* 6d, 5e *vs* 6e,and 5g *vs* 6g). Among pregn-17(20)-en-3-amine derivatives, the activities of 3α-piperidin-1-yl derivatives were better than those of 3β-piperidin1-yl derivatives (5f *vs* 6f, 7f *vs* 8f, and 9f *vs* 10f) (**Figure S1**). According to the results, Qin et al. speculated that the relative configuration of the 3α-piperidine-1-group might be beneficial for some tumor migration targets, and the 3α-piperidin-1-yl group was an effective functional group for the

antimigration activity (13). Shaojie Huo et al. concluded structure–activity relationships by comparing hookerianine A (1) and epipachysamine D (4) that steroidal alkaloids with the phenylacetyl group instead of the benzoyl group at C-3 can enhance the cytotoxicity against SW480, SMMC-7721, PC3, and K562 human cells (**Figure S1**) (12). Paravallarine (16), 7*R*-hydroxyparavallarine (17), gitingensine (18), methylgitingensine (19), and *N*-acetylgitingensine (20) were isolated from *Kibatalia laurifolia* and tested for cytotoxic activity against KB cell lines by Phi et al. The results showed that paravallarine (16) presented cytotoxicity with IC_{50} of 12.8 μM, gitingensine (18) and methylgitingensine (19) displayed weak cytotoxicity with IC_{50} ranged from 21 to 42 μM, and *N*-acetylgitingensine (20) showed no cytotoxicity (IC_{50} > 50 μM) (**Figure S1**). It was observed that the acetylation of C-3 amino reduced the cytotoxic activity against KB cells (16). Since paravallarine (16) was more active than methylgitingensine (19), allowing a conclusion that the configuration of C-3 can influence cytotoxic activity (16). Minorics et al. compared the inhibitory effects of compound 12 having the 3-hydroxy group with compounds 11 and 13 containing the 3-acetate group in HL-60 cells. Compound 12 exhibited more effective inhibition activity than compounds 11 and 13 (**Figure S1**). The results indicated that there was an influence on the biological activity when the C-3 hydroxyl group of ring A is present or absent (14). The cytotoxicity of compounds 21 and 22 were evaluated using the NCI-H187 cell line by Cheenpracha et al. (**Figure S1**). Compound 21 displayed weak cytotoxicity against the NCI-H187 cell line with IC_{50} values of 18.2 μM, whereas compound 22 had no cytotoxicity. Based on the results, the methylamino group at C-3 may be better than the *N, N*-dimethylamino group on cytotoxic activity (17).

There are relatively a few studies on C-7, C-15, and C-21. Through previous studies, the following conclusions can be drawn. Kam et al. investigated the cytotoxicity of holamine (23) and 15*R*-hydroxyholamine (24) in HL-60 cells and P-388 cells. Compound 23 exhibited higher cytotoxicity than compound 24, which showed that the C-15 hydroxyl might slightly reduce the cytotoxic activity (**Figure S1**) (18). In the experiment of Phi et al., paravallarine (16) exhibited cytotoxicity against KB cells exhibiting IC_{50} values of 12.8 μM, whereas, 7*R*-hydroxyparavallarine (17) was not cytotoxic (IC_{50} above 50 μM) (**Figure S1**). It can be inspected that the C-7 hydroxyl group leads to the decrease in cytotoxic activity (16). Minorics et al. concluded that the substituent groups at C-21 were a key factor for cytostatic efficacy when compared with 11, 12, and 13 (14).

CYCLOPREGNANE ALKALOIDS

Cyclopregnane alkaloids are also called C-24 steroidal alkaloids, which contain a characteristic seven-membered system in ring B (1). Among them, cortistatin from marine sponge *Corticium simplex* and cyclopregnane alkaloids from the family Buxus had been widely studied. The schematic diagram of SAR is shown in **Figure 3**.

Cortistatins were first found by Aoki et al., which are compounds with unique structure and potent biological activities, and were isolated from the marine sponge *Corticium simplex* (19). In the reports, Aoki et al. summarized the structure–activity relationships of cortistatin (25-35) (**Figure S2**). Cortistatin E–H (29-32) exhibited weak growth inhibitory activity and poor selective indices against HUVECs, which showed that isoquinoline moiety was essential for potency and selectivity (19). Cortistatin J (33) had more potential with high selectivity than cortistatin K (34) and cortistatin L (35), which suggested that the position of the diene system was of more importance for the activities against HUVECs than the role of the hydroxyl group at the A-ring (**Figure S2**). And it was speculated that the functional group in ring-A and ring-B might play an important role in selective and antiproliferative activity against HUVECs (19). However, cortistatins J (33), K (34), and L (35) showed comparable antiproliferative and selective activities against KB3-1, Neuro2A, K562, and NHDF compared with 25, which indicated that structural modifications of ring-A or ring-B played a role but not a key one (19). Therefore, it is necessary to prove the role of functional groups on ring A in antiproliferative activity through further studies (19).

In 2013, Kotoku et al. converted ring-CD of vitamin D_2 to analogue 36 of cortistatin A (25), obtained analogue **37** (composition of 37a (8,14-cis) and 37b (8,14-trans)) with a CD-cis-fused skeleton accidentally, and evaluated for cortistatin A (25) and their analogues (**Figure S3**). Cortistatin A (25) and analogue 36 with the CD-trans-fused skeleton exerted antiproliferative potency against HUVEC with IC_{50} at 0.0018 and 0.035 μM, respectively. On the other hand, analogue **37** with the CD-cis-fused skeleton only exhibited weak antiproliferative effect (IC_{50}: 1.5 μM) with weak selectivity (ninefold). Furthermore, structures at the CD-ring part of 37a and 37bwere bent, which did not resemble with compound 25 and compound 36 according to molecular mechanics (MM). The results indicated that the stereoscopic structure of the CD-ring of cortistatin A (25) played an essential role in the HUVEC-selective antiproliferative activity (20). Kotoku et al., Aoki et al., and Kobayashi et al. concluded structure–activity relationships through the structure and inhibitory activity of cortistatins B (26) and D (28): the hydroxyl group in ring D led to the decrease in inhibitory activity against HUVECs (**Figure S3**) (19, 21, 22).

The design and synthesis of analogues 38, 39, 40, and 36 of cortistatin A (25) were carried out by Kotoku et al. to improve potent inhibiting activities and antitumor activities (**Figure S3**). Analogues 38 and 40 exhibited moderate growth inhibitory activity against HUVECs (IC_{50}: 2.0 and 15 μM) over KB3-1 cells (IC_{50}: 18 and 20 μM), whereas analogues 39 and 36 exhibited potential growth inhibitory activity against HUVEC (IC_{50}: 0.1 and 0.035 μM) over KB3-1 cells (IC_{50}: 10.5 μM each) (21). Moreover, analogues 39 and 36 (>100-fold) showed more selectivity than analogues 38 (9-fold) and 40 (1.5-fold). Besides, the geometrical isomers of 38 and 40 exhibited weaker antiproliferative and selective activity. The results revealed that

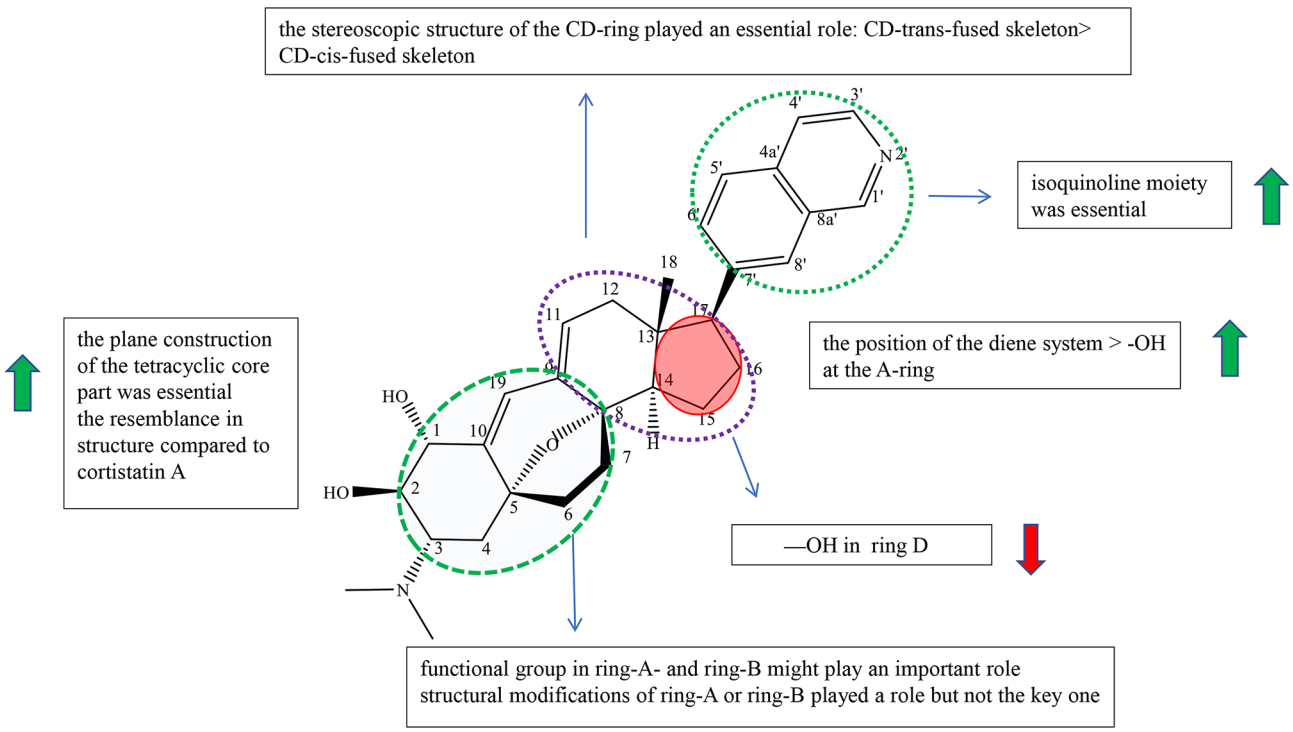

FIGURE 3 | Summary of Structure-activity Relationship of Cyclopregnane Alkaloids.

the plane construction of the tetracyclic core part was essential for selective and antiproliferative activity against HUVECs. The activity of compound 39 was more potential than that of byproduct 41, showing that the resemblance in structure compared to cortistatin A (25) is also an important element (**Figure S3**) (21).

Cyclopregnane alkaloids were mainly found in the genus *Buxus*, containing the basic steroidal skeleton with a cyclopropyl ring at C-9 and C-10. For this kind of compounds, there were a few reports on pharmacological activities, and there are no clear structure–activity relationships for the time being. But according to Qiu's experiment, we can observe that cyclopregnane alkaloids display strong cytotoxic activity against HeG2 and K562 cell lines through compounds 42, 43, 44, 45, and 46 (IC_{50}<6 μM) and showed no cytotoxicity against A549, SW480, SMMC-7721, HL-60, and MCF-7 cell lines through compounds 47, 48, 49, and 50 (IC_{50}>40 μM) (**Figure S4**) (23).

On the other hand, compounds 51 and 52 isolated from the genus *Buxus* having a similar structure of cyclopregnane alkaloids showed relatively good cytotoxicity against A-549 and SW480 cell lines.

CHOLESTANE ALKALOID

Cholestane alkaloid is one type of C-27 steroidal alkaloid found in many plants in families Solanaceae and Liliaceae. According to current studies, we divided cholestane alkaloids into solasodine (including glycoalkaloid and not glycoalkaloid) and others to summarize the SAR. The schematic diagram of SAR of solasodine is shown in **Figure 4** and others are shown in **Figure 5**.

Solasodine (Glycoalkaloid)

Previous studies have indicated that both the aglycone and sugar residues were critical for cytotoxic activity (24, 25). Aglycone was far less inactive than its glycoalkaloid, which showed the essence of sugar moieties (26–28). Some studies also showed that the variation of aglycone did not significantly influence the cytotoxic activity when sugar moieties were kept identical (24, 26, 27). But further study indicated that the activities of some steroidal glycoalkaloid were changed due to the variation of the aglycone. Therefore, it was concluded that the key factors in the activity of solasodine were comprised of two main units, sugar moieties and the substitution of aglycone. The glycosidic moieties included the quantity and the position of α-L-rhamnose, and the type and order of sugar (24, 27, 29).

Ding et al. isolated, purified, and identified SS (compound 53), β_1-solasonine (compound 54), SM (compound 55), β_2-solamargine (compound 56), γ-solamargine (compound 57), and solanigroside P (compound 58) from *Solanum nigrum* L and investigated their anticancer activity against MGC-803 cells by MTT (**Figure S5**). They noted that steroidal alkaloids containing trisaccharides (compounds 53 and 55) showed better results on activity than those containing disaccharides

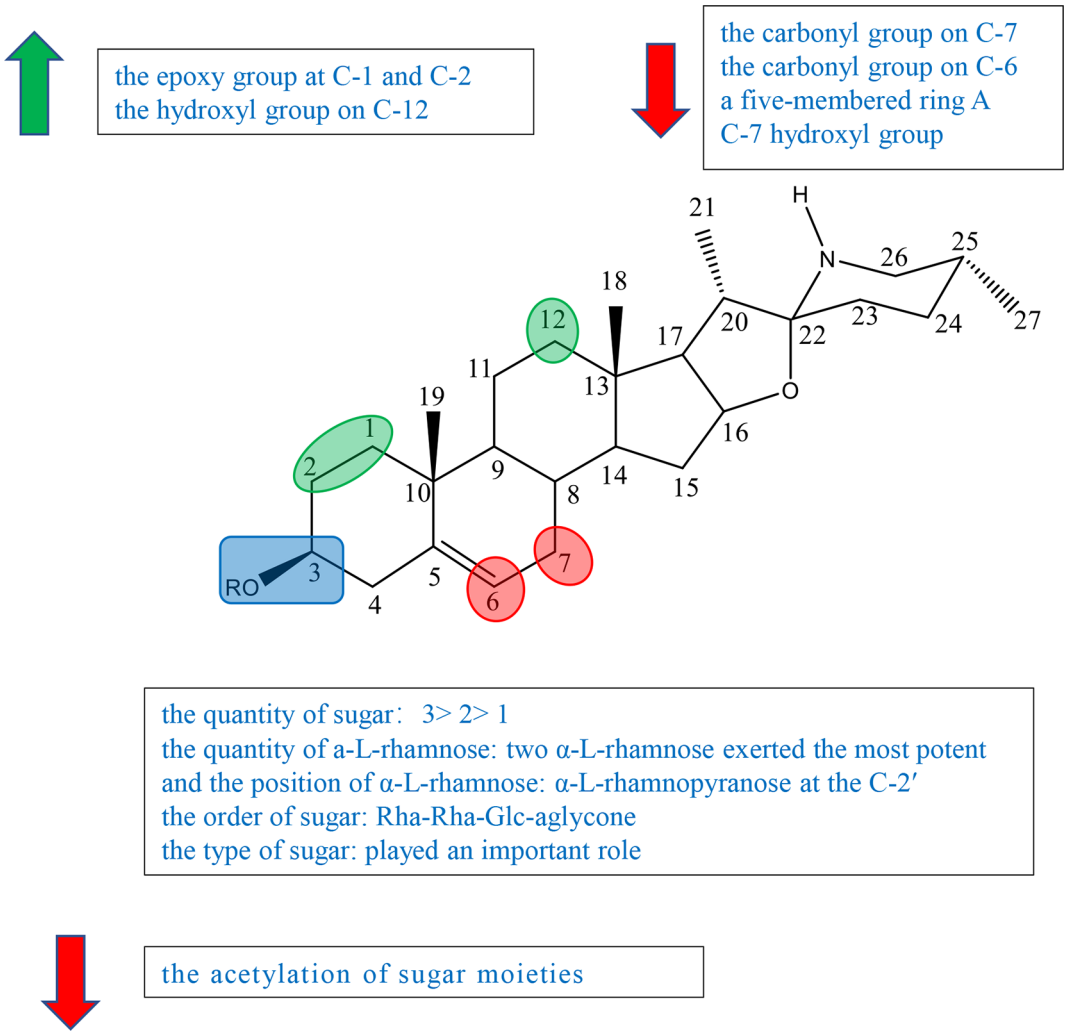

FIGURE 4 | Summary of Structure-activity Relationship of Cholestane Alkaloid—Solasodine (glycoalkaloid).

(compounds 54 and 56) or monosaccharides (compound **57**). Compound 54 containing three sugar units with two α-L-rhamnose had the highest antiproliferative activity among compounds 51–56, which suggested that the quantity of *a*-L-rhamnose was critical for the activity (**Figure S5**) (29). In 2015, Akter et al. isolated SGA 1 (compound 59) from the leaves of *Blumea lacera* and tested the cytotoxicity of SGA 1 and SGA analogues including β-solamargine (compound 60), α-solamargine (compound 61), and khasianine (compound 62) (**Figure S5**). Khasianine exhibited weak cytotoxic effect on MCF-7 cells. SGA 1 and β-solamargine displayed remarkable cytotoxicity against all tested cell lines. A comparison of khasianine, SGA, and β-solamargine was performed, in which aglycone of glycoalkaloids were the same, but the quantity and the position of α-L-rhamnose were varied. The results suggested that the second additional Rha (Rha-Rha-Glc-aglycone) led to the significant enhancement of the activity, and the third additional Rha (Rha-Rha-Glc(Rha)-aglycone) had little further effect on cytotoxicity. Furthermore, it is concluded that two terminal α-L-Rha have positive influence on cytotoxicity (24).

Chang's study indicated that α-solamargine (compound **61**) with (α-L-Rha-(1-2)-α-L-Rha-(1-4)-β-D-Glc-(1-aglycone) showed significant activity against human hepatoma cells, but khasianine (compound 62) with (α-L-Rha-(1-4)-β-D-Glc-(1-aglycone) exhibited weak activation effect. The comparison between α-solamargine and khasianine showed that the 2′-rhamnose moiety may impact significantly on triggering cell death. It was suggested that the enhancement of the biological activity was because the dihedral angle of the glycosidic bond is changed by 2′-rhamnose moiety (26). Among the six compounds isolated from *Blumea lacera* by Ding et al., compounds 53, 54, and 55 having α-L-rhamnopyranose attached to C-2 of β-D-glucose or galactose displayed significant cytotoxic effects against MGC-803 cells. Compound 56 with *a*-L-rhamnopyranose at the C-4 and compound **57** without *a*-L-rhamnopyranose showed little antiproliferative activities. The results inspected that *a*-L-

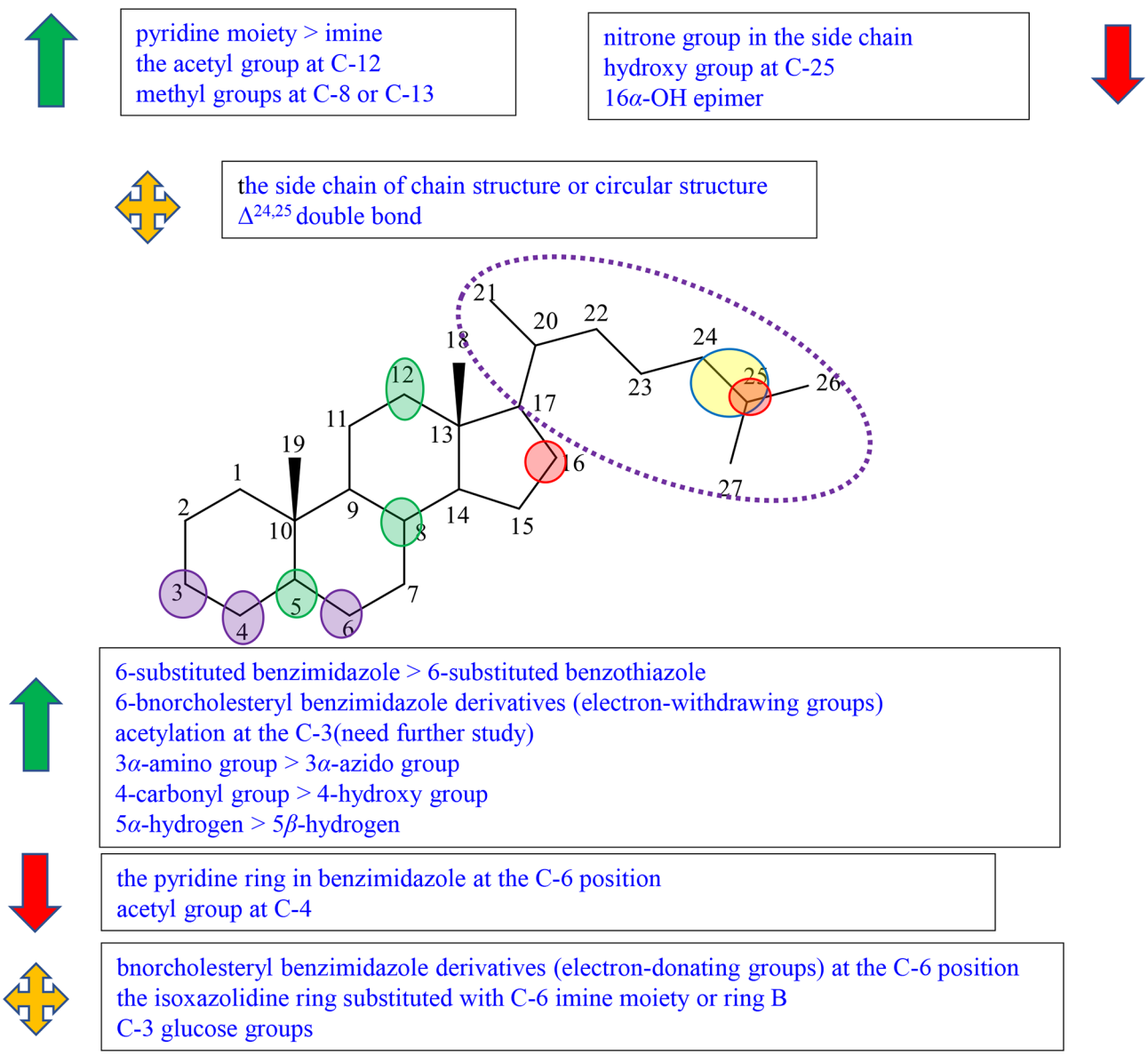

FIGURE 5 | Summary of Structure-activity Relationship of Cholestane Alkaloid (Others).

rhamnopyranose at C-2 was important for inhibition activities (29). Compound 54 had far higher activity than compound 56, suggesting that the type of sugar or the position of rhamnose had an effect on the activity (29). Xiang et al. investigated the cytotoxicity of five steroidal glycoalkaloids isolated from *Solanum nigrum* L. against five human cancer cell lines including HL-60, U-937, Jurkat, K562, and HepG2 cell lines. Compound 66 with the same aglycone as 67 had greatly higher activity than 67, showing that the type of sugar moiety played an important role in cytotoxic activity (**Figure S5**) (29).

Esteves-Souza et al. reported the inhibited cell proliferation evaluation of solasonine (compound 68) and its acetylation. Solasonine (compound 68) showed antiproliferative effect against Ehrlich carcinoma cells with IC_{50} at 74.20 ± 6.26 μM, but 68a furnished by the acetylation of 68 was inactive, suggesting that the acetylation of sugar moieties may reduce the antiproliferative activity (**Figure S5**) (27).

Liu et al. investigated the synthesis of 1-α-hydroxysolanine (compound 69), obtained a series of intermediate products and unexpected products from diosgenin, and tested their cytotoxicity (**Figure S5**). Among the compounds tested [compounds 70, 71–74, and solasodine (75)], only epoxide 75 had moderate inhibiting activities against PC3, Hela, and HepG2 cells lines at the concentration of 10 μM, suggesting that the epoxy group at C-1 and C-2 might impact the cytotoxic activity (**Figure S5**) (30).

In the experiment of Ding et al., compound 58 having the same sugar moieties as compound 56 was more active (IC_{50} = 20.10 μg/ml) than compound 56. The results suggested that the hydroxyl group on C-12 of steroidal alkaloid skeleton may be a factor on the activities (29).

Among steroidal glycoalkaloids tested by Xiang et al., compounds 63–66 contain identical sugars, but the aglycones are variable in rings A and B. Compound 66 showed the most powerful potency to all cell lines, but compounds 63–65 exhibited no cytotoxicity (**Figure S5**). Based on the result, it was speculated that the carbonyl group on C-6/7 (compounds 64 and 65) and the five-membered ring A (compound 63) led to the decrease in anticancer activity (25).

Gu et al. isolated 7α-OH solamargine (compound 76) and 7α-OH solasonine (compound 77) together with known compounds 78 and 79 from the fruits of *Solanum nigrum* (**Figure S5**). Compounds 78 and 79 displayed cytotoxic activities against MGC803, HepG2, and SW480 cell lines with the IC_{50} values ranging from 7.02 ± 0.60 to 23.79 ± 1.42μM. On the other hand, compounds 80 and 81 containing hydroxyl groups located at the C-7 showed no cytotoxicity, suggesting that the C-7 hydroxyl group of the aglycone decreased the cytotoxicity (**Figure S5**) (31).

Solasodine (Not Glycoalkaloid)

In 2012, Zha et al. synthesized novel solasodine derivatives and investigated their cell growth inhibitory effect against PC-3 cell lines. Analogue 91 displayed the highest antiproliferative activity against PC-3 cell line among solasodine derivatives (compounds 82–92), but analogue 90 (3β-hydroxyl) and analogue 92 (3β-*p*-tertbutylbenzoyl) with the similar structure as analogue 91 showed inferior activity (**Figure S6**). The results suggested that substituent groups at C-3 may play a role in inhibitory activities *in vitro*. Moreover, solasodine derivatives that performed etherization and esterization at C-3 (analogues 84–89), except analogue 89 (1-naphthoyl), did not show enhancement of the antiproliferative activity (32). In the same year, Zha et al. also reported a series of structural modification of soladulcidine and tested inhibitory effects of synthetic compounds against PC-3 cell lines *in vitro*. Among the C-3 hydroxyl group modified compounds, soladulcidine 93 showed inhibitory effects against prostate gland adenocarcinoma (PC-3) cell line, and its derivatives 94–100 were inactive, suggesting that hydroxyl groups at C-3 were better than other substituents tested (**Figure S6**) (33).

Others

Sunassee et al. reported the growth inhibition against National Cancer Institute (NCI) 60 cell lines of Plakinamines N (101), O (102) I (103), and J (104), which were isolated from *Corticium niger* by guided separation technology (**Figure S7**). Plakinamines N (101), O (102), and J (104) with a substituted pyrrolidine ring showed potent cytotoxicity against all 60 cell lines with IC_{50} of 11.5, 2.4, and 1.4 μM, while plakinamine I (103) with the fused piperidine ring system displayed only modest activity. It was speculated that the steroidal side chain at C-20 may influence the cytotoxic activity (34). In the experiment performed by Abdel-Kader et al., they tested compounds isolated from *Eclipta alba* cytotoxicity against the M-109 cell line and activity against *Candida albicans* including (20*S*, 25*S*)-22,26-imino-cholesta-5,22(*N*)-dien-3β-ol (verazine, 105) ecliptalbine [(20*R*)-20-pyridyl-cholesta-5-ene-3β,23-diol] (106), and 25β-hydroxyverazine (107) (**Figure S7**). Although they believed that antifungal activity is the main activity of these compounds rather than antitumor activity due to the weak cytotoxicity, it also can be observed the structure–activity relationships of cytotoxicity by Abdel-Kader et al. The cytotoxicity of compound 105 was greater than that of compound 106, which might be due to the change of the imine to a pyridine moiety in the side chain (35). Lee et al. reported the cytotoxicity of lokysterolamine A (108), plakinamine E (109), and plakinamine F (110) isolated from the sponge *Corticium* sp. (**Figure S7**). We can observe that the nitrone group in the side chain slightly reduced cytotoxicity against the human leukemia cell line K562 by comparing plakinamine E (109) with lokysterolamine A (108) (36). Zampella et al. isolated plakinamine I (compound 103) from the marine sponge *Corticium* sp., synthesized their derivatives, compounds 113 and 114, and evaluated for their cytotoxicities against MCF7 cell lines (**Figure S7**). Their results showed that the cytotoxicity of compounds 113 and 114 were relatively good in comparison to plakinamine I (compound 103), suggesting that the side chain of the chain structure or the circular structure exerts no obvious influence on cytotoxicity (37).

Ridley et al. reported the isolation and identification of plakinamine I-K (103, 104, 115) and dihydroplakinamine K (116) from the marine sponge *Corticium niger* (**Figure S7**). These compounds were tested for cytotoxicity against the human colon tumor cell line HCT-116. Plakinamine K (115) and dihydroplakinamine K (116) having the same skeleton apart from the presence of double bond at C-24 and C-25 showed comparable potency against the human colon tumor cell line HCT-116, suggesting that the presence of the $\Delta^{24,25}$ double bond had a little or no effect on cytotoxicity (38). Abdel-Kader et al. compared 25β-hydroxyverazine (107) with verazine (105), concluding that the introduction of the hydroxy group at C-25 reduced the cytotoxic activity against the M-109 cell line (35).

Fedorov et al. synthesized 14 steroidal alkaloids (117–130) containing benzimidazole or benzothiazole moieties, with the compounds from Japanese sponge *Stelletta hiwa aensis* as the parent cores (**Figure S7**). They tested the cell inhibitory effects of these compounds against HeLa and HepG2 cell lines and summarized the structure–activity relationships. The SAR study showed that the 6-substituted benzimidazole compounds were more active than the 6-substituted benzothiazole compounds regarding inhibitory effects by comparing compound 121 with compound 129 (39). Among bnorcholesteryl and benzimidazole derivatives, electron-withdrawing groups led to the decrease in cytotoxicity such as compound 118, compound 120, and compound 122, and electron-donating groups had little influence such as compound 121, compound 123, and compound 125 (39). In comparison with compounds 119, 127, and 128, the isoxazolidine ring substituted with C-6 imine moiety or ring B did not play a positive role in anticancer activity. In

comparison with compounds 121, 127, and 130, the pyridine ring in benzimidazole can reduce the cytotoxic activity (39). It is also at the C-6 position wherein, dendrogenin A (DDA, compound 131) was a potential derivative, which contains imidazol joined with 6-ethylamino founded by Sandrine Silvente-Poirot and co-workers, displaying anticancer properties (40, 41).

Sun et al. isolated 3-*O*-acetylveralkamine (132) and veralkamine (133) from *Veratrum taliense*, and they were evaluated for their cytotoxic effects against HL-60, SMMC-7721, A-549, MCF-7, and SW480 cell lines (**Figure S7**). Compound 132, regarded as the acetylated derivative of compound 133, had higher activity than compound 133, suggesting that acetylation at the C-3 position may enhance the cytotoxic activity (42). This conclusion that compound 121 was more active than compound 122 was also proved in the experiment of Fedorov et al. (**Figure S7**) (39). However, some experimental results did not fit this inference. For example, compounds 118 and 120 with the acetyl group at the C-3 position were less active than compounds 117 and 119 with the hydroxy group at the C-3 position, respectively (**Figure S7**). It was deduced preliminarily that these results may be due to electron-withdrawing groups of the benzimidazole at C-6 (39). Fuchs' team showed that the cytostatic activity of compounds with the acetylated hydroxy group at C-3 was lower than that of derivatives with the free hydroxy group at C-3 (43). Therefore, it is necessary to have further study in order to verify the correctness of the conclusion. Compounds 111 and 112 and their amination products 111a and 112a, the intermediate products in the process of synthesizing derivatives of 19-acetoxy-3α-amino-5α-cholestane, were synthesized by Zampella et al. (**Figure S7**). Compounds 111a and 112a possessed no cytotoxic activity, and compounds 111 and 112 exhibited good cytotoxicity. The results revealed that the 3α-amino group played an important role in observed cytotoxicity rather than the 3α-azido group (37).

In the experiment of Sunassee et al., the comparison between plakinamines O (102) and J (104) indicated that substitution of the acetyl group at C-4 may cause the decrease in cytotoxic activity (**Figure S7**) (34). In the experiment of Lee et al., lokysterolamine A (108) showed superior activity against the human leukemia cell line K562 compared to plakinamine F (110), showing that a 4-hydroxy group may be a better substituent group than the 4-carbonyl group on cytotoxic activity (**Figure S7**) (36).

Among compounds 137–143 (compounds 137–140 with the acetyl group at C-12, compounds 138–140 with the glucose group at C-3) isolated from *Veratrum grandiflorum Loes* and tested for inhibition activities on the Hh pathway by Gao et al., compounds 139–141 and 143 showed prominent inhibitory activity, and compounds 142, 144, and 145 exhibited no inhibitory activities (**Figure S7**). A primary SAR study showed that the acetyl group at C-12 may play an important role on the activity, and the C-3 glucose groups had little influence on the activity (44).

In Zampella's experiment, compound 137 with 5α-hydrogen showed better activities than compound 138 with 5β-hydrogen, which revealed that the relative configuration of hydrogen at C-5 may have an effect on cytotoxicity (**Figure S7**) (37). In order to find compounds with antitumor activity in natural plants, Wang et al. studied the antitumor effects of steroidal alkaloids and extracted them from different solvents including chloroform, *n*-hexane, and water from cultivated Bulbus *Fritillariae ussuriensis*. Verticine as well as imperialine were isolated and investigated their cytotoxicity against LLC, A2780, HepG2, and A549 cells lines. It can be observed that the activity of verticine was far higher than that of imperialine against LLC, and slightly higher against HepG2 and A549 cells lines, implying that methyl groups at C-8 or C-13 can enhance the cytotoxicity (45).

Fuchs' team demonstrated that the configuration of the C-16-OH played an important role in cytotoxic activity. The 16α-OH epimer displayed weak effect on cytotoxicity even at 0.1 μM concentration (43).

C-nor-D-HOMOSTEROIDAL ALKALOIDS

C-nor-D-Homosteroidal alkaloids are the other type of C-27 steroidal alkaloids. According to whether the E-ring is open or not, we divided C-nor-D-Homosteroidal alkaloids into cyclopamines and veratramines. The schematic diagram of SAR of cyclopamine is shown in **Figure 6** and that of veratramine is shown in **Figure 7**.

Cyclopamine

Cyclopamine (**143**) is composed of four rings (named C-nor-D-homosteroid including rings A, B, C, and D) joined at the C-17 position by the cyclic tetrahydrofuran and piperidine systems (namely rings E and F) (**Figure S8**).

A SAR study showed that the parallel fused skeleton of rings C, D, E, and F played a little role in the activity of the compounds, while the complete structure of ring E, the N atom on the F ring, and the α-type lone pair electron were necessary for the activity (46, 47). And the C-17 (*R*)-configuration and the C-22 configuration also are essential elements because these can affect the orientation of piperidinic nitrogen in space (47).

Zhang et al. completed the synthesis of cyclopamine derivatives (144a-k, 145a-k) by the method of "Click" chemistry in order to preliminarily construct a library of carbohydrate–cyclopamine conjugates (**Figure S8**). Compound 145f (IC_{50} = 33 μM) with α-L rhamnose linked to an atom on the F ring of cyclopamine owns higher solubility and antitumor activity against lung cancer cell line A549 than cyclopamine (IC_{50} = 49 μM). However, the antitumor activity of cyclopamine connected with β-D sugar including monosaccharides, disaccharides, and trisaccharides was significantly decreased (145a, 145d, 145k) or even inactive (145b, 145g-j) (46, 48). It can be concluded that the connection of the N atom to L-type sugar moiety by α-L glycosidic moiety can maintain high activity and greatly improve solubility; β-D glycosidic moiety may lead the decrease in activities (46). In 2008, Zheng et al. synthesized the cyclopamine analogues including compounds 146–151 from

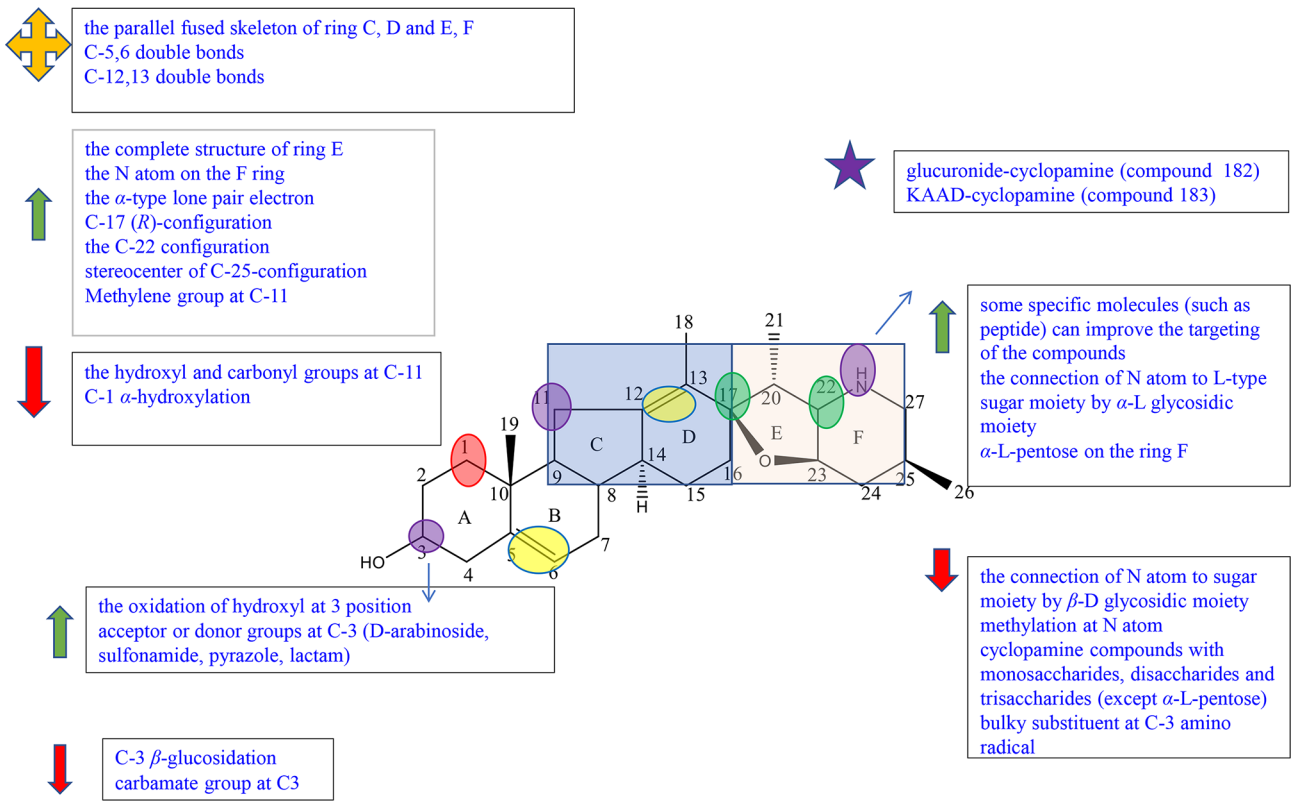

FIGURE 6 | Summary of Structure-activity Relationship of Cyclopamine.

jervine through the methods of reduction, oxidation, and methylation, and tested the activity against human pancreatic cancer Aspc-1 and human gastric cancer SGC-7901. Compound 146 showed prominent inhibition activity against Aspc-1 and SGC-7901 cells, while its methylation products, compound 147 and compound 150, showed no activity, suggesting that methylation at the N atom on the F ring reduced inhibition effects (**Figure S8**) (49). A previous study also proved that the connection of the N atom on ring F to some specific molecules (such as peptide) could improve the targeting of the compound (46).

Exo-cyclopamine (152) with an exo-methylene group at positions 13 and 14 was synthesized by Giannis et al. in 2011, which has good activity and stable acid (**Figure S8**) (50). Because of the advantages, in 2013, Giannis et al. synthesized compounds 153 and 154 for further study, which had the same skeleton as compound 152 except for the substituents at C-25 (**Figure S8**) (51). Compared with compound 143 (cyclopamine) and compound 152 with the C-25 (*R*)-configured methyl group, compound 153 with the C25 (s)-configured methyl group and compound 154 with the $\Delta^{25,27}$ exocyclic double bond showed better inhibition effects against SHh-LIGHT II cells through expressing the Gli1-dependent luciferase. These results suggested that the stereocenter of C-25 configuration affects the Hh inhibition (47).

Jervine (compound 155) is an 11-oxo derivative of cyclopamine (**Figure S8**). In Zheng's experiment, among the three reduction products at C-11 of Jervine (compound 143, compound 156, and compound 157), only cyclopamine (compound 143) with the C-11 methylene group showed good inhibitory activity, while compound 156 and compound 157 with the C-11 hydroxy group showed comparably weak inhibitory activity to Jervine (**Figure S8**). The results showed that the substituents at C-11 were closely related to the antitumor activity. The methylene group at C-11 enhanced the antitumor activity, and the hydroxyl and carbonyl groups decreased the activity (49).

Sinha et al. have reported that the oxidization of the hydroxyl group to a carbonyl moiety at C-3 enhanced the activity (46). Also, in the experiment of Zheng, only compound 146 had relatively good inhibitory activity on Aspc-1 and SGC-7901 cells, whereas the oxidation products and methylation products of Jervine (compounds 146–151) show little activities (**Figure S8**). This result also indicated the conclusion that the oxidation of hydroxyl at the C-3 position may enhance the antitumor activity (49). Khanfar et al. were interested in jervine and veratrum alkaloids due to the reported possible inhibition of the HH signal. They tested the activity of jervine analogues (compounds 158–160) and veratrum alkaloids (155, 161–165) including natural alkaloids, biocatalytic alkaloids, and semisynthetic alkaloids and preliminarily summarized the

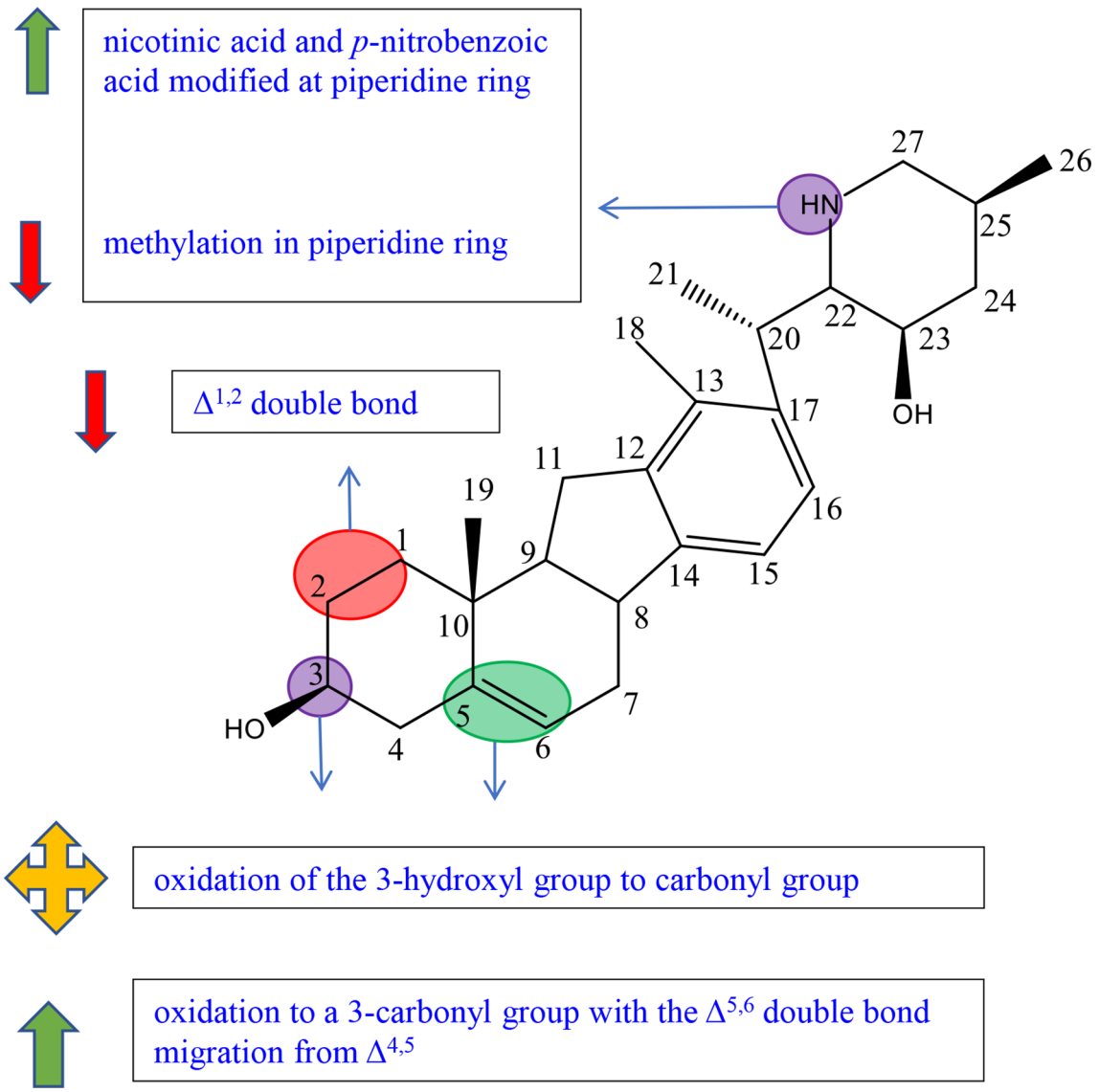

FIGURE 7 | Summary of Structure-activity Relationship of Veratramine.

structure–activity relationships (**Figure S8**). Compound **158** showed no inhibitory effects against PC-3 cells at 50 μM concentration, while most compounds exhibited inhibition activity. The results indicated that C-3 β-glucosidation may reduce the antiproliferative activity (52). Among compounds 155 and 158–165, except compound 158 and compound 165, all compounds exhibited excellent antimigratory activity against PC-3 cells at 50 μM concentration, suggesting that C-3 β-glucosidation (158) or the reduction of $\Delta^{5,6}$ double bond (165) played a negative role in antimigratory activity (52). Thorson et al. established a library of cyclopamine glycosides with the general skeleton of compound 166 to evaluate the effect of nonmetabolic sugars on cyclodopamine (**Figure S8**). In all derivatives, 166 showed better results (3.5–12 times) on the Hh inhibitory effect against lung cancer cell line NCI-H460 than that of cyclopamine (143). Among them, compound 166a with D-arabinoside showed the highest potency (GI_{50} = 6.4 ± 0.5 μM) (53). Compared with compound 167 (EC_{50} = 0.3 ± 0.05 μM), compound 168 with sulfonamide at C-3 (EC_{50} = 0.007 ± 0.002 μM), compound 169 with pyrazole at C-3 (EC_{50} = 0.013 ± 0.008 μM), and compound 170 with lactam at C-3 (EC_{50} = 0.025 ± 0.005 μM) exhibited better efficacy against C3H10T1/2 cell line, suggesting that acceptor or donor groups at C-3 may play an essential role in activities (**Figure S8**) (54).

Gu et al. summarized a SAR exploration according to the collation and analysis of a large number of literatures, indicating that the double bonds at positions 5–6 and 12–13 are not necessary for the activity of the compound (46). However, in the experiment of Tremblay et al., the decreased inhibition activities of C3H10T1/2 cell differentiation of synthetic

compound 171 may be associated with the removal of the C-3 hydroxyl group or the reduction of the $\Delta^{5,6}$ double bond (**Figure S8**) (54).

In the experiment of Khanfar et al., compound 165 showed great inhibitory effects against PC-3 cells at the 50 μM dose, while compound 160 with the same skeleton except α-hydroxylation at C-1 exhibited no antiproliferative activity, implying that the decrease in inhibitory effects may be due to α-hydroxylation at C-1 (**Figure S8**) (52).

Many studies focused on the modification of cyclopamine (143) in order to improve the activities. However, according to the patent of Beachy et al., derivatives of 143 in acidic conditions showed lower biological activities and stabilities. For example, compound 172 with the carbamate group at C-3 and compound 173 with a bulky substituent at amino radical significantly reduced the inhibitory effect of differentiation in C3H10T1/2 cells (**Figure S8**) (55).

In the course of the research, scientists had also found some compounds with potential for development. Compound 145f with α-L-pentose on the ring F synthesized by Zhang et al. had obvious inhibitory activity against lung cancer A450 cells with IC_{50} of 33 μM in the preliminary biological activity test. And 145f had higher inhibitory activity on the Hedgehog signal pathway than that of control (cyclopamine) (48). Compound 174 reported by Goff et al., a glucuronide-cyclopamine compound, significantly reduced the survival rate of malignant glioma U87 cell line with IC_{50} of 21 μM, which had similar effect with cyclopamine in the control group (IC_{50} = 15.5 μM) (**Figure S8**). Compared with cyclopamine, compound 174 showed obvious low toxicity and high effectiveness, having a significant research value *in vivo* activity for further study (56). KAAD-cyclopamine (compound 175) synthesized by Philipp et al. was a derivative substituted on the F ring of cyclopamine, showing higher aqueous solubility, more prominent activity, and lower toxicity (**Figure S8**) (57).

Veratramine

Veratramine (161) has a similar chemical structure with cyclopamine, and the biggest difference is that ring E of veratramine is opened (**Figure S8**).

Guo et al. synthesized and tested five veratrylamine analogues (compounds 176–180) from veratrylamine (161) and preliminarily summarized the structure–activity relationships (**Figure S8**). Compound 176, considered as the oxidation product at C-3 of compound 161 (veratramine), showed comparable antiproliferative activities against SGC-7901 and ASPC-1 compared to compound 161. The result revealed that oxidation of the 3-hydroxyl group to the carbonyl group of compound 161 did not affect the activity (58). It should be pointed out that, in the experiment of Mohammed et al., among veratranes (155, 158-165), only compound 163 exhibited great inhibitory effects at 10 μM, suggesting that oxidation to a C-3 group with the $\Delta^{5,6}$ double bond migration from $\Delta^{4,5}$ led to the enhancement of antiproliferative activities. The chemical modification may remedy the decrease in activity caused by opened ring E (**Figure S8**) (52).

In the experiment of Guo et al., compounds 178, 179, and 180 exhibited comparable or slightly higher activities than cyclopamine or veratramine (**Figure S8**). Moreover, compounds 178 and 179 had significantly higher activity than cyclopamine and veratramine against ASPC-1. The results suggested that the introduction of nicotinic acid and p-nitrobenzoic acid modified at piperidine ring enhanced the inhibitory effects (58).

Guo et al. also reported that the activity of compound 177 determined as the dimethylated product was weaker than that of compound 176 (**Figure S8**). It was speculated that the decrease in activity was because methylation in piperidine ring obscured the possible active groups such as -OH and-NH (58).

Veratrum alkaloids compound 164 reported by Mohammed et al. with $\Delta^{1,2}$ double bond displayed the highest antimigratory activity against the PC-3 cell line, while compound 163 exhibited only moderate activity (**Figure S8**). The results suggest that $\Delta^{1,2}$ double bond played a positive role in antimigratory activity (52).

BIS-STEROIDAL PYRAZINE ALKALOIDS

Bis-steroidal pyrazine alkaloids, including cephalostatins isolated from marine tubeworm *Cephalodiscus gilchristi*, ritterazines isolated from marine organisms *Ritterella tokioka*, and their analogues, are a kind of steroid–alkaloid hybrids with a complex structure (59). The ritterazines and cephalostatins are dense ring compounds, which are fused by two steroidal spirocyclic units with 5/5 or 5/6 spiroketals *via* centra pyrazine heterocycles at C-2 and C-3 and show extremely significant antitumor activity (59–61). The schematic diagram of SAR of cyclopamine is shown in **Figure 8**.

The nonsymmetric structure of bis-steroidal pyrazine alkaloids played an important role in activities. In 2013, Iglesias-Arteaga et al. published a review on cephalostatins and ritterazines by summarizing the literature in 2012 and before. Iglesias-Arteaga et al. reported that symmetrical cephalostatins and ritterazines showed inferior activity, and unsymmetrical compounds were more active. For example, cephalostatin 12 (compound 192) and ritterazine K (compound 210) with polar units as well as ritterazines N (compound 213) and R (compound 217) with nonpolar units showed decreased anticancer activity, although they consist of the most powerful potent core units [including northern and southern hemispheres of cephalostatin 1, southern hemisphere of cephalostatin 7 (compound 187), and northern hemisphere of ritterazine G (compound 206)]. And cephalostatin 13 (compound 193), ritterazines J (compound 209), ritterazines L (compound 211), ritterazines M (compound 212), ritterazines O (compound 214), and ritterazines S (compound 218), which are nearly symmetric, exhibited lower activity (**Figure S9**). In addition, the most potent compounds contained significantly different steroidal portions (62).

Nawasreh continued to study the synthesis of multihydroxylated cephalostatin analogues and synthesized compound 226, compound 227, and borohydride compound

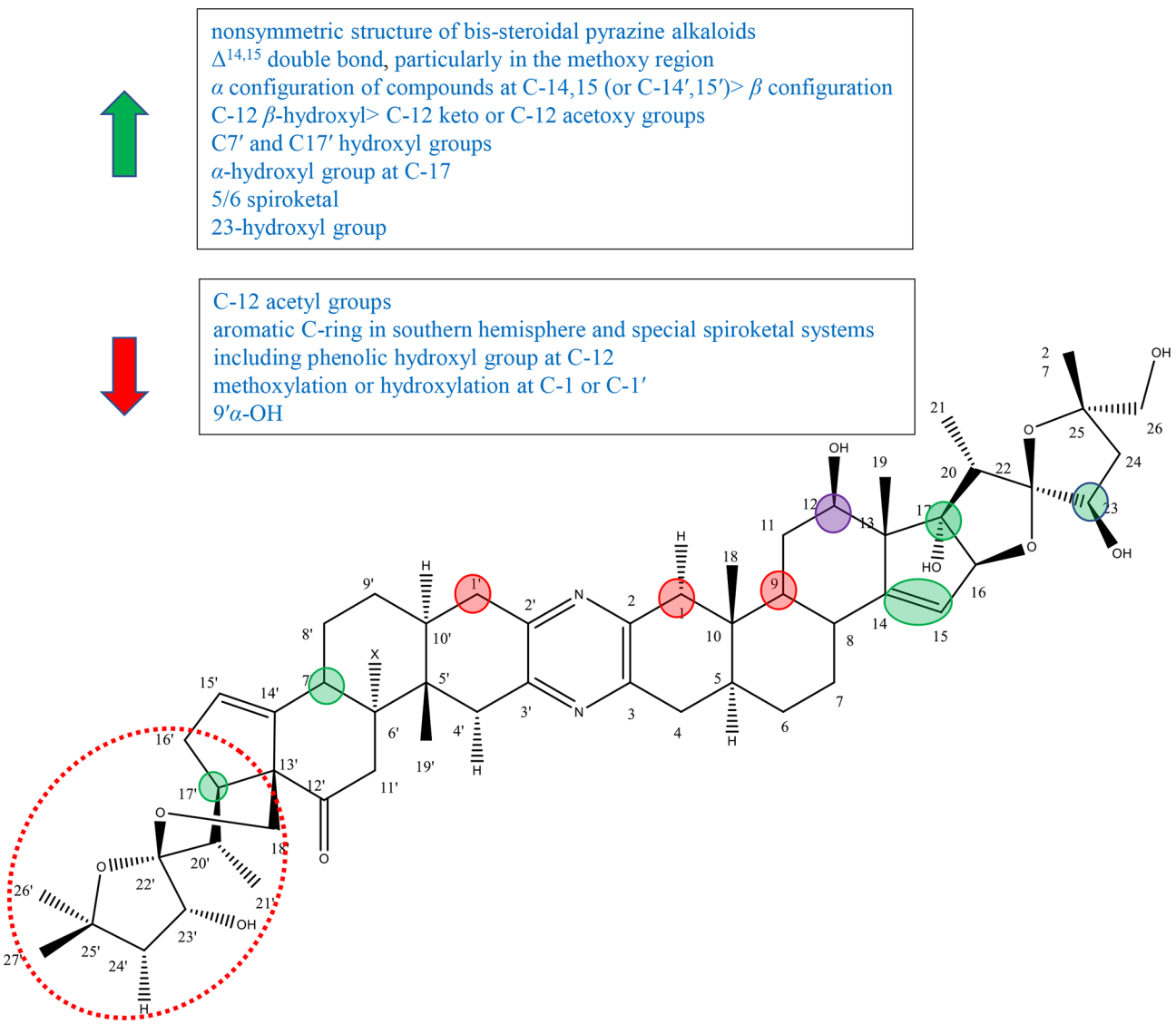

FIGURE 8 | Summary of Structure-activity Relationship of Bis-steroidal Pyrazine Alkaloids.

228 of compound 226. Compound 227 and compound 226 with $\Delta^{14,15}$ double bond showed relatively good activity against HM 02, HEP G2, and MCF 7, while compound 228 lacking it showed very weak activity (**Figure S9**) (63). In addition, in the review of Iglesias-Arteaga et al., most of bis-steroidal pyrazine alkaloids contained $\Delta^{14,15}$ double bond on at least one side, and most cephalostatins contained it on both sides (62). These results suggested that $\Delta^{14,15}$ double bond was important for biological activity, particularly in the methoxy region (62–64). Ritterazine I (compound 208) with 14β-H and 14β-OH was more active than ritterazine Z (compound 225) with 14′α-H or ritterazine U (compound 220) with 14′α-OH. As well as cephalostatin 4 (compound 184) with 14′β,15′β-epoxide was more active than cephalostatins 14 (compound 194) or cephalostatins 15 (compound 195) with 14′α,15′α-epoxides (**Figure S9**). The results suggested that the α configuration of the compounds at C-14,15 (or C-14′,15′) was superior to β configuration (62).

There are five common motifs (I–V) that presented most of alkaloids and three rare motifs (VI–VIII) (**Figure S10**) by Iglesias-Arteaga et al. Compounds with β-hydroxyl or carbonyl groups at 12 and 12′ positions are active. And the hydroxyl group appears to be the intrinsic group of units I, III, and IV, while the ketone group is the intrinsic functional group of units II and V (62). In 1997, Fukuzawa et al. isolated ritterazines N-Z (compounds 212–225) from *Ritterella tokioka* and modified these by reduction, methanolysis, oxidation, and acetylation to obtain compounds 229–236 (**Figure S9**). Ritterazine H (compound 207), determined as the oxidation derivative at C-12 of ritterazine B (compound 201), showed inferior activity to ritterazine B (compound 201), suggesting the importance of the

C-12 hydroxyl group (64). LaCour et al. had reported that C-12 β-hydroxyl in North G played a positive role in the activity, since compounds with C-12 β-hydroxy had invariably higher activity than their counterparts with C-12 keto or C-12 acetoxy groups (65). By comparing with compounds 232–236, Fukuzawa et al. found that the more acetyl groups to introduce, the weaker the activity to exhibit, further proving the importance of the hydroxyl group at C-12 (64). However, in the review of Iglesias-Arteaga et al., compounds containing the aromatic C-ring in the southern hemisphere and special spiroketal systems including the phenolic hydroxyl group at C-12 showed inferior activity, such as cephalostatins 5 (compound 185) and 6 (compound 186) (62).

In the experiment of Fukuzawa et al., ritterazine Y (compound 224) and ritterazine B (compound 201) had the same skeleton except substituent groups at C7′ and C17′. Ritterazine B (compound 201) containing hydroxyl groups at C7′ and C17 was more active than ritterazine B (compound 201) without hydroxyl groups, suggesting that C7′ and C17′ hydroxyl groups may play a positive role in the activity (64). However, Iglesias-Arteaga et al. showed that additional hydroxylation at C-7′ or C-9′ played no or little role in the activity, while it slightly reduced the activity in some situations (9′α-OH) (62). Therefore, it was speculated that the C-17 hydroxyl group plays an important role in the activity and the C7′ hydroxyl group has a little effect.

It was mentioned in Iglesias-Arteaga 's article that the α-hydroxyl group at C-17 was the intrinsic group of core unit I and is often present in unit III (polar domains), but not in units II, IV, and V (nonpolar domains). The active alkaloids contain at least one α-hydroxyl group at C-17 or C-17′ (62). Gryszkiewicz-Wojtkielewicz et al. also reported that the α-hydroxyl group was considered to be a potential functional group (61). By comparing ritterazines T (compound 219) with ritterazines A (compound 200), and ritterazines Y (compound 224) with ritterazines B (compound 201), it can be concluded that the activity of compounds with the 17α-OH group (or 17′α-OH group) was significantly superior to that of analogous compounds without this group (62). In 1998, LaCour et al. synthesized ritterostatin G_N1_N (237), ritterostatin G_N1_S (238), and cephalostatin 1(181) totally for the first time (**Figure S9**). Ritterostatin G_N1_S lacking the 17α-hydroxyl group was far less active than ritterostatin G_N1_N, which further verified the importance of the 17α-hydroxyl group (65).

Fukuzawa et al. reported that 5/6 spiroketal markedly contributed to cytotoxic activity through comparing the cytotoxicity of ritterazines B (compound 201) and C (compound 202). And the cytotoxicity of compounds 229, 230, and 231 also supported this conclusion (**Figure S9**). Therefore, it was speculated that the arrangement of 5/6 spiroketal was important for cytotoxicity (64).

Kumar et al. synthesized 23-deoxy-25-epi ritterostatin G_N1_N (compound 239) and tested the activities against NCI-60 cancer cell lines. The results showed that 25-epi ritterostatin G_N1_N (239) was 50- to 1,000-fold more effective in bioactivity evaluation than that of 23-deoxy-25-epi ritterostatin G_N1_N (compound 240), which suggested that the 23-hydroxyl group of cephalostatin and ritterazine played an important role (**Figure S9**) (61). Iglesias-Arteaga et al. summed up the conclusion through cephalostatins 1 (181), 10 (190), 11 (191), 13 (193), 18 (198), and 19 (199) that methoxylation or hydroxylation at C-1 or C-1′ led to a decrease in the activity (**Figure S9**) (62).

CONCLUSION

Steroidal alkaloids have good anticancer potential. However, due to the imperfect research and its own side effects, the application of steroidal alkaloids is limited. Therefore, there is an urgent need to force us to study the extraction, separation, structural modification, and pharmacological effects of steroidal alkaloids.

To aid the discovery of steroidal alkaloids, we summarize the steroid alkaloids with anticancer activity and conclude the structure–activity relationships. According to the preliminary SAR results, the cytotoxic activity of pregnane alkaloids is affected by C-6, C-7, C-5, C-6, C-3, C-7, C-15, and C-21 substituents. The C-3 position was the most important site to affect the activity; the substituent and configuration of C-3 are both important influential factors. Many scientists had focused on the modification of C-3. According to their results, 10f (IC_{50} value = 0.03 μM) is the most potential compound to treat cancer. Meanwhile, C-16 and C-17 are important active sites. It can be concluded that the double bond at C-16, 17, the epoxidation at C-16, 17, and the hydroxyl group at C-16 can all improve anticancer activities. Besides, the double bond at C-5 and C-6 also can improve anticancer activities, and the substituent groups at C-21 are also key factors for cytostatic efficacy.

The main sources of cyclopregnane alkaloids are cortistatins from marine sponge *Corticium* simplex and cyclopregnane alkaloids from the family Buxus. Research on the anticancer activity of cyclopregnane alkaloids is more focused on cortistatins, but there are a few reports on cyclopregnane alkaloids from the family Buxus. Important factors affecting the activity of cyclopregnane alkaloids include isoquinoline moiety, the plane construction of the tetracyclic core part, and the resemblance in structure compared to cortistatin A.

In terms of structure, cholestane alkaloids are the most variable alkaloids in terms of structure among steroidal alkaloids, which can be divided into solasodine and other types. Both the aglycone and sugar residues are critical for cytotoxic activities. The factors related to sugar residues affect the activity of solasodine including the number of sugars, the number of α-L-rhamnose, the position of α-L-rhamnose, the order of sugar, and the type of sugar. The C-6 position of cholestane is the focus during the research. Scientists changed the substituents at C-6 to compare their activities. Dendrogenin A (DDA) containing imidazol joined with 6-ethylamino is a potential derivative.

For C-nor-D-Homosteroidal alkaloids, people pay more attention to cyclopamine. The high activity of cyclopamine is affected by many factors, including the complete structure of ring E, the N atom on the F ring, the α-type lone pair electron, C17 (*R*)-configuration, the C-22 configuration, and the stereocenter

of C25-configuration. The ways to improve the activity of cyclopamine include methylation at C-11, the oxidation of hydroxyl at C-3, and the presence of acceptor or donor groups at C-3. However, cyclopamine is limited due to its high toxicity. KAAD-cyclopamine is a potential analogue of cyclopamine, showing higher aqueous solubility, more prominent activity, and lower toxicity.

Scientists' research on bis-steroidal pyrazine alkaloids is focused on cephalostatins and ritterazines. According to the preliminary SAR, the ways to improve biological activity are the nonsymmetric structure of bis-steroidal pyrazine alkaloids and the presence of these groups including Δ14,15 double bond, α configuration of compounds at C-14,15 (or C-14′,15′), C-12 β-hydroxyl, C7′ and C17′ hydroxyl groups, α-hydroxyl group at C-17, 5/6 spiroketal, and the 23-hydroxyl group.

The review shows a summary concerning extensive SAR of steroidal alkaloids including pregnane alkaloids, cyclopregnane alkaloids, cholestane alkaloids, C-nor-D-homosteroidal alkaloids, and bis-steroidal pyrazine in the area of anticancer activity. This review is convenient for more scientists to modify steroidal alkaloids and the analogues, as well as to conduct more *in vivo* and preclinical studies to achieve the purpose of reducing toxicity and increasing efficiency. And it greatly saves time to find more active and selective drugs and makes it possible to design new and effective anticancer drugs in the short term.

AUTHOR CONTRIBUTIONS

YZ and HY conceived the project. YH reviewed the literature and drafted the article. GL contributed to classifying the literature. CH and XZ revised the manuscript. All authors contributed to the article and approved the submitted version.

FUNDING

This work was supported by the National Natural Science Foundation of China [No. 81873089] and Scientific Research Projects of Tianjin Education Commission [No. 2018KJ004], the National Key Research and Development Program of China [2021YFE0203100] and the Natural Science Foundation of Liaoning [2021-MS-214]. The funders had no role in the study design, data collection and analysis, decision to publish, or preparation of the manuscript.

SUPPLEMENTARY MATERIAL

The Supplementary Material for this article can be found online at: https://www.frontiersin.org/articles/10.3389/fonc.2021.733369/full#supplementary-material

REFERENCES

1. Jiang Q, Chen M, Cheng K, Yu P, Shi Z. Therapeutic Potential of Steroidal Alkaloids in Cancer and Other Diseases. *Med Res Rev* (2016) 36(1):119–43. doi: 10.1002/med.21346
2. Li S. Review and Expectation of the Study on Quantitative Analysis of Steroidal Alkaloid. *Drug Stanoaros China* (2001) 2(4):8–11. doi: 10.3969/j.issn.1009-3656.2001.04.002
3. Xiaojing L. Thermokinetic Study on the Metabolism of Bacteria by Steroids and Isoquinoline Alkaloids in Traditional Chinese Medicine. *[master's thesis]. [Shan Dong]: Qufu Normal Univ* (2003). doi: 10.7666/d.Y516224
4. Yang BY, Zhen-Peng XU, Liu Y, Kuang HX. Research Progress on Quantitative Analysis Methods of Steroidal Alkaloids. *Chin J Exp Traditional Med Formulae* (2018) 24(16):221–34. doi: 10.13422/j.cnki.syfjx.20181311
5. Dey P, Kundu A, Chakraborty HJ, Kar B, Choi WS, Lee BM, et al. Therapeutic Value of Steroidal Alkaloids in Cancer: Current Trends and Future Perspectives: Steroidal Alkaloids in Cancer. *Int J Cancer* (2018) 145 (7):1721–44. doi: 10.1002/ijc.31965
6. Tantawy MA, Nafie MS, Elmegeed GA, Ali I. Auspicious Role of the Steroidal Heterocyclic Derivatives as a Platform for Anti-Cancer Drugs. *Bioorg Chem* (2017) 73:128. doi: 10.1016/j.bioorg.2017.06.006
7. Lou JS, Yao P, Tism K. Cancer Treatment by Using Traditional Chinese Medicine: Probing Active Compounds in Anti-Multidrug Resistance During Drug Therapy. *Curr Med Chem* (2017) 25(38):5128–41. doi: 10.2174/0929867324666170920161922
8. Peng J, Liang X. Progress in Research on Gold Nanoparticles in Cancer Management. *Medicine* (2019) 98(18):e15311. doi: 10.1097/MD.0000000000015311
9. Coseri S. Natural Products and Their Analogues as Efficient Anticancer Drugs. *Mini Rev Med Chem* (2009) 9(5). doi: 10.2174/138955709788167592
10. Zhidan Z. *Synthesis of Steroidal Alkaloids Solanidine and Demissidine [master's thesis]. [Shang Hai]: Shanghai Normal Univ.*
11. Renghui Y. Research Status and Progress of Steroids. *Technol Wind* (2016) 000(018):260–1. doi: 10.19392/j.cnki.1671-7341.2016180227
12. Huo SJ, Wu JC, He XC, Pan LT, Du J, et al. Two New Cytotoxic Steroidal Alkaloids From Sarcococca Hookeriana. *Mol (Basel Switzerland)* (2018) 24 (1):1–7. doi: 10.3390/molecules24010011
13. Qin N, Jia M, Wu XR, Shou XA, Liu Q, Gan CC, et al. Synthesis and Anti-Metastatic Effects of Pregn-17(20)-En-3-Amine Derivatives. *Eur J Med Chem* (2016) 124:490–9. doi: 10.1016/j.ejmech.2016.08.058
14. Minorics R, Szekeres T, Krupitza G, Saiko P, Giessrigl B, Wolfling J, et al. Antiproliferative Effects of Some Novel Synthetic Solanidine Analogs on Hl-60 Human Leukemia Cells In Vitro - Sciencedirect. *Steroids* (2011) 76(1):156–62. doi: 10.1016/j.steroids.2010.10.006
15. Badmus JA, Ekpo OE, Hussein AA, Meyer M, Hiss DC. Cytotoxic and Cell Cycle Arrest Properties of Two Steroidal Alkaloids Isolated From Holarrhena Floribunda (G. Don) T. Durand & Schinz Leaves. *BMC Complementary Altern Med* (2019) 19(1):1–9. doi: 10.1186/s12906-019-2521-9
16. Phi TD, Pham VC, Mai HT, Litaudon M, Gue Ritte F, Nguyen VH, et al. Cytotoxic Steroidal Alkaloids From Kibatalia Laurifolia. *J Natural Prod* (2011) 74(5):1236–40. doi: 10.1021/np200165t
17. Cheenpracha S, Boapun P, Limtharakul T, Laphookhieo S, Pyne SG. Antimalarial and Cytotoxic Activities of Pregnene-Type Steroidal Alkaloids From Holarrhena Pubescens Roots. *Natural Prod Lett* (2019) 33(6):782–8. doi: 10.1080/14786419.2017.1408108
18. Kam TS, Sim KM, Koyano T, Toyoshima M, Hayashi M, Komiyama K. Cytotoxic and Leishmanicidal Aminoglycosteroids and Aminosteroids From Holarrhena Curtisii. *J Natural Prod* (1998) 61(11):1332–6. doi: 10.1021/np970545f
19. Aoki S, Watanabe Y, Tanabe D, Arai M, Suna H, Miyamoto K, et al. Structure-Activity Relationship and Biological Property of Cortistatins, Anti-Angiogenic Spongean Steroidal Alkaloids. *Bioorg Med Chem* (2007) 15(21):6758–62. doi: 10.1016/j.bmc.2007.08.017
20. Kotoku N, Mizushima K, Tamura S, Kobayashi M. Synthetic Studies of Cortistatin a Analogue From the Cd-Ring Fragment of Vitamin D2. *Chem Pharm Bull* (2013) 61(10):1024–9. doi: 10.1248/cpb.c13-00375
21. Kobayashi M, Kotoku N, Arai M. Search for New Medicinal Seeds From Marine Organisms. In: Shibasaki M, Iino M, Shibasaki H, editors. *Chembiomolecular Science*. Springer, Tokyo (2012). p.93–11. doi: 10.1007/978-4-431-54038-0_9

22. Arai M, Kobayashi M. Search for New Medicinal Seeds From Marine Organisms. *Chembiomol Sci* (2013). doi: 10.1007/978-4-431-54038-0_9
23. Jie Z, Qin XY, Zhang SD, Xu XS, Fu JJ. Chemical Constituents of Plants From the Genus Buxus. *Chem Biodiversity* (2014) 20(9):61–75. doi: 10.1515/hc-2013-0239
24. Akter R, Uddin SJ, Tiralongo J, Darren Grice I, Tiralongo E. A New Cytotoxic Steroidal Glycoalkaloid From the Methanol Extract of Blumea Lacera Leaves. *J Pharm Pharm Sci: Publ Can Soc Pharm Sci Societe Can Des Sci Pharm* (2015) 18(4):616–33. doi: 10.18433/J3161Q
25. Xiang L, Wang Y, Yi X, He X. Steroidal Alkaloid Glycosides and Phenolics From the Immature Fruits of Solanum Nigrum. *Fitoterapia* (2019) 137:104268. doi: 10.1016/j.fitote.2019.104268
26. Li-Ching C, Tong-Rong T, Jeh-Jeng W, Kou-Wha K. The Rhamnose Moiety of Solamargine Plays a Crucial Role in Triggering Cell Death by Apoptosis. *Biochem Biophys Res Commun* (1998) 242(1):21–5. doi: 10.1006/bbrc.1997.7903
27. Andressa ES, Da S, Fernandes A, De C, Raimundo BF, Aurea E. Cytotoxic Activities Against Ehrlich Carcinoma and Human K562 Leukaemia of Alkaloids and Flavonoid From Two Solanum Species. *J Braz Chem Soc* (2002) 13(6):838–42. doi: 10.1590/S0103-50532002000600017
28. Gan KH, Lin CN, Won SJ. Cytotoxic Principles and Their Derivatives of Formosan Solanum Plants. *J Natural Prod* (1993) 56(1):15. doi: 10.1021/np50091a003
29. Xia D, Zhu F, Yang Y, Min L. Purification, Antitumor Activity In Vitro of Steroidal Glycoalkaloids From Black Nightshade (Solanum Nigrum L.). *Food Chem* (2013) 141(2):1181–6. doi: 10.1016/j.foodchem.2013.03.062
30. Liu C, Xie F, Zhao GD, Wang DF, Lou HX, Liu ZP. Synthetic Studies Towards 1α-Hydroxysolasodine From Diosgenin and the Unexpected Tetrahydrofuran Ring Opening in the Birch Reduction Process. *Steroids* (2015) 04:214–9. doi: 10.1016/j.steroids.2015.10.006
31. Xin-Yue G, Xiao-Fei S, Lun W, Zhou-Wei W, Fu L, Bin C, et al. Bioactive Steroidal Alkaloids From the Fruits of Solanum Nigrum. *Phytochemistry* (2018) 147:125–31. doi: 10.1016/j.phytochem.2017.12.020
32. Zha XM, Zhang FR, Shan JQ, Zhang YH, Liu JO, Sun HB, et al. Synthesis and Evaluation of In Vitro Anticancer Activity of Novel Solasodine Derivatives. *Chin Chem Lett* (2010) 20(9):1087–90. doi: 10.1016/j.cclet.2010.04.020
33. Xiao MZ, Fei RZ, Jia QS, Yan KC, Yi HZ, Liu ,J, et al. Synthesis and In Vitro Antitumor Activities of Novel Soladulcidine Derivatives. *J China Pharm Univ* (2010) 41(6):493–8. doi: CNKI:SUN:ZGYD.0.2010-06-006
34. Sunassee SN, Ransom T, Henrich CJ, Beutler JA, Gustafson KR. Steroidal Alkaloids From the Marine Sponge Corticium Niger That Inhibit Growth of Human Colon Carcinoma Cells. *J Natural Prod* (2013) 77(11):2475–80. doi: 10.1055/s-0033-1348635
35. Abdel-Kader MS, Bahler BD, Malone S, Werkhoven M, Troon FV, David, et al. Dna-Damaging Steroidal Alkaloids From Eclipta Alba From the Suriname Rainforest1. *J Natural Prod* (1998) 61(10):1202–8. doi: 10.1021/np970561c
36. Lee HS, Seo Y, Rho JR, Shin J, Paul VJ. New Steroidal Alkaloids From an Undescribed Sponge of the Genus Corticium. *J Natural Prod* (2001) 64 (11):1474. doi: 10.1021/np0101649
37. Zampella A, D'Orsi R, Sepe V, Marino SD, Borbone N, Valentin A, et al. Isolation of Plakinamine I: A New Steroidal Alkaloid From the Marine Sponge Corticium Sp. And Synthesis of an Analogue Model Compound. *Eur J Org Chem* (2005) 2005(20):4359–67. doi: 10.1002/ejoc.200500364
38. Ridley CP, Faulkner DJ. New Cytotoxic Steroidal Alkaloids From the Philippine Sponge Corticium Niger. *J Natural Prod* (2003) 66(12):1536–9. doi: 10.1021/np0302706
39. Fedorov SN, Stonik VA, Honecker F, Dyshlovoy SA. Structure-Activity Relationship Studies of New Marine Anticancer Agents and Their Synthetic Analogues. *Curr Med Chem* (2016) 24(42):4779–99. doi: 10.2174/0929867324666161121115404
40. Silvente-Poirot S, Medina PD, Record M, Poirot M. From Tamoxifen to Dendrogenin a: The Discovery of a Mammalian Tumor Suppressor and Cholesterol Metabolite. *Biochimie* (2016) 30:109–14. doi: 10.1016/j.biochi.2016.05.016
41. Poirot M, Silvente-Poirot S. When Cholesterol Meets Histamine, it Gives Rise to Dendrogenin a: A Tumour Suppressor Metabolite 1. *Biochem Soc Trans* (2016) 44:631–7. doi: 10.1042/bst20150232
42. Yun S, Chen JX, Lin Z, Jia S, Yan L, Qiu MH. Three New Pregnane Alkaloids From Veratrum Taliense. *Helv Chim Acta* (2012) 95(7):1114–20. doi: 10.1002/hlca.201100461
43. Guo C, Lacour TG, Fuchs PL. On the Relationship of Osw-1 to the Cephalostatins. *Bioorg Med Chem Lett* (1999) 9(3):419–24. doi: 10.1016/S0960-894X(98)00743-4
44. Gao LJ, Chen FY, Li XY, Xu SF, Huang WH, Ye YP. Three New Alkaloids From Veratrum Grandiflorum Loes With Inhibition Activities on Hedgehog Pathway. *Bioorg Med Chem Lett* (2016) 26(19):4735–8. doi: 10.1016/j.bmcl.2016.08.040
45. Wang D, Jiang Y, Wu K, Wang S, Wang Y. Evaluation of Antitumor Property of Extracts and Steroidal Alkaloids From the Cultivated Bulbus Fritillariae Ussuriensis and Preliminary Investigation of Its Mechanism of Action. *BMC Complementary Altern Med* (2015) 15(1):29. doi: 10.1186/s12906-015-0551-5
46. Wen-Long GU, Yang Y, Cai J, Min JI. The Antineoplastic Effect of Cyclopamine and its Analogies. *Prog Pharm Sci* (2009) 33(2):631–7. doi: 10.3969/j.issn.1001-5094.2009.02.004
47. Iovine V, Mori M, Calcaterra A, Berardozzi S, Botta B. One Hundred Faces of Cyclopamine. *Curr Pharm Design* (2016) 22(12):16580–81. doi: 10.2174/1381612822666160112130157
48. Zhang J, Garrossian M, Gardner D, Garrossian A, Chang Y-T, Yun Kyung K, et al. Synthesis and Anticancer Activity Studies of Cyclopamine Derivatives. *Bioorg Med Chem Lett* (2008) 18(4):1359–63. doi: 10.1016/j.bmcl.2008.01.017
49. Zheng XH, Guan TW, Han XR, Wang SS, Zhao WJ. Synthesis and Antitumor Activity of Cyclopamine Analogues. *Natural Prod Res Dev* (2015) 27(5):890–5. doi: 10.16333 /j.1001-6880. 2015.05.027
50. Heretsch P, Buttner A, Tzagkaroulaki L, Zahn S, Kirchner B. Exo-Cyclopamine-a Stable and Potent Inhibitor of Hedgehog-Signaling. *Chem Commun R Soc Chem* (2011) 47(26):7362–4. doi: 10.1002/chin.201146188
51. Moschner J, Chentsova A, Eilert N, Rovardi I, Heretsch P, Giannis A. Cyclopamine Analogs Bearing Exocyclic Methylenes Are Highly Potent and Acid-Stable Inhibitors of Hedgehog Signaling. *Beilstein J Org Chem* (2013) 9 (1):2328–35. doi: 10.3762/bjoc.9.267
52. Khanfar MA, Sayed KE. The Veratrum Alkaloids Jervine, Veratramine, and Their Analogues as Prostate Cancer Migration and Proliferation Inhibitors: Biological Evaluation and Pharmacophore Modeling. *Med Chem Res* (2013) 22(10):4775–86. doi: 10.1007/s00044-013-0495-6
53. Goff RD, Thorson JS. Enhancement of Cyclopamine via Conjugation With Nonmetabolic Sugars. *Org Lett* (2012) 14(10):2454–7. doi: 10.1021/ol300703z
54. Tremblay MR, Lescarbeau A, Grogan MJ, Tan E, Lin G, Austad BC, et al. Discovery of a Potent and Orally Active Hedgehog Pathway Antagonist (Ipi-926). *J Med Chem* (2009) 52(14):4400. doi: 10.1021/jm900305z
55. Beachy PA, Chen JK, Taipale A. *Regulators of the Hedgehog Pathway, Compositions and Uses Related Thereto*. Baltimore, MD: U.S. John Hopkins University School of Medicine. U.S. Patent No 9,440,988 B2 (2011).
56. Yang SQ, Feng CL, Wang YC, Min JI. Advances in the Researches on Derivatives of Cyclopamine. *Guangzhou Chem Industry* (2013) 41(9):23–6. doi: 10.3969/j.issn.1001-9677.2013.09.010
57. Taipale J, Chen JK, Cooper MK, Wang B, Mann RK, Milenkovic L, et al. Effects of Oncogenic Mutations in Smoothened and Patched can be Reversed by Cyclopamine. *Nature* (2000) 406(6799):1005–9. doi: 10.1038/35023008
58. Guo XH, Zheng XH, Wang SS, Wang D, Yuan-Yang YU, Zhao WJ. Synthesis of Veratramine Analogs and Evaluation of Their Antiproliferative Activities on Cancer Cell In Vitro. *Fine Chem* (2015) 32(11):1266–70. doi: 10.13550/j.jxhg.2015.11.012
59. Tian W. The Chemistry of Pyrazino - Bis - Steroids. *Chin J Org Chem* (2000) 20(1):11–21. doi: CNKI:SUN:YJHU.0.2000-01-001
60. Fukuzawa S, Matsunaga S, Fusetani N. Isolation and Structure Elucidation of Ritterazines B and C, Highly Cytotoxic Dimeric Steroidal Alkaloids, From the Tunicate Ritterella Tokioka. *J Org Chem* (1995) 60(3):608–14. doi: 10.1021/jo00108a024
61. Kumar RN, Lee S. Synthesis and Bioactivity of Bis-Steroidal Pyrazine 23-Deoxy-25-Epi Ritterostatin Gn1n. *Steroids* (2017) 126:74–8. doi: 10.1016/j.steroids.2017.07.008
62. Iglesiasarteaga MA, Morzycki JW. Cephalostatins and Ritterazines. *Alkaloids Chem Biol* (2013) 72(4):153. doi: 10.1002/9783527619405.ch6a
63. Nawasreh M. Chemo- and Regioselective Hydroboration of Δ14,15 in Certain Cephalostatin Analogue. *Chin Chem Lett* (2008) 19(12):1391–4. doi: 10.1016/j.cclet.2008.09.055

64. Fukuzawa S, Matsunaga S, Fusetani N. Isolation of 13 New Ritterazines From the Tunicate Ritterella Tokioka and Chemical Transformation of Ritterazine B1. *J Org Chem* (1997) 62(13):4484–91. doi: 10.1021/jo970091r
65. Lacour TG, Guo C, Bhandaru S, Boyd MR, Fuchs PL. Interphylal Product Splicing: The First Total Syntheses of Cephalostatin 1, the North Hemisphere of Ritterazine G, and the Highly Active Hybrid Analogue, Ritterostatin G_N1_N. *Printed At Catholic Mission Press* (1998) 120(4):692–707. doi: 10.1021/ja972160p

Conflict of Interest: The authors declare that the research was conducted in the absence of any commercial or financial relationships that could be construed as a potential conflict of interest.

Publisher's Note: All claims expressed in this article are solely those of the authors and do not necessarily represent those of their affiliated organizations, or those of the publisher, the editors and the reviewers. Any product that may be evaluated in this article, or claim that may be made by its manufacturer, is not guaranteed or endorsed by the publisher.

frontiers in Oncology

REVIEW
published: 14 October 2021
doi: 10.3389/fonc.2021.746917

Anti-Tumor Effects of Chinese Medicine Compounds by Regulating Immune Cells in Microenvironment

Fengqian Chen, Jingquan Li, Hui Wang* and Qian Ba**

State Key Laboratory of Oncogenes and Related Genes, Center for Single-Cell Omics, School of Public Health, Shanghai Jiao Tong University School of Medicine, Shanghai, China

As the main cause of death in the world, cancer is one of the major health threats for humans. In recent years, traditional Chinese medicine has gained great attention in oncology due to the features of multi-targets, multi-pathways, and slight side effects. Moreover, lots of traditional Chinese medicine can exert immunomodulatory effects *in vivo*. In the tumor microenvironment, tumor cells, immune cells as well as other stromal cells often coexist. With the development of cancer, tumor cells proliferate uncontrollably, metastasize aggressively, and modulate the proportion and status of immune cells to debilitate the antitumor immunity. Reversal of immunosuppressive tumor microenvironment plays an essential role in cancer prevention and therapy. Immunotherapy has become the most promising strategy for cancer therapy. Chinese medicine compounds can stimulate the activation and function of immune cells, such as promoting the maturation of dendritic cells and inducing the differentiation of myeloid-derived suppressor cells to dendritic cells and macrophages. In the present review, we summarize and discuss the effects of Chinese medicine compounds on immune cells in the tumor microenvironment, including innate immune cells (dendritic cells, natural killer cells, macrophages, and myeloid-derived suppressor cells) and adaptive immune cells ($CD4^+$/$CD8^+$ T lymphocytes and regulatory T cells), and the various immunomodulatory roles of Chinese medicine compounds in cancer therapy such as improving tumor-derived inflammation, enhancing the immunity after surgery or chemotherapy, blocking the immune checkpoints, et al., aiming to provide more thoughts for the anti-tumor mechanisms and applications of Chinese medicine compounds in terms of tumor immunity.

Keywords: Chinese medicine compounds, cancer, immune cell, antitumor immunity, microenvironment

OPEN ACCESS

Edited by:
Lu Chen,
Tianjin University of Traditional Chinese Medicine, China

Reviewed by:
Md Sanaullah Sajib,
United States Food and Drug Administration, United States
Pinaki Misra,
Mayo Clinic, United States

****Correspondence:***
Qian Ba
qba@shsmu.edu.cn
Hui Wang
huiwang@shsmu.edu.cn
Jingquan Li
jqli@shsmu.edu.cn

Specialty section:
This article was submitted to Pharmacology of Anti-Cancer Drugs, a section of the journal Frontiers in Oncology

Received: *25 July 2021*
Accepted: *22 September 2021*
Published: *14 October 2021*

Citation:
Chen F, Li J, Wang H and Ba Q (2021) Anti-Tumor Effects of Chinese Medicine Compounds by Regulating Immune Cells in Microenvironment. Front. Oncol. 11:746917. doi: 10.3389/fonc.2021.746917

INTRODUCTION

Due to high morbidity and mortality, the malignant tumor has long been a hot issue in society. Surgery and chemotherapy are the primary treatments for cancers. Over the past decades, although researchers have devoted themselves to exploiting and exploring more effective treatments for cancers, the morbidity and mortality of malignant tumors are still high all over the world (1). Due to the heterogeneity and complexity of tumors, the cancer treatment focus from single target to multiple targets (2), and the tumor environment (TME) has attracted much attention. There, tumor-infiltrating

immune cells play pivotal roles in tumor immunity and related functions. Chinese medicine compounds refer to the prescription composed of multiple kinds of traditional Chinese medicine (TCM) or the main components of TCM, which are used for treating malignant tumors given the characteristics of multi-pathways, multi-targets, slight side effects, and immunity enhancement (3). More and more Chinese medicine compounds have been recognized for their effects on tumor immunity, such as regulating the proliferation and activation of immune cells and their cytokines (4, 5). However, the impacts and mechanisms of Chinese medicine compounds on distinct immune cells and anti-cancer immunity are diverse and complicated. Herein, we provide an overview of the anti-cancer mechanisms of Chinese medicine compounds by regulating the diverse immune cells (**Figure 1**) and various underlying immunomodulatory pathways in cancer therapy (**Figure 2**).

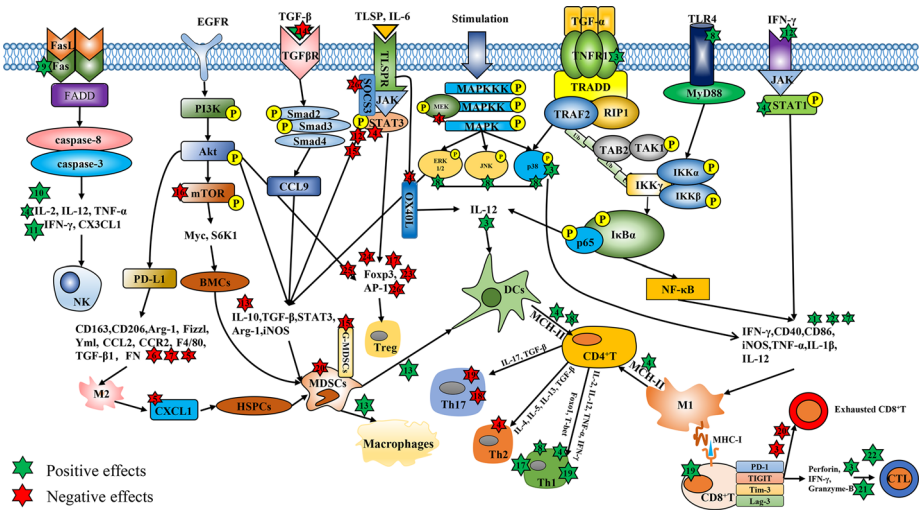

FIGURE 1 | The regulatory effects of Chinese medicine compounds in immune cells. Chinese medicine compounds: 1. Modified Si-Jun-Zi Decoction; 2. Haimufang decoction; 3. Compound kushen injection; 4. Yu-ping-feng; 5. XIAOPI formula; 6. Dahuang Zhechong Pills; 7. Jianpi Yangzheng; 8. Yangyin Wenyang; 9. Jinfukang; 10. Tien-Hsien liquid; 11. ACNO; 12. Yanghe Decoction; 13. Jianpi Huayu Decoction; 14. Baoyuan Jiedu decoction; 15. Ze-Qi-Tang; 16. Shuangshen granules; 17. Quxie capsule; 18. Compound Sophorae Decoction; 19. JC-001 20. Shugan Jianpi formula; 21. Xiao-Ai-Ping; 22. Shenqi Fuzheng Injection; 23. Feiyanning Decoction; 24. Yi-Yi-Fu-Zi-Bai-Jiang-San; 25. Xihuang Pill; 26. Fuzheng Fangai.

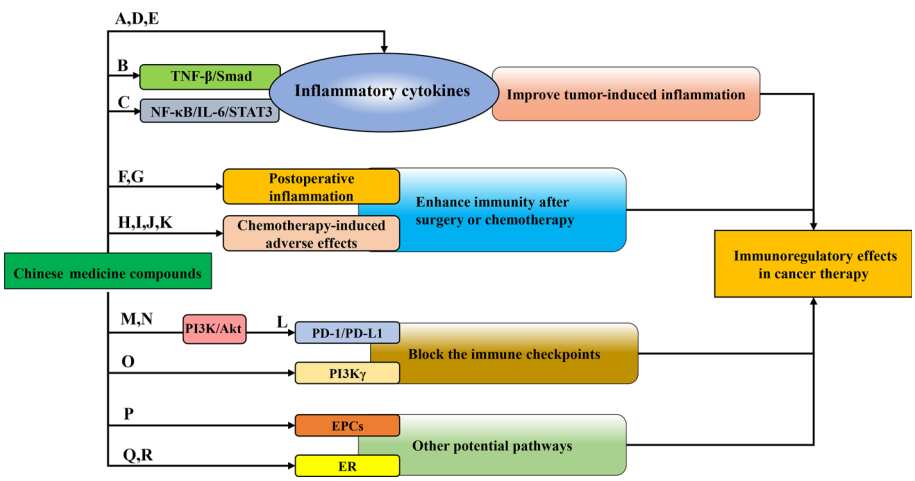

FIGURE 2 | The immunoregulatory patterns of Chinese medicine compounds in cancer therapy. Chinese medicine compounds: **(A)** Banxia Xiexin decoction; **(B)** Compound kushen injection; **(C)** NHE-06; **(D)** Ruyiping+Platycodon grandiflorum; **(E)** Kejinyan decoction; **(F)** DahuangZhechong Pills; **(G)** San Huang decoction; **(H)** PHY906; **(I)** Ciji-Hua'ai-Baosheng; **(J)** Gegen Qinlian decoction; **(K)** Yangyin Fuzheng Decoction; **(L)** Bu Fei Decoction; **(M)** Huoxue Yiqi Recipe-2; **(N)** Bu-zhong-yi-qi decoction; **(O)** Modified Jian-pi-yang-zheng decoction; **(P)** Danggui Buxue decoction; **(Q)** XH formula; **(R)** Shugan Liangxue decoction.

IMMUNE CELLS IN TUMOR MICROENVIRONMENT

TME changes with tumor development and represents diverse immune cell composition and characteristics. Recently, immunotherapy becomes the most promising therapeutic strategy for cancer. In the TME, the functions of diverse immune cell populations function beneficially or harmfully through the local direct/indirect interaction with cancer cells. Typical immune cells in the TME include macrophages, dendritic cells (DCs), natural killer cells (NK cells), and myeloid-derived suppressor cells (MDSCs) in the innate immune system, as well as $CD4^+$/$CD8^+$T lymphocytes and regulatory T cells (Tregs) in the adaptive immune system. As the first defense line against pathogens, macrophages serve as typical antigen-presenting cells (APCs) with the functional capability of phagocytosis and antigen presentation. Tumor-associated macrophages (TAMs), which are recruited into tumors from monocytes in peripheral blood or macrophages in normal tissues, have been proven to assist tumor growth, angiogenesis, and metastasis, thus are considered as a promoter for tumor progression (6). In the TME, TAMs undergo differentiation with distinct properties in response to different stimuli, mainly M1 and M2 phenotypes. M2 macrophages that are activated by alternative pathways play a leading role in TAMs, which are capable of inducing cancer initiation and angiogenesis. Conversely, M1 macrophages are activated classically and have a strong ability of phagocytosis, antigen presentation, and secretion of various pro-inflammatory cytokines such as interleukin-6 (IL-6), IL-12, IL-23, tumor necrosis factor-α (TNF-α) and chemokines to effectively eliminate pathogens or tumor cells in the body (7). DCs are the strongest APCs in human immunity, which enable to efficiently ingest, process, and present antigens to naïve T lymphocytes to initiate adaptive immune responses, acting as a vital bridge linking innate immunity and adaptive immunity (8). Whereas, tumor-infiltrating DCs generally appear to be immature and functional paralysis, thereby failing to initiate or modulate adaptive immunity and gradually leading to immunosuppression (9). NK cells are the cytotoxic lymphocytes of the innate immune system. Although lack antigen receptors, they are regarded as the key cancer defensor due to the cytotoxic ability to quickly kill nearby target cells without antigen in advance. Similarly, there are a variety of endogenous mechanisms to resist NK cells from attack and deep infiltration, leading to the failed cytotoxicity (10). Moreover, MDSCs refer to a heterogeneous population of cells consisting of early myeloprogenitor cells, naïve granulocytes, as well as immature macrophages and DCs with various differentiation degrees, which display strong T-cell suppression function. Pro-inflammatory cytokines could induce the generation of MDSCs in tumor microenvironment and defect the differentiation of MDSCs into mature immune cells. Over the past years, numerous studies have shown that MDSCs could promote cancer progression in terms of cancer cell proliferation and invasion, tumor angiogenesis, and drug resistance (11).

As immunotherapy has been widely studied, $CD4^+$ T lymphocytes, also known as helper T cells (Th), have attached much attention due to the remarkable effects on the adaptive immune system. The naïve T lymphocytes (Th0) differentiate into different subsets, such as Th1, Th2 and Th17. The Th1 immune response can be usually inhibited in a variety of malignant tumors, which manifests as the down-regulation of TNF-α, IL-2, IFN-γ and IL-2, and defecting the proliferation of cytotoxic T cells, macrophages and NK cells. On the contrary, Th2-biased immune response is up-regulated in cancer progression (12). The cytokines IL-4, IL-5 and IL-13 secreted by Th2 cells have been found to facilitate tumor growth (13). In addition, the ratio of Th1/Th2 refers to a crucial factor to maintain the normal immune state, and the imbalance of Th1/Th2 often occurs in immune-related diseases including cancer. Th17 is another helper T cell, which was named from the ability to secrete the pro-inflammatory cytokine IL-17. Th17 has been considered as a potential target for tumor treatment, however, in different tumors, Th17 showed inconsistent effects (14, 15). The subset of $CD8^+$ T lymphocytes, also called cytotoxic T cells (CTLs), is an important guardian of the adaptive immune system. CTLs exert great cytotoxic effects on tumor cells, in other words, they perform cellular immunity by lysing or inducing apoptosis of targeted cells. However, with the infiltration of $CD8^+$ T lymphocytes into tumor tissues, they undergo exhaustion in form of suppressed proliferation and even apoptosis (16). Tregs are a unique subset of $CD4^+CD25^+$ T lymphocytes and are augmented in various cancers. Tregs in the TME serve as a potent immunosuppressive factor and resist anti-tumor immunity (17). Additionally, the balance of Th17/Treg is likely to be disturbed by TAMs in the TME (18). Therefore, it is a feasible immunotherapeutic strategy to reshape TME by modulating the activity and function of immune cells.

THE REGULATORY EFFECTS OF CHINESE MEDICINE COMPOUNDS ON INNATE IMMUNE CELLS

Macrophages

Targeted consumption or regulation of TAMs has become a potential cancer treatment strategy (19), such as activating TAMs towards M1-type polarization, suppressing M2-type polarization, and inducing M2 polarizing to M1. Numerous Chinese medicine compounds have been reported to exert inhibitory effects on tumor growth and metastasis through targeting macrophages (**Figure 1**). Th1 cytokines IFN-γ are conducive to M1 activation in the TME (20). Modified Si-Jun-Zi Decoction stimulated the secretion of GM-CSF, IFN-γ, IL-1α and IL-3, increased the number of macrophages, thus activating the innate immune system to remove colorectal cancer (CRC) cells (21). The elevated expression of phenotypic marker CD86 and CD40 stand for the activation of M1 macrophages to some extent. Ma et al. observed that Haimufang (HMF) decoction

enhanced the generation of nitric oxide (NO) and reactive oxygen species (ROS), the secretion of cytokines TNF-α, IL-1β, IL-12 p70, and IL-6, and the expression of M1 marker CD40 and CD86, with time- and dose-dependent manners in RAW264.7 cells, but had no discernible impact on M2 phenotypic marker CD206. As a result, HMF promoted the M1 polarization and enhanced the phagocytosis ability (22). In hepatocellular carcinoma (HCC), Yang et al. reported that Compound kushen injection (CKI) facilitated the activation of macrophages by stimulating TNF receptor superfamily member 1 (TNFR1)-mediated NF-κB and p38 MAPK signaling pathways, thereby accelerating M1 polarization and alleviating TAMs-mediated immunosuppression (23). Yu-ping-feng (YPF) has usually been prescribed to enhance human immunity, which was reported to up-regulate the secretion of IL-1β and IL-12, the level of iNOS as well as the phosphorylation and activation of signal transducers and activators of transcription 1 (STAT1) in RAW264.7 cells to propel the M1 polarization and enhance M1-induced $CD4^+$T cell activation and Lewis lung cancer (LLC) lysis (24). Furthermore, Chinese medicine compounds could restrain the function of M2 and facilitate the conversion of M2 to M1. XIAOPI (XP) formula remarkably prevented the promoting effect of TAMs on the proliferation and self-renewal activity of breast cancer cell lines (MDA-MB-231 and 4T1) in a co-culture system, and reversed the TAMs-mediated C-X-C Motif Chemokine Ligand 1 (CXCL1) secretion and β-catenin signal, thus attenuating the self-renewal activity and chemotherapy resistance of breast cancer stem cells (CSCs). Moreover, XP weakened the polarization of M2 by down-regulating the expression of CD163, CD206 and Arg1 as well as the transcriptional activity of CXCL1 in a dose-dependent manner (25). C-C Motif Chemokine Ligand-2 (CCL2) refers to an important chemokine for monocyte/macrophage chemotaxis (26). Chen et al. reported that CCL2 boosted the number of macrophages in the liver and induced M2 polarization, which could be prevented by Dahuang Zhechong Pills (DZP) through the suppressed secretion of CCL2 and its receptor CCR2, along with the low level of F4/80, TGF-β1 and FN to attenuate hepatic fibrotic status. DZP also reversed tumor-mediated M2 polarization of macrophages to reshape the immunosuppressive TME and inhibit the liver metastasis of CRC (27). Jianpi Yangzheng (JPYZ), the ingredients for invigorating qi and spleen of Jianpi Yangzheng Xiaozheng decoction, can promote the transformation of M2 to M1 with the elevation of CD86 and reduction of CD206 and CD163. The mRNA levels of M1-related genes (IL-1β, IL-12 and TNF-α) were enhanced by JPYZ while those of M2-related genes (Arg-1, Fizzl and Yml) were attenuated (28). Consequently, Chinese medicine compounds indeed regulate the activation and differentiation of TAMs to exert anti-tumor activity (**Table 1**).

Dendritic Cells (DCs)

Chinese medicine compounds could enhance the maturation and antigen presentation ability of DCs to induce the activation of naïve T lymphocytes and participate in the regulation of T cell differentiation (**Table 1**). IL-12 is closely involved in the antigen presentation function of DCs (41). Zhao et al. optimized a new traditional Chinese medicine formula Yangyin Wenyang (YYWY) on the basis of Jinfukang. YYWY intervention drove the impregnation of DCs, $CD4^+$ and $CD8^+$ T cells in LLC tissues, and raised the mRNA levels of IFN-γ, IL-1β, TNF-α and IL-12. In addition, YYWY stimulated MAPK and NF-κB signaling pathways in bone marrow dendritic cells (BMDCs) to accelerate the maturation of DCs and the proliferation and differentiation of T cells together (29). TSLP, an immune-related factor, can activate DCs and involve in T cell differentiation, which raises the expression of Th2-polarizing molecule CD252 (OX40L), and induces Th2 response (42). Yao et al. reported that YPF reduced the expression of TSLP and OX40L to induce the maturation of DCs and the expression of CD80, CD86, MHC-II as well as IL-12 (12). Furthermore, DCs combine with tumor cells to form fusion cells (FCs), which play an inhibitory role in tumor development. Yang et al. found that fusion cells of dendritic colon cancer stem cells (DC-cCSC FCs) facilitated the proliferation of cytokines induce killer (CIK) cells. The cytotoxicity of DC-cCSC FCs and CIK cells against cCSCs was further improved by IL-12 and could be enhanced by the Chinese medicine CKI (30). In summary, Chinese medicine compounds are capable to activate DCs. Although some studies have proven that Chinese medicine compounds elevate the function of NK cells in the TME by promoting the secretion of IL-12 (**Figure 1**), more researches about the mechanisms are demanded.

Natural Killer Cells (NK Cells)

Recently, the anti-tumor activity of exogenously activated and amplified NK cells has been proved in clinical (43). Some studies have shown that activating NK cells may be an effective approach for Chinese medicine compounds to suppress the advance of tumors (**Table 1**). For example, Luo et al. confirmed that YPF propelled the infiltration, proliferation, and killing activity of NK cells in tumor tissues to prolong the survival of LLC tumor-bearing mice. Elimination of NK cells could remarkably reverse the inhibitory effect of YPF on lung cancer, indicating that NK cells were the potential target cells for YPF-mediated lung cancer treatment (31). Additionally, Que et al. found that Jinfukang was conducive to the secretion of C-X3-C Motif Chemokine Ligand 1 (CX3CL1) in circulating tumor cells (CTCs) and the recruitment of CTCs to NK cells. Meanwhile, Jinfukang significantly accelerated NK cells-mediated CTCs apoptosis and prevented lung cancer metastasis through activating Fas/FasL signaling pathway, manifested as the up-regulated FasL and secretion of TNF-α in NK cells (32). In addition, Tien-Hsien liquid (THL) accelerated the secretion of immune factors including IFN-γ, IL-2 and TNF-α to augment the cytotoxicity of NK cells and CTLs and mitigate the tumor development (33). Finally, Li et al. reported a new traditional Chinese medicine compound anti-cancer No.1 (ACNO) which could dose-dependently enhance the cytotoxicity of NK cells by up-regulating the secretion of IL-2, IL-12, and INF-γ (34) (**Figure 1**). In brief, Chinese medicine compounds can interfere with tumor growth by the way of enhancing the killing activity of NK cells.

TABLE 1 | Innate immune cells impacted by Chinese medicine compounds.

Immune cells	Chinese medicine compounds	Signaling pathway/Cytokines	Specific main effects	Cancer types	Ref
Macrophages	Modified Si-Jun-Zi Decoction	↑GM-CSF, IFN-γ, IL-1α, IL-3,	↑Macrophages	Colorectal cancer	(21)
	Haimufang decoction	↑TNF-α, IL-1β, IL-12 p70, IL-6	↑Macrophages activity and M1	Lewis lung cancer	(22)
	Compound kushen injection	↑NF-κB and p38 MAPK signaling pathway	↑Macrophages activity and M1	Hepatocellular carcinoma	(23)
	Yu-Ping-Feng	↑STAT1 signaling pathway, IL-1β, IL-12, iNOS	↑The number and polarization of M1	Orthotopic lung cancer	(24)
	XIAOPI formula	↓TAMs/CXCL1 signaling pathway	↓Proliferation and polarization of M2	Breast cancer	(25)
	Dahuang Zhechong Pills	↓CCL2, CCR2, F4/80, TGF-β1, FN	↓Function and polarization of M2	Colorectal cancer	(27)
	Jianpi Yangzheng	↑IL-1β, IL-12, TNF-α; ↓Arg-1, Fizzl, Yml	↑The conversion of TAMs from M2 to M1	Gastric cancer	(28)
DCs	Yu-Ping-Feng	↑IL-12	↑The maturation and percentage of DCs	Hepatocellular carcinoma	(12)
	Yangyin Wenyang	↑MAPK, NF-κB signaling pathways	↑The number and maturation of DCs	Non-small cell lung cancer	(29)
	Compound kushen injection	↑IL-12	↑The killing activity of DC-cCSC FCs	Colorectal cancer	(30)
NK cells	Yu-Ping-Feng	↓TGF-β, Indoleamine 2,3-dioxygenase, IL-10; ↑IL-12	↑NK cell tumor infiltration and NK cell cytotoxicity	Lewis lung cancer	(31)
	Jinfukang	↑CX3CL1, TNF-α, Fas/FasL signaling pathway	↑The recruitment and cytotoxicity of NK cells	Lewis lung cancer	(32)
	Tien-Hsien liquid	↑IFN-γ, IL-2, TNF-α	↑The number and tumor-killing activities of NK cells	Colorectal cancer	(33)
	ACNO	↑IL-2, IL-12, INF-γ	↑The number and cytotoxicity of NK cells	Colorectal cancer	(34)
MDSCs	XIAOPI formula	↓TAMs/CXCL1 signaling pathway	↓The differentiation of HSPC into MDSCs	Breast cancer	(25)
	YHD	↓TGF-β and p-STAT3	↓The function of MDSCs		(35)
	Yu-Ping-Feng	↓Arg-1, iNOS, STAT3 ↓p-Akt, p-MEK, p-ERK, p-STAT3	↓The proportions of MDSCs subsets; ↑Apoptosis of MDSCs	Lewis lung cancer	(36)
	Jianpi Huayu Decoction	↓IL-10, TGF - β	↑The differentiation of MDSCs	Hepatocellular carcinoma	(37)
	Baoyuan Jiedu decoction	↓TGF-β/CCL9 signaling pathway	↓The content of G-MDSC and M-MDSC	Breast cancer	(38)
	Ze-Qi-Tang	↓STAT3/S100A9/Bcl-2/caspase-3 signaling pathway	↑The elimination of MDSCs (especially G-MDSCs)	Orthotopic lung cancer	(39)
	Shuangshen granules	↓mTOR/S6K1/Myc signaling pathway	↓The differentiation of BMCs into MDSCs	Lewis lung cancer	(40)

↑, *Up-regulated or enhanced;* ↓, *Down-regulated or inhibited.*

Myeloid-Derived Suppressor Cells (MDSCs)

Researches have suggested that Chinese medicine compounds abated the immunosuppression in the TME by facilitating the apoptosis and differentiation of MDSCs to enhance immune response (**Table 1**). Mao et al. observed that Yanghe Decoction (YHD) had immunomodulatory effects on 4T1 breast tumors, not only boosting the amount of NKT and $CD4^+$ T cells as well as the secretion of IFN-γ and p-STAT1, but also attenuating the recruitment of MDSCs through JAK/STAT3 signaling pathway (35). YPF suppressed the mRNA levels of immunosuppressive genes in MDSCs, including Arg-1, iNOS and STAT3, and decreased the levels of p-Akt, p-MEK, p-ERK and p-STAT3 to prevent MDSCs augment and induce their apoptosis, which further modulated the proportion of T cell subsets by increasing $CD4^+/CD8^+$ T lymphocytes and decreasing Treg proportion, thus reshaping the immune TME and preventing the lung cancer progression (36). Moreover, Xie et al. proved that Jianpi Huayu Decoction (JHD) attenuated the expression of IL-10 and TGF-β in tumor tissues and accelerated the differentiation of MDSCs into macrophages and DCs. JHD decreased the content of ROS in MDSCs, inhibited $CD4^+$ T cells proliferation and the percentages of Th17 and Treg, but elevated the proportion of CTLs and DCs to relieve the MDSCs-mediated immunosuppressive state in HCC (37). Another research reported that Baoyuan Jiedu decoction (BYJD), a traditional Chinese medicine formula composed of Astragalus, Ginseng, Aconite root, Honeysuckle, Angelica, and Licorice, inhibited the TGF-β/CCL9 signaling pathway and reduced the number of MDSCs in peripheral blood and spleen of breast

cancer (4T1)-bearing mice. Furthermore, BYJD blocked the recruitment of MDSCs in lung, the metastatic organ of breast cancer, thereby improving the pre-metastatic niche (PMN) and prolonging the survival of tumor-bearing mice (38). Xu et al. found that the medium dose of Ze-Qi-Tang (ZQT) had the strongest anti-tumor activity. In lung carcinoma *in situ*, ZQT could eliminate MDSCs in a dose-dependent manner, reduce the recruitment of MDSCs, and enhance the infiltration of T cells to reverse MDSCs-mediated immunosuppression. Thoroughly discovered that ZQT suppressed the level of STAT3, p-STAT3 and anti-apoptotic protein Bcl-2, increased the expression of pro-apoptotic protein Bax, cleaved caspase-3 and PARP to induce the apoptosis of G-MDSCs in lung carcinoma *in situ*. However, after G-MDSCs were completely depleted, the cytotoxicity of $CD8^+$ T cells and the inhibitory effect of MDSCs had no significant difference between ZQT group and the control group, suggesting that the anti-tumor activity of ZQT was achieved by targeting G-MDSCs subset (39). Chinese medicine compounds also could decline the generation of MDSCs. Shuangshen granules restrained the expression of mTOR, S6K1 and Myc to block the differentiation of bone marrow cells (BMCs) into MDSCs in a dose-dependent manner, thus preventing lung metastasis (40). XP impaired the activation of hematopoietic stem-progenitor cells (HSPCs) as well as the differentiation of HSPCs into MDSCs through TAMs/CXCL1 signaling pathway to inhibit lung metastasis of breast cancer (25). Therefore, it may be a promising therapeutic way for Chinese medicine compounds to improve TME through targeting MDSCs (**Figure 1**).

THE REGULATORY EFFECTS OF CHINESE MEDICINE COMPOUNDS ON ADAPTIVE IMMUNE CELLS

$CD4^+$ T Lymphocytes

Some Chinese medicine compounds are capable of exerting anti-tumor effects through facilitating $CD4^+$T lymphocytes differentiate to Th1 and attenuating Th2 response (**Table 2**). The activation and differentiation of $CD4^+$ T lymphocytes tend to be affected by APCs, such as macrophages and DCs. YPF enhanced the antigen presentation ability of macrophages by up-regulating the level of MHC II, thereby activating the LLC cell lysis mediated by $CD4^+$ T cells. Meanwhile, YPF enhanced the secretion of Th1 cytokines (IL-2, IL-12) but repressed the level of Th2 cytokines (TGF-β, IL-4) (24). In addition, in H-22 tumor-bearing mice, YPF elevated the ratio of Th1/Th2 (IFN-γ/IL-4) through mature DCs, thus ameliorating Th2-biased immune state (12). Similarly, YYWY exerted the anti-tumor effect by inducing DCs mature, which subsequently activated $CD4^+$ T lymphocytes and enhanced Th1 function (29). Chen et al. found that in CT26 tumor-bearing mice, Quxie capsule (QX) intervention boosted the expression of Foxo1 and T-bet, along with the augment of Th1 and Th1/Th2, to propel the immune response in TME (44). Th17 has been considered as a potential target for tumor treatment in several studies. Deng et al. confirmed that Th17 was conducive to the occurrence of Ulcerative Colitis-Related Colorectal Cancer (UCRCC), however, Compound Sophorae Decoction (CSD) remarkably reversed the increasing number of Th17 and the secretion of IL-17 to relieve inflammation in UCRCC (45). Chuang et al. reported that in the co-culture system of spleen cells and LLC cells, JC-001 enhanced Th1 function and suppressed Th17 function by abating the secretion of TGF-β and IL-17A to prevent tumor progression (46). In liver cancer, JC-001 had the same effects on Th1 and Th17 function, thereby alleviating Treg-mediated immunosuppression (47). Taken together, Chinese medicine compounds control tumor growth by modulating the differentiation of $CD4^+$ T cells, enhancing Th1 immune response as well as restraining the function of Th2 and Th17 (**Figure 1**).

$CD8^+$ T Lymphocytes

Restoring $CD8^+$ T lymphocytes function has always been regarded as an effective method to facilitate tumor immunity (16). Some studies have demonstrated that Chinese medicine compounds lead to the augment of $CD8^+$ T lymphocytes in tumor tissues (29, 33, 36). In addition, Chinese medicine compounds bring vital impacts on the activity and exhaustion of $CD8^+$ T cells (**Table 2**). CKI combined with sorafenib dramatically suppressed function-inhibitory receptors in $CD8^+$ T cells, including lymphocyte-activation gene 3 (Lag-3), programmed cell death protein 1 (PD-1), T-cell immunoreceptor with Ig and ITIM domains (TIGIT), and T-cell immunoglobulin and mucin-domain containing-3 (Tim-3) to reduce the depletion of $CD8^+$ T cell. At the same time, the combination therapy strengthened the cytotoxicity of $CD8^+$ T cells by accelerating the production of TNF-α, Perforin, IFN-γ and Granzyme-B. When $CD8^+$ T lymphocytes were blocked, the anti-tumor activity of combination therapy disappeared, suggesting that $CD8^+$ T cells were necessary for CKI-mediated HCC treatment (23). Lu et al. reported that, in depression breast cancer mice, Shugan Jianpi formula combined with chemotherapy drug gemcitabine (GEM) effectively repressed the apoptosis of $CD8^+$ T cells and significantly reduced MDSCs to enhance the immune surveillance, thereby preventing the progress of breast cancer (48). It has been shown that Xiao-Ai-Ping, an adjuvant injection for tumor therapy, propelled the infiltration and function of $CD8^+$ T cells in the TME of LLC, mainly manifested as the increase in Perforin, IFN-γ and Granzyme-B (49). At last, JC-001 drove the generation of $CD8^+$ T cells in LLC1 tumor and the secretion of IL-12 p70 and IFN-γ to sensitize LLC1 tumor to chemotherapeutic drug cisplatin (CDDP) (46). Jurkat T cell line, a kind of CTLs, has been reported to resist tumor immune escape (55). Du et al. observed that Shenqi Fuzheng Injection (SFI) down-regulated the immunosuppressive cytokines IL-10, TGF-β and VEGF in A375 cells in a concentration-dependent manner. Also, SFI enhanced the cytotoxic and migratory activities of Jurkat T cells in A375 melanoma to reprogram the melanoma microenvironment (50), which demonstrated that CTLs can mediate the anti-tumor effects of Chinese medicine compounds. In conclusion,

TABLE 2 | Adaptive immune cells impacted by Chinese medicine compounds.

Immune cells	Chinese medicine compounds	Signaling pathway/Cytokines	Specific main effects	Cancer types	Ref
$CD4^+$ T lymphocytes	Yu-Ping-Feng	↑IFN-γ/IL-4 ratio↑IL-12, TNF-α, IFN-γ; ↓IL-10, IL-5, IL-4	↓Th2-biased immune state	Hepatocellular carcinoma	(12)
		↑MHC II in Macrophages; ↑IL-2, IL-12; ↓TGF-β, IL-4	↑Th1 immune response; ↑The lysis capacity of $CD4^+$T cells	Orthotopic lung cancer	(24)
			↑The proportion of $CD4^+$T cells	Lewis lung cancer	(36)
	Yangyin Wenyang	↑TNF-α,IL-2,IFN-γ; ↑IFN-γ/IL-4 radio	↑The differentiation of T cells into Th1; ↑The ratio of Th1/Th2	Non-small cell lung cancer	(29)
	Quxie capsule	↑Foxo1, T-bet	↑The ratio of Th1/Th2	Colorectal cancer	(44)
	Compound Sophorae Decoction	↓STAT3, IL-17	↓The proportion of Th17	UCRCC	(45)
	JC-001	↑IL-2, IL-10, TNF-α, IFN-γ; ↓TGF-β, IL-17A	↑Th1 function; ↓Th17 function	Lewis lung cancer	(46)
		↑T-bet, GATA-3	↑Th1 function; ↓Th17 function	Hepatocellular carcinoma	(47)
$CD8^+$ T lymphocytes	Compound kushen injection	↓Lag-3, PD-1, TIGIT,Tim-3; ↑TNF-α, Perforin, IFN-γ, Granzyme-B	↓$CD8^+$T cells exhaustion; ↑$CD8^+$T cells cytotoxicity	Hepatocellular carcinoma	(23)
	Yangyin Wenyang	↑MAPK, NF-κB signaling pathways	↑$CD8^+$T cells generation by mature DCs	Non-small cell lung cancer	(29)
	Tien-Hsien liquid	↑IFN-γ, IL-2, TNF-α	↑The number and cytotoxicity of CTLs	Colorectal Cancer	(33)
	Yu-Ping-Feng		↑The proportion of $CD8^+$T cells	Lewis lung cancer	(36)
	JC-001	↑IL-12 p70, IFN-γ	↑$CD8^+$T cells generation	Lewis lung cancer	(46)
	Shugan Jianpi formula		↓$CD8^+$T cells apoptosis	Breast cancer	(48)
	Xiao-Ai-Ping	↑Perforin, IFN-γ, Granzyme-B	↑$CD8^+$T cells proliferation and function	Lewis lung cancer	(49)
	Shenqi Fuzheng Injection	↓IL-10, TGF-β, VEGF	↑The cytotoxic and migratory activities of Jurkat T cells	Melanoma	(50)
Tregs	Quxie capsule	↓Foxp3 induced by↑Foxo1	↓The proportion of Treg; ↓The ratio of Th17/Treg cells	Colorectal cancer	(44)
	JC-001	↓Foxp3, RORγt	↓Treg function	Hepatocellular carcinoma	(47)
	Feiyanning Decoction	↓Foxp3	↓The number of Tregs	Lewis lung cancer	(51)
	Yi-Yi-Fu-Zi-Bai-Jiang-San	↑IL-6, CCXL13, IL-10	↓Tregs activated by ETBF	Colorectal cancer	(52)
	Xihuang Pill	↓PI3K/Akt/AP-1 signaling pathway	↓The proliferation of Tregs; ↑The apoptosis of Tregs	Breast cancer	(53)
	Fuzheng Fangai	↓IL-17, IL-23, IFN-γ, Foxp3, RORγt, SOCS3, JAK2, STAT3	↓The proportion of Th17 and Treg; Restore the balance of Th17/Treg	Lewis lung cancer	(54)

↑, *Up-regulated or enhanced;* ↓, *Down-regulated or inhibited.*

the restoration and enhancement of the activity of $CD8^+$ T cells are effective ways for Chinese medicine compounds to prevent cancer from deteriorating (**Figure 1**).

Regulatory T Cells (Treg)

Previous researches have shown the potential therapeutic effects of targeting $Foxp3^+$ Tregs for cancer treatment (56). Guo et al. reported that Feiyanning Decoction significantly attenuated the amount of $CD4^+CD25^+$ regulatory T cells in spleen, thymus and tumor tissues in LLC-bearing mice. It decreased the mRNA level of Foxp3, enhanced tumor immune response, and slowed down the progression of lung cancer (51). Yi-Yi-Fu-Zi-Bai-Jiang-San (YYFZBJS), a classical Chinese medicine formula for gastrointestinal diseases, suppressed the number of $CD4^+CD25^+$ $Foxp3^+$ T cells. Although YYFZBJS did not directly affect CRC cells, it was able to down-regulate the proliferation of MC-38 cells through Enterotoxigenic Bacteroides fragilis (ETBF)-primed Tregs and preventing the advance of colon cancer (52). Moreover, Xihuang (XH) Pill reduced the proliferation of Tregs in the TME of breast cancer and induced the apoptosis of Tregs by suppressing PI3K/Akt/AP-1 signaling pathway, thus reversing the immune escape to attenuate the tumor growth (53). The imbalance of Th17/Treg often occurs in autoimmune diseases and inflammation (57), which could be effectively ameliorated by Chinese medicine compounds. CSD restored the balance of Th17/Treg by decreasing the proportion of Th17, Treg and the related inflammatory factors to improve immune function (58).

Inflammation is often closely associated with the advance of cancer, thereby adjusting Th17/Treg balance in cancer may be helpful to relieve tumor-mediated immunosuppression. On the one hand, QX down-regulated Foxo1-mediated Foxp3, reduced Tregs and recovered the balance of Th17/Treg, thus playing a therapeutic role in CRC (44). On the other hand, Liu et al. found that Fuzheng Fangai combined with cyclophosphamide (CTX) effectively decreased the proportion of Th17 and Treg in spleen and tumor tissues of LLC tumor-bearing mice and restored the ratio of Th17/Treg. Meanwhile, the secretion of IL-17, IL-23 and IFN-γ, the mRNA levels of Foxp3 and RORγt as well as the protein levels of SOCS3, JAK2, and STAT3 were remarkably down-regulated by combined therapy compared to CTX alone (54). Summarily, Chinese medicine compounds are capable of suppressing tumor development through the inhibitory effects on Tregs (**Table 2**) (**Figure 1**).

THE IMMUNOREGULATORY PATTERNS OF CHINESE MEDICINE COMPOUNDS IN CANCER THERAPY

Improve Tumor-Induced Inflammation

Chronic inflammation serves as a risk factor for cancers. Tumor-induced inflammation accelerates the enrichment and activity of inflammatory cells in tumor tissue, thereby promoting tumor progression (59). Therefore, it may be feasible to treat cancers through improving inflammation to enhance immune function by Chinese medicine compounds (**Figure 2**). CRC was the third common cancer around the world, the morbidity of which ranked the second. Statistically, the incidence of CRC was higher in transition countries (1). Banxia Xiexin decoction (BXD) has been often applied to treat a variety of inflammatory diseases, including acute and chronic gastritis, oral ulcer, digestive ulcer, and so on. Yan et al. found that BXD enhanced the serum level of pro-inflammatory cytokines IL-1β, TNF-α and IL-6 in colon cancer-bearing nude mice and improve inflammation (60). With the popularization of the hepatitis B vaccine, the total incidence and mortality of liver cancer have been declining in the past three decades, whereas primary liver cancer still continues. HCC is the most common primary liver cancer (1). Hepatic fibrosis is the most vital hazard factor of HCC (61). Yang et al. established chronic liver fibrosis models with CCl_4 or MCD and found that CKI remarkably attenuated the infiltration of macrophages in the livers of these mice, down-regulated the expression of TNF-α and IL-6, thus alleviating the inflammatory response induced by liver fibrosis. Furthermore, Smad7 was identified as a key target of CKI in the treatment of liver fibrosis. CKI up-regulated Smad7, inhibited TNF-βR1, and suppressed TNF-β/Smad signaling pathway to prevent the development of chronic liver fibrosis and HCC (62). NHE-06 exerted a strong anti-inflammatory activity on HCC through the suppression of NF-κB/IL-6/STAT3 signaling and TGF-α and PTSG2. Meanwhile, NHE-06 strengthened the anti-tumor immunity by increasing the infiltration of immune cells and the production of IFN-γ. However, the preventive and therapeutic efficacy against HCC could be merely realized in mice with an intact immune system (63). Breast cancer has become the most common malignant tumor in the world and one of the main causes of death in females (1). Ruyiping (RYP) has been reported as a traditional Chinese medicine formula for breast cancer metastasis. Ye et al. found that in breast cancer 4T1-bearing mice, RYP combined with Platycodon grandiflorum (RP) effectively decreased the content of inflammatory marker Fibrinogen and inflammation-associated cytokines IL-6 and IL-1β in the lung tissue, improved the pulmonary inflammatory microenvironment resulted from breast cancer, and prevented the lung metastasis of breast cancer (64). According to Global Cancer Statistics 2020, lung cancer has become the most deadly malignant tumor in the world, whose morbidity ranked second among all cancers (1). Kejinyan decoction is an empirical prescription of traditional Chinese medicine for lung cancer clinically. Chen et al. reported that, after intervention with Kejinyan decoction, the inflammatory cytokines TNF-α, IFN-γ, IL-6, IL-4 and IL-13 were reduced and the survival of LLC tumor-bearing mice was prolonged (65). In short, Chinese medicine compounds could regulate the secretion of inflammatory cytokines to improve the inflammatory response in cancers.

Enhance Immunity After Surgery or Chemotherapy

Surgery and chemotherapy are the common treatments for cancers. However, side effects are always the major concern and limitation. Surgery tends to trigger inflammation, which leads to various unfavorable prognoses. Chemotherapy can damage the immune system even more. Therefore, Chinese medicine compounds combined with surgery or chemotherapy are typically used in clinical treatments to enhance efficacy and reduce side effects (**Figure 2**). Transcatheter arterial chemoembolization (TACE) has been identified as one of the therapies for HCC (66). Dai et al. reported DZP combined with TACE enhanced the immune functional indexes in serum and the number of $CD4^+/CD8^+$ T cells and reduced VEGF, TGF-β1 and MMP-2 to ameliorate cancer metastasis and other adverse reactions after TACE (67). A clinical trial has demonstrated that San Huang decoction remarkably reduced the volume of exudate after breast cancer surgery and the expression of TNF-α, IL-6, IL-8 and C-reactive protein (CRP) to improve the inflammation. Some studies have illustrated that Chinese medicine compounds could not only enhance the effectiveness of chemotherapy (23, 46, 48), but also alleviate the side effects of chemotherapy, including diarrhea, weight loss and other symptoms of hypoimmunity. PHY906 has been utilized for thousands of years to treat gastrointestinal diseases. In recent years, it has been developed as an adjuvant for cancer. Lam et al. found that PHY906 was capable of accelerating the infiltration of macrophages into tumors by inducing the up-regulation of macrophage cytokines hMCP1, dramatically promoted the conversion of macrophages to M1, and enhanced the anti-tumor effects of Sorafenib (68). In addition, Ciji-Hua'ai-Baosheng improved the immune function of H-22 tumor-bearing mice after

treatment with chemotherapy and alleviated CTX-induced colitis, manifested as elevated lymphocytes in spleen, augmented IL-2, IFN-γ and TNF-α, and the reduced IL-6 in serum and tumor tissues (69). Similarly, Wu et al. found Gegen Qinlian decoction (GQT), a classic Chinese medicine compound widely applys to gastrointestinal inflammatory diseases, assisted the anti-tumor effects of irinotecan (CPT-11) on colon cancer. It reversed the abnormal enhancement of IL-1β, COX-2, ICAM-1, and TNF-α. Moreover, GQT relieved diarrhea in CPT-11-treated patients by restraining hCE2 (70). Tumor suppressor p53 has been considered to be able to regulate immunity. Inactivated p53 may influence the effects of BMCs and T cells (71). Wei et al. reported that Yangyin Fuzheng Decoction promoted the infiltration of inflammatory cells to improve anti-tumor immunity and restore the CDDP-mediated weight loss of mice (72). Thus, Chinese medicine compounds combined with conventional therapy are expected to be a promising treatment for patients suffering from malignant tumors.

Block the Immune Checkpoints

Immune checkpoints represent a series of molecules on immune cells, which are recognized as switches of immune functions. In the TME, immune checkpoints are often overexpressed or activated, leading to the paralysis of the immune system. PD-1 and its ligand 1 (PD-L1) are the pivotal immune checkpoints that promote immune escape and cancer advance. Targeting the PD-1/PD-L1 axis has been effective immunotherapy against cancer (73). The combined therapy of GQT and PD-1 blocker effectively accelerated the proliferation of $CD8^+$ T cells and restored the T-cell function by up-regulating IL-2 and IFN-γ. Moreover, some Chinese medicine compounds themselves exerted blocking effects on immune checkpoints. Bu Fei Decoction adjusted the immunosuppressive TAMs in non-small cell lung cancer (NSCLC) and inhibited its tumor-promoting effect by down-regulating IL-10 and PD-L1 (74). Studies have found that the PI3K/Akt signaling pathway assisted the activation of PD-1/PD-L1 axis. Teng et al. summarized that the active ingredients of Huoxue Yiqi Recipe-2 (HYR-2) targeted PD-L1 signaling pathway in the treatment of lung cancer. HYR-2 could turn M2 to M1 through down-regulating PD-L1 that is closely associated with the blockage of PI3K/Akt signaling pathway (75). Xu et al. observed that Modified Bu-zhong-yi-qi decoction suppressed the expression of PD-L1 through blocking PI3K/Akt signaling pathway in gastric cancer, thereby up-regulating the ratio of $CD4^+/CD8^+$ T cells and the number of $CD8^+PD\text{-}1^+$ T cells as well as decreasing the proportion of $PD\text{-}1^+$ Tregs induced by chemotherapy, representing as a promising therapy for gastric cancer (76). PI3Kγ is an immune checkpoint for macrophages, which can switch the polarization of macrophages to reshape immune microenvironment and control immune suppression in cancers (77). Yuan et al. reported that Modified Jian-pi-yang-zheng decoction down-regulated PI3Kγ remarkably, promoted the secretion of TNF-α and IL-1β while decreased IL-10, accelerated the conversion of M2 to M1 and the differentiation of TAMs, thus prevented the progression and metastasis of gastric cancer (78) (**Figure 2**). Although immune checkpoint has gained great attention in tumor immunotherapy, the impacts of Chinese medicine compounds on immune checkpoints are not fully investigated.

Other Potential Ways

Recently, erythroid progenitor cell (EPC) has been known as the regulator in tumor immune response. In malignant tumors, EPCs did not differentiate into mature red blood cells and have inhibitory effects on tumor immunity (79). Li et al. reported that Danggui Buxue decoction reduced the abnormal accumulation of EPCs in melanoma and accelerated EPCs to differentiate into mature red blood cells, which led to relieving anemia, enhancing tumor immune response, and inhibiting the progression of melanoma (80). Estrogen/estrogen receptor (ER) has also been considered as a possible immunotherapy target for cancers (81). There are two forms of ER, ERα and ERβ. When the increase in ERα level leads to the imbalanced ratio of ERα/ERβ or the mutation rate of ERα augments, it is more likely to induce breast cancer. XH formula has been used for the treatment of breast cancer since 1740, which suppressed the proliferation and activity of breast cancer cells in dose- and time-dependent manners. Hao et al. reported that XH formula bond to ERα and HSP90, promoting the disintegration of ERα, and blocking the transmission of ERα signaling. Through this anti-estrogen-like effect, XH formula inhibited the progression of breast tumors (82). Moreover, it was reported that Shugan Liangxue (SGLX) decoction suppressed the protein levels of ERα and 17β-estradiol (E2) target genes, c-Myc and Bcl-2, in human breast cancer cells. It was speculated that SGLX exerted inhibitory effects on ER^+ breast cancer cells selectively (83) (**Figure 2**).

PERSPECTIVES

There are various ways of Chinese medicine compounds to exert anti-tumor activity, including blocking cell cycle, inhibiting cell viability and proliferation, inducing cell apoptosis, preventing cell invasion and migration, and enhancing the sensitivity of tumor cells to chemotherapy drugs, etc. In recent years, immunotherapy has become the most promising field in cancer therapy. Regulating immune cells has been proved to be a powerful weapon against cancers and is increasingly applied clinically. Traditional Chinese medicine or its extracts have been reported to play a variety of roles in immune cells, thereby enhancing innate and adaptive immunity (84, 85). By the advantages of multi-components and multi-targets, Chinese medicine compounds have more comprehensive effects and mechanisms of regulating tumor immunity. Traditional Chinese medicine compound preparations, such as traditional Chinese medicine patent prescription and Chinese medicine compound injection, have been put into application clinically due to their anti-tumor and anti-inflammatory activity. The studies on mechanisms of Chinese medicine compounds enhancing tumor immunity mostly concentrated on the number and activity of immune cells in the TME, however, more in-depth and systematic researches are still needed and worth being further explored, including but not limited to: the targeted immune cell types which were regulated specifically by Chinese medicine compounds, the direct targets

and pathways, either in immune cells or cancer cells, which mediated the immunotherapeutic effects of Chinese medicine compounds, the different immunomodulatory effects in distinct TME, the combined effect of immunoregulating Chinese medicine compounds with chemotherapy or immunotherapy drugs. Furthermore, the roles of various components in Chinese medicine compounds and their interplay or relationship in different symptoms is another important question. Nowadays, researchers try to depict formulas of traditional Chinese medicine compounds and optimize new formulations with more active ingredients and better therapeutic effects. Therefore, it is necessary to carry out more systematic researches on the immunoregulatory and pharmacological effect of TCM on cancer therapy and the underlying mechanisms to provide the more comprehensive theoretical basis for the clinical application of Chinese medicine compounds in cancer treatment.

AUTHOR CONTRIBUTIONS

FC drafted the manuscript. JL, HW and QB drafted and revised the manuscript. All authors contributed to the article and approved the submitted version.

FUNDING

This study was supported by grants from the National Natural Science Foundation of China (81630086, 82030099, and 81973078), National Key R&D Program of China (2018YFC2000700), Shanghai Municipal Human Resources and Social Security Bureau (2018060), Shanghai Public Health System Construction Three-Year Action Plan (GWV-10.1-XK15), and Innovative Research Team of High-Level Local Universities in Shanghai.

REFERENCES

1. Sung H, Ferlay J, Siegel RL, Laversanne M, Soerjomataram I, Jemal A, et al. Global Cancer Statistics 2020: GLOBOCAN Estimates of Incidence and Mortality Worldwide for 36 Cancers in 185 Countries. *CA Cancer J Clin* (2021) 71(3):209–49. doi: 10.3322/caac.21660
2. Roma-Rodrigues C, Mendes R, Baptista PV, Fernandes AR. Targeting Tumor Microenvironment for Cancer Therapy. *Int J Mol Sci* (2019) 20(4):840. doi: 10.3390/ijms20040840
3. Fan Y, Ma Z, Zhao L, Wang W, Gao M, Jia X, et al. Anti-Tumor Activities and Mechanisms of Traditional Chinese Medicines Formulas: A Review. *BioMed Pharmacother* (2020) 132:110820. doi: 10.1016/j.biopha.2020.110820
4. Dedong C, Huilin X, Anbing H, Ximing X, Wei G. The Effect of ShenQi FuZheng Injection in Combination With Chemotherapy *Versus* Chemotherapy Alone on the Improvement of Efficacy and Immune Function in Patients With Advanced Non-Small Cell Lung Cancer: A Meta-Analysis. *PLoS One* (2016) 11(3):e0152270. doi: 10.1371/journal.pone.0152270
5. Cao ZY, Chen XZ, Liao LM, Peng J, Hu HX, Liu ZZ, et al. Fuzheng Yiliu Granule Inhibits the Growth of Hepatocellular Cancer by Regulating Immune Function and Inducing Apoptosis *In Vivo* and *In Vitro*. *Chin J Integr Med* (2011) 17(9):691–7. doi: 10.1007/s11655-011-0847-3
6. Yang Q, Guo N, Zhou Y, Chen J, Wei Q, Han M. The Role of Tumor-Associated Macrophages (TAMs) in Tumor Progression and Relevant Advance in Targeted Therapy. *Acta Pharm Sin B* (2020) 10(11):2156–70. doi: 10.1016/j.apsb.2020.04.004
7. Rhee I. Diverse Macrophages Polarization in Tumor Microenvironment. *Arch Pharm Res* (2016) 39(11):1588–96. doi: 10.1007/s12272-016-0820-y
8. Ma Y, Shurin GV, Peiyuan Z, Shurin MR. Dendritic Cells in the Cancer Microenvironment. *J Cancer* (2013) 4(1):36–44. doi: 10.7150/jca.5046
9. Tran Janco JM, Lamichhane P, Karyampudi L, Knutson KL. Tumor-Infiltrating Dendritic Cells in Cancer Pathogenesis. *J Immunol* (2015) 194 (7):2985–91. doi: 10.4049/jimmunol.1403134
10. Guillerey C. NK Cells in the Tumor Microenvironment. *Adv Exp Med Biol* (2020) 1273:69–90. doi: 10.1007/978-3-030-49270-0_4
11. Gabrilovich DI. Myeloid-Derived Suppressor Cells. *Cancer Immunol Res* (2017) 5(1):3–8. doi: 10.1158/2326-6066.Cir-16-0297
12. Yao F, Yuan Q, Song X, Zhou L, Liang G, Jiang G, et al. Yupingfeng Granule Improves Th2-Biased Immune State in Microenvironment of Hepatocellular Carcinoma Through TSLP-DC-OX40L Pathway. *Evid Based Complement Alternat Med* (2020) 2020:1263053. doi: 10.1155/2020/1263053
13. Basu A, Ramamoorthi G, Albert G, Gallen C, Beyer A, Snyder C, et al. Differentiation and Regulation of T(H) Cells: A Balancing Act for Cancer Immunotherapy. *Front Immunol* (2021) 12:669474. doi: 10.3389/fimmu.2021.669474
14. Guéry L, Hugues S. Th17 Cell Plasticity and Functions in Cancer Immunity. *BioMed Res Int* (2015) 2015:314620. doi: 10.1155/2015/314620
15. Chang SH. T Helper 17 (Th17) Cells and Interleukin-17 (IL-17) in Cancer. *Arch Pharm Res* (2019) 42(7):549–59. doi: 10.1007/s12272-019-01146-9
16. He QF, Xu Y, Li J, Huang ZM, Li XH, Wang X. CD8+ T-Cell Exhaustion in Cancer: Mechanisms and New Area for Cancer Immunotherapy. *Brief Funct Genomics* (2019) 18(2):99–106. doi: 10.1093/bfgp/ely006
17. Takeuchi Y, Nishikawa H. Roles of Regulatory T Cells in Cancer Immunity. *Int Immunol* (2016) 28(8):401–9. doi: 10.1093/intimm/dxw025
18. Zhou J, Li X, Wu X, Zhang T, Zhu Q, Wang X, et al. Exosomes Released From Tumor-Associated Macrophages Transfer miRNAs That Induce a Treg/Th17 Cell Imbalance in Epithelial Ovarian Cancer. *Cancer Immunol Res* (2018) 6 (12):1578–92. doi: 10.1158/2326-6066.Cir-17-0479
19. Li X, Liu R, Su X, Pan Y, Han X, Shao C, et al. Harnessing Tumor-Associated Macrophages as Aids for Cancer Immunotherapy. *Mol Cancer* (2019) 18 (1):177. doi: 10.1186/s12943-019-1102-3
20. Orecchioni M, Ghosheh Y, Pramod AB, Ley K. Macrophage Polarization: Different Gene Signatures in M1(LPS+) *vs.* Classically and M2(LPS-) *vs.* Alternatively Activated Macrophages. *Front Immunol* (2019) 10:1084. doi: 10.3389/fimmu.2019.01084
21. Zhou JY, Chen M, Wu CE, Zhuang YW, Chen YG, Liu SL. The Modified Si-Jun-Zi Decoction Attenuates Colon Cancer Liver Metastasis by Increasing Macrophage Cells. *BMC Complement Altern Med* (2019) 19(1):86. doi: 10.1186/s12906-019-2498-4
22. Ma WP, Hu SM, Xu YL, Li HH, Ma XQ, Wei BH, et al. Haimufang Decoction, a Chinese Medicine Formula for Lung Cancer, Arrests Cell Cycle, Stimulates Apoptosis in NCI-H1975 Cells, and Induces M1 Polarization in RAW 264.7 Macrophage Cells. *BMC Complement Med Ther* (2020) 20(1):243. doi: 10.1186/s12906-020-03031-1
23. Yang Y, Sun M, Yao W, Wang F, Li X, Wang W, et al. Compound Kushen Injection Relieves Tumor-Associated Macrophage-Mediated Immunosuppression Through TNFR1 and Sensitizes Hepatocellular Carcinoma to Sorafenib. *J Immunother Cancer* (2020) 8(1):e000317. doi: 10.1136/jitc-2019-000317
24. Wang L, Wu W, Zhu X, Ng W, Gong C, Yao C, et al. The Ancient Chinese Decoction Yu-Ping-Feng Suppresses Orthotopic Lewis Lung Cancer Tumor Growth Through Increasing M1 Macrophage Polarization and CD4(+) T Cell Cytotoxicity. *Front Pharmacol* (2019) 10:1333. doi: 10.3389/fphar.2019.01333
25. Zheng Y, Wang N, Wang S, Yang B, Situ H, Zhong L, et al. XIAOPI Formula Inhibits the Pre-Metastatic Niche Formation in Breast Cancer *via* Suppressing TAMs/CXCL1 Signaling. *Cell Commun Signal* (2020) 18(1):48. doi: 10.1186/s12964-020-0520-6
26. Deshmane SL, Kremlev S, Amini S, Sawaya BE. Monocyte Chemoattractant Protein-1 (MCP-1): An Overview. *J Interferon Cytokine Res* (2009) 29(6):313–26. doi: 10.1089/jir.2008.0027
27. Chen C, Yao X, Xu Y, Zhang Q, Wang H, Zhao L, et al. Dahuang Zhechong Pill Suppresses Colorectal Cancer Liver Metastasis *via* Ameliorating Exosomal CCL2 Primed Pre-Metastatic Niche. *J Ethnopharmacol* (2019) 238:111878. doi: 10.1016/j.jep.2019.111878

28. Wu J, Zhang XX, Zou X, Wang M, Wang HX, Wang YH, et al. The Effect of Jianpi Yangzheng Xiaozheng Decoction and its Components on Gastric Cancer. *J Ethnopharmacol* (2019) 235:56–64. doi: 10.1016/j.jep.2019.02.003
29. Zhao B, Hui X, Jiao L, Bi L, Wang L, Huang P, et al. A TCM Formula YYWY Inhibits Tumor Growth in Non-Small Cell Lung Cancer and Enhances Immune-Response Through Facilitating the Maturation of Dendritic Cells. *Front Pharmacol* (2020) 11:798. doi: 10.3389/fphar.2020.00798
30. Yang Y, Ma Y, Wang Z, Wang L, Zhao Y, Hui Y, et al. Compound Kushen Injection Promoted the Killing Effect of Cytokine-Induced Killer Cells Which Was Activated by Dendritic-Colon Cancer Stem Cell Fusion Cells on Colon Cancer Stem Cells. *J Biomater Tissue Eng* (2020) 10(7):957–65. doi: 10.1166/jbt.2020.2362
31. Luo Y, Wu J, Zhu X, Gong C, Yao C, Ni Z, et al. NK Cell-Dependent Growth Inhibition of Lewis Lung Cancer by Yu-Ping-Feng, an Ancient Chinese Herbal Formula. *Mediators Inflamm* (2016) 2016:3541283. doi: 10.1155/2016/3541283
32. Que ZJ, Yao JL, Zhou ZY, Yu P, Luo B, Li HG, et al. Jinfukang Inhibits Lung Cancer Metastasis by Upregulating CX3CL1 to Recruit NK Cells to Kill CTCs. *J Ethnopharmacol* (2021) 275:114175. doi: 10.1016/j.jep.2021.114175
33. Yang PM, Du JL, Wang GN, Chia JS, Hsu WB, Pu PC, et al. The Chinese Herbal Mixture Tien-Hsien Liquid Augments the Anticancer Immunity in Tumor Cell-Vaccinated Mice. *Integr Cancer Ther* (2017) 16(3):319–28. doi: 10.1177/1534735416651492
34. Hong-Fen L, Waisman T, Maimon Y, Shakhar K, Rosenne E, Ben-Eliyahu S. The Effects of a Chinese Herb Formula, Anti-Cancer Number One (ACNO), on NK Cell Activity and Tumor Metastasis in Rats. *Int Immunopharmacol* (2001) 1(11):1947–56. doi: 10.1016/s1567-5769(01)00120-5
35. Mao D, Feng L, Gong H. The Antitumor and Immunomodulatory Effect of Yanghe Decoction in Breast Cancer Is Related to the Modulation of the JAK/STAT Signaling Pathway. *Evid Based Complement Alternat Med* (2018) 2018:8460526. doi: 10.1155/2018/8460526
36. Wang Y, Sun N, Luo Y, Fang Z, Fang Y, Tian J, et al. Yu-Ping-Feng Formula Exerts Antilung Cancer Effects by Remodeling the Tumor Microenvironment Through Regulating Myeloid-Derived Suppressor Cells. *Evid Based Complement Alternat Med* (2021) 2021:6624461. doi: 10.1155/2021/6624461
37. Xie Y, Zhang Y, Wei X, Zhou C, Huang Y, Zhu X, et al. Jianpi Huayu Decoction Attenuates the Immunosuppressive Status of H(22) Hepatocellular Carcinoma-Bearing Mice: By Targeting Myeloid-Derived Suppressor Cells. *Front Pharmacol* (2020) 11:16. doi: 10.3389/fphar.2020.00016
38. Tian S, Song X, Wang Y, Wang X, Mou Y, Chen Q, et al. Chinese Herbal Medicine Baoyuan Jiedu Decoction Inhibits the Accumulation of Myeloid Derived Suppressor Cells in Pre-Metastatic Niche of Lung *via* TGF-β/CCL9 Pathway. *BioMed Pharmacother* (2020) 129:110380. doi: 10.1016/j.biopha.2020.110380
39. Xu ZH, Zhu YZ, Su L, Tang XY, Yao C, Jiao XN, et al. Ze-Qi-Tang Formula Induces Granulocytic Myeloid-Derived Suppressor Cell Apoptosis *via* STAT3/S100A9/Bcl-2/Caspase-3 Signaling to Prolong the Survival of Mice With Orthotopic Lung Cancer. *Mediators Inflamm* (2021) 2021:8856326. doi: 10.1155/2021/8856326
40. Wei H, Guo C, Zhu R, Zhang C, Han N, Liu R, et al. Shuangshen Granules Attenuate Lung Metastasis by Modulating Bone Marrow Differentiation Through mTOR Signalling Inhibition. *J Ethnopharmacol* (2020) 281:113305. doi: 10.1016/j.jep.2020.113305
41. Guéry JC, Ria F, Galbiati F, Adorini L. Antigen Presentation and IL-12 Production by Dendritic Cells *In Vivo*. *Adv Exp Med Biol* (1997) 417:317–21. doi: 10.1007/978-1-4757-9966-8_52
42. Ito T, Wang YH, Duramad O, Hori T, Delespesse GJ, Watanabe N, et al. TSLP-Activated Dendritic Cells Induce an Inflammatory T Helper Type 2 Cell Response Through OX40 Ligand. *J Exp Med* (2005) 202(9):1213–23. doi: 10.1084/jem.20051135
43. Shimasaki N, Jain A, Campana D. NK Cells for Cancer Immunotherapy. *Nat Rev Drug Discov* (2020) 19(3):200–18. doi: 10.1038/s41573-019-0052-1
44. Chen D, Yang Y, Yang P. Quxie Capsule Inhibits Colon Tumor Growth Partially Through Foxo1-Mediated Apoptosis and Immune Modulation. *Integr Cancer Ther* (2019) 18:1534735419846377. doi: 10.1177/1534735419846377
45. Deng S, Tang Q, Duan X, Fan H, Zhang L, Zhu X, et al. Uncovering the Anticancer Mechanism of Compound Sophorae Decoction Against Ulcerative Colitis-Related Colorectal Cancer in Mice. *Evid Based Complement Alternat Med* (2019) 2019:8128170. doi: 10.1155/2019/8128170
46. Chuang MH, Jan MS, Chang JT, Lu FJ. The Chinese Medicine JC-001 Enhances the Chemosensitivity of Lewis Lung Tumors to Cisplatin by Modulating the Immune Response. *BMC Complement Altern Med* (2017) 17(1):210. doi: 10.1186/s12906-017-1728-x
47. Chuang MH, Chang JT, Hsu LJ, Jan MS, Lu FJ. Antitumor Activity of the Chinese Medicine JC-001 Is Mediated by Immunomodulation in a Murine Model of Hepatocellular Carcinoma. *Integr Cancer Ther* (2017) 16(4):516–25. doi: 10.1177/1534735416664173
48. Lu YT, Li J, Qi X, Pei YX, Shi WG, Lin HS. Effects of Shugan Jianpi Formula () on Myeloid-Derived Suppression Cells-Mediated Depression Breast Cancer Mice. *Chin J Integr Med* (2017) 23(6):453–60. doi: 10.1007/s11655-016-2734-4
49. Li W, Yang Y, Ouyang Z, Zhang Q, Wang L, Tao F, et al. Xiao-Ai-Ping, a TCM Injection, Enhances the Antigrowth Effects of Cisplatin on Lewis Lung Cancer Cells Through Promoting the Infiltration and Function of CD8(+) T Lymphocytes. *Evid Based Complement Alternat Med* (2013) 2013:879512. doi: 10.1155/2013/879512
50. Du J, Cheng BC, Fu XQ, Su T, Li T, Guo H, et al. *In Vitro* Assays Suggest Shenqi Fuzheng Injection has the Potential to Alter Melanoma Immune Microenvironment. *J Ethnopharmacol* (2016) 194:15–9. doi: 10.1016/j.jep.2016.08.038
51. Guo J, Wang JY, Zheng Z, Wang Q, Dong CS. [Effects of Chinese Herbal Medicine Feiyanning Decoction on the Ratio of CD4+CD25+ Regulatory T Cells and Expression of Transcription Factor Foxp3 in Mice Bearing Lewis Lung Carcinoma]. *Zhong Xi Yi Jie He Xue Bao* (2012) 10(5):584–90. doi: 10.3736/jcim20120515
52. Sui H, Zhang L, Gu K, Chai N, Ji Q, Zhou L, et al. YYFZBJS Ameliorates Colorectal Cancer Progression in Apc(Min/+) Mice by Remodeling Gut Microbiota and Inhibiting Regulatory T-Cell Generation. *Cell Commun Signal* (2020) 18(1):113. doi: 10.1186/s12964-020-00596-9
53. Su L, Jiang Y, Xu Y, Li X, Gao W, Xu C, et al. Xihuang Pill Promotes Apoptosis of Treg Cells in the Tumor Microenvironment in 4T1 Mouse Breast Cancer by Upregulating MEKK1/SEK1/JNK1/AP-1 Pathway. *BioMed Pharmacother* (2018) 102:1111–9. doi: 10.1016/j.biopha.2018.03.063
54. Liu S, Wang XM, Yang GW. Action Mechanism of Fuzheng Fangai Pill Combined With Cyclophosphamide on Tumor Metastasis and Growth. *Evid Based Complement Alternat Med* (2014) 2014:494528. doi: 10.1155/2014/494528
55. Kassouf N, Thornhill MH. Oral Cancer Cell Lines can Use Multiple Ligands, Including Fas-L, TRAIL and TNF-Alpha, to Induce Apoptosis in Jurkat T Cells: Possible Mechanisms for Immune Escape by Head and Neck Cancers. *Oral Oncol* (2008) 44(7):672–82. doi: 10.1016/j.oraloncology.2007.08.013
56. Saleh R, Elkord E. FoxP3(+) T Regulatory Cells in Cancer: Prognostic Biomarkers and Therapeutic Targets. *Cancer Lett* (2020) 490:174–85. doi: 10.1016/j.canlet.2020.07.022
57. Noack M, Miossec P. Th17 and Regulatory T Cell Balance in Autoimmune and Inflammatory Diseases. *Autoimmun Rev* (2014) 13(6):668–77. doi: 10.1016/j.autrev.2013.12.004
58. Xu M, Duan XY, Chen QY, Fan H, Hong ZC, Deng SJ, et al. Effect of Compound Sophorae Decoction on Dextran Sodium Sulfate (DSS)-Induced Colitis in Mice by Regulating Th17/Treg Cell Balance. *BioMed Pharmacother* (2019) 109:2396–408. doi: 10.1016/j.biopha.2018.11.087
59. Diakos CI, Charles KA, McMillan DC, Clarke SJ. Cancer-Related Inflammation and Treatment Effectiveness. *Lancet Oncol* (2014) 15(11):e493–503. doi: 10.1016/s1470-2045(14)70263-3
60. Yan S, Yue Y, Wang J, Li W, Sun M, Zeng L, et al. Banxia Xiexin Decoction, a Traditional Chinese Medicine, Alleviates Colon Cancer in Nude Mice. *Ann Transl Med* (2019) 7(16):375. doi: 10.21037/atm.2019.07.26
61. Shankaraiah RC, Callegari E, Guerriero P, Rimessi A, Pinton P, Gramantieri L, et al. Metformin Prevents Liver Tumourigenesis by Attenuating Fibrosis in a Transgenic Mouse Model of Hepatocellular Carcinoma. *Oncogene* (2019) 38(45):7035–45. doi: 10.1038/s41388-019-0942-z
62. Yang Y, Sun M, Li W, Liu C, Jiang Z, Gu P, et al. Rebalancing TGF-β/Smad7 Signaling *via* Compound Kushen Injection in Hepatic Stellate Cells Protects Against Liver Fibrosis and Hepatocarcinogenesis. *Clin Transl Med* (2021) 11:e410. doi: 10.1002/ctm2.410
63. Lu X, Wo G, Li B, Xu C, Wu J, Jiang C, et al. The Anti-Inflammatory NHE-06 Restores Antitumor Immunity by Targeting NF-κb/IL-6/STAT3 Signaling in

Hepatocellular Carcinoma. *BioMed Pharmacother* (2018) 102:420–7. doi: 10.1016/j.biopha.2018.03.099
64. Ye Y, Pei L, Wu C, Liu S. Protective Effect of Traditional Chinese Medicine Formula RP on Lung Microenvironment in Pre-Metastasis Stage of Breast Cancer. *Integr Cancer Ther* (2019) 18:1534735419876341. doi: 10.1177/1534735419876341
65. Chen M, Hu C, Gao Q, Li L, Cheng Z, Li Q, et al. Study on Metastasis Inhibition of Kejinyan Decoction on Lung Cancer by Affecting Tumor Microenvironment. *Cancer Cell Int* (2020) 20:451. doi: 10.1186/s12935-020-01540-0
66. Liu J, Yi J. Relationship Between the Changes of VEGF Level and Dendritic Cells in Peripheral Blood of Patients With Hepatocellular Carcinoma After Transcatheter Arterial Chemoembolization. *J Huazhong Univ Sci Technolog Med Sci* (2007) 27(1):58–60. doi: 10.1007/s11596-007-0117-y
67. Dai CM, Jin S, Zhang JZ. Effect of Dahuang Zhechong Pills Combined With TACE on VEGF, MMP-2, TGF-β1 and Immune Function of Patients With Primary Liver Cancer (Blood Stasis and Collaterals Blocking Type). *Zhongguo Zhong Yao Za Zhi* (2021) 46(3):722–9. doi: 10.19540/j.cnki.cjcmm.20200716.501
68. Lam W, Jiang Z, Guan F, Huang X, Hu R, Wang J, et al. PHY906(KD018), an Adjuvant Based on a 1800-Year-Old Chinese Medicine, Enhanced the Anti-Tumor Activity of Sorafenib by Changing the Tumor Microenvironment. *Sci Rep* (2015) 5:9384. doi: 10.1038/srep09384
69. Xi S, Fu B, Loy G, Minuk GY, Peng Y, Qiu Y, et al. The Effects of Ciji-Hua'ai-Baosheng on Immune Function of Mice With H(22) Hepatocellular Carcinoma Receiving Chemotherapy. *BioMed Pharmacother* (2018) 101:898–909. doi: 10.1016/j.biopha.2018.03.027
70. Wu Y, Wang D, Yang X, Fu C, Zou L, Zhang J. Traditional Chinese Medicine Gegen Qinlian Decoction Ameliorates Irinotecan Chemotherapy-Induced Gut Toxicity in Mice. *BioMed Pharmacother* (2019) 109:2252–61. doi: 10.1016/j.biopha.2018.11.095
71. Blagih J, Buck MD, Vousden KH. P53, Cancer and the Immune Response. *J Cell Sci* (2020) 133(5):jcs237453. doi: 10.1242/jcs.237453
72. Wei D, Wang L, Chen Y, Yin G, Jiang M, Liu R, et al. Yangyin Fuzheng Decoction Enhances Anti-Tumor Efficacy of Cisplatin on Lung Cancer. *J Cancer* (2018) 9(9):1568–74. doi: 10.7150/jca.24525
73. Ai L, Xu A, Xu J. Roles of PD-1/PD-L1 Pathway: Signaling, Cancer, and Beyond. *Adv Exp Med Biol* (2020) 1248:33–59. doi: 10.1007/978-981-15-3266-5_3
74. Pang L, Han S, Jiao Y, Jiang S, He X, Li P. Bu Fei Decoction Attenuates the Tumor Associated Macrophage Stimulated Proliferation, Migration, Invasion and Immunosuppression of non-Small Cell Lung Cancer, Partially *via* IL-10 and PD-L1 Regulation. *Int J Oncol* (2017) 51(1):25–38. doi: 10.3892/ijo.2017.4014
75. Teng L, Wang K, Chen W, Wang YS, Bi L. HYR-2 Plays an Anti-Lung Cancer Role by Regulating PD-L1 and Akkermansia Muciniphila. *Pharmacol Res* (2020) 160:105086. doi: 10.1016/j.phrs.2020.105086
76. Xu R, Wu J, Zhang X, Zou X, Li C, Wang H, et al. Modified Bu-Zhong-Yi-Qi Decoction Synergies With 5 Fluorouracile to Inhibits Gastric Cancer Progress *via* PD-1/PD- L1-Dependent T Cell Immunization. *Pharmacol Res* (2020) 152:104623. doi: 10.1016/j.phrs.2019.104623
77. Kaneda MM, Messer KS, Ralainirina N, Li H, Leem CJ, Gorjestani S, et al. Pi3kγ Is a Molecular Switch That Controls Immune Suppression. *Nature* (2016) 539(7629):437–42. doi: 10.1038/nature19834
78. Yuan M, Zou X, Liu S, Xu X, Wang H, Zhu M, et al. Modified Jian-Pi-Yang-Zheng Decoction Inhibits Gastric Cancer Progression via the Macrophage Immune Checkpoint PI3Kγ. *BioMed Pharmacother* (2020) 129:110440. doi: 10.1016/j.biopha.2020.110440
79. Grzywa TM, Justyniarska M, Nowis D, Golab J. Tumor Immune Evasion Induced by Dysregulation of Erythroid Progenitor Cells Development. *Cancers (Basel)* (2021) 13(4):870. doi: 10.3390/cancers13040870
80. Li C, Zhu F, Xu C, Xiao P, Wen J, Zhang X, et al. Dangguibuxue Decoction Abolishes Abnormal Accumulation of Erythroid Progenitor Cells Induced by Melanoma. *J Ethnopharmacol* (2019) 242:112035. doi: 10.1016/j.jep.2019.112035
81. Wang T, Jin J, Qian C, Lou J, Lin J, Xu A, et al. Estrogen/ER in Anti-Tumor Immunity Regulation to Tumor Cell and Tumor Microenvironment. *Cancer Cell Int* (2021) 21(1):295. doi: 10.1186/s12935-021-02003-w
82. Hao J, Jin Z, Zhu H, Liu X, Mao Y, Yang X, et al. Antiestrogenic Activity of the Xi-Huang Formula for Breast Cancer by Targeting the Estrogen Receptor α. *Cell Physiol Biochem* (2018) 47(6):2199–215. doi: 10.1159/000491533
83. Zhou N, Han SY, Chen YZ, Zhou F, Zheng WX, Li PP. Shugan Liangxue Decoction () Down-Regulates Estrogen Receptor α Expression in Breast Cancer Cells. *Chin J Integr Med* (2018) 24(7):518–24. doi: 10.1007/s11655-015-2123-4
84. Wang S, Long S, Deng Z, Wu W. Positive Role of Chinese Herbal Medicine in Cancer Immune Regulation. *Am J Chin Med* (2020) 48(7):1577–92. doi: 10.1142/s0192415x20500780
85. Wang Y, Zhang Q, Chen Y, Liang CL, Liu H, Qiu F, et al. Antitumor Effects of Immunity-Enhancing Traditional Chinese Medicine. *BioMed Pharmacother* (2020) 121:109570. doi: 10.1016/j.biopha.2019.109570

Conflict of Interest: The authors declare that the research was conducted in the absence of any commercial or financial relationships that could be construed as a potential conflict of interest.

Publisher's Note: All claims expressed in this article are solely those of the authors and do not necessarily represent those of their affiliated organizations, or those of the publisher, the editors and the reviewers. Any product that may be evaluated in this article, or claim that may be made by its manufacturer, is not guaranteed or endorsed by the publisher.

GLOSSARY

ACNO	Anti-cancer No.1
Akt	Protein kinase B
AP-1	Activator protein-1
APCs	Antigen presenting cells
Arg-1	Arginase-1
Bax	Bcl2-Associated X
Bcl-2	B-cell lymphoma-2
BMCs	Bone marrow cells
BMDCs	Bone marrow dendritic cells
BXD	Banxia Xiexin decoction
BYJD	Baoyuan Jiedu decoction
CCL2/CCR2	Chemokine (C-C motif) ligand 2/C-C chemokine receptor type 2
CCl_4	Carbon tetrachloride
CCL9	Chemokine (C-C motif) ligand 9
CDDP	Cisplatin
CIK cells	Cytokines induce killer cells
CKI	Compound kushen injection
COX-2	Cyclooxygenase-2
CPT-11	irinotecan
CRC	Colorectal cancer
CRP	C-reactive protein
CSCs	Cancer stem cells
CSD	Compound Sophorae Decoction
CTCs	Circulating tumor cells
CTL/Tc	Cytotoxic T cell
CTX	Cyclophosphamide
CXCL1	Chemokine (C-X-C motif) Ligand 1
CX3CL1	Chemokine (C-X3-C motif) Ligand 1
DCs	Dendritic cells
DC-cCSC FCs	Fusion cells of dendritic colon cancer stem cells
DZP	Dahuang Zhechong Pills
E2	Estradiol
EPC	Erythroid progenitor cell
ER	Estrogen receptor
ERK	Extracellular regulated protein kinases
ETBF	enterotoxigenic bacteroides fragilis
Fas/FasL	Factor associated suicide/Fas Ligand
FCs	Fusion cells
FN	Fibronectin
Foxo1	Forkhead box O1
Foxp3	Forkhead box p3
GEM	gemcitabine
GM-CSF	Granulocyte-macrophage colony stimulating factor
GQT	Gegen Qinlian decoction
HCC	Hepatocellular carcinoma
hCE2	human carboxylesterase 2
hMCP1	Human monocyte chemoattractant protein-1
HMF	Haimufang
HSPCs	Hematopoietic stem-progenitor cells
HSP90	Heat shock protein 90
HYR-2	Huoxue Yiqi Recipe-2
ICAM-1	Intercellular adhesion molecule-1
IFN-γ/INF-γ	Interferon-gamma
IL	Interleukin
iNOS	Inducible nitric oxide synthase
JAK	Janus Kinase
JHD	Jianpi Huayu Decoction
JPYZ	Jianpi Yangzheng
Lag-3	Lymphocyte-activation gene 3
LLC	Lewis lung cancer
MAPK	Mitogen-activated protein kinase
MCD	Methionine-choline deficient
MDSCs	Myeloid-derived suppressor cells
MEK	Mitogen-activated protein kinase kinase
MHC	Major histocompatibility complex
MMP	Matrix metalloproteinase
mTOR	Mechanistic target of rapamycin
Myc	Myelocytomatosis oncogene
NF-κB	nuclear factor kappa-B
NK cells	Natural killer cells
NKT cells	Nature killer T cells
NO	nitric oxide
NSCLC	Non-small cell lung cancer
PARP	Poly ADP-ribose polymerase
PD-1/PD-L1	Programmed cell death protein 1/programmed cell death ligand 1
PI3K	phosphatidylinositol 3 kinase
PMN	Pre-metastatic niche
PTSG2	Prostaglandin-endoperoxide synthase 2
QX	Quxie capsule
ROS	Reactive oxygen species
RORγt	Retinoid-related orphan receptor-gammat
RP	RYP with Platycodon grandiflorum
RYP	Ruyiping
S6K1	Ribsosmal protein S6 kinase 1
SFI	ShenQi FuZheng injection
SGLX	Shugan Liangxue
Smad	Small mothers against decapentaplegic
SOCS3	Suppressor of cytokine signaling 3
STAT	Signal transducer and activator of transcription
T cell	T lymphocyte
TACE	Transcatheter arterial chemoembolization
TAMs	Tumor associated macrophages
TCM	Traditional Chinese medicine
TGF	Transforming growth factor
Th	Helper T lymphocytes
Th0	naïve T lymphocytes
THL	Tien-Hsien liquid
TIGIT	T-cell immunoreceptor with Ig and ITIM domains
Tim-3	T-cell immunoglobulin and mucin-domain containing-3
TME	Tumor microenvironment
TNF	Tumor necrosis factor
TNFR1	Tumor necrosis factor receptor superfamily member 1
Treg	Regulatory T cell
TSLP	Thymic stromal lymphopoietin
UCRCC	Ulcerative Colitis-Related Colorectal Cancer
VEGF	Vascular endothelial growth factor
XP	XIAOPI
XH	Xi Huang
YHD	Yanghe Decoction
YPF	Yu-ping-feng
YYFZBJS	Yi-Yi-Fu-Zi-Bai-Jiang-San
YYWY	Yangyin Wenyang
ZQT	Ze-Qi-Tang

frontiers in Pharmacology

ORIGINAL RESEARCH
published: 16 November 2021
doi: 10.3389/fphar.2021.723147

A System Pharmacology Model for Decoding the Synergistic Mechanisms of Compound Kushen Injection in Treating Breast Cancer

Yi Li[1†], Kexin Wang[2,3†], Yupeng Chen[4,5], Jieqi Cai[4,5], Xuemei Qin[6], Aiping Lu[2], Daogang Guan[4,5], Genggeng Qin[1]* and Weiguo Chen[1]**

[1]Department of Radiology, Nanfang Hospital, Southern Medical University, Guangzhou, China, [2]Institute of Integrated Bioinformedicine and Translational Science, Hong Kong Baptist University, Hong Kong SAR, China, [3]Neurosurgery Center, Guangdong Provincial Key Laboratory on Brain Function Repair and Regeneration, Department of Cerebrovascular Surgery, Engineering Technology Research Center of Education Ministry of China on Diagnosis and Treatment of Cerebrovascular Disease, Zhujiang Hospital, Southern Medical University, Guangzhou, China, [4]Department of Biochemistry and Molecular Biology, School of Basic Medical Sciences, Southern Medical University, Guangzhou, China, [5]Guangdong Key Laboratory of Biochip Technology, Southern Medical University, Guangzhou, China, [6]Modern Research Center for Traditional Chinese Medicine, Shanxi University, Taiyuan, China

OPEN ACCESS

Edited by:
Haiyang Yu,
Tianjin University of Traditional Chinese Medicine, China

Reviewed by:
Wei Wang,
Shanxi Zhendong Pharmaceutical, China
Tara Louise Pukala,
University of Adelaide, Australia

***Correspondence:**
Daogang Guan
guandg0929@hotmail.com
Genggeng Qin
zealotq@smu.edu.cn
Weiguo Chen
chen1999@smu.edu.cn

[†]These authors have contributed equally to this work and share first authorship

Specialty section:
This article was submitted to Pharmacology of Anti-Cancer Drugs, a section of the journal Frontiers in Pharmacology

Received: 10 June 2021
Accepted: 15 October 2021
Published: 16 November 2021

Citation:
Li Y, Wang K, Chen Y, Cai J, Qin X, Lu A, Guan D, Qin G and Chen W (2021) A System Pharmacology Model for Decoding the Synergistic Mechanisms of Compound Kushen Injection in Treating Breast Cancer. Front. Pharmacol. 12:723147. doi: 10.3389/fphar.2021.723147

Breast cancer (BC) is one of the most common malignant tumors among women worldwide and can be treated using various methods; however, side effects of these treatments cannot be ignored. Increasing evidence indicates that compound kushen injection (CKI) can be used to treat BC. However, traditional Chinese medicine (TCM) is characterized by "multi-components" and "multi-targets", which make it challenging to clarify the potential therapeutic mechanisms of CKI on BC. Herein, we designed a novel system pharmacology strategy using differentially expressed gene analysis, pharmacokinetics synthesis screening, target identification, network analysis, and docking validation to construct the synergy contribution degree (SCD) and therapeutic response index (TRI) model to capture the critical components responding to synergistic mechanisms of CKI in BC. Through our designed mathematical models, we defined 24 components as a high contribution group of synergistic components (HCGSC) from 113 potentially active components of CKI based on ADME parameters. Pathway enrichment analysis of HCGSC targets indicated that *Rhizoma Heterosmilacis* and *Radix Sophorae Flavescentis* could synergistically target the PI3K-Akt signaling pathway and the cAMP signaling pathway to treat BC. Additionally, TRI analysis showed that the average affinity of HCGSC and targets involved in the key pathways reached -6.47 kcal/mmol, while *in vitro* experiments proved that two of the three high TRI-scored components in the HCGSC showed significant inhibitory effects on breast cancer cell proliferation and migration. These results demonstrate the accuracy and reliability of the proposed strategy.

Abbreviations: ADME, absorption, distribution, metabolism, and excretion; BC, breast cancer; CKI, compound kushen injection; C-T network, component–target network; DEGs, differentially expressed gene analysis; HCGSC, high contribution group of synergistic components; HPLC, high performance liquid chromatography; HRDR, highly reliable docking relationship; SCD, synergy contribution degree; TCGA, The Cancer Genome Atlas; TCM, traditional Chinese medicine; TRI, therapeutic response index.

Keywords: breast cancer, compound kushen injection, traditional Chinese medicine, molecular docking, synergistic mechanism, system pharmacology

INTRODUCTION

Breast cancer (BC) is the most common cancer in women worldwide and is responsible for the second highest death rate among female patients with cancer (Siegel et al., 2020). Many options are available to treat breast cancer, such as surgical treatment (Zheng et al., 2020), radiation therapy (Balaji et al., 2016), neoadjuvant endocrine therapy (Yao et al., 2019), neoadjuvant chemotherapy (Vaidya et al., 2018), and anti-HER2 therapy (Yao and Fu, 2018). However, side effects of these treatments are often observed. For example, radiation therapy can cause radiation-induced fibrosis (Straub et al., 2015) and radiodermatitis (Singh et al., 2016). Fatigue, pain, and systemic side effects can occur as a result of surgical treatment (Enien et al., 2018). Adjuvant endocrine therapy can cause vasomotor symptoms and musculoskeletal and vulvovaginal symptoms (Condorelli and Vaz-Luis, 2018). These side effects mainly influence the organs and blood system, which aggravates the psychological burden on the patients. Side effect symptoms include loss of appetite, vomiting, diarrhea, nausea, and ulcers (Meng et al., 2017; Recht, 2017; Cochran et al., 2019). In recent years, traditional Chinese medicine (TCM) has become increasingly popular in the treatment of BC. *Ganoderma lucidum* from *Ganoderma* suppresses the proliferation and migration of breast cancer by inhibiting Wnt/β-catenin signaling (Zhang, 2017), while puerarin from *Radix puerariae* inhibits cell migration, invasion, and adhesion of LPS-induced BC by blocking NF-κB and Erk pathways (Liu et al., 2017). In addition to these herbal components, many formulas and proprietary Chinese medicines are widely used in the treatment of BC, such as compound kushen injection (CKI) (Liu et al., 2020), Shugan Jianpi decoction (Jingyuan et al., 2021), and Fangjihuangqi decoction (Guo et al., 2020). Based on these formulas and proprietary Chinese medicines, CKI is a commonly used antitumor treatment in clinical practice.

CKI is a TCM formulae extract from kushen (*Radix Sophorae flavescentis*) and baituling (*Rhizoma Heterosmilacis*) at a ratio of 7: 3, in which exist hundreds of components including alkaloids and flavonoids (Cui et al., 2020). As approved by the China Food and Drug Administration, CKI can be employed for cancer treatment (Guo et al., 2015) and has several pharmacological functions, including anticancer properties, hemostasis, and immunity enhancement (Wang et al., 2015). CKI is widely being used in the treatment of cancers, such as breast cancer (Xu et al., 2011a; Qu et al., 2016; Cui et al., 2019; Nourmohammadi et al., 2019; Cui et al., 2020), acute myeloid leukemia (Jin et al., 2018), and hepatocellular carcinoma (Gao et al., 2018; Yang et al., 2021). Additionally, the function of CKI in treating breast cancer was also proved in *in vitro* and *in vivo* experiments. CKI could reduce the tumor formation rates and tumor volume by the downregulated Wnt/b-catenin pathway in the MCF-7 SP xenograft model (Xu et al., 2011a). Besides, CKI could impair the migration and invasiveness of MDA-MB-231 cell lines (Nourmohammadi et al., 2019) and influence the cell cycle of MDA-MB-231 cell lines in promoting cell death by increasing the proportion of cells in the G1 phase and decreasing the cells in the S and G2/M phase (Cui et al., 2019; Cui et al., 2020), while it could inhibit proliferation and induce cell apoptosis of MCF-7 cell lines (Qu et al., 2016). These *in vitro* and *in vivo* experiments had proved that CKI has anticancer pharmacological function, especially in breast cancer. In CKI, matrine, oxymatrine, and sophocarpine are the main components of *Radix Sophorae flavescentis*, which display antitumor, anti-inflammatory, and antiviral properties, as well as cardiovascular protective abilities (Wang et al., 2015). *Rhizoma Heterosmilacis* may play a role in promoting oxidative stress–induced apoptosis (Liu et al., 2017), reducing oxidative stress (Hong et al., 2014), deoxidation, and dampness relief (Liang et al., 2019). Increasing evidence has shown that CKI can be used to halt cancer migration (Nourmohammadi et al., 2019), reduce anticancer drug resistance (Hy et al., 2014), increase cancer cell apoptosis (Qu et al., 2016), suppress the cancer cell cycle (Cui et al., 2019), and inhibit cancer progression (Wang et al., 2019). Matrine upregulates Bax and downregulates Bcl-2 to inhibit proliferation and increase apoptosis of breast cancer cells (Li et al., 2015) and further downregulates the canonical pathway to suppress human breast cancer stem-like cells (Xu et al., 2011b). Oxymatrine exerts its effects by blocking the cell cycle, initiating apoptosis (Binggang et al., 2002) and suppressing the epithelial–mesenchymal transition (Jiaqin et al., 2018). These sporadic reports suggest that different components of CKI play a role in the treatment of BC, but there is still a lack of systematic and overall research on the synergistic mechanism of different components of *Rhizoma Heterosmilacis* and *Radix Sophorae Flavescentis* in CKI.

Since TCM is characterized by "multi-components" and "multi-targets", it is difficult to reveal the associated mechanisms between herbs, components, genes, and disease through traditional experimental methods. As an effective tool to elucidate the synergistic and potential mechanisms of the networks between component–target and target–disease, systemic pharmacology provides a new perspective on the therapeutic mechanisms of TCM in the treatment of BC at the systematic level.

To explore the therapeutic mechanism of CKI in treating BC, a novel system pharmacology strategy (**Figure 1**), which integrates differentially expressed gene analysis (DEGs), pharmacokinetics synthesis screening, target identification, synergy contribution degree (SCD), network analysis, and therapeutic response index (TRI) calculation, was developed. The Cancer Genome Atlas (TCGA) database was used to explore the DEGs in BC. Subsequently, previously proposed absorption, distribution, metabolism, and excretion (ADME) screening models were employed to select potential active components; online tools were used to predict the targets of these potential active components, and a component–target (C-T) network was used for further network analysis. Network analysis of potential components combined with SCD was used to simulate the treatment effects of each component of CKI in BC and to explore a high contribution group of synergistic components (HCGSC). The virtual docking-aided TRI model was designed to determine whether highly reliable components may have a potential synergistic mechanism. Thereafter, GO enrichment

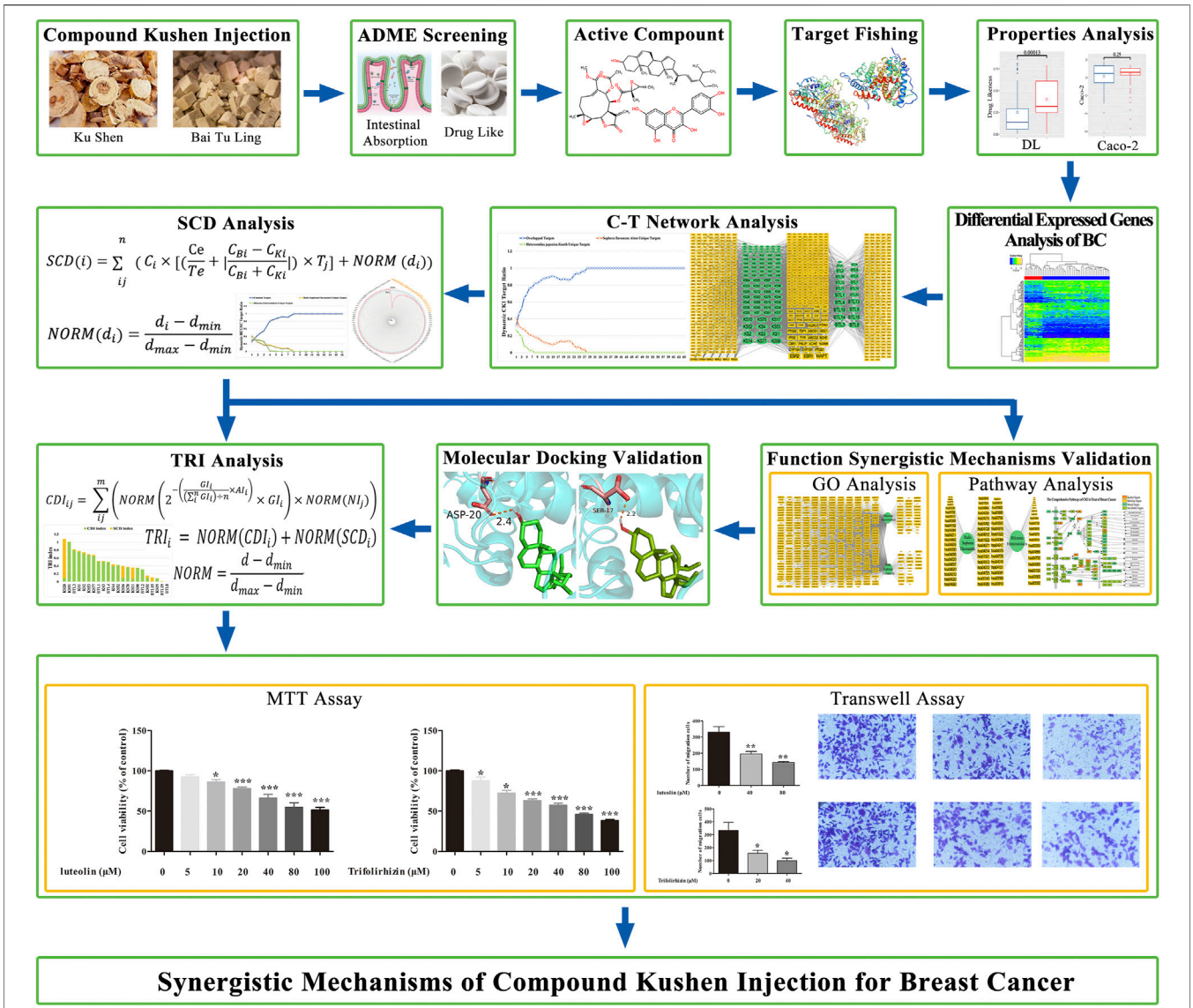

FIGURE 1 | Workflow of the system pharmacology approach.

and KEGG pathway enrichment analysis of BC, CKI, and highly reliable components in HCGSC were discussed to decode the potential synergistic mechanism analysis of CKI in the treatment of BC based on HCGSC. Ultimately, experimental validation was used to confirm the effect of high TRI-scored components in the HCGSC and evaluate the reliability of our model. We hope that these results will provide a strategy to reveal the therapeutic mechanism of TCM at the molecular level.

MATERIALS AND METHODS

Chemical Components Collected From Database

All CKI components were collected from the Traditional Chinese Medicine Systems Pharmacology (TCMSP) database (http://www.tcmspw.com/tcmsp.php). TCMSP includes information from DrugBank, HIT, TTD, and PharmGKB. The pharmacokinetic properties of TCMSP include molecular weight (MW), AlogP, number of acceptor atoms for H-bonds (nHacc), number of donor atoms for H-bonds (nHdon), Caco-2 permeability (Caco-2), oral bioavailability (OB), drug-likeness (DL), blood–brain barrier (BBB), FASA-, and half-life (HL).

ADME Screening

In the process of modern drug development, many drug candidates fail during development because of inadequate ADME properties (Rojas-Aguirre and Medina-Franco, 2014). Therefore, evaluating the ADME of drug components in the early stages has become an essential process. Components with better pharmacokinetic properties can be obtained by ADME screening, and the potential drug–drug interactions can be minimized (Wang et al., 2018). Two ADME-

related models were employed in the present study, namely Caco-2 permeability and drug-likeness, to screen the potential active components of CKI (**Supplementary Figure S1**).

As a model system for intestinal epithelial permeability, the human colon carcinoma cell line (Caco-2) (Ij et al., 1989) is currently considered the gold standard (Jacobsen et al., 2020). The transport rates of components (nm/s) in Caco-2 monolayers represent intestinal epithelial permeability in TCMSP (Ru et al., 2014). Components with Caco-2 < −0.4 are not permeable; thus, Caco-2 > −0.4 were selected as candidate components.

Drug-likeness (DL) may be defined as a complex balance of various molecular properties and structural features that determine whether a particular molecule is similar to known drugs. The drug similarity index of the new compound was calculated using the Tanimoto coefficient, which is defined as

$$f(A,B) = \frac{A \times B}{|A|^2 + |B|^2 - A \times B}$$

In this equation, A represents the molecular descriptor of herbal components, and B is the average molecular property of all components in DrugBank (Tao et al., 2013). Based on the data from TCMSP, the average value of *Radix Sophorae Flavescentis* was 0.40, while that of *Rhizoma Heterosmilacis* was 0.25. Combined with other literature search criteria, we defined DL ≥ 0.18, as the screening criterion of DL.

Target Identification

Three commonly used online tools were employed to identify the targets of active components in CKI, namely, similarity ensemble approach (SEA) (Keiser et al., 2007), HitPick (Liu et al., 2013), and SwissTargetPrediction (Gfeller et al., 2014). Open Babel 3.0.0 (O Boyle et al., 2011) was used to convert the SDF format of all CKI potential active components into the SMILES format. Potential active components in the SMILES format were imported to the SEA, HitPick, and SwissTargetPrediction to predict targets of potential active components. The homologous genes of other species provided by online tools were included in the discussion.

Network Construction and Analysis

The C-T network was used as a frame to uncover the relationship between active components and targets. Cytoscape 3.8.0 (Shannon et al., 2003), an open-source software platform, was employed to visualize the networks.

GO Enrichment and KEGG Pathway Enrichment Analysis

To analyze the main function of targets, clusterProfiler (Yu et al., 2012) in the Bioconductor package (https://bioconductor.org/) based on the R language was used for GO-BP enrichment analysis and KEGG pathway analysis. FDR-adjusted *p* values were set at 0.05, as the cut-off criterion.

Synergy Contribution Degree Calculation

The SCD represents the contribution of a potential active component in the C-T network and its effectiveness in the treatment of BC. To evaluate the effect of CKI on the treatment of BC, we built a mathematical model to calculate the SCD of each active component in CKI:

$$SCD(i) = \sum_{ij}^{n}\left(C_i \times \left[\left(\frac{Ce}{Te} + \left|\frac{C_{Bi} - C_{Ki}}{C_{Bi} + C_{Ki}}\right|\right) \times T_j\right] + NORM\ (d_i)\right),$$

$$NORM\,(d_i) = \frac{d_i - d_{min}}{d_{max} - d_{min}}.$$

In this equation, *i* is the number of components, and *j* is the number of targets. *C* represents the betweenness centrality of each component. *T* represents the betweenness centrality count of all targets of each component. *Ce* represents the edge count of each component. *Te* represents the edge count of all targets of each component. C_B represents the betweenness centrality of each component only in *Rhizoma Heterosmilacis*, and C_K represents the betweenness centrality of each component only in *Radix Sophorae Flavescentis*. If a component consists only of *Radix Sophorae Flavescentis* or *Rhizoma Heterosmilacis*, $|\frac{C_{Bi}-C_{Ki}}{C_{Bi}+C_{Ki}}|$ should be 1. If $|\frac{C_{Bi}-C_{Ki}}{C_{Bi}+C_{Ki}}|$ is zero, we assign 1e-6 to it. *d* represents the dose of each component in CKI, which was extracted using HPLC (**Supplementary Table S1**). *NORM (di)* is the index of min-max normalization to the dose of each component. The betweenness centrality of each component and target was calculated using Cytoscape version 3.8.0. based on the C-T network of the potential active components.

Breast Cancer Differentially Expressed Genes Analysis

The TCGA database (https://portal.gdc.cancer.gov/) was used to explore the DEGs in BC. We used TCGAbiolinks (Colaprico et al., 2016) in the Bioconductor packages to access the HTSeq-Counts number of normal and BC samples from the TCGA-BRCA project of the TCGA program. DESeq (Anders and Huber, 2010) and limma (Ritchie et al., 2015) in the Bioconductor package were used to analyze the DEGs in BC. We set |log2FoldChange|≥2 and FDR adjusted the *p* value < 0.05, as the cut-off criterion. The results are presented and plotted using the gplots (Warnes et al., 2020) package.

Molecular Docking Analysis of HCGSC in the Treatment of BC

The components of HCGSC were collected from the ZINC (Sterling and Irwin, 2015) and PubChem (https://pubchem.ncbi.nlm.nih.gov) databases in the MOL2 format. Human proteins were collected from the Protein Data Bank (PDB) (http://www.rcsb.org). AutoDock Tools (ADT) (Sanner, 1999) was used to pretreat the components and proteins. The pocket of the protein was automatically extracted from the space of the protein. AutoDock Vina (Trott and Olson, 2009) was used for docking. The seed of docking was 10,000, the energy range was 4, and the exhaustiveness was 4. The affinity (kcal/mol) index of each component–protein pair was used to estimate the docking

results. The results were obtained using PyMOL (Schr Odinger, 2015).

Therapeutic Response Index Model Calculation

We developed a mathematical model to calculate the therapeutic response index (TRI) of each component in a highly reliable docking relationship (HRDR) between HCGSC and its targets.

$$CDI_{ij} = \sum_{ij}^{m}\left(NORM\left(2^{-\left(\frac{GI_i}{\left(\sum_i^n GI_i\right)\div n}\times AI_i\right)} \times GI_i \right) \times NORM\left(NI_j\right)\right),$$

$$TRI_i = NORM\left(CDI_i\right) + NORM\left(SCD_i\right),$$

$$NORM = \frac{d - d_{min}}{d_{max} - d_{min}}.$$

In the above model, i is the number of components, j is the number of topology parameters, n is the collection of components, and m is the collection of components and topology parameters. CDI represents the docking index of HRDR. GI represents the number of genes targeted by each component. AI represents the average affinity of all component–protein binding relationships of each component. NI represents the C-T network topology parameters of HCGSC and their targets, including degree, betweenness centrality, closeness centrality, average shortest path length, eccentricity, radiality, neighborhood connectivity, and topological coefficient. SCD is the calculation result for each component from method 2.6. TRI represents the mechanism of CKI in the treatment of BC, which is the sum of normalized CDI and normalized SCD. NORM is a normalized equation.

MATERIALS

High-glucose Dulbecco's modified Eagle medium (DMEM; 4.5 g/L), fetal bovine serum (FBS), 0.25% trypsin, and 3-(4,5-dimethylthiazol-2-yl)-2,5-diphenyltetrazolium bromide (MTT) were purchased from Shanghai Sangon Biotechnology Co., Ltd. (Shanghai, China). The transwell invasion chamber was purchased from Corning costar company (Andover, MA, United States). Matrigel was purchased from BD (Biosciences, Bedford, MA, United States). Luteolin and trifolirhizin (≥98% purity by HPLC) were obtained from Nanjing Jingzu Biotech Co., Ltd. (Nanjing, China).

Cell Culture

The human breast cancer cell line MCF-7 was purchased from Procell Life Science & Technology Co., Ltd. Cells were cultured in an incubator at 37°C in DMEM containing 10% FBS. When the cells reached 80% confluency, they were exposed to different concentrations of luteolin and trifolirhizin (1, 2, and 4 mg/ml) for 24 h.

Cell Viability Assay

MCF-7 cells (1×10^4 cells/well) were seeded in 96-well plates and treated with 0, 5, 10, 20, 40, 80, and 100 μM luteolin and trifolirhizin for 24 h. MTT was added to a 96-well plate for 4 h, and the culture supernatant was removed. Finally, DMSO was used to dissolve the purple crystals. Absorbance at 570 nm was measured using a plate reader.

Transwell Assay

Referring to our previous method (Gao et al., 2018), luteolin (40 and 80 μM) and trifolirhizin (20 and 40 μM) were added to the lower compartments. The migrating cells were observed under a microscope.

Statistical Analysis

The R package ggpubr (Kassambara, 2020) was used to compare the molecular properties of all components in *Rhizoma Heterosmilacis* and *Radix Sophorae Flavescentis*. Data were analyzed using the Student's *t*-test. Differences were considered statistically significant at $p < 0.05$.

RESULTS

Based on the systematic pharmacological model, the mechanism of CKI in BC treatment was clarified and validated. First, DEGs that could be used as potential pathogenic genes were determined based on the data from the TCGA-BRCA project. Second, the CKI components were collected from the TCMSP database, and the ADME method was used to screen active components in CKI. Third, the active components and their targets, which were predicted using three online tools, were used to construct the C-T network. Fourth, a network analysis of potential components combined with SCD was used to explore HCGSC. Thereafter, GO enrichment and KEGG pathway enrichment analysis of BC, CKI, and highly reliable components in HCGSC were discussed to decode the potential synergistic mechanism of CKI in the treatment of BC. Subsequently, the virtual docking-aided TRI model was designed to determine whether highly reliable components may have a synergistic mechanism. Ultimately, experimental validation was used to confirm the effect of high TRI-scored components in HCGSC and evaluate the reliability of our model.

Differentially Expressed Genes Analysis of BC

To further analyze the mechanism of CKI in the treatment of BC, 113 normal breast samples and 1,102 breast cancer samples were extracted from the TCGA-BRCA project. A total of 979 DEGs were upregulated, and 990 were downregulated in cancer (**Supplementary Table S2**). The DEGs were used to determine the gene expression patterns of normal and tumor patients (**Supplementary Figure S2**). The results showed that the DEG

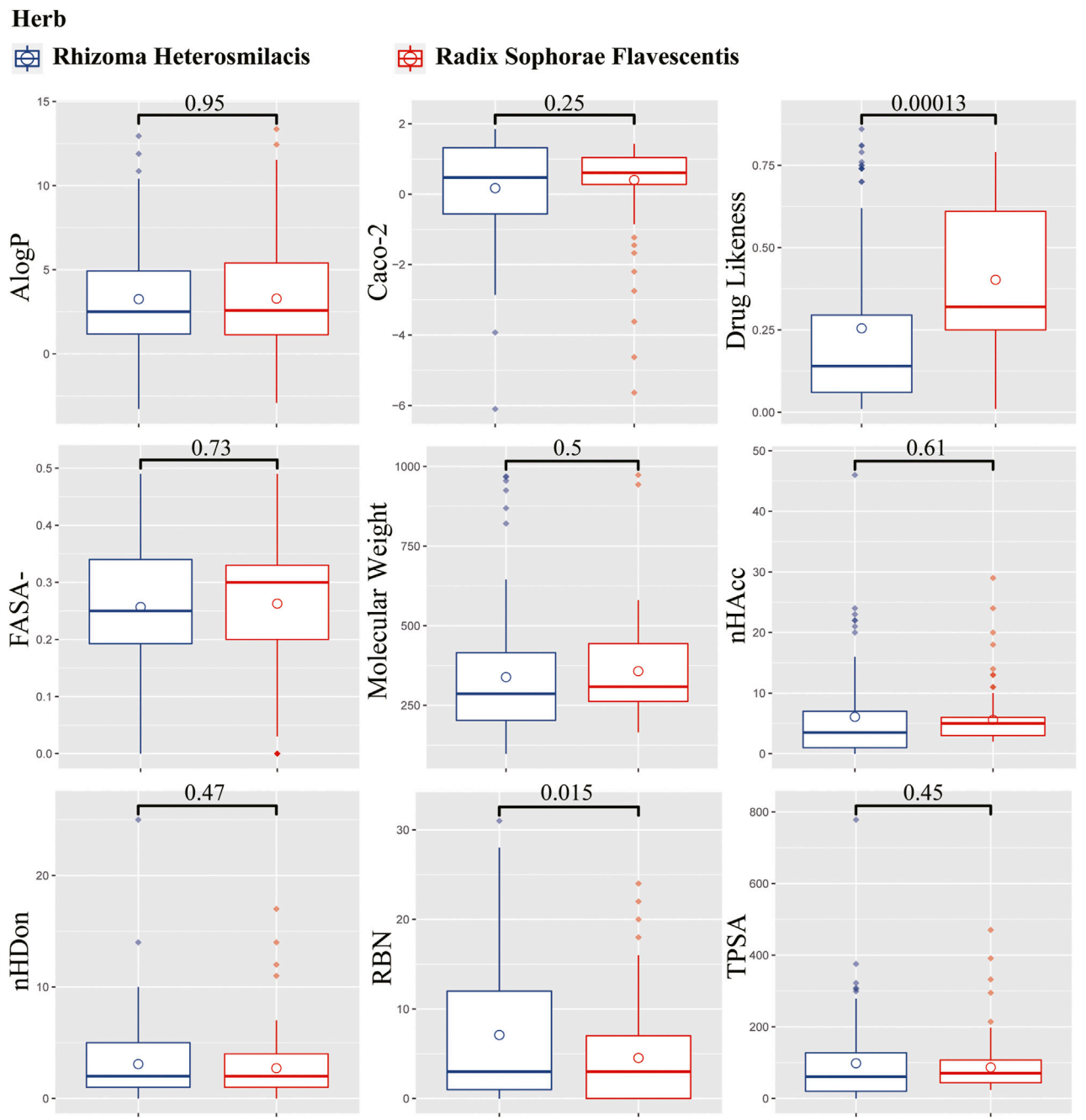

FIGURE 2 | Boxplot of nine properties of the two components. The box in blue represents the value distribution of *Radix Sophorae Flavescentis*, and the box in red represents the value distribution of *Rhizoma Heterosmilacis*.

pattern distinguished between diseased and normal states. From the expression pattern, we identified that the top 10 upregulated genes were *FTHL17, CSAG1, MUC2, COX7B2, CGA, CSAG4, CST4, MAGEA12, MAGEA1*, and *ACTL8*. Among these genes, *MUC2* influences proliferation, apoptosis, and metastasis of breast cancer cells (Astashchanka et al., 2019), while the upregulation of *MAGEA* in patients revealed a higher risk of recurrence (Otte et al., 2001). The top 10 downregulated genes were *LEP, GLYAT, AC087482.1, APOB, TRHDE-AS1, AQP7P2, FP325317.1, PLIN1, CA4*, and *AL845331.2*. *LEP* which inhibit apoptosis of breast cancer cells by coding leptin, while *PLIN1* inhibits invasion, migration, and proliferation of cells (Zhou et al., 2016; Crean-Tate and Reizes, 2018). The literature reports proved that these genes are related to the development of BC, which indicates that the DEGs were more likely to be pathogenic genes.

Component Comparisons in *Rhizoma Heterosmilacis* and *Radix Sophorae Flavescentis*

From the TCMSP database, 187 compounds were retrieved from *Rhizoma Heterosmilacis* (74) and *Radix Sophorae Flavescentis* (113). Detailed information on the components of *Rhizoma Heterosmilacis* and *Radix Sophorae Flavescentis* is provided in **Supplementary Table S3**. To further describe the differences between *Rhizoma Heterosmilacis* and *Radix Sophorae Flavescentis*, we compared nine properties of the two components, including drug likeness (DL), Caco-2, molecular weight (MW), AlogP, TPSA, FASA-, RBN, nHDon, and nHAcc, and drew boxplots using R packages ggplot2 (Wickham, 2016), ggpubr (Kassambara, 2020), and ggsci (Xiao, 2018). The results (**Figure 2**) showed most of chemical composition and properties between *Rhizoma Heterosmilacis* and *Radix Sophorae Flavescentis* had no statistical difference except for DL ($p = 0.00013$) and RBN ($p = 0.015$). These results indicate that *Rhizoma Heterosmilacis* and *Radix Sophorae Flavescentis* have similar chemical properties.

Potential Active Components in *Rhizoma Heterosmilacis* and *Radix Sophorae Flavescentis*

Traditional Chinese medicine uses a combination of herbs, each of which usually contains hundreds of components, and only a few of these components possess satisfactory pharmacodynamic and pharmacokinetic properties. In this study, two ADME-related properties, DL and Caco-2, were used to screen for active components. Through ADME screening, 111 active components (*Radix Sophorae Flavescentis* 90 and *Rhizoma Heterosmilacis* 21) were selected from the 187 components of CKI. Additionally, some components, such as N-methylcytisine and trifolirhizin, did not pass the ADME screening, but were frequently reported in previous studies, so we added them to the list of active components (Xiumei and Cen, 2004; Juan et al., 2007; Yue, 2012; Liang et al., 2013). Therefore, 113 active components (*Radix Sophorae Flavescentis* 92 and *Rhizoma Heterosmilacis* 21) were included for further analysis. Detailed information is provided in **Supplementary Table S4**.

Through ADME screening and literature review, 92 potential components containing ideal pharmacokinetic profiles were selected from *Radix Sophorae Flavescentis*. For example, as one of the major components of CKI, sophoridine (KS18, DL = 0.25, Caco-2 = 1.13) displays antitumor, anti-allergic, anti-inflammatory, anti-arrhythmia, and antiviral properties, and affects the central nervous system (Han et al., 2009; Cuiping, 2010; Huang et al., 2014; Hu et al., 2016). Anagyrine (KS34, DL = 0.24, Caco-2 = 1.16) and (+)-lupanine (KS83, DL = 0.24, Caco-2 = 1.16) inhibit the proliferation and induction of apoptosis in human cervical cancer cells (Merghoub et al., 2011). Oxysophocarpine (KS89, DL = 0.29, Caco-2 = 1.042) suppressed cell proliferation, migration, invasion, and angiogenesis, induced cell cycle arrest, and enhanced apoptosis in oral squamous cell carcinoma (Liu et al., 2018). IDO1 expression can be downregulated by kushenol E (KS76, DL = 0.59, Caco-2 = 0.58) and kushenol F (KS74, DL = 0.61, Caco-2 = 0.45) to inhibit tumor proliferation (Kwon et al., 2019) and induce apoptosis (Kwon et al., 2020).

Among the 74 components in *Rhizoma Heterosmilacis*, 21 components met the screening criteria. For instance, diosgenin (BTL5, DL = 0.81, Caco-2 = 0.82), a steroid compound, has been shown to promote apoptosis and anticancer effects (Romero-Hernández et al., 2015; Jiang et al., 2016). Sitogluside (BTL1, DL = 0.62, Caco-2 = -0.14), beta-sitosterol (BTL2, DL = 0.75, Caco-2 = 1.32), sitosterol (BTL3, DL = 0.75, Caco-2 = 1.32), and stigmasterol (BTL4, DL = 0.75, Caco-2 = 1.45) can inhibit proliferation (Awad et al., 2000; Awad et al., 2003) and promote apoptosis (Awad et al., 2003), cell cycle arrest, and sphingomyelin cycle activation (Jia et al., 2018). Additionally, quercetin (BTL1, DL = 0.28, Caco-2 = 0.05) could be used to inhibit the proliferation of tumor cell lines (Ren et al., 2015) and induce apoptosis of tumor cells (Jia et al., 2018). Taxifolin (BTL13, DL = 0.27, Caco-2 = -0.23) inhibited proliferation, migration, and invasion of breast cancer cells by promoting EMT through β-catenin signal transduction (Li et al., 2019).

Target Prediction and Analysis of *Rhizoma Heterosmilacis* and *Radix Sophorae Flavescentis*

To evaluate the effect of the active components of CKI, we used SEA, HitPick, and SwissTargetPrediction tools to predict the targets of 113 active components of CKI. Finally, 780 targets were obtained from these tools (**Supplementary Table S5**). To explore the mechanism of CKI in the treatment of BC, 113 active components and 780 targets were used to construct the C-T network (**Supplementary Figure S3**). The C-T network results showed that 252 of all 780 targets were overlapped by the target list of *Rhizoma Heterosmilacis* and *Radix Sophorae Flavescentis*, and 320 targets were unique to *Radix Sophorae Flavescentis*, while 208 targets were unique to *Rhizoma Heterosmilacis*. A total of 4,592 component–target associations between 113 active components and 780 targets were contained in the C-T network. The average number of targets per component is 40.64, and the mean number of components per target is 5.89, which shows that CKI has multi-component and multi-target characteristics in treating BC.

Among all components, six components displayed a number of degrees above 120, namely palmitone (BTL15, degree = 149), quercetin (BTL1, degree = 144), quercetin (KS3, degree = 144), norartocarpetin (KS77, degree = 130), apigenin (KS2, degree = 129), and luteolin (KS1, degree = 125), all of which exhibit anticancer functions (Imran et al., 2019), and suppress migration and EMT (Cao et al., 2020). These six high-degree components only accounted for 5.3% of all components but covered 58.3% of all common targets. They all targeted common targets with high degrees, including ESR1 (degree = 65), MAPT (degree = 65), and ESR2 (degree = 63). It is worth noting that the top 25 targets with the highest degree were all dropped in the common targets list between *Rhizoma Heterosmilacis* and *Radix Sophorae Flavescentis*, most of which were related to the pathogenesis or treatment of BC. As the coding genes of the estrogen receptor, methylation of the ESR1

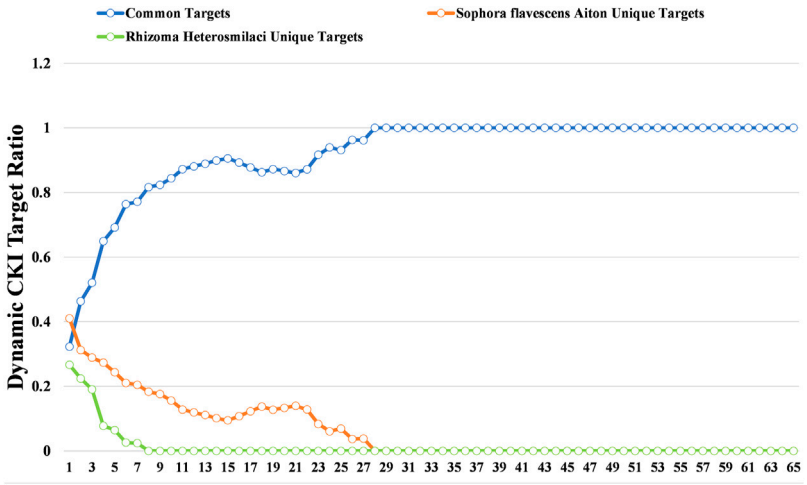

FIGURE 3 | Dynamic ratio changes between common targets and unique targets of *Rhizoma Heterosmilacis* and *Radix Sophorae Flavescentis*.

(degree = 65) promoter may be associated with shorter survival time and increased risk of drug resistance to anti-endocrine therapy (Kirn et al., 2018) and is commonly targeted by oxysophocarpine (KS89), kushenol E (KS76), and kushenol F (KS74) of *Radix Sophorae Flavescentis* and Stigmasterol (BTL5), quercetin (BTL1), and taxifolin (BTL13) of *Rhizoma Heterosmilacis*. Additionally, MAPT (degree = 65) is correlated with microtubule assembly and stabilization (Weingarten et al., 1975), which can promote bicalutamide resistance and is associated with survival in prostate cancer (Sekino et al., 2020). Our data analysis showed that (+)-Lupanine (KS76) and leachianone,g (KS74) from *Radix Sophorae Flavescentis* and quercetin (BTL1) from *Rhizoma Heterosmilacis* could target MAPT. We noted that several components of *Rhizoma Heterosmilacis* and *Radix Sophorae Flavescentis* can both activate common targets to play their role in the treatment of BC. Thus, these results suggest that *Rhizoma Heterosmilacis* and *Radix Sophorae Flavescentis* may act synergistically to treat BC via the common targets based on the "multi-component" and "multi-target" features and provide therapeutic targets for the cooperative treatment of BC.

To further decode the synergistic mechanism between *Radix Sophorae Flavescentis* and *Rhizoma Heterosmilacis*, we investigated the change in common target proportion under the condition of different degrees as thresholds. The results showed that following the increase in degree, the proportion of common target retention maintained a high growth trend. The proportion of common targets increased from 32.31 to 100% when the degree threshold increased from 1 to 28. Additionally, when the degree threshold increased from 1 to 28, the proportion of unique targets of *Rhizoma Heterosmilacis* decreased from 26.76 to 0%; however, when the degree threshold increased from 1 to 8, the proportion of specific targets of *Radix Sophorae Flavescentis* decreased from 41.02 to 0%. The results indicated that the common targets of *Rhizoma Heterosmilacis* and *Radix Sophorae Flavescentis* have relatively high degrees. A higher degree indicates that these targets have a higher influence among all targets, and it also suggests that *Rhizoma Heterosmilacis* and *Radix Sophorae Flavescentis* exert major synergistic effects by targeting common targets, which have a greater influence on the intervention response network.

To further decode the synergistic mechanism between them, we calculated the dynamic ratio change between common targets and unique targets of *Radix Sophorae Flavescentis* and *Rhizoma Heterosmilacis* using degree as the threshold. As shown in **Figure 3**, the proportion of common targets showed an overall upward trend from 32.31% (degree = 1) to 100% (degree = 28). However, the proportion of unique targets of *Rhizoma Heterosmilacis* and *Radix Sophorae Flavescentis* revealed a gradual downward trend. The ratio of unique targets of *Radix Sophorae Flavescentis* changed from 41.02 to 0% with a degree ranging from 1 to 28, while the ratio of unique targets of *Rhizoma Heterosmilacis* changed from 26.67 to 0% with a degree range from 1 to 7.

In the C-T network, nodes with a higher degree usually represent the importance of all nodes. The results indicated that too much background noise may obscure the synergistic mechanism. Therefore, a model should be used to extract the core components.

Synergy Contribution Degree Calculation and Effect Verification

It is worth noting that *Rhizoma Heterosmilacis* and *Radix Sophorae Flavescentis* may play their roles through common targets based on the C-T network. However, the core component groups and mechanisms of synergy require further elucidation. To solve these problems, an SCD calculation method was designed that considers the synergy of both the topology of the components in the C-T network and the dose of the components. The SCD values of the active components of CKI are shown in **Supplementary Table S6**.

According to the calculation results, the top two components with an SCD sum of 49.05% were oxymatrine (KS80) and matrine

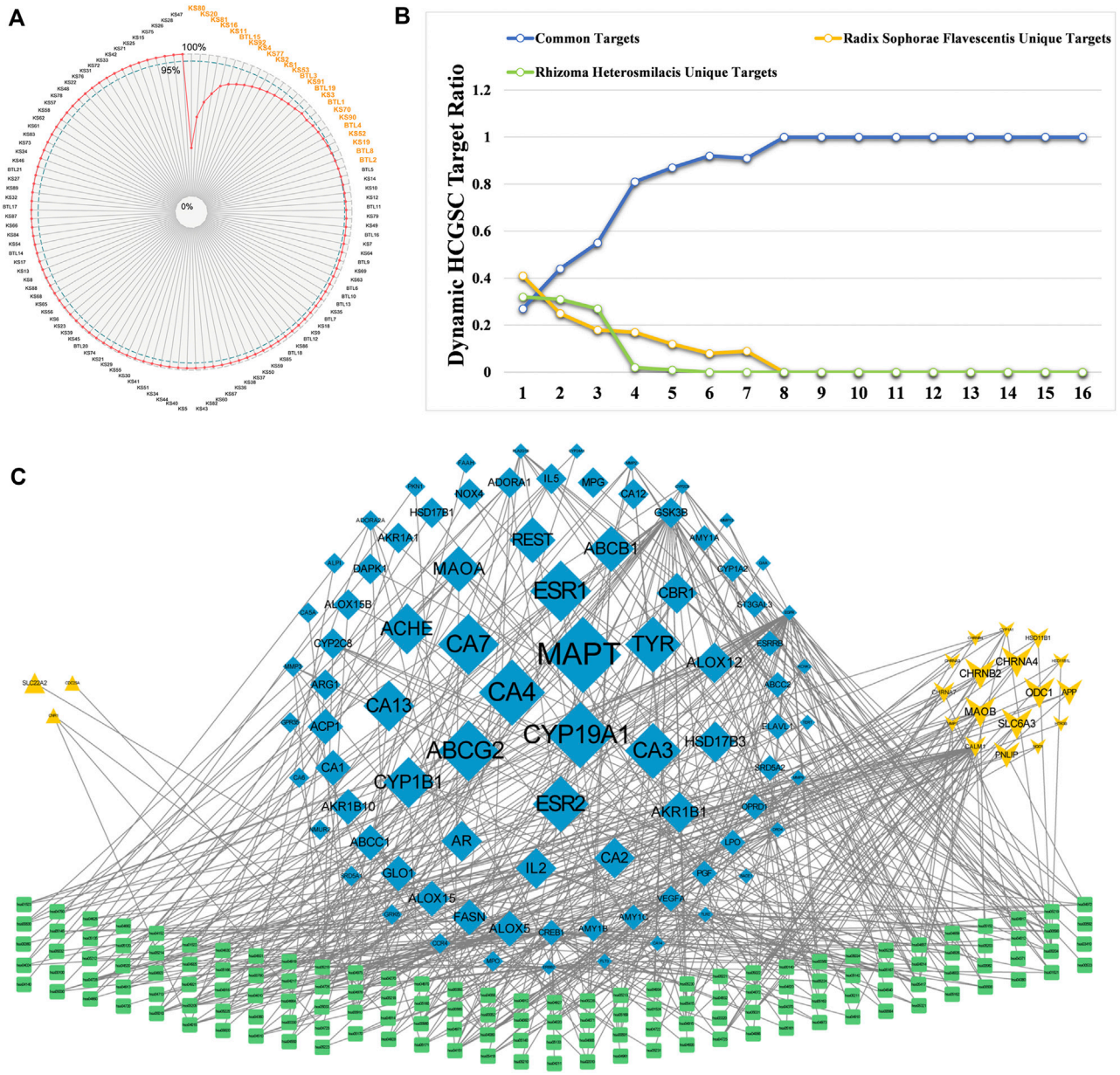

FIGURE 4 | (A) Cumulative radar chart of the ratio between component accumulation targets and the targets of CKI. The label within the chart represented the ratio (%) between component accumulation targets and the targets of CKI. **(B)** The dynamic ratio changes between common targets of HCGSC and unique targets of *Radix Sophorae Flavescentis*, and *Rhizoma Heterosmilacis* of HCGSC. **(C)** The network with targets and their enriched pathways (the degrees of the targets were higher than the third quartile of the targets in the C-T network of HCGSC) and their enriched pathways.

(KS20). Twenty-four components contribute to the effects of CKI on BC, with a total of 95.03%. Surprisingly, 24 components accounted for only 21.23% of all active components in CKI and could cover 631 targets (80.89% of all CKI targets) (**Figure 4A**). Thus, we define these 24 components as the high contribution group of synergistic components (HCGSC). These results show that HCGSC plays key roles in all active components of CKI and may clarify why the herbs in CKI generate synergistic and combination effects on BC.

To evaluate the reliability of HCGSC, we defined two references for further comparison: the first reference was 70 genes, which overlapped with DEGs and CKI targets, and the second reference was the 17 pathways, which are overlapped by enriched DEGs pathways and CKI targets. The targets of HCGSC contained 62 genes, which could cover 88.57% (**Supplementary Figure S4A**) of the first reference, while the HCGSC targets enriched 158 pathways, which could cover 94.11% (**Supplementary Figure S4B**) of the second

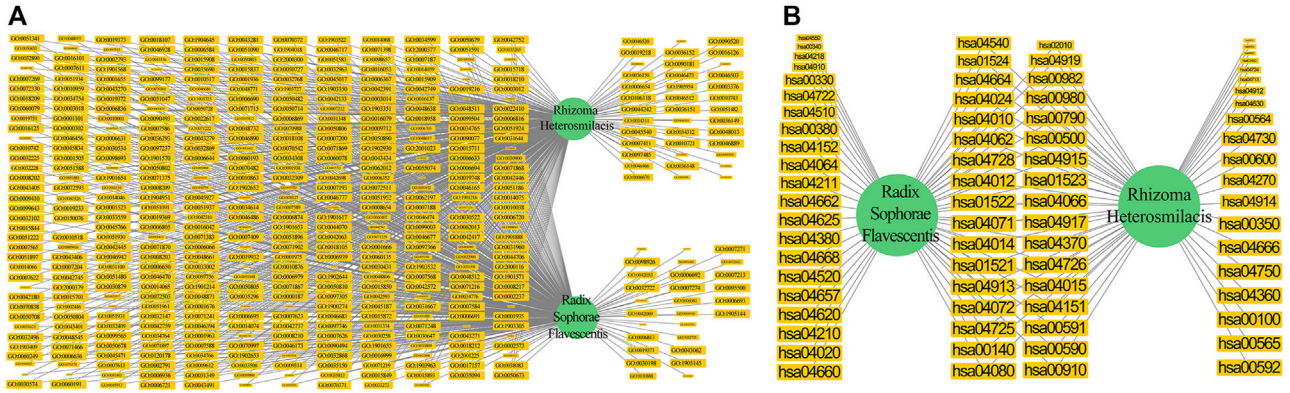

FIGURE 5 | Components were represented in green. The GO-BP terms and pathways were represented in yellow. The size of the pathways was related to the FDR adjust *p* value. The lower FDR adjust *p* value represented the larger size. **(A)** The network of selected GO-BP terms based on the first quartile value of all GO-BP terms FDR adjust *p* value. The left of the network was the commonly enriched GO-BP terms. The upper right of the network was the unique GO-BP terms of *Rhizoma Heterosmilacis*. The lower right of the network was the unique GO-BP terms of *Radix Sophorae Flavescentis*. **(B)** The network of pathways between *Rhizoma Heterosmilacis* and *Radix Sophorae Flavescentis*. The center of the network was the commonly enriched pathways. The right of the network was the unique pathways of *Rhizoma Heterosmilacis*. The left of the network was the unique pathways of *Radix Sophorae Flavescentis*.

reference. Of these 62 overlapped genes, 39 were targeted by *Rhizoma Heterosmilacis*, while 43 were targeted by *Radix Sophorae Flavescentis*. These results confirm the reliability and accuracy of the HCGSC selection model. Two networks were constructed to analyze HCGSC. The first is a C-T network based on 24 components and 631 targets. The second is the target–pathway network based on 532 targets and 158 enriched pathways.

In the first network, the degree of targets ranged from 1 to 16, with the third quartile equal to 3. The change in the proportion of common targets under different conditions showed that the common targets had a higher degree (**Figure 4B**). The proportion of common targets increased from 27.26% to 100%. Additionally, with the increase in the threshold of the degree, the proportion of unique targets of *Rhizoma Heterosmilacis* decreased from 32.17 to 0%, while the proportion of specific targets of *Radix Sophorae Flavescentis* decreased from 40.57 to 0%. In the second network, we assigned the degree from the first network to the targets; targets with a degree higher than 3 (the third quartile of the targets in the C-T network) and their enriched pathways were selected to construct the network (**Figure 4C**). Visualization showed that the size of the target was positively related to the degree. We noted that the common targets (in blue diamond) displayed more connections with pathways and larger sizes than the others. However, the unique targets of *Rhizoma Heterosmilacis* (yellow triangle) and *Radix Sophorae Flavescentis* (yellow arrow) not only showed fewer connections with pathways, but were also smaller than the common targets. These two networks indicated that the common targets of *Rhizoma Heterosmilacis* and *Radix Sophorae Flavescentis* in HCGSC have relatively high degrees, which shows that *Rhizoma Heterosmilacis* and *Radix Sophorae Flavescentis* have a synergistic effect on the nodes with higher influence.

Potential Synergistic Mechanism Analysis of CKI in BC Treatment Based on HCGSC

GO Enrichment Analysis for CKI Based on HCGSC

To further interpret the potential synergistic mechanisms of *Rhizoma Heterosmilacis* and *Radix Sophorae Flavescentis*, we performed GO-BP enrichment analysis for the targets of *Radix Sophorae Flavescentis* and *Rhizoma Heterosmilacis* in HCGSC. *Radix Sophorae Flavescentis* targets in HCGSC were enriched in 1517 GO-BP terms, while *Rhizoma Heterosmilacis* targets in HCGSC were enriched in 1394 GO-BP terms. A total of 927 joint GO-BP terms were found between them (**Supplementary Figure S4C**).

We selected the GO-BP terms with an FDR-adjusted *p* value lower than that of the first quartile of all GO-BP terms to build a network (**Figure 5A**). We found that 86.49% of the selected GO-BP terms belong to the commonly enriched GO-BP terms between the targets of *Radix Sophorae Flavescentis* and *Rhizoma Heterosmilacis* in HCGSC. This suggests that *Rhizoma Heterosmilacis* and *Radix Sophorae Flavescentis* have potential synergistic mechanisms in the treatment of BC through these highly reliable, commonly enriched GO-BP terms based on HCGSC.

It is worth noting that most of the joint GO-BP terms were closely related to BC, such as the steroid metabolic process (GO: 0008202, FDR adjusted *p* value = 2.24E-27) and steroid biosynthetic process (GO:0006694, FDR adjusted *p* value = 1.23E-18). Regarding the genes of these GO terms, estrone (*E1*) can protect women from breast cancer, while estradiol (*E2*) and estriol (*E3*) may enhance the risk (Lemon et al., 1966; Cohn et al., 2017). The expression of *ATGL* is correlated with tumor aggressiveness *in vivo* (Wang et al., 2017), which is related to the lipid catabolic process (GO:0016042, FDR adjust *p* value = 1.46E-22), lipid transport (GO:0006869, FDR adjusted *p* value = 4.04E-17), and lipid localization (GO:0010876, FDR adjusted *p* value = 1.16E-16). Including TRPCs, TPRVs,

TRPMs, TRPA1, TRPPs, and TRPMLs (Berridge et al., 2003; Rohacs, 2005; Monteith et al., 2007; Venkatachalam and Montell, 2007; Doherty et al., 2015; Vangeel and Voets, 2019), calcium homeostasis plays an important role in the occurrence, development, and metastasis of breast cancer, which is related to the response to metal ions (GO:0010038, FDR adjust *p* value = 9.17E-13).

Additionally, the other GO-BP terms of targets for *Radix Sophorae Flavescentis* and *Rhizoma Heterosmilacis* in HCGSC, respectively, are also related to BC treatment. The ERK/MAPK and JAK2/PI3K signaling cascades in breast cancer cells can be activated by α7-nAChR activation (Chen et al., 2006; Nishioka et al., 2011; Kalantari-Dehaghi et al., 2015), while α9-nAChR overexpression is observed in tumor tissues compared with adjacent normal tissues (Lee et al., 2010). These genes are involved in synaptic transmission, cholinergic (GO:0007271, FDR adjust *p* value = 3.54E-19), and acetylcholine receptor signaling pathways (GO:0095500, FDR adjust *p* value = 1.91E-10) of *Radix Sophorae Flavescentis* in HCGSC. For the remaining GO-BP terms of *Rhizoma Heterosmilacis* in HCGSC, some steroid hormones, such as vitamin D, may have anticancer properties, while others may favor cancer progression, including estrogens and androgens (Restrepo-Angulo et al., 2020), which are related to regulation of steroid metabolic processes (GO:0019218, FDR adjusted *p* value = 2.49E-13).

Pathway Analyses Exploring Therapeutic Mechanisms of CKI Based on HCGSC

To further dissect the potential synergistic mechanisms of *Rhizoma Heterosmilacis* and *Radix Sophorae Flavescentis*, we performed the KEGG pathway enrichment analysis for the targets of *Radix Sophorae Flavescentis* and *Rhizoma Heterosmilacis* in HCGSC, respectively. Targets of *Radix Sophorae Flavescentis* in HCGSC were enriched in 55 pathways, while those of *Rhizoma Heterosmilacis* were enriched in 54 pathways. Thirty-four commonly enriched pathways were found between them (**Supplementary Figure S4D**).

We used pathways to build a network (**Figure 5B**). Surprisingly, 45.33% of pathways belonged to the commonly enriched pathways between targets of *Radix Sophorae Flavescentis* and *Rhizoma Heterosmilacis* in HCGSC. This suggests that *Rhizoma Heterosmilacis* and *Radix Sophorae Flavescentis* have potential synergistic mechanisms in the treatment of BC through these commonly enriched pathways based on HCGSC.

As shown in **Figure 5B**, most of the commonly enriched pathways were closely related to BC. Arachidonic acid metabolism (hsa00590, FDR adjusted *p* value = 4.47E-10), as a metabolic process, and the arachidonic acid (AA) pathway play key roles in carcinogenesis (Yarla et al., 2016). Additionally, PLA2s, COXs, LOXs, CYP-dependent monooxygenases, and their metabolites are known to play key roles in carcinogenesis (Tong et al., 2002; Go et al., 2015; Wu et al., 2015; Yarla et al., 2016). The migration and invasion of MDA-MB-231 breast cancer cells may be induced by linoleic acid (Serna-Marquez et al., 2017), which is related to linoleic acid metabolism (hsa00591, FDR adjusted *p* value = 4.47E-10). The PI3K-Akt signaling pathway (hsa04151, FDR adjusted *p* value = 2.78E-07) plays an important role in the tumorigenesis of breast cancer (Yuan and Cantley, 2008), and its activation may promote tumor progression in mice (Mei et al., 2018).

Additionally, other pathways of targets for *Radix Sophorae Flavescentis* and *Rhizoma Heterosmilacis* in HCGSC, respectively, are also related to BC treatment. For other pathways of *Radix Sophorae Flavescentis* in HCGSC, cellular Ca^{2+} signals have been implicated in the induction of apoptosis and regulation of apoptotic pathways (Berridge et al., 1998; Sergeev, 2005), which is related to the calcium signaling pathway (hsa04020, FDR adjusted *p* value = 1.43E-04). Regarding other pathways of *Rhizoma Heterosmilacis* in HCGSC, the higher alpha-linolenic acid content may reduce the risk of breast cancer, which is related to alpha-linolenic acid metabolism (hsa00592, FDR adjusted *p* value = 3.13E-06).

To further explain the synergistic mechanisms, we obtained 34 commonly enriched pathways between targets for *Radix Sophorae Flavescentis* SC and *Rhizoma Heterosmilacis* in HCGSC and 25 DEG-enriched pathways. By analyzing these pathways, we found that five pathways overlapped between 34 and 25 pathways, which we considered highly reliable pathways. These include the PI3K-Akt signaling pathway (hsa04151), cAMP signaling pathway (hsa04024), neuroactive ligand–receptor interaction (hsa04080), dopaminergic synapse (hsa04728), and ABC transporters (hsa02010). The PI3K-Akt and cAMP signaling pathways are reportedly related to BC, with a greater number of published studies (Mei et al., 2018; Dong et al., 2015). Next, we constructed a comprehensive pathway (**Figure 6**), including the PI3K-Akt and cAMP signaling pathways, using CyKEGGParser to explore the synergetic mechanisms of *Rhizoma Heterosmilacis* and *Radix Sophorae Flavescentis* in the treatment of BC using CKI (Nersisyan et al., 2014).

In the PI3K-Akt signaling pathway, *Radix Sophorae Flavescentis* acts on targets of the upstream pathway, such as Ras, GBY, and Syk, while *Rhizoma Heterosmilacis* acts on downstream targets, such as PKCs, SGK, Bcl-2, and Bcl-xL. These results indicate that *Rhizoma Heterosmilacis* and *Radix Sophorae Flavescentis* have synergistic and complementary effects on cell survival, cell cycle progression, metabolism, survival signal, growth and proliferation, actin reorganization, vesicle transport, and glucose uptake. Additionally, in the cAMP signaling pathway, *Rhizoma Heterosmilacis* acts as a target of the upstream pathway, including Gi and PKA, while *Radix Sophorae Flavescentis* acts as a target of the downstream pathway, including FOS, NFKB, and CFTR, which are associated with pathways of hyperexcitability, cell death or survival (hippocampal neuron), and increased testicular AMH output (prepubertal Sertoli cells). As the pathogenic factors of BC are related to metabolism, cell survival, proliferation, cell death, and cell cycle (Jia et al., 2018), the above results suggest that *Rhizoma*

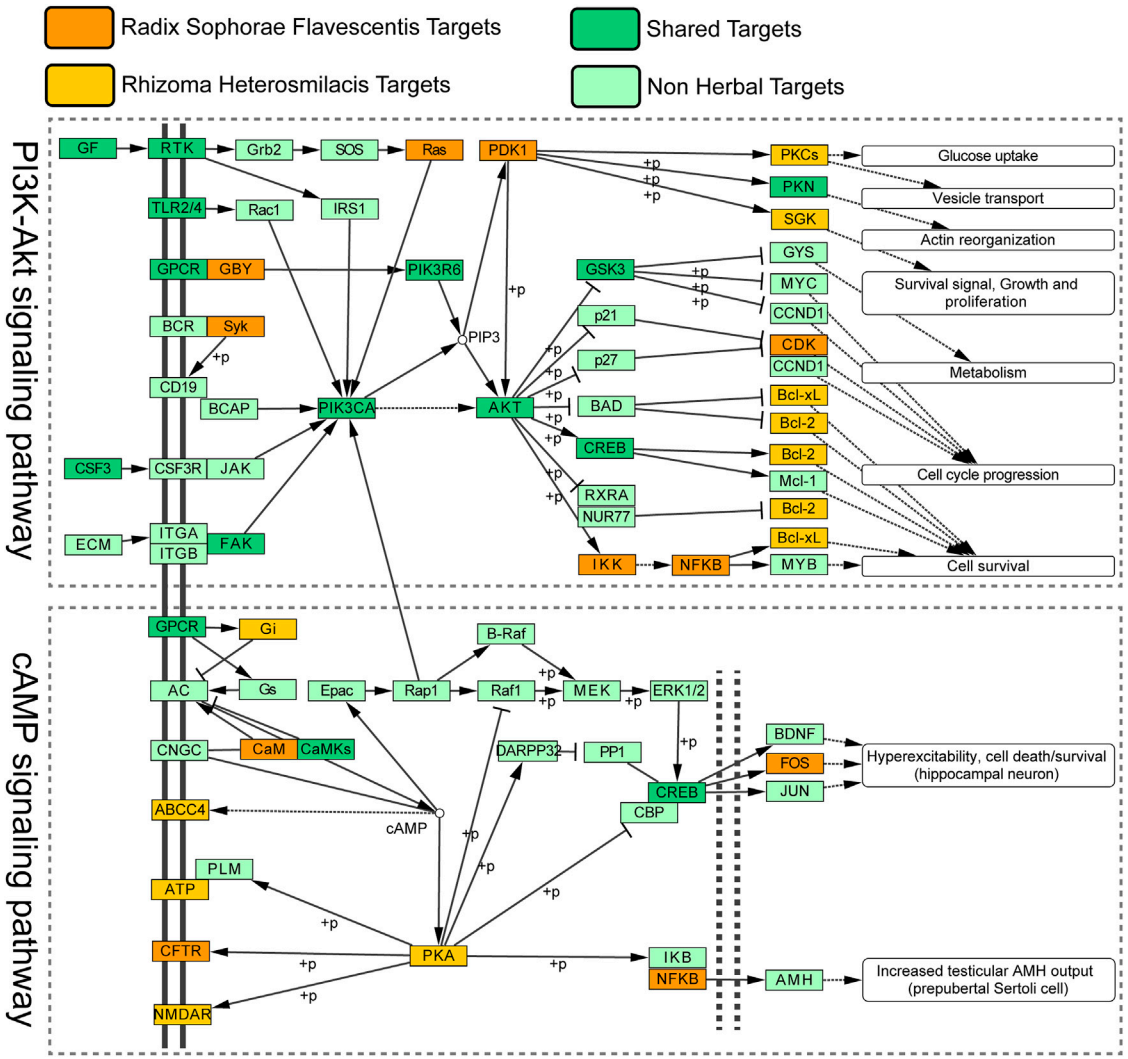

FIGURE 6 | Distribution of target proteins of CKI on the compressed BC pathway. The colors of the blanks represent different types of targets.

Heterosmilacis and *Radix Sophorae Flavescentis* can exert a synergistic effect on BC at multiple pathways.

Molecular Docking Validation of HCGSC in the Treatment of BC

To evaluate the function of HCGSC in BC treatment, molecular docking was employed to simulate the interaction between the ligands and the protein. Twenty-four components from the HCGSC of CKI and 85 proteins coded by 30 genes were used for molecular docking, and 18,254 docking relationships were obtained from the docking results (**Supplementary Table S7**). The result with the lowest affinity value in each component-protein was selected as the best docking relationship (2040 docking relationships), of which the affinity value ranged from −11.3 kcal/mol to −0.5 kcal/mol. Among the best docking relationships, three exhibited affinity values lower than −11.0 kcal/mol, BTL3 and BTL4 had the lowest affinity values of −11.3 kcal/mol, binding with protein 3ovv coded by PKA and protein 2w73 coded by CaM, respectively. BTL3 could bind 2w73 coded by CaM with the affinity values of −11.2 kcal/mol thereafter (**Figures 7A–C**). Based on the literature reports, improved binding between component–protein interactions should have a lower value of affinity (Elhenawy et al., 2019), and the histogram revealed that most of the results were concentrated in the lower affinity value position (**Figure 7D**).

To reduce the influence of background noise of docking relationships with high affinity values, we selected the docking relationships that were lower than the average affinity value (−6.743) from all the best docking relationships as a highly reliable docking relationship (HRDR). Twenty-two components and 82 proteins coded by 29 genes were identified in HRDR with 1,255 docking relationships. Among the 22 components, 15 components were from *Radix Sophorae Flavescentis*, including KS1, KS2, KS3, KS4, KS11, KS16, KS19, KS20, KS52, KS53, KS70, KS77, KS90, KS91, and KS92, and seven

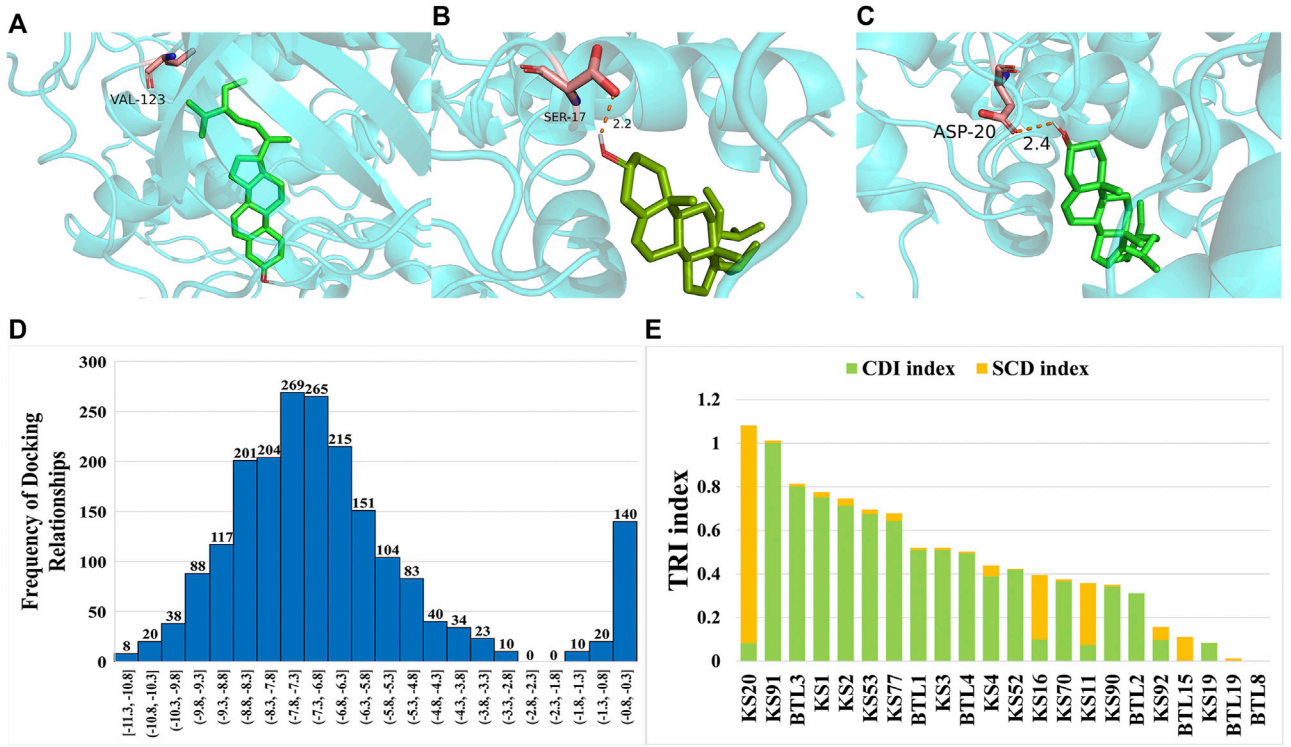

FIGURE 7 | (A) Docking result visualization of BTL3-3ovv (coded by PKA). **(B)** Docking result visualization of BTL4-2w73 (coded by CaM). **(C)** Docking result visualization of BTL3-2w73 (coded by Cam). **(D)** The frequency histogram of the affinity value. **(E)** The bar plot to display the composition of CDI and SCD in each TRI.

components were from *Rhizoma Heterosmilacis*, including BTL1, BTL2, BTL3, BTL4, BTL8, BTL15, and BTL19. The 15 components of *Radix Sophorae Flavescentis* could bind 82 proteins coded by 29 genes, and the seven components of *Rhizoma Heterosmilacis* could bind 81 proteins coded by 29 genes. These results suggest that *Rhizoma Heterosmilacis* and *Radix Sophorae Flavescentis* exert a synergistic effect on BC at multiple pathways.

To evaluate the therapeutic potential of components in HRDR, we designed a mathematical model to calculate the TRI of each component in the HRDR from the HCGSC. To further decode the mechanism of CKI in treating BC comprehensively, we integrated the CDI and SCD to calculate the TRI, which not only considered synergistic effects, but also considered the docking relationship. Detailed information on the TRI is listed in **Supplementary Table S8**. As shown in **Figure 7E**, KS20 (TRI = 1.08), KS91 (TRI = 1.01), BTL3 (TRI = 0.81), and KS1 (TRI = 0.78) were the top four components with TRI scores higher than 0.75. Among these four components, matrine (KS20), with the highest TRI, was confirmed by a number of published studies related to BC therapy (Li et al., 2015). The following three components with higher TRIs were selected for *in vitro* experiments to validate the reliability of our proposed strategy.

Luteolin and Trifolirhizin Inhibited Proliferation and Metastasis of MCF-7 Cells *In Vitro*

Based on the TRI results, trifolirhizin (KS91), beta-sitosterol (BTL3), and luteolin (KS1) were selected for *in vitro* experiments. The *in vitro* experiments proved that two of the three core components of HCGSC showed significant inhibitory effects on breast cancer cell proliferation and migration. The effects of luteolin and trifolirhizin on the viability of MCF-7 cells were determined using the MTT assay. As shown in **Figures 8A,B**, the proliferation of MCF-7 cells was suppressed by luteolin and trifolirhizin in a dose-dependent manner. Subsequently, the effects of luteolin and trifolirhizin on the migration of MCF-7 cells were investigated. As presented in **Figures 7C,D**, luteolin (40 and 80 Mm) and trifolirhizin (20 and 40 Mm) dramatically inhibited the migration of MCF-7 cells. These results indicated that luteolin and trifolirhizin markedly inhibited the proliferation and migration of MCF-7 cells.

DISCUSSION

Breast cancer is one of the most common malignant tumors among women worldwide, with the second highest death rate in female cancer patients (Siegel et al., 2020). At present, research

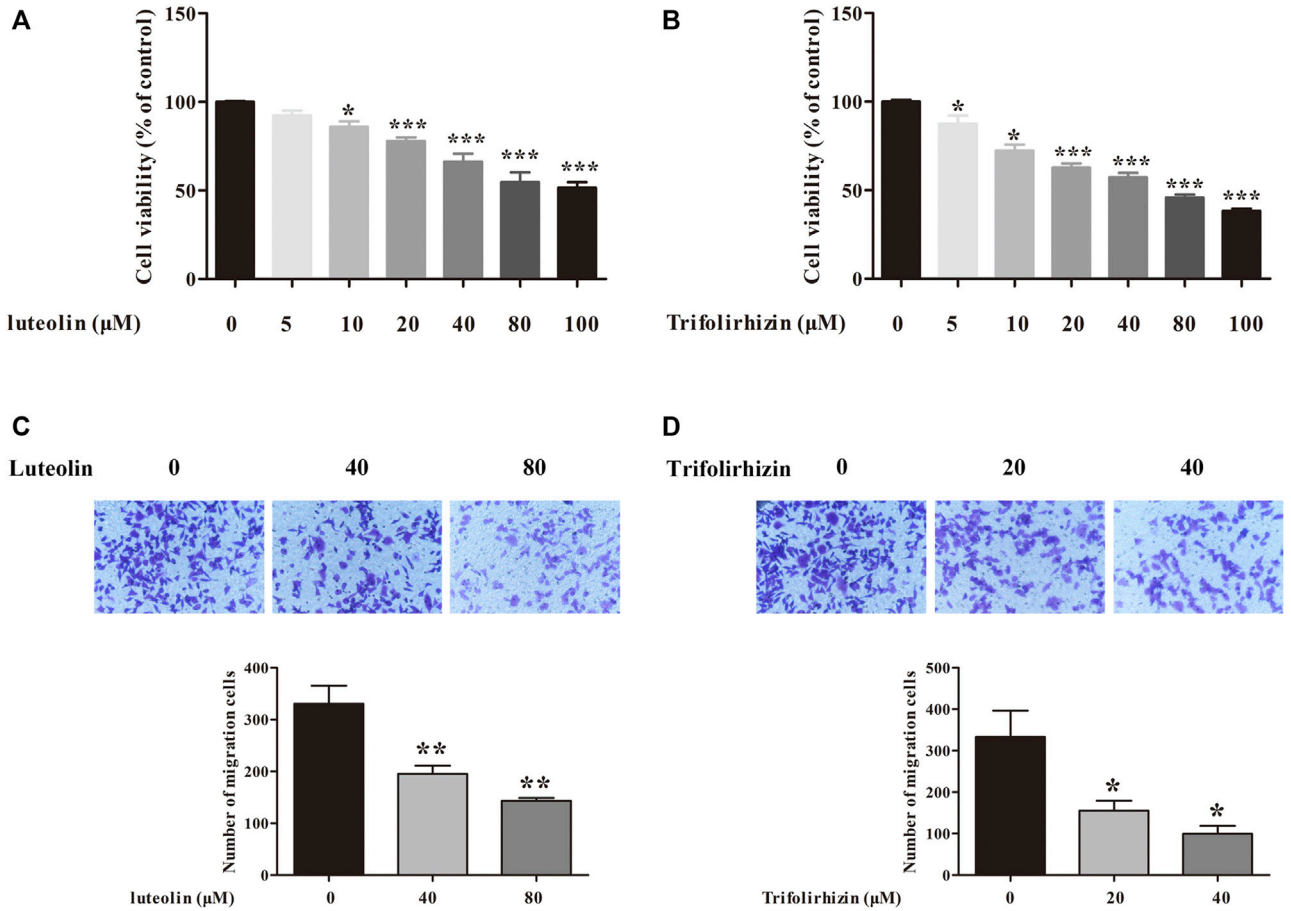

FIGURE 8 | Inhibitory effects of luteolin **(A)** and trifolirhizin **(B)** on the proliferation of MCF-7 cells. Inhibitory effects of luteolin **(C)** and trifolirhizin **(D)** on migration in MCF-7 cells. Data are represented as mean ± SEM (n = 3). $^{*}p < 0.05$, $^{**}p < 0.01$, $^{***}p < 0.001$ as compared with that of the control group.

regarding cancer treatment using TCM is still in the exploratory stage, and CKI has a wide range of applications in the treatment of tumors. However, there are few studies on CKI in the treatment of BC through systematic pharmacology. Therefore, we designed a systematic pharmacology strategy combining differentially expressed gene analysis, pharmacokinetics synthesis screening, target identification, synergy contribution degree, network analysis, therapeutic response index calculation, and experimental validation and provided a reference for this new method.

In this study, we examined the synergistic effect of CKI on BC at three levels. At the first level, the target coincidence of *Rhizoma Heterosmilacis* and *Radix Sophorae Flavescentis* in CKI indicates that *Rhizoma Heterosmilacis* and *Radix Sophorae Flavescentis* may act synergistically to exert a therapeutic effect in treating BC. First, we constructed a C-T network and found that most targets with a higher degree were mapped on the joint targets between *Rhizoma Heterosmilacis* and *Radix Sophorae Flavescentis*. These results suggest that *Rhizoma Heterosmilacis* and *Radix Sophorae Flavescentis* may act synergistically to treat BC *via* common targets and provide therapeutic targets for the cooperative treatment of BC. However, in the complex C-T network, we know neither the key synergistic components in treating BC nor their synergistic mechanisms.

To solve this issue, at the second level, we designed an SCD model with the advantages of reflecting the topology character of the C-T network and the component dose, which implemented a semi-quantitative system pharmacology model. Through the analysis of the SCD model, 24 components compose HCGSC, which can contribute to the effects of CKI on BC with a sum of 95.03% and map 80.89% (631/780) of all targets of CKI. Two references were employed to confirm the reliability and accuracy of the HCGSC selection model, including genes and pathways. The targets of HCGSC contained 62 genes, which could cover 88.57% of the first reference, while the HCGSC targets enriched 81 pathways, which could cover 70.59% of the second reference. Third, we performed GO-BP and KEGG enrichment analysis for *Radix Sophorae Flavescentis* and *Rhizoma Heterosmilacis* targets of HCGSC. We found that most of the overlapped GO-BP terms and pathways between them affect BC treatment, and most of them have a lower FDR adjusted *p* value.

At the third level, to further understand the synergistic mechanisms of CKI and infer the function of synergistic components and verify their effectiveness, three aspects were employed. First, a comprehensive pathway was constructed to explore the synergetic mechanism of *Rhizoma Heterosmilacis* and

Radix Sophorae Flavescentis in the treatment of BC using CKI. In the PI3K-Akt and cAMP signaling pathways, *Rhizoma Heterosmilacis* and *Radix Sophorae Flavescentis* can activate upstream and downstream targets to play their role in the treatment of BC. These results suggest that CKI can produce a combined effect on BC. Second, we designed a TRI model, which provides the results of SCD and docking, to comprehensively evaluate the synergy contribution rate of the components in HCGSC and the binding ability of the components and proteins. TRI calculation results showed that four components displayed a TRI score higher than 0.75, including matrine (KS20, TRI = 1.08), trifolirhizin (KS91, TRI = 1.01), beta-sitosterol (BTL3, TRI = 0.81), and luteolin (KS1, TRI = 0.78), which may be the core components in the treatment of BC with synergistic mechanisms. Third, MTT and Transwell assays were employed to determine the function of luteolin and trifolirhizin. The results showed that they markedly inhibited the proliferation and migration of MCF-7 cells.

In this study, we proposed two novel mathematical models for the speculation of synergistic components and mechanisms. The method provided a methodological reference for decoding the synergistic mechanism of TCM in treating complex diseases. However, several limitations must be mentioned. 1) The precise synergistic mechanisms based on the calculation predictions warrant further validation. 2) Because the interaction between herbs is extremely complex, it may be incomplete to explore the synergistic mechanisms based on our model. Multiple synergistic effects combining with other techniques should be further considered. 3) The TRI model is proposed based on network topology methodology, which is more suitable for the case that herbs have a complex network. This algorithm used undirected network, which ignores the activation or inhibition effects of the disease targets.

DATA AVAILABILITY STATEMENT

Publicly available datasets were analyzed in this study. This data can be found here: https://portal.gdc.cancer.gov/ https://tcmsp-e.com/.

AUTHOR CONTRIBUTIONS

YL and KW contributed equally to this article. Conceptualization: YL, WC, and DG.; methodology: DG and GQ; Software: YL and JC; validation: XQ and AL; investigation: XQ and AL; data curation: YL and YC; writing—original draft: YL and KW; writing—review and editing: DG, WC, and GQ; visualization: YL and KW; funding acquisition: DG and WC. All authors have read and agreed to the published version of the manuscript.

FUNDING

This study was financially supported by the Natural Science Foundation of China (grant No. 82171929), the Natural Science Foundation of Guangdong Province (grant No. 2019A1515011168), the Startup fund from the Southern Medical University (grant No. G820282016), the Natural Science Foundation Council of China (grant No. 31501080, 32070676), the Natural Science Foundation of Guangdong Province (grant No. 2021A1515010737), Hong Kong Baptist University Strategic Development Fund (grant No. SDF13-1209-P01, SDF15-0324-P02(b) and SDF19-0402-P02), Hong Kong Baptist University Interdisciplinary Research Matching Scheme (grant No. RC/IRCs/17-18/04).

SUPPLEMENTARY MATERIAL

The Supplementary Material for this article can be found online at: https://www.frontiersin.org/articles/10.3389/fphar.2021.723147/full#supplementary-material

Supplementary Figure S1 | The process of ADME screening.

Supplementary Figure S2 | The heatmap of DEGs of breast cancer. The red color represents the high expression of the gene and the green color represents the low expression of the gene.

Supplementary Figure S3 | The C-T network of *Rhizoma Heterosmilacis* and *Radix Sophorae Flavescentis*. The targets were in yellow and the components were in the green. The common targets were placed at the center of the network. The targets at the left were the unique targets of *Radix Sophorae Flavescentis*, while those at the right were the unique targets of *Rhizoma Heterosmilacis*. The size of the targets and components were related to the degree. The higher degree represented the larger size.

Supplementary Figure S4 | (A) The Venn diagram of the joint targets between BC and CKI and the targets of HCGSC. **(B)** The Venn diagram of the joint KEGG pathways between BC and CKI and the KEGG pathways of HCGSC. **(C)** The Venn diagram of joint GO-BP terms between *Radix Sophorae Flavescentis* in HCGSC and *Rhizoma Heterosmilacis* in HCGSC. **(D)** The Venn diagram of the joint pathway between *Radix Sophorae Flavescentis* in HCGSC and *Rhizoma Heterosmilacis* in HCGSC.

REFERENCES

Anders, S., and Huber, W. (2010). Differential expression analysis for sequence count data. *Genome Biol.* 11 (10), R106. doi:10.1186/gb-2010-11-10-r106

Astashchanka, A., Shroka, T. M., and Jacobsen, B. M. (2019). Mucin 2 (MUC2) modulates the aggressiveness of breast cancer. *Breast Cancer Res. Treat.* 173 (2), 289–299. doi:10.1007/s10549-018-4989-2

Awad, A. B., Downie, A. C., and Fink, C. S. (2000). Inhibition of growth and stimulation of apoptosis by beta-sitosterol treatment of MDA-MB-231 human breast cancer cells in culture. *Int. J. Mol. Med.* 5 (5), 541–545. doi:10.3892/ijmm.5.5.541

Awad, A. B., Roy, R., and Fink, C. S. (2003). Beta-sitosterol, a plant sterol, induces apoptosis and activates key caspases in MDA-MB-231 human breast cancer cells. *Oncol. Rep.* 10 (2), 497–500. doi:10.3892/or.10.2.497

Balaji, K., Subramanian, B., Yadav, P., Anu Radha, C., and Ramasubramanian, V. (2016). Radiation therapy for breast cancer: Literature review. *Med. Dosim.* 41 (3), 253–257. doi:10.1016/j.meddos.2016.06.005

Berridge, M. J., Bootman, M. D., and Lipp, P. (1998). Calcium--a life and death signal. *Nature* 395 (6703), 645–648. doi:10.1038/27094

Berridge, M. J., Bootman, M. D., and Roderick, H. L. (2003). Calcium signalling: dynamics, homeostasis and remodelling. *Nat. Rev. Mol. Cel Biol* 4 (7), 517–529. doi:10.1038/nrm1155

Binggang, Z., Jing, L., Yuzhuo, F., and Gang, S. (2002). Experimental study on apoptosis of human breast cancer cell line MCF-7 induced by oxymatrine. *Chin. Pharmacol. Bull.* (06), 689–691.

Cao, D., Zhu, G. Y., Lu, Y., Yang, A., Chen, D., Huang, H. J., et al. (2020). Luteolin suppresses epithelial-mesenchymal transition and migration of triple-negative breast cancer cells by inhibiting YAP/TAZ activity. *Biomed. Pharmacother.* 129, 110462. doi:10.1016/j.biopha.2020.110462

Chen, Z. B., Liu, C., Chen, F. Q., Li, S. Y., Liang, Q., and Liu, L. Y. (2006). Effects of tobacco-specific carcinogen 4-(methylnitrosamino)-1-(3-pyridyl)-1-butanone (NNK) on the activation of ERK1/2 MAP kinases and the proliferation of human mammary epithelial cells. *Environ. Toxicol. Pharmacol.* 22 (3), 283–291. doi:10.1016/j.etap.2006.04.001

Cochran, J. M., Busch, D. R., Leproux, A., Zhang, Z., O'Sullivan, T. D., Cerussi, A. E., et al. (2019). Tissue oxygen saturation predicts response to breast cancer neoadjuvant chemotherapy within 10 days of treatment. *J. Biomed. Opt.* 24 (02), 1–11. doi:10.1117/1.JBO.24.2.021202

Cohn, B. A., Cirillo, P. M., Hopper, B. R., and Siiteri, P. K. (2017). Third Trimester Estrogens and Maternal Breast Cancer: Prospective Evidence. *J. Clin. Endocrinol. Metab.* 102 (10), 3739–3748. doi:10.1210/jc.2016-3476

Colaprico, A., Silva, T. C., Olsen, C., Garofano, L., Cava, C., Garolini, D., et al. (2016). TCGAbiolinks: an R/Bioconductor package for integrative analysis of TCGA data. *Nucleic Acids Res.* 44 (8), e71. doi:10.1093/nar/gkv1507

Condorelli, R., and Vaz-Luis, I. (2018). Managing side effects in adjuvant endocrine therapy for breast cancer. *Expert Rev. Anticancer Ther.* 18 (11), 1101–1112. doi:10.1080/14737140.2018.1520096

Crean-Tate, K. K., and Reizes, O. (2018). Leptin Regulation of Cancer Stem Cells in Breast and Gynecologic Cancer. *Endocrinology* 159 (8), 3069–3080. doi:10.1210/en.2018-00379

Cui, J., Qu, Z., Harata-Lee, Y., Nwe Aung, T., Shen, H., Wang, W., et al. (2019). Cell cycle, energy metabolism and DNA repair pathways in cancer cells are suppressed by Compound Kushen Injection. *BMC Cancer* 19 (1), 103. doi:10.1186/s12885-018-5230-8

Cui, J., Qu, Z., Harata-Lee, Y., Shen, H., Aung, T. N., Wang, W., et al. (2020). The effect of compound kushen injection on cancer cells: Integrated identification of candidate molecular mechanisms. *PLoS One* 15 (7), e0236395. doi:10.1371/journal.pone.0236395

Cuiping, Y. (2010). Review on Pharmacological Researches of Sophoridine. *Chin. J. Exp. Traditional Med. Formulae*.

Doherty, A. H., Ghalambor, C. K., and Donahue, S. W. (2015). Evolutionary Physiology of Bone: Bone Metabolism in Changing Environments. *Physiology (Bethesda)* 30 (1), 17–29. doi:10.1152/physiol.00022.2014

Dong, H., Claffey, K. P., Brocke, S., and Epstein, P. M. (2015). Inhibition of breast cancer cell migration by activation of cAMP signaling. *Breast Cancer Res. Treat.* 152 (1), 17–28. doi:10.1007/s10549-015-3445-9

Elhenawy, A. A., Al-Harbi, L. M., El-Gazzar, M. A., Khowdiary, M. M., and Moustfa, A. (2019). Synthesis, molecular properties and comparative docking and QSAR of new 2-(7-hydroxy-2-oxo-2H-chromen-4-yl)acetic acid derivatives as possible anticancer agents. *Spectrochim Acta A. Mol. Biomol. Spectrosc.* 218, 248–262. doi:10.1016/j.saa.2019.02.074

Enien, M. A., Ibrahim, N., Makar, W., Darwish, D., and Gaber, M. (2018). Health-related quality of life: Impact of surgery and treatment modality in breast cancer. *J. Cancer Res. Ther.* 14 (5), 957–963. doi:10.4103/0973-1482.183214

Gao, L., Wang, K. X., Zhou, Y. Z., Fang, J. S., Qin, X. M., and Du, G. H. (2018). Uncovering the anticancer mechanism of Compound Kushen Injection against HCC by integrating quantitative analysis, network analysis and experimental validation. *Sci. Rep.* 8 (1), 624. doi:10.1038/s41598-017-18325-7

Gfeller, D., Grosdidier, A., Wirth, M., Daina, A., Michielin, O., and Zoete, V. (2014). SwissTargetPrediction: a web server for target prediction of bioactive small molecules. *Nucleic Acids Res.* 42, W32–W38. (Web Server issue). doi:10.1093/nar/gku293

Go, R. E., Hwang, K. A., and Choi, K. C. (2015). Cytochrome P450 1 family and cancers. *J. Steroid Biochem. Mol. Biol.* 147, 24–30. doi:10.1016/j.jsbmb.2014.11.003

Guo, Y., Fan, Y., and Pei, X. (2020). Fangjihuangqi Decoction inhibits MDA-MB-231 cell invasion *in vitro* and decreases tumor growth and metastasis in triple-negative breast cancer xenografts tumor zebrafish model. *Cancer Med.* 9 (7), 2564–2578. doi:10.1002/cam4.2894

Guo, Y., Huang, Y., Shen, H., Sang, X., Ma, X., Zhao, Y., and et alXiao, X. (2015). *Efficacy of Compound Kushen Injection in Relieving Cancer-Related Pain: A Systematic Review and Meta-Analysis*. United States: Hindawi Publishing Corporation, 840742–840748.

Han, F. M., Zhu, M. M., Chen, H. X., and Chen, Y. (2009). Identification of Sophoridine and its Metabolites in Rat Urine by Liquid Chromatography-Tandem Mass Spectrometry. *Anal. Lett.* 43 (1), 45–54. doi:10.1080/00032710903276471

Hong, Q., Yu, S., Mei, Y., Lv, Y., Chen, D., Wang, Y., et al. (2014). Smilacis Glabrae Rhizoma Reduces Oxidative Stress Caused by Hyperuricemia via Upregulation of Catalase. *Cell. Physiol. Biochem.* 34 (5), 1675–1685. doi:10.1159/000366369

Hu, S. T., Shen, Y. F., Gong, J. M., and Yang, Y. J. (2016). Effect of sophoridine on Ca^{2+} induced Ca^{2+} release during heart failure. *Physiol. Res.* 65, 43–52. doi:10.33549/physiolres.933052

Huang, X., Li, B., and Shen, L. (20142014). Studies on the Anti-inflammatory Effect and its Mechanisms of Sophoridine. *J. Anal. Methods Chem.* 2014, 502626–6. doi:10.1155/2014/502626

Hy, L., and Qy, H. (2014). Mechanisms of yanshu injection for overcoming multidrug resistance in breast carcinoma MCF-7 cells: an experimental research. *Chin. J. integrated traditional West. Med.* 34 (3), 324–328.

Ij, H., Tj, R., and Rt, B. (1989). Characterization of the human colon carcinoma cell line (Caco-2) as a model system for intestinal epithelial permeability. *Gastroenterology* 96 (3), 736–749.

Imran, M., Rauf, A., Abu-Izneid, T., Nadeem, M., Shariati, M. A., Khan, I. A., et al. (2019). Luteolin, a flavonoid, as an anticancer agent: A review. *Biomed. Pharmacother.* 112, 108612. doi:10.1016/j.biopha.2019.108612

Jacobsen, A. C., Nielsen, S., Brandl, M., and Bauer-Brandl, A. (2020). Drug Permeability Profiling Using the Novel Permeapad® 96-Well Plate. *Pharm. Res.* 37 (6), 93. doi:10.1007/s11095-020-02807-x

Jia, L., Huang, S., Yin, X., Zan, Y., Guo, Y., and Han, L. (2018). Quercetin suppresses the mobility of breast cancer by suppressing glycolysis through Akt-mTOR pathway mediated autophagy induction. *Life Sci.* 208, 123–130. doi:10.1016/j.lfs.2018.07.027

Jiang, S., Fan, J., Wang, Q., Ju, D., Feng, M., Li, J., et al. (2016). Diosgenin induces ROS-dependent autophagy and cytotoxicity via mTOR signaling pathway in chronic myeloid leukemia cells. *Phytomedicine* 23 (3), 243–252. doi:10.1016/j.phymed.2016.01.010

Jiaqin, C., Xiaoxia, W., Xuhui, H., Jie, Z., and Hong, S. (2018). Oxymatrine inhibits invasion and metastasis of triple negative breast cancer cells by regulating epithelial-mesenchymal transformation. *Chin. J. Clin. Pharmacol. Ther.* 23 (01), 13–17.

Jin, Y., Yang, Q., Liang, L., Ding, L., Liang, Y., Zhang, D., et al. (2018). Compound kushen injection suppresses human acute myeloid leukaemia by regulating the Prdxs/ROS/Trx1 signalling pathway. *J. Exp. Clin. Cancer Res.* 37 (1), 277. doi:10.1186/s13046-018-0948-3

Jingyuan, W., Bowen, X., Jie, L., Weilu, C., Taicheng, L., and Luchang, C. (2021). *[Exploring the Molecular Biological Mechanism of Shugan Jianpi Decoction in the Treatment of Depression-related Breast Cancer Based Treatment of Depression-related Breast Cancer Based]*. Hainan: Journal of Hainan Medical University, 1–16. doi:10.13210/j.cnki.jhmu.20210315.001

Juan, T., Weihao, W., Huimin, G., and Zhimin, W. (2007). Determination of matrine, sophoridine and oxymatrine in compound Sophora flavescens injection by HPLC. *China J. Chin. Materia Med.* (03), 222–224.

Kalantari-Dehaghi, M., Parnell, E. A., Armand, T., Bernard, H. U., and Grando, S. A. (2015). The nicotinic acetylcholine receptor-mediated reciprocal effects of the tobacco nitrosamine NNK and SLURP-1 on human mammary epithelial cells. *Int. Immunopharmacol.* 29 (1), 99–104. doi:10.1016/j.intimp.2015.04.041

Kassambara, A. (2020). *ggpubr: 'ggplot2' Based Publication Ready Plots. R package version*.

Keiser, M. J., Roth, B. L., Armbruster, B. N., Ernsberger, P., Irwin, J. J., and Shoichet, B. K. (2007). Relating protein pharmacology by ligand chemistry. *Nat. Biotechnol.* 25 (2), 197–206. doi:10.1038/nbt1284

Kirn, V., Strake, L., Thangarajah, F., Richters, L., Eischeid, H., Koitzsch, U., et al. (2018). ESR1-promoter-methylation status in primary breast cancer and its corresponding metastases. *Clin. Exp. Metastasis* 35 (7), 707–712. doi:10.1007/s10585-018-9935-5

Kwon, M., Jang, M., Kim, G. H., Oh, T., Ryoo, I. J., Ryu, H. W., et al. (2020). Kushenol E inhibits autophagy and impairs lysosomal positioning via VCP/p97 inhibition. *Biochem. Pharmacol.* 175, 113861. doi:10.1016/j.bcp.2020.113861

Kwon, M., Ko, S. K., Jang, M., Kim, G. H., Ryoo, I. J., Son, S., et al. (2019). Inhibitory effects of flavonoids isolated from Sophora flavescens on indoleamine 2,3-dioxygenase 1 activity. *J. Enzyme Inhib. Med. Chem.* 34 (1), 1481–1488. doi:10.1080/14756366.2019.1640218

Lee, C. H., Huang, C. S., Chen, C. S., Tu, S. H., Wang, Y. J., Chang, Y. J., et al. (2010). Overexpression and activation of the alpha9-nicotinic receptor during tumorigenesis in human breast epithelial cells. *J. Natl. Cancer Inst.* 102 (17), 1322–1335. doi:10.1093/jnci/djq300

Lemon, H. M., Wotiz, H. H., Parsons, L., and Mozden, P. J. (1966). Reduced estriol excretion in patients with breast cancer prior to endocrine therapy. *JAMA* 196 (13), 1128–1136. doi:10.1001/jama.1966.03100260066020

Li, H., Li, X., Bai, M., Suo, Y., Zhang, G., and Cao, X. (2015). Matrine inhibited proliferation and increased apoptosis in human breast cancer MCF-7 cells via upregulation of Bax and downregulation of Bcl-2. *Int. J. Clin. Exp. Pathol.* 8 (11), 14793–14799.

Li, J., Hu, L., Zhou, T., Gong, X., Jiang, R., Li, H., et al. (2019). Taxifolin inhibits breast cancer cells proliferation, migration and invasion by promoting mesenchymal to epithelial transition via β-catenin signaling. *Life Sci.* 232, 116617. doi:10.1016/j.lfs.2019.116617

Liang, G., Nie, Y., Chang, Y., Zeng, S., Liang, C., Zheng, X., et al. (2019). Protective effects of Rhizoma smilacis glabrae extracts on potassium oxonate- and monosodium urate-induced hyperuricemia and gout in mice. *Phytomedicine* 59, 152772. doi:10.1016/j.phymed.2018.11.032

Liu, C., Kang, Y., Zhou, X., Yang, Z., Gu, J., and Han, C. (2017). Rhizoma smilacis glabrae protects rats with gentamicin-induced kidney injury from oxidative stress-induced apoptosis by inhibiting caspase-3 activation. *J. Ethnopharmacol.* 198, 122–130. doi:10.1016/j.jep.2016.12.034

Liu, R., Peng, J., Wang, H., Li, L., Wen, X., Tan, Y., et al. (2018). Oxysophocarpine Retards the Growth and Metastasis of Oral Squamous Cell Carcinoma by Targeting the Nrf2/HO-1 Axis. *Cel. Physiol. Biochem.* 49 (5), 1717–1733. doi:10.1159/000493615

Liu, S., Hu, X., Fan, X., Jin, R., Yang, W., Geng, Y., et al. (2020). A Bioinformatics Research on Novel Mechanism of Compound Kushen Injection for Treating Breast Cancer by Network Pharmacology and Molecular Docking Verification. *Evid.-based Compl. Alt.* 2020, 1–14. doi:10.1155/2020/2758640

Liu, X., Vogt, I., Haque, T., and Campillos, M. (2013). HitPick: a web server for hit identification and target prediction of chemical screenings. *Bioinformatics* 29 (15), 1910–1912. doi:10.1093/bioinformatics/btt303

Liu, X., Zhao, W., Wang, W., Lin, S., and Yang, L. (2017). Puerarin suppresses LPS-induced breast cancer cell migration, invasion and adhesion by blockage NF-Kb and Erk pathway. *Biomed. Pharmacother.* 92, 429–436. doi:10.1016/j.biopha.2017.05.102

Mei, Y., Yang, J. P., Lang, Y. H., Peng, L. X., Yang, M. M., Liu, Q., et al. (2018). Global expression profiling and pathway analysis of mouse mammary tumor reveals strain and stage specific dysregulated pathways in breast cancer progression. *Cell Cycle* 17 (8), 963–973. doi:10.1080/15384101.2018.1442629

Meng, G., Tang, X., Yang, Z., Benesch, M. G. K., Marshall, A., Murray, D., et al. (2017). Implications for breast cancer treatment from increased autotaxin production in adipose tissue after radiotherapy. *FASEB J.* 31 (9), 4064–4077. doi:10.1096/fj.201700159R

Merghoub, N., Benbacer, L., El Btaouri, H., Ait Benhassou, H., Terryn, C., Attaleb, M., et al. (2011). *In vitro* antiproliferative effect and induction of apoptosis by Retama monosperma L. extract in human cervical cancer cells. *Cel Mol Biol (Noisy-le-grand)* 57 Suppl (Suppl. l), OL1581–91. doi:10.5772/30025

Miller, K. D., Fidler-Benaoudia, M., Keegan, T. H., Hipp, H. S., Jemal, A., and Siegel, R. L. (2020). Cancer statistics for adolescents and young adults, 2020. *CA Cancer J. Clin.* 70 (1), 443–459. doi:10.3322/caac.2159010.3322/caac.21637

Monteith, G. R., Mcandrew, D., Faddy, H. M., and Roberts-Thomson, S. J. (2007). Calcium and cancer: targeting Ca2+ transport. *Nat. Rev. Cancer* 7 (7), 519–530. doi:10.1038/nrc2171

Nersisyan, L., Samsonyan, R., and Arakelyan, A. (2014). CyKEGGParser: tailoring KEGG pathways to fit into systems biology analysis workflows. *F1000Res* 3, 145. doi:10.12688/f1000research.4410.210.12688/f1000research.4410.1

Nishioka, T., Kim, H. S., Luo, L. Y., Huang, Y., Guo, J., and Chen, C. Y. (2011). Sensitization of epithelial growth factor receptors by nicotine exposure to promote breast cancer cell growth. *Breast Cancer Res.* 13 (6), R113. doi:10.1186/bcr3055

Nourmohammadi, S., Aung, T. N., Cui, J., Pei, J. V., De Ieso, M. L., Harata-Lee, Y., et al. (2019). Effect of Compound Kushen Injection, a Natural Compound Mixture, and its Identified Chemical Components on Migration and Invasion of Colon, Brain, and Breast Cancer Cell Lines. *Front. Oncol.* 9, 314. doi:10.3389/fonc.2019.00314

O'Boyle, N. M., Banck, M., James, C. A., Morley, C., Vandermeersch, T., and Hutchison, G. R. (2011). Open Babel: An open chemical toolbox. *J. Cheminform* 3 (1), 33–14. doi:10.1186/1758-2946-3-33

Otte, M., Zafrakas, M., Riethdorf, L., Pichlmeier, U., Löning, T., Jänicke, F., et al. (2001). MAGE-A gene expression pattern in primary breast cancer. *Cancer Res.* 61 (18), 6682–6687.

Qi, L., Zhang, J., and Zhang, Z. (2013). Determination of four alkaloids in Compound Kushen Injection by high performance liquid chromatography with ionic liquid as mobile phase additive. *Se Pu* 31 (03), 249–253. doi:10.3724/sp.j.1123.2012.10039

Qu, Z., Cui, J., Harata-Lee, Y., Aung, T. N., Feng, Q., Raison, J. M., et al. (2016). Identification of candidate anti-cancer molecular mechanisms of Compound Kushen Injection using functional genomics. *Oncotarget* 7 (40), 66003–66019. doi:10.18632/oncotarget.11788

Recht, A. (2017). Radiation-Induced Heart Disease after Breast Cancer Treatment: How Big a Problem, and How Much Can-and Should-We Try to Reduce it. *J. Clin. Oncol.* 35 (11), 1146–1148. doi:10.1200/JCO.2016.71.4113

Ren, M. X., Deng, X. H., Ai, F., Yuan, G. Y., and Song, H. Y. (2015). Effect of quercetin on the proliferation of the human ovarian cancer cell line SKOV-3 *in vitro*. *Exp. Ther. Med.* 10 (2), 579–583. doi:10.3892/etm.2015.2536

Restrepo-Angulo, I., Bañuelos, C., and Camacho, J. (2020). Ion Channel Regulation by Sex Steroid Hormones and Vitamin D in Cancer: A Potential Opportunity for Cancer Diagnosis and Therapy. *Front. Pharmacol.* 11, 152. doi:10.3389/fphar.2020.00152

Ritchie, M. E., Phipson, B., Wu, D., Hu, Y., Law, C. W., Shi, W., et al. (2015). limma powers differential expression analyses for RNA-sequencing and microarray studies. *Nucleic Acids Res.* 43 (7), e47. doi:10.1093/nar/gkv007

Rohacs, T. (2005). Teaching resources. TRP channels. *Sci. STKE* 2005 (282), tr14. doi:10.1126/stke.2822005tr14

Rojas-Aguirre, Y., and Medina-Franco, J. L. (2014). Analysis of structure-Caco-2 permeability relationships using a property landscape approach. *Mol. Divers.* 18 (3), 599–610. doi:10.1007/s11030-014-9514-x

Romero-Hernández, L. L., Merino-Montiel, P., Montiel-Smith, S., Meza-Reyes, S., Vega-Báez, J. L., Abasolo, I., et al. (2015). Diosgenin-based thio(seleno)ureas and triazolyl glycoconjugates as hybrid drugs. Antioxidant and antiproliferative profile. *Eur. J. Med. Chem.* 99, 67–81. doi:10.1016/j.ejmech.2015.05.018

Ru, J., Li, P., Wang, J., Zhou, W., Li, B., Huang, C., et al. (2014). TCMSP: a database of systems pharmacology for drug discovery from herbal medicines. *J. Cheminform* 6 (1), 13–16. doi:10.1186/1758-2946-6-13

Sanner, M. F. (1999). Python: a programming language for software integration and development. *J. Mol. Graph. Model.* 17 (1), 57–61.

Schr Odinger, L. D. D. (2015). The {PyMOL} Molecular Graphics System. *Version~1*. 8.

Sekino, Y., Han, X., Babasaki, T., Goto, K., Inoue, S., Hayashi, T., et al. (2020). Microtubule-associated protein tau (MAPT) promotes bicalutamide resistance and is associated with survival in prostate cancer. *Urol. Oncol. Semin. Original Invest.* 38, e1–795. doi:10.1016/j.urolonc.2020.04.032

Sergeev, I. N. (2005). Calcium signaling in cancer and vitamin D. *J. Steroid Biochem. Mol. Biol.* 97 (1-2), 145–151. doi:10.1016/j.jsbmb.2005.06.007

Serna-Marquez, N., Diaz-Aragon, R., Reyes-Uribe, E., Cortes-Reynosa, P., and Salazar, E. P. (2017). Linoleic acid induces migration and invasion through FFAR4- and PI3K-/Akt-dependent pathway in MDA-MB-231 breast cancer cells. *Med. Oncol.* 34 (6), 111. doi:10.1007/s12032-017-0969-3

Shannon, P., Markiel, A., Ozier, O., Baliga, N. S., Wang, J. T., Ramage, D., et al. (2003). Cytoscape: a software environment for integrated models of biomolecular interaction networks. *Genome Res.* 13 (11), 2498–2504. doi:10.1101/gr.1239303

Singh, M., Alavi, A., Wong, R., and Akita, S. (2016). Radiodermatitis: A Review of Our Current Understanding. *Am. J. Clin. Dermatol.* 17 (3), 277–292. doi:10.1007/s40257-016-0186-4

Sterling, T., and Irwin, J. J. (2015). ZINC 15--Ligand Discovery for Everyone. *J. Chem. Inf. Model.* 55 (11), 2324–2337. doi:10.1021/acs.jcim.5b00559

Straub, J. M., New, J., Hamilton, C. D., Lominska, C., Shnayder, Y., and Thomas, S. M. (2015). Radiation-induced fibrosis: mechanisms and implications for therapy. *J. Cancer Res. Clin. Oncol.* 141 (11), 1985–1994. doi:10.1007/s00432-015-1974-6

Tao, W., Xu, X., Wang, X., Li, B., Wang, Y., Li, Y., et al. (2013). Network pharmacology-based prediction of the active ingredients and potential targets of Chinese herbal Radix Curcumae formula for application to cardiovascular disease. *J. Ethnopharmacol.* 145 (1), 1–10. doi:10.1016/j.jep.2012.09.051

Tong, W. G., Ding, X. Z., and Adrian, T. E. (2002). The mechanisms of lipoxygenase inhibitor-induced apoptosis in human breast cancer cells. *Biochem. Biophys. Res. Commun.* 296 (4), 942–948. doi:10.1016/S0006-291X(02)02014-4

Trott, O., and Olson, A. J. (2009). AutoDock Vina: Improving the speed and accuracy of docking with a new scoring function, efficient optimization, and multithreading. *J. Comput. Chem.*, NA. doi:10.1002/jcc.21334

Vaidya, J. S., Massarut, S., Vaidya, H. J., Alexander, E. C., Richards, T., Caris, J. A., et al. (2018). Rethinking neoadjuvant chemotherapy for breast cancer. *BMJ* 360, j5913. doi:10.1136/bmj.j5913

Vangeel, L., and Voets, T. (2019). Transient Receptor Potential Channels and Calcium Signaling. *Cold Spring Harb Perspect. Biol.* 11 (6). doi:10.1101/cshperspect.a035048

Venkatachalam, K., and Montell, C. (2007). TRP channels. *Annu. Rev. Biochem.* 76, 387–417. doi:10.1146/annurev.biochem.75.103004.142819

Wang, H., Hu, H., Rong, H., and Zhao, X. (2019). Effects of compound Kushen injection on pathology and angiogenesis of tumor tissues. *Oncol. Lett.* 17 (2), 2278–2282. doi:10.3892/ol.2018.9861

Wang, L. H., Zeng, X. A., Wang, M. S., Brennan, C. S., and Gong, D. (2018). Modification of membrane properties and fatty acids biosynthesis-related genes in Escherichia coli and Staphylococcus aureus: Implications for the antibacterial mechanism of naringenin. *Biochim. Biophys. Acta Biomembr* 1860 (2), 481–490. doi:10.1016/j.bbamem.2017.11.007

Wang, W., You, R. L., Qin, W. J., Hai, L. N., Fang, M. J., Huang, G. H., et al. (2015). Anti-tumor activities of active ingredients in Compound Kushen Injection. *Acta Pharmacol. Sin.* 36 (6), 676–679. doi:10.1038/aps.2015.24

Wang, Y. Y., Attané, C., Milhas, D., Dirat, B., Dauvillier, S., Guerard, A., et al. (2017). Mammary adipocytes stimulate breast cancer invasion through metabolic remodeling of tumor cells. *JCI Insight* 2 (4), e87489. doi:10.1172/jci.insight.87489

Warnes, G. R., Bolker, B., Bonebakker, L., Gentleman, R., Huber, W., Liaw, A., et al. (2020). *gplots: Various R Programming Tools for Plotting Data. R package version 3*.

Weingarten, M. D., Lockwood, A. H., Hwo, S. Y., and Kirschner, M. W. (1975). A protein factor essential for microtubule assembly. *Proc. Natl. Acad. Sci. U S A.* 72 (5), 1858–1862. doi:10.1073/pnas.72.5.1858

Wickham, H. (2016). *ggplot2: Elegant Graphics for Data Analysis*. New York: Springer-Verlag.

Wu, K., Fukuda, K., Xing, F., Zhang, Y., Sharma, S., Liu, Y., et al. (2015). Roles of the Cyclooxygenase 2 Matrix Metalloproteinase 1 Pathway in Brain Metastasis of Breast Cancer. *J. Biol. Chem.* 290 (15), 9842–9854. doi:10.1074/jbc.M114.602185

Xiao, N. (2018). *ggsci: Scientific Journal and Sci-Fi Themed Color Palettes for 'ggplot2'. R package version 2.9*.

Xiumei, Z., and Cen, S. (2004). Simultaneous determination of three Alkaloids in Compound Kushen Injection by HPLC. *China J. Chin. Materia Med.* (07), 99–100.

Xu, W., Lin, H., Zhang, Y., Chen, X., Hua, B., Hou, W., et al. (2011a). Compound Kushen Injection suppresses human breast cancer stem-like cells by down-regulating the canonical Wnt/β-catenin pathway. *J. Exp. Clin. Cancer Res.* 30, 103. doi:10.1186/1756-9966-30-103

Xu, W., Lin, H., Zhang, Y., Chen, X., Hua, B., Hou, W., et al. (2011b). Compound Kushen Injection suppresses human breast cancer stem-like cells by down-regulating the canonical Wnt/β-catenin pathway. *J. Exp. Clin. Cancer Res.* 30, 103. doi:10.1186/1756-9966-30-103

Yang, Y., Sun, M., Li, W., Liu, C., Jiang, Z., Gu, P., et al. (2021). Rebalancing TGF-β/Smad7 signaling via Compound kushen injection in hepatic stellate cells protects against liver fibrosis and hepatocarcinogenesis. *Clin. Transl Med.* 11 (7), e410. doi:10.1002/ctm2.410

Yao, L. T., Wang, M. Z., Wang, M. S., Yu, X. T., Guo, J. Y., Sun, T., et al. (2019). Neoadjuvant endocrine therapy: A potential strategy for ER-positive breast cancer. *World J. Clin. Cases* 7 (15), 1937–1953. doi:10.12998/wjcc.v7.i15.1937

Yao, M., and Fu, P. (2018). Advances in anti-HER2 therapy in metastatic breast cancer. *Chin. Clin. Oncol.* 7 (3), 27. doi:10.21037/cco.2018.05.04

Yarla, N. S., Bishayee, A., Sethi, G., Reddanna, P., Kalle, A. M., Dhananjaya, B. L., et al. (2016). Targeting arachidonic acid pathway by natural products for cancer prevention and therapy. *Semin. Cancer Biol.* 40-41, 48–81. doi:10.1016/j.semcancer.2016.02.001

Yu, G., Wang, L. G., Han, Y., and He, Q. Y. (2012). clusterProfiler: an R Package for Comparing Biological Themes Among Gene Clusters. *OMICS* 16 (5), 284–287. doi:10.1089/omi.2011.0118

Yuan, T. L., and Cantley, L. C. (2008). PI3K pathway alterations in cancer: variations on a theme. *Oncogene* 27 (41), 5497–5510. doi:10.1038/onc.2008.245

Yue, M. (2012). *[Study on Chemical Constituents and Quality Control of Compound Kushen Injection*.

Zhang, Y. (2017). Ganoderma lucidum (Reishi) suppresses proliferation and migration of breast cancer cells via inhibiting Wnt/β-catenin signaling. *Biochem. Biophys. Res. Commun.* 488 (4), 679–684. doi:10.1016/j.bbrc.2017.04.086

Zheng, Y., Zhong, G., Yu, K., Lei, K., and Yang, Q. (2020). Individualized Prediction of Survival Benefit from Locoregional Surgical Treatment for Patients with Metastatic Breast Cancer. *Front. Oncol.* 10, 148. doi:10.3389/fonc.2020.00148

Zhou, C., Wang, M., Zhou, L., Zhang, Y., Liu, W., Qin, W., et al. (2016). Prognostic significance of PLIN1 expression in human breast cancer. *Oncotarget* 7 (34), 54488–54502. doi:10.18632/oncotarget.10239

Conflict of Interest: The authors declare that the research was conducted in the absence of any commercial or financial relationships that could be construed as a potential conflict of interest.

Publisher's Note: All claims expressed in this article are solely those of the authors and do not necessarily represent those of their affiliated organizations, or those of the publisher, the editors, and the reviewers. Any product that may be evaluated in this article, or claim that may be made by its manufacturer, is not guaranteed or endorsed by the publisher.

frontiers in Pharmacology

ORIGINAL RESEARCH
published: 29 November 2021
doi: 10.3389/fphar.2021.775602

Cinobufagin Is a Selective Anti-Cancer Agent against Tumors with EGFR Amplification and PTEN Deletion

Kunyan He[1], Guang-Xing Wang[1], Li-Nan Zhao[1], Xiao-Fang Cui[1], Xian-Bin Su[1], Yi Shi[2], Tian-Pei Xie[3], Shang-Wei Hou[4,5]* and Ze-Guang Han[1,5]**

[1]Key Laboratory of Systems Biomedicine (Ministry of Education), Shanghai Center for Systems Biomedicine, Shanghai Jiao Tong University, Shanghai, China, [2]Key Laboratory for the Genetics of Developmental and Neuropsychiatric Disorders, Bio-X Institutes, Shanghai Jiao Tong University, Shanghai, China, [3]Shanghai Nature Standard Technical Services Co., Ltd., Shanghai, China, [4]Key Laboratory for Translational Research and Innovative Therapeutics of Gastrointestinal Oncology, Department of Anesthesiology, Hongqiao International Institute of Medicine, Shanghai Jiao Tong University School of Medicine Affiliated Tongren Hospital, Shanghai, China, [5]Hangzhou Innovation Institute for Systems Oncology, Hangzhou, China

OPEN ACCESS

Edited by:
Haiyang Yu,
Tianjin University of Traditional Chinese Medicine, China

Reviewed by:
Sreejoyee Ghosh,
University of Texas MD Anderson Cancer Center, United States
Alexander Tikhomirov,
Russian Academy of Medical Sciences, Russia

***Correspondence:**
Kunyan He
khe@sjtu.edu.cn
Shang-Wei Hou
housw@sjtu.edu.cn
Ze-Guang Han
hanzg@sjtu.edu.cn

Specialty section:
This article was submitted to Pharmacology of Anti-Cancer Drugs, a section of the journal Frontiers in Pharmacology

Received: 14 September 2021
Accepted: 22 October 2021
Published: 29 November 2021

Citation:
He K, Wang G-X, Zhao L-N, Cui X-F, Su X-B, Shi Y, Xie T-P, Hou S-W and Han Z-G (2021) Cinobufagin Is a Selective Anti-Cancer Agent against Tumors with EGFR Amplification and PTEN Deletion. Front. Pharmacol. 12:775602. doi: 10.3389/fphar.2021.775602

Glioblastoma multiforme (GBM) is the most common and malignant brain tumor, and almost half of the patients carrying EGFR-driven tumor with PTEN deficiency are resistant to EGFR-targeted therapy. EGFR amplification and/or mutation is reported in various epithelial tumors. This series of studies aimed to identify a potent compound against EGFR-driven tumor. We screened a chemical library containing over 600 individual compounds purified from Traditional Chinese Medicine against GBM cells with EGFR amplification and found that cinobufagin, the major active ingredient of Chansu, inhibited the proliferation of EGFR amplified GBM cells and PTEN deficiency enhanced its anti-proliferation effects. Cinobufagin also strongly inhibited the proliferation of carcinoma cell lines with wild-type or mutant EGFR expression. In contrast, the compound only weakly inhibited the proliferation of cancer cells with low or without EGFR expression. Cinobufagin blocked EGFR phosphorylation and its downstream signaling, which additionally induced apoptosis and cytotoxicity in EGFR amplified cancer cells. *In vivo*, cinobufagin blocked EGFR signaling, inhibited cell proliferation, and elicited apoptosis, thereby suppressing tumor growth in both subcutaneous and intracranial U87MG-EGFR xenograft mouse models and increasing the median survival of nude mice bearing intracranial U87MG-EGFR tumors. Cinobufagin is a potential therapeutic agent for treating malignant glioma and other human cancers expressing EGFR.

Keywords: cinobufagin, EGFR, glioblastoma, PTEN, Chansu

Abbreviations: AKT, v-Akt murine thymoma viral oncogene homolog; CRC, colorectal cancer; EGFR, epidermal growth factor receptor; GBM, glioblastoma multiforme; PTEN, phosphatase and tensin homolog; MEFs, mouse embryonic fibroblasts; NSCLCs, non–small cell lung carcinomas; SAR, structure–activity relationship; STAT3, signal transducers and activators of transcription 3.

INTRODUCTION

Epidermal growth factor receptor (EGFR) amplification and/or mutation exist in different types of cancer and triggers higher interest in EGFR as a cancer therapeutic target. Therefore, the EGFR target therapy has been applied in various epithelial tumors such as lung cancer (Lynch et al., 2004, Hirsch et al., 2008), colorectal cancer (Gibson et al., 2006), and head and neck cancer (Sundvall et al., 2010). Glioblastoma multiforme (GBM) is the most common and malignant brain tumor in adults, with overall survival of 15–16 months and a 5-year survival rate of 5% (Ostrom et al., 2015). Standard of care is surgery followed by radio-chemotherapy and adjuvant chemotherapy (Touat et al., 2017). EGFR amplification, deletion, point mutations, and/or translocation are reported in more than half of glioblastomas (Libermann et al., 1985; Brennan et al., 2013; Eskilsson et al., 2018). GBM still remains a challenge because these tumors are resistant to anti-EGFR therapy, always relapse (Stupp et al., 2009) and recurrent tumors are less sensitive to chemotherapy than the primary tumor, developing novel anti-EGFR agents remains urgent (Campos et al., 2016; Eskilsson et al., 2018). Almost half of the patients carry EGFR-driven tumor with phosphatase and tensin homolog (PTEN) deletion, which are resistant to EGFR target therapy, implying PTEN deficiency plays an important role in resistance to anti-EGFR therapy (Mellinghoff et al., 2007; Arif et al., 2018; Brito et al., 2019). Using PTEN-deficient glioblastoma cell line U87MG-EGFRvIII screening and U87MG-PTEN counter-screening, we have previously reported that G5-7 selectively blocked Janus kinase 2 (Jak2), preventing GBM proliferation (He et al., 2013).

Chansu is extracted from *Bufo bufo gargarizans* Cantor and *Bufo melanostictus* Schneider families, which has been widely used to treat swelling, pain, and heart failure for thousands of years in China (Qi et al., 2018). Cinobufacini (Huachansu), an intravenous formulated extract from toads, has been applied to treat different types of malignant cancers and hepatitis B virus infection (Meng et al., 2009; Cui et al., 2010; Meng et al., 2012; Zhang et al., 2018; Li et al., 2020; Zhang et al., 2020). Cinobufagin, the major bioactive component of Chansu and Huachansu, can inhibit tumor growth through decreasing oncogene expression, blocking the cell cycle, triggering apoptosis, decreasing the new blood vessel formation, enhancing immune response, etc. (Wang et al., 2010; Qi et al., 2011a; Yin et al., 2013; Li et al., 2015; Zhang et al., 2016; Cao et al., 2017; Dai et al., 2018; Zhu et al., 2018; Li et al., 2019; Pan et al., 2019). Cinobufagin's anti-cancer effects have garnered considerable attention in lung cancer, colorectal cancer, liver cancer, and gastric cancer (Qi et al., 2011b; Zhang et al., 2016; Lu et al., 2017; Xiong et al., 2019). Recently, cinobufagin combined with thalidomide was used to treat patients with lung cancer cachexia in a clinical study (Xie et al., 2018). Nonetheless, which types of the malignant tumors are sensitive to cinobufagin and the mechanisms of action remain unknown.

Here, we screened the library from Traditional Chinese Medicine for individual compounds against GBM cells with EGFR amplification and PTEN deletion and successfully identified cinobufagin, the major active ingredient of Chansu. We found that Cinobufagin specifically blocked proliferation of cancer cells with EGFR expression and PTEN deletion enhanced its anti-cell proliferation effects. *In vivo* study showed that cinobufagin suppressed the most malignant glioblastoma, U87MG-EGFR, xenograft tumor growth and extended the life span of nude mice. Cinobufagin might be a therapeutic compound for the treatment of malignant glioma and other human cancers expressing EGFR.

MATERIALS AND METHODS

Cells, Reagents, and Mice

Human glioblastoma cell lines were gifts from Keqiang Ye at Emory University. Liver cancer cell lines (except MHCC97H) were purchased from ATCC. MHCC97H, lung cancer, and colorectal cell lines were from a national collection of authenticated cell cultures of China. All cells were maintained in DMEM or RPMI1640 with 10% FBS and 1× penicillin/streptomycin/glutamine. U87MG was stably transfected with vector control, PTEN, epidermal growth factor receptor variant III (EGFR vIII), and EGFR, and the stable transfected cells were maintained with various antibiotics: 400 μg/ml of G418 for PTEN, 0.7 μg/ml of puromycin for wild-type EGFR, and 150 μg/ml of hygromycin for EGFRvIII. LN229-EGFR and SF763-EGFR stable transfected cells were maintained with 150 μg/ml of hygromycin. All experiments were performed with mycoplasma-free cells. The primary antibodies were from Cell Signaling and the second antibodies were from Invitrogen. The Traditional Chinese Medicine monomer library composed of over 600 natural compounds was provided by Nature Standard of Shanghai. CytoTox 96 Non-Radioactive Cytotoxicity Assay and Caspase-Glo 3/7 Assay were from Promega. Male nude mice (BALB/c nu/nu, 6 weeks of age) and male C57BL/J (MGI Cat# 2160531, 8 weeks of age) mice were obtained from Shanghai SLAC Laboratory Animal Co. Ltd. Mice were housed with a maximum of five per cage and fed autoclaved chow and water with 12 h light and dark cycles. All efforts were made to minimize discomfort to the animals. The animals required physical restraint for injection of tumor cells and delivery of drugs, and measurement of tumor size with a caliper (hand-held). All procedures were approved by the Institutional Animal Care and Use Committee of Shanghai Jiao Tong University and were performed at the Animal Center of Shanghai Jiao Tong University.

In Vitro Proliferation, Cytotoxicity, and Apoptosis Assay

Three thousand cells were seeded in each well of a 96-well plate. The next day, the medium was replaced with fresh medium containing different concentrations of compounds or vehicle. Cells were incubated at 37°C for the indicated times. The cell proliferation, released lactate dehydrogenase (LDH), and caspase 3/7 activity were monitored by cell counting kit 8 (CCK8), CytoTox 96 Non-Radioactive Cytotoxicity, and Caspase-Glo 3/7 assays, respectively, according to the manufacturer's protocols.

Subcutaneous and Intracranial Xenograft Model

Cells (2×10^6) in phosphate buffered saline (PBS) were inoculated subcutaneously into 6-week-old male nude mice. Treatment

commenced once tumors had reached a mean volume of 100 mm^3. The mice were randomly divided into three groups and were treated with vehicle control or cinobufagin (1 and 5 mg kg^{-1}) by daily intraperitoneal injection for indicated days. Tumor volume was calculated using the formula (length × $width^2$)/2, where length is the longest axis and width is the measurement at right angles to the length. For the intracranial model, after anesthetized by intraperitoneal injection of mixture of ketamine/xylazine (95:5 mg/kg), mice were placed in the stereotaxic instrument and cells (1×10^5) were stereotactically inoculated into the right striatum, 3 mm below the dural surface on day 0. On day 7, the mice were intraperitoneally injected with D-luciferin potassium salt and were examined with IVIS Lumina II to confirm tumor formation. Then, the mice were randomly divided into two groups and were daily intraperitoneally injected with vehicle or cinobufagin (5 mg kg^{-1}). Ten days after drug treatment, mice from each group were analyzed by IVIS Lumina II again for tumor luminescence intensity.

Flow Cytometric Analysis

Cells were treated with vehicle or cinobufagin for 24 h, then harvested and washed twice with cold PBS. After fixed in 70% ethanol at −20°C for at least 24 h, the cells were washed with PBS and incubated with propidium iodide (20 μg/ml)/RNase A (20 μg/ml) in PBS for 45 min. The samples were analyzed on a BD&LSR Fortessa.

Immunofluorescence Staining

For immunofluorescence staining, paraffin-embedded tissue sections from intracranial model were deparaffinized in xylene, rehydrated in graded alcohols, and were boiled in 10 mM sodium citrate buffer (pH 6.0) for 10 min. Frozen sections from subcutaneous model were rehydrated in PBS. Then, the sections from both models were permeabilized with PBS+0.1% Triton X-100. The sections were blocked with 1% bovine serum albumin in PBS at 37°C for 30 min followed primary anti-Ki67 (1: 300) or anti-active caspase 3 (1:400) incubation at 4°C overnight. The sections were washed with PBS and incubated with Alexa Fluor 488–labeled goat anti-mouse or anti-rabbit IgG antibody (1: 500) at room temperature for 60 min, followed by rinsing with PBS for 10 min and staining with 4′,6-diamidino-2-phenylindole (DAPI) for another 10 min at room temperature. After mounting, the sections were examined under a fluorescence microscope.

Statistics Analysis

Data are presented as means ± SD. Statistical evaluation was carried out by Student's t-test (two groups) or ANOVA (three groups) plus Bonferroni *post hoc*. Data were considered statistically significant when $p < 0.05$.

RESULTS

Screening Reveals Cinobufagin That Selectively Inhibits Proliferation of EGFR-Amplified, PTEN-Deficient Glioblastoma Cells

To seek compounds effective in treating the most malignant type of GBM with EGFR amplification and PTEN deletion, we developed a cell-based screening assay to identify individual compounds from Traditional Chinese Medicine that specifically block the cell proliferation of U87MG-EGFR with EGFR amplification and PTEN deficiency but mildly inhibit the proliferation of U87MG-PTEN cells without EGFR amplification and with wild-type PTEN. The positive compounds that markedly inhibited the proliferation of U87MG-EGFR cells over 50% were applied to the second-round screening in U87MG-PTEN cells. The compounds that exhibited a robust antiproliferative effect on U87MG-EGFR cells but a weak effect on U87MG-PTEN cells were chosen for further evaluating the cytotoxicity toward mouse embryonic fibroblasts (MEFs). The promising compounds that produced cytotoxicity less than 20% in MEFs were further evaluated. After screening approximately 600 individual compounds of Chinese medicine by this process, we identified two compounds, cinobufagin and resibufogenin, that selectively inhibit U87MG-EGFR not U87MG-PTEN cell proliferation. Interestingly, both cinobufagin and resibufogenin are extracted from Chansu with similar chemical backbones (**Figure 1**).

To search for more effective and selective derivatives, we collected the bioactive compounds of Chansu with similar structure and performed structure–activity relationship (SAR) studies, and found that arenobufagin 3-hemisuberate, cinobufotalin, and cinobufagin at 0.1 μM exhibited more potent antiproliferative effect on U87MG-EGFR cells and almost no effects on other cells derived from the same parent cells, including U87MG-Vehicle, U87MG-PTEN, and U87MG-EGFRvIII. One of the derivatives, resibufogenin, which is another positive hit identified in the screening assay, also exhibited selective antiproliferative activity against U87MG-EGFR at 0.5 μM but no effect at 0.1 μM. Interestingly, cinobufagin and cinobufotalin exhibited potent antiproliferative activity against U87MG-EGFR at both 0.1 and 0.5 μM. They also displayed effective antiproliferative effect on U87MG-EGFRvIII at 0.5 μM, which is often overexpressed in GBM (**Figure 1D**). It is worth noting that cinobufagin, resibufogenin, and cinobufotalin have similar chemical structures except for the acetyl group and hydroxyl groups. Cinobufagin with acetylation was more potent than resibufogenin, implying the acetyl group is critical for its biological effect. Cinobufotalin with an additional 1-hydroxy group was a little bit weak than cinobufagin. So, we selected cinobufagin for further biochemical and pharmacological studies.

Cinobufagin Inhibits EGFR and its Downstream Signaling Cascades, Induces Apoptosis and Cytotoxicity of EGFR Amplified Cells

To explore the potential molecular mechanisms of cinobufagin inhibiting U87MG-EGFR cell proliferation, we conducted the titration assay followed by Western blotting to monitor the signaling pathways mediated by EGFR. Immunoblotting showed that phosphorylation of EGFR at both Tyr1068 and Tyr1173 was inhibited by cinobufagin in U87MG-EGFR cells, which was almost undetectable in U87MG-PTEN cells (**Figure 2A**). Signal transducer and activator of transcription 3 (STAT3), another promising therapeutic target for GBM patients,

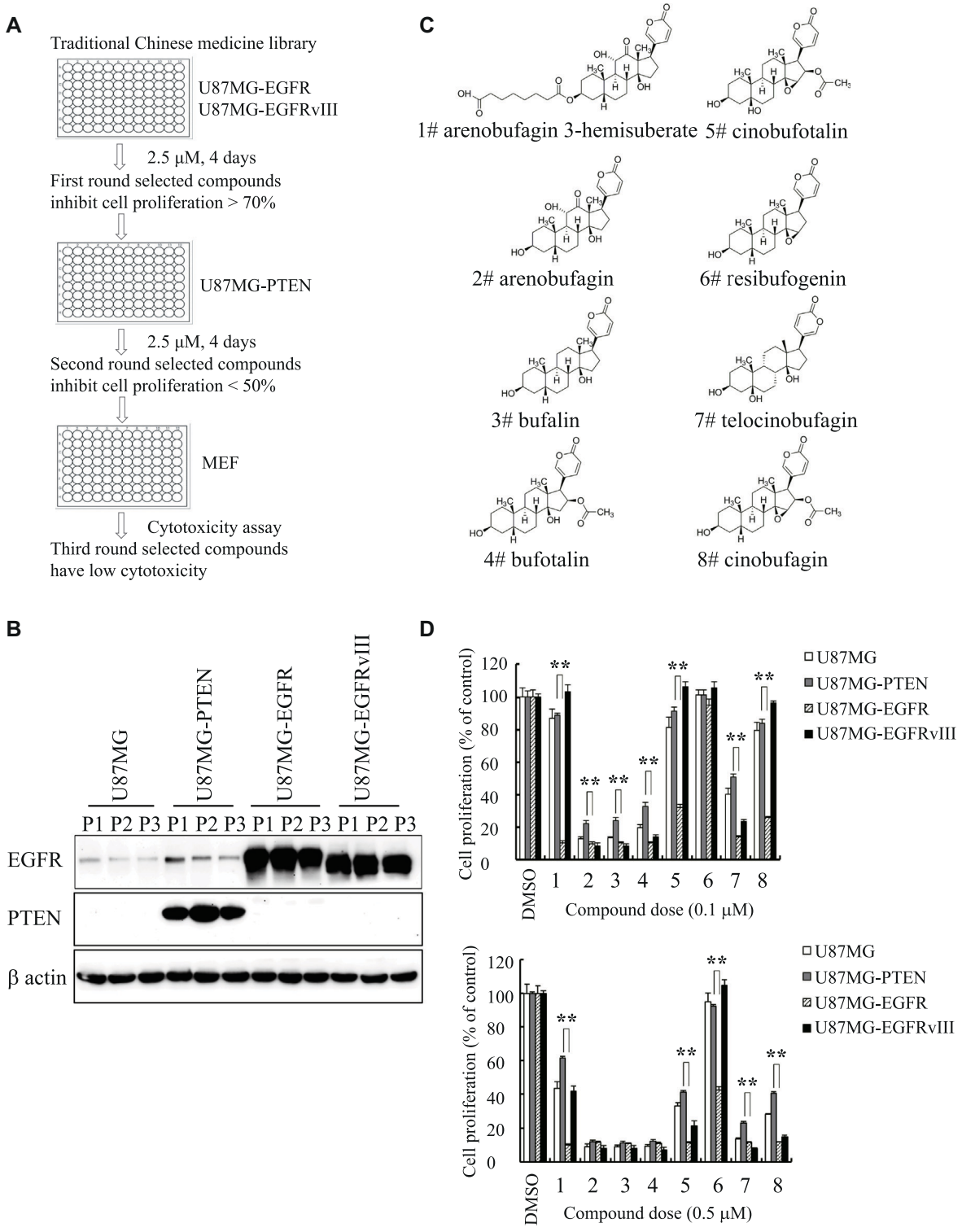

FIGURE 1 | Identification of cinobufagin and its SAR study. **(A)** The diagram of drug screening strategy. **(B)** Expression check of EGFR and PTEN in stable cell lines U87MG-control, U87MG-PTEN, U87MG-EGFR, and U87MG-EGFRvIII from the indicated passages. **(C)** Chemical structures of 8 monomers of Chansu. **(D)** SAR study of Chansu's monomers from **(C)** and their antiproliferative effects on U87MG-control, U87MG-PTEN, U87MG-EGFR, and U87MG-EGFRvIII cells. 1 to 8 in horizontal axis represent the 8 compounds at panel **(C)**. Data are means ± SD.

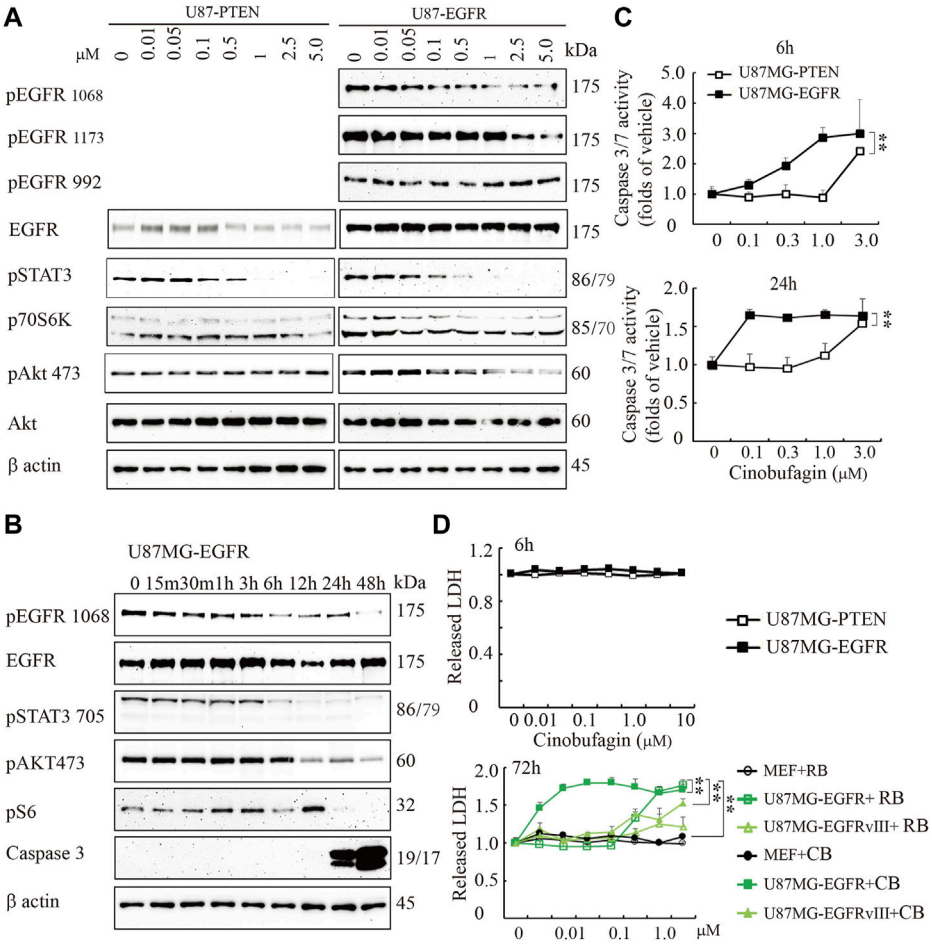

FIGURE 2 | Cinobufagin blocks EGFR phosphorylation and induces cell apoptosis and cytotoxicity. **(A)** Cinobufagin blocks EGFR signaling in a dose-dependent manner. Western blot analysis of U87MG-EGFR and U87MG-PTEN cells treated with different concentrations of cinobufagin for 6 h. Blots are representative of three experiments. **(B)** Cinobufagin blocks EGFR signaling in a time-dependent manner. Western blot analysis of U87MG-EGFR cells treated with 0.5 μM cinobufagin for different times as indicated. Blots are representative of three experiments. **(C)** Cinobufagin specifically induces apoptosis in U87MG-EGFR cells. The cells treated with a range of doses of cinobufagin for 6 or 24 h, then the caspase 3/7 activity was measured with Caspase-Glo 3/7 Assay. **(D)** Cinobufagin specifically induces cytotoxicity of U87MG-EGFR cells. The cells were treated with different doses of cinobufagin (CB) or resibufogenin (RB) for 6 or 72 h, then the released LDH were measured with cytoTox 96 Non-radioactive Cytotoxicity Assay. Data are means ± SD.

is also a critical mediator of EGFR. Inhibition of STAT3 enhances the efficiency of EGFR inhibitor in PTEN-deficient and PTEN-intact GBM cells (Zulkifli et al., 2017). As expected, the phosphorylation of STAT3 was dramatically decreased by cinobufagin in U87MG-EGFR and U87MG-PTEN cells. Consistent with the decreased phosphorylation of EGFR and STAT3, the phosphorylation of downstream molecular, V-akt murine thymoma viral oncogene homolog (Akt), was also decreased by cinobufagin in U87MG-EGFR cells, not in U87MG-PTEN cells (**Figure 2A**). The time-course assay demonstrated that cinobufagin initially blocked EGFR phosphorylation in U87MG-EGFR cells at 15 min, and obviously decreased EGFR and STAT3 phosphorylation from 6 to 48 h (**Figure 2B**). Flow cytometric analysis revealed that cinobufagin substantially arrested cell cycle at G2 and S phases in U87MG-Vehicle, U87MG-EGFRvIII, and U87MG-EGFR cells, except for U87MG-PTEN cells, suggesting that the cell cycle arrest contributes to cinobufagin's antiproliferative effect in GBM cells (**Supplementary Figure S1**).

The time-course assay also showed that cinobufagin at 0.5 μM strongly increased active caspase 3 at 24 and 48 h, detected by Western blotting. The more sensitive luminescence assay for caspase 3/7 activity demonstrated that cinobufagin markedly induced apoptosis of U87MG-EGFR cells at 0.1 μM and reached the highest rate at 1 μM but did not affect U87MG-PTEN cells at 1 μM after 6 h of treatment. When incubation time was extended to 24 h, cinobufagin at 0.1 μM induced the highest apoptosis rate in U87MG-EGFR and did not affect U87MG-PTEN cells except at 1 μM (**Figure 2B,C**). We treated the cells with different doses of cinobufagin for 6 or 72 h. The cytotoxicity assay showed that even 10 μM cinobufagin did not induce cytotoxicity in both U87MG-EGFR and U87MG-PTEN cells after 6 h of incubation. If the incubation time was extended to 72 h, cinobufagin significantly induced stronger

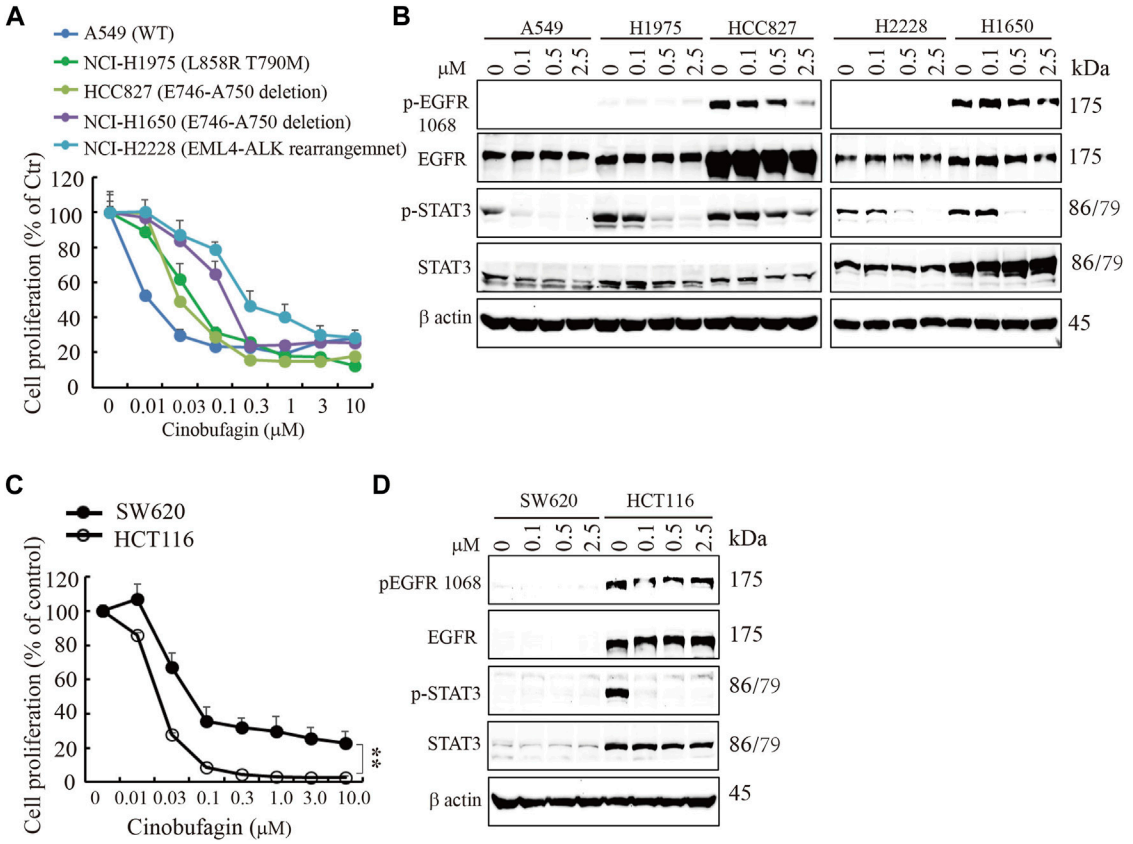

FIGURE 3 | Cinobufagin inhibits proliferation of EGFR expression cancer cells. **(A)** Cinobufagin inhibits proliferation of non–small lung cancer cell lines with EGFR expression. The non–small lung cancer cell lines with different status of EGFR were treated with a range of doses of cinobufagin for 72 h, followed by CCK8 assay. **(B)** EGFR expression and its downstream signaling analysis. The non–small lung cancer cell lines were treated with indicated doses of cinobufagin for 6 h, followed by Western blot analysis of EGFR and its downstream molecules. **(C)** Cinobufagin inhibits proliferation of colorectal cells with EGFR expression. Colorectal cells were treated with cinobufagin for 72 h, then followed by CCK8 assay. **(D)** EGFR expression and its downstream signaling analysis by Western blot. Colorectal cells were treated with indicated doses of cinobufagin for 6 h, followed by Western blot analysis of EGFR and its downstream molecules. Data are means ± SD.

cytotoxicity in U87MG-EGFR cells in a dose-dependent manner than that in U87MG-EGFRvIII cells or MEFs, while its derivative compound resibufogenin induced weak cytotoxicity (**Figure 2D**).

To study whether cinobufagin exerts its anti-cell proliferative effect directly through inhibiting EGFR kinase activity, we performed an *in vitro* kinase assay using the commercial EGFR protein in the presence of different doses of cinobufagin and found that even the high dose of cinobufagin did not affect EGFR kinase activity, while the EGFR inhibitor, erlotinib, robustly blocked the EGFR kinase activity (**Supplementary Figure S2**). The kinase activity profiling and phosphatase activity profiling showed that none of the 83 kinases and 5 phosphatases tested was affected by cinobufagin (**Supplementary Figure S3**, **Supplementary Tables S1, S2**).

Cinobufagin Inhibits Proliferation of EGFR-Expressing Cancer Cells

EGFR is often mutated and/or amplified in various human cancers and is an important target for multiple cancer therapies in the clinical practice (Yarden and Pines, 2012). To characterize whether EGFR-overexpressed or mutated carcinoma cells are sensitive to cinobufagin, we screened more cancer cell lines, including glioblastoma, lung cancer, colorectal cancer (CRC), and liver cancer cell lines, with different status of EGFR. The glioblastoma cell lines without EGFR amplification were less sensitive to cinobufagin compared with the EGFR-overexpressed GBM cells (**Supplementary Figure S4A**). Interestingly, cinobufagin strongly inhibited the proliferation of lung cancer cells with wild-type or mutated EGFR expression. A549 with wild-type EGFR was most sensitive to cinobufagin among these selected lung cancer cells (**Figure 3A,B**). We included two colorectal cancer cell lines to test their sensitivities to cinobufagin. The cell proliferation assays showed that HCT-116 with high EGFR expression was more sensitive to cinobufagin compared with the SW620 with undetectable EGFR (**Figure 3C,D**). We also chose different liver cancer cell lines to test whether their sensitivities to cinobufagin are related to EGFR status. Noticeably, the most sensitive SK-HEP-1 cells expressed high EGFR, while the resistant HepG2 cells expressed undetectable EGFR (**Supplementary**

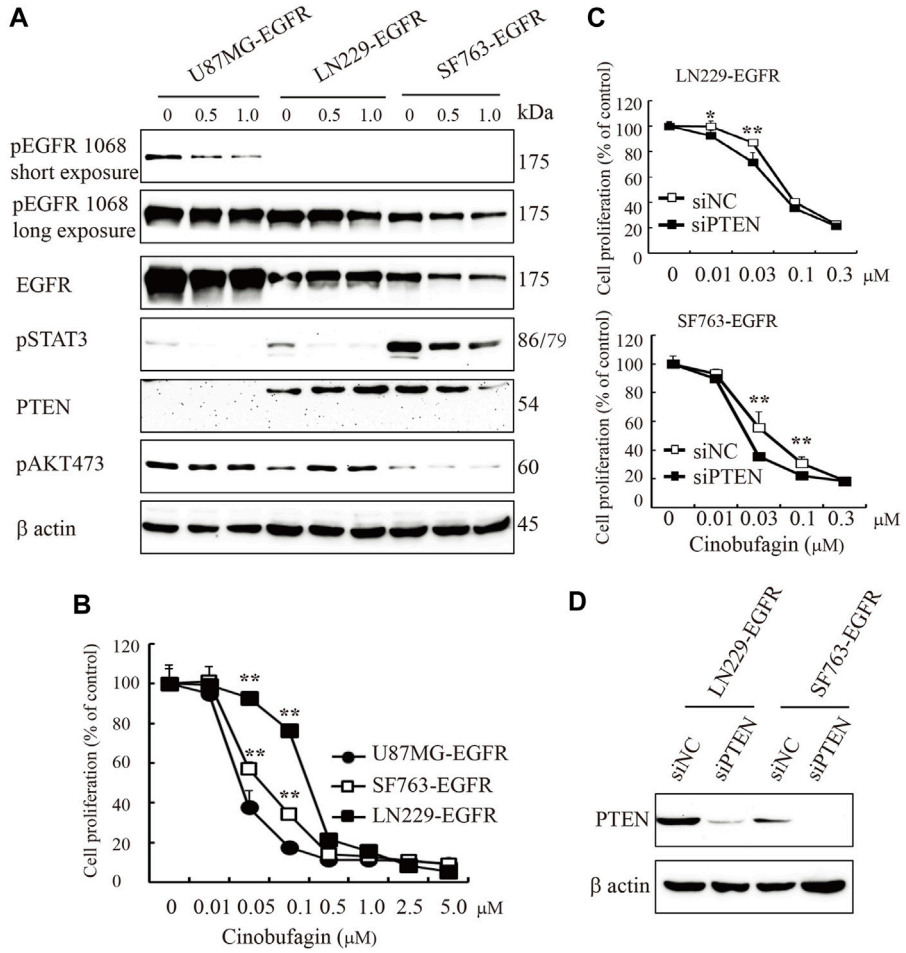

FIGURE 4 | PTEN deficiency enhances cinobufagin's antiproliferation effect. **(A)** PTEN, EGFR expression, and its downstream signaling molecules analyzed by Western blot. U87MG-EGFR, LN229-EGFR, and SF763-EGFR cells were treated with cinobufagin for 6 h, followed by Western blot analysis of PTEN, EGRR, and its downstream molecules. **(B)** Cinobufagin more efficiently inhibits cell proliferation of glioblastoma cell lines with EGFR overexpression and PTEN deficiency. Glioblastoma cells were treated with a range of doses of cinobufagin for 72 h, then followed by CCK8 assay. **(C)** Proliferation of LN229-EGFR and SF763-EGFR cells transfected with control or PTEN siRNA for up to 4 days, followed by CCK8 assay. **(D)** Western blot checks the PTEN expression. Data are means ± SD.

Figure S4B,C). Hence, cinobufagin exerts selective anti-cancer effect toward EGFR-overexpressed cancer cells.

PTEN Deficiency Enhances Cinobufagin's Antiproliferation Effect

EGFR amplification accompanied by loss of PTEN is common in clinical trials; these patients carrying EGFR-driven tumors with PTEN mutation are resistant to anti-EGFR treatment. In the initial screening, we selected the compounds that specifically blocked the most malignant GBM cells' (U87MG-EGFR/PTEN null) proliferation and displayed less or no effects on PTEN normal cells. As expected, we identified cinobufagin as the leading compound, which efficiently blocked U87MG-EGFR cell proliferation and had less effect on U87MG-PTEN cells. We tested the cinobufagin antiproliferation effect on other GBM cells LN229-EGFR and SF763-EGFR, which overexpress EGFR and have normal PTEN, and observed that cinobufagin had less effect on LN229-EGFR and SF763-EGFR than that on PTEN-deficient U87MG-EGFR. To confirm PTEN's role, we further knocked down PTEN at both LN229-EGFR and SF763-EGFR and found that these cells with low PTEN were more sensitive to cinobufagin (**Figure 4**).

Cinobufagin Inhibits Subcutaneous Xenograft Growth in Nude Mice

To study cinobufagin's anti-cancer effect *in vivo*, the U87MG-EGFR cells were subcutaneously inoculated in nude mice. After daily intraperitoneal injection of vehicle or drugs (1 or 5 mg kg^{-1}) for 26 days, tumor growth in the cinobufagin-treated group was much slower than that in the vehicle-treated group (**Figure 5A**). To explore the molecular mechanisms of cinobufagin *in vivo*, we monitored the major signaling effectors

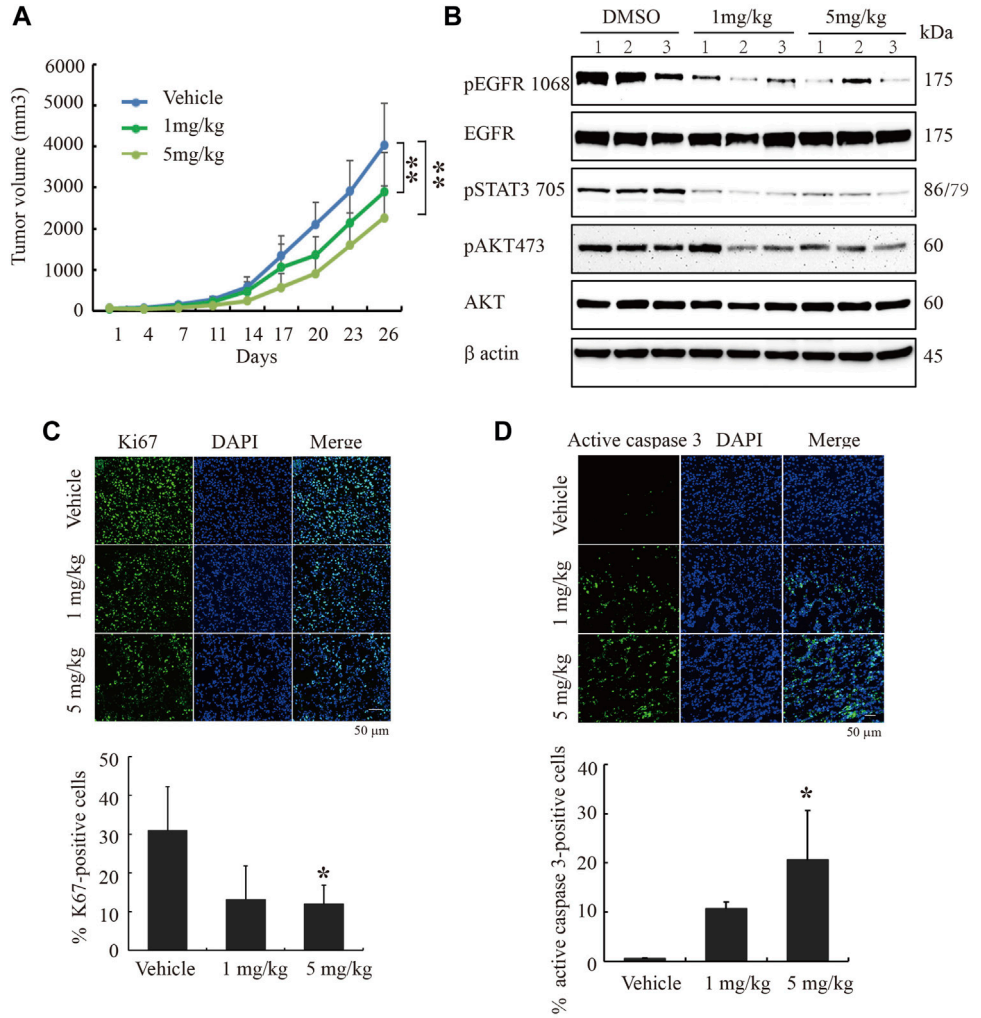

FIGURE 5 | Cinobufagin blocks subcutaneous tumor growth of U87MG-EGFR cells. **(A)** Cinobufagin significantly decreases the tumor volumes in subcutaneous U87MG-EGFR xenograft model. U87MG-EGFR cells were subcutaneously inoculated into nude mice, and after the tumors formed, the nude mice were intraperitoneally injected with vehicle (0.5% cyclodextrin) or cinobufagin at doses of 1 and 5 mg kg^{-1}, respectively. Data represent means ± SD (n = 6/group). **(B)** Cinobufagin inhibits EGFR and STAT3 signaling in subcutaneous tumors. The tumor tissue lysates from vehicle- or drug-treated samples were analyzed by Western blotting with the indicated antibodies. **(C,D)** Cinobufagin inhibits cell proliferation and induces apoptosis in subcutaneous tumors. The immunofluorescence staining of Ki67 and active caspase 3 on tumor sections derived from animals treated with or without cinobufagin. Quantification of Ki67 and active caspase 3–positive cells in subcutaneous tumor. Data represent means ± SD. *p < 0.05; **p < 0.01.

of EGFR and STAT3 in the tumors by Western blotting, and found that *p*-EGFR and its downstream signaling machinery *p*-STAT3 and *p*-Akt were obviously decreased by cinobufagin (**Figure 5B**). The cell proliferation marker (Ki67) staining was also significantly decreased in tumors treated with cinobufagin compared with that in vehicle-treated tumors (**Figure 5C**), suggesting that this compound strongly inhibits tumor cell proliferation *in vivo*. To explore whether this compound also affects tumor growth via triggering apoptosis, the active caspase-3 immunostaining was conducted, and the data showed that the cinobufagin triggered stronger apoptosis, whereas vehicle elicited negligible apoptosis (**Figure 5D**). These data indicated that cinobufagin blocks tumor growth *in vivo* through inhibiting cell proliferation and triggering apoptosis. Thus, cinobufagin inhibits EGFR and STAT3 signaling to block tumor growth in nude mice.

Cinobufagin Decreases Intracranial Tumor Growth and Extends the Life Span of Tumor-Bearing Nude Mice

To further evaluate the therapeutic potential of cinobufagin on the orthotopic glioblastomas, we stereotactically inoculated U87MG-EGFR cells in the corpus striatum of nude mice and monitored tumor growth by luciferase bioluminescence imaging. After confirming tumor formation in the brains on day 7, each group of animals was intraperitoneally injected with vehicle (0.5% β-cyclodextrin) or cinobufagin (5 mg kg^{-1}) once a day. The

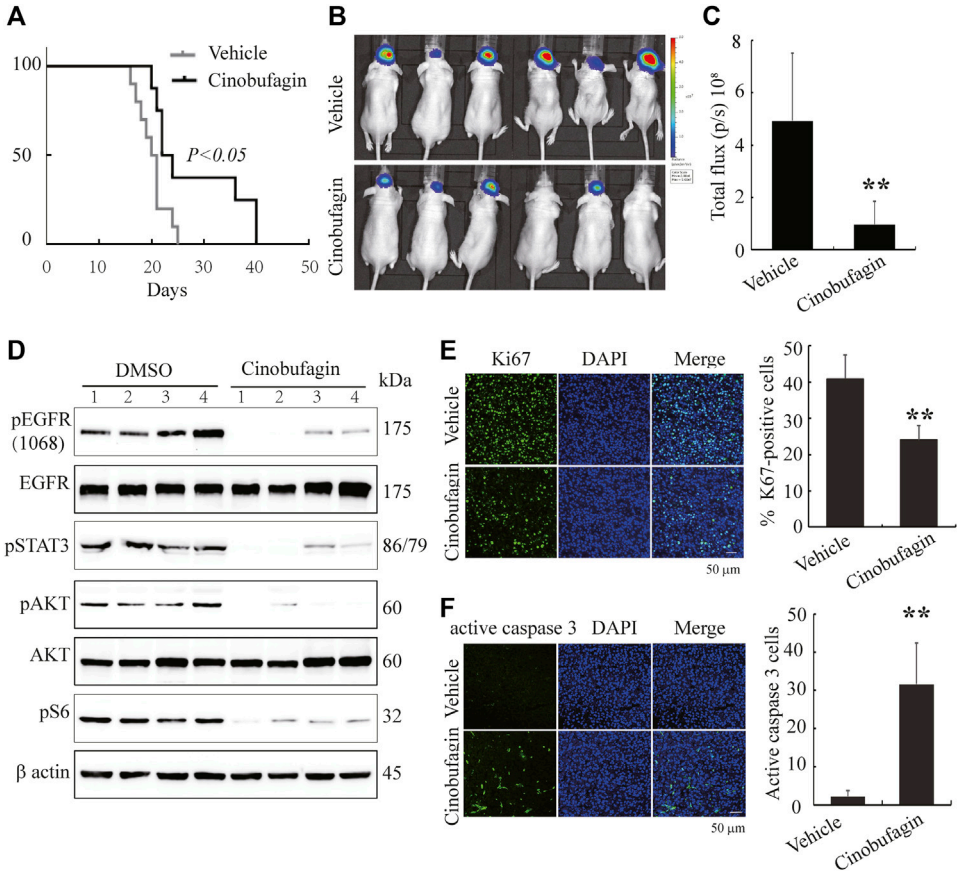

FIGURE 6 | Cinobufagin suppresses tumor growth of U87MG-EGFR cells and elongates nude mice life span. **(A)** Survival curves of brain tumor–bearing mice. After confirmation of brain tumor formation by luminance imaging, mice were intraperitoneally injected with vehicle or cinobufagin once a day until the termination of the experiment ($n = 8$ for vehicle group or 10 for cinobufagin group). The cinobufagin treatment group (23 days) showed a significant improvement in their survival compared with the vehicle treatment group (20.5 days, $p < 0.05$). **(B)** Luminance imaging of individual mice 10 days after cinobufagin treatment. The presence of a glioma is detected through the colorful luminance intensity. **(C)** Quantitative analysis of intracranial tumor luminance intensity in mice treated with vehicle or cinobufagin. Cinobufagin significantly suppressed tumor growth compared with the vehicle. Data represent means ± SD (*$p < 0.05$, $n = 6$). **(D)** Cinobufagin inhibits EGFR and STAT3 signaling in intracranial tumor. The tumor tissue lysates from vehicle or drug-treated mice were analyzed by immunoblotting with the indicated antibodies. **(E,F)** Cinobufagin inhibits cell proliferation and induces apoptosis in intracranial tumor. The immunofluorescence staining of Ki67 **(E)** and active caspase 3 **(F)** on tumor sections derived from animals treated with or without cinobufagin. Quantification of Ki67 and active caspase 3–positive cells in intracranial tumor. Data represent means ± SD. *$p < 0.05$; **$p < 0.01$ compared with the vehicle group.

survival was evaluated by Kaplan–Meier analysis. The median survival time (23 days) for the cinobufagin treatment group was significantly longer than 20.5 days for the vehicle group (**Figure 6A**). The mice were subjected to luciferase bioluminescence imaging 10 days after treatment. The luminescence intensity of brain tumor treated with cinobufagin was decreased about 70% (**Figure 6B,C**).

Next, we tested the signaling molecules in these samples and found that cinobufagin strongly decreased *p*-EGFR, *p*-STAT3, and *p*-Akt levels in the intracranial tumors as compared with the vehicles (**Figure 6D**), which were consistent with what were observed in subcutaneous tumors. Moreover, Ki67 and active caspase-3 immunostaining of intracranial tumors were significantly decreased in cinobufagin-treated group compared with those in the vehicle-treated group (**Figure 6E,F**). Therefore, cinobufagin blocks EGFR/STAT3 signaling in glioblastoma and shrinks brain tumors, elongating nude animal survival.

DISCUSSION

We found cinobufagin, a monomer of Chansu from Traditional Chinese Medicine, that demonstrated selective antiproliferative activity against EGFR-overexpressed and PTEN-deficient GBM cells, compared with normal EGFR and PTEN cells. It also exhibited antiproliferative activity in various carcinoma cancer cells with EGFR expression, including lung cancer cells, colorectal cancer cells, and liver cancer cells. Cinobufagin blocked the oncogenic pathways mediated by EGFR and STAT3, and triggered apoptosis in a dose-dependent manner *in vitro* and *in vivo* (**Figures 2**, **5**, **6**). Intraperitoneal administration of

cinobufagin dose-dependently inhibited the tumor growth of U87MG-EGFR in subcutaneous xenograft model. Moreover, cinobufagin significantly inhibited tumor growth and extended the life span of intracranial xenograft mice, implying that this monomer itself or its metabolites could cross the brain–blood barrier to exert anti-tumor effects (**Figure 6**).

The early studies showed that the anti-cancer activity of cinobufagin is manifested in eliciting apoptosis, inhibiting autophagy, blocking cell cycles, and inhibiting cell proliferation (Zhang et al., 2016; Zhu et al., 2018; Dai et al., 2018; Cao et al., 2017; Zhang et al., 2019). In the study, we demonstrated that cinobufagin exhibited specific antiproliferation effect in the special carcinoma cells with EGFR expression, including glioblastoma cells, lung cancer cells, colorectal cells, and hepatocellular carcinoma cells (**Figures 1A**, **3A**,**C**, **4B**,**C**, **Supplementary Figure S4A,B**). We further characterized that cinobufagin displayed antiproliferation effects on the cells with EGFR mutation, which are resistant to EGFR inhibitor (**Figure 3A**). Zhang et al. and other groups' reports indicate that cinobufagin blocks Akt signaling pathway, decreases Bcl-2, and induces mitochondrial cytochrome *c* release to trigger apoptosis, or inhibits STAT3 and Notch pathways to suppress tumor cell growth (Yin et al., 2013; Zhang et al., 2016; Zhang et al., 2019). Pan et al. reported that cinobufagin arrests cell cycle at G2/M or S phase and induces apoptosis in melanoma and nasopharyngeal carcinoma cells (Pan et al., 2019; Pan et al., 2020). Our work is consistent with these studies and further demonstrated that cinobufagin inhibits EGFR/STAT3 and its downstream signaling to arrest cell cycle at G2/M phase, to inhibit cell proliferation, and to promote apoptosis (**Figures 2A**,**B**, **3B**,**D**). Our work also validated that cinobufagin inhibited tumor growth and elongated nude mice life span via blocking EGFR and STAT3 signaling pathways and inducing apoptosis *in vivo* (**Figures 5B–D**, **6D–F**). Our study demonstrates that the malignant tumors with wild-type or mutated EGFR are sensitive to cinobufagin. Unfortunately, the *in vitro* kinase assay displayed that cinobufagin did not inhibit EGFR and STAT3 activity (**Supplementary Figure S2** and **Supplementary Table S1**). It also cannot affect the EGFR upstream kinase Jak2 or phosphatases activity (**Supplementary Figure S3**, **Supplementary Tables S1, S2**). We failed to identify the cellular target of cinobufagin after screening around 90 kinases and phosphatases (**Supplementary Tables S1, S2**).

Chansu, a traditional medicine from Chinese toad, has been widely used in clinic in Asian countries. Huachansu, which is a water-soluble extract from toad and an intravenous formulated agent, has been used in clinic for treating late-stage liver cancer, lung cancer, and gastric cancer (Gibson et al., 2006; Meng et al., 2009; Zhang et al., 2018; XU and WU, 2017; MA and LU, 2011). Both Chansu and Huachansu are mixtures, which include various bioactive components, such as cinobufagin, bufotalin, bufalin, arenobufagin, and so on, and show potential anti-cancer effect, as well as side effects (Meng et al., 2016). In the current study, we collected the bioactive components of Chansu and performed SAR analysis, and found that each derivative had unique selectivity and antiproliferation efficacy. Among them, cinobufagin, cinobufotalin, and resibufogenin have similar chemical structure except for the acetyl group and hydroxy groups. Cinobufagin and cinobufotalin, having same acetylation and different hydroxy, exhibit better selectivity and higher efficiency against cancer cells with EGFR expression and PTEN deletion than resibufogenin (**Figure 1D**), implying the acetyl group increases the inhibitory effect and 1-hydroxy is not critical. Toma et al. reported that cinobufagin can be metabolized to desacetylcinobufagin (Toma et al., 1987), and our study showed that resibufogenin without the acetyl group had less inhibitory effect, implying that the deacetylation of cinobufagin might contribute to its low anti-cancer efficacy *in vivo*. In the near future, we could focus on cinobufagin and modify it to enhance its anti-cancer efficiency and selectivity *in vitro* and *in vivo*, and to avoid the side effect.

Chansu has been used in clinic for a long time, but its toxicity cannot be ignored. Two preclinical studies showed that intraperitoneal injection of 10 mg kg^{-1} cinobufagin is tolerable in nude mice (Lu et al., 2017). However, in our study, we tried the highest dose of cinobufagin (10 mg kg^{-1}) via intraperitoneal injection and found that one-third of the nude mice were dead, and then reduced the highest dose to 5 mg kg^{-1}. We daily injected C57BL/J mice with 5 mg kg^{-1} cinobufagin up to 1 month and performed complete blood count and did not observed any abnormity and difference between cinobufagin and vehicle-treated groups (**Supplementary Table S3**). We also treated the cells *in vitro* with different doses of cinobufagin and monitored the toxicity and apoptosis. The data showed that cinobufagin did not cause cellular toxicity in MEFs, but triggered significant cell apoptosis after 6 h of treatment, and caused significant cytotoxicity and apoptosis after 72 h of treatment in U87MG-EGFR cells (**Figure 2C,D**). Cinobufagin's structure is similar to ouabain, one of the digitalis drugs used to treat congestive heart failure through targeting Na^+/K^+-ATPase, which can trigger neuron-glia necrosis at high concentration (50–100 μM) (Xiao et al., 2002). However, ouabain inhibits cancer cell proliferation and cannot cause significant changes of intracellular ration of Na^+/K^+ at low concentration (<100 nM) (Kometiani et al., 2005). So cinobufagin might not induce intracellular changes of ratio of Na^+/K^+ to trigger cytotoxicity at low concentration (<0.5 μM). However, it could be possible that cinobufagin triggers acute cytotoxicity due to high concentration at the site of injection, leading to mice death.

At this moment, the cellular targets of cinobufagin remain unclear. Future efforts are necessary to delineate the potential molecular targets for deciphering cinobufagin's anti-cancer effects. Optimization of this compound might warrant a new drug for the treatment of malignant glioma and other human cancers expressing EGFR.

DATA AVAILABILITY STATEMENT

The original contributions presented in the study are included in the article/**Supplementary Material**; further inquiries can be directed to the corresponding authors.

ETHICS STATEMENT

The animal study was reviewed and approved by the Institutional Animal Care and Use Committee of Shanghai Jiao Tong University.

AUTHOR CONTRIBUTIONS

KH: Conceptualization, investigation, writing, funding acquisition. G-XW: Methodology. L-NZ: Methodology. X-FC: Methodology. X-BS: Methodology, writing—review. YS: Methodology, writing—review. T-PX: Resources. S-WH: Writing—review and editing, funding acquisition. Z-GH: Writing—review and editing, resources.

FUNDING

This work was supported by the National Natural Science Foundation of China (81402950, 81761138045, 82073116), Scientific Research Foundation for the Returned Overseas Chinese Scholars of Ministry of Education of China (15Z102050016), Shanghai Pujiang Talent Plan (14PJ1404700), Shanghai Jiao Tong University SMC-Morningstar Young Scholars Award (15X100080059), National Science and Technology Major Project (2017ZX10203207), and National Key Research and Development Program of China (2020YFC2002705).

ACKNOWLEDGMENTS

The authors are most grateful to Dr. Keqiang Ye for helpful advice, discussions, and review of the article.

SUPPLEMENTARY MATERIAL

The Supplementary Material for this article can be found online at: https://www.frontiersin.org/articles/10.3389/fphar.2021.775602/full#supplementary-material

REFERENCES

Arif, S. H., Pandith, A. A., Tabasum, R., Ramzan, A. U., Singh, S., Siddiqi, M. A., et al. (2018). Significant Effect of Anti-tyrosine Kinase Inhibitor (Gefitinib) on Overall Survival of the Glioblastoma Multiforme Patients in the Backdrop of Mutational Status of Epidermal Growth Factor Receptor and PTEN Genes. *Asian J. Neurosurg.* 13, 46–52. doi:10.4103/ajns.AJNS_95_17

Brennan, C. W., Verhaak, R. G., McKenna, A., Campos, B., Noushmehr, H., Salama, S. R., et al. (2013). The Somatic Genomic Landscape of Glioblastoma. *Cell* 155, 462–477. doi:10.1016/j.cell.2013.09.034

Brito, C., Azevedo, A., Esteves, S., Marques, A. R., Martins, C., Costa, I., et al. (2019). Clinical Insights Gained by Refining the 2016 WHO Classification of Diffuse Gliomas with: EGFR Amplification, TERT Mutations, PTEN Deletion and MGMT Methylation. *BMC Cancer* 19, 968. doi:10.1186/s12885-019-6177-0

Campos, B., Olsen, L. R., Urup, T., and Poulsen, H. S. (2016). A Comprehensive Profile of Recurrent Glioblastoma. *Oncogene* 35, 5819–5825. doi:10.1038/onc.2016.85

Cao, Y., Yu, L., Dai, G., Zhang, S., Zhang, Z., Gao, T., et al. (2017). Cinobufagin Induces Apoptosis of Osteosarcoma Cells through Inactivation of Notch Signaling. *Eur. J. Pharmacol.* 794, 77–84. doi:10.1016/j.ejphar.2016.11.016

Cui, X., Inagaki, Y., Xu, H., Wang, D., Qi, F., Kokudo, N., et al. (2010). Anti-hepatitis B Virus Activities of Cinobufacini and its Active Components Bufalin and Cinobufagin in HepG2.2.15 Cells. *Biol. Pharm. Bull.* 33, 1728–1732. doi:10.1248/bpb.33.1728

Dai, G., Zheng, D., Guo, W., Yang, J., and Cheng, A. Y. (2018). Cinobufagin Induces Apoptosis in Osteosarcoma Cells via the Mitochondria-Mediated Apoptotic Pathway. *Cell Physiol Biochem* 46, 1134–1147. doi:10.1159/000488842

Eskilsson, E., Røsland, G. V., Solecki, G., Wang, Q., Harter, P. N., Graziani, G., et al. (2018). EGFR Heterogeneity and Implications for Therapeutic Intervention in Glioblastoma. *Neuro Oncol.* 20, 743–752. doi:10.1093/neuonc/nox191

Gibson, T. B., Ranganathan, A., and Grothey, A. (2006). Randomized Phase III Trial Results of Panitumumab, a Fully Human Anti-epidermal Growth Factor Receptor Monoclonal Antibody, in Metastatic Colorectal Cancer. *Clin. Colorectal Cancer* 6, 29–31. doi:10.3816/CCC.2006.n.01

He, K., Qi, Q., Chan, C. B., Xiao, G., Liu, X., Tucker-Burden, C., et al. (2013). Blockade of Glioma Proliferation through Allosteric Inhibition of JAK2. *Sci. Signal.* 6, ra55. doi:10.1126/scisignal.2003900

Hirsch, F. R., Herbst, R. S., Olsen, C., Chansky, K., Crowley, J., Kelly, K., et al. (2008). Increased EGFR Gene Copy Number Detected by Fluorescent *In Situ* Hybridization Predicts Outcome in Non-small-cell Lung Cancer Patients Treated with Cetuximab and Chemotherapy. *J. Clin. Oncol.* 26, 3351–3357. doi:10.1200/JCO.2007.14.0111

Kometiani, P., Liu, L., and Askari, A. (2005). Digitalis-induced Signaling by Na+/K+-ATPase in Human Breast Cancer Cells. *Mol. Pharmacol.* 67, 929–936. doi:10.1124/mol.104.007302

Li, C., Hashimi, S. M., Cao, S., Qi, J., Good, D., Duan, W., et al. (2015). Chansu Inhibits the Expression of Cortactin in colon Cancer Cell Lines *In Vitro* and *In Vivo*. *BMC Complement. Altern. Med.* 15, 207. doi:10.1186/s12906-015-0723-3

Li, Q., Liang, R. L., Yu, Q. R., Tian, D. Q., Zhao, L. N., Wang, W. W., et al. (2020). Efficacy and Safety of Cinobufacini Injection Combined with Vinorelbine and Cisplatin Regimen Chemotherapy for Stage III/IV Non-small Cell Lung Cancer: A Protocol for Systematic Review and Meta-Analysis of Randomized Controlled Trials. *Medicine (Baltimore)* 99, e21539. doi:10.1097/MD.0000000000021539

Li, X., Chen, C., Dai, Y., Huang, C., Han, Q., Jing, L., et al. (2019). Cinobufagin Suppresses Colorectal Cancer Angiogenesis by Disrupting the Endothelial Mammalian Target of Rapamycin/hypoxia-Inducible Factor 1α axis. *Cancer Sci.* 110, 1724–1734. doi:10.1111/cas.13988

Libermann, T. A., Nusbaum, H. R., Razon, N., Kris, R., Lax, I., Soreq, H., et al. (1985). Amplification, Enhanced Expression and Possible Rearrangement of EGF Receptor Gene in Primary Human Brain Tumours of Glial Origin. *Nature* 313, 144–147. doi:10.1038/313144a0

Lu, X. S., Qiao, Y. B., Li, Y., Yang, B., Chen, M. B., and Xing, C. G. (2017). Preclinical Study of Cinobufagin as a Promising Anti-colorectal Cancer Agent. *Oncotarget* 8, 988–998. doi:10.18632/oncotarget.13519

Lynch, T. J., Bell, D. W., Sordella, R., Gurubhagavatula, S., Okimoto, R. A., Brannigan, B. W., et al. (2004). Activating Mutations in the Epidermal Growth Factor Receptor Underlying Responsiveness of Non-small-cell Lung Cancer to Gefitinib. *N. Engl. J. Med.* 350, 2129–2139. doi:10.1056/NEJMoa040938

Ma, J., and Lu, M. (2011). Clinical Research on 109 Cases of Non-small Cell Lung Cancer Treated by Cinobutacini Injection Plus Gemcitabine and Cisplatin. *J. Traditional Chin. Med.* 52, 2115–2118. doi:10.13288/j.11-2166/r.2011.24.034

Mellinghoff, I. K., Cloughesy, T. F., and Mischel, P. S. (2007). PTEN-mediated Resistance to Epidermal Growth Factor Receptor Kinase Inhibitors. *Clin. Cancer Res.* 13, 378–381. doi:10.1158/1078-0432.CCR-06-1992

Meng, Q., Yau, L. F., Lu, J. G., Wu, Z. Z., Zhang, B. X., Wang, J. R., et al. (2016). Chemical Profiling and Cytotoxicity Assay of Bufadienolides in Toad Venom and Toad Skin. *J. Ethnopharmacol* 187, 74–82. doi:10.1016/j.jep.2016.03.062

Meng, Z., Garrett, C. R., Shen, Y., Liu, L., Yang, P., Huo, Y., et al. (2012). Prospective Randomised Evaluation of Traditional Chinese Medicine

Combined with Chemotherapy: a Randomised Phase II Study of Wild Toad Extract Plus Gemcitabine in Patients with Advanced Pancreatic Adenocarcinomas. *Br. J. Cancer* 107, 411–416. doi:10.1038/bjc.2012.283

Meng, Z., Yang, P., Shen, Y., Bei, W., Zhang, Y., Ge, Y., et al. (2009). Pilot Study of Huachansu in Patients with Hepatocellular Carcinoma, Nonsmall-Cell Lung Cancer, or Pancreatic Cancer. *Cancer* 115, 5309–5318. doi:10.1002/cncr.24602

Ostrom, Q. T., Gittleman, H., Fulop, J., Liu, M., Blanda, R., Kromer, C., et al. (2015). CBTRUS Statistical Report: Primary Brain and Central Nervous System Tumors Diagnosed in the United States in 2008-2012. *Neuro Oncol.* 17 (Suppl. 4), iv1. doi:10.1093/neuonc/nov189

Pan, Z., Luo, Y., Xia, Y., Zhang, X., Qin, Y., Liu, W., et al. (2020). Cinobufagin Induces Cell Cycle Arrest at the S Phase and Promotes Apoptosis in Nasopharyngeal Carcinoma Cells. *Biomed. Pharmacother.* 122, 109763. doi:10.1016/j.biopha.2019.109763

Pan, Z., Zhang, X., Yu, P., Chen, X., Lu, P., Li, M., et al. (2019). Cinobufagin Induces Cell Cycle Arrest at the G2/M Phase and Promotes Apoptosis in Malignant Melanoma Cells. *Front. Oncol.* 9, 853. doi:10.3389/fonc.2019.00853

Qi, F., Inagaki, Y., Gao, B., Cui, X., Xu, H., Kokudo, N., et al. (2011). Bufalin and Cinobufagin Induce Apoptosis of Human Hepatocellular Carcinoma Cells via Fas- and Mitochondria-Mediated Pathways. *Cancer Sci.* 102, 951–958. doi:10.1111/j.1349-7006.2011.01900.x

Qi, F., Li, A., Inagaki, Y., Kokudo, N., Tamura, S., Nakata, M., et al. (2011). Antitumor Activity of Extracts and Compounds from the Skin of the Toad Bufo bufo Gargarizans Cantor. *Int. Immunopharmacol* 11, 342–349. doi:10.1016/j.intimp.2010.12.007

Qi, J., Zulfiker, A. H. M., Li, C., Good, D., and Wei, M. Q. (2018). The Development of Toad Toxins as Potential Therapeutic Agents. *Toxins (Basel)* 10, 336. doi:10.3390/toxins10080336

Stupp, R., Hegi, M. E., Mason, W. P., van den Bent, M. J., Taphoorn, M. J., Janzer, R. C., et al. (2009). Effects of Radiotherapy with Concomitant and Adjuvant Temozolomide versus Radiotherapy Alone on Survival in Glioblastoma in a Randomised Phase III Study: 5-year Analysis of the EORTC-NCIC Trial. *Lancet Oncol.* 10, 459–466. doi:10.1016/S1470-2045(09)70025-7

Sundvall, M., Karrila, A., Nordberg, J., Grénman, R., and Elenius, K. (2010). EGFR Targeting Drugs in the Treatment of Head and Neck Squamous Cell Carcinoma. *Expert Opin. Emerg. Drugs* 15, 185–201. doi:10.1517/14728211003716442

Toma, S., Morishita, S., Kuronuma, K., Mishima, Y., Hirai, Y., and Kawakami, M. (1987). Metabolism and Pharmacokinetics of Cinobufagin. *Xenobiotica* 17, 1195–1202. doi:10.3109/00498258709167411

Touat, M., Idbaih, A., Sanson, M., and Ligon, K. L. (2017). Glioblastoma Targeted Therapy: Updated Approaches from Recent Biological Insights. *Ann. Oncol.* 28, 1457–1472. doi:10.1093/annonc/mdx106

Wang, D. L., Qi, F. H., Xu, H. L., Inagaki, Y., Orihara, Y., Sekimizu, K., et al. (2010). Apoptosis-inducing Activity of Compounds Screened and Characterized from Cinobufacini by Bioassay-Guided Isolation. *Mol. Med. Rep.* 3, 717–722. doi:10.3892/mmr_00000323

Xiao, A. Y., Wei, L., Xia, S., Rothman, S., and Yu, S. P. (2002). Ionic Mechanism of Ouabain-Induced Concurrent Apoptosis and Necrosis in Individual Cultured Cortical Neurons. *J. Neurosci.* 22, 1350–1362. doi:10.1523/jneurosci.22-04-01350.2002

Xie, M., Chen, X., Qin, S., Bao, Y., Bu, K., and Lu, Y. (2018). Clinical Study on Thalidomide Combined with Cinobufagin to Treat Lung Cancer Cachexia. *J. Cancer Res. Ther.* 14, 226–232. doi:10.4103/0973-1482.188436

Xiong, X., Lu, B., Tian, Q., Zhang, H., Wu, M., Guo, H., et al. (2019). Inhibition of Autophagy Enhances Cinobufagin-induced Apoptosis in Gastric Cancer. *Oncol. Rep.* 41, 492–500. doi:10.3892/or.2018.6837

Xu, C., and Wu, Q. (2017). Guiding Journal of Traditional Chinese Medicine and Pharmacology) Advances in the Clinical Study of Cinobufacini for Non-small Cell Lung Cancer. *Guiding J. Traditional Chin. Med. Pharmacol.* 23, 100–103. doi:10.13862/j.cnki.cn43-1446/r.2017.17.035

Yarden, Y., and Pines, G. (2012). The ERBB Network: at Last, Cancer Therapy Meets Systems Biology. *Nat. Rev. Cancer* 12, 553–563. doi:10.1038/nrc3309

Yin, J. Q., Wen, L., Wu, L. C., Gao, Z. H., Huang, G., Wang, J., et al. (2013). The Glycogen Synthase Kinase-3β/nuclear Factor-Kappa B Pathway Is Involved in Cinobufagin-Induced Apoptosis in Cultured Osteosarcoma Cells. *Toxicol. Lett.* 218, 129–136. doi:10.1016/j.toxlet.2012.11.006

Zhang, C., Ma, K., and Li, W. Y. (2019). Cinobufagin Suppresses the Characteristics of Osteosarcoma Cancer Cells by Inhibiting the IL-6-OPN-STAT3 Pathway. *Drug Des. Devel Ther.* 13, 4075–4090. doi:10.2147/DDDT.S224312

Zhang, D., Wang, K., Zheng, J., Wu, J., Duan, X., Ni, M., et al. (2020). Comparative Efficacy and Safety of Chinese Herbal Injections Combined with Transcatheter Hepatic Arterial Chemoembolization in Treatment of Liver Cancer: a Bayesian Network Meta-Analysis. *J. Tradit Chin. Med.* 40, 167–187. doi:10.19852/j.cnki.jtcm.2020.02.001

Zhang, G., Wang, C., Sun, M., Li, J., Wang, B., Jin, C., et al. (2016). Cinobufagin Inhibits Tumor Growth by Inducing Intrinsic Apoptosis through AKT Signaling Pathway in Human Nonsmall Cell Lung Cancer Cells. *Oncotarget* 7, 28935–28946. doi:10.18632/oncotarget.7898

Zhang, X., Yuan, Y., Xi, Y., Xu, X., Guo, Q., Zheng, H., et al. (2018). Cinobufacini Injection Improves the Efficacy of Chemotherapy on Advanced Stage Gastric Cancer: A Systemic Review and Meta-Analysis. *Evid. Based Complement. Alternat Med.* 2018, 7362340. doi:10.1155/2018/7362340

Zhu, L., Chen, Y., Wei, C., Yang, X., Cheng, J., Yang, Z., et al. (2018). Anti-proliferative and Pro-apoptotic Effects of Cinobufagin on Human Breast Cancer MCF-7 Cells and its Molecular Mechanism. *Nat. Prod. Res.* 32, 493–497. doi:10.1080/14786419.2017.1315575

Zulkifli, A. A., Tan, F. H., Putoczki, T. L., Stylli, S. S., and Luwor, R. B. (2017). STAT3 Signaling Mediates Tumour Resistance to EGFR Targeted Therapeutics. *Mol. Cel Endocrinol* 451, 15–23. doi:10.1016/j.mce.2017.01.010

Conflict of Interest: T-PX is an employee of, and may own stock/stock options in Shanghai Nature Standard Technical Services Co., Ltd.

The remaining authors declare that the research was conducted in the absence of any commercial or financial relationships that could be construed as a potential conflict of interest.

Publisher's Note: All claims expressed in this article are solely those of the authors and do not necessarily represent those of their affiliated organizations, or those of the publisher, the editors, and the reviewers. Any product that may be evaluated in this article, or claim that may be made by its manufacturer, is not guaranteed or endorsed by the publisher.

frontiers in Pharmacology

ORIGINAL RESEARCH
published: 09 December 2021
doi: 10.3389/fphar.2021.753068

Compound Kushen Injection Protects Skin From Radiation Injury *via* Regulating Bim

Jianxiao Zheng[1,2†], *Gong Li*[2†], *Juanjuan Wang*[3], *Shujing Wang*[4], *Qing Tang*[1,3], *Honghao Sheng*[1,3], *Wanyin Wu*[1,3*] *and Sumei Wang*[1,3*]

[1]*Department of Oncology, Clinical and Basic Research Team of TCM Prevention and Treatment of NSCLC, the Second Clinical College of Guangzhou University of Chinese Medicine, Guangdong Provincial Hospital of Chinese Medicine, Guangdong Provincial Key Laboratory of Clinical Research on Traditional Chinese Medicine Syndrome, Guangdong-Hong Kong-Macau Joint Lab on Chinese Medicine and Immune Disease Research, Guangzhou University of Chinese Medicine, Guangzhou, China,* [2]*Department of Radiology, Guangdong Provincial Hospital of Chinese Medicine, the Second Clinical Medical College of Guangzhou University of Chinese Medicine, Guangzhou, China,* [3]*State Key Laboratory of Dampness Syndrome of Chinese Medicine, the Second Affiliated Hospital of Guangzhou University of Chinese Medicine, Guangzhou, China,* [4]*The Second Clinical College of Guangzhou University of Chinese Medicine, Guangzhou, China*

OPEN ACCESS

Edited by:
Yuling Qiu,
Tianjin Medical University, China

Reviewed by:
Inamul Hasan Madar,
Korea University, South Korea
Ahm Khurshid Alam,
Rajshahi University, Bangladesh

***Correspondence:**
Wanyin Wu
wwanyin@126.com
Sumei Wang
wangsumei198708@163.com

†*These authors have contributed equally to this work*

Specialty section:
This article was submitted to Pharmacology of Anti-Cancer Drugs, a section of the journal Frontiers in Pharmacology

Received: *04 August 2021*
Accepted: *22 November 2021*
Published: *09 December 2021*

Citation:
Zheng J, Li G, Wang J, Wang S, Tang Q, Sheng H, Wu W and Wang S (2021) Compound Kushen Injection Protects Skin From Radiation Injury via Regulating Bim. Front. Pharmacol. 12:753068. doi: 10.3389/fphar.2021.753068

Background: Radiation-induced skin injury is a major side-effect observed in cancer patients who received radiotherapy. Thus identifying new radioprotective drugs for prevention or treatment of post-irradiation skin injury should be prompted. A large number of clinical studies have confirmed that Compound Kushen injection (CKI) can enhance efficacy and reduce toxicity of radiotherapy. The aim of this study is to confirm the effect of CKI in alleviating radiotherapy injury in the skin and explore the exact mechanism.

Methods: 60 patients who met the inclusion/exclusion criteria were allocated to treatment group (CKI before radiotherapy) or control group (normal saline before radiotherapy) randomly. MTT assay, flow cytometry, Western Blot, and transient transfection were performed to detect the cell viability, cell apoptosis and Bim expression after treatment with CKI or/and radiotherapy.

Results: CKI had the effect of alleviating skin injury in cancer patients who received radiotherapy in clinic. CKI induced cancer cell apoptosis when combined with irradiation (IR), while it reversed the induction of cell apoptosis by IR in human skin fibroblast (HSF) cells. And Bim, as a tumor suppressor, was induced in cancer cells but had no change in HSF cells when treated with CKI. Moreover, the above effect could be attenuated when Bim was silenced by siRNA.

Conclusion: We conclude that CKI represents a promising radio-protective agent with a potential differential beneficial effect on both cancer cells (inducing apoptosis) and HSF cells (providing radio-protection *via* inhibiting IR-induced apoptosis), via regulating Bim. Our study uncovers a novel mechanism by which CKI inhibits human cancer cell while protects skin from radiotherapy, indicating CKI might be a promising radio-protective drug.

Clinical Trial Registration: Chinese Clinical Trial Registry (www.chictr.org.cn), identifier ChiCTR2100049164.

Keywords: compound kushen injection, radiation injury, skin, cancer, Bim

INTRODUCTION

Radiation therapy is an effective non-surgical treatment for human cancers. However, the radiation injury induced by radiation therapy affects the quality of life (QoL) of patients inevitably and seriously. Therefore, prevention and treatment of radiation injury is of great significance. Compound Kushen injection (CKI) is the most used Chinese Herbal injections (CHIs) in human cancers. It has been reported to have the ability to increase QoL and enhance immunity of cancer patients, especially when patients received radiotherapy (Yang et al., 2021). For example, a study showed that CKI combined with radiotherapy is the most preferable and beneficial option for patients with esophageal cancer (EC) in terms of efficacy and safety (Zhang et al., 2019). Since CKI could improve the clinical effectiveness rate and performance status of cancer patients, whether CKI could relieve the radiation injury in the skin at the same time is to be illustrated.

CKI, a Traditional Chinese Medicine (TCM) preparation and a mixture of natural compounds extracted from Kushen (*Sophorae Flavescentis Radix*) and Tufuling (*Smilacis Glabrae Rhixoma*), which have been used for adjuvant anti-cancer clinical therapy for over 20 years (Qu et al., 2016; Cui et al., 2020). Based on the TCM theory, CKI can be used for clearing away heat and dampness, cooling blood and detoxifying and relieving cancer pain, which has been proven to have significant effects against cancer (Guo et al., 2015; Yu et al., 2017). Based on the Western Medicine (WM) theory, CKI suppressed tumor growth by inhibiting cancer cell proliferation and metastasis, promoting cell apoptosis and improving patients' immune system (Wang H. et al., 2019). For example, CKI-primed macrophages obviously promoted the proliferation and the cytotoxic ability of $CD8^+$ T cells and decreased its exhaustion, resulting in HCC (hepatocellular carcinoma) cell apoptosis (Yang et al., 2020). Another study reported that CKI inhibited HCC progression by regulating signaling pathways involving MMP2 (Matrix Metalloproteinase-2) and Caspase-3 and the key pathways of glycometabolism and amino acid metabolism (Gao et al., 2018).

There were researches revealed that the active ingredients from CKI could induce cancer cell apoptosis by regulating p53 and PI3K-Akt pathway (He et al., 2020). Matrine and oxymatrine are main components from *Sophorae Flavescentis Radix*. It has been reported that both matrine and oxymatrine have characteristics of anti-inflammatory, anti-tumor, anti-viral, and cardiovascular protection effects (Ma et al., 2014; Wang et al., 2015). Matrine could suppress the BrCSCs (breast cancer stem cells) differentiation and self-renewal by downregulating Lin28A expression, leading to the inactivation of Wnt pathway in a Let-7b-dependent way (Li et al., 2020). Oxymatrine could inhibit the invasiveness of HCC by reducing the expression of MMP-2/-9 *via* inhibiting the activity of p38 signaling pathway (Chen et al., 2019). Meanwhile, *Smilacis Glabrae Rhixoma* has also been reported to have anti-inflammatory, antiviral, anti-cancer, and immunomodulatory effects (Jiang and Xu, 2003; Ooi et al., 2004; Galhena et al., 2012; Samarakoon et al., 2012). For instance, it could suppress the phosphorylation of Akt (Thr308) and thereby inhibit gastric cancer (GC) cell proliferation and metastasis as well as accelerating GC cell apoptosis through Akt-mediated signaling pathways (Hao et al., 2016).

The above studies emphasized the inhibition role of CKI in human cancers. What's the role of CKI in non-cancerous cells? A previous study showed that cell apoptosis was increased by CKI in breast cancer (BC) but not in non-cancerous lines (Nourmohammadi et al., 2019). Interestingly, our clinic data also showed that CKI had the effect of protecting skin from radiation injury in patients with nasopharyngeal carcinoma (NPC) who received radiotherapy. Therefore, we hypothesized that CKI has differential roles in human cancer and skin cells. In the present study, we'll further identify the role and mechanism of CKI in human cancers including lung cancer (LC) and NPC when combined with radiotherapy, and in human skin fibroblast (HSF) cells.

MATERIALS AND METHODS

Clinical Research Protocol

The clinical research protocol was approved by the Ethics Committee of Guangdong Provincial Hospital of Traditional Chinese Medicine (YF2018-064). Sixty-two patients from the department of Radiotherapy, Guangdong Provincial Hospital of Traditional Chinese Medicine, were identified, screened, and enrolled in the study between June 2014 and January 2018 and all patients provided informed consent. The factors affecting the severity of acute radiation dermatitis, such as age, obesity, KPS (Karnofsky Performance Status) score, stage and other baseline characteristics, were comparable between treatment group and control group. If the subjects would like to withdrawal of consent or fail to adhere to the research protocol or serious adverse events happened, the study of the participant would be suspended and recorded as withdrawn. During the treatment, two patients withdrew from the clinical trial due to personal wishes, and the other sixty patients successfully completed the trial as planned.

Inclusion/Exclusion Criteria

Inclusion Criteria

- Patients who were pathologically diagnosed as Nasopharyngeal Carcinoma (NPC) and planned to receive intensity modulated radiotherapy (IMRT).
- The age is between 18 and 70 years old, regardless of gender.
- Normal bone marrow, liver, kidney, heart, and lung function.
- Patients received the first radical radiotherapy or chemo-radiotherapy.
- Karnofsky's behavior score is above 60.

Exclusion Criteria

- Active repeated cancer.
- Patients suffering from mental disorders.
- Patients with skin infectious diseases.
- Allergic constitution or allergic to the components of the preparation.
- Suspected or true history of alcohol and drug abuse.

- Pregnant or lactating women or those with recent birth planning.
- The researcher believes that it is not suitable to participate in this experiment.

Study Design

In the prospective trial, 60 patients who met the inclusion/exclusion criteria were allocated to treatment group or control group using a computer-generated random sequence.

The Radiation-Induced Skin-Reaction-Assessment-Scale Score

The skin of the neck radiation field was evaluated weekly from baseline using the RISRAS table for a total of 7 weeks. The first part of the RISRAS form is filled in by the patient, which is the subjective symptom evaluation form of the patient, including itching, pain, burning or tension of the skin of the neck radiation field, and the impact of the skin reaction caused by radiotherapy on the patient's daily activities. The patient's response ranges from "none at all" to "very." The higher the score, the more serious the patient's subjective symptoms (**Supplementary Table S1**). The second part is the professional scoring table for medical staff, including erythema (E), dry desquamation (DD), wet desquamation (WD), and necrosis (N). "E" is scored according to the change of skin color of the patient's neck irradiation field, and 0–4 points from "normal" to "deep purple erythema." For "DD," "WD," and "N" the proportion of the area of dermatitis in the whole radiation field skin was evaluated, and 0–4 points were calculated from "normal" to ">75%–100" (**Supplementary Table S2**). Finally, the test observer will summarize the scores of the two scoring tables into the continuous evaluation table to get a final score of each patient.

Intervention

All candidates were treated with standard intensity modulated radiotherapy according to the NPC guidelines of Chinese society of clinical oncology (CSCO). In the treatment group, the candidates received 10 ml of CKI solution intravenously each day before radiotherapy. In the control group, the candidates received normal saline solution intravenously each day before radiotherapy.

Trial Registration

Chinese Clinical Trial Registry Trial registration number: ChiCTR2100049164. Name of registry: Compound Kushen injection alleviates radiation-induced skin injury: randomized controlled trial. Date of registration: 2021-07-24 (1008002 retrospective registration).

Chemicals and Cell Culture

Compound Kushen Injection (CKI, z14021231) was produced by Shanxi Zhendong Pharmaceutical Co., Ltd. (Shanxi, China), and 1 ml CKI contains 0.4 g crude drug. MTT (M5655) and Dimethyl sulfoxide (DMSO) were purchased from Sigma-Aldrich Co. (St. Louis, MO, United States). Monoclonal antibodies specific of Bim, and GAPDH were purchased from Cell Signaling Technology Inc. (Beverly, MA, United States). Lipofectamine 3000 reagent was purchased from Life Technologies (Carlsbad, CA, United States). NSCLC (non-small cell lung caner) cell line H1299 and Human Skin Fibroblast (HSF) cell line were obtained from the Chinese Academy of Sciences Cell Bank of Type Culture Collection (Shanghai, China). Nasopharyngeal Carcinoma cell line CNE-2 was purchased from the Cancer Center of Sun Yat-Sen University (Guangzhou, China). All cells were grown at 37°C, in a humidified 5% CO_2 and 95% air and cultured in RPMI-1640 medium (Life Technologies, Carlsbad, CA, United States) containing 10% FBS (Gibco, United States) and 0.5% penicillin-streptomycin sulfate (Invitrogen Life Technologies, Carlsbad, CA, United States). Cells were counted using the automated cell counter star (Inno-Alliacne Biotech Inc., Denver, CO, United States).

MTT Assay

MTT assay was performed as described previously (Wang S. et al., 2019). Briefly, cells were seeded in 96-well plates at a density of 1×10^4 cells/well and incubated at 37°C for 24 h. After treatment, cells were maintained at 37°C in a humidified atmosphere containing 5% CO_2 for 24 h. The medium was supplemented with 20 μL MTT (5 mg/ml) at 37°C for 4 h. Subsequently, the medium was replaced with 100 μL DMSO. Following incubation for 20 min at room temperature, the absorbance was read by measuring the optical density (OD) at 490 nm in a microplate reader (Molecular Devices, LLC, Sunnyvale, CA, United States). The viability rate was calculated as follows: Viability rate (%) = OD 490 trail/OD 490 blank × 100. The experiment was repeated three times.

Ionizing Radiation

Irradiation was performed at The Second Clinical College of Guangzhou University of Chinese Medicine/Guangdong Provincial Hospital of Traditional Chinese Medicine using MultiRad 225 machine (Faxitron). The cells were divided into the following three groups: Control group, which was cultured in regular medium and without any treatment ; Irradiation group, which was treated with irradiation alone; and CKI combined with irradiation group, which was incubated with CKI before irradiation. After irradiation, cells were maintained at 37°C in a humidified atmosphere containing 5% CO_2 for 24 h for further analysis.

TUNEL Assay

TUNE assay was performed using TUNEL cell apoptosis kit according to the manufacturer's protocol (Beyotime, China). Briefly, cells were fixed with paraformaldehyde for 30 min, and incubated at room temperature with 0.3% Trinton X-100 PBS for 5 min. Wash cells with PBS twice. Samples were added with 50 μL TUNEL detect liquid and incubated at 37°C for 60 min in dark. Finally, samples were sealed with antifluorescence quenched liquid and observed under a fluorescence microscope (Nikon ECLIPSE Ti2-E, Japan).

Confocal Assay of Cell Apoptosis

Cell apoptosis was carried out using cell apoptosis kit according to the manufacturer's protocol (Dojindo, Japan). Briefly, cells were collected, centrifuged for 3 min at 1,000 rpm, and resuspended in 1 × Annexin V binding solution to a final concentration of 1×10^6 cells/ml. Finally, 5 μL Annexin V-FITC and 5 μL PI were added into the cells at room temperature for 15 min. Then 400 μL 1 × Annexin V binding solution were added. The cells were then analyzed using confocal microscope in 1 h (Zeiss LSM 710, German).

Flow Cytometry Analysis

Flow cytometry was performed as described previously (Wang et al., 2018). Cell apoptosis was analyzed by Annexin V-FITC/PI apoptosis detection kit according to the manufacturer's protocol (Sigma-Aldrich Co. St. Louis, MO). Briefly, cells (CNE-2, H1299, and HSF) were seeded in 6-well plates. After 24 h of culture, cells were treated with CKI, IR, or IR combined with CKI, and then incubated at 37°C for 24 h. Afterwards, cells were collected, centrifuged for 5 min at 1,500 rpm, and resuspended in 1 × binding buffer. Finally, 5 μL Annexin V-FITC and 5 μL PI were added into the cells at room temperature for 15 min. The cells were then analyzed using flow cytometer (Beckman FC 500, Beckman Coulter, Inc., CA, United States).

Western Blot Analysis

Western blot analysis was performed as described previously (Wang et al., 2020). Briefly, cells (CNE-2, H1299, and HSF) were harvested, washed and lysed with 1 × RAPI buffer. Protein concentration was determined by the Thermo BCA protein assay Kit. Equal amounts of protein from cell lysates were solubilized in 5 × SDS sample buffer and separated on 8–10% SDS polyacrylamide gels, and transferred onto polyvinylidene fluoride membranes. Membranes were blocked with 5% non-fat milk in TBST and incubated with primary antibodies against Bim and GAPDH proteins at 4°C overnight. Afterwards, the membranes were washed and incubated with a secondary antibody against rabbit IgG for 1 h, followed by washing and transferring into ECL solution (Millipore, Darmstadt, Germany), and scanned under the Bio-Rad ChemiDoc XRS + Chemiluminescence imaging system (Bio-Rad, Hercules, CA, United States). The results were measured by ImageJ software.

Transient Transfection Assays

The cells were seeded in 6-well plates and reached to 50–60% confluence. The negative control and Bim siRNA were obtained from RiboBio (Guangzhou, China). For each well, 10–60 nM NC or Bim siRNA were transfected into the cells using Lipofectamine 3000 reagent (Life Technologies, Carlsbad, CA, United States) for 24 h based on the instruction from the provider.

Statistical Analysis

Statistical analysis was performed using the SPSS statistical software. Statistical evaluation for data analysis used Student's t-test when there were only two groups (two sided) and differences between groups were assessed by one-way ANOVA. RIAPAS data was evaluated using Wilcoxon matched-pairs signed rank test. All data are reported as Means ± SD. Differences between groups were considered significant statistically when $p \leq 0.05$.

RESULTS

CKI Alleviated Radiotherapy Injury in the Skin in Clinic

A prospective randomized controlled clinical trial was conducted to investigate the difference in the severity of radiation injury of skin between the two groups of NPC patients after radiotherapy treated with or without CKI. A total of 62 NPC patients were admitted to the Department of radiotherapy of Guangdong Provincial Hospital of Chinese Medicine, from June 2014 to January 2018. In the course of treatment, 2 patients withdrew from the clinical trial due to their personal wishes. Sixty NPC patients were randomly divided into control and CKI group, both of which were accepted intensity modulated radiotherapy (IMRT). The patients from control group receivednormal saline intravenously before radiotherapy and from CKI group received CKI intravenously before radiotherapy (**Figure 1A**).

At the end of radiotherapy, the incidence of grade III and grade IV radiodermatitis in the CKI-treated group was 30.0 and 13.3%, respectively. While the incidence of grade III and grade IV radiodermatitis in the control group was 56.7 and 20.0%, respectively. Obviously, the data showed that the incidence of severe radiodermatitis in the CKI-treated group was lower than that in the control group, and the difference was statistically significant (p = 0.03, **Table 1**). Moreover, the RISRAS (Radiation-Induced Skin Reaction Assessent Scale) score of the CKI-treated group was also lower than that of the control group, and the difference was statistically significant (p = 0.002, **Table 2**; **Figure 1B**). Therefore, the above clinical results revealed that CKI could alleviate radiotherapy injury in the skin significantly in clinic.

CKI Inhibited Cancer Cell Growth While Promoted HSF Cell Growth

The above clinic data have shown that CKI had the effect of alleviating radiotherapy injury in the skin. To understand the mechanism by which CKI alleviates radiodermatitis, we first performed MTT assay to see the effect of CKI on cancer cells and HSF cells. As shown in **Figures 2A,B**, CKI inhibited human cancer cell growth including NPC and LC, in a both dose- and time-dependent manner. However, in the HSF cells, CKI showed a promotion effect in HSF cell growth (**Figure 2C**). The above results showed a differential role of CKI in human cancer and HSF cells.

Combination of CKI and IR Inhibited Cancer Cell Growth Additively, While Protected HSF From IR Treatment

Whether CKI could influence the effect of cancer radiotherapy? We treated cancer cells and HSF cells with CKI, IR, and the combination of CKI and IR, respectively. Our findings showed an additive effect of CKI and IR in inhibiting cancer cells, as shown

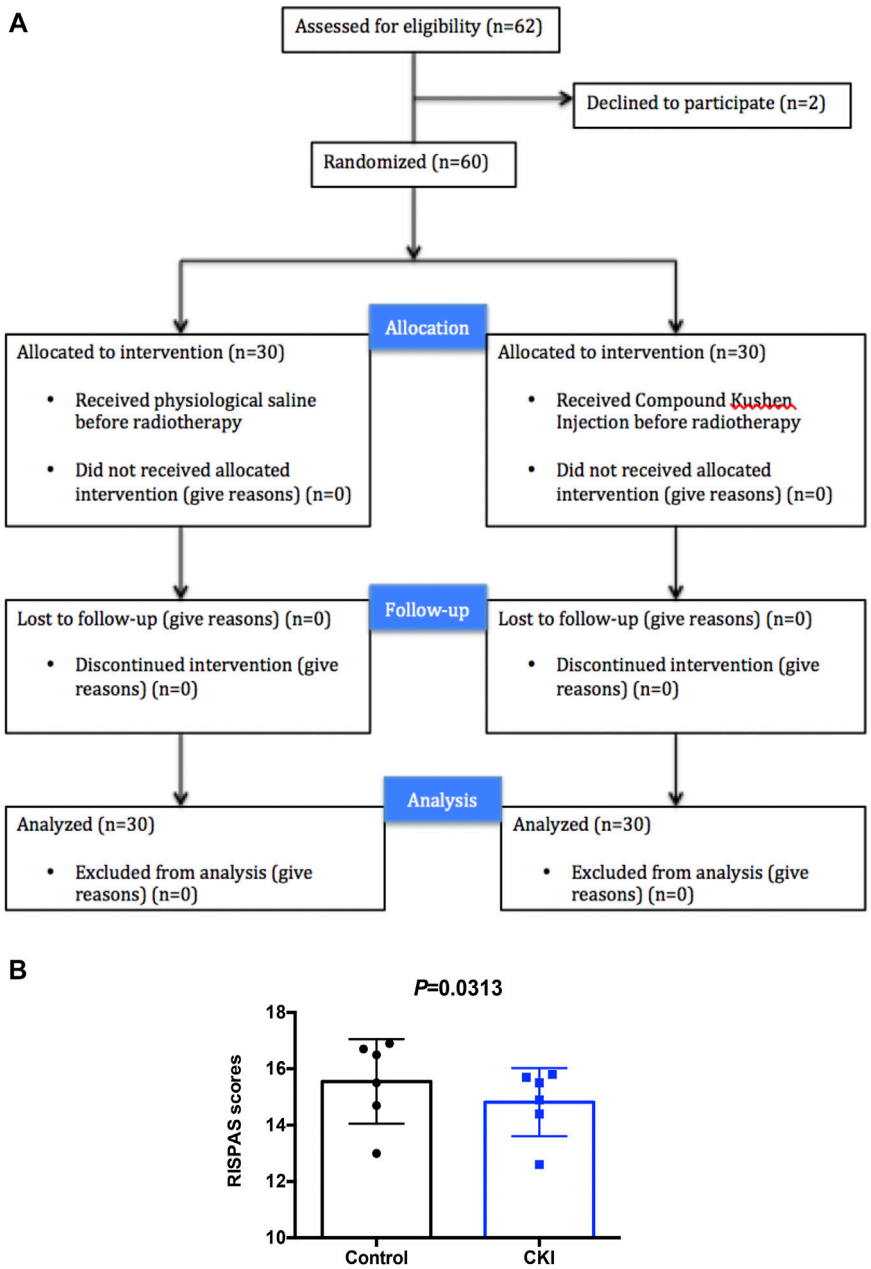

FIGURE 1 | Patients had lower RISPAS scores in the CKI- treated group compared to control group. **(A)** Participant flow through the trial. **(B)** Graph showing RISPAS scores in the CKI and control group. $p = 0.0313$ (< 0.05), indicates a significant difference in the CKI group compared to the untreated control group.

TABLE 1 | Radiation injury of neck skin was alleviated in CKI-treated group.

Groups	Grade-II	Grade-III	Grade-IV	χ^2	*p* value
Control	7	17	6	7.028	0.030
CKI	17	9	5	—	

in **Figures 3A,B**. Nevertheless, there was no inhibition effect seen in the HSF cell growth under the combination treatment of CKI and IR, as shown in **Figure 3C**. The data showed that CKI could reverse the inhibition effect of IR in HSF cells, suggesting a protective role of CKI in HSF cells when treated with IR.

Combination of CKI and IR Promoted Cancer Cell Apoptosis Additively, While Protected HSF From IR Treatment

TUNEL assay was performed to show the effect of CKI on cancer cells (CNE2 and H1299) and HSF cells. The results showed that CKI induced cancer cell apoptosis while has no obvious induction effect of

TABLE 2 | Patients have lower RISPAS scores in the CKI-treated group compared to control group (mean ± SD).

Group	2W	3W	4W	5W	6W	7W	F	*p* value
Control	13.0 ± 0.9	14.7 ± 1.0	15.5 ± 1.2	16.5 ± 1.3	16.7 ± 1.3	16.9 ± 1.2	10.14	0.0313
CKI	12.6 ± 0.8	14.4 ± 0.9	14.9 ± 1.0	15.5 ± 1.2	15.7 ± 1.3	15.8 ± 1.2	—	

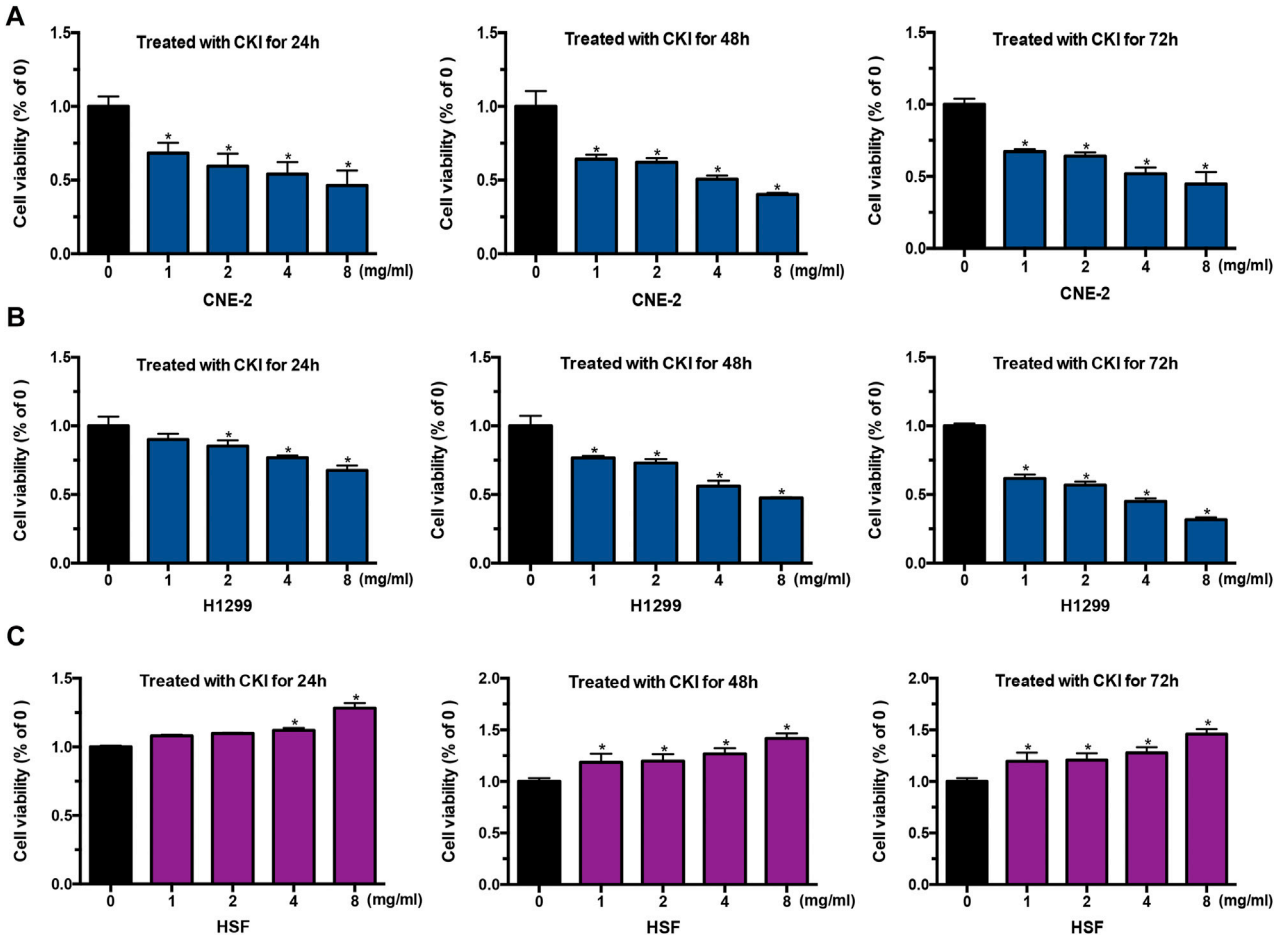

FIGURE 2 | CKI inhibited tumor cell growth while promotes HSF proliferation. **(A–C)** Cancer cells (CNE-2 and H1299) and HSF cells were treated with increased concentrations of CKI for 24, 48, and 72 h. Afterwards, cells were treated with MTT as detailed in Materials and Methods. Values in bar graphs were given as the mean ± SD from three independent experiments performed in triplicate. *Indicates significant difference as compared to the untreated control group (*$p < 0.05$).

HSF cell apoptosis (**Figure 4A**). Meanwhile, PI and FITC annexin-V double staining using confocal microscope was also carried to show that CKI could induce cancer cell apoptosis rather than HSF (**Figure 4B**). To further understand the mechanism by which CKI protects HSF cells from IR treatment. We then performed flow cytometry of cell apoptosis. As expected, CKI combined with IR had an additive effect of promoting cancer cell apoptosis (**Figures 4C,D**). While there was no induction effect of cell apoptosis observed in HSF cells when combined CKI with IR (**Figure 4E**). HSF cell apoptosis was markedly increased following IR alone. While pretreatment with CKI followed by IR resulted in reduced apoptosis levels, which had no significance compared with control group, indicating that CKI could inhibit irradiation-induced apoptosis in HSF cells. In total, the above results showed that CKI could reverse the IR-induced cell apoptosis in HSF cells, indicating a protective role of CKI in the skin.

CKI Increased Bim Expression in Cancer Cells While had No Obvious Effect in HSF Cells

Cell apoptosis was more induced in CKI together with IR group in cancer cells, while no obvious induction of cell apoptosis was

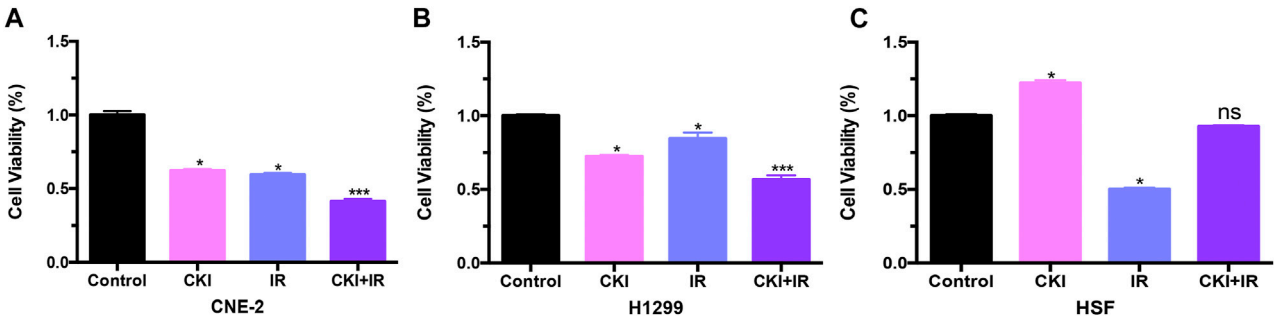

FIGURE 3 | CKI combined with IR inhibited cancer cell growth additively, while had no obvious effect in HSF cells compared to control. **(A–C)** Cancer cells (CNE-2 and H1299) and HSF cells were treated with CKI (4 mg/ml), IR (4Gy), and CKI combined with IR. Afterwards, cell viability was analyzed using MTT assay. Values in bar graphs were given as the mean ± SD from three independent experiments performed in triplicate. *Indicates significant difference as compared to the untreated control group (*$p < 0.05$; ***, $p < 0.001$). ns, not significant, indicates no significant difference as compared to the untreated control group.

found in HSF cell, even a rescue effect of CKI was observed in HSF cells when combined with IR. Apoptosis is a highly conserved form of programmed cell death that can be triggered by extrinsic or intrinsic signals. Bcl-2 family proteins play a decisive role in apoptosis initiated by intrinsic signaling by regulating the integrity of the mitochondrial outer membrane (MOM). It is composed of three classes: pro-survival proteins (BCL-2, MCL-1, BCL-XL, BCL-w, and BFL-1), multi-domain pro-apoptotic proteins (BAX and BAK) that compromise the outer mitochondrial membrane, and BH3- only pro-apoptotic proteins (BIM and NOXA). Among those, the BH3-protein Bim (BCL-2-interacting mediators of cell death) is an important mediator of apoptosis initiated by intracellular stressors. It is related to tumor progression, metastasis, drug resistance, and promotes apoptosis at mitochondria by activating proteins Bax and Bak and by inhibiting the anti-apoptotic proteins Bcl-XL, Bcl-2, and Mcl-1 (Chi et al., 2020).

Therefore, we detected Bim expression in both cancer and HSF cells when treated with CKI. Our results showed that Bim was significantly increased in both NPC and LC cells, while no significant change was observed in HSF cells, with the increased dose of CKI (**Figures 5A–C**). The results indicated that Bim might be a key protein leading to the differential role of CKI in cancer and HSF cells. When combined CKI with IR, a additive increase expression level of Bim was observed in H1299 cells while a slight reverse effect was found in HSF cells (**Figures 5D,E**, left panel). When Bim was silenced by siRNA, the differential expression trends of Bim in H1299 and HSF cells by the treatment with CKI and IR were almost disappeared (**Figures 5D,E**, right panel). The data suggested that Bim plays a crucial role in the differential effect of CKI in human cancer and HSF cells, especially when combined with IR.

Silencing Bim Attenuated the Effect of CKI in Cancer and HSF Cell Apoptosis When Combined with IR

Since the differential expression of Bim almost disappeared when inhibiting Bim in both cancer cells H1299 and HSF cells, whether the cell apoptosis effect could be suppressed when Bim was silenced is to be identified. We then performed flow cytometry to detect the cell apoptosis percentages by inhibiting Bim expression. Our data showed that in H1299 cells, inhibiting Bim could partially reverse the combination effect of CKI and IR in inducing cell apoptosis (**Figure 6A**). And in HSF cells, inhibiting Bim attenuated the effect of CKI combined with IR in reversing the cell apoptosis by IR (**Figure 6B**). This data reconfirmed that Bim is the key protein making CKI functions differently in cancer and HSF cells. Therefore, we concluded that CKI protected skin from radiation injury *via* regulating Bim.

DISCUSSION

Many studies have shown that CKI could relieve acute radiation injury and protect normal tissue of patients. The protective effects of CKI on human dermal fibroblasts suggest that it has potential applications in the protection against irradiation -induced skin injury. However, the mechanism of CKI in reducing radiation injury is unknown. In the present study, we are proposed to uncover the mechanisms by which CKI protect skin against radiation injury.

In the present study, we first identified that CKI had the effect of alleviating radiotherapy injury in the skin in patients with NPC who received IMRT. To discover the mechanism, we then performed a series of *in vitro* experiments. We found that CKI inhibited cancer cell growth by inducing cell apoptosis in NPC CNE-2 cells and LC H1299 cells. At the same time, CKI promoted HSF cell proliferation in a dose- and time-dependent manner. Apoptosis plays a key role in the differential role of CKI in cancer and non-cancerous cells. The induction of apoptosis is a common and required event for different classes of anticancer agents, and disruption of such mechanism can lead to non-specific side effects (Shukla et al., 2017). Our further data found that Bim is the key protein making CKI plays a differential role of in human cancer and HSF cells when combined with IR.

Bim, also known as B-cell chronic lymphocytic leukemia/lymphoma (Bcl-2)-like 11 (BCL2L11), is a member of the Bcl-2 family and a critical modulator of cell apoptosis. Bim encodes the BH3 protein, which activates cell death either by opposing

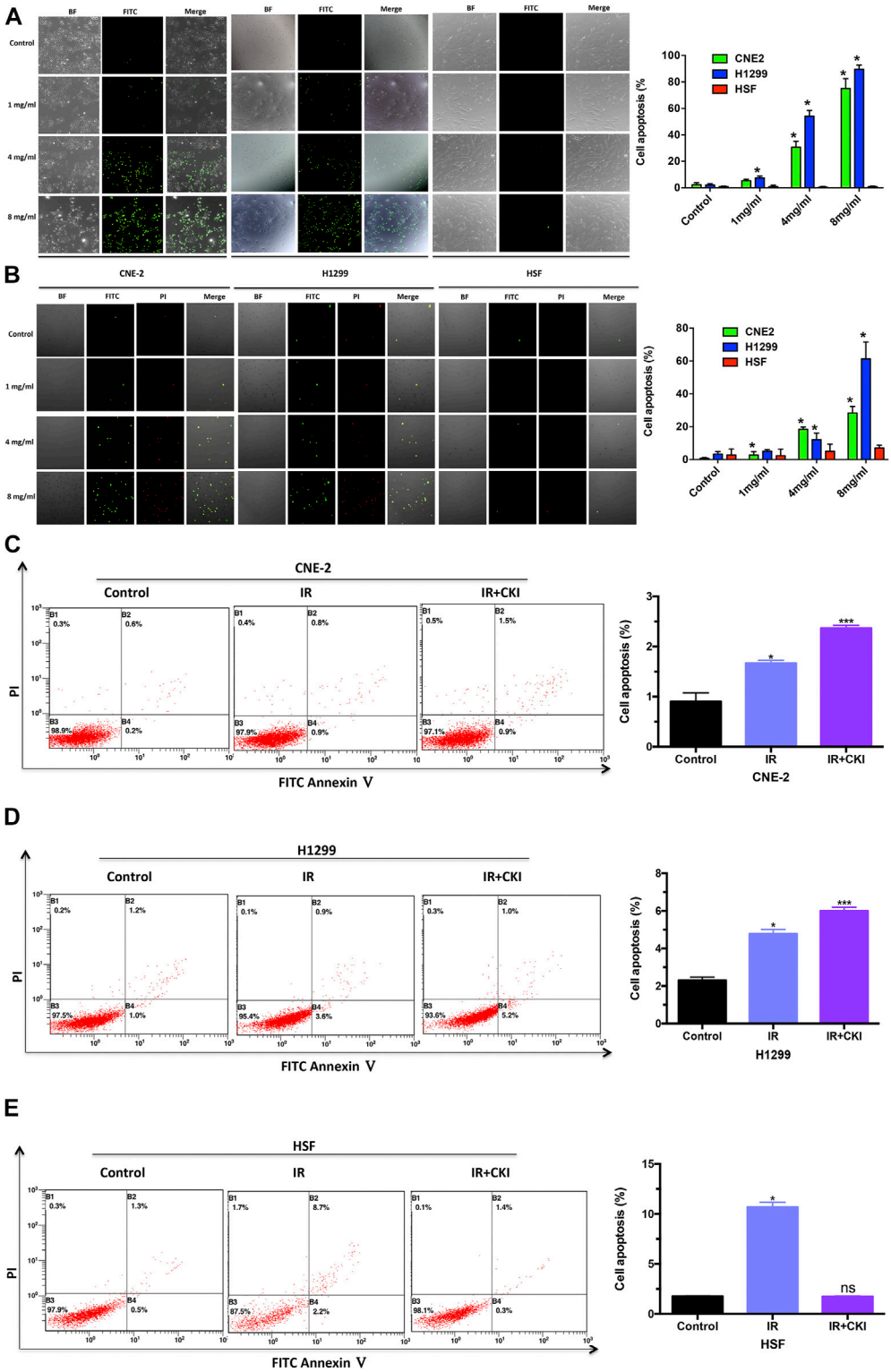

FIGURE 4 | CKI enhanced cancer cell apoptosis by IR, while rescued the HSF cell apoptosis when treated with IR. **(A)** Cancer cells (CNE-2 and H1299) and HSF cells were treated with CKI (0, 1, 4, 8 mg/ml), and cell apoptosis was observed by TUNEL assay. **(B)** Cancer cells (CNE-2 and H1299) and HSF cells were treated with CKI (0, 1, 4, 8 mg/ml), and cell apoptosis was detected by doing PI and FITC annexin-V double staining using confocal microscope. **(C–E)** Cancer cells (CNE-2 and H1299) and HSF cells were treated with IR (4Gy) and CKI (4 mg/ml) combined with IR. Afterwards, cell apoptosis was analyzed using flow cytometry. Values in bar graphs were given as the mean ± SD from three independent experiments performed in triplicate. *Indicates significant difference as compared to the untreated control group (*$p < 0.05$; ***, $p < 0.001$). ns, not significant, indicates no significant difference as compared to the untreated control group.

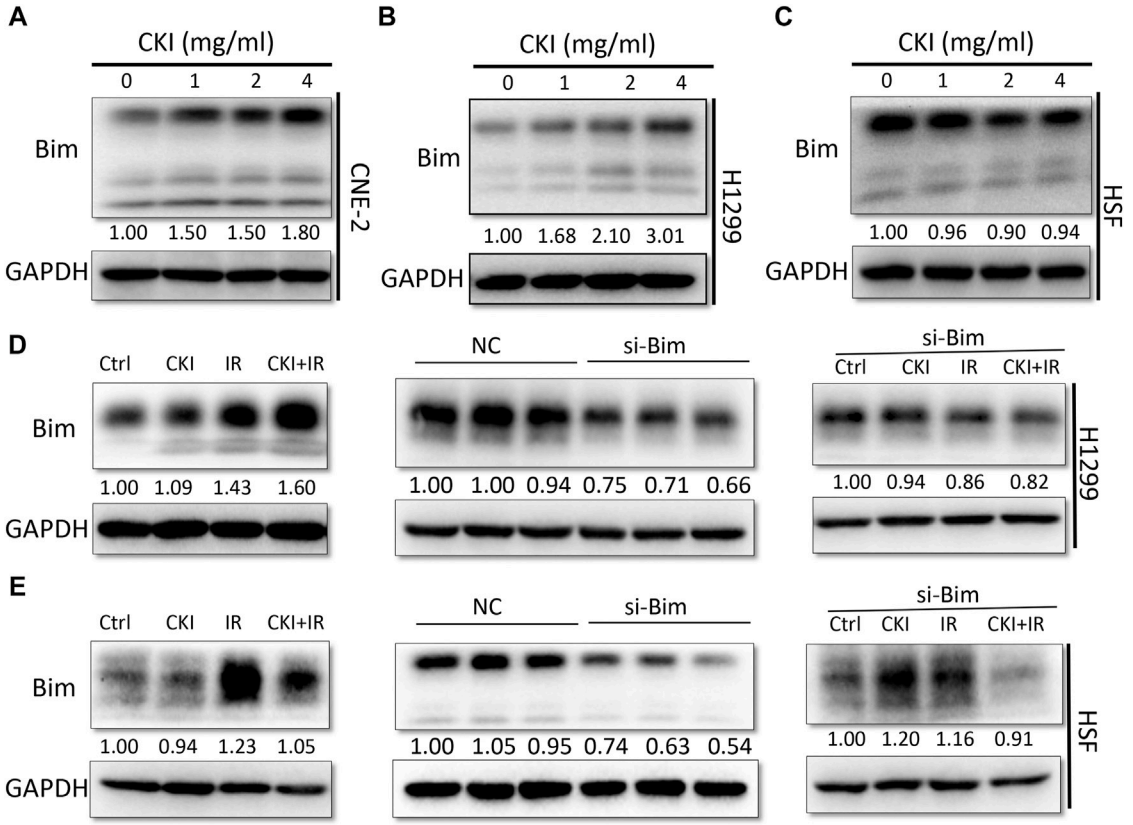

FIGURE 5 | Inhibiting Bim attenuated the differential Bim expression trends caused by the combination of CKI and IR. **(A–C)** Cancer cells (CNE-2 and H1299) and HSF cells were treated with increased dose of CKI. **(D–E)** Cancer cell H1299 and HSF cells were treated with CKI (4 mg/ml), IR (4Gy) and combination of CKI and IR, respectively. Transient transfection was performed to inhibit Bim expression by siRNA. Bim expression was evaluated using Western Blot. GAPDH was used as an external control. The results were measured by ImageJ software.

the pro-survival activities of members of the BCL2 family or by binding to and directly activating pro-apoptotic BCL2 family members. It promotes apoptosis by activating Bax/Bak, and it is regulated at both transcriptional and post-translational levels (Byerly et al., 2020). Induction of Bim triggers cytochrome C release from mitochondria to cytosol. Then, cytosolic cytochrome C induces Caspase cleavage followed by PARP cleavage, finally resulting in cell apoptosis (Akiyama et al., 2009). The overexpression of Bim inhibits tumor growth and drug resistance. Cancer cells suppress Bim expression, associating with tumor promotion, metastasis, and drug resistance (Akiyama et al., 2009; Shukla et al., 2017). For example, Bim plays an important role in sensitizing epidermal growth factor receptor-tyrosine kinase inhibitors (EGFR-TKIs) in EGFR-Positive NSCLC (Incharoen et al., 2019). And modulating Bim transcription is one of the mechanisms by which aspirin overcomes osimertinib resistance in EGFR-mutated NSCLC (Han et al., 2020). A study reported that the homozygous deletion of Bim characterizes it as a novel tumor suppressor in MCL (mantle cell lymphoma) (Tagawa et al., 2005). MCL with high levels of proapoptotic Bim expression are more likely to result in a patient's complete response rather than progressive disease following therapy (Wang JD. et al., 2019). In accordance with other hematopoietic and solid-organ malignancies, Bim's role as a tumor suppressor appears to have prognostic and therapeutic significance. For example, in chronic myeloid leukemia (CML), Bim deletion polymorphisms lengthen the time for patients to achieve a major molecular response on TKIs (Than et al., 2019). Additionally, loss of Bim or its expression in melanoma, colorectal cancer, intrahepatic cholangiocarcinoma, and EGFR-positive NSCLC is associated with worse prognoses (Dai et al., 2008; Sinicrope et al., 2008; Ng et al., 2012; Lee et al., 2015; Zhang et al., 2018). Those data revealed the important role of Bim in human cancers and cancer-related therapies. Here in the present study, Bim serves as a critical protein in protecting skin from radiation injury, with the advent of radiotherapy acting on the cell apoptosis.

CONCLUSION

Our study indicated that CKI represents a promising radioprotective agent with a potential differential beneficial effect on both cancer cells (inducing apoptosis) and HSF cells (providing radio-protection *via* inhibiting IR-induced apoptosis)

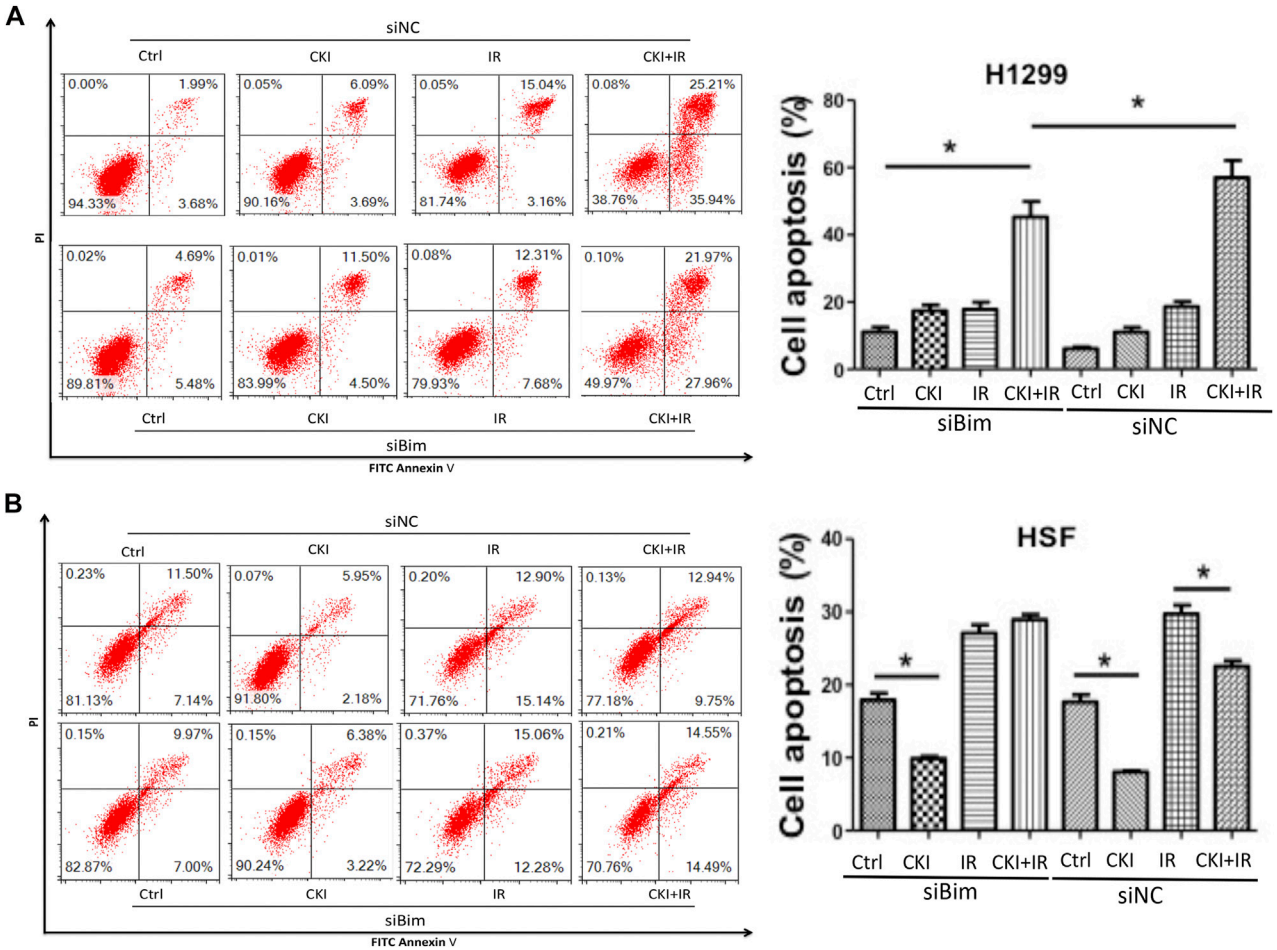

FIGURE 6 | Inhibiting Bim attenuated the differential effect of CKI in cancer and HSF cell apoptosis. **(A, B)** Cancer cell H1299 and HSF cells were treated with CKI (4 mg/ml), IR (4Gy) and combination of CKI and IR, respectively. Cell apoptosis was analyzed using flow cytometry. Values in bar graphs were given as the mean ± SD from three independent experiments performed in triplicate. *Indicates significant difference as compared to the accordingly group (*$p < 0.05$).

as clearly demonstrated through this study, *via* regulation of mitochondria pathway by regulating Bim. Taken together, these results uncover a novel mechanism by which CKI inhibits human cancer while protect skin from radiotherapy.

DATA AVAILABILITY STATEMENT

The raw data supporting the conclusion of this article will be made available by the authors, without undue reservation.

ETHICS STATEMENT

The studies involving human participants were reviewed and approved by the Ethics Committee of Guangdong Provincial Hospital of Traditional Chinese Medicine (YF2018-064). The patients/participants provided their written informed consent to participate in this study. Written informed consent was obtained from the individual(s) for the publication of any potentially identifiable images or data included in this article.

AUTHOR CONTRIBUTIONS

JZ and GL provided the idea and performed some of the experiments. JW, ShW, QT, and HS performed some of the experiments. WW provided some critical suggestions. SuW is responsible for the experiment design and performing the majority of the experiments and the manuscript writing and editing. All authors read and approved the final manuscript.

FUNDING

This work was supported by the grants from the National Natural Science Foundation of China (81903991, 81974543), the Guangdong Natural Science Foundation of China (2019A1515011362, 2021A1515410007), the Guangzhou science and technology plan project (202002030155, 202102010160), the Scientific Research Project in Universities of Guangdong Provincial Department of Education (2020KTSCX029), the Guangdong Provincial Key Laboratory of Clinical Research on Traditional Chinese Medicine Syndrome (ZH2020KF03), the Chinese medicine science and technology research project of Guangdong Provincial Hospital of Chinese Medicine (YN2019MJ09), the Key project of State Key Laboratory of dampness syndrome of Chinese medicine (SZ2021ZZ38), and Science and Technology Planning Project of Guangdong Province (2017B030314166).

SUPPLEMENTARY MATERIAL

The Supplementary Material for this article can be found online at: https://www.frontiersin.org/articles/10.3389/fphar.2021.753068/full#supplementary-material

REFERENCES

Akiyama, T., Dass, C. R., and Choong, P. F. (2009). Bim-targeted Cancer Therapy: a Link between Drug Action and Underlying Molecular Changes. *Mol. Cancer Ther.* 8, 3173–3180. doi:10.1158/1535-7163.MCT-09-0685

Byerly, J. H., Port, E. R., and Irie, H. Y. (2020). PRKCQ Inhibition Enhances Chemosensitivity of Triple-Negative Breast Cancer by Regulating Bim. *Breast Cancer Res.* 22, 72. doi:10.1186/s13058-020-01302-w

Chen, K., Zhu, P., Ye, J., Liao, Y., Du, Z., Chen, F., et al. (2019). Oxymatrine Inhibits the Migration and Invasion of Hepatocellular Carcinoma Cells by Reducing the Activity of MMP-2/-9 via Regulating P38 Signaling Pathway. *J. Cancer* 10, 5397–5403. doi:10.7150/jca.32875

Chi, X., Nguyen, D., Pemberton, J. M., Osterlund, E. J., Liu, Q., Brahmbhatt, H., et al. (2020). The Carboxyl-Terminal Sequence of Bim Enables Bax Activation and Killing of Unprimed Cells. *eLife* 9. doi:10.7554/eLife.44525

Cui, J., Qu, Z., Harata-Lee, Y., Shen, H., Aung, T. N., Wang, W., et al. (2020). The Effect of Compound Kushen Injection on Cancer Cells: Integrated Identification of Candidate Molecular Mechanisms. *PloS one* 15, e0236395. doi:10.1371/journal.pone.0236395

Dai, D. L., Wang, Y., Liu, M., Martinka, M., and Li, G. (2008). Bim Expression Is Reduced in Human Cutaneous Melanomas. *J. Invest. Dermatol.* 128, 403–407. doi:10.1038/sj.jid.5700989

Galhena, P. B., Samarakoon, S. R., Thabrew, M. I., Weerasinghe, G. A. K., Thammitiyagodage, M. G., Ratnasooriya, W. D., et al. (2012). Anti-Inflammatory Activity Is a Possible Mechanism by Which the Polyherbal Formulation Comprised of Nigella Sativa (Seeds), Hemidesmus Indicus (Root), and Smilax Glabra (Rhizome) Mediates its Antihepatocarcinogenic Effects. *Evid. Based Complement. Alternat Med.* 2012, 108626. doi:10.1155/2012/108626

Gao, L., Wang, K. X., Zhou, Y. Z., Fang, J. S., Qin, X. M., and Du, G. H. (2018). Uncovering the Anticancer Mechanism of Compound Kushen Injection against HCC by Integrating Quantitative Analysis, Network Analysis and Experimental Validation. *Sci. Rep.* 8, 624. doi:10.1038/s41598-017-18325-7

Guo, Y. M., Huang, Y. X., Shen, H. H., Sang, X. X., Ma, X., Zhao, Y. L., et al. (2015). Efficacy of Compound Kushen Injection in Relieving Cancer-Related Pain: A Systematic Review and Meta-Analysis. *Evid Based. Complement. Altern. Med.* 2015, 840742. doi:10.1155/2015/840742

Han, R., Hao, S., Lu, C., Zhang, C., Lin, C., Li, L., et al. (2020). Aspirin Sensitizes Osimertinib-Resistant NSCLC Cells *In Vitro* and *In Vivo* via Bim-dependent Apoptosis Induction. *Mol. Oncol.* 14, 1152–1169. doi:10.1002/1878-0261.12682

Hao, G., Zheng, J., Huo, R., Li, J., Wen, K., Zhang, Y., et al. (2016). Smilax Glabra Roxb Targets Akt(p-Thr308) and Inhibits Akt-Mediated Signaling Pathways in SGC7901 Cells. *J. Drug Target.* 24, 557–565. doi:10.3109/1061186X.2015.1113540

He, R., Ou, S., Chen, S., and Ding, S. (2020). Network Pharmacology-Based Study on the Molecular Biological Mechanism of Action for Compound Kushen Injection in Anti-cancer Effect. *Med. Sci. Monit.* 26, e918520. doi:10.12659/MSM.918520

Incharoen, P., Charonpongsuntorn, C., Saowapa, S., Sirachainan, E., Dejthevaporn, T., Kampreasart, K., et al. (2019). Role of BIM Deletion Polymorphism and BIM Expression as Predictive Biomarkers to Maximize the Benefit of EGFR-TKI Treatment in EGFR-Positive NSCLC. *Asian Pac. J. Cancer Prev.* 20, 3581–3589. doi:10.31557/APJCP.2019.20.12.3581

Jiang, J., and Xu, Q. (2003). Immunomodulatory Activity of the Aqueous Extract from Rhizome of Smilax Glabra in the Later Phase of Adjuvant-Induced Arthritis in Rats. *J. Ethnopharmacol* 85, 53–59. doi:10.1016/s0378-8741(02)00340-9

Lee, J. Y., Ku, B. M., Lim, S. H., Lee, M. Y., Kim, H., Kim, M., et al. (2015). The BIM Deletion Polymorphism and its Clinical Implication in Patients with EGFR-Mutant Non-small-cell Lung Cancer Treated with EGFR Tyrosine Kinase Inhibitors. *J. Thorac. Oncol.* 10, 903–909. doi:10.1097/JTO.0000000000000535

Li, X., Liang, T., Chen, S. S., Wang, M., Wang, R., Li, K., et al. (2020). Matrine Suppression of Self-Renewal Was Dependent on Regulation of LIN28A/Let-7 Pathway in Breast Cancer Stem Cells. *J. Cell Biochem* 121, 2139–2149. doi:10.1002/jcb.29396

Ma, Y., Gao, H., Liu, J., Chen, L., Zhang, Q., and Wang, Z. (2014). Identification and Determination of the Chemical Constituents in a Herbal Preparation, Compound Kushen Injection, by Hplc and Lc-Dad-Ms/Ms. *J. Liquid Chromatogr. Relat. Tech.* 37, 207–220. doi:10.1080/10826076.2012.738623

Ng, K. P., Hillmer, A. M., Chuah, C. T., Juan, W. C., Ko, T. K., Teo, A. S., et al. (2012). A Common BIM Deletion Polymorphism Mediates Intrinsic Resistance and Inferior Responses to Tyrosine Kinase Inhibitors in Cancer. *Nat. Med.* 18, 521–528. doi:10.1038/nm.2713

Nourmohammadi, S., Aung, T. N., Cui, J., Pei, J. V., De Ieso, M. L., Harata-Lee, Y., et al. (2019). Effect of Compound Kushen Injection, a Natural Compound Mixture, and its Identified Chemical Components on Migration and Invasion of Colon, Brain, and Breast Cancer Cell Lines. *Front. Oncol.* 9, 314. doi:10.3389/fonc.2019.00314

Ooi, L. S., Sun, S. S., Wang, H., and Ooi, V. E. (2004). New Mannose-Binding Lectin Isolated from the Rhizome of Sarsaparilla Smilax Glabra Roxb. (Liliaceae). *J. Agric. Food Chem.* 52, 6091–6095. doi:10.1021/jf030837o

Qu, Z., Cui, J., Harata-Lee, Y., Aung, T. N., Feng, Q., Raison, J. M., et al. (2016). Identification of Candidate Anti-cancer Molecular Mechanisms of Compound Kushen Injection Using Functional Genomics. *Oncotarget* 7, 66003–66019. doi:10.18632/oncotarget.11788

Samarakoon, S. R., Thabrew, I., Galhena, P. B., and Tennekoon, K. H. (2012). Modulation of Apoptosis in Human Hepatocellular Carcinoma (HepG2 Cells) by a Standardized Herbal Decoction of Nigella Sativa Seeds, Hemidesmus Indicus Roots and Smilax Glabra Rhizomes with Anti- Hepatocarcinogenic Effects. *BMC Complement. Altern. Med.* 12, 25. doi:10.1186/1472-6882-12-25

Shukla, S., Saxena, S., Singh, B. K., and Kakkar, P. (2017). BH3-only Protein BIM: An Emerging Target in Chemotherapy. *Eur. J. Cell Biol* 96, 728–738. doi:10.1016/j.ejcb.2017.09.002

Sinicrope, F. A., Rego, R. L., Okumura, K., Foster, N. R., O'Connell, M. J., Sargent, D. J., et al. (2008). Prognostic Impact of Bim, Puma, and Noxa Expression in Human colon Carcinomas. *Clin. Cancer Res.* 14, 5810–5818. doi:10.1158/1078-0432.CCR-07-5202

Tagawa, H., Karnan, S., Suzuki, R., Matsuo, K., Zhang, X., Ota, A., et al. (2005). Genome-wide Array-Based CGH for Mantle Cell Lymphoma: Identification of

Homozygous Deletions of the Proapoptotic Gene BIM. *Oncogene* 24, 1348–1358. doi:10.1038/sj.onc.1208300

Than, H., Lye, W. K., Sng, C., Allen, J. C., Jr., Ong, S. T., and Chuah, C. (2019). BIM Deletion Polymorphism Profiling Complements Prognostic Values of Risk Scores in Imatinib-Treated Asian Chronic Myeloid Leukemia Patients. *Leuk. Lymphoma* 60, 234–237. doi:10.1080/10428194.2018.1461863

Wang, H., Hu, H., Rong, H., and Zhao, X. (2019a). Effects of Compound Kushen Injection on Pathology and Angiogenesis of Tumor Tissues. *Oncol. Lett.* 17, 2278–2282. doi:10.3892/ol.2018.9861

Wang, J. D., Katz, S. G., Morgan, E. A., Yang, D. T., Pan, X., and Xu, M. L. (2019b). Proapoptotic Protein BIM as a Novel Prognostic Marker in Mantle Cell Lymphoma. *Hum. Pathol.* 93, 54–64. doi:10.1016/j.humpath.2019.08.008

Wang, S., Oh, D. Y., Leventaki, V., Drakos, E., Zhang, R., Sahin, A. A., et al. (2019c). MicroRNA-17 Acts as a Tumor Chemosensitizer by Targeting JAB1/CSN5 in Triple-Negative Breast Cancer. *Cancer Lett.* 465, 12–23. doi:10.1016/j.canlet.2019.08.016

Wang, S., Peng, Z., Li, W., Long, S., Xiao, S., and Wu, W. (2020). Fuzheng Kang-Ai Decoction Enhances the Effect of Gefitinib-Induced Cell Apoptosis in Lung Cancer through Mitochondrial Pathway. *Cancer Cell Int* 20, 185. doi:10.1186/s12935-020-01270-3

Wang, S., Long, S., Xiao, S., Wu, W., and Hann, S. S. (2018). Decoction of Chinese Herbal Medicine Fuzheng Kang-Ai Induces Lung Cancer Cell Apoptosis via STAT3/Bcl-2/Caspase-3 Pathway. *Evid Based. Complement. Altern. Med.* 2018, 8567905. doi:10.1155/2018/8567905

Wang, W., You, R. L., Qin, W. J., Hai, L. N., Fang, M. J., Huang, G. H., et al. (2015). Anti-tumor Activities of Active Ingredients in Compound Kushen Injection. *Acta Pharmacol. Sin* 36, 676–679. doi:10.1038/aps.2015.24

Yang, M., Zhu, S. J., Shen, C., Zhai, R., Li, D. D., Fang, M., et al. (2021). Clinical Application of Chinese Herbal Injection for Cancer Care: Evidence-Mapping of the Systematic Reviews, Meta-Analyses, and Randomized Controlled Trials. *Front. Pharmacol.* 12, 666368. doi:10.3389/fphar.2021.666368

Yang, Y., Sun, M., Yao, W., Wang, F., Li, X., Wang, W., et al. (2020). Compound Kushen Injection Relieves Tumor-Associated Macrophage-Mediated Immunosuppression through TNFR1 and Sensitizes Hepatocellular Carcinoma to Sorafenib. *J. Immunother. Cancer* 8. doi:10.1136/jitc-2019-000317

Yu, L., Zhou, Y., Yang, Y., Lu, F., and Fan, Y. (2017). Efficacy and Safety of Compound Kushen Injection on Patients with Advanced Colon Cancer: A Meta-Analysis of Randomized Controlled Trials. *Evid Based. Complement. Altern. Med.* 2017, 7102514. doi:10.1155/2017/7102514

Zhang, D., Ni, M., Wu, J., Liu, S., Meng, Z., Tian, J., et al. (2019). The Optimal Chinese Herbal Injections for Use with Radiotherapy to Treat Esophageal Cancer: A Systematic Review and Bayesian Network Meta-Analysis. *Front. Pharmacol.* 9, 1470. doi:10.3389/fphar.2018.01470

Zhang, H., Jenkins, S. M., Lee, C. T., Harrington, S. M., Liu, Z., Dong, H., et al. (2018). Bim Is an Independent Prognostic Marker in Intrahepatic Cholangiocarcinoma. *Hum. Pathol.* 78, 97–105. doi:10.1016/j.humpath.2018.04.009

Conflict of Interest: The authors declare that the research was conducted in the absence of any commercial or financial relationships that could be construed as a potential conflict of interest.

Publisher's Note: All claims expressed in this article are solely those of the authors and do not necessarily represent those of their affiliated organizations, or those of the publisher, the editors and the reviewers. Any product that may be evaluated in this article, or claim that may be made by its manufacturer, is not guaranteed or endorsed by the publisher.

frontiers | Frontiers in Oncology

ORIGINAL RESEARCH
published: 30 June 2022
doi: 10.3389/fonc.2022.732860

Sanguinarine Regulates Tumor-Associated Macrophages to Prevent Lung Cancer Angiogenesis Through the WNT/β-Catenin Pathway

Yajing Cui[1†], Yingbin Luo[1†], Qiaohong Qian[2], Jianhui Tian[1], Zhihong Fang[1], Xi Wang[1], Yaoying Zeng[1], Jianchun Wu[1] and Yan Li[1*]*

[1] Department of Oncology, Shanghai Municipal Hospital of Traditional Chinese Medicine, Shanghai University of Traditional Chinese Medicine, Shanghai, China, [2] Department of Integrated Traditional Chinese and Western Medicine, Obstetrics and Gynecology Hospital, Fudan University, Shanghai, China

OPEN ACCESS

Edited by:
Haiyang Yu,
Tianjin University of Traditional Chinese Medicine, China

Reviewed by:
Junhua Mai,
Houston Methodist Research Institute, United States
Nanfang Peng,
Memorial Sloan Kettering Cancer Center, United States
Yu Chong,
Soochow University, China

***Correspondence:**
Jianchun Wu
eq219@126.com
Yan Li
yan.xiaotian@shutcm.edu.cn

[†]These authors have contributed equally to this work and share first authorship

Specialty section:
This article was submitted to Pharmacology of Anti-Cancer Drugs, a section of the journal Frontiers in Oncology

Received: 29 June 2021
Accepted: 27 May 2022
Published: 30 June 2022

Citation:
Cui Y, Luo Y, Qian Q, Tian J, Fang Z, Wang X, Zeng Y, Wu J and Li Y (2022) Sanguinarine Regulates Tumor-Associated Macrophages to Prevent Lung Cancer Angiogenesis Through the WNT/β-Catenin Pathway. Front. Oncol. 12:732860. doi: 10.3389/fonc.2022.732860

Tumor-associated macrophage (TAM)-mediated angiogenesis in the tumor microenvironment is a prerequisite for lung cancer growth and metastasis. Therefore, targeting TAMs, which block angiogenesis, is expected to be a breakthrough in controlling the growth and metastasis of lung cancer. In this study, we found that Sanguinarine (Sang) inhibits tumor growth and tumor angiogenesis of subcutaneously transplanted tumors in Lewis lung cancer mice. Furthermore, Sanguinarine inhibited the proliferation, migration, and lumen formation of HUVECs and the expression of CD31 and VEGF by regulating the polarization of M2 macrophages *in vitro*. However, the inhibitory effect of Sanguinarine on angiogenesis remained *in vivo* despite the clearance of macrophages using small molecule drugs. Further high-throughput sequencing suggested that WNT/β-Catenin signaling might represent the underlying mechanism of the beneficial effects of Sanguinarine. Finally, the β-Catenin activator SKL2001 antagonized the effect of Sanguinarine, indicating that Sanguinarine can regulate M2-mediated angiogenesis through the WNT/β-Catenin pathway. In conclusion, this study presents the first findings that Sanguinarine can function as a novel regulator of the WNT/β-Catenin pathway to modulate the M2 macrophage polarization and inhibit angiogenesis, which has potential application value in immunotherapy and antiangiogenic therapy for lung cancer.

Keywords: lung cancer, angiogenesis, tumor associated macrophages, sanguinarine, Wnt/β- catenin

INTRODUCTION

Primary bronchogenic carcinoma (lung cancer) represents the leading cause of cancer death, accounting for 18% of total cancer deaths (1), and is a public health problem worldwide. Tumoral angiogenesis is a prerequisite for the progression, invasion, and metastasis of solid tumors (2). When the cancer is more significant than 1 to 2 mm, new blood vessels will be formed in the microenvironment (3) to transport nutrients and oxygen to tumor cells and clear metabolites. Lung cancer is a highly vascularized tumor (4)

and refers to a typical vascular-dependent lesion (5), which is related to its poor prognosis. Therefore, anti-angiogenesis is one of the most critical strategies in the treatment of lung cancer. Currently, the clinical efficacy of traditional antiangiogenic agents alone is not ideal. Consequently, it is of great significance to deeply study the mechanism of angiogenesis.

Researchers have found that macrophage infiltration into the tumor microenvironment, namely, tumor-associated macrophages (TAMs) are usually considered to be the key members of the tumor microenvironment (TME) that is correlated with tumor progression (6, 7). A retrospective study involving patients with lung cancer showed that the number of TAMs in tumor nests is more than 50%, which is much higher than the proportion of other cells such as $CD3^+$T cells (8). Accumulating evidence has shown that TAMs trigger "angiogenic switch" (9, 10)by secreting a variety of vascular growth factors (VEGF, Ang2, Tie2, etc.) (11), and matrix metalloproteinases (MMPs) (12), as well as inflammatory factors (TNF-α (13), IL-8 (14), etc.), ultimately resulting in tumor invasion and metastasis. In addition, TAMs are also the cause of treatment failure in chemotherapy (15), radiotherapy, and immunotherapy (16) and are a crucial factor of poor prognoses for lung cancer patients (6). As such, targeting TAMs has gradually become a hot spot at the forefront of tumor research.

Macrophages are characterized by strong heterogeneity and plasticity. M1 type macrophages are activated by lipopolysaccharides (LPS) and the pro-inflammatory cytokine IFN-γ. They exert robust killing activity against pathogens and tumor cells (17) and the promotion of polarized Th1 immune responses by the up-regulation of pro-inflammatory cytokines(TNF-α, IL-1, and IL-6), reactive oxygen species (ROS), and nitric oxide (NO). In contrast, the M2 type is activated by cytokines such as IL-4 or IL-13 and specifically expresses arginase-1 (Arg-1), macrophage mannose receptor (CD206) and YM1 (18), with functions such as inducing the Th2 immune response. Research suggests that M2 macrophages tend to be activated in the tumor microenvironment, and the number of TAMs infiltrating tumor tissues is often positively correlated with poor prognosis in patients. As a result, if the phenotypic transformation of macrophages can be regulated effectively, namely, inhibiting the M2 type and inducing the M1 type, tumor angiogenesis mediated by TAMs can be blocked and the antitumor immune response of the body can be reversed (19).

Sanguinarine, a type of benzophenanthridine alkaloid, possesses various effects, including antibacterial (20), reduce pain (21), and anticancer activities. Current research proves that Sanguinarine has demonstrated significant anticancer effects in a wide variety of tumor types via multiple targets-multiple pathways. Sanguinarine induced apoptosis in pancreatic cancer through the expression Bcl-2 protein levels (22). And, Sanguinarine suppresses the proliferation and migration of gastric cancer cells through the DUSP4/ERK/MMP-9 pathway (23). In hepatocellular carcinoma,Sanguinarine inhibits epithelial-mesenchymal transition(EMT) *via* targeting HIF-1α/TGF-β feed-forward loop (24). In addition, Sanguinarine could inhibit VEGF-mediated angiogenesis through the Akt pathway (25).In summary, Sanguinarine can play an anticancer role through a variety of methods, including inhibiting proliferation and invasion and inducing apoptosis and antiangiogenesis, representing a promising anticancer natural compound with great potential.

However, whether Sanguinarine inhibits angiogenesis through the regulation of macrophages and thereby exerts an anti-lung cancer effect has not yet been reported. In this study, we show for the first time that Sanguinarine can target the WNT/β-Catenin pathway to inhibit the M2 polarization of TAMs and exert antiangiogenic effects on lung cancer and the regulation of immune factors. This finding suggests that Sanguinarine is a potent immunomodulatory agent and angiogenesis inhibitor and has a broad potential in anti-lung cancer applications.

MATERIALS AND METHODS

Cell Culture

The Lewis murine lung adenocarcinoma (Lewis lung cancer cells, LLCs) cell strain and human umbilical vein endothelial cell (HUVEC) strain were both purchased from the Shanghai Cell Bank of Chinese Academy of Sciences; DMEM cell culture medium (KGI Biotechnology Co., Ltd., Jiangsu) with 10% FBS (Gibco, USA) was used to culture the cells in a 37°C incubator.

Selleck Chemicals Co. supplied the Sanguinarine (Catalog: S9032, CAS: 2447-54-3, Chemical Formula: $C_{20}H_{14}NO_4$, Molecular Weight: 332.33, Smiles Structural Formula: C[N+]1=C2C(=C3C=CC4=C(C3=C1)OCO4)C=CC5=CC6=C(C=C52)OCO6). DMSO was used to dilute the Sang into a 10 mM stock solution, which was stored in a -20 refrigerator.

Subcutaneous Transplanted Tumor Model of Lewis Lung Cancer Mice and Macrophage Clearance

The Animal Ethics Committee of Shanghai Traditional Chinese Medicine Hospital approved all the experimental steps. Six-week-old male C57BL/6 mice (20 ± 2 g) were purchased from Shanghai Slack Laboratory Animal Co., Ltd. and were raised in an SPF environment. Each animal was anesthetized with an intraperitoneal injection of sodium pentobarbital (50 mg/kg).Under the right scapula of each mouse, 5×10^5 LLCs were injected subcutaneously. Mice began to receive treatment on the next day (day1) with an intraperitoneal injection of normal saline (0.1 ml/mouse/day), Sanguinarine (2.5 mg/kg/day, 5 mg/kg/day) (26) or Cisplatin (DDP) (2 mg/kg, twice a week).

For the model of subcutaneously transplanted tumors with macrophage clearance in Lewis lung cancer mice, was performed as previously published (27). First, on the day before the transplantation of subcutaneous tumors (day -1), mice were injected intraperitoneally with 200 μl of clodronate liposomes (CLPs; US FormuMax, cat: F70101C-AL) for the exhaustion of mononuclear macrophages in mice *in vivo*. Hereafter, CLPs were injected intraperitoneally into mice twice a week, 100 μl per mouse, to continuously exhaust the mononuclear macrophages in mice *in vivo*. At the end of the experiment, the splenic single-cell suspension was extracted. The ratio of CD11b+F4/80+ macrophages was detected by flow cytometry to evaluate the

efficiency of macrophage clearance. Mice receive treatment with intraperitoneal injections of normal saline (0.1 ml/mouse/day), Sanguinarine (5 mg/kg/day) or Sanguinarine combined with CLPs. A Vernier caliper was used to measure the size of the tumor every 2 days. Three weeks after administration, the mice were sacrificed and tumor tissues were isolated.

Preparation for Splenic Single-Cell Suspension

The spleen tissues of mice were extracted and homogenized to form the single-cell suspensions. These suspensions were filtrated through a 70-μm strainer filter, centrifuged at 1000 rpm at 4°C for 5 minutes, and 1 or 2 volumes of red blood cell lysis buffer (Biosharp, China; Catalog: 143191) were added and incubated at room temperature for 5 minutes. Next, 5 ml PBS was added to terminate the lysis. Afterward, the single-cell suspensions were collected and relevant flow antibodies were incubated at 4°C for 30 minutes in the dark. The data was collected with a flow cytometer (Beckman Coulter Inc, USA) and analyzed with FlowJo software (Ashland, OR, USA).

Paraffin Section Immunostaining

Fresh transplanted tumor tissues in mice were fixed with 4% paraformaldehydeand embedded in paraffin. Tissue sections were stained with anti-mouse CD31 antibody (Bioss, lot: bs-20322R), anti-mouse F4/80 antibody (CST, lot: 30325) and anti-mouse CD206 antibody (CST, lot: 24595). The secondary antibody used in this research was CY3-conjugated AffiniPure goat anti-rabbit IgG (H+L), purchased from Boster (catalog: BA1032). Pictures were taken and recorded using an inverted microscope.

Extraction of Bone Marrow-Derived Macrophages (BMDMs) in Mice and Construction of an M2 Polarization Model

Five-week-old healthy male C57BL/6 mice were purchased from Shanghai Jie-Si-Jie Laboratory Animal Co., Ltd. The experimental program was as described above (28, 29), where mice were sacrificed by cervical dislocation with adequate cleansing using 75% alcohol, and femora and tibiae of mice were separated, of which marrow cavities were flushed with PBS. The flushing fluid collected was filtered through a 70-mesh screen and centrifuged at 20°C at a rate of 1000 rpm. The supernatant liquid was discarded, and the sediments were resuspended in DMEM containing 10% FBS and M-CSF (Pepro Tech, Lot: #0817245) at a final concentration of 20 ng/ml. The liquid was renewed every 48 h, and the cells were cultured continuously for 5 days. Adherent cells from mice were referred to as bone marrow-derived macrophages (BMDMs). On the 5^{th} day of culture, IL-4 (Pepro Tech, Lot: #021749) at a final concentration of 20 ng/ml was added according to the concentration of 1×10^6 cells for stimulation for 24 h. Flow cytometry was used to determine the rate of positive expression in M2 macrophages.

Flow Cytometry and Reagents

FITC anti-mouse CD11b antibody (lot: 101206), PE anti-mouse F4/80 antibody (lot: 12310), and APC anti-mouse CD206 antibody (lot: 141708) were all purchased from BioLegend Co.

After the mature BMDMs were treated under different conditions, the cells were collected under 3% BSA in PBS and blocked at room temperature for 15 minutes. The corresponding flow antibody was added at 4°C and incubated away from light for 30 minutes. The antibody was washed with PBS, and a CytoFLEX flow cytometer (Beckman Coulter Inc, USA) was used for sample detection. FlowJo vX.10 software (Ashland, OR, USA) was used for the analysis of FACS data.

Cell Counting Kit-8 (CCK-8) Assay

BMDMs well-grown were seeded in a 96-well plate at a density of 3×10^4 cells per well. The next day, cells were treated with Sang and incubated for 24 h. And then the culture medium was changed with a medium containing 10% CCK-8 solution (YEASEN Biological Company; Shanghai, lot: 40203ES76) and incubated for 1 to 4 h in an incubator. The optical density(OD) value at 450 nm was detected by a microplate reader. Cell viability was calculated in accordance with the formula in the instructions.

Western Blot

To lyse the cells,RIPA (Beyotime; lot: P0013B) and 1/100 PMSF lysis buffer (Beyotime; lot: ST506) were applied According to the instructions of the BCA quantitative kit (Beyotime; lot: P0010S), the protein content of the samples was measured based on a standard curve of protein. Based on the measured protein content of the sample, 5X loading buffer (Beyotime; lot: P0015) was added(1 μl loading buffer per 4 μl sample)and protein samples were boiled at 100°C for 8 minutes for protein denaturation. Next, 10% gels (Enzyme Biotechnology, Shanghai, China; lot: PG112) were used for SDS-PAGE analysis. Chemiluminescence Substrate (Thermo Fisher Scientific; lot: 32106) was used for immunoblotting, and finally, the images were analyzed using Quantity One software (BIO-RAD; ChemDoxTM XRS+ with image LabTM software). All antibody information is shown in **Supplementary Table 1**.

qRT-PCR

Extraction of the total RNA was performed according to the instructions of the TRIzol reagent (Invitrogen), and the RNA was then reverse-transcribed into cDNA by a reverse transcription kit (Takara, Dalian, China). Next, the SYBR Green PCR kit (Takara) was applied to perform real-time PCR according to the manufacturer's instructions on the QuantStudio 6 Flex real-time PCR system (Thermo Fisher). All the primers were synthesized by Sangon Biotech (Sangon Biotech, Shanghai, China). All the primer sequences used are shown in **Supplementary Table 2**. The $2^{-\triangle\triangle Ct}$ method was applied to analyze the real-time PCR data (30).

Preparation of Conditioned Medium (CM)

The experimental method was performed as previously described (31, 32), mature mononuclear macrophages were treated with IL-4, Sang, or the combination treatment for 24 h and then the original medium was replaced by a serum-free medium to be cultured for another 24h.The liquid supernatant was collected and then filtered twice with a 0.45-μM filter and stored in a -80

refrigerator until use. When used, the macrophage-conditioned medium was mixed with the fresh culture medium at a ratio of 1:1, and 10% FBS was added.

Endothelial Cell Tube Formation Assay

Matrigel (200 μl/well, BD Matrigel matrix, Catalog: 356234) was added to a 24-well plate and incubated at 37°C for 30 minutes for solidification. HUVECs were resuspended in different conditioned media; these cells were inoculated into a 24-well plate at a density of 1.5×10^5 cells/well and cultured in a 37°C incubator to observe tube formation and to photograph.

Scratch Wound Healing Assay

HUVECs were seeded into a 6-well plate at a density of 1×10^6 cells/well; when the cell density reached 80%, 3 parallel scratches was generated in the monolayer with a 200-μl pipette tip. After washing with PBS, the serum-free medium (control group) or macrophage conditioned medium (with or without Sang) was added to the respective wells. Images of the scratch were taken after 0 h, 6 h, 12 h, and 24 h, and the wound area was measured and assessed with the ImageJ software (ImageJ Software Inc., MD, USA).

Transwell Migration Assay

Transwell inserts (CORNING,lot: 3422) were removed, 50 μl of Matrigel was spread in the upper chamber, and these were placed in a 37°C incubator for 30 minutes. After solidification, 5×10^3 HUVECs resuspended in serum-free medium were inoculated. Five hundred microliters of complete conditioned medium (containing 10% FBS) was added to the lower chamber; after 12 h-18 h, the upper chamber was removed and wiped off the cells on the surface of the upper chamber. Next, it was fixed with paraformaldehyde (Boster; lot: AR1069) for 30 minutes, stained with crystal violet (Beyotime, lot: C0121-100 ml) for 30 minutes, washed with distilled water twice, repeatedly washed with water and air dried. The cells that migrated through the membranes for each insert were counted under a microscope.

RNA-Seq Analysis

M0 and M2 cells with good growth status were collected. Three biological replicates were established in each group. After adding TRIzol and blowing repeatedly, they were quickly transferred to an enzyme-free freezing tube. After quick freezing in liquid nitrogen for 30 minutes, they were transferred to a -80°C freezer for long-term preservation; Shanghai Meiji Biotech Co., Ltd. was entrusted to perform eukaryotic mRNA sequencing. Based on the Illumina NovaSeq 6000 sequencing platform, all mRNAs transcribed from cells in each group during the same period were sequenced.

RSEM software package was applied for quantitative statistics of the expression levels of genes and transcripts. Differential gene expression analysis was performed using edgeR and the screening threshold was $|\log2FC| \geq 1$ and p-value <0.05. Finally, differential genes screened were subjected to pathway enrichment analysis using the KEGG database.

Statistical Analysis

All the statistical analyses in this article were completed using SPSS software (Version 21.0), and all the data are presented as the mean ± SD of the results of three independent experiments., A t-test was used for statistical analysis for numerical variables conforming to a normal distribution.A One-way analysis of variance (ANOVA) was performed to test the homogeneity of variances between different groups, followed by a *post hoc* LSD test. Statistically significant differences were by the symbols*p<0.05, **p<0.01, and ***p<0.001). Nonsignificant was denoted as "ns" (p>0.05).

RESULTS

Sanguinarine-Enhanced Tumor Regression and Angiogenesis Inhibition *In Vivo*

To evaluate the effect of Sanguinarine on tumor growth, C56BL/6 Lewis lung cancer mouse models were used. Different doses of Sanguinarine were injected intraperitoneally (i.p.) for 21 days. The results showed high-dose Sanguinarine and DDP significantly inhibited LLC cell tumor growth (**Figure 1A**). The tumors of mice treated with high-dose Sanguinarine (5 mg/kg) and cisplatin were much smaller (**Figure 1B**) and lighter (**Figure 1C**) compared with mice treated with low-dose Sanguinarine (2.5 mg/kg) or control group.In addition, the body weight of mice was also detected. The results showed that mice in the DDP group lost a significant amount of weight, while mice in the low-dose Sanguinarine and high-dose Sanguinarine groups did not have significant weight loss (**Figure S1**), indicating that high-dose Sanguinarine has a better antitumor effect with minor side effects. This was consistent with the results of previous studies (33).

Angiogenesis is necessary for the transport of nutrients and elimination of metabolites for tumor cells. In other words, angiogenesis acts as a bridge for the growth of malignant tumor cells and distant metastasis. CD31, also known as platelet-endothelial cell adhesion molecule (PECAM-1), maintains the migration and survival of endothelial cells and is a direct indicator for the evaluation of angiogenesis (34). To investigate the effect of Sanguinarine on angiogenesis, immunofluorescence was applied to detect the expression of CD31 in the tumor tissues. Compared to the control group, the percentages of CD31+ positive cells were dramatically decreased in the high-dose Sanguinarine group but were unaffected in the low-dose Sanguinarine or the DDP group (**Figures 1D**, **S4A**), indicating that high-dose Sanguinarine can restrain tumor growth and angiogenesis.

Recent research has found that TAMs in the tumor microenvironment induce angiogenesis, which is considered to be the initiating "switch" for tumor angiogenesis and promotes tumor progression. Therefore, we next focused on exploring whether inhibition of tumor angiogenesis by Sanguinarine is related to TAMs from the perspective of the microenvironment. The expression of F4/80, a total macrophage marker, was detected. The results suggested that compared with the control group, there was no dramatic effect on the expression of F4/80 in the Sanguinarine-treated group (**Figures 1E**, **S4B**). Subsequently, the impact of Sanguinarine on CD206, that is, the M2 phenotype, was

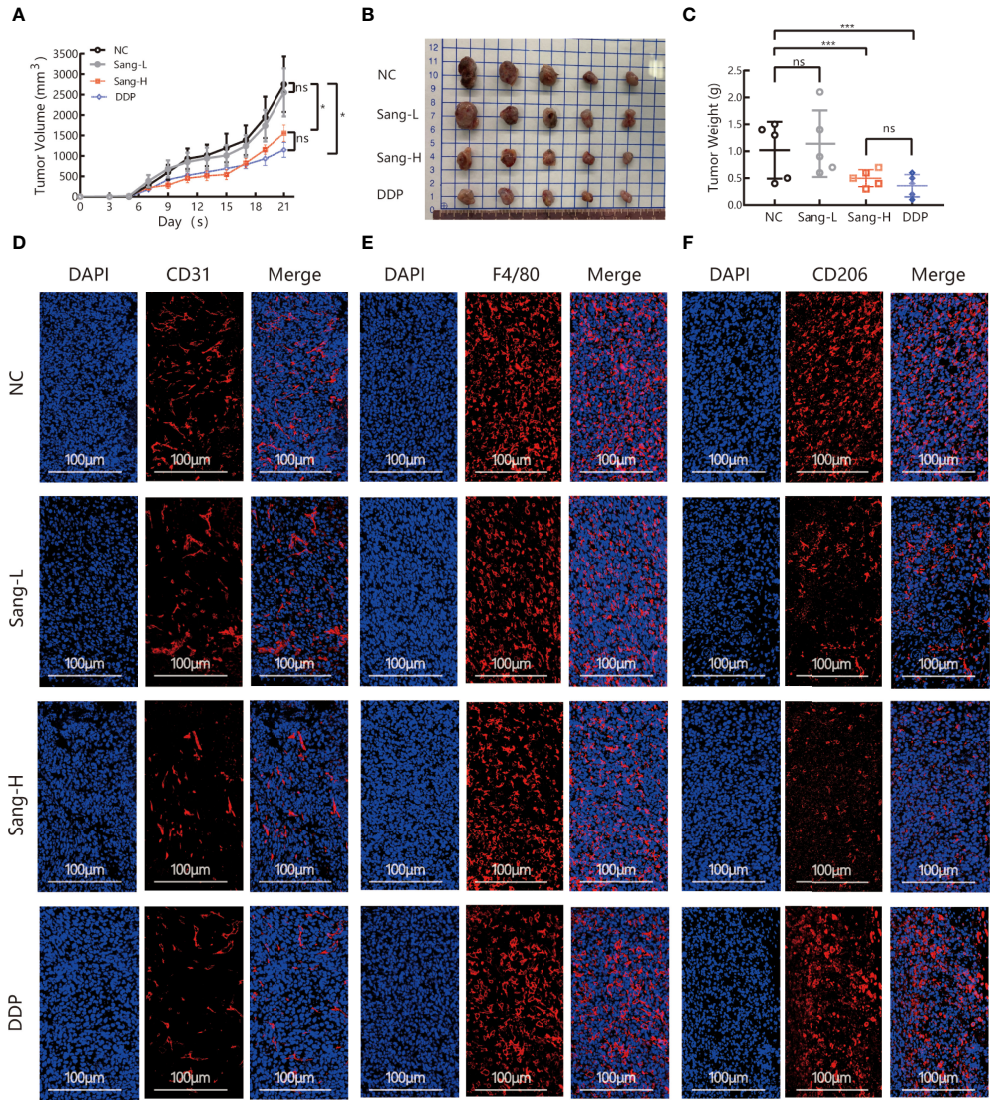

FIGURE 1 | Sang may inhibit tumor growth and angiogenesis in mice through a TAM-dependent mechanism. A total of 5×10^5 LLCs per mouse were subcutaneously injected into the right flank of C57BL/6 mice, and then mice were intraperitoneally injected with saline (0.1 ml/mouse), Sang (2.5 mg/kg, 5 mg/kg) or cisplatin (2 mg/kg) from day 2. Tumor size was measured every 2 days, and following treatment for 3 weeks, the mice were sacrificed, and tumor tissues were isolated. Data are presented as the mean ± SEM of measurements from five mice per group. $^*p < 0.05$; $^{***}p < 0.001$. ns, not statistically significant ($p > 0.05$). **(A)** Tumor volume curves; **(B)** Tumor tissues collected at the end point; and **(C)** Tumor weights. **(D)** The expression of CD31, **(E)** F4/80, and **(F)** CD206 in the subcutaneous tumor tissue of lung cancer mice were revealed by immunofluorescence staining. Nucleus was stained with DAPI solution. Scale bars: 100, 100, and 100 μm, respectively.

observed. The results implied that compared with the control group, percentages of CD206+ positive cells (M2-phenotype) were massively reduced in the Sanguinarine group (**Figures 1F**, **S4C**), indicating that the anticancer effects of Sanguinarine may be correlated with the inhibition of angiogenesis and the regulation of M2-type macrophages.

Inhibition of the M2 Polarization of Macrophages by Sanguinarine

The results of the above *in vivo* study initially revealed that the antiangiogenic effect of Sanguinarine is related to the regulation of TAMs. Further research on the regulation of Sanguinarine on the TAM phenotype was carried out, based on the different roles of M1 and M2 macrophages in tumor angiogenesis. First, bone marrow-derived macrophages (BMDMs) were isolated and cultured in the presence of M-CSF. After flow cytometry, the purity of CD11b+F4/80+ M0 macrophages was 98%, indicating that they developed into mature macrophages. Then, BMDMs were stimulated with IL-4 to induce M2 polarization. The flow cytometry results displayed that compared with the control group, IL-4 treatment markedly enhanced the CD206+ cell proportion(**Figure 2A**). Moreover, after IL-4 induction, the

expression of CD206, an M2-type-specific protein, notably increased (**Figure 2B**). qRT-PCR detected that the mRNA expression of *CD206* and *Arg-1*, both specific markers of M2 macrophages, was increased (**Figure S2B**). In addition, morphological observations suggested that monocytes gradually changed from rounded to flat and spindly under M-CSF culture; the cells became more prolate with pseudopodia after adding IL-4 (morphology of the M2 type) (**Figure S2A**), which is consistent with previous research reports (32). These results suggest that we have successfully established an M2 polarization model of macrophages.

Next, measurements of the IC50 value revealed an IC50 value of 1.81 μM for Sanguinarine-treated BMDMs (**Figure 2C**). Therefore, three types of Sanguinarine concentrations were set for further research that had no obvious effect on BMDM cell proliferation: 0.1 μM, 0.3 μM, and 1μM. The results showed that Sanguinarine markedly suppressed the protein expression of CD206 in M2 macrophages and showed concentration-dependent inhibition, whereas there was no effect on total macrophage CD68 protein expression (**Figure 2D**). The results of flow cytometry suggested that after Sanguinarine intervention, the ratio of F4/80+CD206+ M2 macrophages was 23.23± 5.10%, compared with the untreated F4/80+CD206+ ratio of 41.8 ± 4.47%, with statistical significance (p<0.01) (**Figure 2E**). Similarly, morphological alterations were observed under the microscope, and macrophages after Sanguinarine treatment

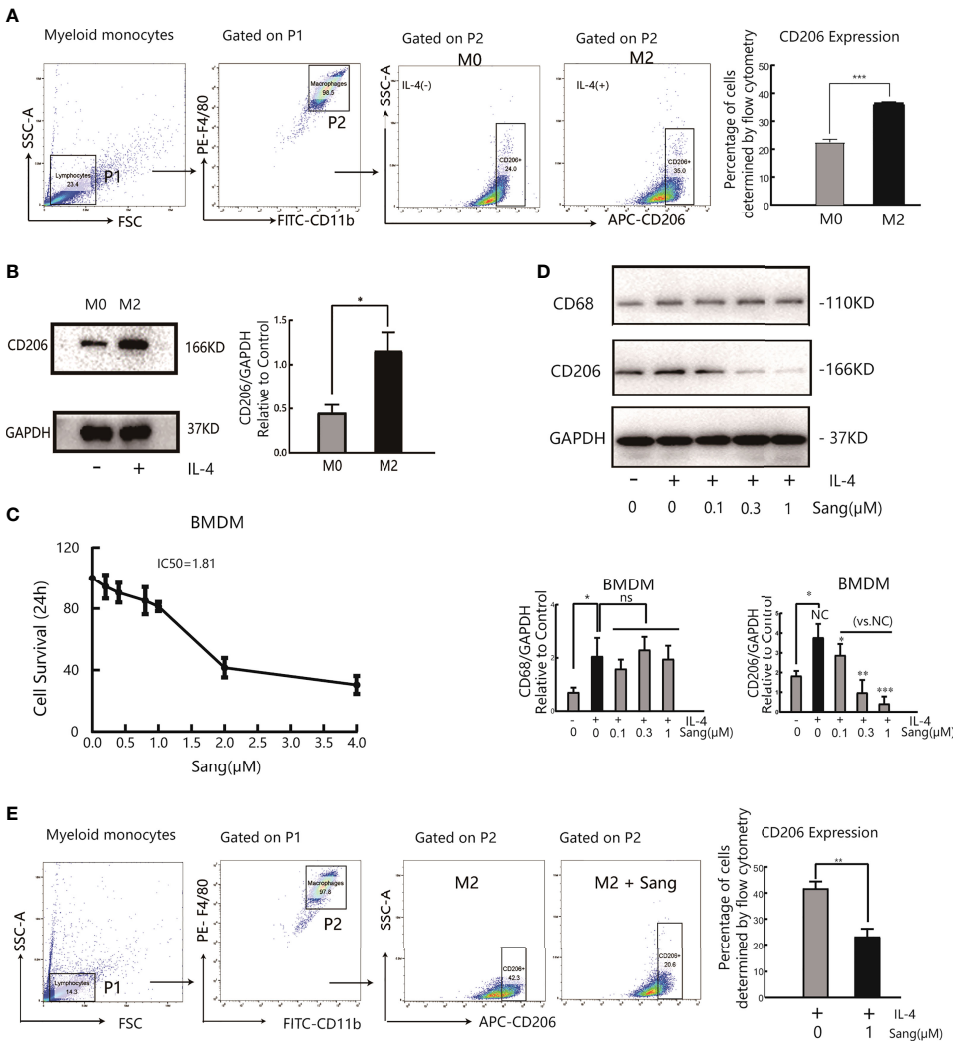

FIGURE 2 | Sang suppresses M2 polarization in macrophages. Bone marrow-derived macrophages (BMDMs) were isolated from mice and treated with IL-4 (20 ng/ml) for 24 h for M2 polarization. **(A)** Flow cytometry analysis of the expression of the M2-like macrophage surface marker CD206. **(B)** Western blot analysis of CD206 protein expression in IL-4- stimulated BMDMs. **(C)** BMDMs were incubated in the presence of Sang at different concentrations (0, 0.2, 0.4, 0.8, 1, 2, and 4 μM) for 24 h, and cell viability was determined by the CCK-8 assay. **(D)** BMDMs in the presence or absence of IL-4 were treated with different concentrations of Sang (0.1, 0.3, and 1 μM), and the expression of CD68 and CD206 proteins was detected through a western blot assay. **(E)** Flow cytometry detection of CD206 expression treated with 1 μM Sang Each experiment was reproduced three times. *p < 0.05; **p < 0.01; ***p < 0.001; ns, not statistically significant (p > 0.05).

became shorter and rounder with fewer pseudopodia and tended to be similar to the morphology before IL-4 polarization (**Figure S2C**). In summary, Sanguinarine can inhibit the polarization of M2 macrophages, thereby affecting their function.

Sanguinarine Inhibits Angiogenesis by Restraining M2 Polarization of Macrophages

We also examined whether the inhibition of M2 macrophage polarization through Sang-mediated would affect angiogenesis in the tumor microenvironment. Tube formation Assay revealed that M2-CM could obviously improve the vascular ring density of HUVECs, while most HUVECs in the M2-CM/Sang group did not have ring formation, with a significantly reduced number and density of vascular rings ($p<0.01$) (**Figure 3A**). Proliferation (35, 36) and migration of endothelial cells are both necessary steps for angiogenesis. The Wound Healing Assay results implied that M2-CM was able to increase the wound-healing rate compared to the untreated control, while this trend was reversed with the treatment of Sang ($p<0.01$) (**Figure 3B**). Transwell experiment results indicated that the number of HUVECs in the M2-CM group passing through the chamber increased significantly, while the number of HUVECs in the M2-CM/Sang group was considerably reduced (**Figure 3C**). The results above indicate that Sanguinarine can inhibit angiogenesis through inhibition of the polarization of M2 macrophages.

Vascular endothelial growth factor (VEGF) is the essential inducing factor for proangiogenesis, and when combined with the VEGF receptor (VEGFR) on endothelial cells, it mediates angiogenesis, changes vascular permeability, and mediates inflammation (37). Experimental results indicated that under M2-CM culture, the expression of CD31 and VEGF in HUVECs was critically increased, while under M2-CM/Sang culture, the expression of CD31 and VEGF in HUVECs was significantly inhibited (**Figure 3D**). Overall, these findings suggest that Sanguinarine may affect capillary like-tube formation of endothelial cells by regulating M2-type macrophage polarization.

Sanguinarine Inhibits Tumor Growth and Angiogenesis in Mice by Regulating the Polarization of M2 Macrophages

The above studies indicate that Sanguinarine can inhibit angiogenesis by regulating M2 macrophage polarization. Furthermore, our next objective was to evaluate if the findings *in vitro* were consistent with the effects *in vivo*. The model of macrophage clearance in Lewis lung cancer mice was constructed, as shown in the experimental flow chart (**Figure 4A**). The results showed that macrophage clearance alone and Sanguinarine treatment alone could inhibit tumor growth, (**Figure 4B**), manifesting in the smallest tumor (**Figure 4C**) and the lightest tumor (**Figure 4D**). The percentage of CD11b+F4/80+ macrophages significantly decreased in the spleen and tumor tissue treated with macrophage clearance (**Figure S3** and **Figures 4F**, **S6B, E**), which is consistent with previous reports (38–40). In addition, the group treated with CLPs effectively decreased tumor size and load (**Figures 4B–D**), indicating that macrophages contribute to neoplastic progression. Unexpectedly, the tumor inhibition effect in the combination group was not significantly different from that in the Sanguinarine alone group, which could be related to the multitarget characteristics of Sanguinarine.

Immunofluorescence co-staining demonstrated that the combination group had significantly reduced CD206 expression, (**Figures 4F**, **S5B**, **S6A–D**), which suggests that Sanguinarine exerts an influence by regulating the M2 phenotype but not reducing the overall population of macrophages.

Expression of the blood vessel marker CD31 in the tumor mass was detected by immunofluorescence. The results showed that clearance of macrophages reduced the signal expression of CD31. After combination therapy of macrophage clearance and Sanguinarine treatment, there was a more significant reduction in the signal expression of CD31 (as shown in **Figures 4E**, **S5A**). As expected, VEGF expression was decreased when treated with CLP and Sanguinarine alone, whereas the combination treatment exhibited a synergistic suppression (**Figures 4G**, **S5C**). Above all, these results suggest that tumor angiogenesis depends on M2 macrophages, and that Sanguinarine exerts an antiangiogenic effect by reducing VEGF expression, which is related to the regulation of M2 macrophages.

High-Throughput Screening of Differentially Expressed Genes of Macrophage Polarization Modulated by Sanguinarine

To clarify the molecular mechanism of Sanguinarine in the regulation of M2, RNA sequencing (RNA-seq) was subsequently applied to detect the whole-genome transcriptome levels of M0 and M2., The screening threshold for the genetic analysis of between-group variance was $|\log2FC| \geq 1$ and a p-value <0.05. We identified 6462 differential genes in the M2 vs. M0 group, of which 3370 were upregulated and 3092 were downregulated (**Figure 5A**). KEGG pathway analysis identified that these differentially expressed genes are mainly involved in the osteoblast differentiation pathway, cancer pathway, Toll-like receptor signaling pathway, cytokine receptor signaling pathway, VEGF signaling pathway, apoptosis, ferroptosis, WNT, etc. (**Figure 5B**).

Multiple literature reports have shown that the WNT/β-Catenin pathway is involved in the differentiation of M2 macrophages (41–43), and prior studies by our group suggested that Sanguinarine might inhibit WNT/β-Catenin pathway activation (44). Therefore, RT-qPCR was applied to evaluate the mRNA levels of *Wnt* ligands. The results suggested that compared with M0 macrophages, the expression of all *Wnt* ligands increased in M2 macrophages, among which the expression of *Wnt1, Wnt7a, Wnt7b, and Wnt10b* improved the most significantly ($p<0.05$); after Sanguinarine intervention, compared with M2 macrophages, the expression of *Wnt* ligands was reduced, among which the expression of *Wnt1 and Wnt7b* was decreased the most significantly ($p<0.01$) (**Figure 5C**). The WNT ligand will bind to its receptor to activate the classic WNT signaling pathway, namely, WNT/β-Catenin, and β-Catenin represents the key switch for signal transmission. Results indicated that the expression of β-Catenin protein increased critically in M2 macrophages ($p<0.05$), while β-Catenin expression was dramatically attenuated after Sanguinarine intervention ($p<0.01$) (**Figure 5D**). The results above imply that WNT signaling is involved in the polarization of M2 macrophages and that

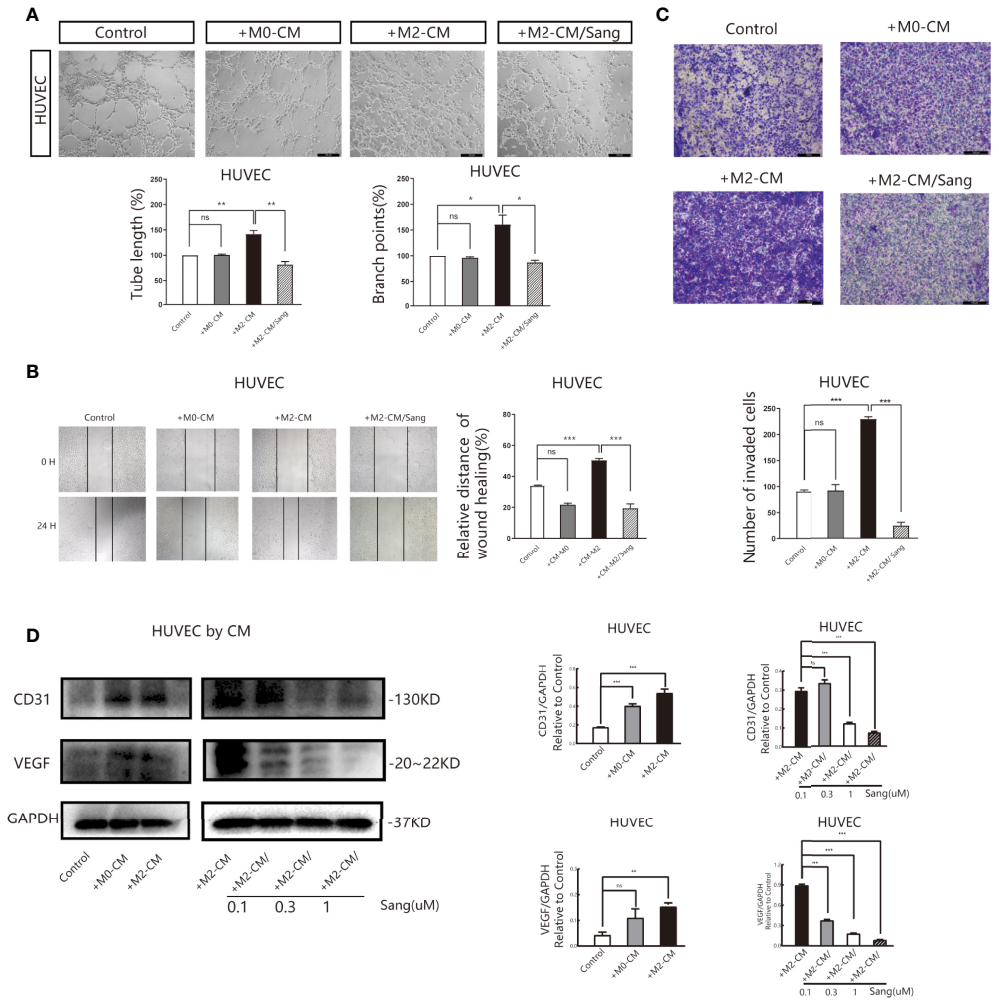

FIGURE 3 | Sang inhibits neovascularization by suppressing M2 macrophage polarization. Conditioned medium (CM) was used to determine the effects of Sang pre-treatment on angiogenesis promoted by M2-like macrophages. **(A)** Representative images of the HUVEC tube formation assay on Matrigel (magnification 20x) and quantification of tubes and branch points. **(B)** Representative images of the HUVECs wound healing assay at 0 h and 24 h, as well as quantitative analysis of the wound healing area. **(C)** HUVECs migration and invasion was detected using a Transwell assay. HUVECs were plated in the upper chamber, and the conditioned medium of macrophages after different treatments was collected and placed in the lower chamber. Representative images of HUVECs invasion, as well as quantification of the number of migrated HUVECs (20X). **(D)** Western blot assay for CD31 and VEGF protein expression in HUVECs that were co-cultured with macrophage-CM, and treated with Sang. Each experiment was reproduced three times. *$p < 0.05$; **$p < 0.01$; ***$p < 0.001$; ns, not statistically significant ($p > 0.05$).

Sanguinarine is highly likely to inhibit the polarization of M2 macrophages through inhibition of the WNT pathway.

Sanguinarine Targets the WNT/β-Catenin Pathway of Macrophages to Restrain M2 Polarization of Macrophages and Lung Cancer Angiogenesis

To further identify the mechanism of Sanguinarine involving the WNT/β-Catenin signaling pathway, the WNT/β-Catenin activator SKL2001 was used. The results agreed with the outcome of **Figure 2C**, showing that the expression of CD206 and β-Catenin was significantly suppressed after Sanguinarine-only treatment of macrophages, while SKL2001-only treatment increased the CD206 and β-Catenin levels. When administered in combination, the efficacy of Sanguinarine was antagonized by SKL2001 (**Figure 6A**).This outcome further proved that the WNT/β-Catenin pathway is involved in M2 polarization and that Sanguinarine can inhibit the WNT/β-Catenin pathway in M2 macrophages as well as the polarization of M2 macrophages.

Moreover, tube formation experiments showed that in HUVECs cultured in SKL2001-CM, the density of vascular rings increased dramatically (p>0.05), while in HUVECs cultured in Sanguinarine together with SKL2001-CM, the number and density of vascular rings decreased dramatically (**Figure 6B**). In addition, the scratch experiment showed that scratches were significantly healed in HUVECs treated with SKL2001-CM (p<0.01), while in HUVECs cultured with Sanguinarine together with SKL2001-CM,

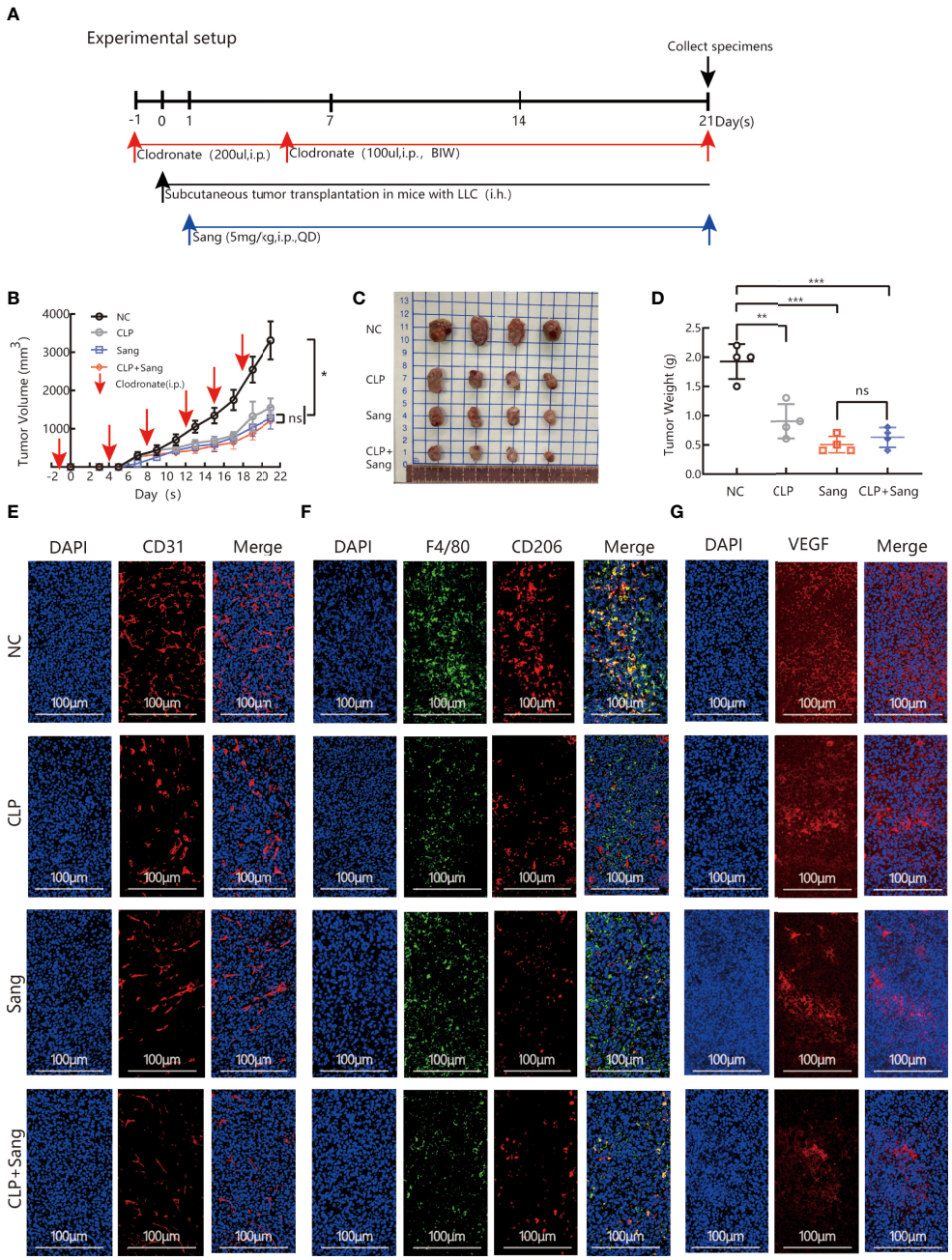

FIGURE 4 | Sang inhibits tumor growth and neovascularization in mice by suppressing macrophage M2 polarization. CLP (200 μl/mouse) was intraperitoneally administered on the day before starting tumor inoculation (day -1). A total of 5 × 105 LLCs per mouse were subcutaneously injected into the right flank of C57BL/6 mice (day 0), and then 100 μl of CLP per mouse was administered by intraperitoneal injection on days 4, 8, 12, 15 and 19 and Sang (5 mg/kg) from day 1. Tumor size was measured every 2 days, and following treatment for 3 weeks, the mice were sacrificed and tumor tissues isolated. Data are presented as the mean ± SEM of measurements from five mice per group. *$p < 0.05$; **$p < 0.01$; ***$p < 0.001$; ns, not statistically significant ($p > 0.05$). **(A)** Experimental setup for depletion of macrophages in the Lewis lung subcutaneous transplantation mouse model. **(B)** Tumor volume curves; **(C)** Tumor tissues collected at the end point; and **(D)** Tumor weights. **(E)** The expression of CD31, **(F)** F4/80 colocalization with CD206, and **(G)** VEGF in the subcutaneous tumor tissue of lung cancer in macrophage-cleared mice was revealed by immunofluorescence staining. Nucleus was stained with DAPI solution. Scale bars: 100, 100, and 100 μm, respectively. *In vivo*, Sang reduced the secretion of VEGF by inhibiting M2 polarization, which ultimately resulted in inhibition of angiogenesis and tumor growth in mice.

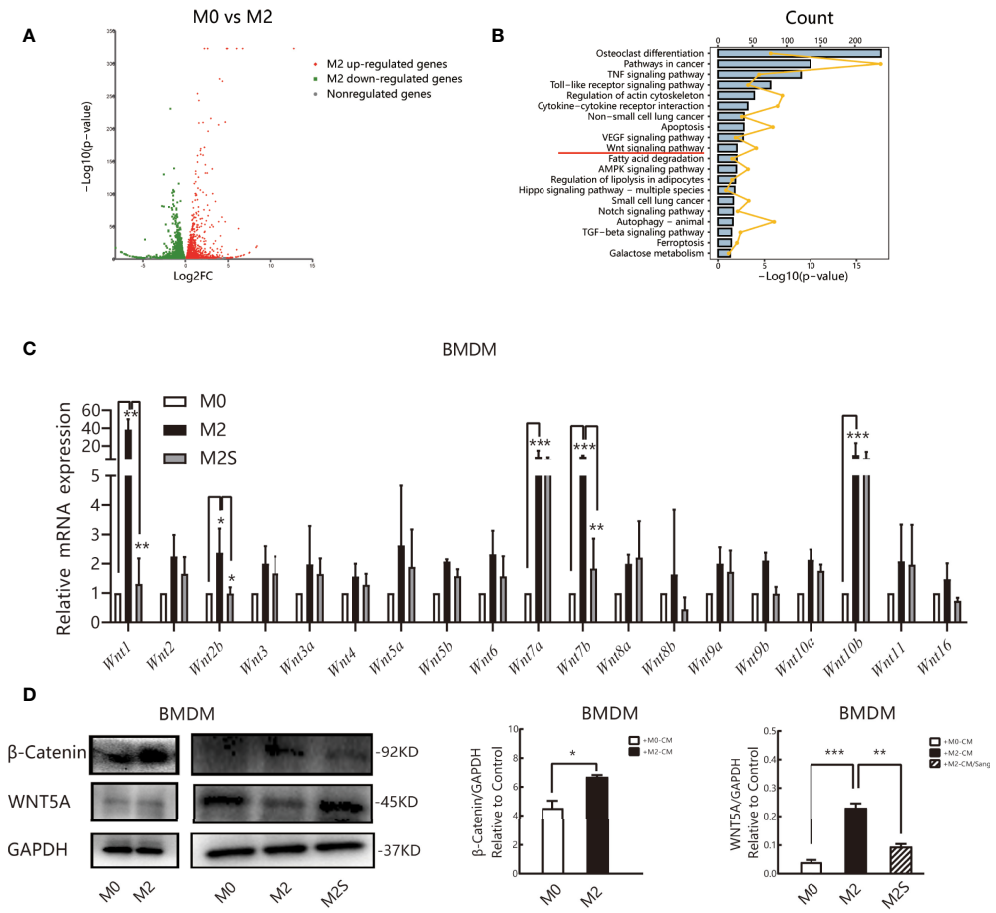

FIGURE 5 | Sang regulates the M2 phenotype of macrophages by the WNT/β-Catenin pathway. RNA sequencing (RNA-Seq) was used to profile genome-wide gene expression and transcriptome changes in M0 and M2 macrophages. |log2FC| >1 and *p*-value<0.05 were taken as thresholds to screen differential genes. **(A)** Volcano plot showing the differentially expressed genes (DEGs) in M0 versus M2, n = 3. FC, fold change. **(B)** KEGG pathway enrichment analysis of differentially expressed genes (DEGs). Each of these blue entries represents a signaling pathway; broken yellow lines indicate the number of differential genes enriched in the pathway. **(C)** qRT-PCR was performed to determine *Wnt* ligand expression in M0, M2, and M2S. **(D)** Western blot assay for WNT5A and β-Catenin in M0, M2, and M2S, are considered to be key proteins in the non-classical and classic WNT/β-Catenin pathway, respectively. $^{*}p < 0.05$; $^{**}p < 0.01$; $^{***}p < 0.001$.

scratch healing was significantly inhibited ($p<0.01$) (**Figure 6C**). In addition, the Transwell experiment showed that HUVEC migration and invasion increased significantly after SKL2001-CM treatment ($p<0.01$), while after treatment with Sanguinarine together with SKL2001-CM, HUVEC migration and invasion were inhibited ($p<0.01$) (**Figure 6D**). In summary, Sanguinarine can inhibit angiogenesis by inhibiting the WNT/β-Catenin pathway of M2 macrophages, which could be proven by the inhibition of the formation of vascular rings, proliferation, and migration of endothelial cells.

DISCUSSION

Targeting tumor angiogenesis refers to an essential treatment strategy to block the invasion and metastasis of malignant tumor cells and to reduce cancer mortality. In this study, Sanguinarine inhibited the growth of tumors in Lewis lung cancer mice and angiogenesis. The antitumor angiogenesis effect of Sanguinarine is related to the regulation of TAMs, which is not linked to the decrease in total macrophage numbers but to the macrophage phenotype. Further research has found that Sanguinarine could exert an antitumor angiogenic effect by restraining the polarization of M2 macrophages and decreasing VEGF expression in endothelial cells. In addition, Sanguinarine reduced the mRNA expression of *Wnt1 and Wnt7b* and the protein expression of β-Catenin, a nuclear transcription factor in M2 macrophages. The results above suggest that Sanguinarine can exert an antitumor angiogenesis effect by targeting the WNT/β-Catenin pathway of macrophages to inhibit the polarization of M2 macrophages.

Studies have found that tumor angiogenesis has been closely related to the tumor microenvironment in recent years. Hypoxia, the growth factors CSF1 and VEGF, and chemotactic factors in

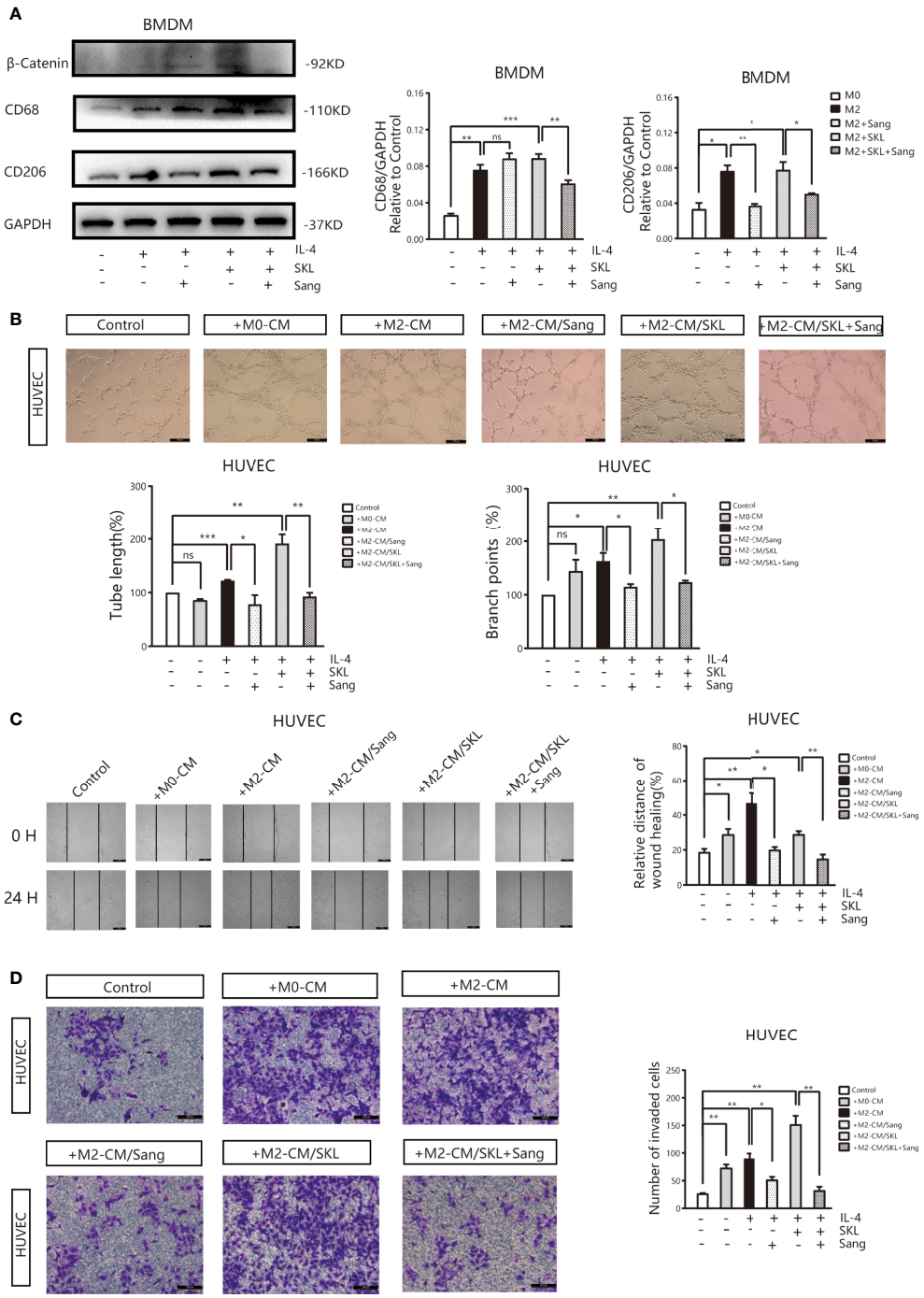

FIGURE 6 | Sang inhibits M2-like polarization of macrophages and M2-mediated angiogenesis by targeting the WNT/β-Catenin pathway in macrophages. **(A)** The WNT/β-Catenin activator SKL2001, alone or in combined with Sang, was utilized to treat BMDMs. Western blotting was performed to detect the protein expression of CD68, CD206, and β-Catenin, and the results indicated that SKL2001 could upregulate β-Catenin and CD206 expression; however, β-Catenin and CD206 were markedly decreased following the SKL2001/Sang combination. **(B–D)** HUVECs were cocultured with M2 macrophages' conditioned medium treated with SKL2001 alone or combined with Sang. **(B)** Representative images of the HUVEC tube formation assay on Matrigel (magnification 20x) and quantification of tubes and branch points. **(C)** Representative images of the wound healing assay of HUVECs at 0 h and 24 h, as well as quantitative analysis of the wound healing area. **(D)** HUVEC migration and invasion was detected using a Transwell assay. HUVECs were plated in the upper chamber, and the conditioned medium of macrophages after different treatments was collected and placed in the lower chamber. Representative images of HUVEC invasion and quantification of the number of migrated HUVECs (20X). Each experiment was reproduced three times. *$p < 0.05$; **$p < 0.01$; ***$p < 0.001$; ns, not statistically significant ($p > 0.05$).

the tumor microenvironment all contribute to increased macrophage recruitment and infiltration into the tumor matrix and blood vessel margins. Research suggests that TAMs are typically M2-polarized immunosuppressive cells in various tumors (45, 46). The M2 TAMs can directly activate angiogenesis through the release of VEGF, bFGF, and PlGF or indirectly activate angiogenesis through the release of matrix metalloproteinases (MMPs) to remodel the extracellular matrix and to improve the migration of endothelial cells (47), which could form new blood vessels and accelerate tumor progression. Therefore, inhibition of the M2 phenotype of macrophages has been proven to be a unique opportunity for effectively blocking tumor angiogenesis (48, 49). The experiments above indicated that inhibition of M2 macrophage polarization could inhibit angiogenesis and VEGF expression. These results are consistent with previous results, which could further confirm that M2-type TAMs promote tumor angiogenesis (31, 50). Previous studies have also found that macrophage clearance therapy alone could not significantly reduce the tumor growth of PDAC homogeneous mice *in situ* (32). However, according to the above findings, Sang and CLP alone significantly inhibited LLC cell tumor growth. Further studies have also shown that the effect of Sanguinarine on tumor suppression is independent of the reduction in the total number of macrophages but is correlated with the inhibition of M2 macrophages. It is considered that it may be due to the sensitivity to CLPs varying between tumor cells and models. In addition, we observed for the first time that the anti-tumor effect was enhanced after treatment by macrophage clearance combined with Sanguinarine. It is believed that TAM phenotypic regulation is not the only target of Sanguinarine. Our previous study pointed to Sanguinarine suppressing lung cancer stem cell (CSC) stemness and inhibiting the proliferation and invasion of lung CSCs (44). In addition, Sanguinarine exhibits multiple antineoplastic characteristics by inhibiting angiogenesis. Therefore, we reasoned that regulating the phenotype of TAMs is only one of the major targets of Sanguinarine action. An apparent synergistic effect is seen when clodronate-liposomes (CLPs) are combined. The results above suggest that Sanguinarine is a promising and exploitable natural anticancer compound with multiple targets and pathways.

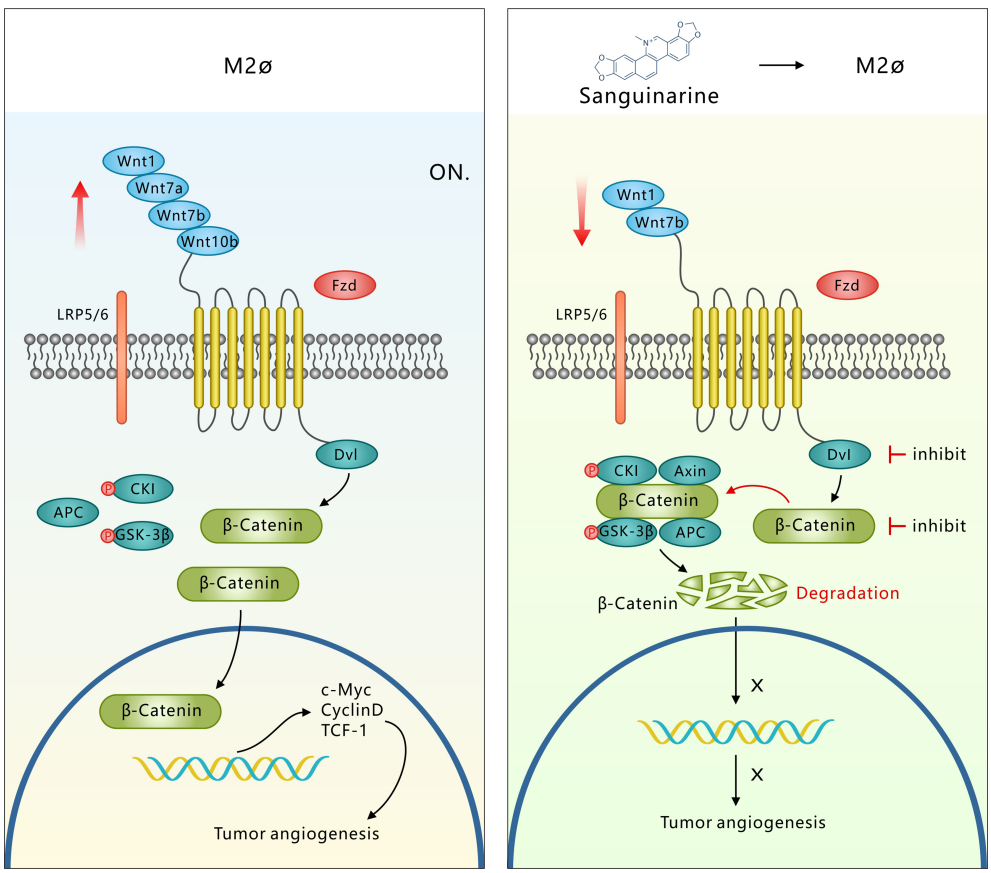

FIGURE 7 | Sang targets the WNT/β-Catenin signaling pathway in TAMs, which represses M2 polarization and thus inhibits TAM-mediated neoangiogenesis. M2-like TAMs show upregulation of WNT ligands (1-7a-7b-10b), leading to transcriptional activation of β-Catenin. β-Catenin translocation into the nucleus induces M2 macrophage polarization, which further promotes the secretion of VEGF protein in HUVECs, leading to the initiation of tumor angiogenesis. However, Sang inhibited WNT/β-Catenin signaling in M2 TAMs by downregulating ligands (*1-7b*) and degrading β-Catenin. β-Catenin could not enter the nucleus to induce M2 macrophage polarization, which thus restrained the secretion of VEGF protein in HUVECs and ultimately suppressed tumor angiogenesis and tumor growth.

The WNT pathway is not only closely related to the invasion and metastasis of lung cancer but also plays a vital role in the maintenance of TAM phenotypes and functions. Therefore, it is a potential clinical molecular target. Previous studies have found (51) that genes from invasive TAMs isolated from transplanted tumors in breast cancer mice were enriched in the WNT signaling pathway. Except for WNT8B, all the other WNT ligands and downstream molecules were increased, with the most obvious ones being WNT7B and 5B. The experiments above indicated that the expression of WNT ligands was significantly increased in M2 macrophages (compared with M0 macrophages), which is consistent with the gene expression analysis of murine myelogenous M2 macrophages in other groups (52). Interestingly, the mRNA levels of *Wnt1, Wnt7a, Wnt7b, and Wnt10b* were higher in M2 macrophages than in M0 macrophages, whereas the expression of *Wnt1 and Wnt7b* dramatically decreased in M2 macrophages after Sanguinarine intervention. These results suggest that macrophages might trigger WNT signaling activation in an autocrine manner to promote the polarization of M2 macrophages. The inhibition of M2 macrophage polarization by Sanguinarine might be related to the inhibition of the WNT pathway.

In addition, the expression of WNT5A in different types of cancers and TAMs remains controversial. In prostate cancer, WNT5A recruits and regulates macrophages through CCL2 to induce castrated prostate cancer (53). In breast cancer, WNT5A from TAMs can induce the expression of MMP-7, resulting in matrix remodeling (54). In contrast, data from our experiments showed that the expression of WNT5A was reduced in M2 macrophages (**Figure 5D**). However, WNT5A has been identified as a promoter protein of the non-classical WNT pathway, induced Ca2+, protein kinase C, Rho-GTPases, and the JNK pathway (55), indicating that the inhibition by Sanguinarine of M2 polarization may depend on the classical WNT/β-Catenin pathway. Among them, β-Catenin represents the key switch for signal transduction to downstream proteins in the classical WNT pathway. The results above showed that the expression of the β-Catenin protein was significantly increased in M2 macrophages, while after Sanguinarine intervention, its expression decreased. Moreover, it was discovered that with SKL2001 intervention, an agonist targeting the β-Catenin signal, the expression of the M2-specific protein CD206 and angiogenesis mediated by M2 increased. However, when the SKL2001 was used for antagonism, the expression of CD206 protein and angiogenesis were reversed, indicating that the WNT signal mediated by TAM-derived β-Catenin plays a central role in the polarization of M2 macrophages, which is consistent with previous research reports (56). Because Sanguinarine attenuated M2 polarization through the WNT/β-Catenin pathway, it is suggested that Sanguinarine is a new type of regulator for the WNT/β-Catenin pathway targeting the polarization of M2 macrophages, which is considered to be a potential strategy for targeted treatment of lung cancer.

Vascular endothelial growth factor (VEGF), as the most specific angiogenesis-inducing factor, plays an essential role in the initiation of tumor angiogenesis (57). Research shows that WNT7B in breast cancer can stimulate endothelial cells to produce VEGF for angiogenesis (58). It is also observed in the experiments above that VEGF expression on HUVECs was upregulated in coculture with M2-CM compared with monocultured HUVECs. This upregulation was significantly weakened by Sang in HUVECs that were co-cultured with M2-CM (**Figure 3D**). At present, we do not yet know the direct relationship between WNT1, WNT7B, and β-Catenin derived from macrophages and VEGF from endothelial cells. This is also a limitation of our current research and will be the direction and focus of our subsequent research. However, the research above suggests that the WNT signal derived from macrophages may be at least partially involved in tumor angiogenesis. Activation of the WNT pathways is essentially engaged in macrophage-mediated angiogenesis and plays a crucial role in tumor invasion and metastasis.

Overall, the tumor microenvironment recruits TAMs to the tumor stroma and blood vessel edges through hypoxia and the release of the growth factor CSF1 or chemotactic factors. TAMs, with the abnormally activated WNT pathway and at the same time through autocrine signaling to promote polarization of the M2 type, secrete a variety of pro-angiogenic factors that eventually induce tumor angiogenesis. However, Sanguinarine can inhibit the occurrence of tumor angiogenesis by targeting the WNT/β-Catenin pathway derived from TAMs to inhibit the polarization of M2 macrophages (**Figure 7**). It was discovered for the first time that Sanguinarine is a new regulator for WNT/β-Catenin pathway that targets the polarization of M2 macrophages. This indicates that Sanguinarine is a promising candidate for targeting the polarization of M2 macrophages for antiangiogenic treatment in lung cancer.

DATA AVAILABILITY STATEMENT

The datasets presented in this study can be found in online repositories. The names of the repository/repositories and accession number(s) can be found below: https://www.ncbi.nlm.nih.gov/ SRP328648, PRJNA745376.

ETHICS STATEMENT

The animal study was reviewed and approved by The Animal Ethics Committee of Shanghai Traditional Chinese Medicine Hospital.

AUTHOR CONTRIBUTIONS

YL and JW conceived and supervised the study; YC, JW, and YL designed experiments; YC and YZ performed the animal work; YC, XW, and QQ carried out all *in vitro* experiments; YC, YL, and ZF analyzed data; YL and JT performed the statistical analysis; YL, JW, and YL provided new tools and reagents; YC wrote the original draft and JW reviewed and edited the manuscript; All authors read and approved the final manuscript.

FUNDING

This work was financially supported by funds from the National Natural Science Foundation of China (No. 81973795, No. 81603590 and No. 82174183), the Shanghai Pujiang Talent Plan (2020PJD057), the Three-year Action Program of Shanghai Municipality for Strengthening Traditional Chinese Medicine Development (2018–2020) (Grant no. ZY CCCX-4001-01) and the Three-year Action Plan Clinical in Hospital Development Centeritals of Shanghai Shenkang (SHDC2020CR4052).

SUPPLEMENTARY MATERIAL

The Supplementary Material for this article can be found online at: https://www.frontiersin.org/articles/10.3389/fonc.2022.732860/full#supplementary-material

REFERENCES

1. Sung H, Ferlay J, Siegel RL, Laversanne M, Soerjomataram I, Jemal A, et al. Global Cancer Statistics 2020: GLOBOCAN Estimates of Incidence and Mortality Worldwide for 36 Cancers in 185 Countries. *CA Cancer J Clin* (2021) 71:209–49. doi: 10.3322/caac.21660
2. Folkman J. Tumor Angiogenesis: Therapeutic Implications. *New Engl J Med* (1971)285(21):1182–6. doi: 10.1056/NEJM197111182852108
3. Cao Y. Tumor Angiogenesis and Molecular Targets for Therapy. *Front Bioscience* (2009) 14:3962–73. doi: 10.2741/3504
4. Daum S, Hagen H, Naismith E, Wolf D, Pircher A. The Role of Anti-Angiogenesis in the Treatment Landscape of Non-Small Cell Lung Cancer - New Combinational Approaches and Strategies of Neovessel Inhibition. *Front Cell Dev Biol* (2020) 8:610903. doi: 10.3389/fcell.2020.610903
5. Mantovani A, Allavena P, Sica A, Balkwill F. Cancer-Related Inflammation. *Nature* (2008) 454(7203):436–44. doi: 10.1038/nature07205
6. Sumitomo R, Hirai T, Fujita M, Murakami H, Otake Y, Huang CL. PD-L1 Expression on Tumor-Infiltrating Immune Cells is Highly Associated With M2 TAM and Aggressive Malignant Potential in Patients With Resected non-Small Cell Lung Cancer. *Lung Canc* (2019) 136:136–44. doi: 10.1016/j.lungcan.2019.08.023
7. Welsh TJ, Green RH, Richardson D, Waller DA, O'Byrne KJ, Bradding P. Macrophage and Mast-Cell Invasion of Tumor Cell Islets Confers a Marked Survival Advantage in non-Small-Cell Lung Cancer. *J Clin Oncol* (2005) 23 (35):8959–67. doi: 10.1200/JCO.2005.01.4910
8. Dora D, Rivard C, Yu H, Pickard SL, Laszlo V, Harko T, et al. Characterization of Tumor-Associated Macrophages and the Immune Microenvironment in Limited-Stage Neuroendocrine-High and -Low Small Cell Lung Cancer. *Biol (Basel)* (2021) 10(6):502. doi: 10.3390/biology10060502
9. De Palma M, Lewis CE. Macrophage Regulation of Tumor Responses to Anticancer Therapies. *Cancer Cell* (2013) 23(3):277–86. doi: 10.1016/j.ccr.2013.02.013
10. Quatromoni J, Eruslanov E. Tumor-Associated Macrophages: Function, Phenotype, and Link to Prognosis in Human Lung Cancer. *Am J Transl Res* (2012) 4(4):376–89. doi: 10.1155/2012/952452
11. Forget MA, Voorhees JL, Cole SL, Dakhlallah D, Patterson IL, Gross AC, et al. Macrophage Colony-Stimulating Factor Augments Tie2-Expressing Monocyte Differentiation, Angiogenic Function, and Recruitment in a Mouse Model of Breast Cancer. *PLoS One* (2014) 9(6):e98623. doi: 10.1371/journal.pone.0098623
12. Li J, Wang JJ, Peng Q, Chen C, Humphrey MB, Heinecke J, et al. Macrophage Metalloelastase (MMP-12) Deficiency Mitigates Retinal Inflammation and Pathological Angiogenesis in Ischemic Retinopathy. *PLoS One* (2012) 7(12): e52699. doi: 10.1371/journal.pone.0052699
13. Torisu H, Ono M, Kiryu H, Furue M, Ohmoto Y, Nakayama J, et al. Macrophage Infiltration Correlates With Tumor Stage and Angiogenesis in Human Malignant Melanoma: Possible Involvement of TNFalpha and IL-1alpha. *Int J Cancer* (2000) 85(2):182–8. doi: 10.1002/(SICI)1097-0215(20000115)85:2%3C182::AID-IJC6%3E3.0.CO;2-M
14. Koch AE, Polverini PJ, Kunkel SL, Harlow LA, DiPietro LA, Elner VM, et al. Interleukin-8 as a Macrophage-Derived Mediator of Angiogenesis. *Sci Advances* (1992) 258:1798–801. doi: 10.1126/science.1281554
15. Baghdadi M, Wada H, Nakanishi S, Abe H, Han N, Putra WE, et al. Chemotherapy-Induced IL34 Enhances Immunosuppression by Tumor-Associated Macrophages and Mediates Survival of Chemoresistant Lung Cancer Cells. *Cancer Res* (2016) 76(20):6030–42. doi: 10.1158/0008-5472.CAN-16-1170
16. Cendrowicz E, Sas Z, Bremer E, Rygiel TP. The Role of Macrophages in Cancer Development and Therapy. *Cancers (Basel)* (2021) 13(8):1946. doi: 10.3390/cancers13081946
17. Lankadasari MB, Mukhopadhyay P, Mohammed S, Harikumar KB. TAMing Pancreatic Cancer: Combat With a Double Edged Sword. *Mol Canc* (2019) 18 (1):48. doi: 10.1186/s12943-019-0966-6
18. Muller U, Stenzel W, Kohler G, Werner C, Polte T, Hansen G, et al. IL-13 Induces Disease-Promoting Type 2 Cytokines, Alternatively Activated Macrophages and Allergic Inflammation During Pulmonary Infection of Mice With Cryptococcus Neoformans. *J Immunol* (2007) 179(8):5367–77. doi: 10.4049/jimmunol.179.8.5367
19. Villalobos-Ayala K, Ortiz Rivera I, Alvarez C, Husain K, DeLoach D, Krystal G, et al. Apigenin Increases SHIP-1 Expression, Promotes Tumoricidal Macrophages and Anti-Tumor Immune Responses in Murine Pancreatic Cancer. *Cancers (Basel)* (2020) 12(12):3631. doi: 10.3390/cancers12123631
20. Anjago WM, Zeng W, Chen Y, Wang Y, Biregeya J, Li Y, et al. The Molecular Mechanism Underlying Pathogenicity Inhibition by Sanguinarine in Magnaporthe Oryzae. *Pest Manag Sci* (2021) 77(10):4669–79. doi: 10.1002/ps.6508
21. Li P, Wang YX, Yang G, Zheng ZC, Yu C. Sanguinarine Attenuates Neuropathic Pain in a Rat Model of Chronic Constriction Injury. *BioMed Res Int* (2021) 2021:3689829. doi: 10.1155/2021/3689829
22. Ahsan H, Reagan-Shaw S, Breur J, Ahmad N. Sanguinarine Induces Apoptosis of Human Pancreatic Carcinoma AsPC-1 and BxPC-3 Cells *via* Modulations in Bcl-2 Family Proteins. *Cancer Lett* (2007) 249(2):198–208. doi: 10.1016/j.canlet.2006.08.018
23. Zhang R, Wang G, Zhang PF, Zhang J, Huang YX, Lu YM, et al. Sanguinarine Inhibits Growth and Invasion of Gastric Cancer Cells *via* Regulation of the DUSP4/ERK Pathway. *J Cell Mol Med* (2017) 21(6):1117–27. doi: 10.1111/jcmm.13043
24. Su Q, Fan M, Wang J, Ullah A, Ghauri MA, Dai B, et al. Sanguinarine Inhibits Epithelial-Mesenchymal Transition *via* Targeting HIF-1alpha/TGF-Beta Feed-Forward Loop in Hepatocellular Carcinoma. *Cell Death Dis* (2019) 10 (12):939. doi: 10.1038/s41419-019-2173-1
25. Eun JP, Koh GY. Suppression of Angiogenesis by the Plant Alkaloid, Sanguinarine. *Biochem Biophys Res Commun* (2004) 317(2):618–24. doi: 10.1016/j.bbrc.2004.03.077
26. Leung EL, Fan XX, Wong MP, Jiang ZH, Liu ZQ, Yao XJ, et al. Targeting Tyrosine Kinase Inhibitor-Resistant Non-Small Cell Lung Cancer by Inducing Epidermal Growth Factor Receptor Degradation *via* Methionine 790 Oxidation. *Antioxid Redox Signal* (2016) 24(5):263–79. doi: 10.1089/ars.2015.6420
27. Lamkin DM, Bradshaw KP, Chang J, Epstein M, Gomberg J, Prajapati KP, et al. Physical Activity Modulates Mononuclear Phagocytes in Mammary Tissue and Inhibits Tumor Growth in Mice. *PeerJ* (2021) 9:e10725. doi: 10.7717/peerj.10725
28. Lee C, Jeong H, Bae Y, Shin K, Kang S, Kim H, et al. Targeting of M2-Like Tumor-Associated Macrophages With a Melittin-Based Pro-Apoptotic Peptide. *J Immunother Canc* (2019) 7(1):147. doi: 10.1186/s40425-019-0610-4
29. Anisiewicz A, Łabędź N, Krauze I, Wietrzyk J. Calcitriol in the Presence of Conditioned Media From Metastatic Breast Cancer Cells Enhances Ex Vivo

Polarization of M2 Alternative Murine Bone Marrow-Derived Macrophages. *Cancers* (2020) 12(11):3485. doi: 10.3390/cancers12113485
30. Livak KJ, Schmittgen TD. Analysis of Relative Gene Expression Data Using Real-Time Quantitative PCR and the 2(-Delta Delta C(T)) Method. *Methods* (2001) 25(4):402–8. doi: 10.1006/meth.2001.1262
31. Wang JC, Sun X, Ma Q, Fu GF, Cong LL, Zhang H, et al. Metformin's Antitumour and Anti-Angiogenic Activities are Mediated by Skewing Macrophage Polarization. *J Cell Mol Med* (2018) 00:1–12. doi: 10.1111/jcmm.13655
32. D'Errico G, Alonso-Nocelo M, Vallespinos M, Hermann PC, Alcala S, Garcia CP, et al. Tumor-Associated Macrophage-Secreted 14-3-3zeta Signals *via* AXL to Promote Pancreatic Cancer Chemoresistance. *Oncogene* (2019) 38 (27):5469–85. doi: 10.1038/s41388-019-0803-9
33. Zhu M, Gong Z, Wu Q, Shi X, Su Q, Zhang YJC, et al. Sanguinarine Suppresses Migration and Metastasis in Colorectal Carcinoma Associated With the Inversion of EMT Through the Wnt/β-Catenin Signaling. *Clin Transl Med* (2020) 10(1):1–12. doi: 10.1002/ctm2.1
34. Lertkiatmongkol P, Liao D, Mei H, Hu Y, Newman PJ. Endothelial Functions of Platelet/Endothelial Cell Adhesion Molecule-1 (Cd31). *Curr Opin Hematol* (2016) 23(3):253–9. doi: 10.1097/MOH.0000000000000239
35. Lugano R, Ramachandran M, Dimberg A. Tumor Angiogenesis: Causes, Consequences, Challenges and Opportunities. *Cell Mol Life Sci* (2020) 77 (9):1745–70. doi: 10.1007/s00018-019-03351-7
36. Plate KH, Scholz A, Dumont DJ. Tumor Angiogenesis and Anti-Angiogenic Therapy in Malignant Gliomas Revisited. *Acta Neuropathol* (2012) 124 (6):763–75. doi: 10.1007/s00401-012-1066-5
37. Ai B, Bie Z, Zhang S, Li A. Paclitaxel Targets VEGF-Mediated Angiogenesis in Ovarian Cancer Treatment. *Am J Cancer Res* (2016) 6(8):1624–35.
38. House IG, Savas P, Lai J, Chen AXY, Oliver AJ, Teo ZL, et al. Macrophage-Derived CXCL9 and CXCL10 Are Required for Antitumor Immune Responses Following Immune Checkpoint Blockade. *Clin Cancer Res* (2020) 26(2):487–504. doi: 10.1158/1078-0432.CCR-19-1868
39. Kim SH, Kim SJ, Park J, Joe Y, Lee SE, Saeidi S, et al. Reprograming of Tumor-Associated Macrophages in Breast Tumor-Bearing Mice Under Chemotherapy by Targeting Heme Oxygenase-1. *Antioxidants (Basel)* (2021) 10(3):470. doi: 10.3390/antiox10030470
40. Ma Y, Li Y, Jiang L, Wang L, Jiang Z, Wang Y, et al. Macrophage Depletion Reduced Brain Injury Following Middle Cerebral Artery Occlusion in Mice. *J Neuroinflamm* (2016) 13:38. doi: 10.1186/s12974-016-0504-z
41. Oguma K, Oshima H, Aoki M, Uchio R, Naka K, Nakamura S, et al. Activated Macrophages Promote Wnt Signalling Through Tumour Necrosis Factor-Alpha in Gastric Tumour Cells. *EMBO J* (2008) 27(12):1671–81. doi: 10.1038/emboj.2008.105
42. Raghavan S, Mehta P, Xie Y, Lei YL, Mehta G. Ovarian Cancer Stem Cells and Macrophages Reciprocally Interact Through the WNT Pathway to Promote Pro-Tumoral and Malignant Phenotypes in 3D Engineered Microenvironments. *J Immunother Canc* (2019) 7(1):190. doi: 10.1186/s40425-019-0666-1
43. Wu X, Deng G, Hao X, Li Y, Zeng J, Ma C, et al. A Caspase-Dependent Pathway is Involved in Wnt/beta-Catenin Signaling Promoted Apoptosis in Bacillus Calmette-Guerin Infected RAW264.7 Macrophages. *Int J Mol Sci* (2014) 15(3):5045–62. doi: 10.3390/ijms15035045
44. Yang J, Fang Z, Wu J, Yin X, Fang Y, Zhao F, et al. Construction and Application of a Lung Cancer Stem Cell Model: Antitumor Drug Screening and Molecular Mechanism of the Inhibitory Effects of Sanguinarine. *Tumour Biol* (2016) 37(10):13871–83. doi: 10.1007/s13277-016-5152-5
45. Sica A, Schioppa T, Mantovani A, Allavena P. Tumour-Associated Macrophages are a Distinct M2 Polarised Population Promoting Tumour Progression: Potential Targets of Anti-Cancer Therapy. *Eur J Canc* (2006) 42 (6):717–27. doi: 10.1016/j.ejca.2006.01.003
46. Yang S, Liu Q, Liao Q. Tumor-Associated Macrophages in Pancreatic Ductal Adenocarcinoma: Origin, Polarization, Function, and Reprogramming. *Front Cell Dev Biol* (2020) 8:607209. doi: 10.3389/fcell.2020.607209
47. Kessenbrock K, Plaks V, Werb Z. Matrix Metalloproteinases: Regulators of the Tumor Microenvironment. *Cell* (2010) 141(1):52–67. doi: 10.1016/j.cell.2010.03.015
48. Chen Y, Jin H, Song Y, Huang T, Cao J, Tang Q, et al. Targeting Tumor-Associated Macrophages: A Potential Treatment for Solid Tumors. *J Cell Physiol* (2021) 236(5):3445–65. doi: 10.1002/jcp.30139
49. Delprat V, Michiels C. A Bi-Directional Dialog Between Vascular Cells and Monocytes/Macrophages Regulates Tumor Progression. *Cancer Metastasis Rev* (2021) 40(2):477–500. doi: 10.1007/s10555-021-09958-2
50. Yin W, Yu X, Kang X, Zhao Y, Zhao P, Jin H, et al. Remodeling Tumor-Associated Macrophages and Neovascularization Overcomes EGFR(T790M) -Associated Drug Resistance by PD-L1 Nanobody-Mediated Codelivery. *Small* (2018) 14(47):e1802372. doi: 10.1002/smll.201802372
51. Ojalvo LS, Whittaker CA, Condeelis JS, Pollard JW. Gene Expression Analysis of Macrophages That Facilitate Tumor Invasion Supports a Role for Wnt-Signaling in Mediating Their Activity in Primary Mammary Tumors. *J Immunol* (2010) 184(2):702–12. doi: 10.4049/jimmunol.0902360
52. Yang Y, Ye Y-C, Chen Y, Zhao J-L, Gao C-C, Han H, et al. Crosstalk Between Hepatic Tumor Cells and Macrophages *via* Wnt/β-Catenin Signaling Promotes M2-Like Macrophage Polarization and Reinforces Tumor Malignant Behaviors. *Cell Death Dis* (2018) 9(8):793. doi: 10.1038/s41419-018-0818-0
53. Lee GT, Kwon SJ, Kim J, Kwon YS, Lee N, Hong JH, et al. WNT5A Induces Castration-Resistant Prostate Cancer *via* CCL2 and Tumour-Infiltrating Macrophages. *Br J Canc* (2018) 118(5):670–8. doi: 10.1038/bjc.2017.451
54. Pukrop T, Klemm F, Hagemann Th., Gradl D, Schulz M, Siemes S, et al. Wnt 5a Signaling is Critical for Macrophage-Induced Invasion of Breast Cancer Cell Lines. *PNAS* (2006) 103:5454–9. doi: 10.1073/pnas.0509703103
55. Bergenfelz C, Medrek C, Ekstrom E, Jirstrom K, Janols H, Wullt M, et al. Wnt5a Induces a Tolerogenic Phenotype of Macrophages in Sepsis and Breast Cancer Patients. *J Immunol* (2012) 188(11):5448–58. doi: 10.4049/jimmunol.1103378
56. Sarode P, Zheng X, Giotopoulou GA, Weigert A, Kuenne C, Günther S, et al. Reprogramming of Tumor-Associated Macrophages by Targeting β-Catenin/FOSL2/ARID5A Signaling: A Potential Treatment of Lung Cancer. *Sci Adv* (2020) 6:eaaz6105. doi: 10.1126/sciadv.aaz6105
57. Bergers G, Benjamin LE, Weigert A, Kuenne C, Günther S. Tumorigenesis and the Angiogenic Switch. *Nat Rev Canc* (2003) 3(6):401–10. doi: 10.1038/nrc1093
58. Yeo EJ, Cassetta L, Qian BZ, Lewkowich I, Li JF, Stefater JA3rd, et al. Myeloid WNT7b Mediates the Angiogenic Switch and Metastasis in Breast Cancer. *Cancer Res* (2014) 74(11):2962–73. doi: 10.1158/0008-5472.CAN-13-2421

Conflict of Interest: The authors declare that the research was conducted in the absence of any commercial or financial relationships that could be construed as a potential conflict of interest.

Advantages of publishing in Frontiers

OPEN ACCESS
Articles are free to read for greatest visibility and readership

FAST PUBLICATION
Around 90 days from submission to decision

HIGH QUALITY PEER-REVIEW
Rigorous, collaborative, and constructive peer-review

TRANSPARENT PEER-REVIEW
Editors and reviewers acknowledged by name on published articles

Frontiers
Avenue du Tribunal-Fédéral 34
1005 Lausanne | Switzerland

Visit us: www.frontiersin.org
Contact us: frontiersin.org/about/contact

REPRODUCIBILITY OF RESEARCH
Support open data and methods to enhance research reproducibility

DIGITAL PUBLISHING
Articles designed for optimal readership across devices

FOLLOW US
@frontiersin

IMPACT METRICS
Advanced article metrics track visibility across digital media

EXTENSIVE PROMOTION
Marketing and promotion of impactful research

LOOP RESEARCH NETWORK
Our network increases your article's readership